FLASH User's Guide

Version 4.4

October 2016 (last updated November 4, 2016)

Flash Center for Computational Science

University of Chicago

License

0.1 Acknowledgments in Publication

All publications resulting from the use of the FLASH Code must acknowledge the Flash Center. Addition of the following text to the paper acknowledgments will be sufficient.

"The software used in this work was in part developed by the DOE NNSA-ASC OASCR Flash Center at the University of Chicago."

The users should visit the bibliography hosted at `flash.uchicago.edu/site/publications/flash_pubs.shtml` to find the relevant papers to cite in their work.

This is a summary of the rules governing the dissemination of the "Flash Code" by the Flash Center for Computational Science to users outside the Center, and constitutes the License Agreement for users of the Flash Code. Users are responsible for following all of the applicable rules described below.

0.2 Full License Agreement

Below is a summary of the rules governing the dissemination of the "FLASH Code" by the Flash Center for Computational Science to users outside the Center, and constitutes the License Agreement for users of the FLASH Code. Users are responsible for following all of the applicable rules described below.

- Public Release. Publicly released versions of the FLASH Code are available via the Center's website. We expect to include any external contributions to the Code in public releases that occur after the end of a negotiated time.
- Decision Process. At present, release of the FLASH Code to users not located at the University of Chicago or at Argonne National Laboratory is governed solely by the Center's Director and Management Committee; decisions related to public release of the FLASH Code will be made in the same manner.
- License and Distribution Rights. The University of Chicago owns the copyright to all Code developed by the members of the Flash Center at the University of Chicago. External contributors may choose to be included in the Copyright Assertion. The FLASH Code, or any part of the code, can only be released and distributed by the Flash Center; individual users of the FLASH Code are not free to re-distribute the FLASH Code, or any of its components, outside the Center. All users of the FLASH Code must sign a hardcopy version of this License Agreement and send it to the Center. Distribution of the FLASH Code can only occur once we receive a signed License Agreement.
- Modifications and Acknowledgments. Users may make modifications to the FLASH Code, and they are encouraged to send such modifications to the Center. Users are not free to distribute the FLASH Code to others, as noted in Section 3 above. As resources permit, we will incorporate such modifications in subsequent releases of the FLASH Code, and we will acknowledge these external contributions. Note that modifications that do not make it into an officially-released version of the FLASH Code will not be supported by us.

Acknowledgments

The Flash Center for Computational Science at the University of Chicago is supported by the DOE NNSA-ASC and NSF. Some of the test calculations described here were performed on machines at LLNL, LANL, San Diego Supercomputing Center, and ANL. The current contributors to the code from the Center include:

Sean Couch, Norbert Flocke, Dongwook Lee, Petros Tzeferacos, and Klaus Weide.
Considerable external and past contributors include:

Katie Antypas, John Bachan, Robi Banerjee, Edward Brown, Peter Brune, Alvaro Caceres, Alan Calder, Christopher Daley, Anshu Dubey, Jonathan Dursi, Milad Fatenejad, Christoph Federrath, Robert Fisher, Bruce Fryxell, Nathan Hearn, Mats Holmström, J. Brad Gallagher, Murali Ganapathy Krishna, Nathan Goldbaum, Shravan K. Gopal, William Gray, Timur Linde, Zarija Lukic, Andrea Mignone, Joshua Miller, Prateeti Mohapatra, Kevin Olson, Salvatore Orlando, Tomek Plewa, Kim Robinson, Lynn Reid, Paul Rich, Paul Ricker, Katherine Riley, Chalence Safranek-Shrader, Anthony Scopatz, Daniel Sheeler, Andrew Siegel, Noel Taylor, Frank Timmes, Dean Townsley, Marcos Vanella, Natalia Vladimirova, Greg Weirs, Richard Wunsch, Mike Zingale, and John ZuHone.

`PARAMESH` was developed under NASA Contracts/Grants NAG5-2652 with George Mason University; NAS5-32350 with Raytheon/STX; NAG5-6029 and NAG5-10026 with Drexel University; NAG5-9016 with the University of Chicago; and NCC5-494 with the GEST Institute. For information on `PARAMESH` please contact its main developers, Peter MacNeice (macneice@alfven.gsfc.nasa.gov) and Kevin Olson (olson@physics.drexel.edu) and see the website
http://www.physics.drexel.edu/~olson/paramesh-doc/Users_manual/amr.html.

Contents

Chapter 1

Introduction

The FLASH code is a modular, parallel multiphysics simulation code capable of handling general compressible flow problems found in many astrophysical environments. It is a set of independent code units put together with a Python language setup tool to form various applications. The code is written in FORTRAN90 and C. It uses the Message-Passing Interface (MPI) library for inter-processor communication and the HDF5 or Parallel-NetCDF library for parallel I/O to achieve portability and scalability on a variety of different parallel computers. FLASH4 has three interchangeable discretization grids: a Uniform Grid, and a block-structured oct-tree based adaptive grid using the `PARAMESH` library, and a block-structured patch based adaptive grid using `Chombo`. Both `PARAMESH` and `Chombo` place resolution elements only where they are needed most.[1] The code's architecture is designed to be flexible and easily extensible. Users can configure initial and boundary conditions, change algorithms, and add new physics units with minimal effort.

The Flash Center was founded at the University of Chicago in 1997 under contract to the United States Department of Energy as part of its Accelerated Strategic Computing Initiative (ASCI) (now the Advanced Simulation and Computing (ASC) Program). The scientific goal of the Center then was to address several problems related to thermonuclear flashes on the surface of compact stars (neutron stars and white dwarfs), in particular Type Ia supernovae, and novae. The software goals of the center were to develop new simulation tools capable of handling the extreme resolution and physical requirements imposed by conditions in these explosions and to make them available to the community through the public release of the FLASH code. Since 2009 the several new scienfic and computational code development projects have been added to the Center, the notable one among them are: Supernova Models, High-Energy Density Physics (HEDP), Fluid-Structure Interaction, and Implicit Solvers for stiff parabolic and hyperbolic systems with AMR.

The FLASH code has become a key hydrodynamics application used to test and debug new machine architectures because of its modular structure, portability, scalability and dependence on parallel I/O libraries. It has a growing user base and has rapidly become a shared code for the astrophysics community and beyond, with hundreds of active users who customize the code for their own research.

1.1 What's New in FLASH4

This Guide describes the release version 4.4 of FLASH4. FLASH4 includes all the well tested capabilities of FLASH3. There were a few modules in the official releases of FLASH2 which were added and tested by local users, but did not have standardized setups that could be used to test them after the migration to FLASH3. Those modules are not included in the official releases of FLASH3 or FLASH4, however, they are being made available to download "as is" from the Flash Center's website. We have ensured that they have been imported into FLASH4 to the extent that they conform to the architecture and compile. We cannot guarantee that they work correctly; they are meant to be useful starting points for users who need their functionality. We also welcome setups contributed by the users that can meaningfully test these units. If such setups become available to us, the units will be released in future.

[1]The `Chombo` grid in FLASH has had limited testing, and supports only a limited set of physics units. At this time the use of Chombo within FLASH for production is not recommended.

In terms of the code architecture, FLASH4 closely follows FLASH3. The major changes from FLASH3 are several new capabilities in both physics solvers and infrastructure. Major effort went into the design of the FLASH3 architecture to ensure that the code can be easily modified and extended by internal as well as external developers. Each code unit in FLASH4, like in FLASH3 has a well defined interface and follows the rules for inheritance and encapsulation defined in FLASH3. One of the largest achievements of FLASH3 was the separation of the discretized 'grid' architecture from the actual physics. This untangling required changes in the deepest levels of the code, but has demonstrated its worth by allowing us to import a new AMR package `Chombo` into the code.

Because of the increasing importance of software verification and validation, the Flash code group has developed a test-suite application for FLASH3. The application is called FlashTest and can be used to setup, compile, execute, and test a series of FLASH code simulations on a regular basis. FlashTest is available without a license and can be downloaded from the Code Support Web Page. There is also a more general open-source version of FlashTest which can be used to test any software in which an application is configured and then executed under a variety of different conditions. The results of the tests can then be visualized in a browser with FlashTestView, a companion to FlashTest that is also open-source.

Many but not all parts of FLASH4 are backwards compatible with FLASH2, and they are all compatible with FLASH3. The Flash code group has written extensive documentation detailing how to make the transition from FLASH2 to FLASH3 as smooth as possible. The user should follow the "Name changes from FLASH2 to FLASH3" link on the Code Support Web Page for help on transitioning to FLASH4 from FLASH2. The transition from FLASH3 to FLASH4 does not require much effort from the users except in any custom implementation they may have.

The new capabilities in FLASH4 that were not included in FLASH3 include

- 3T capabilities in the split and unsplit Hydro solvers. There is support for non-cartesian geometry and the unsplit solver also supports stationary rigid body.
- Upwind biased constrained transport (CT) scheme in the unsplit staggered mesh MHD solver
- Full corner transport upwind (CTU) algorithm in the unsplit hydro/MHD solver
- Cylindrical geometry support in the unsplit staggered mesh MHD solver on UG and AMR. A couple of MHD simulation setups using cylindrical geometry.
- Units for radiation diffusion, conduction, and heat exchange.
- Equation-of state unit includes table based multi-material multi-temperature implementation.
- The Opacities unit with the ability to use hot and cold opacities.
- The laser drive with threading for performance
- Ability to replicate mesh for multigroup diffusion or other similar applications.
- Several important solvers have been threaded at both coarse-grain (one block per thread) and fine-grain (threads within a block) levels.
- Several new HEDP simulation setups.
- A new multipole solver
- Ability to add particles during evolution

The enhancements and bug fixes to the existing capabilities since FLASH4-beta release are :

- The HLLD Riemann solver has been improved to handle MHD degeneracy.
- PARAMESH's handling for face-centered variables in order to ensure divergence-free magnetic fields evolution on AMR now uses `gr_pmrpDivergenceFree=.true.` and `gr_pmrpForceConsistency=.true.` by default.

- The HEDP capabilities of the code have been exercised and are therefore more robust.
- Laser 3D in 2D ray tracing has been added. The code traces rays in a real 3D cylindrical domain using a computational 2D cylindrical domain and is based on a polygon approximation to the angular part.
- In non-fixedblocksize mode, restart with particles did not work when starting with a different processor count. This bug has now been fixed.
- All I/O implementations now support reading/writing 0 blocks and 0 particles.
- There is support for particles and face variables in PnetCDF
- Initializaton of of the computation domain has been optimized by eliminating unnecessary invocations of PARAMESH's "digital orrery" algorithm at simulation startup. It is possible to run the orrery in a reduced communicator in order to speed up FLASH initialization.
- The custom region code and corresponding Grid API routines have been removed.
- PARAMESH4DEV is now the default PARAMESH implementation.

The new capabilities in FLASH4.2 ... FLASH4.2.2 since FLASH4.0.1 include:

- New Core-Collapse Super Nova (CCSN) physics, with complete nuclear EOS routines, local neutrino heating/cooling and multispecies neutrino leakage.
- New unsplit Hydro and MHD implementations, highly optimized for performance. These implementations are now the default option. We have retained the old implementations as an `unsplit_old` alternative for compatibility reasons.
- New support for 3T magnetohydrodynamics, designed for HEDP problems.
- A new magnetic resistivity implementation, `SpitzerHighZ`, for HEDP problems. We have also extended the support for resistivity in cylindrical geometry in the unsplit solver.
- New threading capabilities for unsplit MHD, compatible with all threading strategies followed by the code.
- New, improved multipole Poisson solver, implementing the algorithmic refinements described in http://dx.doi.org/10.1088/0004-637X/778/2/181 and http://arxiv.org/abs/1307.3135.
- Reorganization of the `EnergyDeposition` unit. A new feature has been included that allows EnergyDeposition to be called once every n time steps.

The new capabilities in FLASH4.3 since FLASH4.2.2 include:

- The sink particles implementation now has support for particles to remain active when leaving the grid domain (in case of outflow boundary conditions).
- New Proton Imaging unit: The new unit is a simulated diagnostic of the Proton Radiography used in HEDP experiments.
- Flux-limited-diffusion for radiation (implemented in RadTransMain/MGD) is now available for astrophysical problem setups:
  - MatRad3 (matter+rad [2T] stored in three components) implementations for several Eos types: `Gamma`, `Multigamma`, and (experimentally) `Helmholtz/SpeciesBased`.
  - Implemented additional terms in FLD Rad-Hydro equations to handle streaming and transition-to-streaming regimes better - including radiation pressure. This is currently available as a variant of the unsplit Hydro solver code, under HydroMain/unsplit_rad . We call this RADFLAH - Radiation Flux-Limiter Aware Hydro. Setup with shortcut `+uhd3tR` instead of `+uhd3t` . This has had limited testing, mostly in 1D spherical geometry.

  - New test setups under `Simulation/SimulationMain/radflaHD`: `BondiAccretion`, `RadBlastWave`
  - Various fixes in Eos implementations.
  - New ”outstream” diffusion solver boundary condition for streaming limit. (currently 1D spherical only)
  - Added Levermore-Pomraning flux limiter.
  - More flexible setup combinations are now easily possible - can combine, *e.g.*, species declared on setup command line with SPECIES in Config files and initialized with Simulation_initSpecies, by setup with `ManualSpeciesDirectives=True`.
  - Created an ”`Immediate`” HeatExchange implementation.
  - EXPERIMENTAL: ExpRelax variant of `RadTrans` diffusion solver, implements the algorithm described in Gittings et al (2008) for the RAGE code, good for handling strong matter-radiation coupling; for one group (grey) only.
  - EXPERIMENTAL: Unified variant of RadTrans diffusion solver, for handling several coupled scalar equations with HYPRE.
  - EXPERIMENTAL: More accurate implementation of flux limiting (and evaluation of diffusion coeffs): apply limiter to face values, not cell centered values.

- Gravity can now be used in 3T simulations.

- Laser Energy Deposition: New ray tracing options added based on cubic interpolation techniques. Two variants: 1) Piecewise Parabolic Ray Tracing (PPRT) and 2) Runge Kutta (RK) ray tracing.

- Introduction of new numerical tool units: 1) Interpolate: currently contains the routines to set up and perform cubic interpolations on rectangular 1D,2D,3D grids, 2) Roots: (will) contain all routines that solve $f(x) = 0$ (currently contains quadratic, cubic and quartic polynomial root solvers, 3) Runge Kutta: sets up and performs Runge Kutta integration of arbitrary functions (passed as arguments).

- Unsplit Hydro/MHD: Local CFL factor using `CFL_VAR`. (Declare a ”`VARIABLE cfl`” and initialize it appropriately.)

- Unsplit Hydro/MHD: Significant reorganization.

  - reorganized definition and use of scratch data. Memory savings.
  - use `hy_memAllocScratch` and friends.
  - `hy_fullRiemannStateArrays` (instead of `FLASH_UHD_NEED_SCRATCHVARS`)
  - New runtime parameter hy_fullSpecMsFluxHandling, default TRUE. resulting in flux-corrected handling for species and mass scalars, including USM.
  - Use `shockLowerCFL` instead of `shockDetect` runtime parameter.
  - Revived `EOSforRiemann` option.
  - More accurate handling of geometric effects close to the origin in 1D spherical geometry.

Important changes in FLASH4.4 since FLASH4.3 include:

- The default Hydro implementation has changed from split PPM to unsplit Hydro. A new shortcut `+splitHydro` can be used to request a split Hydro implementation.

- Updated values of many physical constants to 2014 CODATA values. This may cause differences from previously obtained results. The previous values of constants provided by the PhysicalConstants unit can be restored by replacing the file PhysicalCosntants˙init.F90 with an older version; the version from FLASH4.3 is included as `PhysicalConstants_init.F90.flash43`. This should only be done to reproduce previous simulation results to bit accuracy.

- An improved Newton-Raphson search in the 3T Multi-type Eos implemention (MTMMMT, including Eos based on IONMIX tables) can prevent some cases of convergence failure by bounding the search. This implementation follows original improvements made to the `Helmholtz Eos` implementation by Dean Townsley.
- Added new Poisson solvers (Martin-Cartwright Geometric Multigrid and BiPCGStab, which uses multigrid aspreconditioner). Combinations of homogeneous Dirichlet, Neumann, and periodic boundary conditions are supported (although not yet "isolated" boundaries for self-gravity).
- Added the `IncompNS` physics unit, which provides a solver for incompressible flow problems on rectangular domains. Multistep and Runge-Kutta explicit projection schemes are used for time integration. Implementations on staggered grid arrangement for both uniform grid (UG) and adaptive mesh refinement (AMR) are provided. The new Poisson solvers are employed for AMR cases, whereas the homogeneous trigonometric solver + PFFT can be used in UG. Typical velocity boundary conditions for this problem are implemented.
- The ProtonImaging diagnostics code has been improved. Time resolved proton imaging is now possible, where protons are traced through the domain during several time steps. The original version (tracing of protons during one time step with fixed domain) is still available.
- The code for Radiation-Fluxlimiter-Aware Hydro has been updated. Smoothing of the flux-limiter function within the enhanced Hydro implementation has been implemented and has been shown effective in increasing stability in 1D simulations.
- New Opacity implementations: `BremsstrahlungAndThomson` and `OPAL`. These are for gray opacities.
- In addition to the FLASH4.4 release, the publicly available Python module `opacplot2` has received significant development (credit to JT Laune). It can assist in handling EoS/opacity tables, and includes command line tools to convert various table formats to IONMIX and to compare between different tables. More information can be found in the Flash Center's GitHub repository at `https://github.com/flash-center/opacplot2`.

The following features are provided on an EXPERIMENTAL basis. They may only work in limited circumstances and/or have not yet been tested to our satisfaction.

- New Laser - Async communication (experimental).
- Electron-Entropy Advection in Hydro for non-ideal Eos.
- New cubic and quartic equation solvers have been added and are ready to be used. They return only real cubic and quartic roots. The routines can be found in the flashUtilites/general section
- An alternative setup tool "setup_alt" intended to be a compatible replacement with a cleaner structure.

1.2 External Contributions

Here we list some major contributions to FLASH4 from outside the Flash Center that are included in the distribution. For completeness, we also list such contributions in FLASH3 which have long been included in the release.

- Huang-Greengard based multigrid solver, contributed by Paul Ricker. This contribution was first distributed in FLASH3. Reference: `http://adsabs.harvard.edu/abs/2008ApJS..176..293R`
- Direct solvers for Uniform Grid contributed by Marcos Vanella. The solvers have been in the release since FLASH3. Reference: `http://dx.doi.org/10.1002/cpe.2821`
- Additional Poisson solvers (Martin-Cartwright Geometric Multigrid ported from FLASH2, and new BiPCGStab), and Incompressible Navier-Stokes solver unit, from Marcos Vanella; added to the release code in FLASH4.4.

- Hybrid-PIC code, contributed by Mats Holmström. The contribution has been in the distribution since FLASH4-alpha. Reference: `http://adsabs.harvard.edu/abs/2011arXiv1104.1440H`
- Primordial Chemistry contributed by William Gray. This contribution was added in FLASH4.0. Reference: `http://iopscience.iop.org/0004-637X/718/1/417/`.
- Barnes Hut tree gravity solver contributed by Richard Wunsch. This contribution has been further extended in FLASH 4.2.2 and in the current release and has been developed in collaboration with Frantisek Dinnbier (responsible for periodic and mixed boundary conditions) and Stefanie Walch.
- Sink Particles contributed by Christoph Federrath et al. This contribution has received significant updates over several release. Please refer to `http://iopscience.iop.org/0004-637X/713/1/269/` for details.
- Since FLASH4.2.2, there is a new 'FromFile' implementation of the Stir unit, contributed by Christoph Federrath. The new implementations is sitting beside the older 'Generate' implementation.
- New Flame and Turb units contributed by Dean Townsley, with code developed by Aaron Jackson and Alan Calder. A corresponding paper (Jackson, Townsley, & Calder 2014) on modeling turbulent flames has been published, see `http://stacks.iop.org/0004-637X/784/i=2/a=174`. More information can be found in Section 17.6 and Section 17.7.

1.3 Known Issues in This Release

- The outflow boundary condition for face-centered variables in the use of solenoidal magnetic field evolution on AMR fails to ensure the solenoidal constraint at the physical outflow boundaries. However, numerical solutions with respect to this error are still physically correct away from the outflow boundaries. This issue may be resolved in future releases.
- The upwind-biased electric field implementation (i.e., `E_upwind=.true.`) for the unsplit staggered mesh solver in some cases fails to satisfy divergence-free magnetic field evolutions at restart. Users can still use (i.e., `E_upwind=.false.`) in most applications.
- The new multipole solver is missing the ability to treat a non-zero minimal radius for spherical geometries, and the ability to specify a point mass contribution to the potential.
- The “Split” implementation of the diffusion solver is essentially meant for testing purposes. Moreover, it has not been exercised with PARAMESH.
- Some configurations of hydrodynamic test problems with Chombo grid show worse than expected mass and total energy conservation. Please see the Chombo section in the Hydro chapter of this Guide for details.
- We have experienced the following abort when running IsentropicVortex problem with Chombo Grid: "MayDay: TreeIntVectSet.cpp:1995: Assertion 'bxNumPts != 0' failed. !!!" We have been in contact with the Chombo team to resolve this issue.
- The unsplit MHD solver doesn't support the mode "use_GravPotUpdate=.true." for 1D when self-gravity is utilized. The solver will still work if it is set to be .false. In this case the usual reconstruction schemes will be used in computing the gravitational accelerations at the predictor step (i.e., at the n+1/2 step) rather than calling the Poisson solver to compute them.
- Time limiting due to burning, even though has an implementation, is turned off in most simulations by keeping the value of parameter `enucDtFactor` very high. The implementation is therefore not well tested and should be used with care.
- Mesh replication is only supported for parallel HDF5 and the experimental derived data type Parallel-NetCDF (`+pnetTypeIO`) I/O implementations. Flash will fail at runtime if multiple meshes are in use without using one of these I/O implementations.

- The unsplit staggered mesh MHD solver shows slight differences (of relative magnitudes of order 10^{-12}) in restart comparisons (e.g., sfocu comparison), when there are non-zero values of face-centered magnetic fields. With PARAMESH4DEV, the current default Grid implementation, we have observed this problem only with the '`force_consistency`' flag (see Runtime Parameter `gr_pmrpForceConsistency`) turned on.

- In some cases with the default refinement criteria implementation, the refinement pattern at a given point in time of a `PARAMESH` AMR simulation may be slightly different depending on how often plotfiles and checkpoints are written; with resulting small changes in simulation results. The effect is expected to also be present in previous FLASH versions. This is a side effect of `Grid_restrictAllLevels` calls that happen in IO to prepare all grid blocks for being dumped to file. We have determined that this can only impact how quickly coarser blocks next to a refinement boundary are allowed to further derefine when their better resolved neighbors also derefine, in cases where second-derivative criteria applied to the block itself would allow such derefinement. Users who are concerned with this effect may want to replace the call to `amr_restrict` in `Grid_updateRefinement` with a call to `Grid_restrictAllLevels`, at the cost of a slight increase in runtime.

- The PG compiler fails to compile source files which contain OpenMP parallel regions that reference threadprivate data. This happens in the threaded versions of the Multipole solver and the within block threaded version of split hydro. A workaround is to remove "default(none)" from the OpenMP parallel region.

- Absoft compiler (`gcc 4.4.4/Absoft Pro fortran 11.1.x86_64` with `mpich2 1.4.1p1`) generates incorrectly behaving code with some files when used with any optimization. More specifically, we have seen this behavior with gr_markRefineDerefine.F90, but other files may be vulnerable too. An older version (`Absoft Fortran 95 9.0 EP/gcc 4.5.1` with `mpich-1.2.7p1`) works.

- The `-index-reorder` setup flag does not work in all the configurations. If you wish to use it please contact the FLASH team.

- The `-noclobber` setup option will not force a rebuild of all necessary source files in a FLASH application with derived data type I/O (`+hdf5TypeIO` or `+pnetTypeIO`). Do not use `-noclobber` with derived data type I/O.

1.4 About the User's Guide

This User's Guide is designed to enable individuals unfamiliar with the FLASH code to quickly get acquainted with its structure and to move beyond the simple test problems distributed with FLASH, customizing it to suit their own needs. Code users and developers are encouraged to visit the FLASH code documentation page for other references to supplement the User's Guide.

Part I provides a rapid introduction to working with FLASH. Chapter 2 (Quick Start) discusses how to get started quickly with FLASH, describing how to setup, build, and run the code with one of the included test problems and then to examine the resulting output. Users unfamiliar with the capabilities of FLASH, who wish to quickly 'get their feet wet' with the code, should begin with this section. Users who want to get started immediately using FLASH to create new problems of their own will want to refer to Chapter 3 (Setting Up New Problems) and Chapter 5 (The FLASH Configuration Script).

Part II begins with an overview of both the FLASH code architecture and a brief overview of the units included with FLASH. It then describes in detail each of the units included with the code, along with their subunits, runtime parameters, and the equations and algorithms of the implemented solvers. **Important note: We assume that the reader has some familiarity both with the basic physics involved and with numerical methods for solving partial differential equations.** This familiarity is absolutely essential in using FLASH (or any other simulation code) to arrive at meaningful solutions to physical problems. The novice reader is directed to an introductory text, examples of which include

Fletcher, C. A. J. *Computational Techniques for Fluid Dynamics* (Springer-Verlag, 1991)

Laney, C. B. *Computational Gasdynamics* (Cambridge UP, 1998)

LeVeque, R. J., Mihalas, D., Dorfi, E. A., and Müller, E., eds. *Computational Methods for Astrophysical Fluid Flow* (Springer, 1998)

Roache, P. *Fundamentals of Computational Fluid Dynamics* (Hermosa, 1998)

Toro, E. F. *Riemann Solvers and Numerical Methods for Fluid Dynamics, 2nd Edition* (Springer, 1997)

The advanced reader who wishes to know more specific information about a given unit's algorithm is directed to the literature referenced in the algorithm section of the chapter in question.

Part VII describes the different test problems distributed with FLASH. Part VIII describes in more detail the analysis tools distributed with FLASH, including `fidlr` and `sfocu`.

Part I

Getting Started

Chapter 2

Quick Start

This chapter describes how to get up-and-running quickly with FLASH with an example simulation, the Sedov explosion. We explain how to configure a problem, build it, run it, and examine the output using IDL.

2.1 System requirements

You should verify that you have the following:

- A copy of the FLASH source code distribution (as a Unix tar file). To request a copy of the distribution, click on the "Code Request" link on the FLASH Center web site. You will be asked to fill out a short form before receiving download instructions. Please remember the username and password you use to download the code; you will need these to get bug fixes and updates to FLASH.

- A F90 (Fortran 90) compiler and a C compiler. Most of FLASH is written in F90. Information available at the Fortran Company web site can help you select an F90 compiler for your system. FLASH has been tested with many Fortran compilers. For details of compilers and libraries, see the RELEASE-NOTES available in the FLASH home directory.

- An installed copy of the Message-Passing Interface (MPI) library. A freely available implementation of MPI called MPICH is available from Argonne National Laboratory.

- To use the Hierarchical Data Format (HDF) for output files, you will need an installed copy of the freely available HDF library. The serial version of HDF5 is the current default FLASH format. HDF5 is available from the HDF Group (`http://www.hdfgroup.org/`) of the National Center for Supercomputing Applications (NCSA) at `http://www.ncsa.illinois.edu`. The contents of HDF5 output files produced by the FLASH units are described in detail in Section 9.1.

- To use the Parallel NetCDF format for output files, you will need an installed copy of the freely available PnetCDF library. PnetCDF is available from Argonne National Lab at `http://www.mcs.anl.gov/parallel-netcdf/`. For details of this format, see Section 9.1.

- To use Chombo as the (Adaptive Mesh Refinement) AMR option, you will need an installed copy of the library, available freely from Lawrence Berkeley National Lab at `https://seesar.lbl.gov/anag/chombo`. The use of Chombo is described in Section 8.7

- To use the Diffuse unit with HYPRE solvers, you will need to have an installed copy of HYPRE, available for free from Lawrence Livermore National Lab at `https://computation.llnl.gov/casc/hypre/software.html`.

  HYPRE is required for using several critical HEDP capabilities including multigroup radiation diffusion and thermal conduction. Please make sure you have HYPRE installed if you want these capabilities.

- To use the output analysis tools described in this section, you will need a copy of the IDL language from ITT Visual Information Solutions. IDL is a commercial product. It is not required for the analysis of FLASH output, but the `fidlr3.0` tools described in this section require it. (FLASH output formats are described in Section 9.9. If IDL is not available, another visual analysis option is ViSit, described in Chapter 31.) The newest IDL routines, those contained in fidlr3.0, were written and tested with IDL 6.1 and above. You are encouraged to upgrade if you are using an earlier version. Also, to use the HDF5 version 1.6.2, analysis tools included in IDL require IDL 6.1 and above. New versions of IDL come out frequently, and sometimes break backwards compatibility, but every effort will be made to support them.

- The GNU make utility, `gmake`. This utility is freely available and has been ported to a wide variety of different systems. For more information, see the entry for `make` in the development software listing at `http://www.gnu.org/`. On some systems `make` is an alias for `gmake`. GNU make is required because FLASH uses macro concatenation when constructing Makefiles.

- A copy of the Python language, version 2.2 or later is required to run the `setup` script. Python can be downloaded from `http://www.python.org`.

2.2 Unpacking and configuring FLASH for quick start

To begin, unpack the FLASH source code distribution.

```
 tar -xvf FLASHX.Y.tar
```

where *X.Y* is the FLASH version number (for example, use `FLASH4-alpha.tar` for FLASH version 4-alpha, or `FLASH3.1.tar` for FLASH version 3.1). This will create a directory called `FLASH`*X*`/`. Type '`cd FLASH`*X*' to enter this directory. Next, configure the FLASH source tree for the Sedov explosion problem using the `setup` script. Type

```
     ./setup Sedov -auto
```

This configures FLASH for the 2d `Sedov` problem using the default hydrodynamic solver, equation of state, Grid unit, and I/O format defined for this problem, linking all necessary files into a new directory, called '`object/`'. For the purpose of this example, we will use the default I/O format, serial HDF5. In order to compile a problem on a given machine FLASH allows the user to create a file called `Makefile.h` which sets the paths to compilers and libraries specific to a given platform. This file is located in the directory `sites/`*mymachine.myinstitution.mydomain*`/`. The `setup` script will attempt to see if your machine/platform has a `Makefile.h` already created, and if so, this will be linked into the `object/` directory. If one is not created the setup script will use a prototype Makefile.h with guesses as to the locations of libraries on your machine. The current distribution includes prototypes for *AIX*, *IRIX64*, *Linux*, *Darwin*, and *TFLOPS* operating systems. In any case, it is advisable to create a `Makefile.h` specific to your machine. See Section 5.6 for details.

Type the command `cd object` to enter the object directory which was created when you setup the Sedov problem, and then execute `make`. This will compile the FLASH code.

```
cd object
make
```

If you have problems and need to recompile, '`make clean`' will remove all object files from the `object/` directory, leaving the source configuration intact; '`make realclean`' will remove all files and links from `object/`. After '`make realclean`', a new invocation of `setup` is required before the code can be built. The building can take a long time on some machines; doing a parallel build (`make -j` for example) can significantly increase compilation speed, even on single processor systems.

Assuming compilation and linking were successful, you should now find an executable named `flash`*X* in the `object/` directory, where *X* is the major version number (*e.g.*, 4 for $X.Y = 4.0$). You may wish to check that this is the case.

If compilation and linking were not successful, here are a few common suggestions to diagnose the problem:

- Make sure the correct compilers are in your path, and that they produce a valid executable.
- The default Sedov problem uses HDF5 in serial. Make sure you have HDF5 installed. If you do not have HDF5, you can still setup and compile FLASH, but you will not be able to generate either a checkpoint or a plot file. You can setup FLASH without I/O by typing

  ```
  ./setup Sedov -auto +noio
  ```

- Make sure the paths to the MPI and HDF libraries are correctly set in the `Makefile.h` in the `object/` directory.
- Make sure your version of MPI creates a valid executable that can run in parallel.

These are just a few suggestions; you might also check for further information in this guide or at the FLASH web page.

FLASH by default expects to find a text file named `flash.par` in the directory from which it is run. This file sets the values of various runtime parameters that determine the behavior of FLASH. If it is not present, FLASH will abort; `flash.par` must be created in order for the program to run (note: all of the distributed setups already come with a `flash.par` which is *copied* into the `object/` directory at setup time). There is command-line option to use a different name for this file, described in the next section. Here we will create a simple `flash.par` that sets a few parameters and allows the rest to take on default values. With your text editor, edit the `flash.par` in the `object` directory so it looks like Figure 2.1.

```
# runtime parameters

lrefine_max = 5

basenm  = "sedov_"
restart = .false.
checkpointFileIntervalTime = 0.01

nend = 10000
tmax = 0.05

gamma = 1.4

xl_boundary_type = "outflow"
xr_boundary_type = "outflow"

yl_boundary_type = "outflow"
yr_boundary_type = "outflow"

plot_var_1 = "dens"
plot_var_2 = "temp"
plot_var_3 = "pres"
```

Figure 2.1: FLASH parameter file contents for the quick start example.

This example instructs FLASH to use up to five levels of adaptive mesh refinement (AMR) (through the `lrefine_max` parameter) and to name the output files appropriately (`basenm`). We will not be starting from a checkpoint file ("`restart = .false.`" — this is the default, but here it is explicitly set for clarity). Output files are to be written every 0.01 time units (`checkpointFileIntervalTime`) and will be created until $t = 0.05$ or 10000 timesteps have been taken (`tmax` and `nend` respectively), whichever comes first. The ratio of specific heats for the gas (`gamma` = γ) is taken to be 1.4, and all four boundaries of the two-dimensional grid have outflow (zero-gradient or Neumann) boundary conditions (set via the [`xy`][`lr`]`_boundary_type` parameters).

Note the format of the file – each line is of the form *variable* = *value*, a comment (denoted by a hash mark, `#`), or a blank. String values are enclosed in double quotes ("). Boolean values are indicated in the FORTRAN style, `.true.` or `.false.`. Be sure to insert a carriage return after the last line of text. A full list of the parameters available for your current setup is contained in the file `setup_params` located in the `object/` directory, which also includes brief comments for each parameter. If you wish to skip the creation of a `flash.par`, a complete example is provided in the `source/Simulation/SimulationMain/Sedov/` directory.

2.3 Running FLASH

We are now ready to run FLASH. To run FLASH on N processors, type

```
mpirun -np N flashX
```

remembering to replace N and X with the appropriate values. Some systems may require you to start MPI programs with a different command; use whichever command is appropriate for your system. The FLASH4 executable accepts an optional command-line argument for the runtime parameters file. If "`-par_file` *filename*" is present, FLASH reads the file specified on command line for runtime parameters, otherwise it reads `flash.par`.

You should see a number of lines of output indicating that FLASH is initializing the Sedov problem, listing the initial parameters, and giving the timestep chosen at each step. After the run is finished, you should find several files in the current directory:

- `sedov.log` echoes the runtime parameter settings and indicates the run time, the build time, and the build machine. During the run, a line is written for each timestep, along with any warning messages. If the run terminates normally, a performance summary is written to this file.

- `sedov.dat` contains a number of integral quantities as functions of time: total mass, total energy, total momentum, *etc.* This file can be used directly by plotting programs such as `gnuplot`; note that the first line begins with a hash (`#`) and is thus ignored by `gnuplot`.

- `sedov_hdf5_chk_000*` are the different checkpoint files. These are complete dumps of the entire simulation state at intervals of `checkpointFileIntervalTime` and are suitable for use in restarting the simulation.

- `sedov_hdf5_plt_cnt_000*` are plot files. In this example, these files contain density, temperature, and pressure in single precision. If needed, more variables can be dumped in the plotfiles by specifying them in *flash.par*. They are usually written more frequently than checkpoint files, since they are the primary output of FLASH for analyzing the results of the simulation. They are also used for making simulation movies. Checkpoint files can also be used for analysis and sometimes it is necessary to use them since they have comprehensive information about the state of the simulation at a given time. However, in general, plotfiles are preferred since they have more frequent snapshots of the time evolution. Please see Chapter 9 for more information about IO outputs.

We will use the `xflash3` routine under IDL to examine the output. Before doing so, we need to set the values of three environment variables, `IDL_DIR`, `IDL_PATH` and `XFLASH3_DIR`. You should usually have `IDL_DIR` already set during the IDL installation. Under `csh` the two additional variables can be set using the commands

```
setenv XFLASH3_DIR "<flash home dir>/tools/fidlr3.0"
setenv IDL_PATH "${XFLASH3_DIR}:$IDL_PATH"
```

where <*flash home dir*> is the location of the `FLASH`*X.Y* directory. If you get a message indicating that `IDL_PATH` is not defined, enter

```
setenv IDL_PATH "${XFLASH3_DIR}":${IDL_DIR}:${IDL_DIR}/lib
```

where `${IDL_DIR}` points to the directory where IDL is installed. Fidlr assumes that you have a version of IDL with native HDF5 support.

FLASH Transition

Please note! The environment variable used with FLASH3 onwards is `XFLASH3_DIR`. The main routine name for interactive plotting is `xflash3`.

Now run IDL (`idl` or `idl start_linux`) and enter `xflash3` at the `IDL>` prompt. You should see the main widget as shown in Figure 2.2.

Select any of the checkpoint or plot files through the *File/Open Prototype...* dialog box. This will define a prototype file for the dataset, which is used by `fidlr` to set its own data structures. With the prototype defined, enter the suffixes '0000', '0005' and '1' in the three suffix boxes. This tells `xflash3` which files to plot. `xflash3` can generate output for a number of consecutive files, but if you fill in only the beginning suffix, only one file is read. Click the *auto* box next to the data range to automatically scale the plot to the data. Select the desired plotting variable and colormap. Under 'Options,' select whether to plot the logarithm of the desired quantity and select whether to plot the outlines of the computational blocks. For very highly refined grids, the block outlines can obscure the data, but they are useful for verifying that FLASH is putting resolution elements where they are needed.

When the control panel settings are to your satisfaction, click the 'Plot' button to generate the plot. For Postscript or PNG output, a file is created in the current directory. The result should look something like Figure 2.3, although this figure was generated from a run with eight levels of refinement rather than the five used in the quick start example run. With fewer levels of refinement, the Cartesian grid causes the explosion to appear somewhat diamond-shaped. Please see Chapter 34 for more information about visualizing FLASH output with IDL routines.

FLASH is intended to be customized by the user to work with interesting initial and boundary conditions. In the following sections, we will cover in more detail the algorithms and structure of FLASH and the sample problems and tools distributed with it.

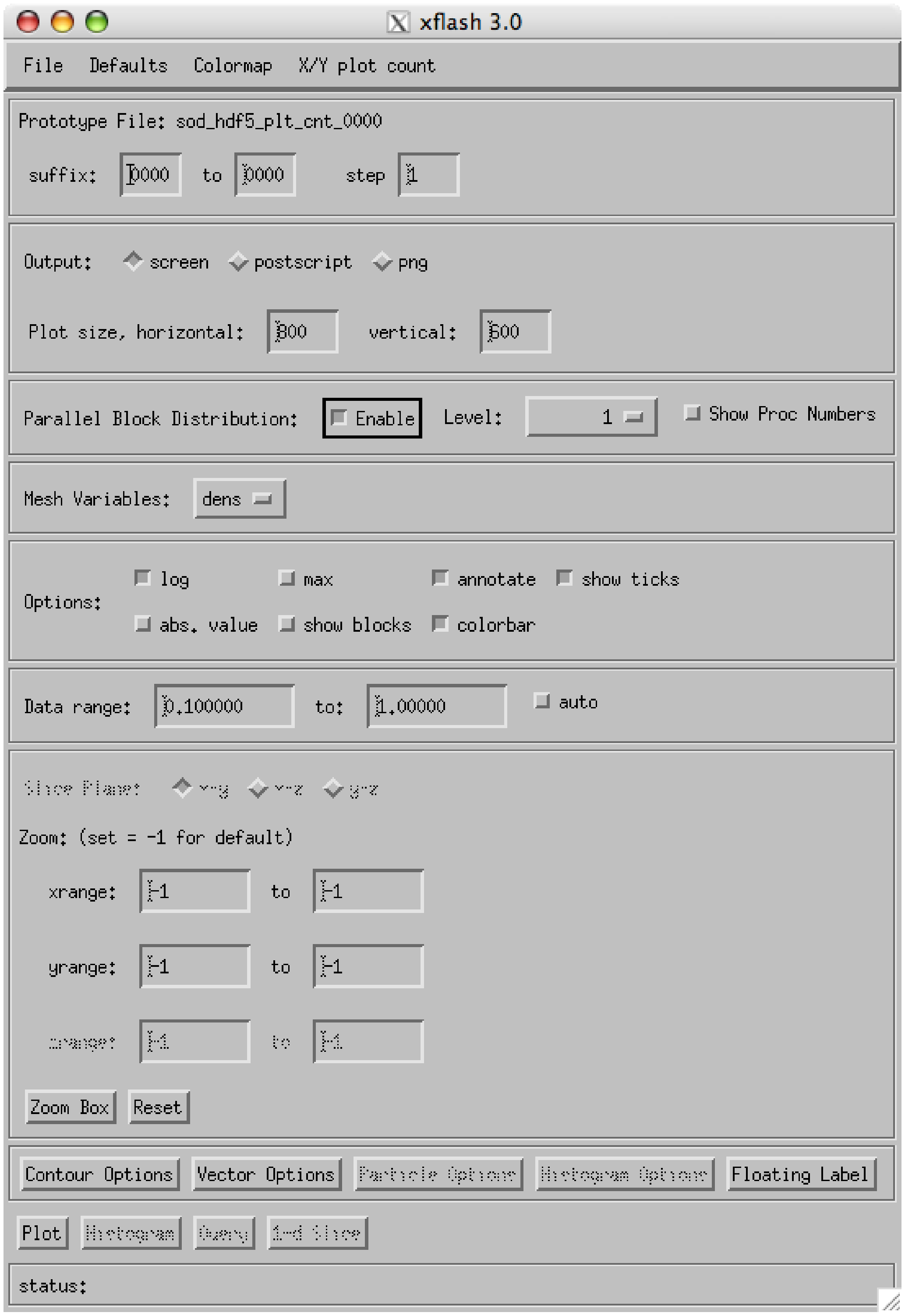

Prototype File: sod_hdf5_plt_cnt_0000

suffix: 0000 to 0000 step 1

Output: screen postscript png

Plot size, horizontal: 800 vertical: 600

Parallel Block Distribution: Enable Level: 1 Show Proc Numbers

Mesh Variables: dens

Options: log max annotate show ticks abs. value show blocks colorbar

Data range: 0.100000 to: 1.00000 auto

Slice Plane: x-y x-z y-z

Zoom: (set = -1 for default)

xrange: -1 to -1

yrange: -1 to -1

zrange: -1 to -1

status:

Figure 2.2: The main `xflash3` widget.

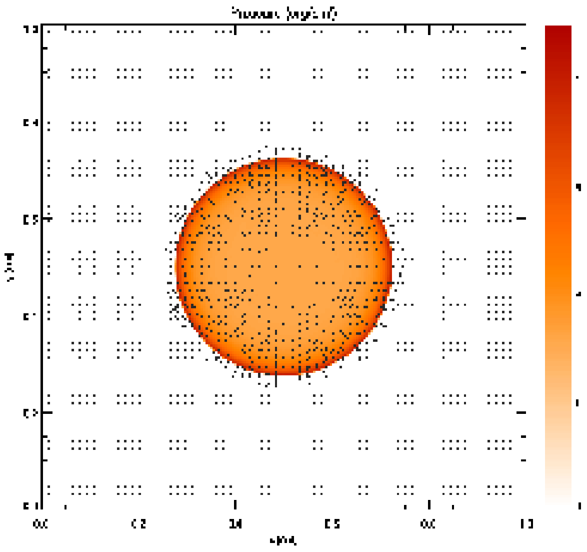

Figure 2.3: Example of `xflash` output for the Sedov problem with eight levels of refinement.

Chapter 3

Setting Up New Problems

A new FLASH problem is created by making a directory for it under `FLASH4/source/Simulation/SimulationMain`. This location is where the FLASH `setup` script looks to find the problem-specific files. The FLASH distribution includes a number of pre-written simulations; however, most FLASH users will want to simulate their own problems, so it is important to understand the techniques for adding a customized problem simulation.

Every simulation directory contains routines to initialize the FLASH grid. The directory also includes a `Config` file which contains information about infrastructure and physics units, and the runtime parameters required by the simulation (see Chapter 5). The files that are usually included in the Simulation directory for a problem are:

`Config`	Lists the units and variables required for the problem, defines runtime parameters and initializes them with default values.
`Makefile`	The `make` include file for the Simulation.
`Simulation_data.F90`	Fortran module which stores data and parameters specific to the Simulation.
`Simulation_init.F90`	Fortran routine which reads the runtime parameters, and performs other necessary initializations.
`Simulation_initBlock.F90`	Fortran routine for setting initial conditions in a single block.
`Simulation_initSpecies.F90`	Optional Fortran routine for initializing species properties if multiple species are being used.
`flash.par`	A text file that specifies values for the runtime parameters. The values in flash.par override the defaults from Config files.

In addition to these basic files, a particular simulation may include some files of its own. These files could provide either new functionality not available in FLASH, or they may include customized versions of any of the FLASH routines. For example, a problem might require a custom refinement criterion instead of the one provided with FLASH. If a customized implementation of `Grid_markRefineDerefine` is placed in the Simulation directory, it will replace FLASH's own implementation when the problem is setup. In general, users are encouraged to put any modifications of core FLASH files in the `SimulationMain` directory in which they are working rather than by altering the default FLASH routines. This encapsulation of personal changes will make it easier to integrate Flash Center patches, and to upgrade to more recent versions of the code. The user might also wish to include data files in the `SimulationMain` necessary for initial conditions. Please see the `LINKIF` and `DATAFILES` keywords in Section 5.5.1 for more information on linking in datafiles or conditionally linking customized implementations of FLASH routines.

The next few paragraphs are devoted to the detailed examination of the basic files for an example setup. The example we describe here is a hydrodynamical simulation of the Sod shock tube problem, which has a one-dimensional flow discontinuity. We construct the initial conditions for this problem by establishing a planar interface at some angle to the x and y axes, across which the density and pressure values are discontinuous. The fluid is initially at rest on either side of the interface. To create a new simulation, we first create a new directory `Sod` in `Simulation/SimulationMain` and then add the `Config`, `Makefile`, `flash.par`, `Simulation_initBlock.F90`, `Simulation_init.F90` and `Simulation_data.F90` files. Since this is a single fluid simulation, there is no need for a `Simulation_initSpecies` file. The easiest way to construct these files is to use files from another setup as templates.

3.1 Creating a `Config` file

The `Config` file for this example serves two principal purposes; (1) to specify the required units and (2) to register runtime parameters.

```
# configuration file for our example problem
REQUIRES Driver
REQUIRES physics/Eos/EosMain/Gamma
REQUIRES physics/Hydro
```

The lines above define the FLASH units required by the Sod problem. Note that we do not ask for particular implementations of the `Hydro` unit, since for this problem many implementations will satisfy the requirements. However, we do ask for the gamma-law equation of state (`physics/Eos/EosMain/Gamma`) specifically, since that implementation is the only valid option for this problem. In FLASH4-alpha, the `PARAMESH` 4 `Grid` implementation is passed to `Driver` by default. As such, there is no need to specify a `Grid` unit explicitly, unless a simulation requires an alternative `Grid` implementation. Also important to note is that we have not explicitly required `IO`, which is included by default. In constructing the list of requirements for a problem, it is important to keep them as general as the problem allows. We recommend asking for specific implementations of units as command line options or in the `Units` file when the problem is being setup, to avoid the necessity of modifying the `Config` files. For example, if there was more than one implementation of `Hydro` that could handle the shocks, any of them could be picked at setup time without having to modify the Config file. However, to change the `Eos` to an implementation other than `Gamma`, the Config file would have to be modified. For command-line options of the setup script and the description of the `Units` file see Chapter 5.

After specifying the units, the `Config` file lists the runtime parameters specific to this problem. The names of runtime parameters are case-insensitive. Note that no unit is constrained to use only the parameters defined in its own `Config` file. It can legitimately access any runtime parameter registered by any unit included in the simulation.

```
PARAMETER sim_rhoLeft   REAL    1.       [0 to ]
PARAMETER sim_rhoRight  REAL    0.125    [0 to ]
PARAMETER sim_pLeft     REAL    1.       [0 to ]
PARAMETER sim_pRight    REAL    0.1      [0 to ]
PARAMETER sim_uLeft     REAL    0.
PARAMETER sim_uRight    REAL    0.
PARAMETER sim_xangle    REAL    0.       [0 to 360]
PARAMETER sim_yangle    REAL    90.      [0 to 360]
PARAMETER sim_posn      REAL    0.5
```

Here we define (`sim_rhoLeft`), (`sim_pLeft`) and (`sim_uLeft`) as density, pressure and velocity to the left of the discontinuity, and (`sim_rhoRight`), (`sim_pRight`) and (`sim_uRight`) as density, pressure and velocity to the right of the discontinuity. The parameters (`sim_xangle`) and (`sim_yangle`) give the angles with respect to the x and y axes, and (`sim_posn`) specifies the intersection between the shock plane and x axis. The quantities in square brackets define the permissible range of values for the parameters. The default value of any parameter (like `sim_xangle`) can be overridden at runtime by including a line (i.e. `sim_xangle = 45.0`) defining a different value for it in the `flash.par` file.

3.2 Creating a `Makefile`

The file `Makefile` included in the Simulation directory does not have the standard Makefile format for make/gmake. Instead, the setup script generates a complete compilation Makefile from the machine/system specific one (see Section 5.6) and the unit Makefiles (see Section 5.7.3).

In general, standard module and routine dependencies are figured out by the `setup` script or are inherited from the directory structure. The `Makefile` for this example is very simple, it only adds the object file for `Simulation_data` to the Simulation unit Makefile. The additional object files such as `Simulation_init.o` are already added in the directory above `SimulationMain`.

3.3 Creating a `Simulation_data.F90`

The Fortran module `Simulation_data` is used to store data specific to the Simulation unit. In FLASH4-alpha there is no central 'database', instead, each unit stores its own data in its `Unit_data` Fortran module. Data needed from other units is accessed through that unit's interface. The basic structure of the `Simulation_data` module is shown below:

```
module Simulation_data
  implicit none

  !! Runtime Parameters
  real, save :: sim_rhoLeft, sim_rhoRight, sim_pLeft, sim_pRight
  real, save :: sim_uLeft, sim_uRight, sim_xAngle, sim_yAngle, sim_posn
  real, save :: sim_gamma, sim_smallP, sim_smallX

  !! Other unit variables
  real, save :: sim_xCos, sim_yCos, sim_zCos

end module Simulation_data
```

Note that all the variables in this data module have the `save` attribute. Without this attribute the storage for the variable is not guaranteed outside of the scope of `Simulation_data` module with many compilers. Also notice that there are many more variables in the data module than in the `Config` file. Some of them, such as 'sim_smallX' etc, are runtime parameters from other units, while others such as 'sim_xCos' are simulation specific variables that are available to all routines in the Simulation unit. The FLASH4-alpha naming convention is that variables that begin with `sim_` are used or "belong" to the Simulation unit.

3.4 Creating a `Simulation_init.F90`

The routine `Simulation_init` is called by the routine `Driver_initFlash` at the beginning of the simulation. `Driver_initFlash` calls Unit_init.F90 routines of every unit to initialize them. In this particular case, the `Simulation_init` routine will get the necessary runtime parameters and store them in the `Simulation_data` Fortran module, and also initialize other variables in the module. More generally, all one-time initialization required by the simulation are implemented in the `Simulation_init` routine.

FLASH Transition

In FLASH2, the contents of the `if (.firstcall.)` clause are now in the Simulation_init routine in FLASH4.

The basic structure of the routine `Simulation_init` should consist of

1. Fortran module `use` statement for the `Simulation_data`
2. Fortran module `use` statement for the `Unit_interfaces` to access the interface of the `RuntimeParameters` unit, and any other units being used.
3. Variable typing `implicit none` statement
4. Necessary `#include` header files
5. Declaration of arguments and local variables.
6. Calls to the `RuntimeParameters` unit interface to obtain the values of runtime parameters.
7. Calls to the `PhysicalConstants` unit interface to initialize any necessary physical constants.
8. Calls to the `Multispecies` unit interface to initialize the species' properties, if there multiple species are in use
9. Initialize other unit scope variables, packages and functions
10. Any other calculations that are needed only once at the beginning of the run.

In this example after the `implicit none` statement we include two files, `"constants.h"`, and `"Flash.h"`. The `"constants.h"` file holds global constants defined in the FLASH code such as `MDIM`, `MASTER_PE`, and `MAX_STRING_LENGTH`. It also stores constants that make reading the code easier, such as `IAXIS`, `JAXIS`, and `KAXIS`, which are defined as 1,2, and 3, respectively. More information is available in comments in the distributed `constants.h`. A complete list of defined constants is available on the Code Support Web Page.

The `"Flash.h"` file contains all of the definitions specific to a given problem. This file is generated by the setup script and defines the indices for the variables in various data structures. For example, the index for density in the cell centered grid data structure is defined as `DENS_VAR`. The `"Flash.h"` file also defines the number of species, number of dimensions, maximum number of blocks, and many more values specific to a given run. Please see Chapter 6 for complete description of the `Flash.h` file.

FLASH Transition

The defined constants in `"Flash.h"` file allows the user direct access to the variable index in '`unk`.' This direct access is unlike FLASH2, where the user would first have to get the integer index of the variable by calling a data base function and then use the integer variable `idens` as the variable index. Previously:

```
idens=dBaseKeyNumber('dens')
ucons(1,i) = solnData(idens,i,j,k)
```

Now, the syntax is simpler:

```
ucons(1,i) = solnData(DENS_VAR,i,j,k)
```

This new syntax also allows discovery of specification errors at compile time.

```
subroutine Simulation_init()

  use Simulation_data
  use RuntimeParameters_interface, ONLY : RuntimeParameters_get
  implicit none
```

```
#include "Flash.h"
#include "constants.h"


  ! get the runtime parameters relevant for this problem

  call RuntimeParameters_get('smallp', sim_smallP)
  call RuntimeParameters_get('smallx', sim_smallX)
  call RuntimeParameters_get('gamma', sim_gamma)
  call RuntimeParameters_get('sim_rhoLeft', sim_rhoLeft)
  call RuntimeParameters_get('sim_rhoRight', sim_rhoRight)
  call RuntimeParameters_get('sim_pLeft', sim_pLeft)
  call RuntimeParameters_get('sim_pRight', sim_pRight)
  call RuntimeParameters_get('sim_uLeft', sim_uLeft)
  call RuntimeParameters_get('sim_uRight', sim_uRight)
  call RuntimeParameters_get('sim_xangle', sim_xAngle)
  call RuntimeParameters_get('sim_yangle', sim_yAngle)
  call RuntimeParameters_get('sim_posn', sim_posn)

  ! Do other initializations
  ! convert the shock angle parameters

  sim_xAngle = sim_xAngle * 0.0174532925 ! Convert to radians.
  sim_yAngle = sim_yAngle * 0.0174532925

  sim_xCos = cos(sim_xAngle)

  if (NDIM == 1) then
     sim_xCos = 1.
     sim_yCos = 0.
     sim_zCos = 0.

  elseif (NDIM == 2) then
     sim_yCos = sqrt(1. - sim_xCos*sim_xCos)
     sim_zCos = 0.

  elseif (NDIM == 3) then
     sim_yCos = cos(sim_yAngle)
     sim_zCos = sqrt( max(0., 1. - sim_xCos*sim_xCos - sim_yCos*sim_yCos) )
  endif

end subroutine Simulation_init
```

3.5 Creating a Simulation_initBlock.F90

The routine Simulation_initBlock is called by the Grid unit to apply initial conditions to the physical domain. If the AMR grid PARAMESH is being used, the formation of the physical domain starts at the lowest level of refinement. Initial conditions are applied to each block at this level by calling Simulation_initBlock. The Grid unit then checks the refinement criteria in the blocks it has created and refines the blocks if the criteria are met. It then calls Simulation_initBlock to initialize the newly created blocks. This process repeats until the grid reaches the required refinement level in the areas marked for refinement. The Uniform Grid has only one level, with same resolution everywhere. Therefore, only one block per processor is created and Simulation_initBlock is called to initialize this single block. It is important to note that a problem's

`Simulation_initBlock` routine is the same regardless of whether `PARAMESH` or Uniform Grid is being used. The `Grid` unit handles these differences, not the Simulation unit.

The basic structure of the routine `Simulation_initBlock` should be as follows:

1. A `use` statement for the Simulation_data
2. One of more `use` statement to access other unit interfaces being used, for example `use Grid_interface, ONLY: Grid_putPointData`
3. Variable typing `implicit none` statement
4. Necessary `#include` header files
5. Declaration of arguments and local variables.
6. Generation of initial conditions either from a file, or directly calculated in the routine
7. Calls to the various `Grid_putData` routines to store the values of solution variables.

We continue to look at the `Sod` setup and describe its `Simulation_initBlock` in detail. The first part of the routine contains all the declarations as shown below. The first statement in routine is the `use` statement, which provides access to the runtime parameters and other unit scope variables initialized in the `Simulation_init` routine. The include files bring in the needed constants, and then the arguments are defined. The declaration of the local variables is next, with allocatable arrays for each block.

```
subroutine Simulation_initBlock(blockID)
  ! get the needed unit scope data
  use Simulation_data, ONLY: sim_posn, sim_xCos, sim_yCos, sim_zCos,&
                             sim_rhoLeft, sim_pLeft, sim_uLeft,     &
                             sim_rhoRight, sim_pRight, sim_uRight,  &
                             sim_smallX, sim_gamma, sim_smallP
  use Grid_interfaces, ONLY : Grid_getBlkIndexLimits, Grid_getCellCoords, &
                              Grid_putPointData
  implicit none

  ! get all the constants
#include "constants.h"
#include "Flash.h"

  ! define arguments and indicate whether they are input or output
  integer, intent(in) :: blockID

  ! declare all local variables.
  integer :: i, j, k, n
  integer :: iMax, jMax, kMax
  real :: xx, yy,  zz, xxL, xxR
  real :: lPosn0, lPosn

  ! arrays to hold coordinate information for the block
  real, allocatable, dimension(:) :: xCenter, xLeft, xRight, yCoord, zCoord

  ! array to get integer indices defining the beginning and the end
  ! of a block.
  integer, dimension(2,MDIM) :: blkLimits, blkLimitsGC
```

```
! the number of grid points along each dimension
integer :: sizeX, sizeY, sizeZ

integer, dimension(MDIM) :: axis
integer :: dataSize
logical :: gcell = .true.

! these variables store the calculated initial values of physical
! variables a grid point at a time.
real :: rhoZone, velxZone, velyZone, velzZone, presZone, &
     enerZone, ekinZone
```

Note that FLASH promotes all floating point variables to double precision at compile time for maximum portability. We therefore declare all floating point variables with `real` in the source code. In the next part of the code we allocate the arrays that will hold the coordinates.

FLASH Transition

FLASH4-alpha supports blocks that are not sized at compile time to generalize the Uniform Grid, and to be able to support different AMR packages in future. For this reason, the arrays are not sized with the static NXB etc. as was the case in FLASH2. Instead they are allocated on a block by block basis in `Simulation_initBlock`. Performance is compromised by the use of allocatable arrays, however, since this part of the code is executed only at the beginning of the simulation, it has negligible impact on the overall execution time in production runs.

```
! get the integer endpoints of the block in all dimensions
! the array blkLimits returns the interior end points
! whereas array blkLimitsGC returns endpoints including guardcells
call Grid_getBlkIndexLimits(blockId,blkLimits,blkLimitsGC)

! get the size along each dimension for allocation and then allocate
sizeX = blkLimitsGC(HIGH,IAXIS)
sizeY = blkLimitsGC(HIGH,JAXIS)
sizeZ = blkLimitsGC(HIGH,KAXIS)
allocate(xLeft(sizeX))
allocate(xRight(sizeX))
allocate(xCenter(sizeX))
allocate(yCoord(sizeY))
allocate(zCoord(sizeZ))
```

The next part of the routine involves setting up the initial conditions. This section could be code for interpolating a given set of initial conditions, constructing some analytic model, or reading in a table of initial values. In the present example, we begin by getting the coordinates for the cells in the current block. This is done by a set of calls to `Grid_getCellCoords` . Next we create loops that compute appropriate values for each grid point, since we are constructing initial conditions from a model. Note that we use the `blkLimits` array from `Grid_getBlkIndexLimits` in looping over the spatial indices to initialize only the interior cells in the block. To initialize the entire block, including the guardcells, the `blkLimitsGC` array should be used.

```
xCoord(:) = 0.0
yCoord(:) = 0.0
zCoord(:) = 0.0
```

```
  call Grid_getCellCoords(IAXIS, blockID, LEFT_EDGE,  gcell, xLeft,   sizeX)
  call Grid_getCellCoords(IAXIS, blockID, CENTER,     gcell, xCenter, sizeX)
  call Grid_getCellCoords(IAXIS, blockID, RIGHT_EDGE, gcell, xRight,  sizeX)
  call Grid_getCellCoords(JAXIS, blockID, CENTER,     gcell, yCoord,  sizeY)
  call Grid_getCellCoords(KAXIS, blockID, CENTER,     gcell, zCoord,  sizeZ)

!------------------------------------------------------------------------------
! loop over all of the zones in the current block and set the variables.
!------------------------------------------------------------------------------
  do k = blkLimits(LOW,KAXIS),blkLimits(HIGH,KAXIS)
     zz = zCoord(k) ! coordinates of the cell center in the z-direction
     lPosn0 = sim_posn - zz*sim_zCos/sim_xCos ! Where along the x-axis
                                              ! the shock intersects
                                              ! the xz-plane at the current z.

     do j = blkLimits(LOW,JAXIS),blkLimits(HIGH,JAXIS)
        yy = yCoord(j) ! center coordinates in the y-direction
        lPosn = lPosn0 - yy*sim_yCos/sim_xCos ! The position of the
                                              ! shock in the current yz-row.
        dataSize = 1  ! for Grid put data function, we are
                      ! initializing a single cell at a time and
                      ! sending it to Grid

        do i = blkLimits(LOW,IAXIS),blkLimits(HIGH,IAXIS)

           xx  = xCenter(i) ! center coordinate along x
           xxL = xLeft(i)   ! left coordinate along y
           xxR = xRight(i)  ! right coordinate along z
```

For the present problem, we create a discontinuity along the shock plane. We do this by initializing the grid points to the left of the shock plane with one value, and the grid points to the right of the shock plane with another value. Recall that the runtime parameters which provide these values are available to us through the Simulation_data module. At this point we can initialize all independent physical variables at each grid point. The following code shows the contents of the loops. Don't forget to *store* the calculated values in the Grid data structure!

```
  if (xxR <= lPosn) then
     rhoZone = sim_rhoLeft
     presZone = sim_pLeft

     velxZone = sim_uLeft * sim_xCos
     velyZone = sim_uLeft * sim_yCos
     velzZone = sim_uLeft * sim_zCos

     ! initialize cells which straddle the shock.  Treat them as though 1/2 of
     ! the cell lay to the left and 1/2 lay to the right.
  elseif ((xxL < lPosn) .and. (xxR > lPosn)) then

     rhoZone = 0.5 * (sim_rhoLeft+sim_rhoRight)
     presZone = 0.5 * (sim_pLeft+sim_pRight)

     velxZone = 0.5 *(sim_uLeft+sim_uRight) * sim_xCos
     velyZone = 0.5 *(sim_uLeft+sim_uRight) * sim_yCos
     velzZone = 0.5 *(sim_uLeft+sim_uRight) * sim_zCos
```

```
    ! initialize cells to the right of the initial shock.
  else

     rhoZone = sim_rhoRight
     presZone = sim_pRight

     velxZone = sim_uRight * sim_xCos
     velyZone = sim_uRight * sim_yCos
     velzZone = sim_uRight * sim_zCos

   endif
   axis(IAXIS) = i   ! Get the position of the cell in the block
   axis(JAXIS) = j
   axis(KAXIS) = k

   ! Compute the gas energy and set the gamma-values
   ! needed for the equation of  state.

   ekinZone = 0.5 * (velxZone**2 + velyZone**2 + velzZone**2)

   enerZone = presZone / (sim_gamma-1.)
   enerZone = enerZone / rhoZone
   enerZone = enerZone + ekinZone
   enerZone = max(enerZone, sim_smallP)

  ! store the variables in the current zone via the Grid_putPointData method

   call Grid_putPointData(blockId, CENTER, DENS_VAR, EXTERIOR, axis, rhoZone)
   call Grid_putPointData(blockId, CENTER, PRES_VAR, EXTERIOR, axis, presZone)
   call Grid_putPointData(blockId, CENTER, VELX_VAR, EXTERIOR, axis, velxZone)
   call Grid_putPointData(blockId, CENTER, VELY_VAR, EXTERIOR, axis, velyZone)
   call Grid_putPointData(blockId, CENTER, VELZ_VAR, EXTERIOR, axis, velzZone)
   call Grid_putPointData(blockId, CENTER, ENER_VAR, EXTERIOR, axis, enerZone)
   call Grid_putPointData(blockId, CENTER, GAME_VAR, EXTERIOR, axis, sim_gamma)
   call Grid_putPointData(blockId, CENTER, GAMC_VAR, EXTERIOR, axis, sim_gamma)
```

When `Simulation_initBlock` returns, the Grid data structures for physical variables have the values of the initial model for the current block. As mentioned before, `Simulation_initBlock` is called for every block that is created as the code refines the initial model.

3.6 Creating a `Simulation_freeUserArrays.F90`

From within `Simulation_init`, the user may create large `allocatable` arrays that are used for initialization within `Simulation_initBlock` or some other routine. An example would be a set of arrays that are used to interpolate fields onto the blocks as they are being created. If these arrays use a lot of allocated memory, the subroutine `Simulation_freeUserArrays` gives the user a chance to free this memory using `deallocate` statements. This subroutine is called after all initalization steps have been performed, and the default implementation is a stub which does nothing. A customized version for a particular setup may be made by copying the stub from the `Simulation` directory and editing it as need be.

3.7 The runtime parameter file (`flash.par`)

The FLASH executable expects a `flash.par` file to be present in the *run* directory, unless another name for the runtime input file is given as a command-line option. This file contains runtime parameters, and thus provides a mechanism for partially controlling the runtime environment. The names of runtime parameters are case-insensitive. Copies of `flash.par` are kept in their respective Simulation directories for easy distribution.

The `flash.par` file for the `example` setup is

```
# Density, pressure, and velocity on either side of interface
sim_rhoLeft = 1.
sim_rhoRight = 0.125

sim_pLeft   = 1.
sim_pRight  = 0.1
sim_uLeft   = 0.
sim_uRight  = 0.

# Angle and position of interface relative to x and y axes
sim_xangle  = 0
sim_yangle = 90.
sim_posn = 0.5

# Gas ratio of specific heats
gamma = 1.4

geometry = cartesian

# Size of computational volume
xmin = 0.
xmax = 1.
ymin = 0.
ymax = 1.

# Boundary conditions

xl_boundary_type = "outflow"
xr_boundary_type = "outflow"

yl_boundary_type = "outflow"
yr_boundary_type = "outflow"


# Simulation (grid, time, I/O) parameters
cfl = 0.8
basenm = "sod_"
restart = .false.

# checkpoint file output parameters
checkpointFileIntervalTime = 0.2
checkpointFileIntervalStep = 0
checkpointFileNumber = 0

# plotfile output parameters
plotfileIntervalTime = 0.
```

```
plotfileIntervalStep = 0
plotfileNumber = 0

nend = 1000
tmax = .2

run_comment = "Sod problem, parallel to x-axis"
log_file = "sod.log"
eint_switch = 1.e-4

plot_var_1 = "dens"
plot_var_2 = "pres"
plot_var_3 = "temp"

# AMR refinement parameters
lrefine_max = 6
refine_var_1 = "dens"

# These parameters are used only for the uniform grid
#iGridSize = 8   #defined as nxb * iprocs
#jGridSize = 8
#kGridSize = 1
iProcs = 1  #number or procs in the i direction
jProcs = 1
kProcs = 1

# When using UG, iProcs, jProcs and kProcs must be specified.
# These are the processors along each of the dimensions
#FIXEDBLOCKSIZE mode ::
# When using fixed blocksize, iGridSize etc are redundant in
# runtime parameters. These quantities are calculated as
# iGridSize = NXB*iprocs
# jGridSize = NYB*jprocs
# kGridSize = NZB*kprocs
#NONFIXEDBLOCKSIZE mode ::
# iGridSize etc must be specified. They constitute the global
# number of grid points in the physical domain without taking
# the guard cell into account. The local blocksize is calculated
# as iGridSize/iprocs  etc.
```

In this example, flags are set to start the simulation from scratch and to set the grid geometry, boundary conditions, and refinement. Parameters are also set for the density, pressure and velocity values on either side of the shock, and also the angles and point of intersection of the shock with the “x” axis. Additional parameters specify details of the run, such as the number of timesteps between various output files, and the initial, minimum and final values of the timestep. The comments and alternate values at the end of the file are provided to help configure uniform grid and variably-sized array situations.

When creating the `flash.par` file, another very helpful source of information is the `setup_params` file which gets written by the `setup` script each time a problem is setup. This file lists all possible runtime parameters and their default values from the `Config` files, as well as a brief description of the parameters. It is located in the `object/` directory created at setup time.

Figure 3.1 shows the initial distribution of density for the 2-d Sod problem as setup by the example described in this chapter.

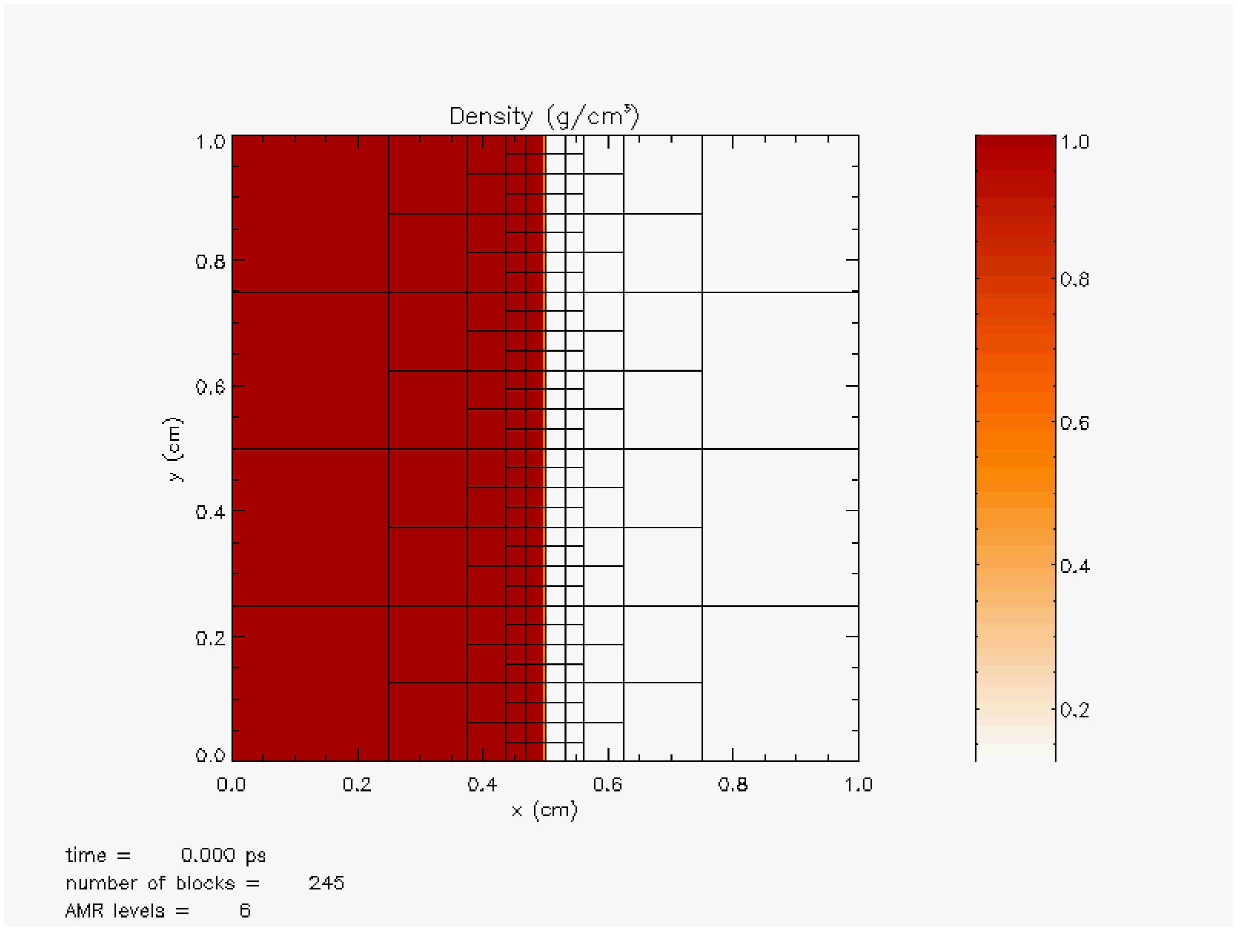

Figure 3.1: Image of the initial distribution of density in `example` setup.

3.8 Running your simulation

You can run your simulation either in the object directory or in a separate run directory.

Running in the object directory is especially convenient for development and testing. The command for starting a FLASH simulation may be system dependent, but typically you would type something like

```
mpirun -np N flash4
```

or

```
mpiexec -n N flash4
```

to start a run on N processing entities. On many systems, you can also simply use

```
./flash4
```

to start a run on 1 processing entity, i.e., without process-level parallelisation.

If you want to invoke FLASH in a separate run directory, the best way is to copy the `flash4` binary into the run directory, and then proceed as above. However, *before* starting FLASH you also need to do the following:

- Copy a FLASH parfile, normally `flash.par`, into the run directory.
- If FLASH was configured with `Paramesh4.0` in `LIBRARY` mode (this is *not* the default): copy the file `amr_runtime_parameters`, into the run directory. This file should have been generated in the object directory by running `./setup`.
- Some code units use additional data or table files, which are also copied into the object directory by `./setup`. (These files typically match one of the patterns `*.dat` or `*_table*`.) copy or move those files into the run directory, too, if your simulation needs them.

Part II

The FLASH Software System

Chapter 4

Overview of FLASH architecture

The files that make up the FLASH source are organized in the directory structure according to their functionality and grouped into components called **units**. Throughout this manual, we use the word 'unit' to refer to a group of related files that control a single aspect of a simulation, and that provide the user with an interface of publicly available functions. FLASH can be viewed as a collection of units, which are selectively grouped to form one application.

A typical FLASH simulation requires only a subset of all of the units in the FLASH code. When the user gives the name of the simulation to the `setup` tool, the tool locates and brings together the units required by that simulation, using the FLASH `Config` files (described in Chapter 5) as a guide. Thus, it is important to distinguish between the entire FLASH source code and a given FLASH application. the FLASH units can be broadly classified into five functionally distinct categories: **infrastructure, physics, monitor, driver,** and **simulation**.

The **infrastructure** category encompasses the units responsible for FLASH housekeeping tasks such as the management of runtime parameters, the handling of input and output to and from the code, and the administration of the grid, which describes the simulation's physical domain.

Units in the **physics** category such as `Hydro` (hydrodynamics), `Eos` (equation of state), and `Gravity` implement algorithms to solve the equations describing specific physical phenomena.

The **monitoring** units `Logfile`, `Profiler`, and `Timers` track the progress of an application, while the `Driver` unit implements the time advancement methods and manages the interaction between the included units.

The **simulation** unit is of particular significance because it defines how a FLASH application will be built and executed. When the setup script is invoked, it begins by examining the simulation's `Config` file, which specifies the units required for the application, and the simulation-specific runtime parameters. Initial conditions for the problem are provided in the routines `Simulation_init` and `Simulation_initBlock`. As mentioned in Chapter 3, the `Simulation` unit allows the user to overwrite any of FLASH's default function implementations by writing a function with the same name in the application-specific directory. Additionally, runtime parameters declared in the simulation's `Config` file override definitions of same-named parameters in other FLASH units. These helpful features enable users to customize their applications, and are described in more detail below in Section 4.1 and online in Architecture Tips. The simulation unit also provides some useful interaces for modifying the behaviour of the application while it is running. For example there is an interface `Simulation_adjustEvolution` which is called at every time step. Most applications would use the null implementation, but its implementation can be placed in the Simulation directory of the application to customize behavior. The API functions of the `Simulation` unit are unique in that except `Simulation_initSpecies`, none of them have any default general implementations. At the API level there are the null implementations, actual implementations exist only for specific applications. The general implementations of `Simulation_initSpecies` exist for different classes of applications, such as those utilizing nuclear burning or ionization.

FLASH Transition

Why the name change from "modules" in FLASH2 to "units" in FLASH3? The term "module" caused confusion among users and developers because it could refer both to a FORTRAN90 module and to the FLASH-specific code entity. In order to avoid this problem, FLASH3 started using the word "module" to refer exclusively to an F90 module, and the word "unit" for the basic FLASH code component. Also, FLASH no longer uses F90 modules to implement units. Fortran's limitation of one file per module is too restrictive for some of FLASH4's units, which are too complex to be described by a single file. Instead, FLASH4 uses interface blocks, which enable the code to take advantage of some of the advanced features of FORTRAN90, such as pointer arguments and optional arguments. Interface blocks are used throughout the code, even when such advanced features are not called for. For a given unit, the interface block will be supplied in the file `"Unit_interface.F90"`. Please note that files containing calls to API-level functions must include the line `use Unit, ONLY: function-name1, function-name2, etc.` at the top of the file.

4.1 FLASH Inheritance

FORTRAN90 is not an object-oriented language like Java or C++, and as such does not implement those languages' characteristic properties of inheritance. But FLASH takes advantage of the Unix directory structure to implement an inheritance hierarchy of its own. Every child directory in a unit's hierarchy inherits all the source code of its parent, thus eliminating duplication of common code. During setup, source files in child directories override same-named files in the parent or ancestor directories.

Similarly, when the `setup` tool parses the source tree, it treats each child or subdirectory as inheriting all of the Config and Makefile files in its parent's directory. While source files at a given level of the directory hierarchy override files with the same name at higher levels, Makefiles and configuration files are cumulative. Since functions can have multiple implementations, selection for a specific application follows a few simple rules applied in order described in Architecture Tips.

However, we must take care that this special use of the directory structure for inheritance does not interfere with its traditional use for organization. We avoid any problems by means of a careful naming convention that allows clear distinction between organizational and namespace directories.

To briefly summarize the convention, which is described in detail online in Architecture Tips, the top level directory of a unit shares its name with that of the unit, and as such always begins with a capital letter. Note, however, that the unit directory may not always exist at the top level of the source tree. A class of units may also be grouped together and placed under an organizational directory for ease of navigation; organizational directories are given in lower case letters. For example the grid management unit, called `Grid`, is the only one in its class, and therefore its path is `source/Grid`, whereas the hydrodynamics unit, `Hydro`, is one of several physics units, and its top level path is `source/physics/Hydro`. This method for distinguishing between organizational directories and namespace directories is applied throughout the entire source tree.

4.2 Unit Architecture

A FLASH unit defines its own Application Programming Interface (API), which is a collection of routines the unit exposes to other units in the code. A unit API is usually a mix of accessor functions and routines which modify the state of the simulation.

A good example to examine is the `Grid` unit API. Some of the accessor functions in this unit are `Grid_getCellCoords`, `Grid_getBlkData`, and `Grid_putBlkData`, while `Grid_fillGuardCells` and `Grid_updateRefinement` are examples of API routines which modify data in the `Grid` unit.

A unit can have more than one implementation of its API. The `Grid` Unit, for example, has both an **Adaptive Grid** and a **Uniform Grid** implementation. Although the implementations are different, they both conform to the **Grid** API, and therefore appear the same to the outside units. This feature allows users to easily swap various unit implementations in and out of a simulation without affecting they way other units communicate. Code does not have to be rewritten if the users decides to implement the uniform grid instead of the adaptive grid.

4.2.1 Stub Implementations

Since routines can have multiple implementations, the **setup** script must select the appropriate implementation for an application. The selection follows a few simple rules described in Architecture Tips. The top directory of every unit contains a **stub** or null implementation of each routine in the Unit's API. The stub functions essentially do nothing. They are coded with just the declarations to provide the same interface to callers as a corresponding "real" implementation. They act as function prototypes for the unit. Unlike true prototypes, however, the stub functions assign default values to the output-only arguments, while leaving the other arguments unaltered. The following snippet shows a simplified example of a stub implementation for the routine Grid_getListOfBlocks.

```
subroutine Grid_getListOfBlocks(blockType, listOfBlocks, count)

  implicit none

  integer, intent(in) :: blockType
  integer,dimension(*),intent(out) :: listOfBlocks
  integer, intent(out) :: count

  count=0
  listOfBlocks(1)=0

  return
end subroutine Grid_getListOfBlocks
```

While a set of null implementation routines at the top level of a unit may seem like an unnecessary added layer, this arrangement allows FLASH to include or exclude units without the need to modify any existing code. If a unit is not included in a simulation, the application will be built with its stub functions. Similarly, if a specific implementation of the unit finds some of the API functions irrelevant, it need not provide any implementations for them. In those situations, the applications include stubs for the unimplemented functions, and full implementations of all the other ones. Since the stub functions do return valid values when called, unexpected crashes from un-initialized output arguments are avoided.

The Grid_updateRefinement routine is a good example of how stub functions can be useful. In the case of a simulation using an adaptive grid, such as PARAMESH, the routine Driver_evolveFlash calls Grid_updateRefinement to update the grid's spacing. The Uniform Grid however, needs no such routine because its grid is fixed. There is no error, however, when Driver_evolveFlash calls Grid_updateRefinement during a Uniform Grid simulation, because the stub routine steps in and simply returns without doing anything. Thus the stub layer allows the same Driver_evolveFlash routine to work with both the Adaptive Grid and Uniform Grid implementations.

FLASH Transition

While the concept of "null" or "stub" functions existed in FLASH2, FLASH3 formalized it by requiring all units to publish their API (the complete Public Interface) at the top level of a unit's directory. Similarly, the inheritance through Unix directory structure in FLASH4 is essentially the same as that of FLASH2, but the introduction of a formal naming convention has clarified it and made it easier to follow. The complete API can be found online at http://flash.uchicago.edu/site/flashcode/user_support/.

4.2.2 Subunits

One or more subunits sit under the top level of a unit. Among them the unit's complete API is implemented. The subunits are considered peers to one another. Each subunit must implement at least one API function, and no two subunits can implement the same API function. The division of a unit into subunits is based upon identifying self-contained subsets of its API. In some instances, a subunit may be completely excluded from a simulation, thereby saving computational resources. For example, the `Grid` unit API includes a few functions that are specific to Lagrangian tracer particles, and are therefore unnecessary to simulations that do not utilize particles. By placing these routines in the `GridParticles` subunit, it is possible to easily exclude them from a simulation. The subunits have composite names; the first part is the unit name, and the second part represents the functionality that the subunit implements. The **primary subunit** is named *Unit*`Main`, which every unit must have. For example, the main subunit of `Hydro` unit is `HydroMain` and that of the `Eos` unit is `EosMain`.

In addition to the subunits, the top level unit directory may contain a subdirectory called *localAPI*. This subdirectory allows a subunit to create a public interface to other subunits within its own unit; all stub implementations of the subunit public interfaces are placed in `localAPI`. External units should *not* call routines listed in the `localAPI`; for this reason these local interfaces are not shown in the general source API tree.

A subunit can have a hierarchy of its own. It may have more than one unit implementation directories with alternative implementations of some of its functions while other functions may be common between them. FLASH exploits the inheritance rules described in Architecture Tips. For example, the `Grid` unit has three implementations for `GridMain`: the Uniform Grid (UG), `PARAMESH` 2, and `PARAMESH` 4. The procedures to apply boundary conditions are common to all three implementations, and are therefore placed directly in `GridMain`. In addition, `GridMain` contains two subdirectories. One is `UG`, which has all the remaining implementations of the API specific to the Uniform Grid. The other directory is organized as `paramesh`, which in turn contains two directories for the package of `PARAMESH` 2 and another organizational directory `paramesh4`. Finally, `paramesh4` has two subdirectories with alternative implementations of the `PARAMESH` 4 package. The directory `paramesh` also contains all the function implementations that are common between `PARAMESH` 2 and `PARAMESH` 4. Following the naming convention described in Architecture Tips, `paramesh` is all lowercase, since it has child directories that have some API implementation. The namespace directories `Paramesh2`, `Paramesh4.0` and`Paramesh4dev` contain functions unique to each implementation. An example of a unit hierarchy is shown in Figure 4.1. The kernels are described below in Section 4.2.4.

4.2.3 Unit Data Modules, `_init`, and `_finalize` routines

Each unit must have a F90 data module to store its unit-scope local data and an `Unit_init` file to initialize it. The `Unit_init` routines are called by the `Driver` unit once by the routine `Driver_initFlash` at the start of a simulation. They get unit specific runtime parameters from the `RuntimeParameters` unit and store them in the unit data module.

Every unit implementation directory of *Unit*`Main`, must either inherit a *Unit*`_data` module, or have its own. There is no restriction on additional unit scope data modules, and individual Units determine how best to manage their data. Other subunits and the underlying computational kernels can have their own data modules, but the developers are encouraged to keep these data modules local to their subunits and kernels for clarity and maintainability of the code. It is strongly recommended that only the data modules in the `Main` subunit be accessible everywhere in the unit. However, no data module of a unit may be known to any other unit. This restriction is imposed to keep the units encapsulated and their data private. If another part of the code needs access to any of the unit data, it must do so through accessor functions.

Additionally, when routines use data from the unit's data module the convention is to indicate what particular data is being used with the `ONLY` keyword, as in `use Unit_data, ONLY : un_someData`. See the snippet of code below for the correct convention for using data from a unit's FORTRAN Data Module.

```
subroutine Driver_evolveFlash()

  use Driver_data, ONLY: dr_myPE, dr_numProcs, dr_nbegin, &
       dr_nend, dr_dt, dr_wallClockTimeLimit, &
```

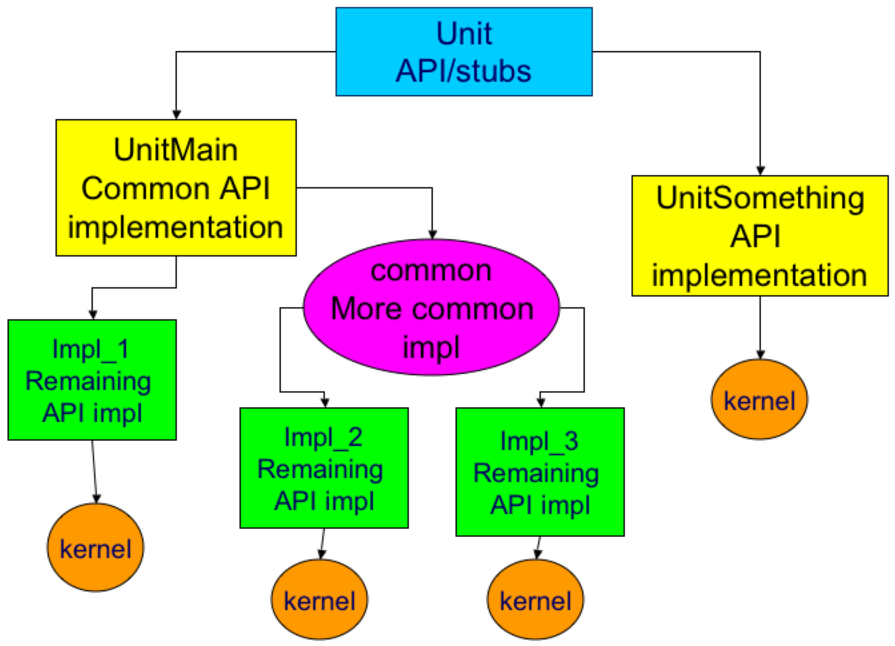

Figure 4.1: The unit hierarchy and inheritance.

```
       dr_tmax, dr_simTime, dr_redshift, &
       dr_nstep, dr_dtOld, dr_dtNew, dr_restart, dr_elapsedWCTime

  implicit none

  integer    :: localNumBlocks
```

Each unit must also have a `Unit_finalize` routine to clean up the unit at the termination of a FLASH run. The finalization routines might deallocate space or write out completion messages.

4.2.4 Private Routines: kernels and helpers

All routines in a unit that do not implement the API are classified as private routines. They are divided into two broad categories: the *kernel* is the collection of routines that implement the unit's core functionality and solvers, and *helper* routines are supplemental to the unit's API and sometimes act as a conduit to its kernel. A helper function is allowed to know the other unit's APIs but is itself known only locally within the unit. The concept of helper functions allows minimization of the unit APIs, which assists in code maintenance. The helper functions follow the convention of starting with an "`un_`" in their name, where "`un`" is in some way derived from the unit name. For example, the helper functions of the `Grid` unit start with `gr_`, and those of `Hydro` unit start with `hy_`. The helper functions have access to the unit's data module, and they are also allowed to query other units for the information needed by the kernel, by using their accessor functions. If the kernel has very specific data structures, the helper functions can also populate them with the collected information. An example of a helper function is `gr_expandDomain`, which refines an AMR block. After refinement, equations of state usually need to be called, so the routine accesses the EOS routines via `Eos_wrapped`.

The concept of kernels, on the other hand, facilitates easy import of third party solvers and software into FLASH. The kernels are not required to follow either the naming convention or the inheritance rules of the FLASH architecture. They can have their own hierarchy and data modules, and the top level of the kernel typically resides at leaf level of the FLASH unit hierarchy. This arrangement allows FLASH to import a solver without having to modify its internal code, since API and helper functions hide the higher level details from it, and hide its details from other units. However, developers are encouraged to follow the helper function naming convention in the kernel where possible to ease code maintenance.

The `Grid` unit and the `Hydro` unit both provide very good examples of private routines that are clearly distinguishable between helper functions and kernel. The AMR version of the `Grid` unit imports the `PARAMESH` version 2 library as a vendor supplied branch in our repository. It sits under the lowest namespace directory `Paramesh2` in `Grid` hierarchy and maintains the library's original structure. All other private functions in the `paramesh` branch of `Grid` are helper functions and their names start with `gr_`. In the `Hydro` unit the entire hydrodynamic solver resides under the directory `PPM`, which was imported from the PROMETHEUS code (see Section 14.1.2). PPM is a directional solver and requires that data be passed to it in vector form. Routines like `hy_sweep` and `hy_block` are helper functions that collect data from the `Grid` unit, and put it in the format required by PPM. These routines also make sure that data stay in thermodynamic equilibrium through calls to the Eos unit. Neither `PARAMESH` 2, nor PPM has any knowledge of units outside their own.

4.3 Unit Test Framework

In keeping with good software practice, FLASH4 incorporates a unit test framework that allows for rigorous testing and easy isolation of errors. The components of the unit test show up in two different places in the FLASH source tree. One is a dedicated path in the `Simulation` unit, `Simulation/SimulationMain/-unitTest/`*UnitTestName*, where *UnitTestName* is the name of a specific unit test. The other place is a subdirectory called `unitTest`, somewhere in the hierarchy of the corresponding unit which implements a function `Unit_unitTest` and any helper functions it may need. The primary reason for organizing unit tests in this somewhat confusing way is that unit tests are special cases of simulation setups that also need extensive access to internal data of the unit being tested. By splitting the unit test into two places, it is possible to meet both requirements without violating unit encapsulation. We illustrate the functioning of the unit test framework with the unit test of the `Eos` unit. For more details please see Section 16.6. The `Eos` unit test needs its own version of the routine `Driver_evolveFlash` which makes a call to its `Eos_unitTest` routine. The initial conditions specification and unit test specific `Driver_evolveFlash` are placed in `Simulation/SimulationMain/unitTest/Eos`, since the `Simulation` unit allows any substitute FLASH function to be placed in the specific simulation directory. The function `Eos_unitTest` resides in `physics/Eos/unitTest`, and therefore has access to all internal `Eos` data structures and helper functions.

Chapter 5

The FLASH configuration script (setup)

The setup script, found in the FLASH root directory, provides the primary command-line interface to configuring the FLASH source code. It is important to remember that the FLASH code is not a single application, but a set of independent code units which can be put together in various combinations to create a multitude of different simulations. It is through the setup script that the user controls how the various units are assembled.

The primary job of the setup script is to

- traverse the FLASH source tree and link necessary files for a given application to the object/ directory
- find the target Makefile.h for a given machine.
- generate the Makefile that will build the FLASH executable.
- generate the files needed to add runtime parameters to a given simulation.
- generate the files needed to parse the runtime parameter file.

More description of how setup and the FLASH4 architecture interact may be found in Chapter 4. Here we describe its usage.

The setup script determines site-dependent configuration information by looking for a directory sites/<hostname> where <hostname> is the hostname of the machine on which FLASH is running.[1] Failing this, it looks in sites/Prototypes/ for a directory with the same name as the output of the uname command. The site and operating system type can be overridden with the -site and -ostype command-line options to the setup command. Only one of these options can be used at one time. The directory for each site and operating system type contains a makefile fragment Makefile.h that sets command names, compiler flags, library paths, and any replacement or additional source files needed to compile FLASH for that specific machine and machine type.

The setup script uses the contents of the problem directory and the site/OS type, together with a Units file, to generate the object/ directory, which contains links to the appropriate source files and makefile fragments. The Units file lists the names of all units which need to be included while building the FLASH application. This file is automatically generated when the user commonly provides the command-line -auto option, although it may be assembled by hand. When -auto option is used, the setup script starts with the Config file of the problem specified, finds its REQUIRED units and then works its way through their Config files. This process continues until all the dependencies are met and a self-consistent set of units has been found. At the end of this automatic generation, the Units file is created and placed in the object/ directory, where it can be edited if necessary. setup also creates the master makefile (object/Makefile) and several FORTRAN include files that are needed by the code in order to parse the runtime parameters. After running setup, the user can create the FLASH executable by running gmake in the object directory.

[1]if a machine has multiple hostnames, setup tries them all

FLASH Transition

In FLASH2, the `Units` file was located in the FLASH root directory. In FLASH4, this file is found in the `object/` directory.

Save some typing

- All the setup options can be shortened to unambiguous prefixes, *e.g.* instead of `./setup -auto <problem-name>` one can just say `./setup -a <problem-name>` since there is only one `setup` option starting with `a`.
- The same abbreviation holds for the problem name as well. `./setup -a IsentropicVortex` can be abbreviated to `./setup -a Isen` assuming that `IsentropicVortex` is the only problem name which starts with `Isen`.
- Unit names are usually specified by their paths relative to the source directory. However, `setup` also allows unit names to be prefixed with an extra "source/", allowing you to use the TAB-completion features of your shell like this

  ```
  ./setup -a Isen -unit=sou<TAB>rce/IO/IOM<TAB>ain/hd<TAB>f5
  ```

- If you use a set of options repeatedly, you can define a shortcut for them. FLASH4 comes with a number of predefined shortcuts that significantly simplify the setup line, particularly when trying to match the Grid with a specific I/O implementation. For more details on creating shortcuts see Section 5.3. For detailed examples of I/O shortcuts please see Section 9.1in the I/O chapter.

Reduce compilation time

- To reuse compiled code when changing setup configurations, use the `-noclobber` setup option. For details see Section 5.2.

5.1 Setup Arguments

The setup script accepts a large number of command line arguments which affect the simulation in various ways. These arguments are divided into three categories:

1. *Setup Options* (example: `-auto`) begin with a dash and are built into the setup script itself. Many of the most commonly used arguments are setup options.
2. *Setup Variables* (example: `species=air,h2o`) are defined by individual units. When writing a `Config` file for any unit, you can define a setup variable. Section 5.4 explains how setup variables can be created and used.
3. *Setup Shortcuts* (example: `+ug`) begin with a plus symbol and are essentially macros which automatically include a set of setup variables and/or setup options. New setup shortcuts can be easily defined, see Section 5.3 for more information.

Table 5.1 shows a list of some of the basic setup arguments that every FLASH user should know about. A comprehensive list of all setup arguments can be found in Section 5.2 alongside more detailed descriptions of these options.

Table 5.1: List of Commonly Used Setup Arguments

Argument	Description
`-auto`	this option should almost always be set
`-unit=<unit>`	include a specified unit
`-objdir=<dir>`	specify a different object directory location
`-debug`	compile for debugging
`-opt`	enable compiler optimization
`-n[xyb]b=#`	specify block size in each direction
`-maxblocks=#`	specify maximum number of blocks per process
`-[123]d`	specify number of dimensions
`-maxblocks=#`	specify maximum number of blocks per process
`+cartesian`	use Cartesian geometry
`+cylindrical`	use cylindrical geometry
`+polar`	use polar geometry
`+spherical`	use spherical geometry
`+noio`	disable IO
`+ug`	use the uniform grid in a fixed block size mode
`+nofbs`	use the uniform grid in a non-fixed block size mode
`+pm2`	use the PARAMESH2 grid
`+pm40`	use the PARAMESH4.0 grid
`+pm4dev`	use the PARAMESH4DEV grid
`+uhd`	use the Unsplit Hydro solver
`+usm`	use the Unsplit Staggered Mesh MHD solver
`+splitHydro`	use a split Hydro solver

5.2 Comprehensive List of Setup Arguments

`-verbose=<verbosity>`

Normally `setup` prints summary messages indicating its progress. Use the `-verbose` to make the messages more or less verbose. The different levels (in order of increasing verbosity) are `ERROR,IMPINFO,WARN,INFO,DEBUG`. The default is `WARN`.

`-auto`

Normally, `setup` requires that the user supply a plain text file called `Units` (in the `object` directory [2]) that specifies the units to include. A sample `Units` file appears in Figure 5.1. Each line is either a comment (preceded by a hash mark (`#`)) or the name of a an include statement of the form `INCLUDE` *unit*. Specific implementations of a unit may be selected by specifying the complete path to the implementation in question; If no specific implementation is requested, `setup` picks the default listed in the unit's `Config` file.

[2]Formerly, (in FLASH2) it was located in the FLASH root directory

The `-auto` option enables `setup` to generate a "rough draft" of a `Units` file for the user. The `Config` file for each problem setup specifies its requirements in terms of other units it requires. For example, a problem may require the perfect-gas equation of state (`physics/Eos/EosMain/Gamma`) and an unspecified hydro solver (`physics/Hydro`). With `-auto`, `setup` creates a `Units` file by converting these requirements into unit include statements. Most users configuring a problem for the first time will want to run `setup` with `-auto` to generate a `Units` file and then to edit it directly to specify alternate implementations of certain units. After editing the `Units` file, the user must re-run `setup` without `-auto` in order to incorporate his/her changes into the code configuration. The user may also use the command-line option `-with-unit=<path>` in conjunction with the `-auto` option, in order to pick a specific implementation of a unit, and thus eliminate the need to hand-edit the `Units` file.

`-[123]d`

By default, `setup` creates a makefile which produces a FLASH executable capable of solving two-dimensional problems (equivalent to `-2d`). To generate a makefile with options appropriate to three-dimensional problems, use `-3d`. To generate a one-dimensional code, use `-1d`. These options are mutually exclusive and cause `setup` to add the appropriate compilation option to the makefile it generates.

`-maxblocks=#`

This option is also used by `setup` in constructing the makefile compiler options. It determines the amount of memory allocated at runtime to the adaptive mesh refinement (AMR) block data structure. For example, to allocate enough memory on each processor for 500 blocks, use `-maxblocks=500`. If the default block buffer size is too large for your system, you may wish to try a smaller number here; the default value depends upon the dimensionality of the simulation and the grid type. Alternatively, you may wish to experiment with larger buffer sizes, if your system has enough memory. A common cause of aborted simulations occurs when the AMR grid creates greater than `maxblocks` during refinement. Resetup the simulation using a larger value of this option.

`-nxb=# -nyb=# -nzb=#`

These options are used by `setup` in constructing the makefile compiler options. The mesh on which the problem is solved is composed of blocks, and each block contains some number of cells. The `-nxb`, `-nyb`, and `-nzb` options determine how many cells each block contains (not counting guard cells). The default value for each is 8. These options do not have any effect when running in Uniform Grid non-fixed block size mode.

`[-debug|-opt|-test]`

The default `Makefile` built by setup will use the optimized setting (`-opt`) for compilation and linking. Using `-debug` will force `setup` to use the flags relevant for debugging (*e.g.*, including `-g` in the compilation line). The user may use the option `-test` to experiment with different combinations of compiler and linker options. Exactly which compiler and linker options are associated with each of these flags is specified in `sites/<hostname>/Makefile*` where `<hostname>` is the hostname of the machine on which FLASH is running.
For example, to tell an Intel Fortran compiler to use real numbers of size 64 when the `-test` option is specified, the user might add the following line to his/her `Makefile.h`:

```
FFLAGS_TEST = -real_size 64
```

`-objdir=<dir>`

Overrides the default `object` directory with `<dir>`. Using this option allows you to have different simulations configured simultaneously in the FLASH4 distribution directory.

`-with-unit=<unit>`, `-unit=<unit>`

Use the specified `<unit>` in setting up the problem.

```
#Units file for Sod generated by setup

INCLUDE Driver/DriverMain/Split
INCLUDE Grid/GridBoundaryConditions
INCLUDE Grid/GridMain/paramesh/interpolation/Paramesh4/prolong
INCLUDE Grid/GridMain/paramesh/interpolation/prolong
INCLUDE Grid/GridMain/paramesh/paramesh4/Paramesh4.0/PM4_package/headers
INCLUDE Grid/GridMain/paramesh/paramesh4/Paramesh4.0/PM4_package/mpi_source
INCLUDE Grid/GridMain/paramesh/paramesh4/Paramesh4.0/PM4_package/source
INCLUDE Grid/GridMain/paramesh/paramesh4/Paramesh4.0/PM4_package/utilities/multigrid
INCLUDE Grid/localAPI
INCLUDE IO/IOMain/hdf5/serial/PM
INCLUDE IO/localAPI
INCLUDE PhysicalConstants/PhysicalConstantsMain
INCLUDE RuntimeParameters/RuntimeParametersMain
INCLUDE Simulation/SimulationMain/Sod
INCLUDE flashUtilities/contiguousConversion
INCLUDE flashUtilities/general
INCLUDE flashUtilities/interpolation/oneDim
INCLUDE flashUtilities/nameValueLL
INCLUDE monitors/Logfile/LogfileMain
INCLUDE monitors/Timers/TimersMain/MPINative
INCLUDE physics/Eos/EosMain/Gamma
INCLUDE physics/Hydro/HydroMain/split/PPM/PPMKernel
```

Figure 5.1: Example of the `Units` file used by `setup` to determine which Units to include

`-curvilinear`

Enable code in `PARAMESH` 4 that implements geometrically correct data restriction for curvilinear coordinates. This setting is automatically enabled if a non-`cartesian` geometry is chosen with the `-geometry` flag; so specifying `-curvilinear` only has an effect in the Cartesian case.

`-defines=<def>[,<def>]...`

`<def>` is of the form `SYMBOL` or `SYMBOL=value`. This causes the specified pre-processor symbols to be defined when the code is being compiled. This is mainly useful for debugging the code. For *e.g.*, `-defines=DEBUG_ALL` turns on all debugging messages. Each unit may have its own `DEBUG_UNIT` flag which you can selectively turn on.

`[-fbs|-nofbs]`

Causes the code to be compiled in fixed-block or non-fixed-block size mode. Fixed-block mode is the default. In non-fixed block size mode, all storage space is allocated at runtime. This mode is available only with Uniform Grid.

`-geometry=<geometry>`

Choose one of the supported geometries `cartesian, cylindrical, spherical,` or `polar`. Some `Grid` implementations require the geometry to be known at compile-time while others don't. This setup option can be used in either case; it is a good idea to specify the geometry here if it is known at `setup`-time. Choosing a non-Cartesian geometry here automatically sets the `-gridinterpolation=monotonic` option below.

`-gridinterpolation=<scheme>`

Select a scheme for `Grid` interpolation. Two schemes are currently supported:

- **monotonic**
  This scheme attempts to ensure that monotonicity is preserved in interpolation, so that interpolation does not introduce small-scale non-monotonicity in the data.
  The `monotonic` scheme is required for curvilinear coordinates and is automatically enabled if a non-`cartesian` geometry is chosen with the `-geometry` flag. For AMR `Grid` implementations, This flag will automatically add additional directories so that appropriate data interpolation methods are compiled it. The `monotonic` scheme is the default (by way of the `+default` shortcut), unlike in FLASH2.

- **native**
  Enable the interpolation that is native to the AMR `Grid` implementation (`PARAMESH` 2 or `PARAMESH` 4) by default. This option is only appropriate for Cartesian geometries.

Change in Interpolation

Note that the default interpolation behavior has changed as of the FLASH3 beta release: the **native** interpolation used to be default.

When to use native Grid interpolation

The **monotonic** interpolation method requires more layers of coarse guard cells next to a coarse guard cell in which interpolation is to be applied. It may therefore be necessary to use the **native** method if a simulation is set up to include fewer than four layers of guard cells.

`-makefile=<extension>`

`setup` normally uses the `Makefile.h` from the directory determined by the hostname of the machine and the `-site` and `-os` options. If you have multiple compilers on your machine you can create `Makefile.h.<extension>` for different compilers. *e.g.*, you can have a `Makefile.h` and `Makefile.h.intel` and `Makefile.h.lahey` for the three different compilers. `setup` will still use the `Makefile.h` file by default, but supplying `-makefile=intel` on the command-line causes `setup` to use `Makefile.h.intel` instead.

`-index-reorder`

Instructs `setup` that indexing of unk and related arrays should be changed. This may be needed in FLASH4 for compatibility with alternative grids. This is supported by both the Uniform Grid as well as PARAMESH, and is currently required for the `Chombo` grid.

`-makehide`

Ordinarily, the commands being executed during compilation of the FLASH executable are sent to standard out. It may be that you find this distracting, or that your terminal is not able to handle these long lines of display. Using the option `-makehide` causes `setup` to generate a `Makefile` so that `gmake` only displays the names of the files being compiled and not the exact compiler call and flags. This information remains available in `setup_flags` in the `object/` directory.

`-noclobber`

`setup` normally removes all code in the `object` directory before linking in files for a simulation. The ensuing `gmake` must therefore compile all source files anew each time `setup` is run. The `-noclobber` option prevents `setup` from removing compiled code which has not changed from the previous `setup` in the same directory. This can speed up the `gmake` process significantly.

`-os=<os>`

If `setup` is unable to find a correct `sites/` directory it picks the `Makefile` based on the operating system. This option instructs `setup` to use the default `Makefile` corresponding to the specified operating system.

`-parfile=<filename>`

This causes `setup` to copy the specified runtime-parameters file in the simulation directory to the `object` directory with the new name `flash.par`

`-particlemethods=TYPE=<particle type>[,INIT=<init method>][,MAP=<map method>][,ADV=<advance method>]`

This option instructs `setup` to adjust the particle methods for a particular particle type. It can only be used when a particle type has already been registered with a `PARTICLETYPE` line in a `Config` file (see Section 6.6.1). A possible scenario for using this option involves the user wanting to use a different passive particle initialization method without modifying the `PARTICLETYPE` line in the simulation `Config` file. In this case, an additional `-particlemethods=TYPE=passive,INIT=cellmass` adjusts the initialization method associated with passive particles in the `setup` generated `Particles_specifyMethods()` subroutine. Since the specification of a method for mapping and initialization requires inclusions of appropriate implementations of `ParticlesMapping` and `ParticlesInitialization` subunits, and the specification of a method for time advancement requires inclusion of an appropriate implementation under `ParticlesMain`, it is the user's responsibility to adjust the included units appropriately. For example a user may want want to override `Config` file defined particle type `passive` using lattice initialization `CellMassBins` density based distribution method using the `setup` command line. Here the user must first specify `-without-unit=Particles/ParticlesInitialization/Lattice` to exclude the lattice initialization, followed by `-with-unit=Particles/ParticlesInitialization/-WithDensity/CellMassBins` specification to include the appropriate implementation. In general, using command line overrides of `-particlemethods` are not recommended, as this option increases the chance of creating an inconsistent simulation setup. More information on multiple particle types can be found in Chapter 20, especially Section 20.3.

`-portable`

This option causes setup to create a portable `object` directory by copying instead of linking to the source files. The resulting `object` directory can be tarred and sent to another machine for actual compilation.

`-site=<site>`

`setup` searches the `sites/` directory for a directory whose name is the hostname of the machine on which setup is being run. This option tells `setup` to use the `Makefile` of the specified site. This option is useful if `setup` is unable to find the right hostname (which can happen on multiprocessor or laptop machines). Also useful when combined with the `-portable` option.

`-unitsfile=<filename>`

This causes `setup` to copy the specified file to the `object` directory as `Units` before setting up the problem. This option can be used when `-auto` is not used, to specify an alternate `Units` file.

`-with-library=<libname>[,args]`, `-library=<libname>[,args]`

This option instructs `setup` to link in the specified library when building the final executable. A *library* is a piece of code which is independent of FLASH. Internal libraries are those libraries whose code is included with FLASH. The `setup` script supports external as well as internal libraries. Information about external libraries is usually found in the site specific Makefile. The additional `args` if any are library-specific and may be used to select among multiple implementations. For more information see Library-HOWTO.

`-tau=<makefile>`

This option causes the inclusion of an additional Makefile necessary for the operation of Tau, which may be used by the user to profile the code. More information on Tau can be found at `http://acts.nersc.gov/tau/`

`-without-library=<libname>`

Negates a previously specified `-with-library=<libname>[,args]`

`-without-unit=<unit>`

This removes all units specified in the command line so far, which are children of the specified unit (including the unit itself). It also negates any REQUESTS keyword found in a `Config` file for units which are children of the specified unit. However it does not negate a REQUIRES keyword found in a `Config` file.

`+default`

This shortcut specifies using basic default settings and is equivalent to the following:
`--with-library=mpi +io +grid-gridinterpolation=monotonic`

`+noio`

This shortcut specifies a simulation without IO and is equivalent to the following:
`--without-unit=physics/sourceTerms/EnergyDeposition/EnergyDepositionMain/Laser/LaserIO`
`--without-unit=IO`

`+io`

This shortcut specifies a simulation with basic IO and is equivalent to the following:
`--with-unit=IO`

`+serialIO`

This shortcut specifies a simulation using serial IO, it has the effect of setting the setup variable
`parallelIO = False`

`+parallelIO`

This shortcut specifies a simulation using serial IO, it has the effect of setting the setup variable
`parallelIO = True`

`+hdf5`

This shortcut specifies a simulation using hdf5 for compatible binary IO output, it has the effect of setting the setup variable
`IO = hdf5`

`+pnetcdf`

This shortcut specifies a simulation using pnetcdf for compatible binary IO output, it has the effect of setting the setup variable
`IO = pnetcdf`

`+hdf5TypeIO`

This shortcut specifies a simulation using hdf5, with parallel io capability for compatible binary IO output, and is equivalent to the following:
`+io +parallelIO +hdf5 typeIO=True`

`+pnetTypeIO`

This shortcut specifies a simulation using pnetcdf, with parallel io capability for compatible binary IO output, and is equivalent to the following:
`+io +parallelIO +pnetcdf typeIO=True`

`+nolog`

This shortcut specifies a simulation without log capability it is equivalent to the following:
`-without-unit=monitors/Logfile`

`+grid`

This shortcut specifies a simulation with the Grid unit, it is equivalent to the following:
`-unit=Grid`

`+ug`

This shortcut specifies a simulation using a uniform grid, it is equivalent to the following:
`+grid Grid=UG`

`+pm2`

This shortcut specifies a simulation using Paramesh2 for the grid, it is equivalent to the following:
`+grid Grid=PM2`

`+pm40`

This shortcut specifies a simulation using Paramesh4.0 for the grid, it is equivalent to the following:
`+grid Grid=PM40`

`+pm3`

This shortcut (for backward compatibility) specifies a simulation using Paramesh4.0 for the grid, it is equivalent to the following:
`+pm40`

`+chombo_ug`

This shortcut specifies a simulation using a Chombo uniform grid, it is equivalent to the following:
```
-unit=Grid/GridMain/Chombo/UG -index-reorder Grid=Chombo -maxblocks=1 -nofbs
-makefile=chombo chomboCompatibleHydro=True
```

`+chombo_amr`

This shortcut specifies a simulation using a Chombo amr grid, it is equivalent to the following:
```
-unit=Grid/GridMain/Chombo/AMR -index-reorder Grid=Chombo -nofbs
-makefile=chombo chomboCompatibleHydro=True
```

`+pm4dev_clean`

This shortcut specifies a simulation using a version of Paramesh 4 that is closer to the version available on sourceforge. It is equivalent to:
`+grid Grid=PM4DEV ParameshLibraryMode=True`

`+pm4dev`

This shortcut specifies a simulation using a modified version of Paramesh 4 that includes a more scalable way of filling the `surr_blks` array. It is equivalent to:
`+pm4dev_clean FlashAvoidOrrery=True`

`+8wave`

This shortcut specifies a MHD simulation using the 8wave mhd solver, which only works with the native interpolation. It is equivalent to:
`--with-unit=physics/Hydro/HydroMain/split/MHD_8Wave +grid -gridinterpolation=native`

`+usm`

This shortcut specifies a MHD simulation using the unsplit staggered mesh hydro solver, if pure hydro mode is used with the USM solver add +pureHydro in the setup line. It is equivalent to:
`--with-unit=physics/Hydro/HydroMain/unsplit/MHD_StaggeredMesh --without-unit=physics/Hydro/HydroMain/split/MHD_8Wave`

`+pureHydro`

This shortcut specifies using pure hydro mode, it is equivalent to:
`physicsMode=hydro`

`+splitHydro`

This shortcut specifies a simulation using a split hydro solver and is equivalent to:
`--unit=physics/Hydro/HydroMain/split -without-unit=physics/Hydro/HydroMain/unsplit SplitDriver=True`

`+unsplitHydro`

This shortcut specifies a simulation using the unsplit hydro solver and is equivalent to:
`--with-unit=physics/Hydro/HydroMain/unsplit/Hydro_Unsplit`

`+uhd`

This shortcut specifies a simulation using the unsplit hydro solver and is equivalent to:
`--with-unit=physics/Hydro/HydroMain/unsplit/Hydro_Unsplit`

`+supportPPMUpwind`

This shortcut specifies a simulation using a specific Hydro method that requires an increased number of guard cells, this may need to be combined with `-nxb=... -nyb=... etc.` where the specified blocksize is greater than or equal to 12 (==2*GUARDCELLS). It is equivalent to:
`SupportPpmUpwind=True`

`+cube64`

This shortcut specifies a simulation with a block size of 64**3, it is equivalent to:
`-nxb=64 -nyb=64 -nzb=64`

`+cube32`

This shortcut specifies a simulation with a block size of 32**3, it is equivalent to:
`-nxb=32 -nyb=32 -nzb=32`

`+cube16`

This shortcut specifies a simulation with a block size of 16**3, it is equivalent to:
`-nxb=16 -nyb=16 -nzb=16`

`+ptio`

This shortcut specifies a simulation using particles and IO for uniform grid, it is equivalent to:
`+ug -with-unit=Particles`

`+rnf`

This shortcut is used for checking FLASH with rectangular block sizes and non-fixed block size. It is equivalent to:
`-3d -nxb=8 -nyb=16 -nzb=32 -nofbs +ug`

`+nofbs`

This shortcut specifies a simulation using a uniform grid with a non-fixed block size. It is equivalent to:
`-nofbs +ug parallelIO=True`

`+curvilinear`

This shortcut specifies a simulation using curvilinear geometry. It is equivalent to:
`-curvilinear`

`+cartesian`

This shortcut specifies a simulation using cartesian geometry. It is equivalent to:
`-geometry=cartesian`

`+spherical`

This shortcut specifies a simulation using spherical geometry. It is equivalent to:
`-geometry=spherical`

`+polar`

This shortcut specifies a simulation using polar geometry. It is equivalent to:
`-geometry=polar`

`+cylindrical`

This shortcut specifies a simulation using cylindrical geometry. It is equivalent to:
`-geometry=cylindrical`

`+curv-pm2`

This shortcut specifies a simulation using curvilinear coordinates along with Paramesh2, it is equivalent to:

```
+pm2 -unit=Grid/GridMain/paramesh/Paramesh2
-with-unit=Grid/GridMain/paramesh/Paramesh2/monotonic
```

`+spherical-pm2`

This shortcut specifies a simulation using spherical coordinates along with Paramesh2, it is equivalent to:
`+pm2 +spherical`

`+ptdens`

This shortcut specifies a simulation using passive particles initialized by density. It is equivalent to:

```
-without-unit=Particles/ParticlesInitialization/Lattice
-without-unit=Particles/ParticlesInitialization/WithDensity/CellMassBins
-unit=Particles/ParticlesMain
-unit=Particles/ParticlesInitialization/WithDensity
-particlemethods=TYPE=passive,INIT=With_Density
```

`+npg`

This shortcut specifies a simulation using NO˙PERMANENT˙GUARDCELLS mode in Paramesh4. It is equivalent to:
`npg=True`

`+mpole`

This shortcut specifies a smilulation using multipole gravity, it is equivalent to:
`-with-unit=physics/Gravity/GravityMain/Poisson/Multipole`

`+longrange`

This shortcut specifies a simulation using long range active particles. It is equivalent to:
```
-with-unit=Particles/ParticlesMain/active/longRange/gravity/ParticleMesh
```

`+gravPfftNofbs`

This shortcut specifies a simulation using FFT based gravity solve on a uniform grid with no fixed block size. It is equivalent to:
```
+ug +nofbs -with-unit=physics/Gravity/GravityMain/Poisson/Pfft
```

`+gravMgrid`

This shortcut specifies a simulation using a multigrid based gravity solve. It is equivalent to:
```
+pm40 -with-unit=physics/Gravity/GravityMain/Poisson/Multigrid
```

`+gravMpole`

This shortcut specifies a smilulation using multipole gravity, it is equivalent to:
```
-with-unit=physics/Gravity/GravityMain/Poisson/Multipole
```

`+noDefaultMpole`

This shortcut specifies a simulation *not* using the multipole based gravity solve. It is equivalent to:
```
-without-unit=Grid/GridSolvers/Multipole
```

`+noMgrid`

This shortcut specifies a simulation *not* using the multigrid based gravity solve. It is equivalent to:
```
-without-unit=physics/Gravity/GravityMain/Poisson/Multigrid
```

`+newMpole`

This shortcut specifies a simulation using the new multipole based gravity solve. It is equivalent to:
```
+noMgrid +noDefaultMpole +gravMpole -with-unit=Grid/GridSolvers/Multipole_new
```

`+mpi1`

This shortcut specifies a simulation using the MPI-1 standard. It is equivalent to:
```
mpi1=True -defines=FLASH_MPI1
```

`+mpi2`

This shortcut specifies a simulation using the MPI-2 standard. It is equivalent to:
```
mpi2=True -defines=FLASH_MPI2
```

`+mtmmmt`

This shortcut specifies use of the MultiTemp/MultiType and Tabulated EOSes (for HEDP simulations). It is equivalent to:
```
-unit=physics/Eos/EosMain/multiTemp/Multitype -unit=physics/Eos/EosMain/Tabulated
Mtmmmt=1
```

`+3t`

This shortcut sets a variable and a preprocessor symbol to request MultiTemp implementations of some units. It is equivalent to:
```
ThreeT=1 -defines=FLASH_3T
```

`+uhd3t`

This shortcut specifies a simulation using unsplit hydro with MultiTemp EOS. It is equivalent to:
```
+3t -without-unit=physics/Hydro/HydroMain/split
-with-unit=physics/Hydro/HydroMain/unsplit/Hydro_Unsplit
```

`+usm3t`

This shortcut specifies a simulation using unsplit MHD with MultiTemp EOS. It is equivalent to:
`+3t -without-unit=physics/Hydro/HydroMain/split`
`--with-unit=physics/Hydro/HydroMain/unsplit/MHD_StaggeredMesh`
`--without-unit=physics/Hydro/HydroMain/split/MHD_8Wave`

`+mgd`

This shortcut specifies a simulation using the MGD (magneto gas dynamic) radiative transfer module. It is equivalent to:
`-unit=physics/materialProperties/Opacity -unit=physics/RadTrans/RadTransMain/MGD`

`+laser`

This shortcut specifies use of source terms for energy deposition. It is equivalent to:
`-unit=physics/sourceTerms/EnergyDeposition/EnergyDepositionMain/Laser`
`-without-unit=Particles`

`+pic`

This shortcut specifies use of proper particle units to perform PIC (particle in cell) method. It is equivalent to:
`+ug -unit=Grid/GridParticles/GridParticlesMove`
`-without-unit=Grid/GridParticles/GridParticlesMove/UG`
`-without-unit=Grid/GridParticles/GridParticlesMove/UG/Directional`

`Grid`

This setup variable can be used to specify which gridding package to use in a simulation:
Name: `Grid`
Type: `String`
Values: `PM4DEV`, `PM40`, `UG`, `PM2`, `Chombo`

`IO`

This setup variable can be used to specify which IO package to use in a simulation:
Name: `IO`
Type: `String`
Values: `hdf5, pnetcdf, MPIHybrid, MPIDump, direct`

`parallelIO`

This setup variable can be used to specify which type of IO strategy will be used. A "parallel" strategy will be used if the value is true, a "serial" strategy otherwise.
Name: `parallelIO`
Type: `Boolean`
Values: `True, False`

`fixedBlockSize`

This setup variable indicates whether or not a fixed block size is to be used. This variable should not be assigned explicitly on the command line. It defaults to `True`, and the setup options `-nofbs` and `-fbs` modify the value of this variable.
Name: `fixedBlockSize`
Type: `Boolean`
Values: `True, False`

`nDim`

This setup variable gives the dimensionality of a simulation. This variable should not be set explicitly on the command line, it is automatically set by the setup options `-1d`, `-2d`, and `-3d`.
Name: `nDim`
Type: `integer`
Values: `1,2,3`

`GridIndexOrder`

This setup variable indicates whether the `-index-reorder` setup option is in effect. This variable should not be assigned explicitly on the command line.
Name: `GridIndexOrder`
Type: `Boolean`
Values: `True, False`

`nxb`

This setup variable gives the number of zones in a block in the X direction. This variable should not be assigned explicitly on the command line, it is automatically set by the setup option `-nxb`.
Name: `nxb`
Type: `integer`

`nyb`

This setup variable gives the number of zones in a block in the Y direction. This variable should not be assigned explicitly on the command line, it is automatically set by the setup option `-nyb`.
Name: `nyb`
Type: `integer`

`nzb`

This setup variable gives the number of zones in a block in the Z direction. This variable should not be assigned explicitly on the command line, it is automatically set by the setup option `-nzb`.
Name: `nzb`
Type: `integer`

`maxBlocks`

This setup variable gives the maximum number of blocks per processor. This variable should not be assigned explicitly on the command line, it is automatically set by the setup option `-maxblocks`.
Name: `maxBlocks`
Type: `integer`

`ParameshLibraryMode`

If true, the setup script will generate file `amr_runtime_parameters` from template `amr_runtime_parameters.tpl` found in either the object directory (preferred) or the setup script (bin) directory. Selects whether Paramesh4 should be compiled in LIBRARY mode, i.e., with the preprocessor symbol LIBRARY defined.
Name: `ParameshLibraryMode`
Type: `Boolean`
Values: `True, False`

`PfftSolver`

PfftSolver selects a PFFT solver variant when the hybrid (*i.e.*, Multigrid with PFFT) Poisson solver is used.
Name: `PfftSolver`
Type: `String`
Values: `DirectSolver` (default), `HomBcTrigSolver`, others (unsupported) if recognized in `source/Grid/GridSolvers/Multigrid/PfftTopLevelSolve/Config`

`SplitDriver`

If True, a `Split Driver` implementation is requested.
Name: `SplitDriver`
Type: `Boolean`

`Mtmmmt`

Automatically set `True` by `+mtmmmt` shortcut. When true, this option activates the MTMMMT EOS.
Name: `Mtmmmt`
Type: `Boolean`

`mgd_meshgroups`

mgd˙meshgroups * meshCopyCount sets the MAXIMUM number of radiation groups that can be used in a simulation. The ACTUAL number of groups (which must be less than mgd˙meshgroups * meshCopyCount) is set by the rt˙mgdNumGroups runtime parameter.
Name: `mgd_meshgroups`
Type: `Integer`

`species`

This setup variable can be used as an alternative specifying species using the SPECIES Config file directive by listing the species in the setup command. Some units, like the Multispecies Opacity unit, will ONLY work when the species setup variable is set. This is because they use the species name to automatically create runtime paramters which include the species names.
Name: `species`
Type: `String`, comma seperated list of strings (*e.g.*, `species=air,sf6)`

`ed_maxPulses`

Name: `ed_maxPulses`
Type: `integer`
Remark: Maximum number of laser pulses (defaults to 5)

`ed_maxBeams`

Name: `ed_maxBeams`
Type: `integer`
Remark: Maximum number of laser beams (defaults to 6)

`threadHydroBlockList`

This is used to turn on block list OPENMP threading of hydro routines.
Name: `threadHydroBlockList`
Type: `Boolean`
Values: `True, False`

`threadMpoleBlockList`

This is used to turn on block list OPENMP threading of the multipole routine.
Name: `threadMpoleBlockList`
Type: `Boolean`
Values: `True, False`

`threadRayTrace`

This is used to turn on block list OPENMP threading of Enery Deposition source term routines.
Name: `threadRayTrace`
Type: `Boolean`
Values: `True, False`

`threadHydroWithinBlock`

This is used to turn on within block OPENMP threading of hydro routines.
Name: `threadHydroWithinBlock`
Type: `Boolean`
Values: `True, False`

`threadEosWithinBlock`

This is used to turn on within block OPENMP threading of Eos routines.
Name: `threadEosWithinBlock`
Type: `Boolean`
Values: `True, False`

`threadMpoleWithinBlock`

This is used to turn on within block OPENMP threading of then multipole routine.
Name: `threadMpoleWithinBlock`
Type: `Boolean`
Values: `True, False`

Dependencies among libraries

If you have some libraries which depend on other libraries, create a `lib/<libname>/Config` which declares the dependencies. Libraries can have their own `Config` files, but the format is a little different. For details see Library-HOWTO.

5.3 Using Shortcuts

Apart from the various setup options the `setup` script also allows you to use shortcuts for frequently used combinations of options. For example, instead of typing in

```
 ./setup -a Sod -with-unit=Grid/GridMain/UG
```

you can just type

```
./setup -a Sod +ug
```

The `+ug` or any setup option starting with a '+' is considered as a shortcut. By default, setup looks at `bin/setup_shortcuts.txt` for a list of declared shortcuts. You can also specify a ":" delimited list of files in the environment variable `SETUP_SHORTCUTS` and `setup` will read all the files specified (and ignore those which don't exist) for shortcut declarations. See Figure 5.2 for an example file.

The shortcuts are replaced by their expansions in place, so options which come after the shortcut override (or conflict with) options implied by the shortcut. A shortcut can also refer to other shortcuts as long as there are no cyclic references.

The "default" shortcut is special. `setup` always prepends `+default` to its command line thus making `./setup -a Sod` equivalent to `./setup +default -a Sod`. Thus changing the default IO to "hdf5/parallel", is as simple as changing the definition of the "default" shortcut.

Some of the more commonly used shortcuts are described below:

5.4 Setup Variables and Preprocessing `Config` Files

`setup` allows you to assign values to "Setup Variables". These variables can be string-valued, integer-valued, or boolean. A `setup` call like

```
./setup -a Sod Foo=Bar Baz=True
```

sets the variable "Foo" to string "Bar" and "Baz" to boolean True[3]. `setup` can conditionally include and exclude parts of the `Config` file it reads based on the values of these variables. For example, the `IO/IOMain/hdf5/Config` file contains

[3]All non-integral values not equal to True/False/Yes/No/On/Off are considered to be string values

```
# comment line

# each line is of the form # shortcut:arg1:arg2:...:
# These shortcuts can refer to each other.

default:--with-library=mpi:-unit=IO/IOMain:-gridinterpolation=monotonic

# io choices
noio:--without-unit=IO/IOMain:
io:--with-unit=IO/IOMain:

# Choice of Grid
ug:-unit=Grid/GridMain/UG:
pm2:-unit=Grid/GridMain/paramesh/Paramesh2:
pm40:-unit=Grid/GridMain/paramesh/paramesh4/Paramesh4.0:
pm4dev:-unit=Grid/GridMain/paramesh/paramesh4/Paramesh4dev:

# frequently used geometries
cube64:-nxb=64:-nyb=64:-nzb=64:
```

Figure 5.2: A sample `setup_shortcuts.txt` file

Table 5.5: Shortcuts for often-used options

Shortcut	Description
+cartesian	use cartesian geometry
+cylindrical	use cylindrical geometry
+noio	omit IO
+nolog	omit logging
+pm2	use the PARAMESH2 grid
+pm40	use the PARAMESH4.0 grid
+pm4dev	use the PARAMESH4DEV grid
+polar	use polar geometry
+spherical	use spherical geometry
+ug	use the uniform grid in a fixed block size mode
+nofbs	use the uniform grid in a non-fixed block size mode
+usm	use the Unsplit Staggered Mesh MHD solver
+8wave	use the 8-wave MHD solver
+splitHydro	use a split Hydro solver

Table 5.6: Shortcuts for HEDP options

Shortcut	Description
+mtmmmt	Use the 3-T, multimaterial, multitype EOS
+uhd3t	Use the 3-T version of Unsplit Hydro
+usm3t	Use the 3-T version of Unsplit Staggered Mesh MHD
+mgd	Use Multigroup Radiation Diffusion and Opacities
+laser	Use the Laser Ray Trace package

```
DEFAULT serial

USESETUPVARS parallelIO

IF parallelIO
   DEFAULT parallel
ENDIF
```

The code sets IO to its default value of "serial" and then resets it to "parallel" if the setup variable "parallelIO" is True. The `USESETUPVARS` keyword in the `Config` file instructs setup that the specified variables must be defined; undefined variables will be set to the empty string.

Through judicious use of setup variables, the user can ensure that specific implementations are included or the simulation is properly configured. For example, the setup line `./setup -a Sod +ug` expands to `./setup -a Sod -unit=Grid/GridMain/ Grid=UG`. The relevant part of the `Grid/GridMain/Config` file is given below:

```
# Requires use of the Grid SetupVariable
USESETUPVARS Grid

DEFAULT paramesh

IF Grid=='UG'
   DEFAULT UG
ENDIF
IF Grid=='PM2'
   DEFAULT paramesh/Paramesh2
ENDIF
```

The `Grid/GridMain/Config` file defaults to choosing `PARAMESH`. But when the setup variable Grid is set to "UG" through the shortcut `+ug`, the default implementation is set to "UG". The same technique is used to ensure that the right IO unit is automatically included.

See `bin/Readme.SetupVars` for an exhaustive list of Setup Variables which are used in the various Config files. For example the setup variable `nDim` can be test to ensure that a simulation is configured with the appropriate dimensionality (see for example `Simulation/SimulationMain/unitTest/Eos/Config`).

5.5 `Config` Files

Information about unit dependencies, default sub-units, runtime parameter definitions, library requirements, and physical variables, etc. is contained in plain text files named `Config` in the different unit directories. These are parsed by `setup` when configuring the source tree and are used to create the code needed to register unit variables, to implement the runtime parameters, to choose specific sub-units when only a generic unit has been specified, to prevent mutually exclusive units from being included together, and to flag problems when dependencies are not resolved by some included unit. Some of the Config files contain additional information about unit interrelationships. As mentioned earlier, `setup` starts from the `Config` file in the Simulation directory of the problem being built.

5.5.1 Configuration file syntax

Configuration files come in two syntactic flavors: static text and python. In static mode, configuration directives are listed as lines in a plain text file. This mode is the most readable and intuitive of the two, but it lacks flexibility. The python mode has been introduced to circumvent this inflexibility by allowing the configuration file author to specify the configuration directives as a function of the setup variables with a python procedure. This allows the content of each directive and the number of directives in total to be amenable to general programming.

The rule the setup script uses for deciding which flavor of configuration file it's dealing with is simple. Python configuration files have as their first line `##python:genLines`. If the first line does not match this string, then static mode is assumed and each line of the file is interpreted verbatim as a directive.

If python mode is triggered, then the entire file is considered as valid python source code (as if it were a .py). From this python code, a function of the form `def genLines(setupvars)` is located and executed to generate the configuration directives as an array (or any iterable collection) of strings. The sole argument to genLines is a dictionary that maps setup variable names to their corresponding string values.

As an example, here is a configuration file in python mode that registers runtime parameters named indexed˙parameter˙x where x ranges from 1 to NP and NP is a setup line variable.

```
##python:genLines

# We define genLines as a generator with the very friendly "yield" syntax.
# Alternatively, we could have genLines return an array of strings or even
# one huge multiline string.
def genLines(setupvars):
    # emit some directives that dont depend on any setup variables
    yield """
REQUIRES Driver
REQUIRES physics/Hydro
REQUIRES physics/Eos
"""
    # read a setup variable value from the dictionary
    np = int(setupvars("NP")) # must be converted from a string
    # loop from 0 to np-1
    for x in xrange(np):
        yield "PARAMETER indexed_parameter_\%d REAL 0." \% (x+1)
```

When setting up a problem with NP=5 on the setup command line, the following directives will be processed:

```
REQUIRES Driver
REQUIRES physics/Hydro
REQUIRES physics/Eos
PARAMETER indexed_parameter_1 REAL 0.
PARAMETER indexed_parameter_2 REAL 0.
PARAMETER indexed_parameter_3 REAL 0.
PARAMETER indexed_parameter_4 REAL 0.
PARAMETER indexed_parameter_5 REAL 0.
```

5.5.2 Configuration directives

The syntax of the configuration directives is described here. Arbitrarily many spaces and/or tabs may be used, but all keywords must be in uppercase. Lines not matching an admissible pattern will raise an error when running setup.

- `# comment`
  A comment. Can appear as a separate line or at the end of a line.

- `DEFAULT` *sub-unit*
  Every unit and sub-unit designates one implementation to be the "default", as defined by the keyword `DEFAULT` in its `Config` file. If no specific implementation of the unit or its sub-units is selected by the application, the designated default implementation gets included. For example, the `Config` file for the `EosMain` specifies Gamma as the default. If no specific implementation is explicitly included (*i.e.*, `INCLUDE physics/Eos/EosMain/Multigamma`), then this command instructs `setup` to include the Gamma implementation, as though `INCLUDE physics/Eos/EosMain/Gamma` had been placed in the `Units` file.

- `EXCLUSIVE` *implementation...*
  Specifies a list of implementations that cannot be included together. If no `EXCLUSIVE` instruction is given, it is perfectly legal to simultaneously include more than one implementation in the code. Using "`EXCLUSIVE` *" means that at most one implementation can be included.

- `CONFLICTS` *unit1[/sub-unit[/implementation...]] ...*
  Specifies that the current unit, sub-unit, or specific implementation is not compatible with the list of units, sub-units or other implementations that follows. `setup` issues an error if the user attempts a conflicting unit configuration.

- `REQUIRES` *unit[/sub-unit[/implementation...]] [* `OR` *unit[/sub-unit...]]...*
  Specifies a unit requirement. Unit requirements can be general, without asking for a specific implementation, so that unit dependencies are not tied to particular algorithms. For example, the statement `REQUIRES physics/Eos` in a unit's `Config` file indicates to `setup` that the physics/Eos unit is needed, but no particular equation of state is specified. As long as an `Eos` implementation is included, the dependency will be satisfied. More specific dependencies can be indicated by explicitly asking for an implementation. For example, if there are multiple species in a simulation, the `Multigamma` equation of state is the only valid option. To ask for it explicitly, use `REQUIRES physics/Eos/EosMain/Multigamma`. Giving a complete set of unit requirements is helpful, because `setup` uses them to generate the units file when invoked with the -auto option.

- `REQUESTS` *unit[/sub-unit[/implementation...]]*
  Requests that a unit be added to the Simulation. All requests are upgraded to a "REQUIRES" if they are not negated by a "-without-unit" option from the command line. If negated, the `REQUEST` is ignored. This can be used to turn off profilers and other "optional" units which are included by default.

- `SUGGEST` *unitname unitname ...*
  Unlike `REQUIRES`, this keyword suggests that the current unit be used along with one of the specified units. The setup script will print details of the suggestions which have been ignored. This is useful in catching inadvertently omitted units before the run starts, thus avoiding a waste of computing resources.

- `PARAMETER` *name type [*`CONSTANT`*] default* [*range-spec*]
  Specifies a runtime parameter. Parameter names are unique up to 20 characters and may not contain spaces. Admissible types include `REAL`, `INTEGER`, `STRING`, and `BOOLEAN`. Default values for `REAL` and `INTEGER` parameters must be valid numbers, or the compilation will fail. Default `STRING` values must be enclosed in double quotes ("). Default `BOOLEAN` values must be `.true.` or `.false.` to avoid compilation errors. Once defined, runtime parameters are available to the entire code. Optionally, any

parameter may be specified with the `CONSTANT` attribute (*e.g.*, `PARAMETER foo REAL CONSTANT 2.2`). If a user attempts to set a constant parameter via the runtime parameter file, an error will occur.

The range specification is optional and can be used to specify valid ranges for the parameters. The range specification is allowed only for `REAL, INTEGER, STRING` variables and must be enclosed in '[]'.

For a `STRING` variable, the range specification is a comma-separated list of strings (enclosed in quotes). For a `INTEGER, REAL` variable, the range specification is a comma-separated list of (closed) intervals specified by `min ... max`, where min and max are the end points of the interval. If min or max is omitted, it is assumed to be $-\infty$ and $+\infty$ respectively. Finally `val` is a shortcut for `val ... val`. For example

```
PARAMETER pres REAL 1.0 [ 0.1 ... 9.9, 25.0 ... ]
PARAMETER coords STRING "polar" ["polar","cylindrical","2d","3d"]
```

indicates that `pres` is a REAL variable which is allowed to take values between 0.1 and 9.9 or above 25.0. Similarly `coords` is a string variable which can take one of the four specified values.

- `D` *parameter-name comment*
  Any line in a `Config` file is considered a parameter comment line if it begins with the token `D`. The first token after the comment line is taken to be the parameter name. The remaining tokens are taken to be a description of the parameter's purpose. A token is delineated by one or more white spaces. For example,

  ```
  D SOME_PARAMETER The purpose of this parameter is whatever
  ```

  If the parameter comment requires additional lines, the `&` is used to indicate continuation lines. For example,

  ```
  D SOME_PARAMETER The purpose of this parameter is whatever
  D &              This is a second line of description
  ```

  You can also use this to describe other variables, fluxes, species, etc. For example, to describe a species called "xyz", create a comment for the parameter "xyz_species". In general the name should be followed by an underscore and then by the lower case name of the keyword used to define the name.

  Parameter comment lines are special because they are used by `setup` to build a formatted list of commented runtime parameters for a particular problem. This information is generated in the file `setup_params` in the `object` directory.

- `VARIABLE` *name [*`TYPE:` *vartype] [eosmap-spec]*
  Registers variable with the framework with name *name* and a variable type defined by *vartype*. The `setup` script collects variables from all the included units, and creates a comprehensive list with no duplications. It then assigns defined constants to each variable and calculates the amount of storage required in the data structures for storing these variables. The defined constants and the calculated sizes are written to the file `Flash.h`.

  The possible types for *vartype* are as follows:

  – `PER_VOLUME`
    This solution variable is represented in **conserved** form, *i.e.*, it represents the density of a conserved extensive quantity. The prime example is a variable directly representing mass density. Energy densities, momentum densities, and partial mass densities would be other examples (but these quantities are usually represented in `PER_MASS` form instead).

  – `PER_MASS`
    This solution variable is represented in **mass-specific** form, *i.e.*, it represents quantities whose nature is extensive quantity per mass unit. Examples are specific energies, velocities of material (since they are equal to momentum per mass unit), and abundances or mass fractions (partial density divided by density).

- `GENERIC`
  This is the default *vartype* and need not be specified. This type should be used for any variables that do not clearly belong to one of the previous two categories.

In the current version of the code, the `TYPE` attribute is only used to determine which variables should be converted to conservative form for certain `Grid` operations that may require interpolation (*i.e.*, prolongation, guardcell filling, and restriction) when one of the runtime parameters `convertToConsvdForMeshCalls` or `convertToConsvdInMeshInterp` is set `true`. Only variables of type `PER_MASS` are converted: values are multiplied cell-by-cell with the value of the `"dens"` variable, and potential interpolation results are converted back by cell-by-cell division by `"dens"` values after interpolation.

Note that therefore

- variable types are irrelevant for uniform grids,
- variable types are irrelevant if neither `convertToConsvdForMeshCalls` nor `convertToConsvdInMeshInterp` is `true`, and
- variable types (and conversion to and from conserved form) only take effect if a

  `VARIABLE dens ...`

  exists.

An *eosmap-spec* has the syntax `EOSMAP:` *eos-role* | ([`EOSMAPIN:` *eos-role*] [`EOSMAPOUT:` *eos-role*]), where *eos-role* stands for a **role** as defined in `Eos_map.h`. These roles are used within implementations of the `Eos_wrapped` interface, via the subroutines `Eos_getData` and `Eos_putData`, to map variables from `Grid` data structures to the `eosData` array that `Eos` understands, and back. For example,

```
VARIABLE eint TYPE: PER_MASS EOSMAPIN: EINT
```

means that within `Eos_wrapped`, the `EINT_VAR` component of `unk` will be treated as the grid variable in the "internal energy" role for the purpose of constructing input to `Eos`, and

```
VARIABLE gamc EOSMAPOUT: GAMC
```

means that within `Eos_wrapped`, the `GAMC_VAR` component of `unk` will be treated as the grid variable in the `EOSMAP_GAMC` role for the purpose of returning results from calling `Eos` to the grid. The specification

```
VARIABLE pres EOSMAP: PRES
```

has the same effect as

```
VARIABLE pres EOSMAPIN: PRES EOSMAPOUT: PRES
```

Note that not all roles defined in `Eos_map.h` are necessarily meaningful or actually used in a given `Eos` implementation. An *eosmap-spec* for a `VARIABLE` is only used in an `Eos_wrapped` invocation when the optional `gridDataStruct` argument is absent or has a value of `CENTER`.

- `FACEVAR` *name [eosmap-spec]*
  This keyword has the same meaning for face-centered variables, that `VARIABLE` does for cell-centered variables. It allocates space in the grid data structure that contains face-centered physical variables for "name". See Section 6.1 for more information

  For *eosmap-spec*, see above under `VARIABLE`. An *eosmap-spec* for `FACEVAR` is only used when `Eos_wrapped` is called with an optional `gridDataStruct` argument of `FACEX`, `FACEY`, or `FACEZ`.

- `FLUX` *name*
  Registers flux variable *name* with the framework. When using an adaptive mesh, flux conservation is needed at fine-coarse boundaries. `PARAMESH` uses a data structure for this purpose, the flux variables provide indices into that data structure. See Section 6.3 for more information.

- `SCRATCHCENTERVAR` *name [eosmap-spec]*
  This keyword is used in connection with the grid scope scratch space for cell-centered data supported by FLASH. It allows the user to ask for scratch space with "name". The scratch variables do not participate in the process of guardcell filling, and their values become invalid after a grid refinement step. While users can define scratch variables to be written to the plotfiles, they are not by default written to checkpoint files. Note this feature wasn't available in FLASH2. See Section 6.4 for more information.

- `SCRATCHFACEVAR` *name [eosmap-spec]*
  This keyword is used in connection with the grid scope scratch space for face-centered data, it is identical in every other respect to `SCRATCHCENTERVAR`.

- `SCRATCHVAR` *name [eosmap-spec]*
  This keyword is used for specifying instances of general purpose grid scope scratch space. The same space can support cell-centered as well as face-centered data. Like other scratch data structures, the variables in this data structure can also be asked with "name" and do not participate in guardcell filling.

  For *eosmap-spec*, see above under `VARIABLE`. An *eosmap-spec* for `SCRATCHVAR` is only used when `Eos_wrapped` is called with an optional `gridDataStruct` argument of `SCRATCH`.

- `MASS_SCALAR` *name [RENORM: group-name] [eosmap-spec]*
  If a quantity is defined with keyword MASS_SCALAR, space is created for it in the grid "unk" data structure. It is treated like any other variable by `PARAMESH`, but the hydrodynamic unit treats it differently. It is advected, but other physical characteristics don't apply to it. If the optional "RENORM" is given, this mass-scalar will be added to the renormalization group of the accompanying group name. The hydrodynamic solver will renormalize all mass-scalars in a given group, ensuring that all variables in that group will sum to 1 within an individual cell. See Section 6.2

  For *eosmap-spec*, see above under `VARIABLE`. An *eosmap-spec* for a `MASS_SCALAR` may be used in an `Eos_wrapped` invocation when the optional `gridDataStruct` argument is absent or has a value of `CENTER`.

  Avoid Confusion!

  It is inadvisable to name variables, species, and mass scalars with the same prefix, as post-processing routines have difficulty deciphering the type of data from the output files. For example, don't create a variable "temp" to hold temperature and a mass scalar "temp" indicating a temporary variable. Although the `Flash.h` file can distinguish between these two types of variables, many plotting routines cannot.

- `PARTICLETYPE` *particle-type* `INITMETHOD` *initialization-method* `MAPMETHOD` *map-method* `ADVMETHOD` *time-advance-method*
  This keyword associates a **particle type** with mapping and initialization sub-units of `Particles` unit to operate on this particle type during the simulation. Here, *map-method* describes the method used to map the particle properties to and from the mesh (see Section 20.2), *initialization-method* describes the method used to distribute the particles at initialization, and *time-advance-method* describes the method used to advance the associated particle type in time (see Section 20.1, and in general Section 20.3). This keyword has been introduced to facilitate inclusion of multiple particle types in the same simulation. It imposes certain requirements on the use of the `ParticlesMapping` and `ParticlesInitialization` subunits. Particles (of any type, whether called `passive` or anything else) do not have default methods for initialization, mapping, or time integration, so a `PARTICLETYPE` directive in a `Config` file (or an equivalent `-particlemethods=` setup option, see Table 5.4) is the only way to specify the appropriate implementations of the `Particles` subunits to be used. The declaration should be accompanied by appropriate "REQUESTS" or "REQUIRES" directives to specify the paths of the appropriate subunit

implementation directories to be included. For clarity, our technique has been to include this information in the simulation directory `Config` files only. All the currently available mapping and initialization methods have a corresponding identifier in the form of preprocessor definition in `Particles.h`. The user may select any *particle-type* name, but the *map-method*, *initialization-method* and *time-advance-method* must correspond to existing identifiers defined in `Particles.h`. This is necessary to navigate the data structure that stores the particle type and its associated mapping and initialization methods. Users desirous of adding new methods for mapping or initialization should also update the `Particles.h` file with additional identifiers and their preprocessor definitions. Note, it is possible to use the same methods for different particle types, but each particle type name must only appear once. Finally, the Simulations `Config` file is also expected to request appropriate implementations of mapping and initialization subunits using the keyword `REQUESTS`, since the corresponding Config files do not specify a default implementation to include. For example, to include `passive` particle types with `Quadratic` mapping, `Lattice` initialization,and `Euler` for advancing in time the following code segment should appear in the `Config` file of the `Simulations` directory.

```
PARTICLETYPE passive INITMETHOD lattice MAPMETHOD quadratic ADVMETHOD Euler
REQUIRES Particles/ParticlesMain
REQUESTS Particles/ParticlesMain/passive/Euler
REQUESTS Particles/ParticlesMapping/Quadratic
REQUESTS Particles/ParticlesInitialization/Lattice
```

- `PARTICLEPROP` *name type*
  This keyword indicates that the particles data structure will allocate space for a sub-variable "NAME_-PART_PROP." For example if the Config file contains

  ```
  PARTICLEPROP dens
  ```

  then the code can directly access this property as

  ```
  particles(DENS_PART_PROP,1:localNumParticles) = densInitial
  ```

  type may be REAL or INT, however INT is presently unused. See Section 6.6 for more information and examples.

- `PARTICLEMAP` TO *partname* FROM *vartype varname*
  This keyword maps the value of the particle property *partname* to the variable *varname*. *vartype* can take the values VARIABLE, MASS_SCALAR, SPECIES, FACEX, FACEY, FACEZ, or one of SCRATCH types (SCRATCHVAR/ SCRATCHCENTERVAR, SCRATCHFACEXVAR. SCRATCHFACEYVAR, SCRATCHFACEZVAR) These maps are used to generate `Simulation_mapParticlesVar`, which takes the particle property *partname* and returns *varname* and *vartype*. For example, to have a particle property tracing density:

  ```
  PARTICLEPROP dens REAL
  PARTICLEMAP TO dens FROM VARIABLE dens
  ```

  or, in a more advanced case, particle properties tracing some face-valued function Mag:

  ```
  PARTICLEPROP Mag_x REAL
  PARTICLEPROP Mag_y REAL
  PARTICLEPROP Mag_z REAL
  PARTICLEMAP TO Mag_x FROM FACEX Mag
  PARTICLEMAP TO Mag_y FROM FACEY Mag
  PARTICLEMAP TO Mag_z FROM FACEZ Mag
  ```

  Additional information on creating `Config` files for particles is obtained in Section 20.3.2.

- `SPECIES` *name* [TO *number of ions*]
  An application that uses multiple species uses this keyword to define them. See Section 6.2 for more

information. The user may also specify an optional number of ions for each element, *name*. For example, `SPECIES` *o* TO *8* creates 9 spaces in `unk` for Oxygen, that is, a single space for Oxygen and 8 spaces for each of its ions. This is relevant to simulations using the `ionize` unit. (Omitting the optional `TO` specifier is equivalent to specifying `TO` 0).

- `DATAFILES` *wildcard*
  Declares that all files matching the given wildcard in the unit directory should be copied over to the object directory. For example,

  ```
  DATAFILES *.dat
  ```

  will copy all the ".dat" files to the object directory.

- `KERNEL` *[subdir]*
  Declares that all subdirectories must be recursively included. This usually marks the end of the high level architecture of a unit. Directories below it may be third party software or a highly optimized solver, and are therefore not required to conform to FLASH architecture.

  Without a *subdir*, the current directory (*i.e.*, the one containing the `Config` file with the `KERNEL` keyword) is marked as a kernel directory, so code from all its subdirectories (with the exception of subdirectories whose name begins with a dot) is included. When a *subdir* is given, then that subdirectory must exist, and it is treated as a kernel directory in the same way.

  Note that currently the `setup` script can process only one `KERNEL` directive per `Config` file.

- `LIBRARY` *name*
  Specifies a library requirement. Different FLASH units require different libraries, and they must inform `setup` so it can link the libraries into the executable. Some valid library names are `HDF5, MPI`. Support for external libraries can be added by modifying the site-specific `Makefile.h` files to include appropriate Makefile macros. It is possible to use internal libraries, as well as switch libraries at setup time. To use these features, see
  Library-HOWTO.

- `LINKIF` *filename unitname*
  Specifies that the file *filename* should be used only when the unit *unitname* is included. This keyword allows a unit to have multiple implementations of any part of its functionality, even down to the kernel level, without the necessity of creating children for every alternative. This is especially useful in Simulation setups where users may want to use different implementations of specific functions based upon the units included. For instance, a user may wish to supply his/her own implementation of `Grid_markRefineDerefine.F90`, instead of using the default one provided by FLASH. However, this function is aware of the internal workings of `Grid`, and has different implementations for different grid packages. The user could therefore specify different versions of his/her own file that are intended for use with the different grids. For example, adding

  ```
   LINKIF Grid_markRefineDerefine.F90.ug Grid/GridMain/UG
   LINKIF Grid_markRefineDerefine.F90.pmesh Grid/GridMain/paramesh
  ```

  to the `Config` file ensures that if the application is built with `UG`, the file `Grid_markRefineDerefine.F90.ug` will be linked in as `Grid_markRefineDerefine.F90`, whereas if it is built with `Paramesh2` or `Paramesh4.0` or `Paramesh4dev`, then the file `Grid_markRefineDerefine-.F90.pmesh` will be linked in as `Grid_markRefineDerefine.F90`. Alternatively, the user may want to provide only one implementation specific to, say, `PARAMESH`. In this case, adding

  ```
   LINKIF Grid_markRefineDerefine.F90 Grid/GridMain/paramesh
  ```

  to the Config file ensures that the user-supplied file is included when using `PARAMESH` (either version), while the default FLASH file is included when using `UG`.

- `PPDEFINE` *sym1 sym2 ...*
  Instructs setup to add the PreProcessor symbols *SYM1* and *SYM2* to the generated `Flash.h`. Here *SYM1* is *sym1* converted to uppercase. These pre-process symbols can be used in the code to distinguish between which units have been used in an application. For example, a Fortran subroutine could include

  ```
  #ifdef FLASH_GRID_UG
    ug specific code
  #endif

  #ifdef FLASH_GRID_PARAMESH3OR4
    pm3+ specific code
  #endif
  ```

  By convention, many preprocessor symbols defined in Config files included in the FLASH code distribution start with the prefix "FLASH_".

- `USESETUPVARS` *var1, var2, ...*
  This tells `setup` that the specified "Setup Variables" are being used in this `Config` file. The variables initialize to an empty string if no values are specified for them. Note that commas are required if listing several variables.

- `CHILDORDER` *child1 child2 ...*
  When `setup` links several implementations of the same function, it ensures that implementations of children override that of the parent. Its method is to lexicographically sort all the names and allow implementations occurring later to override those occurring earlier. This means that if two siblings implement the same code, the names of the siblings determine which implementation wins. Although it is very rare for two siblings to implement the same function, it does occur. This keyword permits the `Config` file to override the lexicographic order by one preferred by the user. Lexicographic ordering will prevail as usual when deciding among implementations that are not explicitly listed.

- `GUARDCELLS` *num*
  Allows an application to choose the stencil size for updating grid points. The stencil determines the number of guardcells needed. The PPM algorithm requires 4 guardcells, hence that is the default value. If an application specifies a smaller value, it will probably not be able to use the default `monotonic` AMR Grid interpolation; see the `-gridinterpolation setup` flag for additional information.

- `SETUPERROR` *`error message`*
  This causes `setup` to abort with the specified error message. This is usually used only inside a conditional IF/ENDIF block (see below).

- `IF, ELSEIF, ELSE, ENDIF`
  A conditional block is of the following form:

  ```
  IF cond
     ...
  ELSEIF cond
     ...
  ELSE
     ...
  ENDIF
  ```

  where the `ELSEIF` and `ELSE` blocks are optional. There is no limit on the number of `ELSEIF` blocks. "..." is any sequence of valid `Config` file syntax. The conditional blocks may be nested. "cond" is any boolean valued Python expression using the setup variables specified in the `USESETUPVARS`.

- `NONREP` *unktype name localmax globalparam ioformat*
  Declares an array of `UNK` variables that will be partitioned across the replicated meshes. Using various preprocessor macros in Flash.h each copy of the mesh can determine at runtime its own subset of indexes into this global array. This allows an easy form of parallelism where regular "replicated" mesh variables are computed redundantly across processors, but the variables in the "non-replicated" array are computed in parallel.

  – *unktype*: must be either `MASS_SCALAR` or `VARIABLE`

  – *name*: the name of this variable array. It is suggested that it be all capital letters, and must conform to what the C preprocessor will consider as a valid symbol for use in a `#define` statement.

  – *localmax*: a positive integer specifying the maximum number of elements from the global variable array a mesh can hold. This is the actual number of `UNK` variables that are allocated on each processor, though not all of them will necessarily be used.

  – *globalparam*: the name of a runtime parameter which dictates the size of this global array of variables.

  – *ioformat*: a string representing how the elements of the array will be named when written to the output files. The question mark character `?` is used as a placeholder for the digits of the array index. As an example, the format string `x???` will generate the dataset names `x001`, `x002`, `x003`, etc. This string must be no more than four characters in length.

The number of meshes is dictated by the runtime parameter `meshCopyCount`. The following constraint must be satisfied or FLASH will fail at runtime:

$$globalparam \le meshCopyCount * localmax$$

The reason for this restriction is that `localmax` is the maximum number of array elements a mesh can be responsible for, and `meshCopyCount` is the number of meshes, so their product bounds the size of the array.

Example:

Config file:

```
NONREP MASS_SCALAR A 4 numA a???
NONREP MASS_SCALAR B 5 numB b???
```

flash.par file:

```
meshCopyCount = 3
numA = 11
numB = 15
```

In this case two non-replicated mass-scalar arrays are defined, `A` and `B`. Their lengths are specified by the runtime parameters `numA` and `numB` respectively. `numB` is set to its maximum value of $5 * meshCopyCount = 15$, but `numA` is one less than its maximum value of $4 * meshCopyCount = 12$ so at runtime one of the meshes will not have all of its `UNK` variables in use. The dataset names generated by IO will take the form `a001 ...a011` and `b001 ...b015`.

The preprocessor macros defined in `Flash.h` for these arrays will have the prefixes `A_` and `B_` respectively. For details about these macros and how they will distribute the array elements across the meshes see Section 6.7.

5.6 Creating a Site-specific `Makefile`

If `setup` does not find your hostname in the `sites/` directory it picks a default `Makefile` based on the operating system. This `Makefile` is not always correct but can be used as a template to create a `Makefile` for your machine. To create a Makefile specific to your system follow these instructions.

- Create the directory `sites/<hostname>`, where `<hostname>` is the hostname of your machine.
- Start by copying `os/<your os>/Makefile.h` to `sites/<hostname>`
- Use `bin/suggestMakefile.sh` to help identify the locations of various libraries on your system. The script scans your system and displays the locations of some libraries. You must note the location of `MPI` library as well. If your compiler is actually an mpi-wrapper (*e.g.*`mpif90`), you must still define `LIB_MPI` in your site specific `Makefile.h` as the empty string.
- Edit `sites/<hostname>/Makefile.h` to provide the locations of various libraries on your system.
- Edit `sites/<hostname>/Makefile.h` to specify the FORTRAN and C compilers to be used.

Actual Compiler or MPI wrapper?

If you have `MPI` installed, you can either specify the actual compiler (*e.g.*`f90`) or the mpi-wrapper (*e.g.*`mpif90`) for the "compiler" to be used on your system. Specifying the actual compiler and the location of the MPI libraries in the site-specific Makefile allows you the possibility of switching your MPI implementation. For more information see Library-HOWTO.

Compilation warning

The Makefile.h *must* include a compiler flag to promote Fortran `Reals` to `Double Precision`. FLASH performs all `MPI` communication of Fortran `Reals` using `MPI_DOUBLE_PRECISION` type, and assumes that Fortran `Reals` are interoperable with C `doubles` in the I/O unit.

5.7 Files Created During the `setup` Process

When `setup` is run it generates many files in the `object` directory. They fall into three major categories:

(a) Files not required to build the FLASH executable, but which contain useful information,

(b) Generated F90 or C code, and

(c) Makefiles required to compile the FLASH executable.

5.7.1 Informational files

These files are generated before compilation by `setup`. Each of these files begins with the prefix `setup_` for easy identification.

`setup_call`	contains the options with which `setup` was called and the command line resulting after shortcut expansion
`setup_libraries`	contains the list of libraries and their arguments (if any) which was linked in to generate the executable
`setup_units`	contains the list of all units which were included in the current setup
`setup_defines`	contains a list of all pre-process symbols passed to the compiler invocation directly
`setup_flags`	contains the exact compiler and linker flags
`setup_params`	contains the list of runtime parameters defined in the `Config` files processed by `setup`
`setup_vars`	contains the list of variables, fluxes, species, particle properties, and mass scalars used in the current setup, together with their descriptions.

5.7.2 Code generated by the `setup` call

These routines are generated by the setup call and provide simulation-specific code.

`setup_buildstamp.F90`	contains code for the subroutine `setup_buildstamp` which returns the setup and build time as well as code for `setup_systemInfo` which returns the *uname* of the system used to setup the problem
`setup_buildstats.c`	contains code which returns build statistics including the actual `setup` call as well as the compiler flags used for the build
`setup_getFlashUnits.F90`	contains code to retrieve the number and list of flashUnits used to compile code
`setup_flashRelease.F90`	contains code to retrieve the version of FLASH used for the build
`Flash.h`	contains simulation specific preprocessor macros, which change based upon setup unlike `constants.h`. It is described in Chapter 6
`Simulation_mapIntToStr.F90`	contains code to map an index described in `Flash.h` to a string described in the `Config` file.
`Simulation_mapStrToInt.F90`	contains code to map a string described in the `Config` file to an integer index described in the `Flash.h` file.
`Simulation_mapParticlesVar.F90`	contains a mapping between particle properties and grid variables. Only generated when particles are included in a simulation.
`Particles_specifyMethods.F90`	contains code to make a data structure with information about the mapping and initialization method for each type of particle. Only generated when particles are included in a simulation.

5.7.3 Makefiles generated by `setup`

Apart from the master `Makefile`, `setup` generates a makefile for each unit, which is "included" in the master `Makefile`. This is true even if the unit is not included in the application. These unit makefiles are named `Makefile.Unit` and are a concatenation of all the Makefiles found in unit hierarchy processed by `setup`.

For example, if an application uses `Grid/GridMain/paramesh/paramesh4/Paramesh4.0`, the file `Makefile.Grid` will be a concatenation of the Makefiles found in

- `Grid`,
- `Grid/GridMain`,
- `Grid/GridMain/paramesh`,
- `Grid/GridMain/paramesh/paramesh4`, and
- `Grid/GridMain/paramesh/paramesh4/Paramesh4.0`

As another example, if an application does not use `PhysicalConstants`, then `Makefile.PhysicalConstants` is just the contents of `PhysicalConstants/Makefile` at the API level.

Since the order of concatenation is arbitrary, the behavior of the Makefiles should not depend on the order in which they have been concatenated. The makefiles inside the units contain lines of the form:

```
Unit += file1.o file2.o ...
```

where `Unit` is the name of the unit, which was `Grid` in the example above. Dependency on data modules files *need not be specified* since the setup process determines this requirement automatically.

5.8 Setup a hybrid MPI+OpenMP FLASH application

There is the experimental inclusion of FLASH multithreading with OpenMP in the FLASH4 beta release. The units which have support for multithreading are split hydrodynamics 14.1.2, unsplit hydrodynamics 14.1.3, Gamma law and multigamma EOS 16.2, Helmholtz EOS 16.3, Multipole Poisson solver (improved version (support for 2D cylindrical and 3D cartesian)) 8.10.2.2 and energy deposition 17.4.

The FLASH multithreading requires a MPI-2 installation built with thread support (building with an MPI-1 installation or an MPI-2 installation without thread support is possible but strongly discouraged). The FLASH application requests the thread support level `MPI_THREAD_SERIALIZED` to ensure that the MPI library is thread-safe and that any OpenMP thread can call MPI functions safely. You should also make sure that your compiler provides a version of OpenMP which is compliant with at least the OpenMP 2.5 (200505) standard (older versions may also work but I have not checked).

In order to make use of the multithreaded code you must setup your application with one of the setup variables `threadBlockList`, `threadWithinBlock` or `threadRayTrace` equal to `True`, e.g.

```
./setup Sedov -auto threadBlockList=True
./setup Sedov -auto threadBlockList=True +mpi1 (compatible with MPI-1 - unsafe!)
```

When you do this the setup script will insert `USEOPENMP = 1` instead of `USEOPENMP = 0` in the generated Makefile. If it is equal to 1 the Makefile will prepend an OpenMP variable to the `FFLAGS`, `CFLAGS`, `LFLAGS` variables.

Makefile.h variables

In general you should not define `FLAGS`, `CFLAGS` and `LFLAGS` in your `Makefile.h`. It is much better to define `FFLAGS_OPT`, `FFLAGS_TEST`, `FFLAGS_DEBUG`, `CFLAGS_OPT`, `CFLAGS_TEST`, `CFLAGS_DEBUG`, `LFLAGS_OPT`, `LFLAGS_TEST` and `LFLAGS_DEBUG` in your `Makefile.h`. The setup script will then initialize the `FFLAGS`, `CFLAGS` and `LFLAGS` variables in the Makefile appropriately for an optimized, test or debug build.

The OpenMP variables should be defined in your `Makefile.h` and contain a compiler flag to recognize OpenMP directives. In most cases it is sufficient to define a single variable named `OPENMP`, but you may encounter special situations when you need to define `OPENMP_FORTRAN`, `OPENMP_C` and `OPENMP_LINK`. If you want to build FLASH with the GNU Fortran compiler `gfortran` and the GNU C compiler `gcc` then your `Makefile.h` should contain

```
OPENMP = -fopenmp
```

If you want to do something more complicated like build FLASH with the Lahey Fortran compiler `lf90` and the GNU C compiler `gcc` then your `Makefile.h` should contain

```
OPENMP_FORTRAN = --openmp -Kpureomp
OPENMP_C = -fopenmp
OPENMP_LINK = --openmp -Kpureomp
```

When you run the hybrid FLASH application it will print the level of thread support provided by the MPI library and the number of OpenMP threads in each parallel region

```
[Driver_initParallel]: Called MPI_Init_thread - requested level   2, given level   2
[Driver_initParallel]: Number of OpenMP threads in each parallel region  4
```

Note that the FLASH application will still run if the MPI library does not provide the requested level of thread support, but will print a warning message alerting you to an unsafe level of MPI thread support. There is no guarantee that the program will work! I strongly recommend that you stop using this FLASH application - you should build a MPI-2 library with thread support and then rebuild FLASH.

Log file stamp	**safe**	**unsafe (1)**	**unsafe (2)**	**unsafe (3)**
Number of MPI tasks:	1	1	1	1
MPI version:	2	1	2	2
MPI subversion:	2	2	1	2
MPI thread support:	T	F	F	F
OpenMP threads/MPI task:	2	2	2	2
OpenMP version:	200805	200505	200505	200805
Is "_OPENMP" macro defined:	T	T	T	F

Table 5.7: Log file entries showing safe and unsafe threaded FLASH applications

We record extra version and runtime information in the FLASH log file for a threaded application. Table 5.7 shows log file entries from a threaded FLASH application along with example safe and unsafe values. All cells colored red show unsafe values.

The FLASH applications in Table 5.7 are unsafe because

1. we are using an MPI-1 implementation.
2. we are using an MPI-2 implementation which is not built with thread support - the "MPI thread support in OpenMPI" Flash tip may help.
3. we are using a compiler that does not define the macro `_OPENMP` when it compiles source files with OpenMP support (see OpenMP standard). I have noticed that Absoft 64-bit Pro Fortran 11.1.3 for Linux x86_64 does not define this macro. We use this macro in `Driver_initParallel.F90` to conditionally initialize MPI with `MPI_Init_thread`. If you find that `_OPENMP` is not defined you should define it in your `Makefile.h` in a manner similar to the following:

   ```
   OPENMP_FORTRAN = -openmp -D_OPENMP=200805
   ```

MPI thread support in OpenMPI

A default installation of OpenMPI-1.5 (and earlier) does not provide any level of MPI thread support. To include MPI thread support you must configure OpenMPI-1.5 with `--enable-mpi-thread-multiple` or `--enable-opal-multi-threads`. We prefer to configure with `--enable-mpi-thread-multiple` so that we can (in future) use the highest level of thread support. The configure option is named `--enable-mpi-threads` in earlier versions of OpenMPI.

MPI-IO issues when using a threaded FLASH application

The ROMIO in older versions of MPICH2 and OpenMPI is known to be buggy. We have encountered a segmentation fault on one platform and a deadlock on another platform during MPI-IO when we used OpenMPI-1.4.4 with a multithreaded FLASH application. We solved the error by using OpenMPI-1.5.4 (it should be possible to use OpenMPI-1.5.2 or greater because the release notes for OpenMPI-1.5.2 state "- Updated ROMIO from MPICH v1.3.1 (plus one additional patch).". We have not tested to find the minimum version of MPICH2 but MPICH2-1.4.1p1 works fine. If it is not possible to use a newer MPI implementation you can avoid MPI-IO altogether by setting up your FLASH application with `+serialIO`.

You should not setup a FLASH application with both `threadBlockList` and `threadWithinBlock` equal to `True` - nested OpenMP parallelism is not supported. For further information about FLASH multithreaded applications please refer to Chapter 38.

5.9 Setup a FLASH+Chombo application

5.9.1 Overview

In FLASH4 we have introduced a new grid implementation that makes use of Chombo library (Section 8.7). This allows us to create FLASH applications that use an adaptive patch-based mesh for the first time.

You can create a FLASH application using Chombo mesh with the standard FLASH setup script and the designated shortcuts `+chombo_ug` or `+chombo_amr`. These shortcuts instruct the setup script to:

- Add the appropriate FLASH C++ source files that interact with Chombo library to the object directory. There are different C++ wrapper classes for a uniform grid (`+chombo_ug`) and adaptive grid (`+chombo_amr`) configuration.
- Reorder the arrays so that FLASH blocks normally accessed with solnData(v,i,j,k) are now accessed with solnData(i,j,k,v). This is a pre-processing step that is described in Section 5.2.
- Undefine the `FIXEDBLOCKSIZE` macro in Flash.h so that the code in FLASH source files does not assume that blocks contain a fixed number of cells.
- Define a setup variable named `chomboCompatibleHydro`. This variable is used in Hydro Config files to include a version of Hydro that is compatible with Chombo flux correction. At the current time we have only implemented flux correction with Chombo library for Split Hydro.
- Use the Makefile header file named `Makefile.h.chombo` instead of `Makefile.h`.

The shortcuts are used in FLASH setup lines as follows:

```
./setup Sedov -auto +chombo_ug -parfile=test_chombo_ug_2d.par
./setup Sod -auto +chombo_amr -parfile=test_chombo_amr_2d.par
```

The setup lines for all the problems that we have ever tested can be found in the file
`sites/code.uchicago.edu/flash_test/test.info`.

5.9.2 Build procedure

A FLASH application that makes use of Chombo library has the following dependencies:

- C++ compiler
- Fortran compiler with C interoperability features
- MPI build of Chombo
- parallel HDF5

The mixed-language Fortran/C interoperability features are critical for this project. Not all Fortran compilers have working C interoperability as this is a new feature that was introduced in the Fortran 2003 standard. Before spending time building Chombo and customizing FLASH Makefile headers, you should use our standalone unit test to determine whether your compilers have the basic mixed-language functionality needed by this project. The unit test is at `source/Grid/GridMain/Chombo/wrapper/unit_tests/1` and is independent of FLASH. It is a standalone Fortran application that uses the `iso_c_binding` function `c_f_pointer` to construct a Fortran pointer object given a raw C memory address and a shape argument. To build, enter this directory and execute `make "compiler name"`, where ”compiler name” is gnu, intel, ibm, sun.

Old compilers, such as gfortran version 4.1.2, will give a compile-time error because `iso_c_binding` module is not available, and at least one version of gfortran, namely gfortran version 4.4.0, has an array indexing run-time bug that is detected by this unit test. The array indexing bug is documented at **GCC bugzilla 40962** and gives the following incorrect answers shown in Figure 5.3.

```
We expect to pick up the complete set of integer values
from 0 to 23 in contiguous memory locations
Fortran array element:  1  1  1  1.   Expected:     0, actual:    0.
Fortran array element:  1  2  1  1.   Expected:     1, actual:    1.
Fortran array element:  1  1  2  1.   Expected:     2, actual:    2.
Fortran array element:  1  2  2  1.   Expected:     3, actual:    3.
Fortran array element:  1  1  3  1.   Expected:     4, actual:    4.
Fortran array element:  1  2  3  1.   Expected:     5, actual:    5.
Fortran array element:  1  1  1  2.   Expected:     6, actual:    3.
Fortran array element:  1  2  1  2.   Expected:     7, actual:    4.
Fortran array element:  1  1  2  2.   Expected:     8, actual:    5.
Fortran array element:  1  2  2  2.   Expected:     9, actual:    6.
Fortran array element:  1  1  3  2.   Expected:    10, actual:    7.
Fortran array element:  1  2  3  2.   Expected:    11, actual:    8.
Fortran array element:  1  1  1  3.   Expected:    12, actual:    6.
Fortran array element:  1  2  1  3.   Expected:    13, actual:    7.
Fortran array element:  1  1  2  3.   Expected:    14, actual:    8.
Fortran array element:  1  2  2  3.   Expected:    15, actual:    9.
Fortran array element:  1  1  3  3.   Expected:    16, actual:   10.
Fortran array element:  1  2  3  3.   Expected:    17, actual:   11.
Fortran array element:  1  1  1  4.   Expected:    18, actual:    9.
Fortran array element:  1  2  1  4.   Expected:    19, actual:   10.
Fortran array element:  1  1  2  4.   Expected:    20, actual:   11.
Fortran array element:  1  2  2  4.   Expected:    21, actual:   12.
Fortran array element:  1  1  3  4.   Expected:    22, actual:   13.
Fortran array element:  1  2  3  4.   Expected:    23, actual:   14.
FAILURE!  Picked up unexpected C++ assigned values
```

Figure 5.3: Unit test stdout for gfortran versions affected by GCC bug 40962.

```
CXX             = icpc
FC              = ifort
MPI             = TRUE
MPICXX          = /home/cdaley/software/mpich2/1.3.1/intel/bin/mpicxx
USE_64          = TRUE
USE_HDF         = TRUE
HDFINCFLAGS     = -I/home/cdaley/software/hdf5/1.8.5-patch1/intel/include -DH5_USE_16_API
HDFLIBFLAGS     = -L/home/cdaley/software/hdf5/1.8.5-patch1/intel/lib -lhdf5
HDFMPIINCFLAGS = -I/home/cdaley/software/hdf5/1.8.5-patch1/intel/include -DH5_USE_16_API
HDFMPILIBFLAGS = -L/home/cdaley/software/hdf5/1.8.5-patch1/intel/lib -lhdf5
USE_MT          = FALSE
syslibflags     = -lstdc++ -lz
```

Figure 5.4: Example macro definitions used to build Chombo in a FLASH-compatible way.

If this test fails at compile-time or run-time then FLASH-Chombo applications will not work! You can save a lot of time and frustration by running this unit test before continuing with the build process.

In contrast to Paramesh, the Chombo source code is not included in the FLASH source tree. This means that you, the user, must manually download and then build Chombo before building FLASH applications that make use of Chombo. You should download version 3.0 or 3.1 of Chombo from `https://seesar.lbl.gov/anag/chombo/` as these are the only versions of Chombo that have been tested with FLASH. Please refer to their user guide which is available from the same download page for help building Chombo. It contains a very clear and detailed build procedure along with a Chombo support email address that you can contact if you experience problems building Chombo.

You should build 1D,2D and 3D versions of Chombo library in a MPI configuration (`MPI = TRUE`) with parallel HDF5 (`USE_HDF = TRUE`). A parallel HDF5 implementation means a HDF5 installation that is configured with `--enable-parallel`. You can check whether you have a parallel HDF5 build using the following command line:

```
grep "Parallel HDF5" /path/to/hdf5/lib/libhdf5.settings
```

You should also explicitly turn off Chombo memory tracking (`USE_MT = FALSE`) because it is a feature that does not work with FLASH's usage of Chombo. Note that it is not always sufficient to set `USE_MT = FALSE` in your `Make.defs.local`; for Intel compiler we also had to remove `USE_MT = TRUE` from the default compiler settings in `./lib/mk/compiler/Make.defs.Intel`.

Only after you have successfully built and run the Chombo unit tests described in their user guide should you have any expectation that FLASH will work with Chombo library. For your reference we show the `Make.defs.local` macro definitions that we have used to build Chombo on a x86_64 machine in a FLASH-compatible way in Figure 5.4 .

Compiling Chombo on IBM BG/P

The file src/BaseTools/ClockTicks.H from the Chombo-3.0 distribution needs to be modified in order to compile Chombo on IBM BG/P. Change line 51 from

```
#elif defined(_POWER) || defined(_POWERPC) || defined(__POWERPC__)
```

to

```
#elif defined(_POWER) || defined(_POWERPC) || defined(__POWERPC__) ||
defined(__powerpc__)
```

At this stage you can optionally build and run the unit test `source/Grid/GridMain/Chombo/wrapper/-unit_tests/2`. This is a standalone Fortran MPI application that uses Chombo library to create a distributed mesh over 4 MPI processes. It can be built by entering this directory and then executing the command `make all`. We expect that this program will be helpful for debugging mixed-language programming issues between FLASH and Chombo (especially on untested architectures / compiler combinations) independently of a full-blown FLASH application. Note that you will need to edit the Makefile appropriately for your installation of Chombo.

In order to build a FLASH application with Chombo you must create a custom FLASH `Makefile.h` named `Makefile.h.chombo`. We use a new file named `Makefile.h.chombo` because it includes convenience shell functions (described later) that will fail if a Chombo package is not available. At minimum the FLASH `Makefile.h.chombo` must include definitions for the new macros `CFLAGS_CHOMBO` and `LIB_CHOMBO`. These can be manually defined, but this is not recommended because it does not guarantee that FLASH's C++ wrapper classes are built the same way as the Chombo library. Example macro definitions for a FLASH 2D simulations are shown below:

```
CFLAGS_CHOMBO: -I/home/cdaley/flash/chomboForFlash/current/lib/include
-DCH_SPACEDIM=2 -DCH_Linux -DCH_IFC -DCH_MPI -DMPICH_SKIP_MPICXX
-ULAM_WANT_MPI2CPP -DMPI_NO_CPPBIND -DCH_USE_SETVAL -DCH_USE_COMPLEX
-DCH_USE_64 -DCH_USE_DOUBLE -DCH_USE_HDF5
-I/home/cdaley/software/hdf5/1.8.5-patch1/intel/include
-DH5_USE_16_API -DCH_FORT_UNDERSCORE
-I/home/cdaley/flash/chomboForFlash/current/lib/src/BaseTools
-DCH_LANG_CC

LIB_CHOMBO: -L/home/cdaley/flash/chomboForFlash/current/lib
-lamrtimedependent2d.Linux.64.mpicxx.ifort.DEBUG.MPI
-lamrtools2d.Linux.64.mpicxx.ifort.DEBUG.MPI
-lboxtools2d.Linux.64.mpicxx.ifort.DEBUG.MPI
-lbasetools2d.Linux.64.mpicxx.ifort.DEBUG.MPI -lstdc++
```

This is obviously hugely inconvenient because the macros must be kept in sync with the current Chombo build and also the Chombo library names are dimension dependent. Our mechanism in FLASH4 to hide this build complexity is to add shell functions in `Makefile.h.chombo` that extract:

- application dimensionality from `Flash.h`.
- information about the Chombo build from the `make vars` rule in the main Chombo Makefile for the specified application dimensionality.

The shell functions appear in the `Makefile.h.chombo` in `sites/code.uchicago.edu`, so this file should be used as your reference. A subset of this file is shown in Figure 5.5.

Notice that there are several temporary macros (`_DIM, _MPI, _CPP, _LIB, _PHDF_INC, _PHDF_LIB`) that store information about the Chombo build at location `CHOMBO_PATH`. These temporary macros are later used to give values for macros referenced in the actual FLASH Makefile.

You should now be ready to setup and build FLASH applications with Chombo mesh package.

```
CHOMBO_PATH = /home/cdaley/flash/chomboForFlash/current

#----------------------------------------------------------------------------
# Extract dimensionality from Flash.h.
# The code in this section should not need to be modified.
#----------------------------------------------------------------------------

_DIM := \$(shell grep "define NDIM" Flash.h | cut -d " " -f 3)

#----------------------------------------------------------------------------
# Extract Chombo build information from the Makefile at CHOMBO_PATH.
# The code in this section should not need to be modified.
#----------------------------------------------------------------------------

_MPI := \$(shell make vars DIM=\${_DIM} -C \${CHOMBO_PATH}/lib | \
         awk -F 'MPICXX=' '/^MPICXX/{print \$\$2}')

ifeq (\$(strip \$(_MPI)),)
  \$(error "Chombo MPICXX variable is empty")
endif

_CPP := \$(shell make vars DIM=\${_DIM} -C \${CHOMBO_PATH}/lib | \
         awk -F 'CPPFLAGS=' '/^CPPFLAGS/{print \$\$2}')
_LIB := \$(shell make vars DIM=${_DIM} -C \${CHOMBO_PATH}/lib | \
         awk -F 'config=' '/^config/{print \$\$2}')
_PHDF_INC := \$(shell make vars DIM=\${_DIM} -C \${CHOMBO_PATH}/lib | \
         awk -F 'HDFMPIINCFLAGS=' '/^HDFMPIINCFLAGS/{print \$\$2}')
_PHDF_LIB := \$(shell make vars DIM=${_DIM} -C \${CHOMBO_PATH}/lib | \
         awk -F 'HDFMPILIBFLAGS=' '/^HDFMPILIBFLAGS/{print \$\$2}')

#----------------------------------------------------------------------------
# Use Chombo build information to get consistent macro values for the FLASH build.
#----------------------------------------------------------------------------

# Use two passes of dirname to strip the bin/mpicxx
MPI_PATH   := \$(shell dirname \$(shell dirname \$(shell which \$(_MPI))))
FCOMP   = \${MPI_PATH}/bin/mpif90
CCOMP   = \${MPI_PATH}/bin/mpicc
CPPCOMP = \${MPI_PATH}/bin/mpicxx
LINK    = \${MPI_PATH}/bin/mpif90

CFLAGS_CHOMBO = -I\${CHOMBO_PATH}/lib/include \${_CPP} -DCH_LANG_CC
CFLAGS_HDF5 = \$(_PHDF_INC)

LIB_CHOMBO = -L\$(CHOMBO_PATH)/lib \
-lamrtimedependent\${_LIB} \
-lamrtools\${_LIB} \
-lboxtools\${_LIB} \
-lbasetools\${_LIB} \
-lstdc++
LIB_HDF5 = \$(_PHDF_LIB) -lz
```

Figure 5.5: gmake shell functions to build FLASH and Chombo consistently.

Chapter 6

The `Flash.h` file

`Flash.h` is a critical header file in FLASH4 which holds many of the key quantities related to the particular simulation. The `Flash.h` file is written by the setup script and should not be modified by the user. The `Flash.h` file will be different for various applications. When the setup script is building an application, it parses the `Config` files, collects definitions of variables, fluxes, grid vars, species, and mass scalars, and writes a symbol (an index into one of the data structures maintained by the `Grid` unit) for each defined entity to the `Flash.h` header file. This chapter explains these symbols and some of the other important quantities and indices defined in the `Flash.h` file.

6.1 `UNK`, `FACE(XYZ)` Dimensions

Variables in a simulation are stored and manipulated by the `Grid` unit. The basic data structures in the `Grid` unit are 5-dimensional arrays: `unk`, `facex`, `facey`, and `facez`. The array `unk` stores the cell-centered values of various quantities (density, pressure, etc.). The `facex`, `facey` and `facez` variables store face-centered values of some or all of the same quantities. Face centered variables are commonly used in Magnetohydrodynamics (MHD) simulations to hold vector-quantity fields. The first dimension of each of these arrays indicates the variable, the 2nd, 3rd, and 4th dimensions indicate the cell location in a block, and the 5th dimension is the block identifier for the local processor. The size of the block, dimensions of the domain, and other parameters which influence the `Grid` data structures are defined in `Flash.h`.

`NXB,NYB,NZB`

The number of interior cells in the x,y,z-dimension per block

`MAXCELLS`

The maximum of (NXB,NYB,NZB)

`MAXBLOCKS`

The maximum number of blocks which can be allocated in a single processor

`GRID_(IJK)LO`

The index of the lowest numbered cell in the x,y,z-direction in a block (not including guard cells)

`GRID_(IJK)HI`

The index of the highest numbered cell in the x,y,z-direction in a block (not including guard cells)

`GRID_(IJK)LO_GC`

The index of the lowest numbered cell in the x,y,z-direction in a block (including guard cells)

`GRID_(IJK)HI_GC`

The index of the highest numbered cell in the x,y,z-direction in a block (including guard cells)

`NGUARD`

The number of guard cells in each dimension.

All of these constants have meaning when operating in FIXEDBLOCKSIZE mode only. FIXEDBLOCKSIZE mode is when the sizes and the block bounds are determined at compile time. In NONFIXEDBLOCKSIZE mode, the block sizes and the block bounds are determined at runtime. `PARAMESH` always runs in FIXEDBLOCKSIZE mode, while the Uniform Grid can be run in either FIXEDBLOCKSIZE or NONFIXEDBLOCKSIZE mode. See Section 5.2 and Section 8.5.2 for more information.

6.2 Property Variables, Species and Mass Scalars

The `unk` data structure stores, in order, property variables (like density, pressure, temperature), the mass fraction of species, and mass scalars [1]. However, in FLASH4 the user does not need to be intimately aware of the `unk` array layout, as starting and ending indices of these groups of quantities are defined in `Flash.h`. The following pre-processor symbols define the indices of the various quantities related to a given cell. These symbols are primarily used to perform some computation with all property variables, species mass fractions, or all mass scalars.

`NPROP_VARS`

The number of property variables in the simulation

`NSPECIES`

The total number of species in the simulation

`NMASS_SCALARS`

The number of mass scalars in the simulation

`NUNK_VARS`

The total number of quantities stored for each cell in the simulation. This equals `NPROP_VARS + NSPECIES + NMASS_SCALARS`

`PROP_VARS_BEGIN,PROP_VARS_END`

The indices in the `unk` array used for property variable data

`SPECIES_BEGIN,SPECIES_END`

The indices in the `unk` array used for species data

`MASS_SCALARS_BEGIN,MASS_SCALARS_END`

The indices in the `unk` array used for mass scalars data

`UNK_VARS_BEGIN,UNK_VARS_END`

The low and high indices for the `unk` array

The indices where specific properties (*e.g.*, density) are stored can also be accessed via pre-processor symbols. All properties are declared in `Config` files and consist of 4 letters. For example, if a `Config` file declares a "dens" variable, its index in the `unk` array is available via the pre-processor symbol `DENS_VAR` (append `_VAR` to the uppercase name of the variable) which is guaranteed to be an integer. The same is true for species and mass scalars. In the case of species, the pre-processor symbol is created by appending `_SPEC` to the uppercase name of the species (*e.g.*, `SF6_SPEC`, `AIR_SPEC`). Finally, for mass scalars, `_MSCALAR` is appended to the uppercase name of the mass scalars.

It is inadvisable to name variables, species, and mass scalars with the same prefix as post-processing routines have difficulty deciphering the type of data from the output files. For example, don't create

[1] See (14.9) for more information about mass scalars

a variable "temp" to hold temperature and a mass scalar "temp" indicating a temporary variable. Although the `Flash.h` file can distinguish between these two types of variables, many plotting routines such as `fidlr3.0`cannot.

6.3 Fluxes

The fluxes are stored in their own data structure and are only necessary when an adaptive grid is in use. The index order works in much the same way as with the `unk` data structure. There are the traditional property fluxes, like density, pressure, *etc.* Additionally, there are species fluxes and mass scalars fluxes. The name of the pre-processor symbol is assembled by appending `_FLUX` to the uppercase name of the declared flux (*e.g.*, `EINT_FLUX`, `U_FLUX`). For flux species and flux mass scalars, the suffix `_FLUX_SPECIES` and `_FLUX_MSCALAR` are appended to the uppercase names of flux species and flux mass scalars, respectively, as declared in the `Config` file. Useful defined variables are calculated as follows:

`NPROP_FLUX`

The number of property variables in the simulation

`NSPECIES_FLUX`

The total number of species in the simulation

`NMASS_SCALARS_FLUX`

The number of mass scalars in the simulation

`NFLUXES`

The total number of quantities stored for each cell in the simulation. This equals `(NPROP_FLUX + NSPECIES_FLUX + NMASS_SCALARS_FLUX)`

`PROP_FLUX_BEGIN,PROP_FLUX_END`

The indices in the `fluxes` data structure used for property variable data

`SPECIES_FLUX_BEGIN,SPECIES_FLUX_END`

The indices in the `fluxes` data structure used for species data

`MASS_SCALARS_FLUX_BEGIN,MASS_SCALARS_FLUX_END`

The indices in the `fluxes` data structure used for mass scalars data

`FLUXES_BEGIN`

The first index for the `fluxes` data structure

6.4 Scratch Vars

In FLASH4 the user is allowed to declare 'scratch' space for grid scope variables which resemble cell-centered or face-centered in shape and are dimensioned accordingly, but are not advected or transformed by the usual evolution steps. They do not participate in the guard-cell filling or regridding processes. For example a user could declare a scratch variable to store the temperature change on the grid from one timestep to another.They can be requested using keyword `SCRATCHCENTERVAR` for cell-centered scratch variables, or `SCRATCHFACEVAR` for face-centered scratch variables. A special case is `SCRATCHVAR`, which has one extra cell than the cell-centered variables along every dimension. We have provided this data structure to enable the reuse of the same scratch space by both cell-centered and each of the face-centered variables. Similar to the mesh variables used in the evolution, the scratch data structures are 4-dimensional arrays per block, where the first dimension enumerates the variables and the next three dimensions are the spatial dimensions. Scratch variables are indexed by postpending one of `_SCRATCH_GRID_VAR`, `_SCRATCH_CENTER_VAR` or `_SCRATCH_FACEX/Y/Z_VAR` to the capitalized four letter variable defined in the `Config` file. Similarly to property variables, `NSCRATCH_CENTER_VARS`, `SCRATCH_CENTER_VARS_BEGIN`, and `SCRATCH_CENTER_VARS_END` are defined to hold the number and endpoints of the cell-centered scratch variables. For face-centered scratch variables the CENTER is in the above terms is replaced with FACEX/Y/Z while for SCRATCHVARS, the CENTER is replace with GRID.

6.5 Fluid Variables Example

The snippet of code below shows a `Config` file and parts of a corresponding `Flash.h` file.

```
# Config file for explicit split PPM hydrodynamics.
# source/physics/Hydro/HydroMain/split/PPM

REQUIRES physics/Hydro/HydroMain/utilities
REQUIRES physics/Eos

DEFAULT PPMKernel

VARIABLE dens TYPE: PER_VOLUME       # density
VARIABLE velx TYPE: PER_MASS         # x-velocity
VARIABLE vely TYPE: PER_MASS         # y-velocity
VARIABLE velz TYPE: PER_MASS         # z-velocity
VARIABLE pres TYPE: GENERIC          # pressure
VARIABLE ener TYPE: PER_MASS         # specific total energy (T+U)
VARIABLE temp TYPE: GENERIC          # temperature
VARIABLE eint TYPE: PER_MASS         # specific internal energy

FLUX rho
FLUX u
FLUX p
FLUX ut
FLUX utt
FLUX e
FLUX eint

SCRATCHVAR otmp
SCRATCHCENTERVAR ftmp
.....
```

The `Flash.h` files would declare the property variables, fluxes and scratch variables as: (The setup script alphabetizes the names.)

```
#define DENS_VAR 1
#define EINT_VAR 2
#define ENER_VAR 3
#define PRES_VAR 4
#define TEMP_VAR 5
#define VELX_VAR 6
#define VELY_VAR 7
#define VELZ_VAR 8

#define E_FLUX 1
#define EINT_FLUX 2
#define P_FLUX 3
#define RHO_FLUX 4
#define U_FLUX 5
```

```
#define UT_FLUX 6
#define UTT_FLUX 7

#define OTMP_SCRATCH_GRID_VAR 1

#define FTMP_SCRATCH_CENTER_VAR 1
```

6.6 Particles

6.6.1 Particles Types

FLASH4 now supports the co-existence of multiple particle types in the same simulation. To facilitate this ability, the particles are now defined in the `Config` files with `PARTICLETYPE` keyword, which is also accompanied by an associated initialization and mapping method. The following example shows a Config file with passive particles, and the corresponding generated `Flash.h` lines

```
Config file :

PARTICLETYPE passive INITMETHOD lattice MAPMETHOD quadratic ADVMETHOD rungekutta

REQUIRES Particles/ParticlesMain
REQUESTS Particles/ParticlesMain/passive/RungeKutta
REQUESTS Particles/ParticlesMapping/Quadratic
REQUESTS Particles/ParticlesInitialization/Lattice
REQUESTS IO/IOMain/
REQUESTS IO/IOParticles

Flash.h :

#define PASSIVE_PART_TYPE 1
#define PART_TYPES_BEGIN CONSTANT_ONE
#define NPART_TYPES 1
#define PART_TYPES_END (PART_TYPES_BEGIN + NPART_TYPES - CONSTANT_ONE)
```

One line desribing the type, initialization, and mapping methods must be provided for *each* type of particle included in the simulation.

6.6.2 Particles Properties

Particle properties are defined within the `particles` data structure. The individual properties will be listed in `Flash.h` if the `Particles` unit is defined in a simulation. The variables `NPART_PROPS`, `PART_PROPS_BEGIN` and `PART_PROPS_END` indicate the number and location of particle properties indices. For example if a Config file has the following specifications

```
PARTICLEPROP dens
PARTICLEPROP pres
PARTICLEPROP velx
```

then the relevant portion of `Flash.h` will contain

```
#define DENS_PART_PROP 1
#define PRES_PART_PROP 2
#define VELX_PART_PROP 3
...
#define PART_PROPS_BEGIN CONSTANT_ONE
#define NPART_PROPS 3
#define PART_PROPS_END (PART_PROPS_BEGIN + NPART_PROPS - CONSTANT_ONE)
```

6.7 Non-Replicated Variable Arrays

For each non-replicated variable array defined in the `Config` file (see Section 5.5.1), various macros and constants are defined to assist the user in retrieving the information from the `NONREP` line as well as determining the distribution of array element variables across the meshes.

6.7.1 Per-Array Macros

For each non-replicated variable array *FOO* as defined by the following `Config` line:
`NONREP` *unktype* `FOO` *localmax globalparam ioformat*
the following will be placed into `Flash.h`:

- `#define` *FOO*`_NONREP`
  An integer constant greater than zero to be used as an id for this array. The user should rarely ever need to use this value. Instead, it is much more likely that the user would just query the preprocessor for the existence of this symbol (via `#ifdef` *FOO*`_NONREP`) to enable sections of code.

- `#define` *FOO*`_NONREP_LOC2UNK(loc)`
  Given the 1-based index into this mesh's local subset of the global array, returns the `UNK` index where that variable is stored.

- `#define` *FOO*`_NONREP_MAXLOCS`
  The integer constant *localmax* as supplied in the `Config` file `NONREP` line.

- `#define` *FOO*`_NONREP_RPCOUNT`
  The string literal value of *globalparam* from the `NONREP` line.

6.7.2 Array Partitioning Macros

These are the macros used to calculate the subset of indices into the global variable array each mesh is responsible for:

- `#define NONREP_NLOCS(mesh,meshes,globs)`
  Returns the number of elemenets in the mesh's local subset. This value will always be less than or equal to *FOO*˙NONREP˙MAXLOCS.

- `#define NONREP_LOC2GLOB(loc,mesh,meshes)`
  Maps an index into a mesh's local subset to its index in the global array.

- `#define NONREP_GLOB2LOC(glob,mesh,meshes)`
  Maps an index of the global array to the index into a mesh's local subset. If the mesh provided does not have that global element the result is undefined.

- `#define NONREP_MESHOFGLOB(glob,meshes)`
  Returns the mesh that owns a given global array index.

Descriptions of arguments to the above macros:

- `loc`: 1-based index into the mesh-local subset of the global array's indices.

- `glob`: 1-based index into the global array.

- `globs`: Length of the global array. This should be the value read from the array's runtime parameter *FOO*˙NONREP˙RPCOUNT.
- `mesh`: 0-based index of the mesh in question. For a processor, this is its rank in the `MESH_ACROSS_COMM` communicator.

- `meshes`: The number of meshes. This should be the value of the runtime parameter `meshCopyCount`, or equivalently the number of processors in the `MESH_ACROSS_COMM` communicator.

6.7.3 Example

In this example the global array `FOO` has eight elements, but there are three meshes, so two of the meshes will receive three elements of the array and one will get two. How that distribution is decided is hidden from the user. The output datasets will contain variables `foo1 ...foo8`.

Config:

```
NONREP MASS_SCALAR FOO 3 numFoo foo?
```

flash.par:

```
meshCopyCount = 3
numFoo = 8
```

Fortran 90:

```
\#include "Flash.h"\\
! this shows how to iterate over the UNKs corresponding to this
! processor's subset of FOO
integer :: nfooglob, nfooloc ! number of foo vars, global and local
integer :: mesh, nmesh ! this mesh number, and total number of meshes
integer :: fooloc, fooglob ! local and global foo indices
integer :: unk\\
call Driver_getMype(MESH_ACROSS_COMM, mesh)
call Driver_getNumProcs(MESH_ACROSS_COMM, nmesh)
call RuntimeParameters_get(FOO_NONREP_RPCOUNT, nfooglob)
nfooloc = NONREP_NLOCS(mesh, nmesh, nfooglob)\\
! iterate over the local subset for this mesh
do fooloc=1, nfooloc
    ! get the location in UNK
    unk = FOO_NONREP_LOC2UNK(fooloc)
    ! get the global index
    fooglob = NONREP_LOC2GLOB(fooloc, mesh, nmesh)\\
    ! you have what you need, do your worst...
end do
```

6.8 Other Preprocessor Symbols

The constants FIXEDBLOCKSIZE and NDIM are both included for convenience in this file. NDIM gives the dimensionality of the problem, and FIXEDBLOCKSIZE is defined if and only if fixed blocksize mode is selected at compile time.

Each Config file can include the PPDEFINE keyword to define additional preprocessor symbols. Each "PPDEFINE *symbol [value]*" gets translated to a "#define *symbol [value]*". This mechanism can be used to write code that depends on which units are included in the simulation. See Section 5.5.1 for concrete usage examples.

Part III

Driver Unit

Chapter 7

Driver Unit

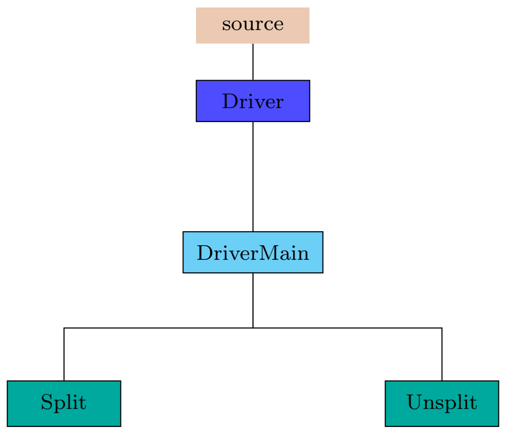

Figure 7.1: The `Driver` unit directory tree.

The `Driver` unit controls the initialization and evolution of FLASH simulations. In addition, at the highest level, the `Driver` unit organizes the interaction between units. Initialization can be from scratch or from a stored checkpoint file. For advancing the solution, the drivers can use either an operator-splitting technique adapted to directionally split physics operators like split `Hydro` (`Split`), or a more generic "`Unsplit`" implementation. The `Driver` unit also calls the `IO` unit at the end of every timestep to produce checkpoint files, plot files, or other output.

7.1 Driver Routines

The most important routines in the `Driver` API are those that initialize, evolve, and finalize the FLASH program. The file `Flash.F90` contains the main FLASH program (equivalent to `main()` in C). The default top-level program of FLASH, `Simulation/Flash.F90`, calls `Driver` routines in this order:

```
program Flash

  implicit none

  call Driver_initParallel()
  call Driver_initFlash()
  call Driver_evolveFlash( )
  call Driver_finalizeFlash ( )
```

```
end program Flash
```

Therefore the no-operation stubs for these routines in the `Driver` source directory must be overridden by an implementation function in a unit implementation directory under the `Driver` or `Simulation` directory trees, in order for a simulation to perform any meaningful actions. The most commonly used implementations for most of these files are located in the `Driver/DriverMain` unit implementation directory, with a few specialized ones in either `Driver/DriverMain/Split` or `Driver/DriverMain/Unsplit`.

7.1.1 Driver_initFlash

The first of these routines is `Driver_initParallel`, which initializes the parallel environment for the simulation. New in FLASH4 is an ability to replicate the mesh where more than one copy of the discretized mesh may exist with some overlapping and some non-overlapping variables. Because of this feature, the parallel environment differentiates between global and mesh communicators. All the necessary communicators, and the attendant meta-data is generated in this routine. Also because of this modification, runtime parameters such as iProcs, jProcs etc, which were under the control of the Grid unit in FLASH3, are now under the control of the Driver unit. Several new accessor interface allow other code units to query the driver unit for this information. The `Driver_initFlash`, the next routine, in general calls the initialization routines in each of the units. If a unit is not included in a simulation, its stub (or empty) implementation is called. Having stub implementations is very useful in the `Driver` unit because it allows the user to avoid writing a new driver for each simulation. For a more detailed explanation of stub implementations please see Section 4.2. It is important to note that when individual units are being initialized, order is often very important and the order of initialization is different depending on whether the run is from scratch or being restarted from a checkpoint file.

7.1.2 Driver_evolveFlash

The next routine is `Driver_evolveFlash` which controls the timestepping of the simulation, as well as the normal termination of FLASH based on time. `Driver_evolveFlash` checks the parameters `tmax`, `nend` and `zFinal` to determine that the run should end, having reached a particular point in time, a certain number of steps, or a particular cosmological redshift, respectively. Likewise the initial simulation time, step number and cosmological redshift for a simulation can be set using the runtime parameters `tmin`, `nbegin`, and `zInitial`. This version of FLASH includes versions of `Driver_evolveFlash` for directionally-split and unsplit staggered mesh operators.

7.1.2.1 Strang Split Evolution

The code in the `Driver/DriverMain/Split` unit implementation directory has been the default time update method up to FLASH4.3, and can still be be used for many setups that can be configured with FLASH. The routine `Driver_evolveFlash` implements a Strang-split method of time advancement where each physics unit updates the solution data for two equal timesteps – thus the sequence of calls to physics and other units in each time step goes something like this: `Hydro`, diffusive terms, source terms, `Particles`, `Gravity`; `Hydro`, diffusive terms, source terms, `Particles`, `Gravity`, `IO` (for output), `Grid` (for grid changes). The hydrodynamics update routines take a "sweep order" argument since they must be directionally split to work with this driver. Here, the first call usually uses the ordering $x - y - z$, and the second call uses $z - y - x$. Each of the update routines is assumed to directly modify the solution variables. At the end of one loop of timestep advancement, the condition for updating the mesh refinement pattern is tested if the adaptive mesh is being used, and a refinement update is carried out if required.

7.1.2.2 Unsplit Evolution

The driver implementation in the `Driver/DriverMain/Unsplit` directory is the default since FLASH4.4. It is required specifically for the two unsplit solvers: unsplit staggered mesh MHD solver (Section 14.3.3) and the unsplit gas hydrodynamics solver (Section 14.1.3). This implementation in general calls each of the physics routines only once per time step, and each call advances solution vectors by one timestep. At the end of one loop of timestep advancement, the condition for updating the adaptive mesh refinement pattern is tested and applied.

7.1.2.3 Super-Time-Stepping (STS)

A new timestepping method implemented in FLASH4 is a technique called Super-Time-Stepping (STS). The STS is a simple explicit method which is used to accelerate restrictive parabolic timestepping advancements ($\Delta t_{\text{CFL\_para}} \approx \Delta x^2$) by relaxing the CFL stability condition of parabolic equation system.

The STS has been proposed by Alexiades et al., (1996), and used in computational astrophysics and sciences recenly (see Mignone et al., 2007; O'Sullivan & Downes, 2006; Commerçon et al., 2011; Lee, D. et al, 2011) for solving systems of parabolic PDEs numerically. The method increases its effective time steps Δt_{sts} using two properties of stability and optimality in Chebychev polynomial of degree n. These properties optimally maximize the time step Δt_{sts} by which a solution vector can be evolved. A stability condition is imposed only after each time step Δt_{sts}, which is further subdivided into smaller N_{sts} sub-time steps, τ_i, that is, $\Delta t_{\text{sts}} = \sum_{i=1}^{N_{\text{sts}}} \tau_i$, where the sub-time step is given by

$$\tau_i = \Delta t_{\text{CFL\_para}} \big[(-1+\nu_{\text{sts}}) cos\big(\frac{\pi(2j-1)}{2N_{\text{sts}}} + 1 + \nu_{\text{sts}}\big)\big]^{-1}, \tag{7.1}$$

where $\Delta t_{\text{CFL\_para}}$ is an explicit time step for a given parabolic system based on the CFL stability condition. ν (`nuSTS`) is a free parameter less than unity. For $\nu \to 0$, STS is asymptotically N_{sts} times faster than the conventional explicit scheme based on the CFL condition. During the N_{sts} sub-time steps, the STS method still solves solutions at each intermediate step τ_i; however, such solutions should not be considered as meaningful solutions.

Extended from the original STS method for accelerating parabolic timestepping, our STS method advances advection and/or diffusion (hyperbolic and/or parabolic) system of equations. This means that the STS algorithm in FLASH invokes a single Δt_{sts} for both advection and diffusion, and does not use any sub-cycling for diffusion based on a given advection time step. In this case, τ_i is given by

$$\tau_i = \Delta t_{\text{CFL}} \big[(-1+\nu_{\text{sts}}) cos\big(\frac{\pi(2j-1)}{2N_{\text{sts}}} + 1 + \nu_{\text{sts}}\big)\big]^{-1}, \tag{7.2}$$

where Δt_{CFL} can be an explicit time step for advection ($\Delta t_{\text{CFL\_adv}}$) or parabolic ($\Delta t_{\text{CFL\_para}}$) systems. In cases of advection-diffusion system, Δt_{CFL} takes ($\Delta t_{\text{CFL\_para}}$) when it is smaller than ($\Delta t_{\text{CFL\_adv}}$); otherwise, FLASH's timestepping will proceed without using STS iterations (i.e., using standard explicit timestepping that is either Strang split evolution or unsplit evolution.

Since the method is explicit, it works equally well on both a uniform grid and AMR grids without modification. The STS method is first-order accurate in time.

Both directionally-split and unsplit hydro solvers can use the STS method, simply by invoking a runtime parameter `useSTS = .true.` in `flash.par`. There are couple of runtime parameters that control solution accuracy and stability. They are decribed in Table 7.1.

7.1.2.4 Runtime Parameters

The `Driver` unit supplies certain runtime parameters regardless of which type of driver is chosen. These are described in the online `Runtime Parameters Documentation page`.

Table 7.1: Runtime parameters for STS

Variable	Type	Default	Description
`useSTS`	logical	.false.	Enable STS
`nstepTotalSTS`	integer	5	Suggestion: $\sim$ 5 for hyperbolic; $\sim$ 10 for parabolic
`nuSTS`	real	0.2	Suggestion: $\sim$ 0.2 for hyperbolic; $\sim$ 0.01 for parabolic. It is known that a very low value of ν may result in unstable temporal integrations, while a value close to unity can decrease the expected efficiency of STS.
`useSTSforDiffusion`	logical	.false.	This setup will use the STS for overcoming small diffusion time steps assuming $\Delta t_{\mathrm{CFL\_adv}} > \Delta t_{\mathrm{CFL\_para}}$. In implementation, it will set $\Delta t_{\mathrm{CFL}} = \Delta t_{\mathrm{CFL\_para}}$ in Eqn. 7.2. Do not allow to turn on this switch when there is no diffusion (viscosity, conductivity, and magnetic resistivity) used.
`allowDtSTSDominate`	logical	.false.	If true, this will allow to have $\tau_i > \Delta t_{\mathrm{CFL\_adv}}$, which may result in unstable integrations.

FLASH Transition

The `Driver` unit no longer provides runtime parameters, physical constants, or logfile management. Those services have been placed in separate units. The `Driver` unit also does not declare boolean values to include a unit in a simulation or not. For example, in FLASH2, the `Driver` declared a runtime parameter `iburn` to turn on and off burning.

```
if(iburn) then
    call burning ....
end if
```

In FLASH4 the individual unit declares a runtime parameter that determines whether the unit is used during the simulation *e.g.*, the `Burn` unit declares `useBurn` within the `Burn` unit code that turns burning on or off. This way the `Driver` is no longer responsible for knowing what is included in a simulation. A unit gets called from the `Driver`, and if it is not included in a simulation, a stub gets called. If a unit, like `Burn`, is included but the user wants to turn burning off, then the runtime parameter declared in the `Burn` unit would be set to false.

7.1.3 Driver_finalizeFlash

Finally, the the `Driver` unit calls `Driver_finalizeFlash` which calls the finalize routines for each unit. Typically this involves deallocating memory and any other necessary cleanup.

7.1.4 Driver accessor functions

In FLASH4 the `Driver` unit also provides a number of accessor functions to get data stored in the `Driver` unit, for example `Driver_getDt`, `Driver_getNStep`, `Driver_getElapsedWCTime`, `Driver_getSimTime`.

FLASH Transition

In FLASH4 most of the quantities that were in the FLASH2 database are stored in the `Grid` unit or are replaced with functionality in the `Flash.h` file. A few scalars quantities like `dt`, the current timestep number `nstep`, simulation time and elapsed wall clock time, however, are now stored in the `Driver_data` FORTRAN90 module.

The `Driver` unit API also defines two interfaces for halting the code, `Driver_abortFlash` and `Driver_abortFlashC.c`. The 'c' routine version is available for calls written in C, so that the user does not have to worry about any name mangling. Both of these routines print an error message and call `MPI_Abort`.

Part IV

Infrastructure Units

Chapter 8

Grid Unit

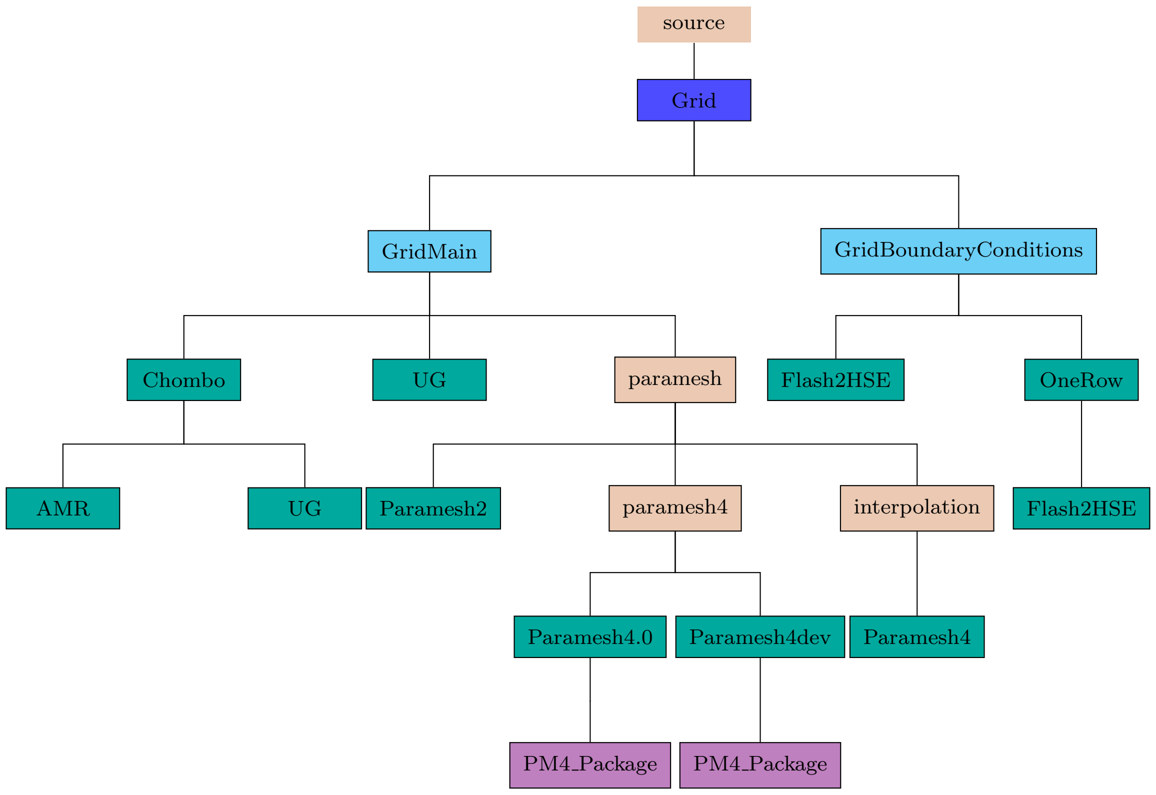

Figure 8.1: The `Grid` unit: structure of `GridMain` and `GridBoundaryCondition` subunits.

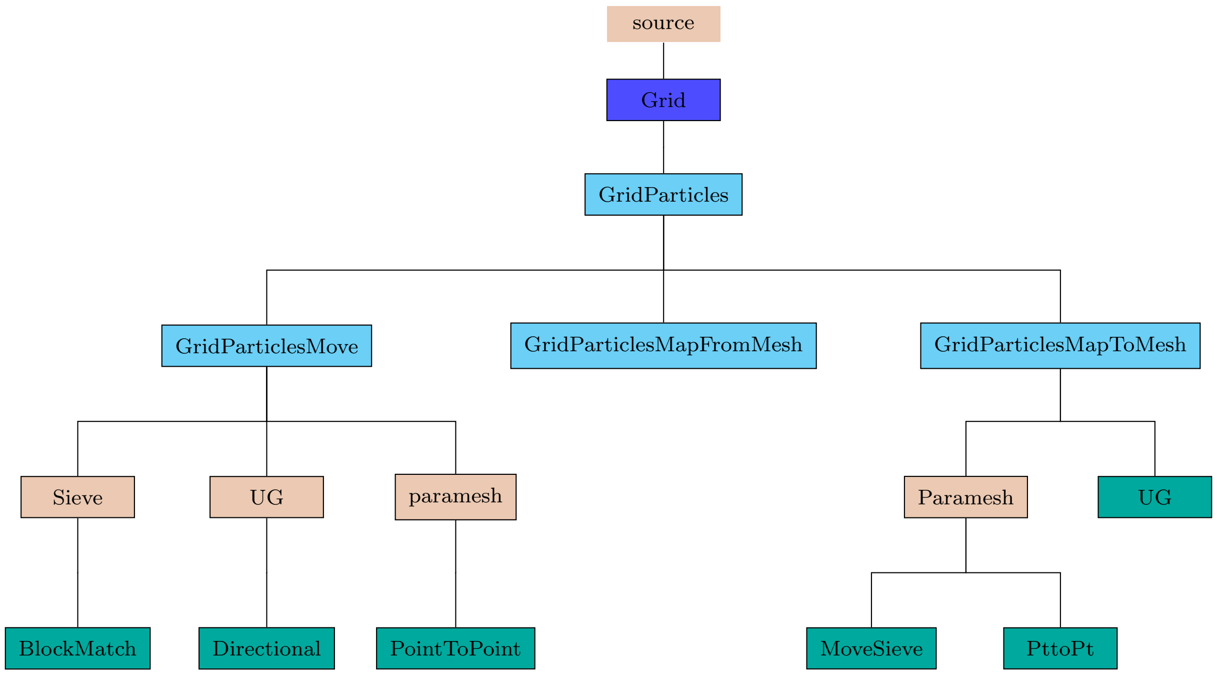

Figure 8.2: The `Grid` unit: structure of `GridParticles` subunit.

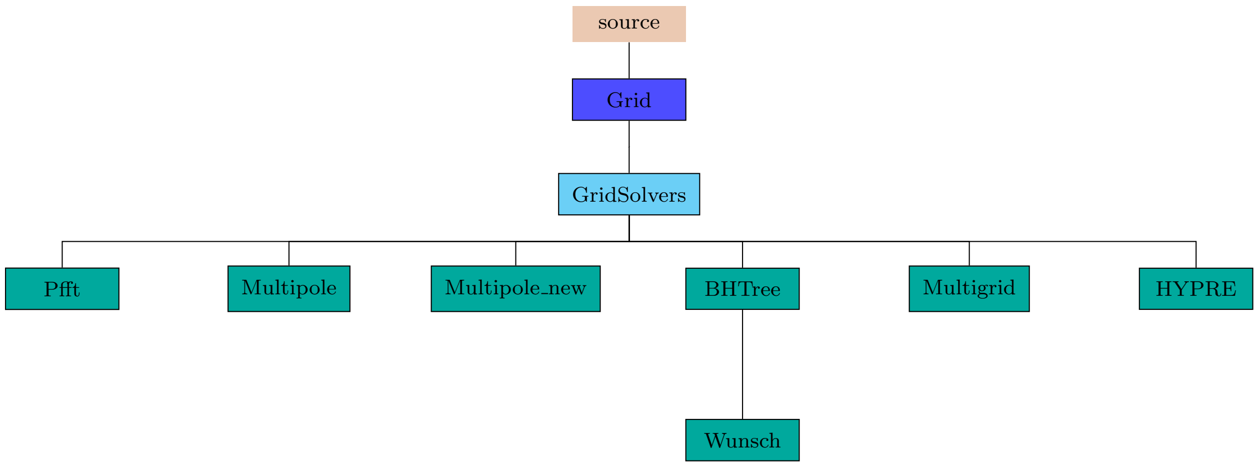

Figure 8.3: The `Grid` unit: structure of `GridSolvers` subunit.

8.1 Overview

The `Grid` unit has four subunits: `GridMain` is responsible for maintaining the Eulerian grid used to discretize the spatial dimensions of a simulation; `GridParticles` manages the data movement related to active, and Lagrangian tracer particles; `GridBoundaryConditions` handles the application of boundary conditions at the physical boundaries of the domain; and `GridSolvers` provides services for solving some types of partial differential equations on the grid. In the Eulerian grid, discretization is achieved by dividing the computational domain into one or more sub-domains or blocks, and using these blocks as the primary computational entity visible to the physics units. A block contains a number of computational cells (`nxb` in the x-direction, `nyb` in the y-direction, and `nzb` in the z-direction). A perimeter of guardcells, of width `nguard` cells in each coordinate direction, surrounds each block of local data, providing it with data from the neighboring blocks or with boundary conditions, as shown in Figure 8.4. Since the majority of physics solvers used in FLASH are explicit, a block with its surrounding guard cells becomes a self-contained computational domain. Thus the physics units see and operate on only one block at a time, and this abstraction is reflected in their design.

Therefore any mesh package that can present a self contained block as a computational domain to a client unit can be used with FLASH. However, such interchangeability of grid packages also requires a careful design of the `Grid` API to make the underlying management of the discretized grid completely transparent to outside units. The data structures for physical variables, the spatial coordinates, and the management of the grid are kept private to the `Grid` unit, and client units can access them only through accessor functions. This strict protocol for data management along with the use of blocks as computational entities enables FLASH to abstract the grid from physics solvers and facilitates the ability of FLASH to use multiple mesh packages.

Any unit in the code can retrieve all or part of a block of data from the `Grid` unit along with the coordinates of corresponding cells; it can then use this information for internal computations, and finally return the modified data to the `Grid` unit. The `Grid` unit also manages the parallelization of FLASH. It consists of a suite of subroutines which handle distribution of work to processors and guard cell filling. When using an adaptive mesh, the Grid unit is also responsible for refinement/derefinement and conservation of flux across block boundaries.

FLASH can interchangeably use either a **uniform** or **adaptive grid** for most problems. Additionally, a new feature in FLASH4 is an option to replicate the mesh; that is processors are assumed to be partitioned into groups, each group gets a copy of the entire domain mesh. This feature is useful when it is possible to decompose the computation based upon certain compute intensive tasks that apply across the domain. One such example is radiation transfer with multigroup flux limited diffusion where each group needs an implicit solve. Here the state variable of the mesh are replicated on each group of processors, while the groups are unique. Thus at the cost of some memory redundancy, it becomes possible to compute a higher

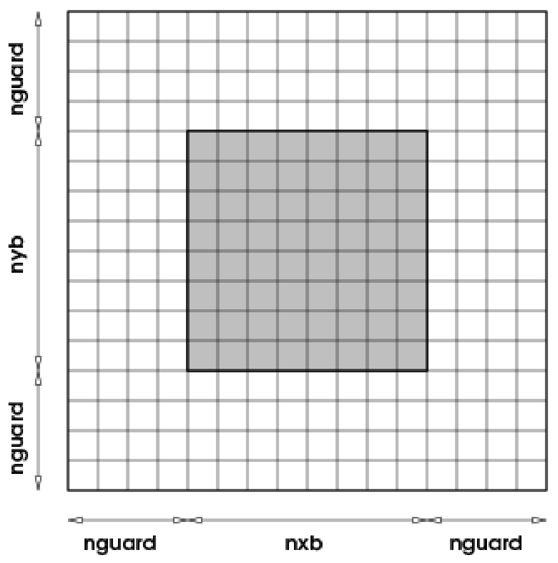

Figure 8.4: A single 2-D block showing the interior cells (shaded) and the perimeter of guard cells.

fidelity problem (see Chapter 24 for an example). Because of this feature, the parallel environment of the simulation is now controlled by the Driver which differentiates between global communicators and mesh communicators. The Grid unit queries the Driver unit for mesh communicators. In all other respects this change is transparent to the Grid unit. Mesh replication can be invoked through the runtime parameter `meshCopyCount`

The uniform grid supported in FLASH discretizes the physical domain by placing grid points at regular intervals defined by the geometry of the problem. The grid configuration remains unchanged throughout the simulation, and exactly one block is mapped per processor. An adaptive grid changes the discretization over the course of the computation, and several blocks can be mapped to each computational processor. Two AMR packages are currently supported in FLASH for providing adaptive grid capbility. The block-structured oct-tree based AMR package, `PARAMESH` has been the work horse since the beginning of the code. Version 2 and Version 4 of paramesh are both supported, version 2 is kept mostly to enable cross checking against FLASH2 results. FLASH4, for the first time, includes patch based `Chombo` as an alternative AMR package. By default, `PARAMESH` 4 is chosen when setting up an application, unless another implementation is explicitly specified. The use of paramesh 2 is deprecated, and `Chombo` has not so far been used for production at the Flash Center.

FLASH Transition

The following two commands will create the same (identical) application: a simulation of a Sod shock tube in 3 dimensions with PARAMESH 4 managing the grid.

```
./setup Sod -3d -auto

./setup Sod -3d -auto -unit=Grid/GridMain/paramesh/paramesh4/Paramesh4.0
```

However, if the command is changed to

```
./setup Sod -3d -auto -unit=Grid/GridMain/UG
```

the application is set up with a uniform grid instead. Additionally, because two different grids types are supported in FLASH, the user must match up the correct IO alternative implementation with the correct Grid alternative implementation. Please see Chapter 9 for more details. Note that the setup script has capabilities to let the user set up shortcuts, such as "+ugio", which makes sure that the appropriate branch of IO is included when the uniform grid is being used. Please see Section 5.3 for more information. Also see grid tips for shortcuts useful for the Grid unit.

8.2 GridMain Data Structures

The Grid unit is the most extensive infrastructure unit in the FLASH code, and it owns data that most other units wish to fetch and modify. Since the data layout in this unit has implications on the manageability and performance of the code, we describe it in some detail here.

FLASH can be run with a grid discretization that assumes cell-centered data, face-centered data, or a combination of the two. Paramesh and Uniform Grid store physical data in multidimensional F90 arrays; cell-centered variables in unk, short for "unknowns", and face-centered variables in arrays called facevarx, facevary, and facevarz, which contain the face-centered data along the x, y, and z dimensions, respectively. The cell-centered array unk is dimensioned as array(NUNK_VARS,nxb,nyb,nzb,*blocks*), where nxb, nyb, nzb are the spatial dimensions of a single block, and *blocks* is the number of blocks per processor (MAXBLOCKS for PARAMESH and 1 for UG). The face-centered arrays have one extra data point along the dimension they are representing, for example facevarx is dimensioned as array(NFACE_VARS,nxb+1,nyb,nzb,*blocks*). Some or all of the actual values dimensioning these arrays are determined at application setup time. The number of variables and the value of MAXBLOCKS are always determined at setup time. The spatial dimensions nxb,nyb,nzb can either be fixed at setup time, or they may be determined at runtime. These two modes are referred to as FIXEDBLOCKSIZE and NONFIXEDBLOCKSIZE. Chombo, which is written in C++, maintains its internal data very differently. However, through the wrapper layer provided by Grid, the Chombo data structures mimic the data layout understood by the FLASH solvers. Details of Grid implementation with Chombo are described in section Section 8.7

All values determined at setup time are defined as constants in a file Flash.h generated by the setup tool. This file contains all application-specific global constants such as the number and naming of physical variables, number and naming of fluxes and species, *etc.*; it is described in detail in Chapter 6.

For cell-centered variables, the Grid unit also stores a **variable type** that can be retrieved using the Simulation_getVarnameType routine; see Section 5.5.1 for the syntax and meaning of the optional TYPE attribute that can be specified as part of a VARIABLE definition read by the setup tool.

In addition to the primary physical variables, the Grid unit has another set of data structures for storing auxiliary fluid variables. This set of data structures provides a mechanism for storing such variables whose spatial scope is the entire physical domain, but who do not need to maintain their guard cells updated at all times. The data structures in this set include: SCRATCHCENTERVAR, which has the same shape as the cell centered variables data structure; and SCRATCHFACEXVAR, SCRATCHFACEYVAR and SCRATCHFACEZVAR, which have the same shape as the corresponding face centered variables data structures. Early releases of

FLASH3 had `SCRATCHVAR`, dimensioned `array(NSCRATCH_GRID_VARS,nxb+1,nyb+1,nzb+1,blocks)`, as the only grid scope scratch data structure. For reasons of backward compatibility, and to maximize reusability of space, `SCRATCHVAR` continues to exist as a supported data structure, though its use is deprecated. The datastructures for face variables, though supported, are not used anywhere in the released code base. The unsplit MHD solver `StaggeredMesh` discussed in Section 14.3.3 gives an example of the use of some of these data structures. It is important to note that there is no guardcell filling for the scratch variables, and the values in the scratch variables become invalid after a grid refinement step. While users can define scratch variables to be written to the plotfiles, they are not by default written to checkpoint files. The `Grid` unit also stores the metadata necessary for work distribution, load balancing, and other housekeeping activities. These activities are further discussed in Section 8.5 and Section 8.6, which describe individual implementations of the `Grid` unit.

8.3 Computational Domain

The size of the computational domain in physical units is specified at runtime through the (`xmin`, `xmax`), (`ymin`, `ymax`), and (`zmin`, `zmax`) runtime parameters. When working with curvilinear coordinates (see below in Section 8.11), the extrema for angle coordinates are specified in degrees. Internally all angles are represented in radians, so angles are converted to radians at `Grid` initialization.

FLASH Transition

The convention for specifying the ranges for angular coordinates has changed from FLASH2, which used units of π instead of degrees for angular coordinates.

The physical domain is mapped into a computational domain at problem initialization through routine `Grid_initDomain` in `PARAMESH` and `Chombo`, and `Grid_init` in `UG`.When using the uniform grid `UG`, the mapping is easy: one block is created for each processor in the run, which can be sized either at build time or runtime depending upon the mode of UG use. [1] Further description can be found in Section 8.5. When using the AMR grid `PARAMESH`, the mapping is non-trivial. The adaptive mesh `gr_createDomain` function creates an initial mesh of `nblockx * nblocky * nblockz` top level blocks, where `nblockx`, `nblocky`, and `nblockz` are runtime parameters which default to 1.[2] The resolution of the computational domain is usually very coarse and unsuitable for computation after the initial mapping. The `gr_expandDomain` routine remedies the situation by applying the refinement process to the initial domain until a satisfactory level of resolution is reached everywhere in the domain. This method of mapping the physical domain to computational domain is effective because the resultant resolution in any section is related to the demands of the initial conditions there.

[1]Note that the term processor, as used here and elsewhere in the documentation, does not necessarily correspond to a separate hardware processor. It is also possible to have several logical "processors" mapped to the same hardware, which can be useful for debugging and testing; this is a matter for the operating environment to regulate.

[2]The `gr_createDomain` function also can remove certain blocks of this initial mesh, if this is requested by a non-default `Simulation_defineDomain` implementation.

FLASH Transition

FLASH2 supported only an AMR grid with paramesh 2. At initialization, it created the coarsest level initial blocks covering the domain using an algorithm called "sequential" divide domain. A uniform grid of blocks on processor zero was created, and until the first refinement, all blocks were on processor zero. FLASH3 onwards the paramesh based implementation of the Grid uses a "parallel" domain creation algorithm that attempts to create the initial domain in blocks that are distributed amongst all processors according to the same Morton ordering used by `PARAMESH`.
First, the parallel algorithm computes a Morton number for each block in the coarsest level uniform grid, producing a sorted list of Morton numbers for all blocks to be created. Each processor will create the blocks from a section of this list, and each processor determines how big its section will be. After that, each processor loops over all the blocks on the top level, computing Morton numbers for each, finding them in the sorted list, and determining if this block is in its own section. If it is, the processor creates the block. Parallel divide domain is especially useful in three-dimensional problems where memory constraints can sometimes force the initial domain to be unrealistically coarse with a sequential divide domain algorithm.

8.4 Boundary Conditions

Much of the FLASH3 code within the `Grid` unit that deals with implementing boundary conditions has been organized into a separate subunit, `GridBoundaryConditions`. Note that the following aspects are still handled elsewhere:

- Recognition of bounday condition names as strings (in runtime parameters) and constants (in the source code); these are defined in `RuntimeParameters_mapStrToInt` and in `constants.h`, respectively.
- Handling of periodic boundary conditions; this is done within the underlying `GridMain` implementation. When using `PARAMESH`, the subroutine `gr_createDomain` is responsible for setting the neighbors of top-level blocks (to either other top-level blocks or to external boundary conditions) at initialization, after `Nblockx` $\times$ `Nblocky` $\times$ `Nblockz` root blocks have been created. periodic (wrap-around) boundary conditions are initially configured in this routine as well. If periodic boundary conditions are set in the x-direction, for instance, the first blocks in the x-direction are set to have as their left-most neighbor the blocks that are last in the x-direction, and *vice versa*. Thus, when the guard cell filling is performed, the periodic boundary conditions are automatically maintained.
- Handling of user-defined boundary conditions; this should be implemented by code under the `Simulation` directory.
- Low-level implementation and interfacing, such as are part of the `PARAMESH` code.
- Behavior of particles at a domain boundary. This is based on the boundary types described below, but their handling is implemented in `GridParticles`.

Although the `GridBoundaryConditions` subunit is included in a setup by default, it can be excluded (if no `Config` file "`REQUIRES`" it) by specifying `-without-unit=Grid/GridBoundaryConditions`. This will generally only make sense if all domain boundaries are to be treated as periodic. (All relevant runtime parameters `xl_boundary_type` *etc.* need to be set to `"periodic"` in that case.)

8.4.1 Boundary Condition Types

Boundary conditions are determined by the physical problem. Within FLASH, the parallel structure of blocks means that each processor works independently. If a block is on a physical boundary, the guard cells are filled by calculation since there are no neighboring blocks from which to copy values. Boundaries are selected by setting runtime parameters such as `xl_boundary_type` (for the 'left' X–boundary) to one of the supported boundary types (Section 8.4.1) in `flash.par`. Even though the runtime parameters for specifying boundary condition types are strings, the `Grid` unit understands them as defined integer constants defined in the file `constants.h`, which contains all global constants for the code. The translation from the string specified in "flash.par" to the constant understood by the `Grid` unit is done by the routine `RuntimeParameters_mapStrToInt`.

*ab*_**boundary_type**	**Description**
`periodic`	Periodic ('wrap-around')
`reflect`	Non-penetrating boundaries; plane symmetry, the normal vector components change sign
`outflow`	Zero-gradient boundary conditions; allows shocks to leave the domain
`diode`	like outflow, but fluid velocities are never allowed to let matter flow into the domain: normal velocity components are forced to zero in guard cells if necessary
`axisymmetric`	like reflect, but both normal and toroidal vector components change sign. Typically used with cylindrical geometry (R-Z) for the Z symmetry axis.
`eqtsymmetric`	like reflect for velocities but the magnetic field components, poloidal and toroidal, change sign. The sign of the normal magnetic field component remains the same. Typically used with cylindrical geometry (R-Z) for the R axis to emulate equatorial symmetry.
`hydrostatic-f2`	Hydrostatic boundary handling as in FLASH2. See remark in text.
`hydrostatic-f2+nvrefl`, `hydrostatic-f2+nvout`, `hydrostatic-f2+nvdiode`	Variants of `hydrostatic-f2`, where the **n**ormal **v**elocity is handled specially in various ways, analogous to `reflect`, `outflow`, and `diode` boundary conditions, respectively. See remark in text.
`user-defined` or `user`	The user must implement the desired boundary behavior; see text.

Table 8.1: Hydrodynamical boundary conditions supported by FLASH. Boundary type *ab* may be replaced with a={x,y,z} for direction and b={l,r} for left/right edge. All boundary types listed except the last (`user`) have an implementation in `GridBoundaryConditions`.

To use any of the `hydrostatic-f2*` boundary conditions, the setup must include `Grid/GridBoundary-Conditions/Flash2HSE`. This must usually be explicitly requested, for example with a line

```
REQUIRES Grid/GridBoundaryConditions/Flash2HSE
```

in the simulation directory's `Config` file.

Note that the `grav_boundary_type` runtime parameter is used by some implementations of the `Gravity` unit to define the type of boundary for solving a self-gravity (Poisson) problem; see `Gravity_init`. This runtime parameter is separate from the *ab*_**boundary_type** ones interpreted by `GridBoundaryConditions`, and its recognized values are not the same (although there is some overlap).

8.4.2 Boundary Conditions at Obstacles

The initial coarse grid of root blocks can be modified by removing certain blocks. This is done by providing a non-trivial implementation of `Simulation_defineDomain`. Effectively this creates additional domain boundaries at the interface between blocks removed and regions still included. All boundary conditions other than

*ab*_boundary_type	Constant	Remark
isolated	—	used by Gravity only for grav_boundary_type
—	DIRICHLET	used for multigrid solver
—	GRIDBC_MG_EXTRAPOLATE	for use by multigrid solver
—	PNEUMANN	(for use by multigrid solver)
hydrostatic	HYDROSTATIC	Hydrostatic, other implementation than FLASH2
hydrostatic+nvrefl	HYDROSTATIC_NVREFL	Hydrostatic variant, other impl. than FLASH2
hydrostatic+nvout	HYDROSTATIC_NVOUT	Hydrostatic variant, other impl. than FLASH2
hydrostatic+nvdiode	HYDROSTATIC_NVDIODE	Hydrostatic variant, other impl. than FLASH2

Table 8.2: Additional boundary condition types recognized by FLASH. Boundary type *ab* may be replaced with a={x,y,z} for direction and b={l,r} for left/right edge. These boundary types are either reserved for implementation by users and/or future FLASH versions for a specific purpose (as indicate by the remarks), or are for special uses within the Grid unit.

periodic are possible at these additional boundaries, and are handled there in the same way as on external domain boundaries. This feature is only available with PARAMESH. See the documentation and example in Simulation_defineDomain for more details and some caveats.

8.4.3 Implementing Boundary Conditions

Users may need to implement boundary conditions beyond those provided with FLASH3, and the Grid-BoundaryConditions subunit provides several ways to achieve this. Users can provide an implementation for the user boundary type; or can provide or override an implementation for one of the other recognized types.

The simple boundary condition types reflect, outflow, diode are implemented in the Grid_bcApplyToRegion.F90 file in Grid/GridBoundaryConditions. A users can add or modify the handling of some boundary condition types in a version of this file in the simulation directory, which overrides the regular version. There is, however, also the interface Grid_bcApplyToRegionSpecialized which by default is only provided as a stub and is explicitly intended to be implemented by users.
A Grid_bcApplyToRegionSpecialized implementation gets called before Grid_bcApplyToRegion and can decide to either handle a specific combination of boundary condition type, direction, grid data structure, *etc.*, or leave it to Grid_bcApplyToRegion. These calls operate on a region of one block's cells at a time. FLASH will pass additional information beyond that needed for handling simple boundary conditions to Grid_bcApplyToRegionSpecialized, in particular a block handle through which an implementation can retrieve coordinate information and access other information associated with a block and its cells.

The GridBoundaryConditions subunit also provides a simpler kind of interface if one includes Grid/-GridBoundaryConditions/OneRow in the setup. When using this style of interface, users can implement guard cell filling one row at a time. FLASH passes to the implementation one row of cells at a time, some of which are interior cells while the others represent guard cells outside the boundary that are to be modified in the call. A row here means a contiguous set of cells along a line perpendicular to the boundary surface. There are two versions of this interface: Grid_applyBCEdge is given only one fluid variable at a time, but can also handle data structures other than unk; whereas Grid_applyBCEdgeAllUnkVars handles all variables of unk along a row in one call. Cell coordinate information is included in the call arguments. FLASH invokes these functions through an implementation of Grid_bcApplyToRegionSpecialized in Grid/GridBoundaryConditions/OneRow which acts as a wrapper. GridBoundaryConditions/OneRow also provides a default implementation of Grid_applyBCEdge (which implements the simple boundary conditions) and Grid_applyBCEdgeAllUnkVars (which calls Grid_applyBCEdge) each. Another implementation of Grid_applyBCEdgeAllUnkVars can be found in GridBoundaryConditions/OneRow/Flash2HSE, this one calls Grid_applyBCEdge or, for FLASH2-type hydrostatic boundaries, the code for handling them. These can be used as templates for overriding implementations under Simulation. It is not recommended to try to mix both Grid_bcApplyToRegion*-style and Grid_applyBCEdge*-style overriding implementations in a simulation directory, since this could become confusing.

Note that in all of these cases, *i.e.*, whether boundary guard cell filling for a boundary type is implemented in Grid_bcApplyToRegion, Grid_bcApplyToRegionSpecialized, Grid_applyBCEdge, or Grid_applyBCEdgeAllUnkVars, the implementation does not fill guard cells in permanent data storage (the unk array and similar data structures) directly, but operates on buffers. FLASH3 fills some parts of the buffers with current values for interior cells before the call, and copies updated guardcell data from some (other) parts of the buffers back into unk (or similar) storage after the handling routine returns.

All calls to handlers for boundary conditions are for one face in a given dimension at a time. Thus for each of the IAXIS, JAXIS, and KAXIS dimensions there can be up to two series of calls, once for the left, *i.e.*, "LOW," and once for the right, *i.e.*, "HIGH," face. PARAMESH 4 makes additional calls for filling guard cells in edge and corner regions of blocks, these calls result in additional Grid_bcApplyToRegion* invocations for those cells that lie in diagonal directions from the block interior.

The boundary condition handling interfaces described so far can be implemented (and will be used!) independent of the Grid implementation chosen. At a lower level, the various implementations of GridMain have different ways of requesting that boundary guard cells be filled. The GridBoundaryConditions subunit collaborates with GridMain implementations to provide to user code uniform interfaces that are agnostic of lower-level details. However, it is also possible — but not recommended — for users to replace a routine that is located deeper in the Grid unit. For PARAMESH 4, the most relevant routine is amr_1blk_bcset.F90, for PARAMESH 2 it is tot_bnd.F90, and for uniform grid UG it is gr_bcApplyToAllBlks.F90.

8.4.3.1 Additional Concerns with PARAMESH 4

Boundary condition handling has become significantly more complex in FLASH3. In part this is so because PARAMESH 4 imposes requirements on guard cell filling code that do not exist in the other GridMain implementations:

1. In other Grid implementations, filling of domain boundary guard cells is under control of the "user" (in this context, the user of the grid implementation, *i.e.*, FLASH): These cells can be filled for all blocks at a time that is predictable to the user code, as a standard part of handling Grid_fillGuardCells, only. With PARAMESH 4, the user-provided amr_1blk_bcset routine can be called from within the depths of PARAMESH on individual blocks (and cell regions, see below) during guard cell filling and at other times when the user has called a PARAMESH routine. It is not easy to predict when and in which sequence this will happen.

2. PARAMESH 4 does not want all boundary guard cells filled in one call, but requests individual regions in various calls.

3. PARAMESH 4 does not let the user routine amr_1blk_bcset operate on permanent storage (unk *etc.*) directly, but on (regions of) one-block buffers.

4. PARAMESH 4 occasionally invokes amr_1blk_bcset to operate on regions of a block that belongs to a remote processor (and for which data has been cached locally). Such block data is not associated with a valid local blockID, making it more complicated for user code to retrieve metadata that may be needed to implement the desired boundary handling.

Some consequences of this for FLASH3 users:

- User code that implements boundary conditions for the grid inherits the requirement that it must be ready to be called at various times (when certain Grid routines are called).

- User code that implements boundary conditions for the grid inherits the requirement that it must operate on a region of the cells of a block, where the region is specified by the caller.

- Such user code must not assume that it operates on permanent data (in unk *etc.*). Rather, it must be prepared to fill guardcells for a block-shaped buffer that may or may not end up being copied back to permanent storage.

  User code also is not allowed to make certain PARAMESH 4 calls while a call to amr_1blk_bcset is active, namely those that would modify the same one-block buffers that the current call is working on.

- The user code must not assume that the block data it is acting on belongs to a local block. The data may not have a valid `blockID`. The code will be passed a "block hande" which can be used in some ways, but not all, like a valid `blockID`.

Caveat Block Handles

See the `README` file in `Grid/GridBoundaryConditions` for more information on how a block handle can be used.

8.5 Uniform Grid

The Uniform Grid has the same resolution in all the blocks throughout the domain, and each processor has exactly one block. The uniform grid can operate in either of two modes: fixed block size (FIXEDBLOCKSIZE) mode, and non-fixed block size (NONFIXEDBLOCKSIZE) mode. The default fixed block size grid is statically defined at compile time and can therefore take advantage of compile-time optimizations. The non-fixed block size version uses dynamic memory allocation of grid variables.

8.5.1 FIXEDBLOCKSIZE Mode

`FIXEDBLOCKSIZE` mode, also called static mode, is the default for the uniform grid. In this mode, the block size is specified at compile time as `NXB`×`NYB`×`NZB`. These variables default to 8 if the dimension is defined and 1 otherwise – *e.g.*for a two-dimensional simulation, the defaults are `NXB`$= 8$, `NYB`$= 8$, `NZb`$= 1$. To change the static dimensions, specify the desired values on the command line of the `setup` script; for example

```
./setup Sod -auto -3d -nxb=12 -nyb=12 -nzb=4 +ug
```

The distribution of processors along the three dimensions is given at run time as $iprocs \times jprocs \times kprocs$ with the constraint that this product must be equal to the number of processors that the simulation is using. The global domain size in terms of number of grid points is `NXB`$*iprocs \times$ `NYB`$*jprocs \times$ `NZB`$*kprocs$. For example, if $iprocs = jprocs = 4$ and $kprocs = 1$, the execution command should specify $np = 16$ processors.

```
mpirun -np 16 flash3
```

When working in static mode, the simulation is constrained to run on the same number of processors when restarting, since any different configuration of processors would change the domain size.

At Grid initialization time, the domain is created and the communication machinery is also generated. This initialization includes MPI communicators and datatypes for directional guardcell exchanges. If we view processors as arranged in a three-dimensional processor grid, then a row of processors along each dimension becomes a part of the same communicator. We also define MPI datatypes for each of these communicators, which describe the layout of the block on the processor to MPI. The communicators and datatypes, once generated, persist for the entire run of the application. Thus the `MPI_SEND/RECV` function with specific communicator and its corresponding datatype is able to carry out all data exchange for guardcell fill in the selected direction in a single step.

Since all blocks exist at the same resolution in the Uniform Grid, there is no need for interpolation while filling the guardcells. Simple exchange of correct data between processors, and the application of boundary conditions where needed is sufficient. The guard cells along the face of a block are filled with the layers of the interior cells of the block on the neighboring processor if that face is shared with another block, or calculated based upon the boundary conditions if the face is on the physical domain boundary. Also, because there are no jumps in refinement in the Uniform Grid, the flux conservation step across processor boundaries is unnecessary. For correct functioning of the Uniform Grid in FLASH, this conservation step should be explicitly turned off with a runtime parameter `flux_correct` which controls whether or not to run the flux conservation step in the PPM Hydrodynamics implementation. AMR sets it by default to true, while UG sets it to false. Users should exercise care if they wish to override the defaults via their "`flash.par`" file.

8.5.2 NONFIXEDBLOCKSIZE mode

Up ot version 2, FLASH always ran in a mode where all blocks have exactly the same number of grid points in exactly the same shape, and these were fixed at compile time. FLASH was limited to use the fixed block size mode described above. With FLASH3 this constraint was eliminated through an option at setup time. The two main reasons for this development were: one, to allow a uniform grid based simulation to be able to restart with different number of processors, and two, to open up the possibility of using other AMR packages with FLASH. Patch-based packages typically have different-sized block configurations at different times. This mode, called the "NONFIXEDBLOCKSIZE" mode, can currently be selected for use with Uniform Grid, and is the default mode with `Chombo`. To run an application in "NONFIXEDBLOCKSIZE" mode, the "`-nofbs`" option must be used when invoking the setup tool; see Chapter 5 for more information. For example:

```
./setup Sod -3d -auto -nofbs
```

Note that `NONFIXEDBLOCKSIZE` mode requires the use of its own IO implementation, and a convenient shortcut has been provided to ensure that this mode is used as in the example below:

```
./setup Sod -3d -auto +nofbs
```

In this mode, the blocksize in UG is determined at execution from runtime parameters `iGridSize`, `jGridSize` and `kGridSize`. These parameters specify the global number of grid points in the computational domain along each dimension. The blocksize then is $(iGridSize/iprocs) \times (jGridSize/jprocs) \times (kGridSize/kprocs)$.

Unlike `FIXEDBLOCKSIZE` mode, where memory is allocated at compile time, in the `NONFIXEDBLOCKSIZE` mode all memory allocation is dynamic. The global data structures are allocated when the simulation initializes and deallocated when the simulation finalizes, whereas the local scratch space is allocated and deallocated every time a unit is invoked in the simulation. Clearly there is a trade-off between flexibility and performance as the `NONFIXEDBLOCKSIZE` mode typically runs about 10-15% slower. We support both to give choice to the users. The amount of memory consumed by the Grid data structure of the Uniform Grid is $\texttt{nvar} \times (2 * \texttt{nguard} + \texttt{nxb}) \times (2 * \texttt{nguard} + \texttt{nyb}) \times (2 * \texttt{nguard} + \texttt{nzb})$ irrespective of the mode. Note that this is not the total amount of memory used by the code, since fluxes, temporary variables, coordinate information and scratch space also consume a large amount of memory.

The example shown below gives two possible ways to define parameters in `flash.par` for a 3d problem of global domain size $64 \times 64 \times 64$, being run on 8 processors.

```
iprocs = 2
jprocs = 2
kprocs = 2
iGridSize = 64
jGridSize = 64
kGridSize = 64
```

This specification will result in each processor getting a block of size $32 \times 32 \times 32$. Now consider the following specification for the number of processors along each dimension, keeping the global domain size the same.

```
iprocs = 4
jprocs = 2
kprocs = 1
```

In this case, each processor will now have blocks of size $16 \times 32 \times 64$.

8.6 Adaptive Mesh Refinement (AMR) Grid with Paramesh

The default package in FLASH is `PARAMESH` (MacNeice *et al.* 1999) for implementing the adaptive mesh refinement (AMR) grid. `PARAMESH` uses a block-structured adaptive mesh refinement scheme similar to others in the literature (*e.g.*, Parashar 1999; Berger & Oliger 1984; Berger & Colella 1989; DeZeeuw & Powell 1993).

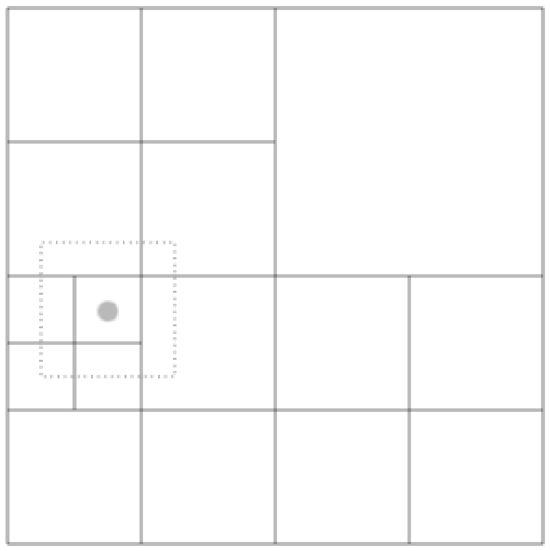

Figure 8.5: A simple computational domain showing varying levels of refinement in a total of 16 blocks. The dotted lines outline the guard cells for the block marked with a circle.

It also shares ideas with schemes which refine on an individual cell basis (Khokhlov 1997). In block-structured AMR, the fundamental data structure is a block of cells arranged in a logically Cartesian fashion. "Logically Cartesian" implies that each cell can be specified using a block identifier (processor number and local block number) and a coordinate triple (i, j, k), where $i = 1 \ldots$ `nxb`, $j = 1 \ldots$ `nyb`, and $k = 1 \ldots$ `nzb` refer to the x-, y-, and z-directions, respectively. It does not require a physically rectangular coordinate system; for example a spherical grid can be indexed in this same manner.

The complete computational grid consists of a collection of blocks with different physical cell sizes, which are related to each other in a hierarchical fashion using a tree data structure. The blocks at the root of the tree have the largest cells, while their children have smaller cells and are said to be refined. Three rules govern the establishment of refined child blocks in `PARAMESH`. First, a refined child block must be one-half as large as its parent block in each spatial dimension. Second, a block's children must be nested; *i.e.*, the child blocks must fit within their parent block and cannot overlap one another, and the complete set of children of a block must fill its volume. Thus, in d dimensions a given block has either zero or 2^d children. Third, blocks which share a common border may not differ from each other by more than one level of refinement.

A simple two-dimensional domain is shown in Figure 8.5, illustrating the rules above. Each block contains `nxb` $\times$ `nyb` $\times$ `nzb` interior cells and a set of guard cells. The guard cells contain boundary information needed to update the interior cells. These can be obtained from physically neighboring blocks, externally specified boundary conditions, or both. The number of guard cells needed depends upon the interpolation schemes and the differencing stencils used by the various physics units (usually hydrodynamics). For the explicit PPM algorithm distributed with FLASH, four guard cells are needed in each direction, as illustrated in Figure 8.4. The blocksize while using the adaptive grid is fixed at compile time, resulting in static memory allocation. The total number of blocks a processor can manage is determined by `MAXBLOCKS`, which can be overridden at setup time with the `setup ...-maxblocks=#` argument. The amount of memory consumed by the Grid data structure of code when running with `PARAMESH` is `NUNK_VARS` $\times$ $(2 *$ `nguard` $+$ `nxb`$)$ $\times$ $(2 *$ `nguard` $+$ `nyb`$)$ $\times$ $(2 *$ `nguard` $+$ `nzb`$)$ $\times$ `MAXBLOCKS`. `PARAMESH` also needs memory to store its tree data structure for adaptive mesh management, over and above what is already mentioned with Uniform Grid. As the levels of refinement increase, the size of the tree also grows.

`PARAMESH` handles the filling of guard cells with information from other blocks or, at the boundaries of the physical domain, from an external boundary routine (see Section 8.4). If a block's neighbor exists and has the same level of refinement, `PARAMESH` fills the corresponding guard cells using a direct copy

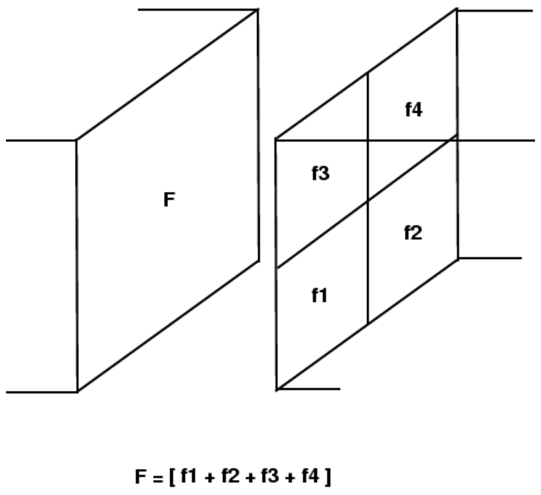

Figure 8.6: Flux conservation at a jump in refinement. The fluxes in the fine cells are added and replace the coarse cell flux (F).

from the neighbor's interior cells. If the neighbor has a different level of refinement, the data from the neighbor's cells must be adjusted by either interpolation (to a finer level of resolution) or averaging (to a coarser level)—see Section 8.6.2 below for more information. If the block and its neighbor are stored in the memory of different processors, `PARAMESH` handles the appropriate parallel communications (blocks are never split between processors). The filling of guard cells is a global operation that is triggered by calling `Grid_fillGuardCells`.

Grid Interpolation is also used when filling the blocks of children newly created in the course of automatic refinement. This happens during `Grid_updateRefinement` processing. Averaging is also used to regularly update the solution data in at least one level of parent blocks in the oct-tree. This ensures that after leaf nodes are removed during automatic refinement processing (in regions of the domain where the mesh is becoming coarser), the new leaf nodes automatically have valid data. This averaging happens as an initial step in `Grid_fillGuardCells` processing.

`PARAMESH` also enforces flux conservation at jumps in refinement, as described by Berger and Colella (1989). At jumps in refinement, the fluxes of mass, momentum, energy (total and internal), and species density in the fine cells across boundary cell faces are summed and passed to their parent. The parent's neighboring cell will be at the same level of refinement as the summed flux cell because `PARAMESH` limits the jumps in refinement to one level between blocks. The flux in the parent that was computed by the more accurate fine cells is taken as the correct flux through the interface and is passed to the corresponding coarse face on the neighboring block (see Figure 8.6). The summing allows a geometrical weighting to be implemented for non-Cartesian geometries, which ensures that the proper volume-corrected flux is computed.

8.6.1 Additional Data Structures

`PARAMESH` maintains much additional information about the mesh. In particular, oct-tree related information is kept in various arrays which are declared in a F90 module called "`tree`". It includes the physical coordinate of a block's center, its physical size, level of refinement, and much more. These data structures also acts as temporary storage while updating refinement in the grid and moving the blocks. This metadata should in general not be accessed directly by application code. The `Grid` API contains subroutines for accessing the most important pars of this metadata on a block by block basis, like `Grid_getBlkBoundBox`, `Grid_getBlkCenterCoords`, `Grid_getBlkPhysicalSize`, `Grid_getBlkRefineLevel`, and `Grid_getBlkType`.

FLASH has its own `oneBlock` data structure that stores block specific information. This data structure keeps the physical coordinates of each cell in the block. For each dimension, the coordinates are stored for the `LEFT_EDGE`, the `RIGHT_EDGE` and the center of the cell. The coordinates are determined from "*cornerID*" which is also a part of this data structure.

The concept of `cornerID` was introduced in FLASH3; it serves three purposes. First, it creates a unique global identity for every cell that can come into existence at any time in the course of the simulation. Second, it can prevent machine precision error from creeping into the spatial coordinates calculation. Finally, it can help pinpoint the location of a block within the oct-tree of `PARAMESH`. Another useful integer variable is the concept of a *stride*. A stride indicates the spacing factor between one cell and the cell directly to its right when calculating the cornerID. At the maximum refinement level, the stride is 1, at the next higher level it is 2, and so on. Two consecutive cells at refinement level n are numbered with a stride of $2^{lrefine\_max-n}$ where $1 \leq n \leq lrefine\_max$.

The routine `Grid_getBlkCornerID` provides a convenient way for the user to retrieve the location of a block or cell. A usage example is provided in the documentation for that routine. The user should retrieve accurate physical and grid coordinates by calling the routines `Grid_getBlkCornerID`, `Grid_getCellCoords`, `Grid_getBlkCenterCoords` and `Grid_getBlkPhysicalSize`, instead of calculating their own from local block information, since they take advantage of the `cornerID` scheme, and therefore avoid the possibility of introducing machine precision induced numerical drift in the calculations.

8.6.2 Grid Interpolation (and Averaging)

The adaptive grid requires data **interpolation** or **averaging** when the refinement level (*i.e.*, mesh resolution) changes in space or in time. [3] If during guardcell filling a block's neighbor has a coarser level of refinement, the neighbor's cells are used to **interpolate** guard cell values to the cells of the finer block. Interpolation is also used when filling the blocks of children newly created in the course of automatic refinement. Data **averaging** is used to adapt data in the opposite direction, *i.e.*, from fine to coarse.

In the AMR context, the term **prolongation** is used to refer to data interpolation (because it is used when the tree of blocks grows longer). Similarly, the term **restriction** is used to refer to fine-to-coarse data averaging.

The algorithm used for restriction is straightforward (equal-weight) averaging in Cartesian coordinates, but has to take cell volume factors into account for curvilinear coordinates; see Section 8.11.5.

`PARAMESH` supports various interpolation schemes, to which user-specified interpolation schemes can be added. FLASH4 currently allows to choose between two interpolation schemes:

1. monotonic
2. native

The choice is made at `setup` time, see Section 5.2.

The versions of `PARAMESH` supplied with FLASH4 supply their own default interpolation scheme, which is used when FLASH4 is configured with the `-gridinterpolation=native setup` option (see Section 5.2). The default schemes are only appropriate for Cartesian coordinates. If FLASH4 is configured with curvilinear support, an alternative scheme (appropriate for all supported geometries) is compiled in. This so-called "**monotonic**" interpolation attempts to ensure that interpolation does not introduce small-scale non-monotonicity in the data. The order of "monotonic" interpolation can be chosen with the `interpol_order` runtime parameter. See Section 8.11.5 for some more details on prolongation for curvilinear coordinates. At setup time, monotonic interpolation is the default interpolation used.

8.6.2.1 Interpolation for mass-specific solution variables

To accurately preserve the total amount of conserved quantities, the interpolation routines have to be applied to solution data in **conserved**, *i.e.*, volume-specific, form. However, many variables are usually stored in the `unk` array in mass-specific form, *e.g.*, specific internal and total energies, velocities, and mass fractions. See Section 5.5.1 for how to use the optional `TYPE` attribute in a `Config` file's `VARIABLE` definitions to inform the `Grid` unit which variables are considered mass-specific.

FLASH4 provides three ways to deal with this:

[3] Particles and Physics units may make additional use of interpolation as part of their function, and the algorithms may or may not be different. This subsection only discusses interpolation automatically performed by the `Grid` unit on the fluid variables in a way that should be transparent to other units.

1. Do nothing—*i.e.*, assume that ignoring the difference between mass-specific and conserved form is a reasonable approximation. Depending on the smoothness of solutions in regions where refinement, derefinement, and jumps in refinement level occur, this assumption may be acceptable. This behavior can be forced by setting the `convertToConsvdInMeshInterp` runtime parameter to `.false.`

2. Convert mass-specific variables to conserved form *in all blocks throughout the physical domain* before invoking a `Grid` function that may result in some data interpolation or restriction (refinement, derefinement, guardcell filling); and convert back after these functions return. Conversion is done by cell-by-cell multiplication with the density (*i.e.*, the value of the "`dens`" variable, which should be declared as

   ```
   VARIABLE dens TYPE: PER_VOLUME
   ```

   in a `Config` file).

   This behavior is available in both `PARAMESH` 2 and `PARAMESH` 4. It is enabled by setting the `convertToConsvdForMeshCalls` runtime parameter and corresponds roughly to FLASH2 with `conserved_var` enabled.

3. Convert mass-specific variables to conserved form only where and when necessary, from the `Grid` user's point of view *as part of data interpolation.* Again, conversion is done by cell-by-cell multiplication with the value of density. In the actual implementation of this approach, the conversion and back-conversion operations are closely bracketing the interpolation (or restriction) calls. The implementation avoids spurious back-and-forth conversions (*i.e.*, repeated successive multiplications and divisions of data by the density) in blocks that should not be modified by interpolation or restriction.

   This behavior is available only for `PARAMESH` 4. As of FLASH4, this is the default behavior whenever available. It can be enabled explicitly (only necessary in setups that change the default) by setting the `convertToConsvdInMeshInterp` runtime parameter.

8.6.3 Refinement

8.6.3.1 Refinement Criteria

The refinement criterion used by `PARAMESH` is adapted from Löhner (1987). Löhner's error estimator was originally developed for finite element applications and has the advantage that it uses a mostly local calculation. Furthermore, the estimator is dimensionless and can be applied with complete generality to any of the field variables of the simulation or any combination of them.

FLASH Transition

FLASH4 does not define any refinement variables by default. Therefore simulations using AMR have to make the appropriate runtime parameter definitions in `flash.par`, or in the simulation's `Config` file. If this is not done, the program generates a warning at startup, and no automatic refinement will be performed. The mistake of not specifying refinement variables is thus easily detected. To define a refinement variable, use `refine_var_#` (where `#` stands for a number from 1 to 4) in the `flash.par` file.

Löhner's estimator is a modified second derivative, normalized by the average of the gradient over one computational cell. In one dimension on a uniform mesh, it is given by

$$E_i = \frac{\mid u_{i+1} - 2u_i + u_{i-1} \mid}{\mid u_{i+1} - u_i \mid + \mid u_i - u_{i-1} \mid + \epsilon [\mid u_{i+1} \mid + 2 \mid u_i \mid + \mid u_{i-1} \mid]} \,, \tag{8.1}$$

where u_i is the refinement test variable's value in the ith cell. The last term in the denominator of this expression acts as a filter, preventing refinement of small ripples, where ϵ should be a small constant.

When extending this criterion to multidimensions, all cross derivatives are computed, and the following generalization of the above expression is used

$$E_{i_1 i_2 i_3} = \left\{ \frac{\sum_{pq} \left(\frac{\partial^2 u}{\partial x_p \partial x_q} \Delta x_p \Delta x_q \right)^2}{\sum_{pq} \left[\left(\left| \frac{\partial u}{\partial x_p} \right|_{i_p+1/2} + \left| \frac{\partial u}{\partial x_p} \right|_{i_p-1/2} \right) \Delta x_p + \epsilon \frac{\partial^2 |u|}{\partial x_p \partial x_q} \Delta x_p \Delta x_q \right]^2} \right\}^{1/2} , \tag{8.2}$$

where the sums are carried out over coordinate directions, and where, unless otherwise noted, partial derivatives are evaluated at the center of the $i_1 i_2 i_3$-th cell.

The estimator actually used in FLASH4's default refinement criterion is a modification of the above, as follows:

$$E_i = \frac{| u_{i+2} - 2u_i + u_{i-2} |}{| u_{i+2} - u_i | + | u_i - u_{i-2} | + \epsilon [| u_{i+2} | + 2 | u_i | + | u_{i-2} |]} , \tag{8.3}$$

where again u_i is the refinement test variable's value in the ith cell. The last term in the denominator of this expression acts as a filter, preventing refinement of small ripples, where ϵ is a small constant.

When extending this criterion to multidimensions, all cross derivatives are computed, and the following generalization of the above expression is used

$$E_{i_X i_Y i_Z} = \left\{ \frac{\sum_{pq} \left(\frac{\partial^2 u}{\partial x_p \partial x_q} \right)^2}{\sum_{pq} \left[\frac{1}{2\,\Delta x_q} \left(\left| \frac{\partial u}{\partial x_p} \right|_{i_q+1} + \left| \frac{\partial u}{\partial x_p} \right|_{i_q-1} \right) + \epsilon \frac{|\bar{u}_{pq}|}{\Delta x_p \Delta x_q} \right]^2} \right\}^{1/2} , \tag{8.4}$$

where again the sums are carried out over coordinate directions, where, unless otherwise noted, partial derivatives are actually finite-difference approximations evaluated at the center of the $i_X i_J i_K$-th cell, and $|\bar{u}_{pq}|$ stands for an *average* of the values of $|u|$ over several neighboring cells in the p and q directions.

The constant ϵ is by default given a value of 10^{-2}, and can be overridden through the refine_filter_# runtime parameters. Blocks are marked for refinement when the value of $E_{i_X i_Y i_Z}$ for any of the block's cells exceeds a threshold given by the runtime parameters refine_cutoff_#, where the number # matching the number of the refine_var_# runtime parameter selecting the refinement variable. Similarly, blocks are marked for derefinement when the values of $E_{i_X i_Y i_Z}$ for *all* of the block's cells lie below another threshold given by the runtime parameters derefine_cutoff_#.

Although PPM is formally second-order and its leading error terms scale as the third derivative, we have found the second derivative criterion to be very good at detecting discontinuities and sharp features in the flow variable u. When Particles (active or tracer) are being used in a simulation, their count in a block can also be used as a refinement criterion by setting refine_on_particle_count to true and setting max_particles_per_blk to the desired count.

8.6.3.2 Refinement Processing

Each processor decides when to refine or derefine its blocks by computing a user-defined error estimator for each block. Refinement involves creation of either zero or 2^d refined child blocks, while derefinement involves deletion of all of a parent's child blocks (2^d blocks). As child blocks are created, they are temporarily placed at the end of the processor's block list. After the refinements and derefinements are complete, the blocks are redistributed among the processors using a work-weighted Morton space-filling curve in a manner similar to that described by Warren and Salmon (1987) for a parallel treecode. An example of a Morton curve is shown in Figure 8.7.

During the distribution step, each block is assigned a weight which estimates the relative amount of time required to update the block. The Morton number of the block is then computed by interleaving the bits of its integer coordinates, as described by Warren and Salmon (1987). This reordering determines its location

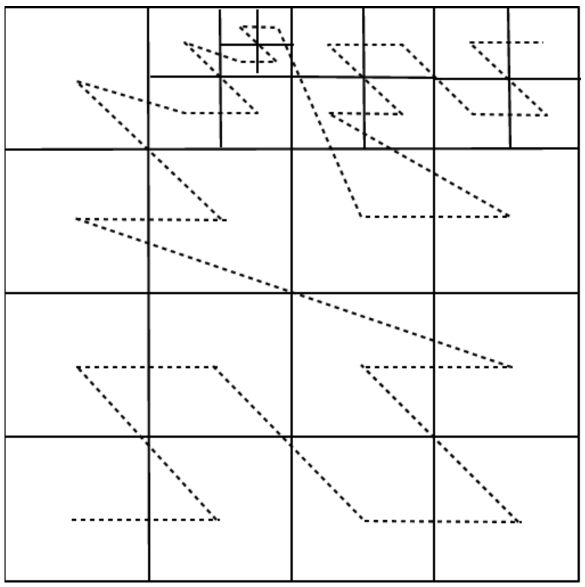

Figure 8.7: Morton space-filling curve for adaptive mesh grids.

along the space-filling curve. Finally, the list of all blocks is partitioned among the processors using the block weights, equalizing the estimated workload of each processor. By default, all leaf-blocks are weighted twice as heavily as all other blocks in the simulation.

8.6.3.3 Specialized Refinement Routines

Sometimes, it may be desirable to refine a particular region of the grid independent of the second derivative of the variables. This criterion might be, for example, to better resolve the flow at the boundaries of the domain, to refine a region where there is vigorous nuclear burning, or to better resolve some smooth initial condition. For curvilinear coordinates, regions around the coordinate origin or the polar z-axis may require special consideration for refinement. A collection of methods that can refine a (logically) rectangular region or a circular region in Cartesian coordinates, or can automatically refine by using some variable threshold, are available through the `Grid_markRefineSpecialized`. It is intended to be called from the `Grid_markRefineDerefine` routine. The interface works by allowing the calling routine to pick one of the routines in the suite through an integer argument. The calling routine is also expected to populate the data structure `specs` before making the call. A copy of the file `Grid_markRefineDerefine.F90` should be placed in the `Simulation` directory, and the interface file `Grid_interface.F90` should be used in the header of the function.

Warning

This collection of specialized refinement routines have had limited testing. The routine that refines in a specified region has been tested with some of the setups included in the release. All the other routines should be used mostly as guidelines for the user's code.

FLASH3.2 added additional support in the standard implementation of refinement routine `Grid_markRefineDerefine` for enforcing a maximum on refinement based on location or simulation time. These work by effectively lowering the absolute ceiling on refinement level represented by `lrefine_max`. See the following runtime parameters:

- `gr_lrefineMaxRedDoByLogR`

- gr_lrefineMaxRedRadiusFact
- gr_lrefineMaxRedDoByTime
- gr_lrefineMaxRedTimeScale
- gr_lrefineMaxRedTRef
- gr_lrefineMaxRedLogBase

8.7 Chombo

We have included an experimental Grid implementation which makes use of Chombo library in FLASH4. Since this is very much a work in progress it should not be considered as production grade yet. We expect new developments and improvement to happen at a rapid pace, so please contact us if you would like to use the latest snapshots of our Chombo integration in FLASH before our next major code release.

Most flash.par parameters relevant to the Grid unit will continue to work; the differences are described later in this section. There are some important restrictions to be aware of when using this Grid implementation.

- Only Cartesian geometries are handled.
- Only cell-centered solution variables are supported, i.e. those variables defined with keywords VARIABLE and SCRATCHCENTERVAR in Config files.

FLASH does not include the source code for Chombo library and so Chombo must be independently downloaded and then built using the instructions given in Section 5.9. Please also see the restrictions in Hydro Section 14.1.5 and I/O Section 9.12.

Our integration of FLASH with Chombo is slightly unusual because we do not use the higher-level Chombo classes for solving time-dependent problems on an AMR mesh. The reason is that these higher level classes also "drive" the simulation, that is, control the initialization and evolution of simulations. These are tasks that already happen in a FLASH application in the Driver unit. Our approach is therefore to use the lower-level Chombo classes so that Chombo library is only responsible for Grid related tasks.

The actual patch-based mesh is allocated and managed in Chombo library. Each individual patch is stored in contiguous memory locations with the slowest varying dimension being the solution variable. This has allowed us to create a Grid_getBlkPtr that builds a 4D Fortran pointer object from the memory address of the first element of a specified patch. The patch is treated as a standard FLASH block in the physics units of FLASH. The Grid unit obtains the memory address and other metadata such as patch size, coordinates, index limits, cell spacing and refinement level through non-decorated C++ function calls which query Chombo objects.

8.7.1 Using Chombo in a UG configuration

This is a Grid implementation that operates in the same way as the standard FLASH uniform grid mode in which there is one block per MPI process. The parameters accepted are identical to those described for a non fixed blocksize uniform grid in Section 8.5.2. The only difference is that the checkpoint file is written in Chombo file layout rather than FLASH file layout. Setup a simulation using:

```
./setup Sedov -auto +chombo_ug -parfile=test_chombo_ug_2d.par
```

8.7.2 Using Chombo in a AMR configuration

The real motivation for integrating Chombo into FLASH is for its adaptive mesh which is patch-based rather than an oct-tree like Paramesh. It has several desirable features including:

- refinement can happen cell-by-cell rather than block-by-block.

- blocks (or patches in Chombo terminology) are not limited to a fixed number of cells.
- refinement jumps of greater than 2 can happen between neighboring blocks.

A major difference in the generated meshes is that there is no longer the concept of "LEAF" blocks which cover the global domain. This was useful in Paramesh because a union of the space covered by the children of a block cover is exactly equal to the space covered by the parent block. It is therefore possible to evolve solution only on leaf blocks. Such complete overlap is not guaranteed in Chombo, in fact it rarely happens. Therefore, to be compatible with Chombo, physics units must evolve a solution on all blocks. For reference, the LEAF definition in Flash.h for FLASH-Chombo application now means all blocks.

A FLASH application with Chombo uses the refinement criteria similar to the one described in Section 8.6.3. The slight modification is that the $i_X i_Y i_Z$-th cell is tagged when $E_{i_X i_Y i_Z}$ exceeds a threshold value. Recall that in the Paramesh, the entire block is tagged for refinement when the error estimator of *any* of cells within a block exceeds a given threshold. As a further extension to this cell tagging procedure we also tag all cells within a small radius of a given tagged cell. The tagging radius is set using the runtime parameter tagradius; a value of 1 means that 1 cell to the left and right of a tagged cell in each dimension is also tagged. Values below the default value of 2 may cause problems because of introduction of fine-coarse interfaces in regions of the domain where there are steep gradients. For example, a Sod problem does not converge in Riemann solver when the value is 0.

The runtime parameters are described below:

- **lrefine_max** Used in an identical way to Paramesh. It is still a unit-based parameter and not zero-based. Defaults to 1.
- **igridsize,jgridsize,kgridsize** The global number of cells on the coarsest level of the adaptive mesh. Varying igridsize gives the same level of control as the unused Paramesh parameters lrefine_min and nblockx. Defaults to 16.
- **maxBlockSize** The maximum number of cells along a single dimension of a block. Defaults to 16.
- **BRMeshRefineBlockFactor** The minimum number of cells along a single dimension of a block. See BRMeshRefine class in Chombo user-guide. Defaults to 8.
- **BRMeshRefineFillRatio** Overall grid efficiency to be generated. If this number is set low, the grids will tend to be larger and less filled with tags. If this number is set high, the grids will tend to be smaller and more filled with tags. See BRMeshRefine class in Chombo user-guide. Defaults to 0.75.
- **BRMeshRefineBufferSize** Proper nesting buffer size. This will be the minimum number of level l cells between any level l+1 cell and a level l-1 cell. See BRMeshRefine class in Chombo user-guide. Defaults to 1.
- **verbosity** The verbosity of debugging output written to local log files - higher values mean progressively more debugging output. As a rough guide 0 means no debugging output, 2 means debugging output from FLASH objects, and values above 2 add debugging output from Chombo objects. Defaults to 0.
- **refRatio** The refinement jump between fine-coarse levels, typically 2, 4 or 8. Defaults to 2.
- **restrictBeforeGhostExchange** Invokes a full mesh restriction before guard cells are exchanged. This is to make the guard cell exchange behave the same way as Paramesh guard cell exchange. We do not know yet if it is necessary. Defaults to True.
- **tagRadius** The radius of cells around a tagged cell that should also be tagged. Defaults to 2.

Set convertToConsvdForMeshCalls runtime parameter to .true. to interpolate mass specific solution variables (see Section 8.6.2.1). We have not yet added code for convertToConsvdInMeshInterp runtime parameter and so it should not be used.

Setup a simulation using:

```
./setup Sedov -auto +chombo_amr -parfile=test_chombo_amr_2d.par
```

The GridParticles and GridSolvers sub-unit do not interoperate with Chombo yet.

8.8 GridMain Usage

The `Grid` unit has the largest API of all units, since it is the custodian of the bulk of the simulation data, and is responsible for most of the code housekeeping. The `Grid_init` routine, like all other `Unit_init` routines, collects the runtime parameters needed by the unit and stores values in the data module. If using UG, the `Grid_init` also creates the computational domain and the housekeeping data structures and initializes them. If using AMR, the computational domain is created by the `Grid_initDomain` routine, which also makes a call to mesh package's own initialization routine. The physical variables are all owned by the `Grid` unit, and it initializes them by calling the `Simulation_initBlock` routine which applies the specified initial conditions to the domain. If using an adaptive grid, the initialization routine also goes through a few refinement iterations to bring the grid to desired initial resolution, and then applies the `Eos` function to bring all simulation variables to thermodynamic equilibrium. Even though the mesh-based variables are under `Grid`'s control, all the physics units can operate on and modify them.

A suite of `get/put` accessor/mutator functions allows the calling unit to fetch or send data by the block. One option is to get a pointer `Grid_getBlkPtr`, which gives unrestricted access to the whole block and the client unit can modify the data as needed. The more conservative but slower option is to get some portion of the block data, make a local copy, operate on and modify the local copy and then send the data back through the "put" functions. The `Grid` interface allows the client units to fetch the whole block (`Grid_getBlkData`), a partial or full plane from a block (`Grid_getPlaneData`), a partial or full row (`Grid_getRowData`), or a single point (`Grid_getPointData`). Corresponding "put" functions allow the data to be sent back to the `Grid` unit after the calling routine has operated on it. Various `getData` functions can also be used to fetch some derived quantities such as the cell volume or face area of individual cells or groups of cells. There are several other accessor functions available to query the housekeeping information from the grid. For example `Grid_getListOfBlocks` returns a list of blocks that meet the specified criterion such as being "LEAF" blocks in `PARAMESH`, or residing on the physical boundary.

FLASH Transition

The `Grid_getBlkData` and `Grid_putBlkData` functions replace the `dBaseGetData` and `dBasePutData` functions in FLASH2. The bulk of the dBase functionality from FLASH2 is now handled by the `Grid` unit. For example, the global mesh data structures "`unk`" and "`tree`" now belong to `Grid`, and any information about them is queried from it. However, `dBase` and `Grid` are not identical. `dBase` was a central storage for all data, whereas in FLASH4 some of the data, such as simulation parameters like `dt` and simulation time are owned by the `Driver` unit instead of the `Grid` unit.

FLASH Transition

In FLASH2, variables *nxb*, *nyb* and *nzb* traditionally described blocksize. From FLASH3 on, the symbols `NXB`, `NYB`, and `NYB` are intended not to be used directly except in the `Grid` unit itself. The variables like `iHi_gc` and `iHi` *etc.* that marked the endpoints of the blocks were replaced in FLASH3 with in their new incarnation (`GRID_IHI_GC` *etc.*) Again, these new variables are used only in sizing arrays in declaration headers. Even when they are used for array sizing, they are enclosed in preprocessor blocks that can be eliminated at compile time. This separation was done to compartmentalize the FLASH3 code. The grid layout is not required to be known in any other unit (with the exception of `IO`). FLASH3 provides an API function `Grid_getBlkIndexLimits` that fetches the block endpoints from the `Grid` unit for each individual block. The fetched values are then used as `do` loop end points in all $\langle i, j, k \rangle$ loops in all the client units. When working in `NONFIXEDBLOCKSIZE` mode, the same fetched values are also used to size and allocate arrays. We have retained `GRID_IHI_GC` *etc.* for array sizing as compile time option for performance reasons. Statically allocated arrays allow better compiler optimization.

In addition to the functions to access the data, the `Grid` unit also provides a collection of routines that drive some housekeeping functions of the grid without explicitly fetching any data. A good example of such routines is `Grid_fillGuardCells`. Here no data transaction takes place between `Grid` and the calling unit. The calling unit simply instructs the `Grid` unit that it is ready for the guard cells to be updated, and doesn't concern itself with the details. The `Grid_fillGuardCells` routine makes sure that all the blocks get the right data in their guardcells from their neighbors, whether they are at the same, lower or higher resolution, and if instructed by the calling routine, also ensures that `EOS` is applied to them.

In large-scale, highly parallel FLASH simulations with AMR, the processing of `Grid_fillGuardCells` calls may take up a significant part of available resource like CPU time, communication bandwidth, and buffer space. It can therefore be important to optimize these calls in particular. From FLASH3.1, `Grid_fillGuardCells` provides ways to

- operate on only a subset of the variables in `unk` (and `facevarx`, `facevary`, and `facevarz`), by masking out other variables;
- fill only some the `nguard` layers of guard cells that surround the interior of a block (while possibly excepting a "sweep" direction);
- combine guard cell filling with EOS calls (which often follow guard cell exchanges in the normal flow of execution of a simulation in order to ensure thermodynamical consistency in all cells, and which may also be very expensive), by letting `Grid_fillGuardCells` make the calls on cells where necessary;
- automatically determine masks and whether to call EOS, based on the set of variables that the calling code actually needs updated. by masking out other variables.

These options are controlled by `OPTIONAL` arguments, see `Grid_fillGuardCells` for documentation. When these optional arguments are absent or when a `Grid` implementation does not support them, FLASH falls back to safe default behavior which may, however, be needlessly expensive.

Another routine that may change the global state of the grid is `Grid_updateRefinement`. This function is called when the client unit wishes to update the grid's resolution. again, the calling unit does not need to know any of the details of the refinement process.

FLASH Transition

As mentioned in Chapter 4, FLASH allows every unit to identify scalar variables for checkpointing. In the `Grid` unit, the function that takes care of consolidating user specified checkpoint variable is `Grid_sendOutputData`. Users can select their own variables to checkpoint by including an implementation of this function specific to their requirements in their Simulation setup directory.

8.9 GridParticles

FLASH is primarily an Eulerian code, however, there is support for tracing the flow using Lagrangian particles. In FLASH4 we have generalized the interfaces in the Lagrangian framework of the Grid unit in such a way that it can also be used for miscellaneous non-Eulerian data such as tracing the path of a ray through the domain, or tracking the motion of solid bodies immersed in the fluid. FLASH also uses active particles with mass in cosmological simulations, and charged particles in a hybrid PIC solver. Each particle has an associated data structure, which contains fields such as its physical position and velocity, and relevant physical attributes such as mass or field values in active particles. Depending upon the time advance method, there may be other fields to store intermediate values. Also, depending upon the requirements of the simulation, other physical variables such as temperature *etc.* may be added to the data structure. The `GridParticles` subunit of the `Grid` unit has two sub-subunits of its own. The `GridParticlesMove` sub-subunit moves the data structures associated with individual particles when the particles move between blocks; the actual movement of the particles through time advancement is the responsibility of the `Particles`

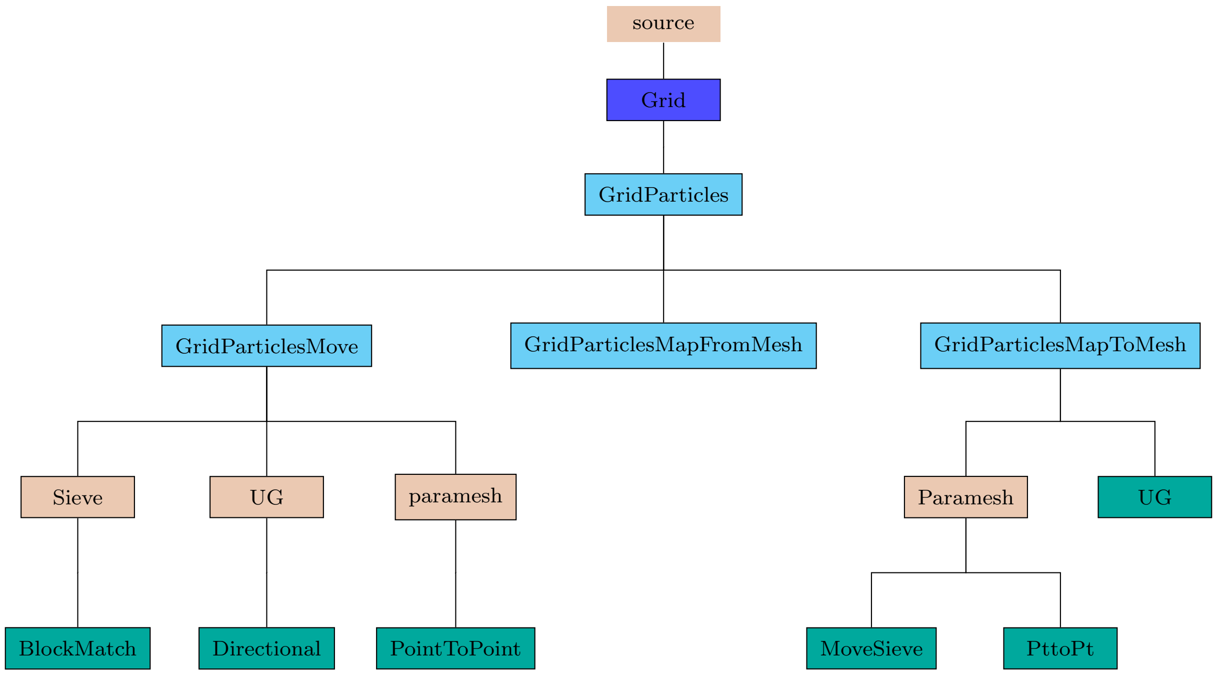

Figure 8.8: The `Grid` unit: structure of `GridParticles` subunit.

unit. Particles move from one block to another when their time advance places them outside their current block. In AMR, the particles can also change their block through the process of refinement and derefinement. The `GridParticlesMap` sub-subunit provides mapping between particles data and the mesh variables. The mesh variables are either cell-centered or face-centered, whereas a particle's position could be anywhere in the cell. The `GridParticlesMap` sub-subunit calculates the particle's properties at its position from the corresponding mesh variable values in the appropriate cell . When using active particles, this sub-subunit also maps the mass of the particles onto the specified mesh variable in appropriate cells. The next sections describe the algorithms for moving and mapping particles data.

8.9.1 GridParticlesMove

FLASH4 has implementations of three different parallel algorithms for moving the particles data when they are displaced from their current block. FLASH3 had an additional algorithm, `Perfect Tree Level` which made use of the oct-tree structure. However, because in all performance experiments it performed significantly worse than the other two algorithms, it is not supported currently in FLASH4. The simplest algorithm, `Directional algorithm` is applicable only to the uniform grid when it is configured with one block per processor. This algorithm uses directional movement of data, and is easy because the directional neighbors are trivially known. The movement of particles data is much more challenging with AMR even when the grid is not refining. Since the blocks are at various levels of refinement at any given moment, a block may have more than one neighbor along one or more of its faces. The distribution of blocks based on space-filling curve is an added complication since the neighboring blocks along a face may reside at a non-neighboring processor The remaining two algorithmss included in FLASH4 implement `GridParticlesMove` subunit for the adaptive mesh; `Point to Point` and `Sieve`, of which only the `Sieve` algorithm is able to move the data when the mesh refines. Thus even when a user opts for the `PointToPoint` implementation for moving particles with time evolution, some part of the `Sieve` implementation must necessarily be included to successfully move the data upon refinement.

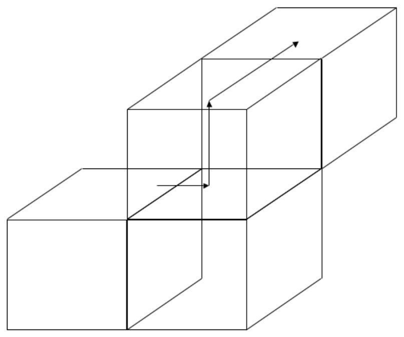

Figure 8.9: Moving one particle to a neighbor on the corner.

8.9.1.1 Directional Move

The Directional Move algorithm for moving particles in a Uniform Grid minimizes the number of communication steps instead of minimizing the volume of data moved. Its implementation has the following steps:

1. Scan particle positions. Place all particles with their x coordinate value greater than the block bounding box in the Rightmove bin, and place those with x coordinate less than block bounding box in Leftmove bin.
2. Exchange contents of Rightbin with the right block neighbor's Leftbin contents, and those of the Leftbin with left neightbor's Rightbin contents.
3. Merge newly arrived particles from step 2 with those which did not move outside their original block.
4. Repeat steps 1-3 for the y direction.
5. Repeat step 1-2 for the z direaction.

At the end of these steps, all particles will have reached their destination blocks, including those that move to a neighbor on the corner. Figure 8.9 illustrates the steps in getting a particle to its correct destination.

8.9.1.2 Point To Point Algorithm

As a part of the data cached by Paramesh, there is wealth of information about the neighborhood of all the blocks on a processor. This information includes the processor and block number of all neighbors (face and corners) if they are at the same refinement level. If those neighbors are at lower refinement level, then the neighbor block is in reality the current block's parent's neighbor, and the parent's neighborhood information is part of the cached data. Similarly, if the neighbor is at a higher resolution then the current blocks neighbor is in reality the parent of the neighbor. The parent's metadata is also cached, from which information about all of its children can be derived. Thus it is possible to determine the processor and block number of the destination block for each particle. The PointToPoint implementation finds out the destinations for every particles that is getting displaced from its block. Particles going to local destination blocks are moved first. The remaining particles are sorted based on their destination processor number, followed by a couple of global operations that allow every processor to determine the number of particles it is expected to receive from all of the other processors. A processor then posts asynchronous receives for every source processor that had at least one particle to send to it. In the next step, the processor cycles through the sorted list of particles and sends them to the appropriate destinations using synchronous mode of communition.

8.9.1.3 Sieve Algorithm

The `Sieve` algorithm does not concern itself with the configuration of the underlying mesh at any time. It also does not distinguish between data movements due to time evolution or regridding, and is therefore the only usable implementation when the particles are displaced as a consequence of mesh refinement. The sieve implementation works with two bins, one collects particles that have to be moved off-processor, and the other receives particles sent to it by other processors. The following steps broadly describe the algorithm:

1. For each particle, find if its current position is on the current block
2. If not, find if its current position is on another block on the same processor. If it is move the particle to that block, otherwise put it in the send bin.
3. Send contents of the send bin to the designated neighbor, and receive contents of another neighbor's send bin into my receive bin.
4. Repeat step 2 on the contents of the receive bin, and step 3 until all particles are at their destination.
5. For every instance of step 3, the designated send and receive neighbors are different from any of the previous steps.

In this implementation, the trick is to use an algorithm to determine neighbors in such a way that all the particles reach their destination in minimal number of hops. Using $MyPE + n * (-1)^{n+1}$ as the destination processor and $MyPE + n * (-1)^{n}$ as the source processor in modulo *numProcs* arithmetic meets the requirements. Here $MyPE$ is the local processor number and *numProcs* is the number of processors.

8.9.2 GridParticlesMapToMesh

FLASH4 provides support for particles that can experience forces and contribute to the problem dynamics. These are termed *active* particles, and are described in detail in Chapter 20. As these particles may move independently of fluid flow, it is necessary to update the grid by mapping an attribute of the particles to the cells of the grid. We use these routines, for example, during the PM method to assign the particles' mass to the particle density solution variable `pden`. The hybrid PIC method uses its own variation for mapping appropriate physical quantities to the mesh.

In general the mapping is performed using the grid routines in the `GridParticlesMapToMesh` directory and the particle routines in the `ParticlesMapping` directory. Here, the particle subroutines map the particles' attribute into a temporary array which is independent of the current state of the grid, and the grid subroutines accumulate the mapping from the array into valid cells of the computational domain. This means the grid subroutines accumulate the data according to the grid block layout, the block refinement details, and the simulation boundary conditions. As these details are closely tied with the underlying grid, there are separate implementations of the grid mapping routines for UG and `PARAMESH` simulations.

The implementations are required to communicate information in a relatively non-standard way. Generally, domain decomposition parallel programs do not write to the guard cells of a block, and only use the guard cells to represent a sufficient section of the domain for the current calculation. To repeat the calculation for the next time step, the values in the guard cells are refreshed by taking updated values from the internal section of the relevant block. In FLASH4, `PARAMESH` refreshes the values in the guard cells automatically, and when instructed by a `Grid_fillGuardCells` call.

In contrast, the guard cell values are mutable in the particle mapping problem. Here, it is possible that a portion of the particle's attribute is accumulated in a guard cell which represents an internal cell of another block. This means the value in the updated guard cell must be communicated to the appropriate block. Unfortunately, the mechanism to communicate information in this direction is not provided by `PARAMESH` or UG grid. As such, the relevant communication is performed within the grid mapping subroutines directly.

In both `PARAMESH` and UG implementations, the particles' attribute is "smeared" across a temporary array by the generic particle mapping subroutine. Here, the temporary array represents a single leaf block from the local processor. In simulations using the `PARAMESH` grid, the temporary array represents each LEAF block from the local processor in turn. We assign a particle's attribute to the temporary array when that particle exists in the same space as the current leaf block. For details about the attribute assignment schemes available to the particle mapping sub-unit, please refer to Section 20.2.

After particle assignment, the `Grid` sub-unit applies simulation boundary conditions to those temporary arrays that represent blocks next to external boundaries. This may change the quantity and location of particle assignment in the elements of the temporary array. The final step in the process involves accumulating values from the temporary array into the correct cells of the computational domain. As mentioned previously, there are different strategies for UG and `PARAMESH` grids, which are described in Section 8.9.2.1 and Section 8.9.2.2, respectively.

FLASH Transition

The particle mapping routines can be run in a custom debug mode which can help spot data errors (and even detect possible bugs). In this mode we inspect data for inconsistencies. To use, append the following line to the setup script:

```
-defines=DEBUG_GRIDMAPPARTICLES
```

8.9.2.1 Uniform Grid

The Uniform Grid algorithm for accumulating particles' attribute on the grid is similar to the particle redistribution algorithm described in Section 8.9.1.1. We once again apply the concept of directional movement to minimize the number of communication steps:

1. Take the accumulated temporary array and iterate over all elements that correspond to the x-axis guard cells of the low block face. If a guard cell has been updated, determine its position in the neighboring block of the low block face. Copy the guard cell value and a value which encodes the destination cell into the send buffer.

2. Send the buffer to the low-side processor, and receive a buffer from the high-side processor. For processors next to a domain boundary assume periodic conditions because all processors must participate. If the simulation does not have periodic boundary conditions, there is still periodic communication at the boundaries, but the send buffers do not contain data.

3. Iterate over the elements in the receive buffer and accumulate the values into the local temporary array at the designated cells. It is possible to accumulate values in cells that represent internal cells and guard cells. A value accumulated in a guard cell will be repacked into the send buffer during the next directional (y or z) sweep.

4. Repeat steps 1-3 for the high block face.

5. Repeat steps 1-4 for the y-axis, and then the z-axis.

When the guard cell's value is packed into the send buffer, a single value is also packed which is a 1-dimensional representation of the destination cell's N-dimensional position. The value is obtained by using an array equation similar to that used by a compiler when mapping an array into contiguous memory. The receiving processor applies a reverse array equation to translate the value into N-dimensional space. The use of this communication protocol is designed to minimize the message size.

At the end of communication, each local temporary buffer contains accumulated values from guard cells of another block. The temporary buffer is then copied into the solution array.

8.9.2.2 Paramesh Grid

There are two implementations of the AMR algorithms for accumulating particles' attribute on the grid. They are inspired by a particle redistribution algorithms `Sieve` and `Point to Point` described in Section 8.9.1.3 and Section 8.9.1.2 respectively.

The `MoveSieve` implementation of the mapping algorithm uses the same back and forth communication pattern as `Sieve` to minimize the number of message exchanges. That is, processor $MyPE$ sends to $MyPE + n * (-1)^{n+1}$ and receives from $MyPE + n * (-1)^n$, where, $MyPE$ is the local processor number and n is the count of the buffer exchange round. As such, this communication pattern involves a processor exchanging data with its nearest neighbor processors first. This is appropriate here because the block distribution generated by the space filling curve should be high in data locality, *i.e.*, nearest neighbor blocks should be placed on the same processor or nearest neighbor processors.

Similarly, the `Point to Point` implementation of the mapping algorithm exploits the cached neighborhood knowledge, and uses a judicious combination of global communications with asynchronous receives and synchronous sends, as described in Section 8.9.1.2. Other than their communication patterns, the two implementations are very similar as described below.

1. Accumulate the temporary array values into the central section of the corresponding leaf block.
2. Divide the leaf block guard cells into guard cell regions. Determine whether the neighbor(s) to a particular guard cell region exist on the same processor.
3. If a neighbor exists on the same processor, the temporary array values are accumulated into the central cells of that leaf block. If the neighbor exists off processor, all temporary array values corresponding to a single guard cell region are copied into a send buffer. Metadata is also packed into the send buffer which describes the destination of the updated values.
4. Repeat steps 1-3 for each leaf block.
5. Carry out data exchange with off-processor destinations as described in the Section 8.9.1.3 or Section 8.9.1.2

The guard cell region decomposition described in Step 2 is illustrated in Figure 8.10. Here, the clear regions correspond to guard cells and the gray region corresponds to internal cells. Each guard cell region contains cells which correspond to the internal cells of a single neighboring block at the same refinement.

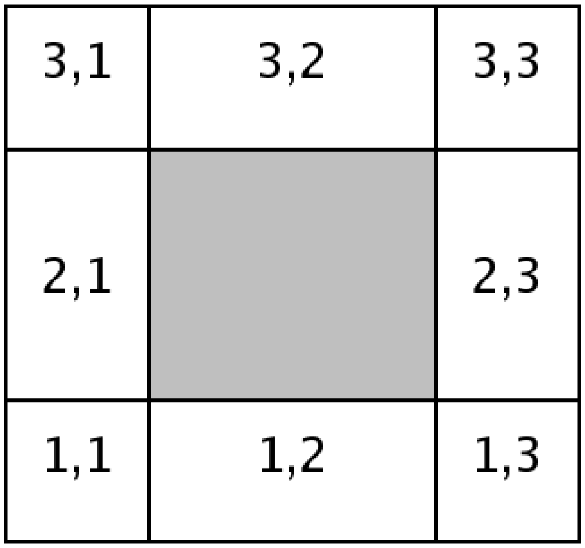

Figure 8.10: A single 2-D block showing how guard cells are divided into regions.

We use this decomposition as it makes it possible to query public `PARAMESH` data structures which contain the block and process identifier of the neighboring block at the same refinement. However, at times this is not enough information for finding the block neighbor(s) in a refined grid. We therefore categorize neighboring blocks as: Existing on the same processor, existing on another processor and the block and process ID are known, and existing on another processor and the block and process ID are unknown. If the block and process identifier are unknown we use the FLASH4 corner ID. This is a viable alternative as the corner ID of a neighboring block can always be determined.

The search process also identifies the refinement level of the neighboring block(s). This is important as the guard cell values cannot be directly accumulated into the internal cells of another block if the blocks are at a different refinement levels. Instead the values must be operated on in processes known as restriction and prolongation (see Section 8.6.2). We perform these operations directly in the `GridParticlesMapToMesh` routines, and use quadratic interpolation during prolongation.

Guard cell data is accumulated in blocks existing on the same processor, or packed into a send buffer ready for communication. When packed into the send buffer, we keep values belonging to the same guard cell region together. This enables us to describe a whole region of guard cell data by a small amount of metadata. The metadata consists of: Destination block ID, destination processor ID, block refinement level difference, destination block corner ID (IAXIS, JAXIS, KAXIS) and start and end coordinates of destination cells (IAXIS, JAXIS, KAXIS). This is a valid technique because there are no gaps in the guard cell region, and is sufficient information for a receiving processor to unpack the guard cell data correctly.

We size the send / receive buffers according to the amount of data that needs to be communicated between processors. This is dependent upon how the `PARAMESH` library distributes blocks to processors. Therefore, in order to size the communication buffers economically, we calculate the number of guard cells that will accumulate on blocks belonging to another processor. This involves iterating over every single guard cell region, and keeping a running total of the number of off-processor guard cells. This total is added to the metadata total to give the size of the send buffer required on each processor. We use the maximum of the send buffer size across all processors as the local size for the send / receive buffer. Choosing the maximum possible size prevents possible buffer overflow when an intermediate processor passes data onto another processor.

After the point to point communication in step 6, the receiving processor scans the destination processor identifier contained in each metadata block. If the data belongs to this processor it is unpacked and accumulated into the central cells of the relevant leaf block. As mentioned earlier, it is possible that some guard cell sections do not have the block and processor identifier. When this happens, the receiving processor attempts to find the same corner ID in one of its blocks by performing a linear search over each of its leaf blocks. Should there be a match, the guard cells are copied into the matched block. If there is no match, the guard cells are copied from the receive buffer into the send buffer, along with any guard cell region explicitly designated for another processor. The packing and unpacking will continue until all send buffers are empty, as indicated by the result of the collective communication.

It may seem that the algorithm is unnecessarily complicated, however, it is the only viable algorithm when the block and process identifiers of the nearest block neighbors are unknown. This is the situation in FLASH3.0, in which some data describing block and process identifiers are yet to be extracted from `PARAMESH`. As an aside, this is different to the strategy used in FLASH2, in which the entire `PARAMESH` tree structure was copied onto each processor. Keeping a local copy of the entire `PARAMESH` tree structure on each processor is an unscalable approach because increase in the levels of resolution increases the meta-data memory overhead, which restricts the size of active particle simulations. Therefore, Point to Point method is a better option for larger simulations, and significantly, simulations that run on massively parallel processing (MPP) hardware architectures.

In FLASH3.1 we added a routine which searches non-public `PARAMESH` data to obtain **all** neighboring block and process identifiers. This discovery greatly improves the particle mapping performance because we no longer need to perform local searches on each processor for blocks matching a particular corner ID.

As another consequence of this discovery, we are able to experiment with alternative mapping algorithms that require all block and process IDs. From FLASH3.1 on we also provide a non-blocking point to point implementation in which off-processor cells are sent directly to the appropriate processor. Here, processors receive messages at incremented positions along a data buffer. These messages can be received in any order, and their position in the data buffer can change from run to run. This is very significant because the mass accumulation on a particular cell can occur in any order, and therefore can result in machine precision discrepancies. Please be aware that this can actually lead to slight variations in end-results between two runs of the exact same simulation.

8.10 GridSolvers

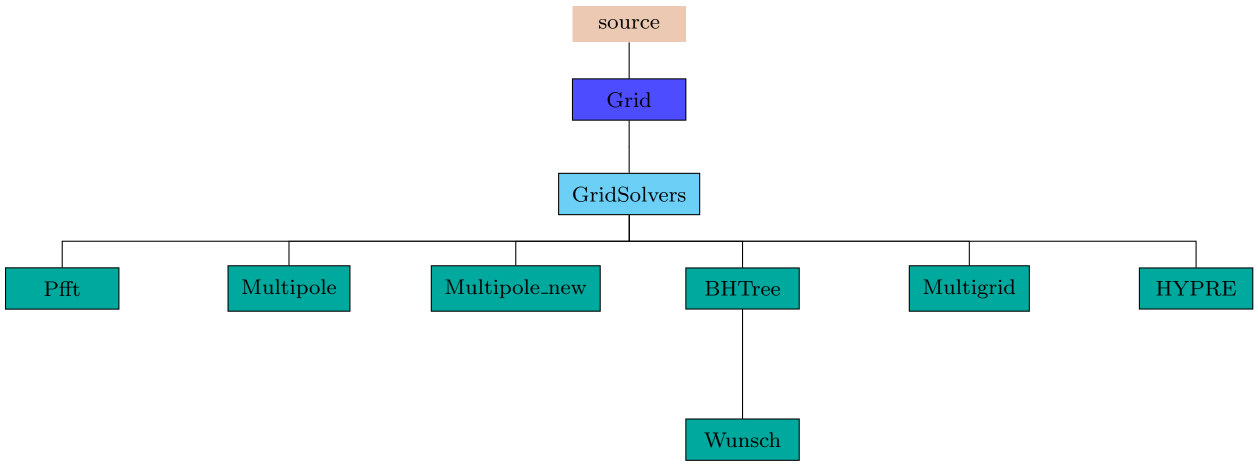

Figure 8.11: The `Grid` unit: structure of `GridSolvers` subunit.

The `GridSolvers` unit groups together subunits that are used to solve particular types of differential equations. Currently, there are two types of solvers: a parallel Fast Fourier Transform package (Section 8.10.1) and various solvers for the Poisson equation (Section 8.10.2).

8.10.1 Pfft

`Pfft` is a parallel frame work for computing a Fast Fourier Transform (FFT) on uniform grids. It can also be combined with the Multigrid solver described below in Section 8.10.2.6 to let the composite solver scale to thousands of processors.

`Pfft` has a layered architecture where the lower layer contains functions implementing basic tasks and primary data structures. The upper layer combines pieces from the lowest layer to interface with FLASH and create the parallel transforms. The computational part of `Pfft` is handled by sequential 1-dimensional FFT's, which can be from a native, vendor supplied scientific library, or from public domain packages. The current distribution of FLASH uses `fftpack` from NCAR for the 1-D FFTs, since that package also contains transforms that are useful with non-periodic boundary conditions.

The lowest layer has three distinct components. The first component redistributes data. It includes routines for distributed transposes for two and three dimensional data. The second component provides a uniform interface for FFT calls to hide the details of individual libraries. The third component is the data structures. There are global data structures to keep track of the type of transform, number of data dimensions, and physical and transform space information about each dimension. The dimensional information includes the start and end point of data (useful when the dimension is spread over more than one processor), the MPI communicator, the coordinates of the node in the processor grid etc. The structures also include pointers to the trigonometric tables and work space needed by the sequential FFT calls.

The upper layer of PFFT combines the lower layer routines to create end-to-end transforms in a variety of ways. The available one dimensional transforms include real-to-complex, complex-to-complex, sine and cosine transforms. They can be combined to create two or three dimensional tranforms for different configuration of the domain. The two dimensional transforms support parallelization of one dimension (or a one dimensional grid of processors). The three dimensional transforms support one or two dimensional grid of processors. All transforms must have at least one dimension within the processor at all times. The data distribution changes during the computation. However, a complete cycle of forward and inverse transform restores the data distribution.

The computation of a forward three dimensional FFT in parallel involves following steps :

1. Compute 1-D transforms along **x**.

2. Reorder, or transpose from **x-y-z** to **y-z-x**
3. Compute 1-D transforms along **y**. If the transform along **x** was real-to-complex, this one must be a complex-to-complex transform.
4. Transpose from **y-z-x** to **z-x-y**
5. Compute 1-D FFTs along **z**. If the transform along **x** or **y** was real-to-complex, this must be a complex-to-complex transform.

The inverse transform can be computed by carrying out the steps described above in reverse order. The more commonly used domain decomposition in FFT based codes assumes a one dimensional processor grid:

$$N_1 \times N_2 \times N_3 / P, \tag{8.5}$$

where $N_1 \times N_2 \times N_3$ is the global data size and P is the number of processors. Here, the first transpose is local, while the second one is distributed. The internode communication is limited to one distributed transpose involving all the processors. However, there are two distinct disadvantages of this distribution of work:

- The size of the problem imposes an upper limit on the number of processors, in that the largest individual dimension is also the largest number of active processors. A three dimensional problem is forced to have modest individual dimensions to fit in the processor memory.
- As the machine size grows, the internode exchanges become long range, and the possibility of contention grows.

We have chosen a domain decomposition where each subdomain is a column of size

$$\begin{gathered} N_1 \times N_2/P_1 \times N_3/P_2 \\ P = P_1 \times P_2. \end{gathered} \tag{8.6}$$

With this distribution both the transposes are distributed in parallel. The data exchange along any one processor grid dimension is a collection of disjointed distributed transposes. Here, the contention and communication range is reduced, while the volume of data exchange is unaltered. The distributed transposes are implemented using collective **MPI** operation **alltoall**. In a slabwise distribution, the upper limit on the number of processors is determined by the smallest of $< N_1, N_2, N_3 >$, where as in our distribution, the upper limit on the number of processors is the smallest of $< N_1 * N_2, N_2 * N_3, N_1 * N_3 >$.

8.10.1.1 Using `Pfft`

`Pfft` can only be used with a pencil grid, with the constraint that the number of processors along the `IAXIS` must be 1. This is because all one dimensional transforms are computed locally within a processor. However, FLASH contains a set of data movement subroutines that generate a usable pencil grid from any UG grid or any level of a PM grid. These routines are briefly explained in Section 8.10.1.2.

During the course of a simulation, `Pfft` can be used in two different modes. In the first mode, every instance of Pfft use will be exactly identical to every other instance in terms of domain size and the type of transforms. In this mode, the user can set the runtime parameter `pfft_setupOnce` to true, which enables the `FLASH` initialization process to also create and initialize all the data structures of `Pfft`. The finalization of the `Pfft` subunit is also done automatically by the `FLASH` shutdown process in this mode. However, if a simulation needs to use `Pfft` in different configurations at different instances of its use, then each set of calls to `Grid_pfft` for computing the transforms must be preceded by a call to `Grid_pfftInit` and followed by a call to `Grid_pfftFinalize`. In addition, the runtime parameter `pfft_setupOnce` should be set to false. A few other helper routines are available in the subunit to allow the user to query `Pfft` about the dimensioning of the domain, and also to map the Mesh variables from the `unk` array to and from `Pfft` compatible (single dimensional) arrays. `Pfft` also provides the location of wave numbers in the parallel domain; information that users can utilize to develop their own customized PDE solvers using FFT based techniques.

8.10.1.2 `Pfft` data movement subroutines

Mesh reconfiguration subroutines are available to generate a pencil grid for the `Pfft` unit from another mesh configuration. Two different implementations are available at `Grid/GridSolvers/Pfft/MeshReconfiguration/-PtToPt` and `Grid/GridSolvers/Pfft/MeshReconfiguration/Collective`, with the `PtToPt` implementation being the default. Both implementations are able to generate an appropriate pencil grid in UG and PM mode. The pencil processor grid is automatically selected, but can be overridden by passing optional arguments to `Grid_pfftInit`. In UG mode they are invoked when the number of processors in the `IAXIS` of the `FLASH` grid is greater than one, and in PM mode they are always invoked. In PM mode they generate a pencil grid from a single level of the AMR grid, which may be manually specified or automatically selected as the maximum level that is fully-refined (i.e. has blocks that completely cover the computational domain at this level).

The pencil grid processor topology is stored in an `MPI` communicator, and the communicator may contain fewer processors than are used in the simulation. This is to ensure the pencil grid points are never distributed too finely over the processors, and naturally handles the case where the user may wish to obtain a pencil grid at a very coarse level in the AMR grid. If there are more blocks than processors then we are safe to distribute the pencil grid over **all** processors, otherwise we must remove a number of processors. Currently, we eliminate those processors that own **zero** `FLASH` blocks at this level, as this is a simple calculation that can be computed locally.

Both mesh reconfiguration implementations generate a map describing the data movement before moving any grid data. The map is retained between calls to the `Pfft` routines and is only regenerated when the grid changes. This avoids repeating the same global communications, but means communication buffers are left allocated between calls to `Pfft`.

In the `Collective` implementation, the map coordinates are used to specify where the `FLASH` data is copied into a send communication buffer. Two `MPI_Alltoall` calls then move this data to the appropriate pencil processor at coordinates (J,K). Here, the first `MPI_Alltoall` moves data to processor (J,0), and the second `MPI_Alltoall` moves data to processor (J,K). The decision to use `MPI_Alltoalls` simplifies the `MPI` communication, but leads to very large send / receive communication buffers on each processor which consume:

```
Memory(bytes) = sizeof(REAL) * total grid points at solve level * 2
```

The `PtToPt` implementation consumes less memory compared to the `Collective` implementation, and communicates using point to point `MPI` messages. It is based upon using nodes in a linked list which contain metadata (a map) and a communication buffer for a single block fragment. There are two linked lists: one for the `FLASH` block fragments and one for `Pfft` block fragments. Metadata information about each `FLASH` block fragment is placed in separate messages and sent using `MPI_Isend` to the appropriate destination pencil grid processor.

Each destination pencil grid processor repeatedly invokes `MPI_Iprobe` using `MPI_ANY_SOURCE`, and creates a node in its `Pfft` list whenever it discovers a message. The `MPI` message is received into a metadata region of the freshly allocated node, and a communication buffer is also allocated according to the size specified in the metadata. The pencil processor continues probing for messages until the cumulative size of its node's communication buffers is equal to the pencil grid points it has been assigned. At this stage, grid data is communicated by traversing the `Pfft` list and posting `MPI_Irecvs`, and then traversing the `FLASH` list and sending block fragment using `MPI_Isends`. After performing `MPI_Waits`, the received data in the nodes of the `Pfft` list is copied into internal `Pfft` arrays.

Note, the linked list is constructed using an include file stored at `flashUtilities/datastructures/-linkedlist`. The file is named `ut_listMethods.includeF90` and is meant to be included in any `Fortran90` module to create lists with nodes of a user-defined type. Please see the README file, and the unit test example at `flashUtilities/datastructures/linkedlist/UnitTest`.

8.10.1.3 Unit Test

The unit test for Pfft solver solves the following equation:

$$\nabla^2(\mathbf{F}) = -13.0 * \cos 2x * \sin 3y \tag{8.7}$$

The simplest analytical solution of this equation assuming no constants is

$$F = \cos 2x * \sin 3y \tag{8.8}$$

We discretize the domain by assuming $xmin, ymin, zmin = 0$, and $xmax, ymax, zmax = 2\pi$. The equation satisfies periodic boundary conditions in this formulation and FFT based poisson solve techniques can be applied. In the unit test we initialize one variable of the solution data with the function F, and another one with the right hand side of (8.7). We compute the forward real-to-complex transform of the solution data variable that is initialized with the right hand side of (8.7). This variable is then divided by $({k_i}^2 + {k_j}^2 + {k_k}^2)$ where k_i, k_j and k_k are the wavenumbers at any point i,j,k in the domain. An inverse complex-to-real transform after the division should give the function F as result. Hence the unit test is considered successful if both the variables have matching values within the specified tolerance.

8.10.2 Poisson equation

The `GridSolvers` subunit contains several different algorithms for solving the general Poisson equation for a potential $\phi(\mathbf{x})$ given a source $\rho(\mathbf{x})$

$$\nabla^2 \phi(\mathbf{x}) = \alpha \rho(\mathbf{x}) \ . \tag{8.9}$$

Here α is a constant that depends upon the application. For example, when the gravitational Poisson equation is being solved, $\rho(\mathbf{x})$ is the mass density, $\phi(\mathbf{x})$ is the gravitational potential, and $\alpha = 4\pi G$, where G is Newton's gravitational constant.

8.10.2.1 Multipole Poisson solver (original version)

This section describes the multipole Poisson solver that has been included in all the past releases of FLASH. It is included in the current release also, however, certain limitations found in this solver lead to a new implementation described in Section 8.10.2.2. This version is retained in FLASH4, because the new version is missing the ability to treat a non-zero minimal radius for spherical geometries and the ability to specify a point mass contribution to the potential. This will be implemented for the next coming release.

The multipole Poisson solver is appropriate for spherical or nearly-spherical source distributions with isolated boundary conditions (Müller (1995)). It currently works in 1D and 2D spherical, 2D axisymmetric cylindrical (r, z), and 3D Cartesian and axisymmetric geometries. Because of the imposed symmetries, in the 1D spherical case, only the monopole term ($\ell = 0$) makes sense, while in the axisymmetric and 2D spherical cases, only the $m = 0$ moments are used (*i.e.*, the basis functions are Legendre polynomials).

The multipole algorithm consists of the following steps. First, find the center of mass $\mathbf{x}_{\rm cm}$

$$\mathbf{x}_{\rm cm} = \frac{\int d^3\mathbf{x}\, \mathbf{x} \rho(\mathbf{x})}{\int d^3\mathbf{x}\, \rho(\mathbf{x})} \ . \tag{8.10}$$

We will take $\mathbf{x}_{\rm cm}$ as our origin. In integral form, Poisson's ((8.9)) is

$$\phi(\mathbf{x}) = -\frac{\alpha}{4\pi} \int d^3\mathbf{x}' \, \frac{\rho(\mathbf{x}')}{|\mathbf{x} - \mathbf{x}'|} \ . \tag{8.11}$$

The Green's function for this equation satisfies the relationship

$$\frac{1}{|\mathbf{x} - \mathbf{x}'|} = 4\pi \sum_{\ell=0}^{\infty} \sum_{m=-\ell}^{\ell} \frac{1}{2\ell + 1} \frac{r_<^\ell}{r_>^{\ell+1}} Y_{\ell m}^*(\theta', \varphi') Y_{\ell m}(\theta, \varphi) \ , \tag{8.12}$$

where the components of $\mathbf{x}$ and $\mathbf{x}'$ are expressed in spherical coordinates (r, θ, φ) about $\mathbf{x}_{\rm cm}$, and

$$\begin{aligned} r_< &\equiv \min\{|\mathbf{x}|, |\mathbf{x}'|\} \\ r_> &\equiv \max\{|\mathbf{x}|, |\mathbf{x}'|\} \ . \end{aligned} \tag{8.13}$$

Here $Y_{\ell m}(\theta,\varphi)$ are the spherical harmonic functions

$$Y_{\ell m}(\theta,\varphi) \equiv (-1)^m \sqrt{\frac{2\ell+1}{4\pi}\frac{(\ell-m)!}{(\ell+m)!}} P_{\ell m}(\cos\theta) e^{im\varphi} \ . \tag{8.14}$$

$P_{\ell m}(x)$ are Legendre polynomials. Substituting (8.12) into (8.11), we obtain

$$\begin{aligned}\phi(\mathbf{x}) &= -\alpha \sum_{\ell=0}^{\infty}\sum_{m=-\ell}^{\ell} \frac{1}{2\ell+1}\Bigg\{ Y_{\ell m}(\theta,\varphi) \times \\ &\left[r^\ell \int_{r<r'} d^3\mathbf{x}' \frac{\rho(\mathbf{x}')Y^*_{\ell m}(\theta',\varphi')}{r'^{\ell+1}} + \frac{1}{r^{\ell+1}} \int_{r>r'} d^3\mathbf{x}' \rho(\mathbf{x}') Y^*_{\ell m}(\theta',\varphi') r'^{\ell} \right]\Bigg\} \ .\end{aligned} \tag{8.15}$$

In practice, we carry out the first summation up to some limiting multipole $\ell_{\max}$. By taking spherical harmonic expansions about the center of mass, we ensure that the expansions are dominated by low-multipole terms, so that for a given value of $\ell_{\max}$, the error created by neglecting high-multipole terms is minimized. Note that the product of spherical harmonics in (8.15) is real-valued

$$\begin{aligned}\sum_{m=-\ell}^{\ell} Y^*_{\ell m}(\theta',\varphi') Y_{\ell m}(\theta,\varphi) &= \frac{2\ell+1}{4\pi}\Bigg[P_{\ell 0}(\cos\theta)P_{\ell 0}(\cos\theta') + \\ & 2\sum_{m=1}^{\ell} \frac{(\ell-m)!}{(\ell+m)!} P_{\ell m}(\cos\theta) P_{\ell m}(\cos\theta') \cos\left(m(\varphi-\varphi')\right)\Bigg] \ .\end{aligned} \tag{8.16}$$

Using a trigonometric identity to split up the last cosine in this expression and substituting for the inner sums in (8.15), we obtain

$$\begin{aligned}\phi(\mathbf{x}) &= -\frac{\alpha}{4\pi}\sum_{\ell=0}^{\infty} P_{\ell 0}(\cos\theta)\left[r^\ell \mu^{\rm eo}_{\ell 0}(r) + \frac{1}{r^{\ell+1}}\mu^{\rm ei}_{\ell 0}(r)\right] - \\ & \frac{\alpha}{2\pi}\sum_{\ell=1}^{\infty}\sum_{m=1}^{\ell} P_{\ell m}(\cos\theta)\Bigg[(r^\ell \cos m\varphi)\mu^{\rm eo}_{\ell m}(r) + (r^\ell \sin m\varphi)\mu^{\rm oo}_{\ell m}(r) + \\ & \frac{\cos m\varphi}{r^{\ell+1}}\mu^{\rm ei}_{\ell m}(r) + \frac{\sin m\varphi}{r^{\ell+1}}\mu^{\rm oi}_{\ell m}(r)\Bigg] \ .\end{aligned} \tag{8.17}$$

The even (e)/odd (o), inner (i)/outer (o) source moments in this expression are defined to be

$$\mu^{\rm ei}_{\ell m}(r) \equiv \frac{(\ell-m)!}{(\ell+m)!}\int_{r>r'} d^3\mathbf{x}'\, r'^{\ell} \rho(\mathbf{x}') P_{\ell m}(\cos\theta')\cos m\varphi' \tag{8.18}$$

$$\mu^{\rm oi}_{\ell m}(r) \equiv \frac{(\ell-m)!}{(\ell+m)!}\int_{r>r'} d^3\mathbf{x}'\, r'^{\ell} \rho(\mathbf{x}') P_{\ell m}(\cos\theta')\sin m\varphi' \tag{8.19}$$

$$\mu^{\rm eo}_{\ell m}(r) \equiv \frac{(\ell-m)!}{(\ell+m)!}\int_{r<r'} d^3\mathbf{x}'\, \frac{\rho(\mathbf{x}')}{r'^{\ell+1}} P_{\ell m}(\cos\theta')\cos m\varphi' \tag{8.20}$$

$$\mu^{\rm oo}_{\ell m}(r) \equiv \frac{(\ell-m)!}{(\ell+m)!}\int_{r<r'} d^3\mathbf{x}'\, \frac{\rho(\mathbf{x}')}{r'^{\ell+1}} P_{\ell m}(\cos\theta')\sin m\varphi' \ . \tag{8.21}$$

The procedure is thus to compute the moment integrals ((8.18) − (8.21)) for a given source field $\rho(\mathbf{x})$, and then to use these moments in (8.17) to compute the potential.

In practice, the above procedure must take account of the fact that the source and the potential are assumed to be cell-averaged quantities discretized on a block-structured mesh with varying cell size. Also, because of the radial dependence of the multipole moments of the source function, these moments must be tabulated as functions of distance from $\mathbf{x}_{\rm cm}$, with an implied discretization. The solver allocates storage for moment samples spaced a distance Δ apart in radius

$$\mu^{\rm ei}_{\ell m,q} \equiv \mu^{\rm ei}_{\ell m}(q\Delta) \qquad \mu^{\rm eo}_{\ell m,q} \equiv \mu^{\rm eo}_{\ell m}((q-1)\Delta) \tag{8.22}$$

$$\mu^{\rm oi}_{\ell m,q} \equiv \mu^{\rm oi}_{\ell m}(q\Delta) \qquad \mu^{\rm oo}_{\ell m,q} \equiv \mu^{\rm oo}_{\ell m}((q-1)\Delta) \ . \tag{8.23}$$

The sample index q varies from 0 to N_q ($\mu^{\rm eo}_{\ell m,0}$ and $\mu^{\rm oo}_{\ell m,0}$ are not used). The sample spacing Δ is chosen to be one-half the geometric mean of the x, y, and z cell spacings at the highest level of refinement, and N_q is chosen to be large enough to span the diagonal of the computational volume with samples.

Determining the contribution of individual cells to the tabulated moments requires some care. To reduce the error caused by the grid geometry, in each cell ijk an optional subgrid can be establish (see mpole_subSample) consisting of N' points at the locations $\mathbf{x}'_{i'j'k'}$, where

$$x'_{i'} = x_i + (i' - 0.5(N'-1))\frac{\Delta x_i}{N'}\ , \qquad i' = 0\ldots N'-1 \tag{8.24}$$

$$y'_{j'} = y_j + (j' - 0.5(N'-1))\frac{\Delta y_j}{N'}\ , \qquad j' = 0\ldots N'-1 \tag{8.25}$$

$$z'_{k'} = z_k + (k' - 0.5(N'-1))\frac{\Delta z_k}{N'}\ , \qquad k' = 0\ldots N'-1\ , \tag{8.26}$$

and where $\mathbf{x}_{ijk}$ is the center of cell ijk. (For clarity, we have omitted ijk indices on $\mathbf{x}'$ as well as all block indices.) For each subcell, we assume $\rho(\mathbf{x}'_{i'j'k'}) \approx \rho_{ijk}$ and then apply

$$\mu^{\rm ei}_{\ell m,q\geq q'} \leftarrow \mu^{\rm ei}_{\ell m,q\geq q'} + \frac{(\ell-m)!}{(\ell+m)!}\frac{\Delta x_i \Delta y_j \Delta z_k}{N'^3} r'^{\ell}_{i'j'k'}\rho(\mathbf{x}'_{i'j'k'})P_{\ell m}(\cos\theta'_{i'j'k'})\cos m\varphi'_{i'j'k'} \tag{8.27}$$

$$\mu^{\rm oi}_{\ell m,q\geq q'} \leftarrow \mu^{\rm oi}_{\ell m,q\geq q'} + \frac{(\ell-m)!}{(\ell+m)!}\frac{\Delta x_i \Delta y_j \Delta z_k}{N'^3} r'^{\ell}_{i'j'k'}\rho(\mathbf{x}'_{i'j'k'})P_{\ell m}(\cos\theta'_{i'j'k'})\sin m\varphi'_{i'j'k'} \tag{8.28}$$

$$\mu^{\rm eo}_{\ell m,q\leq q'} \leftarrow \mu^{\rm eo}_{\ell m,q\leq q'} + \frac{(\ell-m)!}{(\ell+m)!}\frac{\Delta x_i \Delta y_j \Delta z_k}{N'^3} \frac{\rho(\mathbf{x}'_{i'j'k'})}{r'^{\ell+1}_{i'j'k'}}P_{\ell m}(\cos\theta'_{i'j'k'})\cos m\varphi'_{i'j'k'} \tag{8.29}$$

$$\mu^{\rm oo}_{\ell m,q\leq q'} \leftarrow \mu^{\rm oo}_{\ell m,q\leq q'} + \frac{(\ell-m)!}{(\ell+m)!}\frac{\Delta x_i \Delta y_j \Delta z_k}{N'^3} \frac{\rho(\mathbf{x}'_{i'j'k'})}{r'^{\ell+1}_{i'j'k'}}P_{\ell m}(\cos\theta'_{i'j'k'})\sin m\varphi'_{i'j'k'}\ , \tag{8.30}$$

where

$$q' = \left\lfloor \frac{|\mathbf{x}'_{i'j'k'}|}{\Delta} \right\rfloor + 1 \tag{8.31}$$

is the index of the radial sample within which the subcell center lies. These expressions introduce (hopefully) small errors when compared to ((8.18)) – (8.21), because the subgrid volume elements are not spherical. These errors are greatest when $r' \sim \Delta x$; hence, using a subgrid reduces the amount of source affected by these errors. An error of order Δ^2 is also introduced by assuming the source profile within each cell to be flat. Note that the total source computed by this method ($\mu^{\rm ei}_{\ell m,N_q}$) is exactly equal to the total implied by ρ_{ijk}.

Another way to reduce grid geometry errors when using the multipole solver is to modify the AMR refinement criterion to refine all blocks containing the center of mass (in addition to other criteria that may be used, such as the second-derivative criterion supplied with PARAMESH). This ensures that the center-of-mass point is maximally refined at all times, further restricting the volume which contributes errors to the moments because $r' \sim \Delta x$.

The default value of N' is 1; note that large values of this parameter very quickly increase the amount of time required to evaluate the multipole moments (as N'^3). In order to speed up the moment summations, the sines and cosines in ((8.27)) – (8.30) are evaluated using trigonometric recurrence relations, and the factorials are pre-computed and stored at the beginning of the run.

When computing the cell-averaged potential, we again employ a subgrid, but here the subgrid points fall on cell boundaries to improve the continuity of the result. Using $N'+1$ subgrid points per dimension, we have

$$x'_{i'} = x_i + (i' - 0.5N'))\frac{\Delta x_i}{N'}\ , \qquad i' = 0\ldots N' \tag{8.32}$$

$$y'_{j'} = y_j + (j' - 0.5N'))\frac{\Delta y_j}{N'}\ , \qquad j' = 0\ldots N' \tag{8.33}$$

$$z'_{k'} = z_k + (k' - 0.5N'))\frac{\Delta z_k}{N'}\ , \qquad k' = 0\ldots N'\ . \tag{8.34}$$

The cell-averaged potential in cell ijk is then

$$\phi_{ijk} = \frac{1}{N'^3} \sum_{i'j'k'} \phi(\mathbf{x}'_{i'j'k'}) \ , \tag{8.35}$$

where the terms in the sum are evaluated via (8.17) up to the limiting multipole order $\ell_{\max}$.

8.10.2.2 Multipole Poisson solver (improved version)

The multipole Poisson solver is based on a multipolar expansion of the source (mass for gravity, for example) distribution around a conveniently chosen center of expansion. The angular number L entering this expansion is a measure of how detailed the description of the source distribution will be on an angular basis. Higher L values mean higher angular resolution with respect to the center of expansion. The multipole Poisson solver is thus appropriate for spherical or nearly-spherical source distributions with isolated boundary conditions. For problems which require high spatial resolution throughout the entire domain (like, for example, galaxy collision simulations), the multipole Poisson solver is less suited, unless one is willing to go to extremely (computationally unfeasible) high L values. For stellar evolution, however, the multipole Poisson solver is the method of choice.

The new implementation of the multipole Poisson solver is located in the directory

`source/Grid/GridSolvers/Multipole_new.`

This implementation improves upon the original implemention in many ways: i) efficient memory layout ii) elimination of numerical over- and underflow errors for large angular momenta when using astrophysical (dimensions $\approx 10^9$) domains iii) elimination of subroutine call overhead (1 call per cell), iv) minimization of error due to non-statistical distributions of moments near the multipolar origin. The following paragraphs explain the new approach to the multipole solver and an explanation of the above improvements. Details about the theory of the new implementation of the Poisson solver can be found in Couch et al. (2013).

The multipole Poisson solver is appropriate for spherical or nearly-spherical source distributions with isolated boundary conditions. It currently works in 1D spherical, 2D spherical, 2D cylindrical, 3D Cartesian and 3D cylindrical. Symmetries can be specified for the 2D spherical and 2D cylindrical cases (a horizontal symmetry plane along the radial axis) and the 3D Cartesian case (assumed axisymmetric property). Because of the radial symmetry in the 1D spherical case, only the monopole term ($\ell = 0$) contributes, while for the 3D Cartesian axisymmetric, the 2D cylindrical and 2D spherical cases only the $m = 0$ moments need to be used (the other $m \neq 0$ moments effectively cancel out).

The multipole algorithm consists of the following steps. First, the center of the multipolar expansion $\mathbf{x}_{\text{cen}}$ is determined via density-squared weighted integration over position:

$$\mathbf{x}_{\text{cen}} = \frac{\int \mathbf{x}\rho^2(\mathbf{x})\, d\mathbf{x}}{\int \rho^2(\mathbf{x})\, d\mathbf{x}}. \tag{8.36}$$

We will take $\mathbf{x}_{\text{cen}}$ as our origin. In integral form, Poisson's equation (8.9) becomes

$$\phi(\mathbf{x}) = -\frac{\alpha}{4\pi} \int \frac{\rho(\mathbf{x}')}{|\mathbf{x}-\mathbf{x}'|}\, d\mathbf{x}'. \tag{8.37}$$

The inverse radial distance part can be expanded in terms of Legendre polynomials

$$\frac{1}{|\mathbf{x}-\mathbf{x}'|} = \sum_{\ell=0}^{\infty} \frac{x_<^{\ell}}{x_>^{\ell+1}} P_\ell(\cos\gamma), \tag{8.38}$$

where $x_<$ ($x_>$) indicate the smaller (larger) of the magnitudes and γ denotes the angle between $\mathbf{x}$ and $\mathbf{x}'$. Note, that this definition includes those cases where both magnitudes are equal. The expansion is always convergent if $\cos\gamma < 1$. Expansion of the Legendre polynomials in terms of spherical harmonics gives

$$P_\ell(\cos\gamma) = \frac{4\pi}{2\ell+1} \sum_{m=-\ell}^{+\ell} Y^*_{\ell m}(\theta',\phi') Y_{\ell m}(\theta,\phi), \tag{8.39}$$

where θ, ϕ and θ', ϕ' are the spherical angular components of $\mathbf{x}$ and $\mathbf{x}'$ about $\mathbf{x}_{\text{cen}}$. Defining now the regular $R_{\ell m}$ and irregular $I_{\ell m}$ solid harmonic functions

$$R_{\ell m}(x_<) = \sqrt{\frac{4\pi}{2\ell+1}} x_<^{\ell} Y_{\ell m}(\theta, \phi) \tag{8.40}$$

$$I_{\ell m}(x_>) = \sqrt{\frac{4\pi}{2\ell+1}} \frac{Y_{\ell m}(\theta, \phi)}{x_>^{\ell+1}}, \tag{8.41}$$

we can rewrite Eq.(8.37) in the form

$$\phi(\mathbf{x}) = -\frac{\alpha}{4\pi} \int \sum_{\ell m} R_{\ell m}(x_<) I^*_{\ell m}(x_>) \rho(\mathbf{x}')\, d\mathbf{x}', \tag{8.42}$$

where the summation sign is a shorthand notation for the double sum over all the allowed ℓ and m values. In FLASH both the source and the potential are assumed to be cell-averaged quantities discretized on a block-structured mesh with varying cell size. The integration must hence be replaced by a summation over all leaf cells

$$\phi(q) = -\frac{\alpha}{4\pi} \sum_{q'} \sum_{\ell m} R_{\ell m}(q_<) I^*_{\ell m}(q_>) m(q'), \tag{8.43}$$

where m denotes the cell's mass. Note, that the symbol q stands for cell index as well as its defining distance position from the expansion center in the computational domain. This discrete Poisson equation is incorrect. It contains the divergent $q' = q$ term on the rhs. The $q' = q$ contribution to the potential corresponds to the cell self potential $\phi_{Self}(q)$ and is divergent in our case because all the cell's mass is assumed to be concentrated at the cell's center. The value of this divergent term can easily be calculated from Eq.(8.38) by setting $\cos\gamma = 1$:

$$\phi_{Self}(q) = m(q) \frac{L+1}{x_q}, \tag{8.44}$$

where m is the cell's mass, L the highest angular number considered in the expansion and x_q the radial distance of the cell center from the expansion center. To avoid this divergence problem, we evaluate the potentials on each face of the cell and form the average of all cell face potentials to get the cell center potential. Eq.(8.43) will thus be replaced by

$$\phi(q) = \frac{1}{n_F} \sum_F \phi(\mathbf{x}_F) \tag{8.45}$$

and

$$\phi(\mathbf{x}_F) = -\frac{\alpha}{4\pi} \sum_{q'} \sum_{\ell m} R_{\ell m}([q', x_F]_<) I^*_{\ell m}([q', x_F]_>) m(q'), \tag{8.46}$$

where $\mathbf{x}_F$ is the cell face radial distance from the expansion center and $[q', x_F]_<$ denotes the larger of the magnitudes between the cell center radial distance q' and the cell face radial distance x_F. Splitting the summation over cells in two parts

$$\phi(\mathbf{x}_F) = -\frac{\alpha}{4\pi} \left\{ \sum_{q' \le x_F} \sum_{\ell m} \left[R_{\ell m}(q') m(q')\right] I^*_{\ell m}(\mathbf{x}_F) + \sum_{q' > x_F} \sum_{\ell m} R_{\ell m}(\mathbf{x}_F) \left[I^*_{\ell m}(q') m(q')\right] \right\}, \tag{8.47}$$

and defining the two moments

$$M^R_{\ell m}(\mathbf{x}_F) = \sum_{q' \le x_F} R_{\ell m}(q') m(q') \tag{8.48}$$

$$M^I_{\ell m}(\mathbf{x}_F) = \sum_{q' > x_F} I_{\ell m}(q') m(q'), \tag{8.49}$$

we obtain

$$\phi(\mathbf{x}_F) = -\frac{\alpha}{4\pi}\left[\sum_{\ell m} M^R_{\ell m}(\mathbf{x}_F) I^*_{\ell m}(\mathbf{x}_F) + \sum_{\ell m} M^{I*}_{\ell m}(\mathbf{x}_F) R_{\ell m}(\mathbf{x}_F)\right] \tag{8.50}$$

and using vector notation

$$\phi(\mathbf{x}_F) = -\frac{\alpha}{4\pi}\left[\mathbf{M}^R(\mathbf{x}_F)\cdot\mathbf{I}^*(\mathbf{x}_F) + \mathbf{M}^{I*}(\mathbf{x}_F)\cdot\mathbf{R}(\mathbf{x}_F)\right]. \tag{8.51}$$

We now change from complex to real formulation. We state this for the regular solid harmonic functions, the same reasoning being applied to the irregular solid harmonic functions and all their derived moments. The regular solid harmonic functions can be split into a real and imaginary part

$$R_{\ell m} = R^c_{\ell m} + i\, R^s_{\ell m}. \tag{8.52}$$

The labels 'c' and 's' are shorthand notations for 'cosine' and 'sine', reflecting the nature of the azimuthal function of the corresponding real spherical harmonics. When inserting (8.52) into (8.51) all cosine and sine mixed terms of the scalar products cancel out. Also, due to the symmetry relations

$$R^c_{\ell,-m} = (-1)^m R^c_{\ell m} \tag{8.53}$$
$$R^s_{\ell,-m} = -(-1)^m R^s_{\ell m} \tag{8.54}$$

we can restrict ourselves to the following polar angle number ranges

$$c \;:\; \ell \geq 0 \;,\; \ell \geq m \geq 0 \tag{8.55}$$
$$s \;:\; \ell \geq 1 \;,\; \ell \geq m \geq 1. \tag{8.56}$$

The real formulation of (8.51) becomes then

$$\phi(\mathbf{x}_F) = -\frac{\alpha}{4\pi}\left\{\begin{bmatrix}\mathbf{M}^{Rc}(\mathbf{x}_F)\\ \mathbf{M}^{Rs}(\mathbf{x}_F)\end{bmatrix}\cdot\boldsymbol{\Delta}\begin{bmatrix}\mathbf{I}^c(\mathbf{x}_F)\\ \mathbf{I}^s(\mathbf{x}_F)\end{bmatrix} + \begin{bmatrix}\mathbf{M}^{Ic}(\mathbf{x}_F)\\ \mathbf{M}^{Is}(\mathbf{x}_F)\end{bmatrix}\cdot\boldsymbol{\Delta}\begin{bmatrix}\mathbf{R}^c(\mathbf{x}_F)\\ \mathbf{R}^s(\mathbf{x}_F)\end{bmatrix}\right\}, \tag{8.57}$$

which, when compared to (8.51), shows, that all vectors now contain a cosine and a sine section. The $\boldsymbol{\Delta}$ matrix is a diagonal matrix whose elements are equal to 2 for $m \neq 0$ and 1 otherwise, i.e.:

$$\boldsymbol{\Delta} = diag(2 - \delta_{m0}). \tag{8.58}$$

The recursion relations for calculating the solid harmonic vectors are

$$R^c_{00} = 1 \tag{8.59}$$
$$R^c_{\ell\ell} = -\frac{xR^c_{\ell-1,\ell-1} - yR^s_{\ell-1,\ell-1}}{2\ell} \tag{8.60}$$
$$R^s_{\ell\ell} = -\frac{yR^c_{\ell-1,\ell-1} + xR^s_{\ell-1,\ell-1}}{2\ell} \tag{8.61}$$
$$R^{c/s}_{\ell m} = \frac{(2\ell-1)zR^{c/s}_{\ell-1,m} - r^2 R^{c/s}_{\ell-2,m}}{(\ell+m)(\ell-m)}, \quad 0 \leq m < \ell \tag{8.62}$$

and

$$I^c_{00} = \frac{1}{r} \tag{8.63}$$
$$I^c_{\ell\ell} = -(2\ell-1)\frac{xI^c_{\ell-1,\ell-1} - yI^s_{\ell-1,\ell-1}}{r^2} \tag{8.64}$$
$$I^s_{\ell\ell} = -(2\ell-1)\frac{yI^c_{\ell-1,\ell-1} + xI^s_{\ell-1,\ell-1}}{r^2} \tag{8.65}$$
$$I^{c/s}_{\ell m} = \frac{(2\ell-1)zI^{c/s}_{\ell-1,m} - \left[(\ell-1)^2 - m^2\right] I^{c/s}_{\ell-2,m}}{r^2}, \quad 0 \leq m < \ell \tag{8.66}$$

in which x, y, z are the cartesian location coordinates of the cell face and $r^2 = x^2 + y^2 + z^2$. For geometries depending on polar angles one must first calculate the corresponding cartesian coordinates for each cell before applying the recursions. In FLASH, the order of the two cosine and sine components for each solid harmonic vector is such that ℓ precedes m. This allows buildup of the vectors with maximum number of unit strides. The same applies of course for the assembly of the moments. For 2D cylindrical and 2D spherical geometries only the $m = 0$ parts of both recursions are needed, involving only the cartesian z coordinate and r^2. Symmetry along the radial axes of these 2D geometries inflicts only the sign change $z \rightarrow -z$, resulting in the symmetry relations $R^c_{\ell 0} \rightarrow R^c_{\ell 0}$ for even ℓ and $R^c_{\ell 0} \rightarrow -R^c_{\ell 0}$ for odd ℓ, the same holding for the irregular solid harmonic vector components. Thus symmetry in 2D can effectively be treated by halving the domain size and multiplying each even ℓ moments by a factor of 2 while setting the odd ℓ moments equal to 0. For 3D cartesian geometries introduction of symmetry is far more complicated since all m components need to be taken into account. It is not sufficient to simply reduce the domain to the appropriate size and multiply the moments by some factor, but rather one would have to specify the exact symmetry operations intended (generators of the symmetry group O_h or one of its subgroups) in terms of their effects on the x, y, z cartesian basis. The resulting complications in calculating symmetry adapted moments outweighs the computational gain that can be obtained from it. Options for 3D symmetry are thus no longer available in the improved FLASH multipole solver. The 'octant' symmetry option from the old multipole solver, using only the monopole $\ell = 0$ term, was too restrictive in its applicability (exact only for up to angular momenta $\ell = 3$ due to cancellation of the solid harmonic vector components).

From the above recursion relations (8.59-8.66), the solid harmonic vector components are functions of $x^i y^j z^k$ monomials, where $i + j + k = \ell$ for the $\mathbf{R}$ and (formally) $i + j + k = -(\ell + 1)$ for the $\mathbf{I}$. For large astrophysical coordinates and large ℓ values this leads to potential computational over- and underflow. To get independent of the size of both the coordinates and ℓ we introduce a damping factor Dx, Dy, Dz for the coordinates for each solid harmonic type before entering the recursions. D will be chosen such that for the highest specified $\ell = L$ we will have approximately a value close to 1 for both solid harmonic components:

$$R^{c/s}_{Lm} \approx 1 \tag{8.67}$$

$$I^{c/s}_{Lm} \approx 1. \tag{8.68}$$

This ensures proper handling of size at the solid harmonic function evaluation level and one does not have to rely on size cancellations at a later stage when evaluating the potential via Eq.(8.57). We next state the evaluation of the damping factor D. Due to the complicated nature of the recursions, the first step is to find solid harmonic components which have a simple structure. To do this, consider a cell face with $x, y = 0$ and $z \neq 0$. Then $r^2 = z^2$, $|z| = r$ and only the $m = 0$ components are different from zero. An explicit form can be stated for the absolute values of these components in terms of r:

$$|R_{\ell 0}| = \frac{r^\ell}{\ell!} \tag{8.69}$$

$$|I_{\ell 0}| = \frac{\ell!}{r^{\ell+1}}. \tag{8.70}$$

Since $r = \sqrt{x^2 + y^2 + z^2}$, damping of the coordinates with D results in a damped radial cell face distance Dr. Inserting this result into (8.69) and (8.70) and imposing conditions (8.67) and (8.68) results in

$$D_R = \frac{1}{r}\sqrt[L]{L!} \approx \frac{1}{r}\frac{L}{e}\sqrt[2L]{2\pi L} \tag{8.71}$$

$$D_I = \frac{1}{r}\sqrt[L+1]{L!} \approx \frac{1}{r}\frac{L}{e}\sqrt[2L+2]{\frac{2\pi e^2}{L}}, \tag{8.72}$$

where the approximate forms are obtained by using Stirling's factorial approximation formula for large L. In FLASH only the approximate forms are computed for D_R and D_I to avoid having to deal with factorials of large numbers.

From the moment defining equations (8.48) and (8.49) we see, that the moments are sums over subsets of cell center solid harmonic vectors multiplied by the corresponding cell mass. From Eq.(8.57) it follows that for highest accuracy, the moments should be calculated and stored for each possible cell face. For high refinement levels and/or 3D simulations this would result in an unmanageable request for computer memory. Several cell face positions have to be bundled into radial bins Q defined by lower and upper radial bounds. Once a cell center solid harmonic vector pair $\mathbf{R}(q)$ and $\mathbf{I}(q)$ for a particular cell has been calculated, its radial bin location $q \rightarrow Q$ is determined and its contribution is added to the radial bin moments $\mathbf{M}^R(Q)$ and $\mathbf{M}^I(Q)$. The computational definition of the radial bin moments is

$$\mathbf{M}^R(Q) = \sum_{q \leq Q} \mathbf{R}(q)m(q) \tag{8.73}$$

$$\mathbf{M}^I(Q) = \sum_{q \geq Q} \mathbf{I}(q)m(q), \tag{8.74}$$

where $q \leq Q$ means including all cells belonging to Q and all radial bins with lower radial boundaries than Q. The two basic operations of the multipole solver are thus: i) assembly of the radial bin moments and ii) formation of the scalar products via Eq.(8.57) to obtain the potentials. The memory declaration of the moment array should reflect the way the individual moment components are addressed and the most efficient layout puts the angular momentum indices in rows and the radial bin indices in columns.

How do we extract moments $\mathbf{M}^R(\mathbf{x})$ and $\mathbf{M}^I(\mathbf{x})$ at any particular position $\mathbf{x}$ inside the domain (and, in particular, at the cell face positions $\mathbf{x}_F$), which are ultimately needed for the potential evaluation at that location? Assume that the location $\mathbf{x}$ corresponds to a particular radial bin $\mathbf{x} \rightarrow Q$. Consider the three consecutive radial bins $Q-1$, Q and $Q+1$, together with their calculated moments:

$$\begin{array}{r|c|l} \mathbf{M}^R(Q-1) & \mathbf{M}^R(Q) & \mathbf{M}^R(Q+1) \\ \mathbf{M}^I(Q-1) & \mathbf{M}^I(Q) & \mathbf{M}^I(Q+1) \end{array} \tag{8.75}$$

Let us concentrate on the Q bin, whose lower and upper radial limits are shown as solid vertical lines. The radial distance corresponding to $\mathbf{x}$ splits the Q bin into two parts: the left fractional part, denoted R_{frac}, and the right fractional part, denoted I_{frac}. Since both $\mathbf{M}^R(Q-1)$ and $\mathbf{M}^I(Q+1)$ are completely contained respectively in $\mathbf{M}^R(Q)$ and $\mathbf{M}^I(Q)$, the moments at $\mathbf{x}$ be approximately evaluated as:

$$\mathbf{M}^R(\mathbf{x}) = \mathbf{M}^R(Q-1) + R_{frac}\left[\mathbf{M}^R(Q) - \mathbf{M}^R(Q-1)\right] \tag{8.76}$$

$$\mathbf{M}^I(\mathbf{x}) = \mathbf{M}^I(Q+1) + I_{frac}\left[\mathbf{M}^I(Q) - \mathbf{M}^I(Q+1)\right], \tag{8.77}$$

The extraction of the moments via (8.76) and (8.77) is of course an approximation that relies on the statistically dense distribution of the individual cell center moments inside each radial bin. For bins which are reasonably far away from the expansion center this statistical approximation is valid but for those close to the expansion center the statistical distribution does not hold and calculating the moments via the above scheme introduces a large statistical error. The way out of this problem is to move from a statistical radial bin description around the expansion center to a more discrete one, by constructing very narrow isolated radial bins. The code is thus forced to analyze the detailed structure of the geometrical domain grid surrounding the expansion center and to establish the inner radial zone of discrete distributed radial bins. The statistical radial bins are then referred to as belonging to the outer radial zone(s).

While the structure of the inner radial zone is fixed due to the underlying geometrical grid, the size of each radial bin in the outer radial zones has to be specified by the user. There is at the moment no automatic derivation of the optimum (accuracy vs memory cost) bin size for the outer zones. There are two types of radial bin sizes defined for the FLASH multipole solver: i) exponentially and/or ii) logarthmically growing:

$$\text{exponential bin size upper radial limit} = s \cdot \Delta r \cdot Q^t \tag{8.78}$$

$$\text{logarithmic bin size upper radial limit} = s \cdot \Delta r \cdot \frac{e^{tQ}-1}{e^t-1}. \tag{8.79}$$

In these definitions, Δr is a small distance 'atomic' (basic unit) radial measure, defined as half the geometric mean of appropriate cell dimensions at highest refinement level, s is a scalar factor to optionally increase or decrase the atomic unit radial measure and $Q = 1, 2, \ldots$ is a local bin index counter for each outer zone.

The atomic radial distance Δr is calculated for each individual domain geometry as follows:

Domain Geometry	Δr
3D cartesian	$\frac{1}{2}\sqrt[3]{\Delta x \Delta y \Delta z}$
3D cylindrical	$\frac{1}{2}\sqrt{\Delta R \Delta z}$
2D cylindrical	$\frac{1}{2}\sqrt{\Delta R \Delta z}$
2D spherical	$\frac{1}{2}\Delta R$
1D spherical	$\frac{1}{2}\Delta R$

, (8.80)

where $\Delta x, \Delta y, \Delta z$ are the usual cartesian cell dimensions and ΔR is the radial cell dimension. Note, that since Δr measures a basic radial unit along the radial distance from the expansion center (which, for approximate spherical problems, is located close to the domain's geometrical origin), only those cell dimensions for calculating each Δr are taken, which are directly related to radial distances from the geometrical domain origin. For 3D cylindrical domain geometries for example, only the radial cylindrical and z-coordinate cell dimensions determine the 3D radial distance from the 3D cylindrical domain origin. The angular coordinate is not needed. Likewise for spherical domains only the radial cell coordinate is of importance. Definitions (8.78) and (8.79) define the upper limit of the radial bins. Hence in order to obtain the true bin size for the Q-th bin one has to subtract its upper radial limit from the corresponding one of the $(Q-1)$-th bin:

$$Q\text{-th exponential bin size} = s \cdot \Delta r \cdot \left[Q^t - (Q-1)^t\right] \tag{8.81}$$

$$Q\text{-th logarithmic bin size} = s \cdot \Delta r \cdot e^{t(Q-1)}. \tag{8.82}$$

In principle the user can specify as many outer zone types as he/she likes, each having its own exponential or logarithmic parameter pair $\{s, t\}$.

Multithreading of the code is currently enabled in two parts: 1) during moment evaluation and 2) during potential evaluation. The threading in the moment evaluation section is achieved by running multiple threads over separate, non-conflicting radial bin sections. Moment evaluation is thus organized as a single loop over all relevant radial bins on each processor. Threading over the potential evaluation is done over blocks, as these will address different non-conflicting areas of the solution vector.

The improved multipole solver was extensively tested and several runs have been performed using large domains ($> 10^{10}$) and extremely high angular numbers up to $L = 100$ for a variety of domain geometries. Currently, the following geometries can be handled: 3D cartesian, 3D cylindrical, 2D cylindrical, 2D spherical and 1D spherical. The structure of the code is such that addition of new geometries, should they ever be needed by some applications, can be done rapidly.

8.10.2.3 Multipole Poisson solver unit test (MacLaurin spheroid)

The first unit test for the multipole Poisson solver is based on the MacLaurin spheroid analytical gravitational solution given in section 30.3.4. The unit test sets up a spheroid with uniform unit density and determines both the analytical and numerical gravitational fields. The absolute relative error based on the analytical solution is formed for each cell and the maximum of all the absolute errors is compared to a predefined error tolerance value for a particular uniform refinement level. The multipole unit test runs in 2D cylindrical, 2D spherical, 3D cartesian and 3D cylindrical geometries and threaded multipole unit tests are also available.

8.10.2.4 Tree Poisson Solver

The tree solver is based on the Barnes & Hut (1986, Nature, 324, 446) tree code for calculation of gravity forces in N-body simulations. However, it is more general and it includes some more modern features described for instance in Salmon & Warren (1994, J. Comp. Phys, 136, 155), Springel (2005, MNRAS, 364, 1105) and other works. It builds a global octal tree over the whole computational domain, communicates its part to all processors and uses it for calculations of various physical problems provided as separate units in source/physics directory. The global tree is an extension of the AMR mesh octal tree down to individual cells. The communication of the tree is implemented so that only parts of the tree that are needed for the calculation of the potential on a given processor are sent to it. The calculation of physical problems is done by walking the tree for each grid cell (hereafter *point-of-calculation*) and evaluating whether the tree node should be used for calculation or whether its children should be open.

The tree solver is connected to physical units by several wrapper subroutines that are called at specific places of the tree build and tree walk, and that call corresponding subroutines of physical units. In this way, physical units can include arbitrary quantity into the tree, and then, use it to calculate some other physical quantity by integrating contributions of all tree nodes during the tree walk. In this version, the only working unit implementation is `physics/Gravity/GravityMain/Poisson/BHTree`, which calculates the gravitational potential.

The tree solver algorithm consists of four parts. The first one, communication of block properties, is called only if the AMR grid changes. The other three, building of the tree, communication of the tree and calculation of the potential, are called in each time-step.

Communication of block properties. In recent version, each processor needs to know some basic information about all blocks in the simulation. It includes arrays: `nodetype`, `lrefine` and `child`. These arrays are distributed from each processor to all the other processors. They can occupy a substantial amount of memory on large number of processors (memory required for statically allocated arrays of the tree solver can be calculated by a script `tree_mem_use.py`).

Building the tree. The global tree is constructed from bottom and the process consists of three steps. In the first one, the so-called *block-tree* is constructed in each leaf block on a given processor. The *block-trees* are 1-dimensional dynamically allocated arrays (see Figure 8.12) and pointers to them are stored in array `gr_bhTreeArray`. In the second step, top nodes of block-trees (corresponding to whole blocks) are distributed to all processors and stored in array `gr_bhTreeParentTree`. In the last step, higher nodes of the parent tree are calculated by each processor and stored in the `gr_bhTreeParentTree` array. At the end, each processor holds information about the global tree down to the level of leaf blocks. During the whole process of tree building, 5 subroutines providing the interface to physical units are called: `gr_bhFillBotNode`, `gr_bhAccBotNode`, `gr_bhAccNode`, `gr_bhNormalizeNode` and `gr_bhPostprocNode` (see their auto-documentation and source code for details). Each of them calls a corresponding subroutine of all physical units with a name where the first two letters 'gr' are replaced with the name of the unit (e.g. `Gravity_bhFillBotNode`).

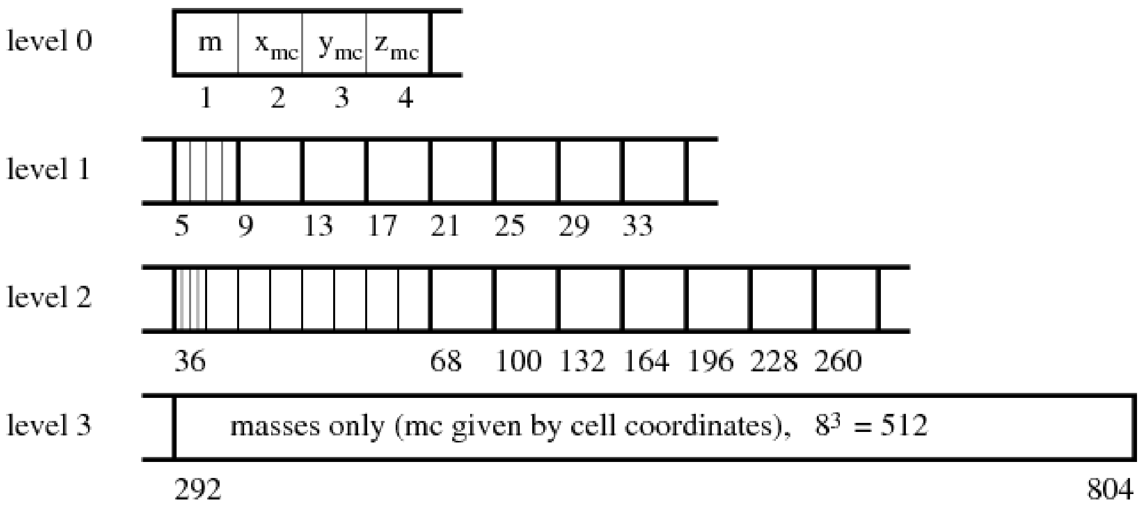

Figure 8.12: Example of a block-tree in case of `nxb=nyb=nzb=8` and in case physical units do not store any further information to tree nodes (masses and mass centre positions are included by the tree solver itself).

Communication of the tree. Most of the tree data is contained on the bottom levels in individual *block-trees*. In order to save memory and communication time, only parts of *block-trees* that are needed on a given processor are sent to it. The procedure consists of three steps. In the first one, a level down to which each *block-tree* has to be sent to each processor is determined. For a given *block-tree*, it is done by evaluating the criterion for the node acceptance (traditionally called multipole acceptance criterion, shortly MAC) for all blocks on a remote processor, searching for the maximum level down to which the evaluated node will be needed on a given remote processor. In the second step, information about the *block-tree* levels which are going to be communicated is sent to all processors. This information is needed for allocation of arrays in which *block-trees* are stored on remote processors. In the third step, the *block-tree* arrays are allocated, all *block-trees* for a given processor are packed into a single message and the messages are communicated.

The MAC is implemented in subroutine `gr_bhMAC` which includes only a simple geometrical MAC used also by Barnes & Hut. The node is accepted for calculation if

$$\frac{S_{\rm node}}{D} < \texttt{gr\_bhTreeLimAngle}\ , \tag{8.83}$$

where $S_{\rm node}$ is the node size (defined as the largest edge of the corresponding cuboid) and D is the distance between the node and the *point-of-calculation.* Additionally, `gr_bhMAC` checks that the *point-of-calculation* is not located within the node itself enlarged by factor `gr_bhTreeSafeBox`. On the top of that, `gr_bhMAC` calls MACs of physical units and the node is accepted only if all criteria are fulfilled.

Tree walk. The tree is traversed from the top to the bottom, evaluating MAC of each node and in case it is not fulfilled, continuing the tree walk with its children. If the node's MAC is fulfilled, the node is accepted for the calculation and subroutine `gr_bhBotNodeContrib` or `gr_bhNodeContrib` is called, depending on whether it is a bottom-most node (i.e. a single grid cell) or higher node, respectively. These subroutines only call the corresponding subroutines of physical units (*e.g.*, `Gravity_bhNodeContrib`). This is the most CPU-intensive part of the tree solver, it usually takes more than 90% of the total tree solver time. It is completely parallel and it does not include any communication (apart from sending some statistics to the main processor at the end).

The tree solver includes several implementations of the tree walk. The default algorithm is the Barnes-Hut like tree walk in which the whole tree is traversed from the top down to nodes fulfilling MAC for each cell separately. This algorithm is used in case the runtime parameter `gr_bhUnifiedTreeWalk` is true (default). If it this parameter is set to false, another algorithm is used in which instead of walking the whole tree for each cell individually, MAC is at first evaluated for whole mesh block (interacting with some node). If the node is accepted and if the node is a parent node (i.e. corresponding to whole mesh block), the node is accepted for all cells of the block and the contribution of the node is added to them. However, the node contribution is calculated separately for each cell, because the distance between the node and individual cells differs. The third tree walk algorithm is an implementation of the so called `SumSquare` MAC described by Salmon & Warren (1994). The tree is traversed using the priority queue, taking contribution of the most important nodes first. This algorithm provides much better error control, however, the implementation in this code version is highly experimental.

The tree solver supports isolated and periodic boundary conditions that can be set independently in each direction. In the latter case, when a node is considered for MAC evaluation and eventually calculation by calling `Gravity_bhNodeContrib`, periodic copies of the node are checked, and the minimum distance among the node periodic copies is taken in account. This allows for instance to calculate gravitational potential with periodic boundary conditions using the Ewald method (see description of the Gravity unit).

8.10.2.5 Tree Poisson solver unit test

The unit test for the tree gravity solver calculates the gravitational potential of the Bonnor-Ebert sphere (Bonnor, W. B., 1956, MNRAS, 116, 351) and compares it to the analytical potential. The density distribution and the analytical potential are calculated by the python script `bes-generator.py`. The simulation setup only reads the file with radial profiles of these quantities and sets it on the grid. It also normalizes the analytical potential (adds a constant to it) so that the minimum values of the analytical and numerical potential are the same. The error of the gravitational potential calculated by the tree code is stored in the field array PERR (written into the PlotFile). The maximum absolute and relative errors are written into the log file.

8.10.2.6 Multigrid Poisson solver

This section of the User's Guide is taken from a paper by Paul Ricker, "A Direct Multigrid Poisson Solver for Oct-Tree Adaptive Meshes" (2008). Dr. Ricker wrote an original version of this multigrid algorithm for FLASH2. The Flash Center adapted it to FLASH3.

Structured adaptive mesh refinement provides some challenges for the implementation of effective, parallel multigrid methods. In the case of patch-based meshes, Huang & Greengard (2000) presents an algorithm which works by using the coarse-grid solution to impose boundary values on the fine grid. Discontinuities in the solution caused by jumps in refinement are resolved through iterative calculation of the residual and subsequent correction. While this is not a multigrid method in the standard sense, it still provides significant convergence acceleration.

The adaptation of this method to the FLASH grid structure (Ricker, 2008) requires a few modifications. The original formulation required that there be shared points between the coarse and fine patches. Contrast this with finite-volume, nested-cell, cell-averaged grids as used in FLASH(Figure 8.13). This is overcome by the exchange of guardcells from coarse to fine using monotonic interpolation (Section 8.6.2) and external boundary extrapolation for the calculation of the residual.

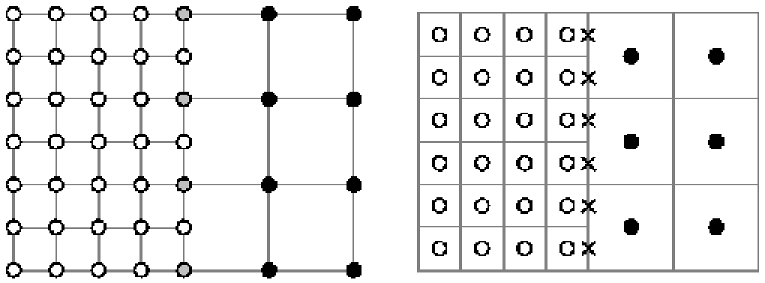

Figure 8.13: Contrast between jumps of refinement in meshes used in the original paper (left) and the oct-tree adapted method (right).

Another difference between the method of (Ricker 2008) and Huang & Greengard is that an oct-tree undoubtedly has neighboring blocks of the same refinement, while a patch-based mesh would not. This problem is solved through uniform prolongation of boundaries from coarse-to-fine, with simple relaxation done to eliminate the slight error introduced between adjacent cells.

One final change between the two methods is that the original computes new sources at the boundary between corrections, while the propagation here is done through nested solves on various levels.

The entire algorithm requires that the PARAMESH grid be reset such that all blocks at refinement above some level ℓ are set as temporarily nonexistent. This is required so that guardcell filling can occur at only that level, neglecting blocks at a higher level of refinement. This requires some global communication by PARAMESH.

The method requires three basic operators over the solution ϕ on the grid: taking the residual, restricting a fine-level function to coarser-level blocks, and prolonging values from the coarse level to the faces of fine level blocks in order to impose boundary values for the fine mesh problems.

The residual is calculated such that:

$$R(\mathbf{x}) \equiv 4\pi G\rho(\mathbf{x}) - \nabla^2\tilde{\phi}(\mathbf{x}) \ . \tag{8.84}$$

This is accomplished through the application of the finite difference laplacian, defined on level ℓ with length-scales Δx_ℓ, Δy_ℓ and Δz_ℓ.

$$\mathcal{D}_\ell\tilde{\phi}^{b\ell}_{ijk} \equiv \frac{1}{\Delta x_\ell^2}\left(\tilde{\phi}^{b\ell}_{i+1,jk} - 2\tilde{\phi}^{b\ell}_{ijk} + \tilde{\phi}^{b\ell}_{i-1,jk}\right) + \frac{1}{\Delta y_\ell^2}\left(\tilde{\phi}^{b\ell}_{i,j+1,k} - 2\tilde{\phi}^{b\ell}_{ijk} + \tilde{\phi}^{b\ell}_{i,j-1,k}\right) \tag{8.85}$$

$$+\frac{1}{\Delta z_\ell^2}\left(\tilde{\phi}^{b\ell}_{ij,k+1} - 2\tilde{\phi}^{b\ell}_{ijk} + \tilde{\phi}^{b\ell}_{ij,k-1}\right) \ . \tag{8.86}$$

The restriction operator $\mathcal{R}_\ell$ for block interior zones (i,j,k) is:

$$(\mathcal{R}_\ell\tilde{\phi})^{\mathcal{P}(c),\ell}_{ijk} \equiv \frac{1}{2^d}\sum_{i'j'k'}\tilde{\phi}^{c,\ell+1}_{i'j'k'} \ , \tag{8.87}$$

where the indices (i',j',k') refer to the zones in block c that lie within zone (i,j,k) of block $\mathcal{P}(c)$. We apply the restriction operator throughout the interiors of blocks, but its opposite, the prolongation operator $\mathcal{I}_\ell$, need only be defined on the edges of blocks, because it is only used to set boundary values for the direct single-block Poisson solver:

$$(\mathcal{I}_\ell\tilde{\phi})^{c,\ell+1}_{i'j'k'} \equiv \sum_{p,q,r=-2}^{2} \alpha_{i'j'k'pqr}\tilde{\phi}^{\mathcal{P}(c),\ell}_{i+p,j+q,k+r} \tag{8.88}$$

When needed, boundary zone values are set as for the difference operator. We use conservative quartic interpolation to set edge values, then solve with homogeneous Dirichlet boundary conditions after using second-order boundary-value elimination. The coefficients α determine the interpolation scheme. For the $-x$ face in 3D,

$$\begin{aligned}
\alpha_{1/2,j'k'pqr} &= \beta_p\gamma_{j'q}\gamma_{k'r} \\
(\beta_p) &= \left(-\frac{1}{12},\frac{7}{12},\frac{7}{12},-\frac{1}{12},0\right) \\
(\gamma_{j'q}) &= \begin{cases} \left(-\frac{3}{128},\frac{11}{64},1,-\frac{11}{64},\frac{3}{128}\right) & j' \text{ odd} \\ \left(\frac{3}{128},-\frac{11}{64},1,\frac{11}{64},-\frac{3}{128}\right) & j' \text{ even} \end{cases}
\end{aligned} \tag{8.89}$$

Interpolation coefficients are defined analogously for the other faces. Note that we use half-integer zone indices to refer to averages over the faces of a zone; integer zone indices refer to zone averages.

8.10.2.7 The direct solver

In the case of problems with Dirichlet boundary conditions, a d-dimensional fast sine transform is used. The transform-space Green's Function for this is:

$$G^\ell_{ijk} = -16\pi G\left[\frac{1}{\Delta x_\ell^2}\sin^2\left(\frac{i\pi}{2n_x}\right)+\frac{1}{\Delta y_\ell^2}\sin^2\left(\frac{j\pi}{2n_y}\right)+\frac{1}{\Delta z_\ell^2}\sin^2\left(\frac{k\pi}{2n_z}\right)\right]^{-1} . \tag{8.90}$$

However, to be able to use the block solver in a general fashion, we must be able to impose arbitrary boundary conditions per-block. In the case of nonhomogenous Dirichlet boundary values, boundary value elimination may be used to generalize the solver. For instance, at the $-x$ boundary:

$$\rho_{1jk} \rightarrow \rho_{1jk} - \frac{2}{\Delta x_\ell^2}\phi(x_{1/2},y_j,z_k) . \tag{8.91}$$

For periodic problems only the coarsest block must be handled differently; block adjacency for finer levels is handled naturally. The periodic solver uses a real-to-complex FFT with the Green's function:

$$G^\ell_{ijk} = \begin{cases} -16\pi G\left[\frac{1}{\Delta x_\ell^2}\sin^2\left(\frac{(i-1)\pi}{n_x}\right)+\frac{1}{\Delta y_\ell^2}\sin^2\left(\frac{(j-1)\pi}{n_y}\right)+\frac{1}{\Delta z_\ell^2}\sin^2\left(\frac{(k-1)\pi}{n_z}\right)\right]^{-1} \\ \qquad\qquad i,j,\ \text{or}\ k\neq 1 \\ 0 \qquad\qquad i=j=k=1 \end{cases} \tag{8.92}$$

This solve requires that the source be zero-averaged; otherwise the solution is non-unique. Therefore the source average is subtracted from all blocks. In order to decimate error across same-refinement-level boundaries, Gauss-Seidel relaxations to the outer two layers of zones in each block are done after applying the direct solver to all blocks on a level. With all these components outlined, the overall solve may be described by the following algorithm:

1. Restrict the source function $4\pi G\rho$ to all levels. Subtract the global average for the `periodic` case.

2. *Interpolation step:* For ℓ from 1 to $\ell_{\max}$,

(a) Reset the grid so that ℓ is the maximum refinement level

(b) Solve $\mathcal{D}_\ell \tilde{\phi}^{b\ell}_{ijk} = 4\pi G \rho^{b\ell}_{ijk}$ for all blocks b on level ℓ.

(c) Compute the residual $R^{b\ell}_{ijk} = 4\pi G \rho^{b\ell}_{ijk} - \mathcal{D}_\ell \tilde{\phi}^{b\ell}_{ijk}$

(d) For each block b on level ℓ that has children, prolong face values for $\tilde{\phi}^{b\ell}_{ijk}$ onto each child block.

3. *Residual propagation step:* Restrict the residual $R^{b\ell}_{ijk}$ to all levels.

4. *Correction step:* Compute the discrete L_2 norm of the residual over all leaf-node blocks and divide it by the discrete L_2 norm of the source over the same blocks. If the result is greater than a preset threshold value, proceed with a correction step: for each level ℓ from 1 to $\ell_{\max}$,

   (a) Reset the grid so that ℓ is the maximum refinement level

   (b) Solve $\mathcal{D}_\ell C^{b\ell}_{ijk} = R^{b\ell}_{ijk}$ for all blocks b on level ℓ.

   (c) Overwrite $R^{b\ell}_{ijk}$ with the new residual $R^{b\ell}_{ijk} - \mathcal{D}_\ell C^{b\ell}_{ijk}$ for all blocks b on level ℓ.

   (d) Correct the solution on all leaf-node blocks b on level ℓ: $\tilde{\phi}^{b\ell}_{ijk} \rightarrow \tilde{\phi}^{b\ell}_{ijk} + C^{b\ell}_{ijk}$.

   (e) For each block b on level ℓ that has children, interpolate face boundary values of $C^{b\ell}_{ijk}$ for each child.

5. If a correction step was performed, return to the residual propagation step.

The above procedure requires storage for $\tilde{\phi}$, C, R, and ρ on each block, for a total storage requirement of $4n_x n_y n_z$ values per block. Global communication is required in computing the tolerance-based stopping criterion.

8.10.2.8 A Hybrid Poisson Solver: Interfacing PFFT with Multigrid

We can improve the performance of the Multigrid solver in Section 8.10.2.6 by replacing single block FFTs with a parallel FFT at a specified coarse level, where, the coarse level is any level which is fully refined, i.e. containing blocks that completely cover the computational domain. Currently, we automatically select the maximum refinement level that is fully refined.

There is load imbalance in the Multigrid solver because each processor performs single block FFTs on the blocks it owns. At the coarse levels there are relatively few blocks compared to available processors which means many processors are effectively idle during the coarse level solves. The introduction of PFFT, and creation of a hybrid solver, eliminates some of the coarse level solves.

The performance characteristics of the hybrid solver are described in "Optimization of multigrid based elliptic solver for large scale simulations in the FLASH code" (2012) which is available online at `http://onlinelibrary.wiley.com/doi/10.1002/cpe.2821/pdf`. Performance results are obtained using the PFFT_PoissonFD unit test.

8.10.3 Using the Poisson solvers

The `GridSolvers` subunit solves the Poisson equation ((8.9)). Two different elliptic solvers are supplied with FLASH: a multipole solver, suitable for approximately spherical source distributions, and a multigrid solver, which can be used with general source distributions. The multipole solver accepts only isolated boundary conditions, whereas the multigrid solver supports Dirichlet, given-value, Neumann, periodic, and isolated boundary conditions. Boundary conditions for the Poisson solver are specified using an argument to the `Grid_solvePoisson` routine which can be set from different runtime parameters depending on the physical context in which the Poisson equation is being solved. The `Grid_solvePoisson` routine is the primary entry point to the Poisson solver module and has the following interface

```
call Grid_solvePoisson (iSoln, iSrc,  bcTypes(6), bcValues(2,6), poisfact) ,
```

Table 8.3: Runtime parameters used with `poisson/multipole`.

Variable	Type	Default	Description
`mpole_lmax`	integer	10	Maximum multipole moment
`quadrant`	logical	`.false.`	Use symmetry to solve a single quadrant in 2D axisymmetric cylindrical (r, z) coordinates, instead of a half domain.

where *iSoln* and *iSrc* are the integer-valued indices of the solution and source (density) variables, respectively. *bcTypes(6)* is an integer array specifying the type of boundary conditions to employ on each of the (up to) 6 sides of the domain. Index 1 corresponds to the -x side of the domain, 2 to +x, 3 to -y, 4 to +y, 5 to -z, and 6 to +z. The following values are accepted in the array

bcTypes	Type of boundary condition
0	Isolated boundaries
1	Periodic boundaries
2	Dirichlet boundaries
3	Neumann boundaries
4	Given-value boundaries

Not all boundary types are supported by all solvers. In this release, *bcValues(2,6)* is not used and can be filled arbitrarily. Given-value boundaries are treated as Dirichlet boundaries with the boundary values subtracted from the outermost interior cells of the source; for this case the solution variable should contain the boundary values in its first layer of boundary cells on input to `Grid_solvePoisson`. It should be noted that if `PARAMESH` is used, the values must be set for all levels. Finally, *poisfact* is real-valued and indicates the value of α multiplying the source function in ((8.9)).

When solutions found using the Poisson solvers are to be differenced (*e.g.*, in computing the gravitational acceleration), it is strongly recommended that for AMR meshes, quadratic (or better) spatial interpolation at fine-coarse boundaries is chosen. (For PARAMESH, this is automatically the case by default, and is handled correctly for Cartesian as well as the supported curvilinear geometries. But note that the default interpolation implementation may be changed at configuration time with the '`-gridinterpolation=`...' setup option; and with the default implementation, the interpolation order may be lowered with the `interpol_order` runtime parameter.) If the order of the gridinterpolation of the mesh is not of at least the same order as the differencing scheme used in places like `Gravity_accelOneRow`, unphysical forces will be produced at refinement boundaries. Also, using constant or linear grid interpolation may cause the multigrid solver to fail to converge.

8.10.3.1 Multipole (original version)

The `poisson/multipole` sub-module takes two runtime parameters, listed in Table 8.3. Note that storage and CPU costs scale roughly as the square of `mpole_lmax`, so it is best to use this module only for nearly spherical matter distributions.

8.10.3.2 Multipole (improved version)

To include the new multipole solver in a simulation, the best option is to use the shortcut `+newMpole` at setup command line, effectively replacing the following setup options :

```
-with-unit=Grid/GridSolvers/Multipole_new
-with-unit=physics/Gravity/GravityMain/Poisson/Multipole
-without-unit=Grid/GridSolvers/Multipole
```

The improved multipole solver currently accepts only two setup parameters, either one switching on multithreading:

- **threadBlockList**: enables multithreaded compilation and execution.
- **threadWithinBlock**: enables multithreaded compilation and execution.

The names of these two setup parameters are missleading, since there is only one universal threading strategy used. The use of these two setup parameters is a temporary solution and will be replaced in near future by only one setup parameter.

The improved multipole solver takes several runtime parameters, whose functions are explained in detail below, together with comments about expected time and memory scaling.

- `mpole_Lmax`: The maximum angular moment L to be used for the multipole Poisson solver. Depending on the domain geometry, the memory and time scaling factors due to this variable alone are: i) 3D cartesian, 3D cylindrical $\rightarrow (L+1)(L+1)$, ii) 3D cartesian axisymmetric, 2D cylindrical, 2D spherical $\rightarrow (L+1)$, iii) 1D spherical $\rightarrow 1$. Assuming no memory limitations, the multipole solver is numerically stable for very large L values. Runs up to $L = 100$ for 3D cartesian domains have been performed. For 2D geometries, $L = 1000$ was the maximum tested.

- `mpole_2DSymmetryPlane`: In 2D coordinates, this runtime parameter enables the user to specify a plane of symmetry along the radial part of the domain coordinates. In effect, this allows a reduction of the computational domain size by one half. The code internally computes the multipole moments as if the other symmetric part is present, i.e. no memory or execution time savings can be achieved by this runtime parameter.

- `mpole_3DAxisymmetry`: Forces rotational invariance around the main (z) axis in 3D cartesian domains. The assumed rotational invariance in the (x, y) plane effectively cancels all $m \neq 0$ multipole moments and one can restrict the calculation to the $m = 0$ multipole moments only. The time and memory savings compared to a asymmetric 3D cartesian run is thus about a factor of $(L+1)$. For 3D cylindrical domains, rotational invariance in the (x, y) plane is equivalent of setting up the corresponding 2D cylindrical domain, hence this runtime parameter is not honored for 3D cylindrical domains, and the user is informed about the 3D to 2D cylindrical domain reduction possibility.

- `mpole_DumpMoments`: This parameter is meant mainly for debugging purposes. It prints the entire moment array for each radial bin for each time step. This option should be used with care and for small problems only. The output is printed to a text file named '<basenm>_dumpMoments.txt', where $< basenm >$ is the base name given for the output files.

- `mpole_PrintRadialInfo`: This parameter enables showing all detailed radial bin information at each time step. This option is especially useful for optimizing the radial bin sizes. The output is written to the text file '<basenm>_printRadialInfo.txt'.

- `mpole_IgnoreInnerZone`: Controls switching on/off the radial inner zone. If it is set .true., the inner zone will not be recognized and all inner zone radii will be treated statistically. This parameter is meant only for performing some error analysis. For production runs it should always be at its default value of false. Otherwise errors will be introduced in calculating the moments near the expansion center.

- `mpole_InnerZoneSize`: The size defining the discrete inner zone. The size is given in terms of the inner zone smallest (atomic) radius, which is determined at each time step by analyzing the domain grid structure around the multipolar origin (expansion center). Only very rarely will this value ever have to be changed. The default setting is very conservative and only under unusual circumstances (ex: highly nonuniform grid around the expansion center) this might be necessary. This value needs to be an integer, as it is used by the code to define dimensions of certain arrays. Note, that by giving this runtime parameter a large integer value (¿ 1000 for domain refinement levels up to 5) one can enforce the code to use only non-statistical radial bins.

- `mpole_InnerZoneResolution`: Defines the inner zone radial bin size for the inner zone in terms of the inner zone smallest (atomic) radius. Two inner zone radii will be considered different, if they are more than this resolution value apart. A very tiny number (for example 10^{-8}) will result in a complete separation of all inner zone radii into separate radial bins. The default value of 0.1 should never be surpassed, and any attempt to do so will stop the program with the appropriate information to the user. Likewise with a meaningless resolution value of 0.

- `mpole_MaxRadialZones`: The maximum number of outer radial zones to be used. In contrast to the inner radial zone, the outer radial zones are much more important for the user. Their layout defines the performance of the multipole solver both in cpu time spent and accuracy of the potential obtained at each cell. The default value of 1 outer radial zone at maximum refinement level leads to high accuracy, but at the same time can consume quite a bit of memory, especially for full 3D runs. In these cases the user can specify several outer radial zones each having their own radial bin size determination rule.

- `mpole_ZoneRadiusFraction_n`: The fraction of the maximum domain radius defining the n-th outer zone maximum radial value. The total number of fractions given must match the maximum number of outer radial zones specified and the fractions must be in increasing order and less than unity as we move from the 1st outer zone upwards. The last outer zone must always have a fraction of exactly 1. If not, the code will enforce it.

- `mpole_ZoneType_n`: String value containing the outer radial zone type for the n-th outer zone. If set to 'exponential', the radial equation $r(Q) = s \cdot \Delta r \cdot Q^t$, defining the upper bound radius of the Q-th radial bin in the n-th outer zone, is used. If set to 'logarithmic', the radial equation $r(Q) = s \cdot \Delta r \cdot (e^{Qt} - 1)/(e^t - 1)$ is used. In these equations Q is a local radial bin counting index for each outer zone and s, t are parameters defining size and growth of the outer zone radial bins (see below).

- `mpole_ZoneScalar_n`: The scalar value s in the n-th outer radial zone equation $r(Q) = s \cdot \Delta r \cdot Q^t$ or $r(Q) = s \cdot \Delta r \cdot (e^{Qt} - 1)/(e^t - 1)$. The scalar is needed to be able to increase (or decrease) the size of the first radial bin with respect to the default smallest outer zone radius Δr.

- `mpole_ZoneExponent_n`: The exponent value t in the n-th outer radial zone equations $r(Q) = s \cdot \Delta r \cdot Q^t$ or $r(Q) = s \cdot \Delta r \cdot (e^{Qt} - 1)/(e^t - 1)$. The exponent controls the growth (shrinkage) in size of each radial bin with increasing bin index. For the first equation, growing will occur for $t > 1$, shrinking for $t < 1$ and same size for $t = 1$. For the logarithmic equation, growing will occur for $t > 0$, shrinking for $t < 0$, but the same size option $t = 0$ will not work because the denominator becomes undefined. The same size option must hence be treated using the exponential outer zone type choice.

- **Runtime parameter types, defaults and options**:

Parameter	Type	Default	Options
`mpole_Lmax`	integer	0	> 0
`mpole_2DSymmetryPlane`	logical	false	true
`mpole_3DAxisymmetry`	logical	false	true
`mpole_DumpMoments`	logical	false	true
`mpole_PrintRadialInfo`	logical	false	true
`mpole_IgnoreInnerZone`	logical	false	true
`mpole_InnerZoneSize`	integer	16	> 0
`mpole_InnerZoneResolution`	real	0.1	less than 0.1 and > 0.0
`mpole_MaxRadialZones`	integer	1	> 1
`mpole_ZoneRadiusFraction_n`	real	1.0	less than 1.0 and > 0.0
`mpole_ZoneType_n`	string	"exponential"	"logarithmic"
`mpole_ZoneScalar_n`	real	1.0	> 0.0
`mpole_ZoneExponent_n`	real	1.0	> 0.0 (exponential)
	real	-	any $\neq 0$ (logarithmic)

8.10.3.3 Tree Poisson solver

The tree gravity solver can be included by `setup` or a `Config` file by requesting `physics/Gravity/GravityMain/Poisson/BHTree`

The current implementation works only in 3D Cartesian coordinates, and blocks have to be logically cubic (*i.e.*, `nxb`=`nyb`=`nzb`). Physical dimensions of blocks can be arbitrary, however, some multipole acceptance criteria can provide inaccurate error estimates with non-cubic blocks. The computational domain can have arbitrary dimensions, and there can be more blocks with `lrefine`=1 (*i.e.*, `nblockx`, `nblocky` and `nblockz` can have different values).

Runtime parameters `gr_bhPhysMACTW` and `gr_bhPhysMACComm` control whether MACs of physical units are used in tree walk and communication, respectively. If one of them (or both) is set `.false.`, only purely geometric MAC is used for a corresponding part of the tree solver. It is not allowed to set `gr_bhPhysMACTW` = `.false.` and `gr_bhPhysMACComm` = `.true.`.

Runtime parameter `gr_bhTreeLimAngle` allows to set the limit opening angle for the purely geometrical MAC. Another condition controlling the acceptance of the node for the calculations is that the *point-of-calculation* must lie out of the box obtained by increasing the considered node by factor `gr_bhTreeSafeBox`.

Parameter `gr_bhUseUnifiedTW` controls whether the Barnes-Hut like tree walk algorithm is used (`.true.`) or whether an alternative algorithm is used which checks the MAC only once for whole block for interactions with parent blocks (`.false.`; see 8.10.2.4 for more details). The latter one is $10 - 20\%$ faster, however, it may lead to higher errors at block boundaries, in particular if the gravity modules calculates the potential which is subsequently differentiated to obtain gravitational acceleration. The tree walk algorithm base on the priority queue is used if `grv_bhMAC` is set to `"SumSquare"`.

Variable	Type	Default	Description
`gr_bhPhysMACTW`	logical	.false.	whether physical MAC should be used in tree walk
`gr_bhPhysMACComm`	logical	.false.	whether physical MAC should be used in communication
`gr_bhTreeLimAngle`	real	0.5	limiting opening angle
`gr_bhTreeSafeBox`	real	1.2	relative size of restricted volume around node where the point-of-calculation is not allowed to be located
`gr_bhUseUnifiedTW`	logical	.true.	whether Barnes-Hut like tree walk algorithm should be used
`gr_bhTWMaxQueueSize`	integer	.true.	maximum length of the priority queue

8.10.3.4 Multigrid

The `Grid/GridSolvers/Multigrid` module is appropriate for general source distributions. It solves Poisson's equation for 1, 2, and 3 dimensional problems with Cartesian geometries. It only supports the `PARAMESH` Grid with one block at the coarsest level. For any other mesh configuration it is advisable to use the hybrid solver, which switches to a uniform grid exact solve when the specified level of coarsening has been achieved. In most use cases for FLASH, the multigrid solver will be used to solve for Gravity (see: Chapter 19). It may be included by `setup` or `Config` by including:

`physics/Gravity/GravityMain/Poisson/Multigrid`

The multigrid solver may also be included stand-alone using:

`Grid/GridSolvers/Multigrid`

In which case the interface is as described above. The supported boundary conditions for the module are periodic, Dirichlet, given-value, and isolated. Due to the nature of the FFT block solver, the same type of boundary condition must be used in all directions. Therefore, only the value of *bcTypes(1)* will be considered in the call to `Grid_solvePoisson`.

The multigrid solver requires the use of two internally-used grid variables: `isls` and `icor`. These are used to store the calculated residual and solved-for correction, respectively. If it is used as a Gravity solver with isolated boundary conditions, then two additional grid variables, `imgm` and `imgp`, are used to store the image mass and image potential.

Table 8.4: Runtime parameters used with `Grid/GridSolvers/Multigrid`.

Variable	Type	Default	Description
`mg_MaxResidualNorm`	real	1×10^{-6}	Maximum ratio of the norm of the residual to that of the right-hand side
`mg_maxCorrections`	integer	100	Maximum number of iterations to take
`mg_printNorm`	real	`.true.`	Print the norm ratio per-iteration
`mpole_lmax`	integer	4	The number of multipole moments used in the isolated case

8.10.3.5 Hybrid (Multigrid with PFFT)

The hybrid solver can be used in place of the Multigrid solver for problems with

- all-periodic
- 2 periodic and 1 Neumann
- 1 periodic and 2 Neumann

boundary conditions, if the default PFFT solver variant (called DirectSolver) is used. To use the hybrid solver in this way, add `Grid/GridSolvers/Multigrid/PfftTopLevelSolve` to your setup line or request the solver in your Simulation Config file (see e.g. unitTest/PFFT_PoissonFD). The following setup lines create a unit test that uses first the hybrid solver and then the standard Multigrid solver

```
./setup unitTest/PFFT_PoissonFD -auto -3d -parfile=flash_pm_3d.par -maxblocks=800 +noio

./setup unitTest/PFFT_PoissonFD -auto -3d -parfile=flash_pm_3d.par -maxblocks=800 +noio
--without-unit=Grid/GridSolvers/Multigrid/PfftTopLevelSolve
--with-unit=Grid/GridSolvers/Multigrid
```

It is also possible to select a different PFFT solver variant. In that case, different combinations of boundary conditions for the Poisson problem may be supported. The `HomBcTrigSolver` variant supports the largest set of combinations of boundary conditions. Use the `PfftSolver` setup variable to choose a variant. Thus, appending `PfftSolver=HomBcTrigSolver` to the `setup` chooses the `HomBcTrigSolver` variant. When using the hybrid solver with the PFFT variants `HomBcTrigSolver` or `SimplePeriodicSolver`, the runtime parameter `gr_pfftDiffOpDiscretize` should be set to 1.

The `Multigrid` runtime parameters given in the previous section also apply.

8.10.4 HYPRE

As a part of implicit time advancement we end up with a system of equations that needs to be solved at every time step. In FLASH4 the HYPRE linear algebra package is used to solve these systems of equations. Therefore it is necessary to install Hypre if this capability of FLASH is to be used.

`Grid_advanceDiffusion` is the API function which solves the system of equations. This API is provided by both the split and unsplit solvers. The unsplit solver uses HYPRE to solve the system of equations and split solver does a direct inverse using Thomas algorithm. Note that the split solver relies heavily on PFFT infrastructure for data exchange and a significant portion of work in split `Grid_advanceDiffusion` involves PFFT routines. In the unsplit solver the data exchange is implicitly done within HYPRE and is hidden.

The steps in unsplit `Grid_advanceDiffusion` are as follows:

- Setup HYPRE grid object
- Exchange Factor B
- Set initial guess
- Compute HYPRE Matrix M such that B = MX
- Compute RHS Vector B
- Compute matrix A
- Solve system AX = B
- Update solution (in FLASH4)

Mapping UG grid to HYPRE matrix is trivial, however mapping PARAMESH grid to a HYPRE matrix can be quite complicated. The process is simplified using the grid interfaces provided by HYPRE.

- Struct Grid interface
- SStruct Grid interface
- IJ System interface

The choice of an interface is tightly coupled to the underlying grid on which the problem is being solved. We have chosen the SSTRUCT interface as it is the most compatible with the block structured AMR mesh in FLASH4. Two terms commonly used in HYPRE terminology are part and box. We define these terms in equivalent FLASH4 terminology. A HYPRE box object maps directly to a leaf block in FLASH4. The block is then defined by it's extents. In FLASH4 this information can be computed easily using a combination of `Grid_getBlkCornerID` and `Grid_getBlkIndexLimits`.All leaf blocks at a given refinement level form a HYPRE part. So number of parts in a typical FLASH4 grid would be give by,

```
nparts = leaf_block(lrefine_max) - leaf_block(lrefine_min) + 1
```

So, if a grid is fully refined or UG, nparts = 1. However, there could still be more then one box object.

Setting up the HYPRE grid object is one of the most important step of the solution process. We use the SSTRUCT interface provided in HYPRE to setup the grid object. Since the HYPRE Grid object is mapped directly with FLASH4 grid, whenever the FLASH4 grid changes the HYPRE grid object needs to be updated. Consequentlywith AMR the HYPRE grid setup might happen multiple times.

Setting up a HYPRE grid object is a two step process,

- Creating stenciled relationships.
- Creating Graph relationships.

Stenciled relationships typically exist between leaf blocks at same refinement level (intra part) and graph relationships exist between leaf blocks at different refinement levels (inter part). The fine-coarse boundary is handled in such a way that fluxes are conserved at the interface (see Chapter 18 for details). UG does not require any graph relationships.

Whether a block needs a graph relationship depends on the refinement level of it's neighbor. While this information is not directly available in PARAMESH, it is possible to determine whether the block neighbor is coarser or finer. Combining this information with the constraint of at best a factor of two jump in refinement at block boundaries, it is possible to compute the part number of a neighbor block, which in turn determines whether we need a graph. Creating a graph involves creating a link between all the cells on the block boundary.

Once the grid object is created, the matrix and vector objects are built on the grid object. The diffusion solve needs uninterpolated data from neighbor blocks even when there is a fine-coarse boundary, therefore it cannot rely upon the guardcell fill process. A two step process is used to handle this situation,

- Since HYPRE has access to X(at n, *i.e.*, initial guess), the RHS vector B can be computed as MX where M is a modified Matrix.
- Similarly the value of Factor B can be shared across the fine-coarse boundary by using `Grid_conserveFluxes`,the fluxes need to be set in a intuitive to way to achieve the desired effect.

With the computation of Vector B (RHS), the system can be solved using HYPRE and UNK can be updated.

8.10.4.1 HYPRE Solvers

In FLASH4 we use the HYPRE PARCSR storage format as this exposes the maximum number of iterative solvers.

Table 8.5: Solvers, Preconditioners combinations used with `Grid/GridSolvers/HYPRE`.

Solver	Preconditioner
PCG	AMG, ILU(0)
BICGSTAB	AMG, ILU(0)
GMRES	AMG, ILU(0)
AMG	-
SPLIT	-

Parallel runs: One issue that has been observed is that there is a difference in the results produced by HYPRE using one or more processors. This would most likely be due to use of CG (krylov subspace methods), which involves an MPI_SUM over the dot product of the residue. We have found this error to be dependent on the type of problem. One way to get across this problem is to use direct solvers in HYPRE like SPLIT. However we have noticed that direct solvers tend to be slow. THe released code has an option to use the SPLIT solver, but this solver has not been extensively tested and was used only for internal debugging purposes and the usage of the HYPRE SPLIT solver in FLASH4 is purely experimental.

Customizing solvers: HYPRE exposes a lot more parameters to tweak the solvers and preconditioners mentioned above. We have only used those which are applicable to general diffusion problems. Although in general these settings might be good enough it is by no means complete and might not be applicable to all class of problems. Use of additional HYPRE parameters might require direct manipulation of FLASH4 code.

Symmetric Positive Definite (SPD) Matrix: PCG has been noticed to have convergence issues which might be related to (not necessarily),

- A non-SPD matrix generated due to round of errors (only).
- Use of BoomerAMG as PC (refer to HYPRE manual).

The default settings use PCG as the solver with AMG as preconditioner. The following parameters can be tweaked at run time,

Table 8.6: Runtime parameters used with `Grid/GridSolvers/HYPRE`.

Variable	Type	Default	Description
`gr_hyprePCType`	string	`"hypre_amg"`	Algebraic Multigrid as Preconditioner
`gr_hypreMaxIter`	integer	10000	Maximum number of iterations
`gr_hypreRelTol`	real	1×10^{-8}	Maximum ratio of the norm of the residual to that of the initial residue
`gr_hypreSolverType`	string	`"hypre_pcg"`	Type of linear solver, Preconditioned Conjugate gradient
`gr_hyprePrintSolveInfo`	boolean	FALSE	enables/disables some basic solver information (for e.g number of iterations)
`gr_hypreInfoLevel`	integer	1	Verbosity level of solver diagnostics (refer HYPRE manual).
`gr_hypreFloor`	real	1×10^{-12}	Used to floor the end solution.
`gr_hypreUseFloor`	boolean	TRUE	whether to apply gr_hypreFloor to floor results from HYPRE.

8.11 Grid Geometry

FLASH can use various kinds of coordinates (“**geometries**”) for modeling physical problems. The available geometries represent different (orthogonal) curvilinear coordinate systems.

The geometry for a particular problem is set at runtime (after an appropriate invocation of `setup`) through the `geometry` runtime parameter, which can take a value of `"cartesian"`, `"spherical"`, `"cylindrical"`, or `"polar"`. Together with the dimensionality of the problem, this serves to completely define the nature of the problem's coordinate axes (Table 8.7). Note that not all `Grid` implementations support all geometry/dimension combinations. Physics units may also be limited in the geometries supported, some may only work for cartesian coordinates.

The core code of a `Grid` implementation is not concerned with the mapping of cell indices to physical coordinates; this is not required for under-the-hood `Grid` operations such as keeping track of which blocks are neighbors of which other blocks, which cells need to be filled with data from other blocks, and so on. Thus the physical domain can be logically modeled as a rectangular mesh of cells, even in curvilinear coordinates.

There are, however, some areas where geometry needs to be taken into consideration. The correct implementation of a given geometry requires that gradients and divergences have the appropriate area factors and that the volume of a cell is computed properly for that geometry. Initialization of the grid as well as AMR operations (such as restriction, prolongation, and flux-averaging) must respect the geometry also. Furthermore, the hydrodynamic methods in FLASH are finite-volume methods, so the interpolation must also be conservative in the given geometry. The default mesh refinement criteria of FLASH4 also currently take geometry into account, see Section 8.6.3 above.

A **convention:** in this section, Small letters x, y, and z are used with their usual meaning in designating coordinate directions for specific coordinate systems: *i.e.*, x and y refer to directions in cartesian coordinates, and z may refer to a (linear) direction in either cartesian or cylindrical coordinates.

On the other hand, capital symbols X, Y, and Z are used to refer to the (up to) three directions of any coordinate system, *i.e.*, the directions corresponding to the `IAXIS`, `JAXIS`, and `KAXIS` dimensions in FLASH4, respectively. Only in the cartesian case do these correspond directly to their small-letter counterparts. For other geometries, the correspondence is given in Table 8.7.

Table 8.7: Different geometry types. For each geometry/dimensionality combination, the "support" column lists the `Grid` implementations that support it: pm4 stands for `PARAMESH` 4.0 and `PARAMESH` 4dev, pm2 for `PARAMESH` 2, UG for Uniform Grid implementations, respectively.

name	dimensions	support	axisymmetric	X-coord	Y-coord	Z-coord
cartesian	1	pm4,pm2,UG	n	x		
cartesian	2	pm4,pm2,UG	n	x	y	
cartesian	3	pm4,pm2,UG	n	x	y	z
cylindrical	1	pm4,UG	y	r		
cylindrical	2	pm4,pm2,UG	y	r	z	
cylindrical	3	pm4,UG	n	r	z	ϕ
spherical	1	pm4,pm2,UG	y	r		
spherical	2	pm4,pm2,UG	y	r	θ	
spherical	3	pm4,pm2,UG	n	r	θ	ϕ
polar	1	pm4,UG	y	r		
polar	2	pm4,pm2,UG	n	r	ϕ	
"polar + z" (cylindrical with a different ordering of coordinates)	3	—	n	r	ϕ	z

8.11.1 Understanding Curvilinear Coordinates

In the context of FLASH, curvilinear coordinates are most useful with 1-d or 2-d simulations, and this is how they are commonly used. But what does it mean to apply curvilinear coordinates in this way? Physical reality has three spatial dimensions (as far as the physical problems simulated with FLASH are concerned). In cartesian coordinates, it is relatively straightforward to understand what a 2-d (or 1-d) simulation means: "Just leave out one (or two) coordinates." This is less obvious for other coordinate systems, therefore some fundamental discussion follows.

A reduced dimensionality (RD) simulation can be naively understood as taking a cut (or, for 1-d, a linear probe) through the real 3-d problem. However, there is also an assumption, not always explicitly stated, that is implied in this kind of simulation: namely, that the cut (or line) is representative of the 3-d problem. This can be given a stricter meaning: it is assumed that the physics of the problem do not depend on the omitted dimension (or dimensions). A RD simulation can be a good description of a physical system only to the degree that this assumption is warranted. Depending on the nature of the simulated physical system, non-dependence on the omitted dimensions may mean the absence of force and/or momenta vector components in directions of the omitted coordinate axes, zero net mass and energy flow out of the plane spanned by the included coordinates, or similar.

For omitted dimensions that are lengths — z and possibly y in cartesian, and z in cylindrical and polar RD simulations — one may think of a 2-d cut as representing a (possibly very thin) layer in 3-d space sandwiched between two parallel planes. there is no *a priori* definition of the thickness of the layer, so it is not determined what 3-d volume should be asigned to a 2-d cell in such coordinates. We can thus arbitrarily assign the length "1" to the edge length of a 3-d cell volume, making the volume equal to the 2-d area. We can understand generalizations of "volume" to 1-d, and of "face areas" to 2-d and 1-d RD simulations with omitted linear coordinates, in an equivalent way: just set the length of cell edges along omitted dimensions to 1.

For omitted dimensions that are angles — the θ and ϕ coordinates on spherical, cylindrical, and polar geometries — it is easier to think of omitting an angle as the equivalent of integrating over the full range of that angle coordinate (under the assumption that all physical solution variables are independent of that angle). Thus omitting and angle ϕ in these geometries implies the assumption of axial symmetry, and this is noted in Table 8.7. Similarly, omitting both ϕ and θ in spherical coordinates implies an assumption of complete spherical symmetry. When ϕ is omitted, a 2-d cell actually represents the 3-d object that is generated by rotating the 2-d area around a z-axis. Similarly, when only r is included, 1-d cells (*i.e.*, r intervals) represent hollow spheres or cylinders. (If the coordinate interval begins at $r_l = 0.0$, the sphere or cylinder is massive instead of hollow.)

As a result of these considerations, the measures for cell (and block) volumes and face areas in a simulation depends on the chosen geometry. Formulas for the volume of a cell dependent on the geometry are given in the geometry-specific sections further below.

As discussed in Figure 8.6, to ensure conservation at a jump in refinement in AMR grids, a flux correction step is taken. The fluxes leaving the fine cells adjacent to a coarse cell are used to determine more accurately the flux entering the coarse cell. This step takes the coordinate geometry into account in order to accurately determine the areas of the cell faces where fine and coarse cells touch. By way of example, an illustration is provided below in the section on cylindrical geometry.

8.11.2 Choosing a Geometry

The user chooses a geometry by setting the `geometry` runtime parameter in `flash.par`. The default is `"cartesian"` (unless overridden in a simulation's `Config` file). Depending on the `Grid` implementation used and the way it is configured, the geometry may also have to be compiled into the program executable and thus may have to be specified at configuration time; the `setup` flag `-geometry` should be used for this purpose, see Section 5.2.

The `geometry` runtime parameter is most useful in cases where the geometry does not have to be specified at compile-time, in particular for the Uniform Grid. The runtime parameter will, however, always be considered at run-time during `Grid` initialization. If the `geometry` runtime parameter is inconsistent with a geometry specified at setup time, FLASH will then either override the geometry specified at setup time (with a warning) if that is possible, or it will abort.

This runtime parameter is used by the `Grid` unit and also by hydrodynamics solvers, which add the necessary geometrical factors to the divergence terms. Next we describe how user code can use the runtime parameter's value.

8.11.3 Getting Geometry Information in Program Code

The `Grid` unit provides an accessor `Grid_getGeometry` property that returns the geometry as an integer, which can be compared to the symbols {`CARTESIAN, SPHERICAL, CYLINDRICAL, POLAR`} defined in `"constants.h"` to determine which of the supported geometries we are using. A unit writer can therefore determine flow-control based on the geometry type (see Figure 8.14). Furthermore, this provides a mechanism for a unit to determine at runtime whether it supports the current geometry, and if not, to abort.

Coordinate information for the mesh can be determined via the `Grid_getCellCoords` routine. This routine can provide the coordinates of cells at the left edge, right edge, or center. The width of cells can be determined via the `Grid_getDeltas` routine. Angle values and differences are given in radians. Coordinate information for a block of cells as a whole is available through `Grid_getBlkCenterCoords` and `Grid_getBlkPhysicalSize`.

The volume of a single cell can be obtained via the `Grid_getSingleCellVol` or the `Grid_getPointData` routine. Use the `Grid_getBlkData`, `Grid_getPlaneData`, or `Grid_getRowData` routines with argument `dataType=CELL_VOLUME` To retrieve cell volumes for more than one cell of a block. To retrieve cell face areas, use the same `Grid_get*Data` interfaces with the appropriate `dataType` argument.

Note the following difference between the two groups of routines mentioned in the previous two paragraphs: the routines for volumes and areas take the chosen geometry into account in order to return geometric measures of physical volumes and faces (or their RD equivalents). On the other hand, the routines for coordinate values and widths return values for X, Y, and Z directly, without converting angles to (arc) lengths.

8.11.4 Available Geometries

Currently, all of FLASH's physics support one-, two-, and (with a few exceptions explicitly stated in the appropriate chapters) three-dimensional Cartesian grids. Some units, including the FLASH `Grid` unit and PPM hydrodynamics unit (Chapter 15), support additional geometries, such as two-dimensional cylindrical

```
#include "constants.h"

integer :: geometry

call Grid_getGeometry(geometry)

select case (geometry)

case (CARTESIAN)

! do Cartesian stuff here ...

case (SPHERICAL)

! do spherical stuff here ...

case (CYLINDRICAL)

! do cylindrical stuff here ...

case (POLAR)

! do polar stuff here ...

end select
```

Figure 8.14: Branching based on geometry type

(r, z) grids, one/two-dimensional spherical $(r)/(r, \theta)$ grids, and two-dimensional polar (r, ϕ) grids. Some specific considerations for each geometry follow.

The following tables use the convention that r_l and r_r stand for the values of the r coordinate at the "left" and "right" end of the cell's r-coordinate range, respectively (*i.e.*, $r_l < r_r$ is always true), and $\Delta r = r_r - r_l$; and similar for the other coordinates.

8.11.4.1 Cartesian geometry

FLASH uses Cartesian (plane-parallel) geometry by default. This is equivalent to specifying

```
geometry = "cartesian"
```

in the runtime parameter file.

Cell Volume in Cartesian Coordinates

1-d	Δx
2-d	$\Delta x \Delta y$
3-d	$\Delta x \Delta y \Delta z$

8.11.4.2 Cylindrical geometry

To run FLASH with cylindrical coordinates, the `geometry` parameter must be set thus:

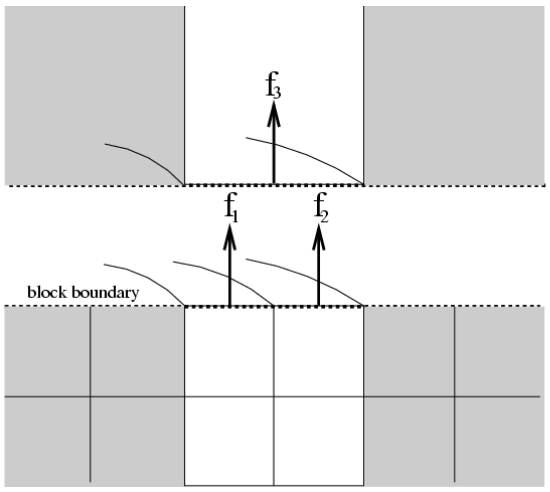

Figure 8.15: Diagram showing two fine cells and a coarse cell at a jump in refinement in the cylindrical 'z' direction. The block boundary has been cut apart here for illustrative purposes. The fluxes out of the fine blocks are shown as f_1 and f_2. These will be used to compute a more accurate flux entering the coarse flux f_3. The area that the flux passes through is shown as the annuli at the top of each fine cell and the annulus below the coarse cell.

```
geometry = "cylindrical"
```

Cell Volume in Cylindrical Coordinates

1-d	$\pi(r_r^2 - r_l^2)$
2-d	$\pi(r_r^2 - r_l^2)\Delta z$
3-d	$\frac{1}{2}(r_r^2 - r_l^2)\Delta z\Delta\phi$

As in other non-cartesian geometries, if the minimum radius is chosen to be zero (`xmin = 0.`), the left-hand boundary type should be reflecting. Of all supported non-cartesian geometries, the cylindrical is in 2-d most similar to a 2-d coordinate system: it uses two linear coordinate axes (r and z) that form a rectangular grid physically as well as logically.

As an illustrative example of the kinds of considerations necessary in curved coordinates, Figure 8.15 shows a jump in refinement along the cylindrical 'z' direction. When performing the flux correction step at a jump in refinement, we must take into account the area of the annulus through which each flux passes to do the proper weighting. We define the cross-sectional area through which the z-flux passes as

$$A = \pi(r_r^2 - r_l^2) \ . \tag{8.93}$$

The flux entering the coarse cell above the jump in refinement is corrected to agree with the fluxes leaving the fine cells that border it. This correction is weighted according to the areas

$$f_3 = \frac{A_1 f_1 + A_2 f_2}{A_3} \ . \tag{8.94}$$

For fluxes in the radial direction, the cross-sectional area is independent of the height, z, so the corrected flux is simply taken as the average of the flux densities in the adjacent finer cells.

8.11.4.3 Spherical geometry

One or two dimensional spherical problems can be performed by specifying

```
geometry = "spherical"
```

in the runtime parameter file.

Cell Volume in Spherical Coordinates

1-d	$\frac{4}{3}\pi(r_r^3 - r_l^3)$
2-d	$\frac{2}{3}\pi(r_r^3 - r_l^3)(\cos(\theta_l) - \cos(\theta_r))$
3-d	$\frac{1}{3}(r_r^3 - r_l^3)(\cos(\theta_l) - \cos(\theta_r))\Delta\phi$

If the minimum radius is chosen to be zero (`xmin = 0.`), the left-hand boundary type should be reflecting.

8.11.4.4 Polar geometry

Polar geometry is a 2-D subset of 3-D cylindrical configuration without the "z" coordinate. Such geometry is natural for studying objects like accretion disks. This geometry can be selected by specifying

```
geometry = "polar"
```

in the runtime parameter file.

Cell Volume in Polar Coordinates

1-d	$\pi(r_r^2 - r_l^2)$
2-d	$\frac{1}{2}(r_r^2 - r_l^2)\Delta\phi$
3-d	$\frac{1}{2}(r_r^2 - r_l^2)\Delta\phi\Delta z$ (not supported)

As in other non-cartesian geometries, if the minimum radius is chosen to be zero (`xmin = 0.`), the left-hand boundary type should be reflecting.

8.11.5 Conservative Prolongation/Restriction on Non-Cartesian Grids

When blocks are refined, we need to initialize the child data using the information in the parent cell in a manner which preserves the cell-averages in the coordinate system we are using. When a block is derefined, the parent block (which is now going to be a leaf block) needs to be filled using the data in the child blocks (which are soon to be destroyed). The first procedure is called prolongation. The latter is called restriction. Both of these procedures must respect the geometry in order to remain conservative. Prolongation and restriction are also used when filling guard cells at jumps in refinement.

8.11.5.1 Prolongation

When using a supported non-Cartesian geometry, FLASH has to use geometrically correct prolongation routines. These are located in:

- `source/Grid/GridMain/paramesh/Paramesh2/monotonic` (for `PARAMESH` 2)
- `source/Grid/GridMain/paramesh/interpolation/Paramesh4/prolong` (for `PARAMESH` 4)

These paths will be be automatically added by the `setup` script when the `-gridinterpolation=monotonic` option is in effect (which is the case by default, unless `-gridinterpolation=native` was specified). The "monotonic" interpolation scheme used in both cases is taking geometry into consideration and is appropriate for all supported geometries.

FLASH Transition

Some more specific PARAMESH 2 interpolation schemes are included in the distribution and might be useful for compatibility with FLASH2:

- `source/Grid/GridMain/paramesh/Paramesh2/quadratic_cartesian` (for cartesian coordinates)
- `source/Grid/GridMain/paramesh/Paramesh2/quadratic_spherical` (for spherical coordinates)

Other geometry types and prolongation schemes can be added in a manner analogous to the ones implemented here.
These routines could be included by specifying the correct path in your `Units` file, or by using appropriate `-unit=` flags for `setup`. However, their use is not recommended.

8.11.5.2 Restriction

The default restriction routines understand the supported geometries by default. A cell-volume weighted average is used when restricting the child data up to the parent. For example, in 2-d, the restriction would look like

$$\langle f \rangle_{i,j} = \frac{V_{ic,jc}\,\langle f \rangle_{ic,jc} + V_{ic+1,jc}\,\langle f \rangle_{ic+1,jc} + V_{ic,jc+1}\,\langle f \rangle_{ic,jc+1} + V_{ic+1,jc+1}\,\langle f \rangle_{ic+1,jc+1}}{V_{i,j}} \,, \tag{8.95}$$

where $V_{i,j}$ is the volume of the cell with indices, i, j, and the ic, jc indices refer to the children.

8.12 Unit Test

The `Grid` unit test has implementations to test Uniform Grid and PARAMESH. The Uniform Grid version of the test has two parts; the latter portion is also tested in PARAMESH. The test initializes the grid with a sinusoid function $\sin(x) \times \cos(y) \times \cos(z)$, distributed over a number of processors. Knowing the configuration of processors, it is possible to determine the part of the sinusoid on each processor. Since guardcells are filled either from the interior points of the neighboring processor, or from boundary conditions, it is also possible to predict the values expected in guard cells on each processor. The first part of the UG unit test makes sure that the actual received values of guard cell match with the predicted ones. This process is carried out for both cell-centered and face-centered variables.

The second part of the UG test, and the only part of the PARAMESH test, exercises the get and put data functions. Since the `Grid` unit has direct access to all of its own data structures, it can compare the values fetched using the getData functions against the directly accessible values and report an error if they do not match. The testing of the `Grid` unit is not exhaustive, and given the complex nature of the unit, it is difficult to devise tests that would do so. However, the more frequently used functions are exercised in this test.

Chapter 9

IO Unit

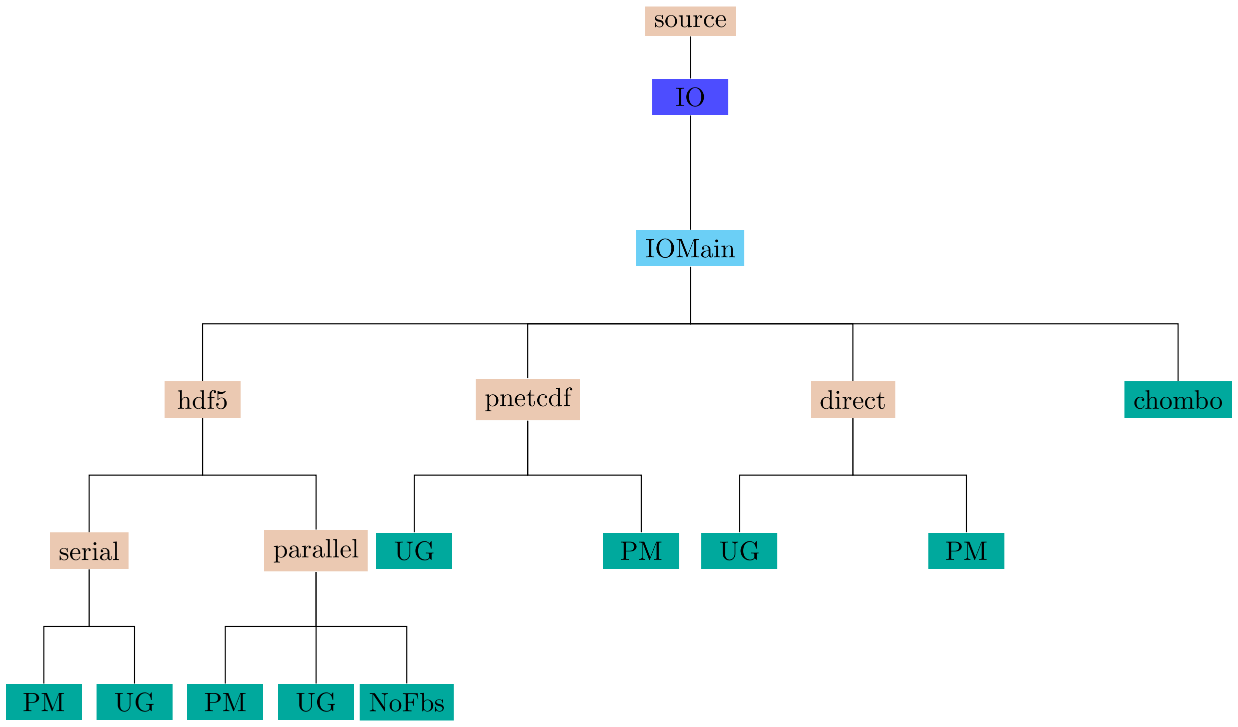

Figure 9.1: The `IO` unit: IOMain subunit directory tree.

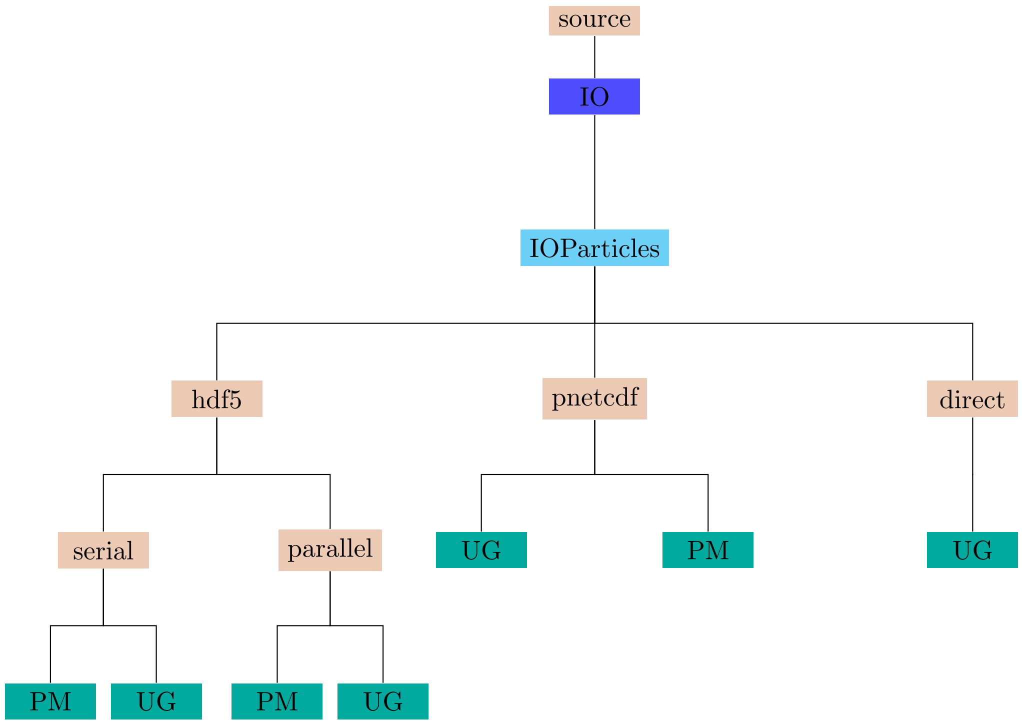

Figure 9.2: The `IO` unit: IOParticles subunit tree.

FLASH uses parallel input/output (IO) libraries to simplify and manage the output of the large amounts of data usually produced. In addition to keeping the data output in a standard format, the parallel IO libraries also ensure that files will be portable across various platforms. The mapping of FLASH data-structures to records in these files is controlled by the FLASH IO unit. FLASH can output data with two parallel IO libraries, HDF5 and Parallel-NetCDF. The data layout is different for each of these libraries. Since FLASH3 we also offer direct serial FORTRAN IO, which can be used as a last resort if no parallel library is available. However, FLASH post-processing tools such as fidlr (Chapter 34) and sfocu (Chapter 32) do not support the direct IO format.

Note:

This release supports both HDF5 and Parallel-NetCDF, including particle IO for both implementations.

Various techniques can be used to write the data to disk when running a parallel simulation. The first is to move all the data to a single processor for output; this technique is known as serial IO. Secondly, each processor can write to a separate file, known as direct IO. As a third option, each processor can use parallel access to write to a single file in a technique known as parallel IO. Finally, a hybrid method can be used where clusters of processors write to the same file, though different clusters of processors output to different files. In general, parallel access to a single file will provide the best parallel IO performance unless the number of processors is very large. On some platforms, such as Linux clusters, there may not be a parallel file system, so moving all the data to a single processor is the only solution. Therefore FLASH supports HDF5 libraries in both serial and parallel forms, where the serial version collects data to one processor before writing it, while the parallel version has every processor writing its data to the same file.

9.1 IO Implementations

FLASH4 supports multiple IO implementations: direct, serial and parallel implementations as well as support for different parallel libraries. In addition, FLASH4 also supports multiple (Chapter 8) `Grid` implementations. As a consequence, there are many permutations of the IO API implementation, and the selected implementation must match not only the correct IO library, but also the correct grid. Although there are many IO options, the `setup` script in FLASH4 is quite 'smart' and will not let the user setup a problem with incompatible `IO` and `Grid` unit implementations. Table 9.1 summarizes the different implementation of the FLASH IO unit in the current release.

Table 9.1: IO implementations available in FLASH. All implementations begin at the /source directory.

Implementation Path	Description
`IO/IOMain/HDF5/parallel/PM`	Hierarchical Data Format (HDF) 5 output. A single HDF5 file is created, with each processor writing its data to the same file simultaneously. This relies on the underlying MPIIO layer in HDF5. This particular implementation only works with the `PARAMESH` grid package.
`IO/IOMain/hdf5/parallel/UG`	Hierarchical Data Format (HDF) 5 output. A single HDF5 file is created, with each processor writing its data to the same file simultaneously. This relies on the underlying MPIIO layer in HDF5. This particular implementation only works with the Uniform Grid.
`IO/IOMain/hdf5/parallel/NoFbs`	Hierarchical Data Format (HDF) 5 output. A single HDF5 file is created, with each processor writing its data to the same file simultaneously. All data is written out as one block. This relies on the underlying MPIIO layer in HDF5. This particular implementation only works in non-fixedblocksize mode.
`IO/IOMain/hdf5/serial/PM`	Hierarchical Data Format (HDF) 5 output. Each processor passes its data to processor 0 through explicit MPI sends and receives. Processor 0 does all of the writing. The resulting file format is identical to the parallel version; the only difference is how the data is moved during the writing. This particular implementation only works with the `PARAMESH` grid package.
`IO/IOMain/hdf5/serial/UG`	Hierarchical Data Format (HDF) 5 output. Each processor passes its data to processor 0 through explicit MPI sends and receives. Processor 0 does all of the writing. The resulting file format is identical to the parallel version; the only difference is how the data is moved during the writing. This particular implementation only works with the Uniform Grid.
`IO/IOMain/pnetcdf/PM`	ParallelNetCDF output. A single file is created with each processor writing its data to the same file simultaneously. This relies on the underlying MPI-IO layer in PNetCDF. This particular implementation only works with the `PARAMESH` grid package.

Table 9.1: FLASH IO implementations (continued).

Implementation path	Description
`IO/IOMain/pnetcdf/UG`	ParallelNetCDF output. A single file is created with each processor writing its data to the same file simultaneously. This relies on the underlying MPI-IO layer in PNetCDF. This particular implementation only works with the Uniform Grid.
`IO/IOMain/direct/UG`	Serial FORTRAN IO. Each processor writes its own data to a separate file. Warning! This choice can lead to many many files! Use only if neither HDF5 or Parallel-NetCDF is available. The FLASH tools are not compatible with the direct IO unit.
`IO/IOMain/direct/PM`	Serial FORTRAN IO. Each processor writes its own data to a separate file. Warning! This choice can lead to many many files! Use only if neither HDF5 or Parallel-NetCDF is available. The FLASH tools are not compatible with the direct IO unit.
`IO/IOMain/chombo`	Hierarchical Data Format (HDF) 5 output. The subroutines provide an interface to the `Chombo` I/O routines that are part of the standard `Chombo` release. This implementation can only be used in applications built with `Chombo Grid`. The `Chombo` file layout is incompatible with tools, such as `fidlr` and `sfocu`, that depend on FLASH file layout.

FLASH4 also comes with some predefined setup **shortcuts** which make choosing the correct IO significantly easier; see Chapter 5 for more details about shortcuts. In FLASH4 HDF5 serial IO is included by default. Since `PARAMESH` 4.0 is the default grid, the included IO implementations will be compatible with `PARAMESH` 4.0. For clarity, a number or examples are shown below.

An example of a basic setup with HDF5 serial IO and the `PARAMESH` grid, (both defaults) is:

```
./setup Sod -2d -auto
```

To include a parallel implementation of HDF5 for a `PARAMESH` grid the `setup` syntax is:

```
./setup Sod -2d -auto -unit=IO/IOMain/hdf5/parallel/PM
```

using the already defined shortcuts the `setup` line can be shortened to

```
./setup Sod -2d -auto +parallelio
```

To set up a problem with the Uniform Grid and HDF5 serial IO, the `setup` line is:

```
./setup Sod -2d -auto -unit=Grid/GridMain/UG -unit=IO/IOMain/hdf5/serial/UG
```

using the already defined shortcuts the `setup` line can be shortened to

```
./setup Sod -2d -auto +ug
```

To set up a problem with the Uniform Grid and HDF5 parallel IO, the complete `setup` line is:

```
./setup Sod -2d -auto -unit=Grid/GridMain/UG -unit=IO/IOMain/hdf5/parallel/UG
```

using the already defined shortcuts the `setup` line can be shortened to

```
./setup Sod -2d -auto +ug  +parallelio
```

If you do *not* want to use IO, you need to *explicitly* specify on the `setup` line that it should not be included, as in this example:

```
./setup Sod -2d -auto +noio
```

To setup a problem using the Parallel-NetCDF library the user should include either

```
-unit=IO/IOMain/pnetcdf/PM or -unit=IO/IOMain/pnetcdf/UG
```

to the setup line. The predefined shortcut for including the Parallel-NetCDF library is

```
+pnetcdf
```

Note that Parallel-NetCDF IO unit does not have a serial implementation.
If you are using non-fixedblocksize the shortcut

```
+nofbs
```

will bring in both Uniform Grid,set the mode to nonfixed blocksize, and choose the appropriate IO.

Note:

Presently, nonfixed blocksize is only supported by HDF5 parallel IO.

In keeping with the FLASH code architecture, the F90 module `IO_data` stores all the data with `IO` unit scope. The routine `IO_init` is called once by `Driver_initFlash` and initializes `IO` data and stores any runtime parameters. See Chapter 10.

9.2 Output Files

The IO unit can output 4 different types of files: checkpoint files, plotfiles, particle files and flash.dat, a text file holding the integrated grid quantities. FLASH also outputs a logfile, but this file is controlled by the Logfile Unit; see Chapter 25 for a description of that format.

There are a number of runtime parameters that are used to control the output and frequency of IO files. A list of all the runtime parameters and their descriptions for the `IO` unit can be found online `all of them`. Additional description is located in Table 9.2 for checkpoint parameters, Table 9.3 for plotfile parameters, Table 9.4 for particle file parameters, Table 9.5 for flash.dat parameters, and Table 9.6 for genereal IO parameters.

9.2.1 Checkpoint files - Restarting a Simulation

Checkpoint files are used to restart a simulation. In a typical production run, a simulation can be interrupted for a number of reasons— *e.g.*, if the machine crashes, the present queue window closes, the machine runs out of disk space, or perhaps (gasp) there is a bug in FLASH. Once the problem is fixed, a simulation can be restarted from the last checkpoint file rather than the beginning of the run. A checkpoint file contains all the information needed to restart the simulation. The data is stored at full precision of the code (8-byte reals) and includes all of the variables, species, grid reconstruction data, scalar values, as well as meta-data about the run.

The API routine for writing a checkpoint file is `IO_writeCheckpoint`. Users usually will not need to call this routine directly because the FLASH IO unit calls `IO_writeCheckpoint` from the routine `IO_output` which checks the runtime parameters to see if it is appropriate to write a checkpoint file at this time. There are a number of ways to get FLASH to produce a checkpoint file for restarting. Within the flash.par, runtime parameters can be set to dump output. A checkpoint file can be dumped based on elapsed simulation time, elapsed wall clock time or the number of timesteps advanced. A checkpoint file is also produced when the simulation ends, when the max simulation time tmax, the minimum cosmological redshift, or the total number of steps nend has been reached. A user can force a dump to a checkpoint file at another time by creating a file named `.dump_checkpoint` in the output directory of the master processor. This manual action causes FLASH to write a checkpoint in the next timestep. Checkpoint files will continue to be dumped after every timestep as long as the code finds a `.dump_checkpoint` file in the output directory, so the user must remember to remove the file once all the desired checkpoint files have been dumped. Creating a file named `.dump_restart` in the output directory will cause FLASH to output a checkpoint file and then stop the simulation. This technique is useful for producing one last checkpoint file to save time evolution since the last checkpoint, if the machine is going down or a queue window is about to end. These different methods can be combined without problems. Each counter (number of timesteps between last checkpoint, amount of simulation time single last checkpoint, the change in cosmological redshift, and the amount of wall clock time elapsed since the last checkpoint) is independent of the others, and are not influenced by the use of a `.dump_checkpoint` or `.dump_restart`.

Runtime Parameters used to control checkpoint file output include:

Table 9.2: Checkpoint IO parameters.

Parameter	Type	Default value	Description
`checkpointFileNumber`	INTEGER	0	The number of the initial checkpoint file. This number is appended to the end of the filename and incremented at each subsequent output. When restarting a simulation, this indicates which checkpoint file to use.
`checkpointFileIntervalStep`	INTEGER	0	The number of timesteps desired between subsequent checkpoint files.
`checkpointFileIntervalTime`	REAL	1.	The amount of simulation time desired between subsequent checkpoint files.
`checkpointFileIntervalZ`	REAL	HUGE(1.)	The amount of cosmological redshift change that is desired between subsequent checkpoint files.
`rolling_checkpoint`	INTEGER	10000	The number of checkpoint files to keep available at any point in the simulation. If a checkpoint number is greater than `rolling_checkpoint`, then the checkpoint number is reset to 0. There will be at most `rolling_checkpoint` checkpoint files kept. This parameter is intended to be used when disk space is at a premium.
`wall_clock_checkpoint`	REAL	43200.	The maximum amount of wall clock time (seconds) to elapse between checkpoints. When the simulation is started, the current time is stored. If `wall_clock_checkpoint` seconds elapse over the course of the simulation, a checkpoint file is stored. This is useful for ensuring that a checkpoint file is produced before a queue closes.

Table 9.2: Checkpoint IO parameters (continued).

Parameter	Type	Default value	Description
`restart`	`BOOLEAN`	`.false.`	A logical variable indicating whether the simulation is restarting from a checkpoint file (`.true.`) or starting from scratch (`.false.`).

FLASH is capable of restarting from any of the checkpoint files it produces. The user should make sure that the checkpoint file is valid (*e.g.*, the code did not stop while outputting). To tell FLASH to restart, set the `restart` runtime parameter to `.true.` in the `flash.par`. Also, set `checkpointFileNumber` to the number of the file from which you wish to restart. If plotfiles or particle files are being produced set `plotfileNumber` and `particleFileNumber` to the number of the *next* plotfile and particle file you want FLASH to output. In FLASH4 plotfiles and particle file outputs are forced whenever a checkpoint file is written. Sometimes several plotfiles may be produced after the last valid checkpoint file. Resetting `plotfileNumber` to the first plotfile produced after the checkpoint from which you are restarting will ensure that there are no gaps in the output. See Section 9.2.2 for more details on plotfiles.

9.2.2 Plotfiles

A plotfile contains all the information needed to interpret the grid data maintained by FLASH. The data in plotfiles, including the grid metadata such as coordinates and block sizes, are stored at single precision to preserve space. This can, however, be overridden by setting the runtime parameters `plotfileMetadataDP` and/or `plotfileGridQuantityDP` to true to set the grid metadata and the quantities stored on the grid (dens, pres, temp, etc.) to use double precision, respectively. Users must choose which variables to output with the runtime parameters `plot_var_1`, `plot_var_2`, *etc.*, by setting them in the `flash.par` file. For example:

```
plot_var_1 = "dens"
plot_var_2 = "pres"
```

Currently, we support a number of plotvars named `plot_var_`*n* up to the number of `UNKVARS` in a given simulation. Similarly, scratch variables may be output to plot files Section 9.6. At this time, the plotting of face centered quantities is not supported.

FLASH Transition

In FLASH2 a few variables like density and pressure were output to the plotfiles by default. Because FLASH4 supports a wider range of simulations, it makes no assumptions that density or pressure variables are even included in the simulation. In FLASH4 a user *must* define plotfile variables in the `flash.par` file, otherwise the plotfiles will not contain any variables.

The interface for writing a plotfile is the routine `IO_writePlotfile`. As with checkpoint files, the user will not need to call this routine directly because it is invoked indirectly through calling `IO_output` when, based on runtime parameters, FLASH4 needs to write a plotfile. FLASH can produce plotfiles in much the same manner as it does with checkpoint files. They can be dumped based on elapsed simulation time, on steps since the last plotfile dump or by forcing a plotfile to be written by hand by creating a`.dump_plotfile` in the output directory. A plotfile will also be written at the termination of a simulation as well.

If plotfiles are being kept at particular intervals (such as time intervals) for purposes such as visualization or analysis, it is also possible to have FLASH denote a plotfile as “forced”. This designation places the word forced between the basename and the file format type identifier (or the split number if splitting is used). These files are numbered separately from normal plotfiles. By default, plotfiles are considered forced if output for any reason other than the change in simulation time, change in cosmological redshift, change in step number, or the termination of a simulation from reaching `nend` , `zFinal`, or `tmax`. This option can be disabled by setting `ignoreForcedPlot` to true in a simulations `flash.par` file. The following runtime parameters pertain to controlling plotfiles:

Table 9.3: Plotfile IO parameters.

Parameter	Type	Default value	Description
`plotFileNumber`	`INTEGER`	`0`	The number of the starting (or restarting) plotfile. This number is appended to the filename.
`plotFileIntervalTime`	`REAL`	`1.`	The amount of simulation time desired between subsequent plotfiles.
`plotFileIntervalStep`	`INTEGER`	`0`	The number of timesteps desired between subsequent plotfiles.
`plotFileIntervalZ`	`INTEGER`	`HUGE(1.)`	The change in cosmological redshift desired between subsequent plotfiles.
`plot_var_1, ..., plot_var_n`	`STRING`	`"none"`	Name of the variables to store in a plotfile. Up to 12 variables can be selected for storage, and the standard 4-character variable name can be used to select them.
`ignoreForcedPlot`	`BOOLEAN`	`.false.`	A logical variable indicating whether or not to denote certain plotfiles as forced.
`forcedPlotfileNumber`	`INTEGER`	`0`	An integer that sets the starting number for a forced plotfile.
`plotfileMetadataDP`	`BOOLEAN`	`.false.`	A logical variable indicating whether or or not to output the normally single-precision grid metadata fields as double precision in plotfiles. This specifically affects `coordinates`, `block size`, and `bounding box`.
`plotfileGridQuantityDP`	`BOOLEAN`	`.false.`	A logical variable that sets whether or not quantities stored on the grid, such as those stored in `unk`, are output in single precision or double precision in plotfiles.

9.2.3 Particle files

When Lagrangian particles are included in a simulation, the ParticleIO subunit controls input and output of the particle information. The particle files are stored in double precision. Particle data is written to the checkpoint file in order to restart the simulation, but is not written to plotfiles. Hence analysis and metadata about particles is also written to the particle files. The particle files are intended for more frequent dumps. The interface for writing the particle file is `IO_writeParticles`. Again the user will not usually call this function directly because the routine `IO_output` controls particle output based on the runtime parameters controlling particle files. They are controlled in much of the same way as the plotfiles or checkpoint files and can be dumped based on elapsed simulation time, on steps since the last particle dump or by forcing a particle file to be written by hand by creating a `.dump_particle_file` in the output directory. The following runtime parameters pertain to controlling particle files:

Table 9.4: Particle File IO runtime parameters.

Parameter	Type	Default value	Description
`particleFileNumber`	`INTEGER`	`0`	The number of the starting (or restarting) particle file. This number is appended to the end of the filename.
`particleFileIntervalTime`	`REAL`	`1.`	The amount of simulation time desired between subsequent particle file dumps.
`particleFileIntervalStep`	`INTEGER`	`0`	The number of timesteps desired between subsequent particle file dumps.
`particleFileIntervalZ`	`REAL`	`HUGE(1.)`	The change in cosmological redshift desired between subsequent particle file dumps.

FLASH Transition

From FLASH3 on each particle dump is written to a separate file. In FLASH2 the particles data structure was broken up into real and integer parts, where as in FLASH3 all particle properties are real values. See Section 9.9 and Chapter 20 for more information about the particles data structure in FLASH4. Additionally, filtered particles are not implemented in FLASH4.

All the code necessary to output particle data is contained in the `IO` subunit called `IOParticles`. Whenever the `Particles` unit is included in a simulation the correct `IOParticles` subunit will also be included. For example as setup:

```
./setup IsentropicVortex -2d -auto -unit=Particles +ug
```

will include the `IO` unit `IO/IOMain/hdf5/serial/UG` and the correct `IOParticles` subunit `IO/IOParticles/hdf5/serial/UG`. The shortcuts `+parallelio`, `+pnetcdf`, `+ug` will also cause the setup script to pick up the correct `IOParticles` subunit as long as a `Particles` unit is included in the simulation.

9.2.4 Integrated Grid Quantities – flash.dat

At each simulation time step, values which represent the overall state (*e.g.*, total energy and momentum) are computed by calculating over all cells in the computations domain. These integral quantities are written to the ASCI file `flash.dat`. A default routine `IO_writeIntegralQuantities` is provided to output standard measures for hydrodynamic simulations. The user should copy and modify the routine

`IO_writeIntegralQuantities` into a given simulation directory to store any quantities other than the default values. Two runtime parameters pertaining to the `flash.dat` file are listed in the table below.

Table 9.5: flash.dat runtime parameters.

Parameter	Type	Default value	Description
`stats_file`	`STRING`	`"flash.dat"`	Name of the file to which the integral quantities are written.
`wr_integrals_freq`	`INTEGER`	`1`	The number of timesteps to elapse between outputs to the scalar/integral data file (`flash.dat`)

9.2.5 General Runtime Parameters

There are several runtime parameters that pertain to the general IO unit or multiple output files rather than one particular output file. They are listed in the table below.

Table 9.6: General IO runtime parameters.

Parameter	Type	Default value	Description
`basenm`	`STRING`	`"flash_"`	The main part of the output filenames. The full filename consists of the base name, a series of three-character abbreviations indicating whether it is a plotfile, particle file or checkpoint file, the file format, and a 4-digit file number. See Section 9.8 for a description of how FLASH output files are named.
`output_directory`	`STRING`	`""`	Output directory for plotfiles, particle files and checkpoint files. The default is the directory in which the executable sits. `output_directory` can be an absolute or relative path.
`memory_stat_freq`	`INTEGER`	`100000`	The number of timesteps to elapse between memory statistic dumps to the log file (`flash.log`).
`useCollectiveHDF5`	`BOOLEAN`	`.true.`	When using the parallel HDF5 implementation of IO, will enable collective mode for HDF5.
`summaryOutputOnly`	`BOOLEAN`	`.false.`	When set to .true. write an integrated grid quantities file only. Checkpoint, plot and particle files are not written unless the user creates a .dump_plotfile, .dump_checkpoint, .dump_restart or .dump_particle file.

9.3 Restarts and Runtime Parameters

FLASH4 outputs the runtime parameters of a simulation to all checkpoint files. When a simulation is restarted, these values are known by the `RuntimeParameters` unit while the code is running. On a restart, all values from the checkpoint used in the restart are stored as previous values in the lists kept by the `RuntimeParameters` unit. All current values are taken from the defaults used by FLASH4 and any simulation parameter files (*e.g.*, `flash.par`). If needed, the previous values from the checkpoint file can be obtained using the routines `RuntimeParameters_getPrev`.

9.4 Output Scalars

In FLASH4, each unit has the opportunity to request scalar data to be output to checkpoint or plotfiles. Because there is no central database, each unit "owns" different data in the simulation. For example, the `Driver` unit owns the timestep variable `dt`, the simulation variable `simTime`, and the simulation step number `nStep`. The `Grid` unit owns the sizes of each block, `nxb`, `nyb`, and `nzb`. The `IO` unit owns the variable `checkpointFileNumber`. Each of these quantities are output into checkpoint files. Instead of hard coding the values into checkpoint routines, FLASH4 offers a more flexible interface whereby each unit sends its data to the `IO` unit. The `IO` unit then stores these values in a linked list and writes them to the checkpoint file or plotfile. Each unit has a routine called "*Unit*`_sendOutputData`", *e.g.*, `Driver_sendOutputData` and `Grid_sendOutputData`. These routines in turn call `IO_setScalar`. For example, the routine `Grid_sendOutputData` calls

```
IO_setScalar("nxb", NXB)
IO_setScalar("nyb", NYB)
IO_setScalar("nzb", NZB)
```

To output additional simulation scalars in a checkpoint file, the user should override one of the "*Unit*`_sendOutputData`" or `Simulation_sendOutputData`.

After restarting a simulation from a checkpoint file, a unit might call `IO_getScalar` to reset a variable value. For example, the `Driver` unit calls `IO_getScalar("dt", dr_dt)` to get the value of the timestep `dt` reinitialized from the checkpoint file. A value from the checkpoint file can be obtained by calling `IO_getPrevScalar`. This call can take an optional argument to find out if an error has occurred in finding the previous value, most commonly because the value was not found in the checkpoint file. By using this argument, the user can then decide what to do if the value is not found. If the scalar value is not found and the optional argument is not used, then the subroutine will call `Driver_abortFlash` and terminate the run.

9.5 Output User-defined Arrays

Often in a simulation the user needs to output additional information to a checkpoint or plotfile which is not a grid scope variable. In FLASH2 any additional information had to be hard coded into the simulation. In FLASH4, we have provided a general interface `IO_writeUserArray` and `IO_readUserArray` which allows the user to write and read any generic array needed to be stored. The above two functions do not have any implementation and it is up to the user to fill them in with the needed calls to the HDF5 or pnetCDF C routines. We provide implementation for reading and writing integer and double precision arrays with the helper routines `io_h5write_generic_iarr`, `io_h5write_generic_rarr`, `io_ncmpi_write_generic_iarr`, and `io_ncmpi_write_generic_rarr`. Data is written out as a 1-dimensional array, but the user can write multidimensional arrays simply by passing a reference to the data and the total number of elements to write. See these routines and the simulation `StirTurb` for details on their usage.

9.6 Output Scratch Variables

In FLASH4 a user can allocate space for a scratch or temporary variable with grid scope using one of the `Config` keywords `SCRATCHVAR`, `SCRATCHCENTERVAR`, `SCRATCHFACEXVAR`,`SCRATCHFACEYVAR` or `SCRATCHFACEZVAR` (see Section 5.5.1). To output these scratch variables, the user only needs to set the values of the runtime parameters `plot_grid_var_1`, `plot_grid_var_2`, *etc.*, by setting them in the `flash.par` file. For example to output the magnitude of vorticity with a declaration in a `Config` file of `SCRATCHVAR mvrt`:

```
plot_grid_var_1 = "mvrt"
```

Note that the post-processing routines like `fidlr` do not display these variables, although they are present in the output file. Future implementations may support this visualization.

9.7 Face-Centered Data

Face-centered variables are now output to checkpoint files, when they are declared in a configuration file. Presently, up to nine face-centered variables are supported in checkpoint files. Plotfile output of face-centered data is not yet supported.

9.8 Output Filenames

FLASH constructs the output filenames based on the user-supplied basename, (runtime parameter `basenm`) and the file counter that is incremented after each output. Additionally, information about the file type and data storage is included in the filename. The general checkpoint filename is:

$$\texttt{basename\_s0000\_}\left\{\begin{array}{c}\texttt{hdf5}\\ \texttt{ncmpi}\end{array}\right\}\texttt{\_chk\_0000}\ ,$$

where `hdf5` or `ncmpi` (prefix for PnetCDF) is picked depending on the particular IO implementation, the number following the “s” is the split file number, if split file IO is in use, and the number at the end of the filename is the current checkpointFileNumber. (The PnetCDF function prefix ”`ncmpi`” derived from the serial NetCDF calls beginning with ”`nc`”)

The general plotfile filename is:

$$\texttt{basename\_s0000\_}\left\{\begin{array}{c}\texttt{hdf5}\\ \texttt{ncmpi}\end{array}\right\}\texttt{\_plt\_}\left\{\begin{array}{c}\texttt{crn}\\ \texttt{cnt}\end{array}\right\}\texttt{\_0000}\ ,$$

where `hdf5` or `ncmpi` is picked depending on the IO implementation used, `crn` and `cnt` indicate data stored at the cell corners or centers respectively, the number following “s” is the split file number, if used, and the number at the end of the filename is the current value of `plotfileNumber`. `crn` is reserved, even though corner data output is not presently supported by FLASH4’s IO.

FLASH Transition

In FLASH2 the correct format of the names of the checkpoint, plotfile and particle file were necessary in order to read the files with the FLASH fidlr visualization tool. In FLASH4 the name of the file is irrelevant to fidlr3.0 (see Chapter 34). We have kept the same naming convention for consistency but the user is free to rename files. This can be helpful during post-processing or when comparing two files.

9.9 Output Formats

HDF5 is our most most widely used IO library although Parallel-NetCDF is rapidly gaining acceptance among the high performance computing community. In FLASH4 we also offer a serial direct FORTRAN IO which is currently only implemented for the uniform grid. This option is intended to provide users a way to output data if they do not have access to HDF5 or PnetCDF. Additionally, if HDF5 or PnetCDF are not performing well on a given platform the direct IO implementation can be used as a last resort. Our tools, fidlr and sfocu (Part X), do not currently support the direct IO implementation, and the output files from this mode are not portable across platforms.

9.9.1 HDF5

HDF5 is supported on a large variety of platforms and offers large file support and parallel IO via MPI-IO. Information about the different versions of HDF can be found at `http://www.ncsa.illinois.edu/`. The IO in FLASH4 implementations require HDF5 1.4.0 or later. Please note that HDF5 1.6.2 requires IDL 1.6 or higher in order to use fidlr3.0 for post processing.

Implementations of the `HDF5 IO` unit use the HDF application programming interface (API) for organizing data in a database fashion. In addition to the raw data, information about the data type and byte ordering (little- or big-endian), rank, and dimensions of the dataset is stored. This makes the HDF format extremely portable across platforms. Different packages can query the file for its contents without knowing the details of the routine that generated the data.

FLASH provides different HDF5 IO unit implementations – the serial and parallel versions for each supported grid, Uniform Grid and `PARAMESH`. It is important to remember to match the IO implementation with the correct grid, although the `setup` script generally takes care of this matching. `PARAMESH` 2, `PARAMESH` 4.0, and `PARAMESH` 4dev all work with the `PARAMESH` (PM) implementation of IO. Nonfixed blocksize IO has its own implementation in parallel, and is presently not supported in serial mode. Examples are given below for the five different HDF5 IO implementations.

```
./setup Sod -2d -auto -unit=IO/IOMain/hdf5/serial/PM (included by default)
./setup Sod -2d -auto -unit=IO/IOMain/hdf5/parallel/PM
./setup Sod -2d -auto -unit=Grid/GridMain/UG -unit=IO/IOMain/hdf5/serial/UG
./setup Sod -2d -auto -unit=Grid/GridMain/UG -unit=IO/IOMain/hdf5/parallel/UG
./setup Sod -2d -auto -nofbs -unit=Grid/GridMain/UG -unit=IO/IOMain/hdf5/parallel/NoFbs
```

The default IO implementation is `IO/IOMain/hdf5/serial/PM`. It can be included simply by adding `-unit=IO` to the `setup` line. In FLASH4, the user can set up shortcuts for various implementations. See Chapter 5 for more information about creating shortcuts.

The format of the HDF5 output files produced by these various IO implementations is identical; only the method by which they are written differs. It is possible to create a checkpoint file with the parallel routines and restart FLASH from that file using the serial routines or vice-versa. (This switch would require resetting up and compiling a code to get an executable with the serial version of IO.) When outputting with the Uniform Grid, some data is stored that isn't explicitly necessary for data analysis or visualization, but is retained to keep the output format of `PARAMESH` the same as with the Uniform Grid. See Section 9.9.1.3 for more information on output data formats. For example, the refinement level in the Uniform Grid case is always equal to 1, as is the nodetype array. A tree structure for the Uniform Grid is 'faked' for visualization purposes. In a similar way, the non-fixedblocksize mode outputs all of the data stored by the grid as though it is one large block. This allows restarting with differing numbers of processors and decomposing the domain in an arbitrary fashion in Uniform Grid.

Parallel HDF5 mode has two runtime parameters useful for debugging: `chkGuardCellsInput` and `chkGuardCellsOutput`. When these runtime parameters are true, the FLASH4 input and output routines read and/or output the guard cells in addition to the normal interior cells. Note that the HDF5 files produced are *not* compatible with the visualization and analysis tools provided with FLASH4.

9.9.1.1 Collective Mode

By default, the parallel mode of HDF5 uses an independent access pattern for writing datasets and performs IO without aggregating the disk access for writing. Parallel HDF5 can also be run so that the writes to the file's datasets are aggregated, allowing the data from multiple processors to be written to disk in fewer operations. This can greatly increase the performance of IO on filesystems that support this behavior. FLASH4 can make use of this mode by setting the runtime parameter `useCollectiveHDF5` to true.

FLASH Transition

We recommend that HDF5 version 1.6 or later be used with the HDF5 IO implementations with FLASH4. While it is possible to use any version of HDF5 1.4.0 or later, files produced with versions predating version 1.6 will not be compatible with code using the libraries post HDF5 1.6.

Caution

If you are using version HDF5 >= 1.8 then you must explicitly use HDF5 1.6 API bindings. Either build HDF5 library with "–with-default-api-version=v16" configure option or compile FLASH with the C preprocessor definition H5_USE_16_API. Our preference is to set CFLAGS_HDF5 Makefile.h variable, e.g., for a GNU compilation:

```
CFLAGS_HDF5 = -I\${HDF5_PATH}/include -DH5_USE_16_API
```

9.9.1.2 Machine Compatibility

The HDF5 modules have been tested successfully on the ASC platforms and on a Linux clusters. Performance varies widely across the platforms, but the parallel version is usually faster than the serial version. Experience on performing parallel IO on a Linux Cluster using PVFS is reported in Ross *et al.* (2001). Note that for clusters without a parallel filesystem, you should not use the parallel HDF5 IO module with an NFS mounted filesystem. In this case, all of the information will still have to pass through the node from which the disk is hanging, resulting in contention. It is recommended that a serial version of the HDF5 unit be used instead.

9.9.1.3 HDF5 Data Format

The HDF5 data format for FLASH4 is identical to FLASH2 for all grid variables and datastructures used to recreate the tree and neighbor data with the exception that `bounding box`, `coordinates`, and `block size` are now sized as `mdim`, or the maximum dimensions supported by FLASH's grids, which is three, rather than `ndim`. `PARAMESH` 4.0 and `PARAMESH` 4dev, however, do requires a few additional tree data structures to be output which are described below. The format of the metadata stored in the HDF5 files has changed to reduce the number of 'writes' required. Additionally, scalar data, like `time, dt, nstep`, *etc.*, are now stored in a linked list and written all at one time. Any unit can add scalar data to the checkpoint file by calling the routine `IO_setScalar`. See Section 9.4 for more details. The FLASH4 HDF5 format is summarized in Table 9.7.

Table 9.7: FLASH HDF5 file format.

Record label	Description of the record
Simulation Meta Data: included in all files	

Table 9.7: HDF5 format (continued).

Record label	Description of the record
sim info	Stores simulation meta data in a user defined C structure. Structure datatype and attributes of the structure are described below.

```
typedef struct sim_info_t {
  int file_format_version;
  char setup_call[400];
  char file_creation_time[MAX_STRING_LENGTH];
  char flash_version[MAX_STRING_LENGTH];
  char build_date[MAX_STRING_LENGTH];
  char build_dir[MAX_STRING_LENGTH];
  char build_machine[MAX_STRING_LENGTH];
  char cflags[400];
  char fflags[400];
  char setup_time_stamp[MAX_STRING_LENGTH];
  char build_time_stamp[MAX_STRING_LENGTH];
} sim_info_t;

sim_info_t sim_info;
```

`sim_info.file_format_version`:	An integer giving the version number of the HDF5 file format. This is incremented anytime changes are made to the layout of the file.
`sim_info.setup_call`:	The complete syntax of the `setup` command used when creating the current FLASH executable.
`sim_info.file_creation_time`:	The time and date that the file was created.
`sim_info.flash_version`:	The version of FLASH used for the current simulation. This is returned by routine `setup_flashVersion`.
`sim_info.build_date`:	The date and time that the FLASH executable was compiled.
`sim_info.build_dir`:	The complete path to the FLASH root directory of the source tree used when compiling the FLASH executable. This is generated by the subroutine `setup_buildstats` which is created at compile time by the Makefile.
`sim_info.build_machine`:	The name of the machine (and anything else returned from `uname -a`) on which FLASH was compiled.
`sim_info.cflags`:	The c compiler flags used in the given simulation. The routine `setup_buildstats` is written by the `setup` script at compile time and also includes the `fflags` below.
`sim_info.fflags`:	The f compiler flags used in the given simulation.

Table 9.7: HDF5 format (continued).

Record label	Description of the record
`sim_info.setup_time_stamp`:	The date and time the given simulation was setup. The routine `setup_buildstamp` is created by the `setup` script at compile time.
`sim_info.build_time_stamp`:	The date and time the given simulation was built. The routine `setup_buildstamp` is created by the `setup` script at compile time.

RuntimeParameter and Scalar data
Data are stored in linked lists with the nodes of each entry for each type listed below.

```
typedef struct int_list_t {
  char name[MAX_STRING_LENGTH];
  int value;
} int_list_t;

typedef struct real_list_t {
  char name[MAX_STRING_LENGTH];
  double value;
} real_list_t;

typedef struct str_list_t {
  char name[MAX_STRING_LENGTH];
  char value[MAX_STRING_LENGTH];
} str_list_t;

typedef struct log_list_t {
  char name[MAX_STRING_LENGTH];
  int value;
} log_list_t;

int_list_t  *int_list;
real_list_t  *real_list;
str_list_t  *str_list;
log_list_t  *log_list;
```

integer runtime parameters	`int_list_t int_list(numIntParams)` A linked list holding the names and values of all the integer runtime parameters.
real runtime parameters	`real_list_t real_list(numRealParams)` A linked list holding the names and values of all the real runtime parameters.
string runtime parameters	`str_list_t str_list(numStrParams)` A linked list holding the names and values of all the string runtime parameters.

Table 9.7: HDF5 format (continued).

Record label	Description of the record
logical runtime parameters	`log_list_t log_list(numLogParams)` A linked list holding the names and values of all the logical runtime parameters.
integer scalars	`int_list_t int_list(numIntScalars)` A linked list holding the names and values of all the integer scalars.
real scalars	`real_list_t real_list(numRealScalars)` A linked list holding the names and values of all the real scalars.
string scalars	`str_list_t str_list(numStrScalars)` A linked list holding the names and values of all the string scalars.
logical scalars	`log_list_t log_list(numLogScalars)` A linked list holding the names and values of all the logical scalars.
Grid data: included only in checkpoint files and plotfiles	
unknown names	`character*4 unk_names(nvar)` This array contains four-character names corresponding to the first index of the `unk` array. They serve to identify the variables stored in the 'unknowns' records.
refine level	`integer lrefine(globalNumBlocks)` This array stores the refinement level for each block.
node type	`integer nodetype(globalNumBlocks)` This array stores the node type for a block. Blocks with node type 1 are leaf nodes, and their data will always be valid. The leaf blocks contain the data which is to be used for plotting purposes.
gid	`integer gid(nfaces+1+nchild,globalNumBlocks)` This is the global identification array. For a given block, this array gives the block number of the blocks that neighbor it and the block numbers of its parent and children.
coordinates	`real coord(mdim,globalNumBlocks)` This array stores the coordinates of the center of the block. `coord(1,blockID)` = x-coordinate `coord(2,blockID)` = y-coordinate `coord(3,blockID)` = z-coordinate

Table 9.7: HDF5 format (continued).

Record label	Description of the record
block size	`real size(mdim,globalNumBlocks)` This array stores the dimensions of the current block. `size(1,blockID)` = x size `size(2,blockID)` = y size `size(3,blockID)` = z size
bounding box	`real bnd_box(2,mdim,globalNumBlocks)` This array stores the minimum (`bnd_box(1,:,:)`) and maximum (`bnd_box(2,:,:)`) coordinate of a block in each spatial direction.
which child (*Paramesh4.0 and Paramesh4dev only!*)	`integer which_child(globalNumBlocks)` An integer array identifying which part of the parents' volume this child corresponds to.
variable	`real unk(nxb,nyb,nzb,globalNumBlocks)` `nx` = number of cells/block in x `ny` = number of cells/block in y `nz` = number of cells/block in z This array holds the data for a single variable. The record label is identical to the four-character variable name stored in the record *unknown names*. Note that, for a plot file with `CORNERS=.true.` in the parameter file, the information is interpolated to the cell corners and stored.
Particle Data: included in checkpoint files and particle files	
localnp	`integer localnp(globalNumBlocks)` This array holds the number of particles on each processor.
particle names	`character*24 particle_labels(NPART_PROPS)` This array contains twenty four-character names corresponding to the attributes in the particles array. They serve to identify the variables stored in the 'particles' record.
tracer particles	`real particles(NPART_PROPS, globalNumParticles` Real array holding the particles data structure. The first dimension holds the various particle properties like, velocity, tag etc. The second dimension is sized as the total number of particles in the simulation. Note that all the particle properties are real values.

9.9.1.4 Split File IO

On machines with large numbers of processors, IO may perform better if, all processors write to a limited number of separate files rather than one single file. This technique can help mitigate IO bottlenecks and contention issues on these large machines better than even parallel-mode IO can. In addition this technique has the benefit of keeping the number of output files much lower than if every processor writes its own file. Split file IO can be enabled by setting the `outputSplitNum` parameter to the number of files desired (i.e. if `outputSplitNum` is set to 4, every checkpoint, plotfile and parfile will be broken into 4 files, by processor number). This feature is only available with the HDF5 parallel IO mode, and is still experimental. Users should use this at their own risk.

9.9.2 Parallel-NetCDF

Another implementation of the IO unit uses the Parallel-NetCDF library available at `http://www.mcs.anl.gov/parallel-netcdf/`. At this time, the FLASH code requires version 1.1.0 or higher. Our testing shows performance of PNetCDF library to be very similar to HDF5 library when using collective I/O optimizations in parallel I/O mode.

There are two different PnetCDF IO unit implementations. Both are parallel implementations, one for each supported grid, the Uniform Grid and `PARAMESH`. It is important to remember to match the IO implementation with the correct grid. To include PnetCDF IO in a simulation the user should add `-unit=IO/IOMain/pnetcdf.....` to the `setup` line. See examples below for the two different PnetCDF IO implementations.

```
./setup Sod -2d -auto -unit=IO/IOMain/pnetcdf/PM
./setup Sod -2d -auto -unit=Grid/GridMain/UG -unit=IO/IOMain/pnetcdf/UG
```

The paths to these IO implementations can be long and tedious to type, users are advised to set up shortcuts for various implementations. See Chapter 5 for information about creating shortcuts.

To the end-user, the PnetCDF data format is very similar to the HDF5 format. (Under the hood the data storage is quite different.) In HDF5 there are datasets and dataspaces, in PnetCDF there are dimensions and variables. All the same data is stored in the PnetCDF checkpoint as in the HDF5 checkpoint file, although there are some differences in how the data is stored. The grid data is stored in multidimensional arrays, as it is in HDF5. These are unknown names, refine level, node type, gid, coordinates, proc number, block size and bounding box. The particles data structure is also stored in the same way. The simulation metadata, like file format version, file creation time, `setup` command line, *etc.*, are stored as global attributes. The runtime parameters and the output scalars are also stored as attributes. The `unk` and particle labels are also stored as global attributes. In PnetCDF, all global quantities must be consistent across all processors involved in a write to a file, or else the write will fail. All IO calls are run in a collective mode in PnetCDF.

9.9.3 Direct IO

As mentioned above, the direct IO implementation has been added so users can always output data even if the HDF5 or pnetCDF libraries are unavailable. The user should examine the two helper routines `io_writeData` and `io_readData`. Copy the base implementation to a simulation directory, and modify them in order to write out specifically what is needed. To include the direct IO implementation add the following to your setup line:

```
-unit=IO/IOMain/direct/UG or -unit=IO/IOMain/direct/PM
```

9.9.4 Output Side Effects

In FLASH4 when plotfiles or checkpoint files are output by `IO_output`, the grid is fully restricted and user variables are computed prior to writing the file. `IO_writeCheckpoint` and `IO_writePlotfile` by default, do not do this step themselves. The restriction can be forced for all writes by setting runtime parameter `alwaysRestrictCheckpoint` to true and the user variables can always be computed prior to output by setting `alwaysComputeUserVars` to true.

9.10 Working with Output Files

The checkpoint file output formats offer great flexibility when visualizing the data. The visualization program does not have to know the details of how the file was written; rather it can query the file to find the number of dimensions, block sizes, variable data etc that it needs to visualize the data. `IDL` routines for reading HDF5 and PnetCDF formats are provided in `tools/fidlr3/`. These can be used interactively though the `IDL` command line (see Chapter 34). In addition, ViSit version 10.0 and higher (see Chapter 31) can natively read FLASH4 HDF5 output files by using the command line option `-assume_format FLASH`.

9.11 Unit Test

The `IO` unit test is provided to test IO performance on various platforms with the different FLASH IO implementations and parallel libraries.

FLASH Transition

The `IO` unit test replaces the simulation setup `io_benchmark` in FLASH2.

The `unitTest` is setup like any other FLASH4 simulation. It can be run with any IO implementation as long as the correct Grid implementation is included. This `unitTest` writes a checkpoint file, a plotfile, and if particles are included, a particle file. Particles IO can be tested simply by including particles in the simulation. Variables needed for particles should be uncommented in the `Config` file.

Example setups:

```
#setup for PARAMESH Grid and serial HDF5 io
./setup unitTest/IO -auto

#setup for PARAMESH Grid with parallel HDF5 IO (see shortcuts docs for explanation)
./setup unitTest/IO -auto +parallelIO     (same as)
./setup unitTest/IO -auto -unit=IO/IOMain/hdf5/parallel/PM

#setup for Uniform Grid with serial HDF5 IO, 3d problem, increasing default number of zones
./setup unitTest/IO -3d -auto +ug -nxb=16 -nyb=16 -nzb=16  (same as)
./setup unitTest/IO -3d -auto -unit=Grid/GridMain/UG -nxb=16 -nyb=16 -nzb=16


#setup for PM3 and parallel netCDF, with particles
./setup unitTest/IO -auto -unit=Particles +pnetcdf


#setup for UG and parallel netCDF
./setup unitTest/IO -auto +pnetcdf +ug
```

Run the test like any other FLASH simulation:

```
mpirun -np numProcs flash3
```

There are a few things to keep in mind when working with the IO unit test:

- The Config file in unitTest/IO declares some dummy grid scope variables which are stored in the unk array. If the user wants a more intensive IO test, more variables can be added. Variables are initialized to dummy values in `Driver_evolveFlash`.
- Variables will only be output to the plotfile if they are declared in the `flash.par` (see the example `flash.par` in the unit test).

- The only units besides the simulation unit included in this simulation are `Grid, IO, Driver, Timers, Logfile, RuntimeParameters` and `PhysicalConstants`.
- If the `PARAMESH` Grid implementation is being used, it is important to note that the grid will not refine on its own. The user should set `lrefine_min` to a value > 1 to create more blocks. The user could also set the runtime parameters `nblockx`, `nblocky`, `nblockz` to make a bigger problem.
- Just like any other simulation, the user can change the number of zones in a simulation using `-nxb=-numZones` on the setup line.

9.12 Chombo

In FLASH4 we introduced a new `Grid` implementation that depends on `Chombo` library (see Section 8.7). An application built with this `Grid` implementation will include `IO/IOMain/chombo` by default. No other I/O implementation is compatible with `Chombo Grid` implementation. As before, I/O can be excluded from an application using the `+noio` setup shortcut.

Data files are written in standard `Chombo` file layout in HDF5 format. The visualization tool `VisIt` supports `Chombo` file layout, but other tools, such as `fidlr` and `sfocu`, are incompatible with Chombo file layout.

9.13 Derived data type I/O

In FLASH4 we introduced an alternative I/O implementation for both HDF5 and Parallel-NetCDF which is a slight spin on the standard parallel I/O implementations. In this new implementation we select the data from the mesh data structures directly using HDF5 hyperslabs (HDF5) and MPI derived datatypes (Parallel-NetCDF) and then write the selected data to datasets in the file. This eliminates the need for manually copying data into a FLASH allocated temporary buffer and then writing the data from the temporary buffer to disk.

You can include derived data type I/O in your FLASH application by adding the setup shortcuts `+hdf5TypeIO` for HDF5 and `+pnetTypeIO` for Parallel-NetCDF to your setup line. If you are using the HDF5 implementation then you need a parallel installation of HDF5. All of the runtime parameters introduced in this chapter should be compatible with derived data type I/O.

A nice property of derived data type I/O is that it eliminates a lot of the I/O code duplication which has been spreading in the FLASH I/O unit over the last decade. The same code is used for UG, NoFBS and Paramesh FLASH applications and we have also shared code between the HDF5 and Parallel-NetCDF implementations. A technical reason for using the new I/O implementation is that we provide more information to the I/O libraries about the exact data we want to read from / write to disk. This allows us to take advantage of recent enhancements to I/O libraries such as the nonblocking APIs in the Parallel-NetCDF library. We discuss experimentation with this API and other ideas in the paper "A Case Study for Scientific I/O: Improving the FLASH Astrophysics Code" `www.mcs.anl.gov/uploads/cels/papers/P1819.pdf`

The new I/O code has been tested in our internal FLASH regression tests from before the FLASH4 release and there are no known issues, however, it will probably be in the release following FLASH4 when we will recommend using it as the default implementation. We have made the research ideas from our case study paper usable for all FLASH applications, however, the code still needs a clean up and exhaustive testing with all the FLASH runtime parameters introduced in this chapter.

Chapter 10

Runtime Parameters Unit

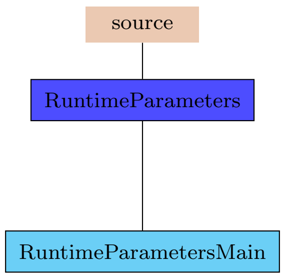

Figure 10.1: The `RuntimeParameters` unit directory tree.

The `RuntimeParameters` Unit stores and maintains a global linked lists of runtime parameters that are used during program execution. Runtime parameters can be added to the lists, have their values modified, and be queried. This unit handles adding the default runtime parameters to the lists as well as reading any overwritten parameters from the `flash.par` file.

10.1 Defining Runtime Parameters

All parameters must be declared in a `Config` file with the keyword declaration `PARAMETER`. In the `Config` file, assign a data type and a default value for the parameter. If possible, assign a range of valid values for the parameter. You can also provide a short description of the parameter's function in a comment line that begins with D.

```
#section of Config file for a Simulation
D myParameter Description of myParameter
PARAMETER myParameter REAL 22.5  [20 to 60]
```

To change the runtime parameter's value from the default, assign a new value in the flash.par for the simulation.

```
#snippet from a flash.par
myParameter = 45.0
```

See Section 5.5 for more information on declaring parameters in a `Config` file.

10.2 Identifying Valid Runtime Parameters

The values of runtime parameters are initialized either from default values defined in the `Config` files, or from values explicitly set in the file `flash.par`. Variables that have been changed from default are noted in the

```
=======================================================
RuntimeParameters:
=======================================================
pt_numx                      =        10 [CHANGED]
pt_numy                      =         5 [CHANGED]
checkpointfileintervalstep   =         0
```

Figure 10.2: Section of output log showing runtime parameters values

```
physics/Eos/EosMain/Multigamma
    gamma [REAL] [1.6667]
        Valid Values: Unconstrained
        Ratio of specific heats for gas

physics/Hydro/HydroMain
    cfl [REAL] [0.8]
        Valid Values: Unconstrained
        Courant factor
```

Figure 10.3: Portion of a `setup_params` file from an object directory.

simulation's output log. For example, the RuntimeParameters section of the output log shown in Figure 10.2 indicates that `pt_numx` and `pt_numy` have been read in from `flash.par` and are different than the default values, whereas the runtime parameter `checkpointFileIntervalStep` has been left at the default value of 0.

After a simulation has been configured with a `setup` call, all possible valid runtime parameters are listed in the file `setup_params` located in the `object` directory (or whatever directory was chosen with `-objdir=`) with their default values. This file groups the runtime parameters according to the units with which they are associated and in alphabetical order. A short description of the runtime parameter, and the valid range or values if known, are also given. See Figure 10.3 for an example listing.

10.3 Routine Descriptions

The Runtime Parameters unit is included by default in all of the provided FLASH simulation examples, through a dependence within the `Driver` unit. The main FLASH initialization routine (`Driver_initFlash`) and the initialization code created by `setup` handles the creation and initialization of the runtime parameters, so users will mainly be interested in querying parameter values. Because the RuntimeParameters routines are overloaded functions which can handle character, real, integer, or logical arguments, the user *must* make sure to `use` the interface file `RuntimeParameters_Interfaces` in the calling routines.

The user will typically only have to use one routine from the Runtime Parameters API, `RuntimeParameters_get`. This routine retrieves the value of a parameter stored in the linked list in the `RuntimeParameters_data` module. In FLASH4 the value of runtime parameters for a given unit are stored in that unit's `Unit_data` Fortran module and they are typically initialized in the unit's `Unit_init` routine. Each unit's 'init' routine is only called once at the beginning of the simulation by `Driver_initFlash`. For more documentation on the FLASH code architecture please see Chapter 4. It is important to note that even though runtime parameters are declared in a specific unit's `Config` file, the runtime parameters linked list is a global space and so any unit can fetch a parameter, even if that unit did not declare it. For example, the `Driver` unit declares the logical parameter `restart`, however, many units, including the `IO` unit get `restart` parameter with the `RuntimeParameters_get` interface. If a section of the code asks for a runtime parameter that was not declared in a `Config` file and thus is not in the runtime parameters linked list, the FLASH code will call `Driver_abortFlash` and stamp an error to the `logfile`. The other RuntimeParameter routines in the API are not generally called by user routines. They exist because various other units within FLASH need to access parts of the RuntimeParameters interface. For example, the input/output unit `IO` needs `RuntimeParameters_set`. There are no user-defined parameters which affect the `RuntimeParameters` unit.

FLASH Transition

FLASH no longer distinguishes between contexts as in FLASH2. All runtime parameters are stored in the same context, so there is no need to pass a 'context' argument.

10.4 Example Usage

An implementation example from the `IO_init` is straightforward. First, use the module containing definitions for the unit (for `_init` subroutines, the usual `use Unit_data, ONLY:` structure is waived). Next, use the module containing interface definitions of the `RuntimeParameters` unit, *i.e.*, `use RuntimeParameters_-interface, ONLY:`. Finally, read the runtime parameters and store them in unit-specific variables.

```
subroutine IO_init()

  use IO_data
  use RuntimeParamters_interface, ONLY : RuntimeParameters_get
  implicit none



  call RuntimeParameters_get('plotFileNumber',io_plotFileNumber)
  call RuntimeParameters_get('checkpointFileNumber',io_checkpointFileNumber)

  call RuntimeParameters_get('plotFileIntervalTime',io_plotFileIntervalTime)
  call RuntimeParameters_get('plotFileIntervalStep',io_plotFileIntervalStep)
  call RuntimeParameters_get('checkpointFileIntervalTime',io_checkpointFileIntervalTime)
  call RuntimeParameters_get('checkpointFileIntervalStep',io_checkpointFileIntervalStep)

  !! etc ...
```

Note that the parameters found in the `flash.par` or in the `Config` files, for example `plotFileNumber`, are generally stored in a variable of the same name with a unit prefix prepended, for example `io_plotFileNumber`. In this way, a program segment clearly indicates the origin of variables. Variables with a unit prefix (*e.g.*, `io_` for `IO`, `pt_` for particles) have been initialized from the `RuntimeParameters` database, and other variables are locally declared. When creating new simulations, runtime parameters used as variables should be prefixed with `sim_`.

Chapter 11

Multispecies Unit

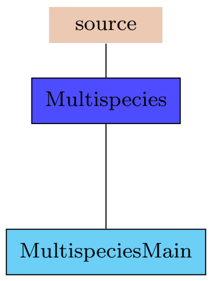

Figure 11.1: The `Multispecies` unit directory tree.

FLASH has the ability to track multiple fluids, each of which can have its own properties. The `Multispecies` unit handles setting and querying on the properties of fluids, as well as some common operations on properties. The advection and normalization of species is described in the context of the Hydro unit in Chapter 15.

11.1 Defining Species

The names and properties of fluids are accessed by using their constant integer values defined in the `Flash.h` header file. The species names are defined in a `Config` file. The names of the species, for example `AIR`, `NI56`, are given in the `Config` file with keyword `SPECIES`.

In the traditional method for defining species, this `Config` would typically be the application's `Config` file in the `Simulation` unit. In the alternative method described below in Section 11.4, `SPECIES` are normally not listed explicitly in the `Simulation` unit `Config`, but instead are automatically generated by `Multispecies/MultispeciesMain/Config` based on the contents of the `species` setup variable. Either way, the `setup` procedure transforms those names into accessor integers with the appended description `_SPEC`.

These names are stored in the `Flash.h` file. The total number of species defined is also defined within `Flash.h` as `NSPECIES`, and the integer range of their definition is given by `SPECIES_BEGIN` and `SPECIES_END`. To access the species in your code, use the index listed in `Flash.h`, for example `AIR_SPEC`, `NI56_SPEC`.

Note that `NSPECIES`, `SPECIES_BEGIN`, and `SPECIES_END` are always defined, whether a simulation uses multiple species or not (and whehter the simulation includes the `Multispecies` unit or not). However, if `NSPECIES`$= 0$, `SPECIES_END` will be less than `SPECIES_BEGIN`, and then neither of them should be used as an index into solution vectors.

As an illustration, Figures Figure 11.2 and Figure 11.3 are snippets from a configuration file and the corresponding section of the FLASH header file, respectively. For more information on `Config` files, see

```
# Portion of a Config file for a Simulation
SPECIES AIR
SPECIES SF6
```

Figure 11.2: Sample `Config` file showing how to define required fluid species.

```
#define SPECIES_BEGIN (NPROP_VARS + CONSTANT_ONE)
#define AIR_SPEC 11
#define SF6_SPEC 12
#define NSPECIES 2
#define SPECIES_END (SPECIES_BEGIN + NSPECIES - CONSTANT_ONE)
```

Figure 11.3: Sample excerpt from header file `Flash.h` showing integer definition of fluid species.

Section 5.5; for more information on the `setup` procedure, see Chapter 5; for more information on the structure of the main header file `Flash.h`, see Chapter 6.

FLASH Transition

In FLASH2, you found the integer index of a species by using `find_fluid_index`. In FLASH4, the species index is always available because it is defined in `Flash.h`. Use the index directory, as in `xIn(NAME_SPEC - SPECIES_BEGIN + 1) = solnData(NAME_SPEC,i,j,k)`. But be careful that the species name is really defined in your simulation! You can test with

```
if (NAME_SPEC /= NONEXISTENT) then
    okVariable = solnData(NAME_SPEC,i,j,k)
endif
```

The available properties of an individual fluid are listed in Table 11.1 and are defined in file `Multispecies.h`. In order to reference the properties in code, you must `#include` the file `Multispecies.h`. The initialization of properties is described in the following section.

11.2 Initializing Species Information in `Simulation_initSpecies`

Before you can work with the properties of a fluid, you must initialize the data in the `Multispecies` unit. Normally, initialization is done in the routine `Simulation_initSpecies`. An example procedure is shown below and consists of setting relevant properties for all fluids/`SPECIES` defined in the `Config` file. Fluids do not have to be isotopes; any molecular substance which can be defined by the properties shown in Figure 11.4 is a valid input to the Multispecies unit.

FLASH Transition

For nuclear burning networks, a `Simulation_initSpecies` routine is already predefined. It automatically initializes all isotopes found in the `Config` file. To use this shortcut, `REQUIRE` the module `Simulation/SimulationComposition` in the `Config` file.

Table 11.1: Properties available through the Multispecies unit.

Property Name	Description	Data type
A	Number of protons and neutrons in nucleus	real
Z	Atomic number	real
N	Number of neutrons	real
E	Number of electrons	real
BE	Binding Energy	real
GAMMA	Ratio of heat capacities	real
MS_ZMIN	Minimum allowed average ionization	real
MS_EOSTYPE	EOS type to use for MTMMMT EOS	integer
MS_EOSSUBTYPE	EOS subtype to use for MTMMMT EOS	integer
MS_EOSZFREEFILE	Name of file with ionization data	string
MS_EOSENERFILE	Name of file with internal energy data	string
MS_EOSPRESFILE	Name of file with pressure data	string
MS_NUMELEMS	Number of elements comprising this species	integer
MS_ZELEMS	Atomic number of each species element	array(integer)
MS_AELEMS	Mass number of each species element	array(real)
MS_FRACTIONS	Number fraction of each species element	array(real)
MS_OPLOWTEMP	Temperature at which cold opacities are used	real

```
  subroutine Simulation_initSpecies()

implicit none
#include "Multispecies.h"
#include "Flash.h"

! These two variables are defined in the Config file as
! SPECIES SF6 and SPECIES AIR
  call Multispecies_setProperty(SF6_SPEC, A, 146.)
  call Multispecies_setProperty(SF6_SPEC, Z, 70.)
  call Multispecies_setProperty(SF6_SPEC, GAMMA, 1.09)

  call Multispecies_setProperty(AIR_SPEC, A, 28.66)
  call Multispecies_setProperty(AIR_SPEC, Z, 14.)
  call Multispecies_setProperty(AIR_SPEC, GAMMA, 1.4)
end subroutine Simulation_initSpecies
```

Figure 11.4: A Simulation_initSpecies.F90 file showing Multispecies initialization

```
#include "Flash.h"
#include "Multispecies.h"

! Create arrays to store constituent element data. Note that these
! arrays are always of length MS_MAXELEMS.
real :: aelems(MS_MAXELEMS)
real :: fractions(MS_MAXELEMS)
integer :: zelems(MS_MAXELEMS)

call Multispecies_setProperty(H2O_SPEC, A, 18.0/3.0) ! Set average mass number
call Multispecies_setProperty(H2O_SPEC, Z, 10.0/3.0) ! Set average atomic number
call Multispecies_setProperty(H2O_SPEC, GAMMA, 5.0/3.0)
call Multispecies_setProperty(H2O_SPEC, MS_NUMELEMS, 2)

aelems(1) =  1.0 ! Hydrogen
aelems(2) = 16.0 ! Oxygen
call Multispecies_setProperty(H2O_SPEC, MS_AELEMS, aelems)

zelems(1) = 1 ! Hydrogen
zelems(2) = 8 ! Oxygen
call Multispecies_setProperty(H2O_SPEC, MS_ZELEMS, zelems)

fractions(1) = 2.0/3.0 ! Two parts Hydrogen
fractions(2) = 1.0/3.0 ! One part Oxygen
call Multispecies_setProperty(H2O_SPEC, MS_FRACTIONS, fractions)
```

Figure 11.5: A `Simulation_initSpecies.F90` file showing Multispecies initialization

11.3 Specifying Constituent Elements of a Species

A species can represent a specific isotope or a single element or a more complex material. Some units in FLASH require information about the elements that constitute a single species. For example, water is comprised of two elements: Hydrogen and Oxygen. The `Multispecies` database can store a list of the atomic numbers, mass numbers, and relative number fractions of each of the elements within a given species. This information is stored in the array properties `MS_ZELEMS`, `MS_AELEMS`, and `MS_FRACTIONS` respectively. The property `MS_NUMELEMS` contains the total number of elements for a species (`MS_NUMELEMS` would be two for water since water is made of Hydrogen and Oxygen). There is an upper bound on the number of elements for a single species which is defined using the preprocessor symbol `MS_MAXELEMS` in the “Flash.h” header file and defaults to six. The value of `MS_MAXELEMS` can be changed using the `ms_maxelems` setup variable. Figure 11.5 shows an example of how the constituent elements for water can be set using the `Simulation_initSpecies` subroutine.

The constituent element information is optional and is only needed if a particular unit of interest requires it. At present, only the analytic cold opacities used in the `Opacity` unit make use of the constituent element information.

11.4 Alternative Method for Defining Species

Section 11.1 described how species can be defined by using the `SPECIES` keyword in the `Config` file. Section 11.2 then described how the properties of the species can be set using various subroutines defined in the `Multispecies` unit. There is an alternative to these approaches which uses setup variables to define the species, then uses runtime parameters to set the properties of each species. This allows users to change the number and names of species without modifying the `Config` file and also allows users to change properties without recompiling the code.

Table 11.2: Automatically Generated `Multispecies` Runtime Parameters

Property Name	Runtime Parameter Name
`A`	`ms_<spec>A`
`Z`	`ms_<spec>Z`
`N`	`ms_<spec>Neutral`
`E`	`ms_<spec>Negative`
`BE`	`ms_<spec>BindEnergy`
`GAMMA`	`ms_<spec>Gamma`
`MS_ZMIN`	`ms_<spec>Zmin`
`MS_EOSTYPE`	`eos_<spec>EosType`
`MS_EOSSUBTYPE`	`eos_<spec>SubType`
`MS_EOSZFREEFILE`	`eos_<spec>TableFile`
`MS_EOSENERFILE`	`eos_<spec>TableFile`
`MS_EOSPRESFILE`	`eos_<spec>TableFile`
`MS_NUMELEMS`	`ms_<spec>NumElems`
`MS_ZELEMS`	`ms_<spec>ZElems_<N>`
`MS_AELEMS`	`ms_<spec>AElems_<N>`
`MS_FRACTIONS`	`ms_<spec>Fractions_<N>`
`MS_OPLOWTEMP`	`op_<spec>LowTemp`

Species can be defined using the `species` setup variable. For example, to create two species called `AIR` and `SF6` one would specify `species=air,sf6` in the simulation setup command. Using this setup variable and using the `SPECIES` keyword in the `Config` file are mutually exclusive. Thus, the user must choose which method they wish to use for a given simulation. Certain units, such as the `Opacity` unit, requires the use of the setup variable.

When species are defined using the setup variable approach, the `Multispecies` unit will automatically define several runtime parameters for each species. These runtime parameters can be used set the properties shown in Table 11.1. The runtime parameter names contain the species name. Table 11.2 shows an example of the mapping between runtime parameters and `Multispecies` properties, where `<spec>` is replaced by the species name as specified in the species setup argument list. Some of these runtime parameters are arrays, and thus the `<N>` is a number ranging from 1 to `MS_MAXELEMS`. The `Simulation_initSpecies` subroutine can be used to override the runtime parameter settings.

11.5 Routine Descriptions

We now briefly discuss some interfaces to the multifluid database that are likely of interest to the user. Many of these routines include optional arguments.

- `Multispecies_setProperty` This routine sets the value species property. It should be called within the subroutine `Simulation_initSpecies` for all the species of interest in the simulation problem, and for all the required properties (any of A, Z, N, E, EB, GAMMA).

FLASH Transition

In FLASH2, you could set multiple properties at once in a call to `add_fluid_to_db`. In FLASH4, individual calls are required. If you are setting up a nuclear network, there is a precoded `Simulation_initSpecies` to easily initialize all necessary species. It is located in the unit `Simulation/SimulationComposition`, which must be listed in your simulation `Config` file.

- `Multispecies_getProperty` Returns the value of a requested property.
- `Multispecies_getSum` Returns a weighted sum of a chosen property of species. The total number of species can be subset. The weights are optional, but are typically the mass fractions X_i of each of the fluids at a point in space. In that case, if the selected property (one of A_i, Z_i, ..., γ_i) is denoted $\mathcal{P}_i$, the sum calculated is

$$\sum_i X_i \mathcal{P}_i \quad .$$

- `Multispecies_getAvg` Returns the weighted average of the chosen property. As in `Multispecies_getSum`, weights are optional and a subset of species can be chosen. If the weights are denoted w_i and the selected property (one of A_i, Z_i, ..., γ_i) is denoted $\mathcal{P}_i$, the average calculated is

$$\frac{1}{N}\sum_i^N w_i \mathcal{P}_i \quad ,$$

  where N is the number of species included in the sum; it may be less than the number of all defined species if an average over a subset is requested.

- `Multispecies_getSumInv` Same as `Multispecies_getSum`, but compute the weighted sum of the inverse of the chosen property. If the weights are denoted w_i and the selected property (one of A_i, Z_i, ..., γ_i) is denoted $\mathcal{P}_i$, the sum calculated is

$$\sum_i^N \frac{w_i}{\mathcal{P}_i} \quad .$$

  For example, the average atomic mass of a collection of fluids is typically defined by

$$\frac{1}{\bar{A}} = \sum_i \frac{X_i}{A_i} \ , \tag{11.1}$$

  where X_i is the mass fraction of species i, and A_i is the atomic mass of that species. To compute $\bar{A}$ using the multifluid database, one would use the following lines

```
call Multispecies_getSumInv(A, abarinv, xn(:))
abar = 1.e0 / abarinv
```

  where `xn(:)` is an array of the mass fractions of each species in FLASH. This method allows some of the mass fractions to be zero.

- `Multispecies_getSumFrac` Same as `Multispecies_getSum`, but compute the weighted sum of the chosen property divided by the total number of particles (A_i). If the weights give the mass fractions X_i of the fluids at a point in space and the selected property (one of A_i, Z_i, ..., γ_i) is denoted $\mathcal{P}_i$, the sum calculated is

$$\sum_i \frac{X_i}{A_i}\mathcal{P}_i \quad .$$

- `Multispecies_getSumSqr` Same as `Multispecies_getSum`, but compute the weighted sum of the squares of the chosen property values. If the weights are denoted w_i and the selected property (one of A_i, Z_i, ..., γ_i) is denoted $\mathcal{P}_i$, the sum calculated is

$$\sum_i^N w_i {\mathcal{P}_i}^2 \quad .$$

- `Multispecies_list` List the contents of the multifluid database in a snappy table format.

11.6 Example Usage

In general, to use Multispecies properties in a simulation, the user must only properly initialize the species as described above in the `Simulation_init` routine. But to program with the Multispecies properties, you must do three things:

- `#include` the `Flash.h` file to identify the defined species
- `#include` the `Multispecies.h` file to identify the desired property
- use the Fortran interface to the Multispecies unit because the majority of the routines are overloaded.

The example below shows a snippet of code to calculate the electron density.

```
...
#include Flash.h
#include Multispecies.h

    USE Multispecies_interface, ONLY:  Multispecies_getSumInv, Multispecies_getSumFrac
...
    do k=blkLimitsGC(LOW,KAXIS),blkLimitsGC(HIGH,KAXIS)
        do j=blkLimitsGC(LOW,JAXIS),blkLimitsGC(HIGH,JAXIS)
           do i=blkLimitsGC(LOW,IAXIS),blkLimitsGC(HIGH,IAXIS)
              call Multispecies_getSumInv(A,abar_inv)
              abar = 1.e0 / abar_inv
              call Multispecies_getSumFrac(Z,zbar)
              zbar = abar * zbar
              ye(i,j,k) = abar_inv*zbar
           enddo
        enddo
     enddo
...
```

11.7 Unit Test

The unit test for `Multispecies` provides a complete example of how to call the various API routines in the unit with all variations of arguments. Within `Multispecies_unitTest`, incorrect usage is also indicated within commented-out statements.

Chapter 12

Physical Constants Unit

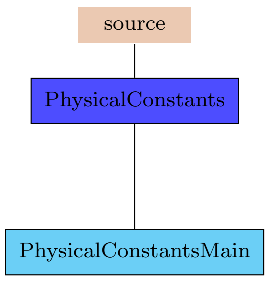

Figure 12.1: The `PhysicalConstants` unit directory tree.

The Physical Constants unit provides a set of common constants, such as Pi and the gravitational constant, in various systems of measurement units. The default system of units is CGS, so named for having a length unit in centimeters, a mass unit in grams, and a time unit in seconds. In CGS, the charge unit is the esu, and the temperature unit is the Kelvin. The constants can also be obtained in the standard MKS system of units, where length is in meters, mass in kilograms, and time in seconds. For MKS units, charge is in Coloumbs, and temperature in Kelvin.

FLASH Transition

For ease of usage, the constant PI=3.14159.... is defined in the header file `constants.h`. Including this file with #include "constants.h" is an alternate way to access the value of π, rather than needing to include the `PhysicalConstants` unit.

Any constant can optionally be converted from the standard units into any other available units. This facility makes it easy to ensure that all parts of the code are using a consistent set of physical constant values and unit conversions.

For example, a program using this unit might obtain the value of Newton's gravitational constant G in units of Mpc^3 Gyr$^{-2}M_\odot^{-1}$ by calling

```
call PhysicalConstants_get ("Newton", G, len_unit="Mpc",
                            time_unit="Gyr", mass_unit="Msun")
```

In this example, the local variable `G` is set equal to the result, 4.4983×10^{-15} (to five significant figures).

Physical constants are taken from K. Nahamura *et al.* (Particle Data Group), J. Phys. G **37**, 075021 (2010).

Table 12.1: Available Physical Constants

String Constant	**Description**
Newton	Gravitational constant G
speed of light	Speed of light
Planck	Planck's constant
electron charge	charge of an electron
electron mass	mass of an electron
proton mass	Mass of a proton
fine-structure	fine-structure constant
Avogadro	Avogadro's Mole Fraction
Boltzmann	Boltzmann's constant
ideal gas constant	ideal gas constant
Wien	Wien displacement law constant
Stefan-Boltzmann	Stefan-Boltzman constant
pi	Pi
e	e
Euler	Euler-Mascheroni constant

12.1 Available Constants and Units

There are many constants and units available within FLASH3, see Table 12.1 and Table 12.2. Should the user wish to add additional constants or units to a particular setup, the routine `PhysicalConstants_init` should be overridden and the new constants added within the directory of the setup.

12.2 Applicable Runtime Parameters

There is only one runtime parameter used by the Physical Constants unit: `pc_unitsBase` selects the default system of units for returned constants. It is a three-character string set to "CGS" or "MKS"; the default is CGS.

12.3 Routine Descriptions

The following routines are supplied by this unit.

- `PhysicalConstants_get` Request a physical constant given by a string, and returns its real value. This routine takes optional arguments for converting units from the default. If the constant name or any of the optional unit names aren't recognized, a value of 0 is returned.
- `PhysicalConstants_init` Initializes the Physical Constants Unit by loading all constants. This routine is called by `Driver_initFlash` and must be called before the first invocation of `PhysicalConstants_get`. In general, the user does not need to invoke this call.
- `PhysicalConstants_list` Lists the available physical constants in a snappy table.
- `PhysicalConstants_listUnits` Lists all the units available for optional conversion.
- `PhysicalConstants_unitTest` Lists all physical constants and units, and tests the unit conversion routines.

Table 12.2: Available Units for Conversion of Physical Constants

Base unit	**String Constant**	**Value in CGS units**	**Description**
length	cm	1.0	centimeter
time	s	1.0	second
temperature	K	1.0	degree Kelvin
mass	g	1.0	gram
charge	esu	1.0	ESU charge
length	m	`1.0E2`	meter
length	km	`1.0E5`	kilometer
length	pc	`3.0856775807E18`	parsec
length	kpc	`3.0856775807E21`	kiloparsec
length	Mpc	`3.0856775807E24`	megaparsec
length	Gpc	`3.0856775807E27`	gigaparsec
length	Rsun	`6.96E10`	solar radius
length	AU	`1.49597870662E13`	astronomical unit
time	yr	`3.15569252E7`	year
time	Myr	`3.15569252E13`	megayear
time	Gyr	`3.15569252E16`	gigayear
mass	kg	`1.0E3`	kilogram
mass	Msun	`1.9889225E33`	solar mass
mass	amu	`1.660538782E-24`	atomic mass unit
charge	C	`2.99792458E9`	Coulomb
	Cosmology-friendly units using $H_0 = 100$ km/s/Mpc:		
length	LFLY	`3.0856775807E24`	1 Mpc
time	TFLY	`2.05759E17`	$\frac{2}{3H_0}$
mass	MFLY	`9.8847E45`	`5.23e12` Msun

FLASH Transition

The header file `PhysicalConstants.h` must be included in the calling routine due to the optional arguments of `PhysicalConstants_get`.

12.4 Unit Test

The `PhysicalConstants` unit test `PhysicalConstants_unitTest` is a simple exercise of the functionality in the unit. It does not require time stepping or the grid. “Correct” usage is indicated, as is erroneous usage.

Part V

Physics Units

Chapter 13

3T Capabilities for Simulation of HEDP Experiments

The FLASH code has been extended with numerous capabilities to allow it to simulate laser-driven High Energy Density Physics (HEDP) experiments. These experiments often require a multi-temperature treatment of the plasma where the ion temperature, $T_{\rm ion}$ and the electron temperature $T_{\rm ele}$ are not necessarily equal. Thermal radiation effects are also important in many High Energy Density (HED) plasmas. If the radiation field has a total energy density given by $u_{\rm rad}(\boldsymbol{x}, t)$ then the radiation temperature is defined as $T_{\rm rad} = (u_{\rm rad}/a)^{1/4}$. The radiation field is not in equilibrium with the plasma and thus $T_{\rm rad} \neq T_{\rm ele} \neq T_{\rm ion}$. We refer to this treatment, where these three temperatures are not necessarily equal, as a 3T treatment. This chapter is intended to describe the basic theory behind FLASH's 3T implementation to direct users to other parts of the manual and simulations which provide further details on how to use these new capabilities in FLASH.

The term "3T" is not meant to imply in any way that a gray treatment of the radiation field is being assumed. The radiation temperature is only used to represent the total energy density, which is integrated over all photon frequencies. The radiation temperature never directly enters the calculation. Thus, 3T refers to the fact that FLASH is being run in a mode where 3 independent components (ions, electrons, radiation) are being modeled. The radiation field is usually treated in a frequency dependent way through multigroup radiation diffusion as described below and in Chapter 24.

The equations which FLASH solves to describe the evolution of an unmagnetized 3T plasma are:

$$\frac{\partial \rho}{\partial t} + \nabla \cdot (\rho \boldsymbol{v}) = 0, \tag{13.1a}$$

$$\frac{\partial}{\partial t}(\rho \boldsymbol{v}) + \nabla \cdot (\rho \boldsymbol{v}\boldsymbol{v}) + \nabla P_{\rm tot} = 0, \tag{13.1b}$$

$$\frac{\partial}{\partial t}(\rho E_{\rm tot}) + \nabla \cdot \left[(\rho E_{\rm tot} + P_{\rm tot})\, \boldsymbol{v}\right] = Q_{\rm las} - \nabla \cdot \boldsymbol{q}, \tag{13.1c}$$

where:

- ρ is the total mass density
- $\boldsymbol{v}$ is the average fluid velocity
- $P_{\rm tot}$ is the total pressure defined as the sum over the ion, electron, and radiation pressures:

$$P_{\rm tot} = P_{\rm ion} + P_{\rm ele} + P_{\rm rad} \tag{13.2}$$

- $E_{\rm tot}$ is the total specific energy which includes the specific internal energies of the electrons, ions, and radiation field along with the specific kinetic energy. Thus:

$$E_{\rm tot} = e_{\rm ion} + e_{\rm ele} + e_{\rm rad} + \frac{1}{2}\boldsymbol{v} \cdot \boldsymbol{v} \tag{13.3}$$

- $\boldsymbol{q}$ is the total heat flux which is assumed to have a radiation and electron conductivity component:

$$\boldsymbol{q} = \boldsymbol{q}_{\text{ele}} + \boldsymbol{q}_{\text{rad}} \tag{13.4}$$

- Q_{las} represents the energy source due to laser heating

Since the plasma is not assumed to have a single temperature, additional equations must be evolved to describe the change in specific internal energies of the ions, electrons, and radiation field. For the electrons and ions these equations are:

$$\frac{\partial}{\partial t}(\rho e_{\text{ion}}) + \nabla\cdot(\rho e_{\text{ion}}\boldsymbol{v}) + P_{\text{ion}}\nabla\cdot\boldsymbol{v} = \rho\frac{c_{v,\text{ele}}}{\tau_{ei}}(T_{\text{ele}} - T_{\text{ion}}), \tag{13.5a}$$

$$\frac{\partial}{\partial t}(\rho e_{\text{ele}}) + \nabla\cdot(\rho e_{\text{ele}}\boldsymbol{v}) + P_{\text{ele}}\nabla\cdot\boldsymbol{v} = \rho\frac{c_{v,\text{ele}}}{\tau_{ei}}(T_{\text{ion}} - T_{\text{ele}}) - \nabla\cdot\boldsymbol{q}_{\text{ele}} + Q_{\text{abs}} - Q_{\text{emis}} + Q_{\text{las}}, \tag{13.5b}$$

$$\frac{\partial}{\partial t}(\rho e_{\text{rad}}) + \nabla\cdot(\rho e_{\text{rad}}\boldsymbol{v}) + P_{\text{rad}}\nabla\cdot\boldsymbol{v} = \nabla\cdot\boldsymbol{q}_{\text{rad}} - Q_{\text{abs}} + Q_{\text{emis}}, \tag{13.5c}$$

where:

- $c_{v,\text{ele}}$ is the electron specific heat
- τ_{ei} is the ion/electron equilibration time
- Q_{abs} represents the increase in electron internal energy due to the total absorption of radiation
- Q_{emis} represents the decrease in electron internal energy due to the total emission of radiation

The 3T equation of state in FLASH connects the internal energies, temperatures, and pressures of the components. Many different equations of state options exist in FLASH. These are described in Section 16.4. A full-physics HEDP simulation using FLASH will solve equations (13.1) and (13.5) using the 3T equation of state. These equations are somewhat redundant since (13.1c) can be written as a sum of the other equations. These equations are also not yet complete, since it has not been described how many of the terms above are defined and computed in FLASH. The remainder of this chapter will describe this and direct readers to the appropriate sections of the manual where examples and further information can be found.

A series of operator splits is used to solve (13.1) and (13.5) in FLASH. First, all of the terms on the left hand sides of these equations are split off and solved in various code units. The remaining equations:

$$\frac{\partial\rho}{\partial t} + \nabla\cdot(\rho\boldsymbol{v}) = 0, \tag{13.6a}$$

$$\frac{\partial}{\partial t}(\rho\boldsymbol{v}) + \nabla\cdot(\rho\boldsymbol{v}\boldsymbol{v}) + \nabla P_{\text{tot}} = 0, \tag{13.6b}$$

$$\frac{\partial}{\partial t}(\rho E_{\text{tot}}) + \nabla\cdot[(\rho E + P_{\text{tot}})\,\boldsymbol{v}] = 0, \tag{13.6c}$$

$$\frac{\partial}{\partial t}(\rho e_{\text{ion}}) + \nabla\cdot(\rho e_{\text{ion}}\boldsymbol{v}) + P_{\text{ion}}\nabla\cdot\boldsymbol{v} = 0, \tag{13.6d}$$

$$\frac{\partial}{\partial t}(\rho e_{\text{ele}}) + \nabla\cdot(\rho e_{\text{ele}}\boldsymbol{v}) + P_{\text{ele}}\nabla\cdot\boldsymbol{v} = 0, \tag{13.6e}$$

$$\frac{\partial}{\partial t}(\rho e_{\text{rad}}) + \nabla\cdot(\rho e_{\text{rad}}\boldsymbol{v}) + P_{\text{rad}}\nabla\cdot\boldsymbol{v} = 0, \tag{13.6f}$$

describe the advection of conserved quantities and the effect of work. (13.6) is solved by the `Hydro` unit. Chapter 15 describes the hydrodynamics solvers in a general way where only equations for conservation of total mass, momentum, and energy are considered. The extension of the FLASH hydrodynamics solvers to 3T is described in Section 14.1.4. Note that these equations are not in a conservative form because of the presence of the work terms in (13.6d), (13.6e), and (13.6f). These work terms are divergent at shocks and cannot be directly evaluated. Two techniques are described in Section 14.1.4 for coping with this issue.

The electron, ion, and radiation internal energy equations in the absence of the hydrodynamic terms are shown in (13.7). The density is updated in the hydrodynamic update so for the remaining equations the density is assumed to be constant, and we remove the density from the time derivatives.

$$\rho \frac{\partial e_{\text{ion}}}{\partial t} = \rho \frac{c_{v,\text{ele}}}{\tau_{ei}} (T_{\text{ele}} - T_{\text{ion}}), \tag{13.7a}$$

$$\rho \frac{\partial e_{\text{ele}}}{\partial t} = \rho \frac{c_{v,\text{ele}}}{\tau_{ei}} (T_{\text{ion}} - T_{\text{ele}}) - \nabla \cdot \boldsymbol{q}_{\text{ele}} + Q_{\text{abs}} - Q_{\text{emis}} + Q_{\text{las}}, \tag{13.7b}$$

$$\rho \frac{\partial e_{\text{rad}}}{\partial t} = \nabla \cdot \boldsymbol{q}_{\text{rad}} - Q_{\text{abs}} + Q_{\text{emis}}. \tag{13.7c}$$

The first term on the right hand side of (13.7a) and (13.7b) describes the exchange of internal energy between ions and electrons through collisions. This term will force the ion and electron temperatures to equilibrate over time. The `Heatexchange` unit, described in Section 17.5.1, solves for this part of (13.7). Specifically, it updates the ion and electron temperatures according to:

$$\frac{\partial e_{\text{ion}}}{\partial t} = \frac{c_{v,\text{ele}}}{\tau_{ei}} (T_{\text{ele}} - T_{\text{ion}}), \tag{13.8a}$$

$$\frac{\partial e_{\text{ele}}}{\partial t} = \frac{c_{v,\text{ele}}}{\tau_{ei}} (T_{\text{ion}} - T_{\text{ele}}). \tag{13.8b}$$

The electron specific heat, $c_{v,\text{ele}}$ is computed through calls to the equation of state. The ion/electron equilibration time is computed in the `Heatexchange` unit.

The second term on the right hand side of (13.7b) represents the transport of energy through electron thermal conduction. Thus the heat flux is defined as:

$$\boldsymbol{q}_{\text{ele}} = -K_{\text{ele}} \nabla T_{\text{ele}}, \tag{13.9}$$

where K_{ele} is the electron thermal conductivity and is computed in the `Conductivity` unit (see Section 22.1). The `Diffuse` unit, described in Chapter 18, is responsible for including the effect of conduction in FLASH simulations. Again, using operator splitting, the `Diffuse` unit solves the following equation over a time step:

$$\rho \frac{\partial e_{\text{ele}}}{\partial t} = \nabla \cdot K_{\text{ele}} \nabla T_{\text{ele}}. \tag{13.10}$$

This equation can be solved implicitly over the time step to avoid time-step constraints. The electron conductivity is evaluated using a flux limiter to give more a physically realistic heat flux in regions where the electron temperature gradient is very large.

The remaining terms describe radiation transport. FLASH incorporates radiation effects using multigroup diffusion (MGD) theory. The total radiation flux, emission, and absorption terms which appear in (13.7) contain contributions from each energy group. For group g, where $1 \le g \le N_g$, the total quantities can be written as summations over each group:

$$Q_{\text{abs}} = \sum_{g=1}^{N_g} Q_{\text{ele},g}, \; Q_{\text{emis}} = \sum_{g=1}^{N_g} Q_{\text{emis},g}, \; \boldsymbol{q}_{\text{rad}} = \sum_{g=1}^{N_g} \boldsymbol{q}_g. \tag{13.11}$$

The change in the radiation energy density for each group, u_g, is described by:

$$\frac{\partial u_g}{\partial t} + \nabla \cdot (u_g \boldsymbol{v}) + \left(\frac{u_g}{e_{\text{rad}} \rho} \right) P_{\text{rad}} \nabla \cdot \boldsymbol{v} = -\nabla \cdot \boldsymbol{q}_g + Q_{\text{emis},g} - Q_{\text{abs},g} \tag{13.12}$$

The total specific radiation energy is related to u_g through:

$$\rho e_{\text{rad}} = \sum_{g=1}^{N_g} u_g \tag{13.13}$$

The `RadTrans` unit is responsible for solving the radiation diffusion equations for each energy group. The `RadTrans` unit solves these diffusion equations implicitly by using the `Diffuse` unit. While the work term for the total radiation energy is computed in the `Hydro` unit, the distribution of that work amongst each energy group is performed in the `RadTrans` unit. Chapter 24 describes in detail how the multigroup radiation diffusion package in FLASH functions. The group radiation flux, emission, and absorption terms are all defined in that chapter. These terms are functions of the material opacity which is computed by the `Opacity` unit and is described in Section 22.4.

The only remaining term in (13.7) is Q_{las} which represents the deposition of energy by lasers into the electrons. The `Laser` implementation in the `EnergyDeposition` unit is responsible for computing Q_{las}. The geometrics optics approximation to laser energy deposition is used in FLASH. Section 17.4 describes the theory and usage of the laser ray-tracing model in FLASH in detail.

As has been described above, the HEDP capabilities in FLASH are divided amongst many units including:

- `Hydro`: Responsible for the 3T hydrodynamic update
- `Eos`: Computes 3T equation of state
- `Heatexchange`: Implements ion/electron equilibration
- `Diffuse`: Responsible for implementing implicit diffusion solvers and computes effect of electron conduction
- `RadTrans`: Implements multigroup radiation diffusion
- `Opacity`: Computes opacities for radiation diffusion
- `Conductivity`: Computes electron thermal conductivities
- `EnergyDeposition`: Computes the laser energy deposition

Several simulations are included with FLASH which demonstrate the usage of the HEDP capabilities and, taken together, exercise all of the units listed above. These simulations are described briefly below. Chapter 30 describes all of the simulations in detail. Below, the relevant simulations listed with brief descriptions.

- `MGDInfinite` simulation, described in Section 30.6.1: Simple 0D test of the exchange of energy between electrons, ions, and the radiation field
- `MGDStep` simulation, described in Section 30.6.2: Simple 1D test of electron conduction, ion/electron equilibration, and MGD
- `ShafranovShock` simulation, described in Section 30.8.1: Simple 1D verification test of the structure of a shock in a radiationless plasma with $T_{\text{ele}} \neq T_{\text{ion}}$.
- `GrayDiffRadShock` simulation, described in Section 30.8.2: Simple 1D verification test of the structure of a radiating shock
- `ReinickeMeyer` simulation, described in Section 30.8.3: Verification test of a spherical blast wave with thermal conduction
- `LaserSlab` simulation, described in Section 30.7.5: Full physics 2D simulation which includes 3T hydrodynamics, tabulated EOS and opacity, MGD, electron conduction, and laser ray-tracing. This simulation is meant to demonstrate how to set up a complex simulation of an HEDP experiment

Chapter 14

Hydrodynamics Units

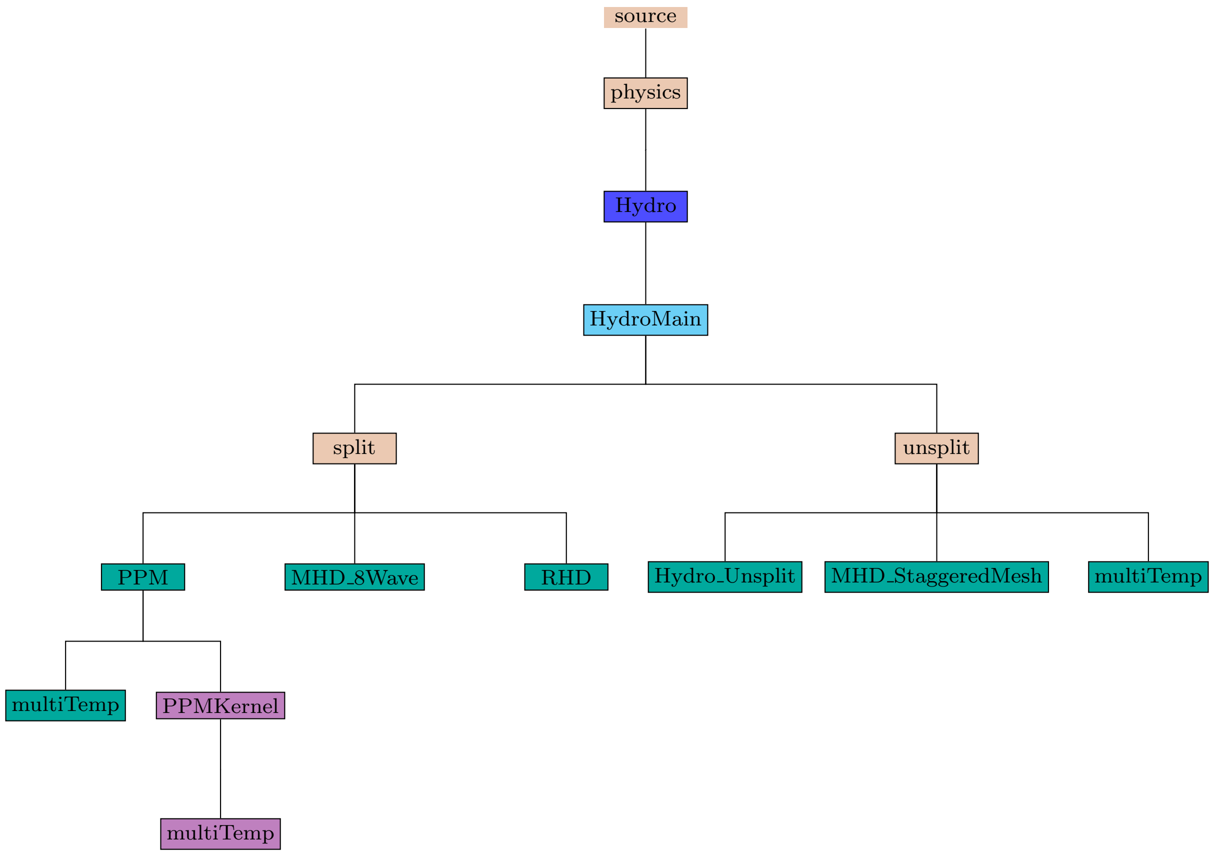

Figure 14.1: The `Hydro` unit directory tree.

The `Hydro` unit solves Euler's equations for compressible gas dynamics in one, two, or three spatial dimensions. We first describe the basic functionality; see implementation sections below for various extensions.

The Euler equations can be written in conservative form as

$$\frac{\partial \rho}{\partial t} + \nabla \cdot (\rho \mathbf{v}) = 0 \tag{14.1}$$

$$\frac{\partial \rho \mathbf{v}}{\partial t} + \nabla \cdot (\rho \mathbf{v}\mathbf{v}) + \nabla P = \rho \mathbf{g} \tag{14.2}$$

$$\frac{\partial \rho E}{\partial t} + \nabla \cdot [(\rho E + P)\,\mathbf{v}] = \rho \mathbf{v} \cdot \mathbf{g}\ , \tag{14.3}$$

where ρ is the fluid density, $\mathbf{v}$ is the fluid velocity, P is the pressure, E is the sum of the internal energy ϵ and kinetic energy per unit mass,

$$E = \epsilon + \frac{1}{2}|\mathbf{v}|^2\ , \tag{14.4}$$

$\mathbf{g}$ is the acceleration due to gravity, and t is the time coordinate. The pressure is obtained from the energy and density using the equation of state. For the case of an ideal gas equation of state, the pressure is given by

$$P = (\gamma - 1)\rho\epsilon\ , \tag{14.5}$$

where γ is the ratio of specific heats. More general equations of state are discussed in Section 16.2 and Section 16.3.

In regions where the kinetic energy greatly dominates the total energy, computing the internal energy using

$$\epsilon = E - \frac{1}{2}|\mathbf{v}|^2 \tag{14.6}$$

can lead to unphysical values, primarily due to truncation error. This results in inaccurate pressures and temperatures. To avoid this problem, we can separately evolve the internal energy according to

$$\frac{\partial \rho\epsilon}{\partial t} + \nabla \cdot [(\rho\epsilon + P)\,\mathbf{v}] - \mathbf{v} \cdot \nabla P = 0\ . \tag{14.7}$$

If the internal energy is a small fraction of the kinetic energy (determined via the runtime parameter `eintSwitch`), then the total energy is recomputed using the internal energy from (14.7) and the velocities from the momentum equation. Numerical experiments using the PPM solver included with FLASH showed that using (14.7) when the internal energy falls below 10^{-4} of the kinetic energy helps avoid the truncation errors while not affecting the dynamics of the simulation.

For reactive flows, a separate advection equation must be solved for each chemical or nuclear species

$$\frac{\partial \rho X_\ell}{\partial t} + \nabla \cdot (\rho X_\ell \mathbf{v}) = 0\ , \tag{14.8}$$

where X_ℓ is the mass fraction of the ℓth species, with the constraint that $\sum_\ell X_\ell = 1$. FLASH will enforce this constraint if you set the runtime parameter `irenorm` equal to 1. Otherwise, FLASH will only restrict the abundances to fall between `smallx` and 1. The quantity ρX_ℓ represents the partial density of the ℓth fluid. The code does not explicitly track interfaces between the fluids, so a small amount of numerical mixing can be expected during the course of a calculation.

The `hydro` unit has a capability to advect mass scalars. Mass scalars are field variables advected with density, similar to species mass fractions,

$$\frac{\partial \rho \phi_\ell}{\partial t} + \nabla \cdot (\rho \phi_\ell \mathbf{v}) = 0\ , \tag{14.9}$$

where ϕ_ℓ is the ℓth mass scalar. Note that mass scalars are optional variables; to include them specify the name of each mass scalar in a `Config` file using the `MASS_SCALAR` keyword. Mass scalars are not renormalized in order to sum to 1, except when they are declared to be part of a renormalization group. See Section 5.5.1 for more details.

Table 14.1: Runtime parameters used with the hydrodynamics (`Hydro`) unit.

Variable	Type	Default	Description
`eintSwitch`	real	0	If $\epsilon <$ `eintSwitch` $\cdot \frac{1}{2}|\mathbf{v}|^2$, use the internal energy equation to update the pressure
`irenorm`	integer	0	If equal to one, renormalize multifluid abundances following a hydro update; else restrict their values to lie between `smallx` and 1.
`cfl`	real	0.8	Courant-Friedrichs-Lewy (CFL) factor; must be less than 1 for stability in explicit schemes

Table 14.2: Solution variables used with the hydrodynamics (`Hydro`) unit.

Variable	Type	Description
`dens`	PER_VOLUME	density
`velx`	PER_MASS	x-component of velocity
`vely`	PER_MASS	y-component of velocity
`velz`	PER_MASS	z-component of velocity
`pres`	GENERIC	pressure
`ener`	PER_MASS	specific total energy $(T + U)$
`temp`	GENERIC	temperature

14.1 Gas hydrodynamics

14.1.1 Usage

The two gas hydrodynamic solvers supplied in the release of FLASH4 are organized into two different operator splitting methods: directionally split and unsplit. The directionally split piecewise-parabolic method (PPM) makes use of second-order Strang time splitting, and the new directionally unsplit solver is based on Monotone Upstream-centered Scheme for Conservation Laws (MUSCL) Hancock type second-order scheme.

The algorithms are described in Section 14.1.2 and Section 14.1.3 and implemented in the directory tree under `physics/Hydro/HydroMain/split/PPM` and `physics/Hydro/HydroMain/unsplit/Hydro_Unsplit`. Extensions for multitemperature applications are described in Section 14.1.4.

Current and future implementations of `Hydro` use the runtime parameters and solution variables described in Table 14.1 and Table 14.2. Additional runtime parameters used either solely by the PPM method or the unsplit hydro solver are described in `HydroMain`.

14.1.2 The piecewise-parabolic method (PPM)

FLASH includes a directionally split piecewise-parabolic method (PPM) solver descended from the `PROMETHEUS` code (Fryxell, Müller, and Arnett 1989). The basic PPM algorithm is described in detail in Woodward and Colella (1984) and Colella and Woodward (1984). It is a higher-order version of the method developed by Godunov (1959). FLASH implements the Direct Eulerian version of PPM.

Godunov's method uses a finite-volume spatial discretization of the Euler equations together with an explicit forward time difference. Time-advanced fluxes at cell boundaries are computed using the numerical solution to Riemann's shock tube problem at each boundary. Initial conditions for each Riemann problem are determined by assuming the non-advanced solution to be piecewise-constant in each cell. Using the Riemann solution has the effect of introducing explicit nonlinearity into the difference equations and permits the calculation of sharp shock fronts and contact discontinuities without introducing significant nonphysical oscillations into the flow. Since the value of each variable in each cell is assumed to be constant, Godunov's method is limited to first-order accuracy in both space and time.

PPM improves on Godunov's method by representing the flow variables with piecewise-parabolic functions. It also uses a monotonicity constraint rather than artificial viscosity to control oscillations near discontinuities, a feature shared with the MUSCL scheme of van Leer (1979). Although these choices could lead to a method which is accurate to third order, PPM is formally accurate only to second order in both space and time, as a fully third-order scheme proved not to be cost-effective. Nevertheless, PPM is considerably more accurate and efficient than most formally second-order algorithms.

PPM is particularly well-suited to flows involving discontinuities, such as shocks and contact discontinuities. The method also performs extremely well for smooth flows, although other schemes which do not perform the extra work necessary for the treatment of discontinuities might be more efficient in these cases. The high resolution and accuracy of PPM are obtained by the explicit nonlinearity of the scheme and through the use of intelligent dissipation algorithms, such as monotonicity enforcement and interpolant flattening. These algorithms are described in detail by Colella and Woodward (1984).

A complete description of PPM is beyond the scope of this guide. However, for comparison with other codes, we note that the implementation of PPM in FLASH uses the Direct Eulerian formulation of PPM and the technique for allowing non-ideal equations of state described by Colella and Glaz (1985). For multidimensional problems, FLASH uses second-order operator splitting (Strang 1968). We note below the extensions to PPM that we have implemented.

The PPM algorithm includes a steepening mechanism to keep contact discontinuities from spreading over too many cells. Its use requires some care, since under certain circumstances, it can produce incorrect results. For example, it is possible for the code to interpret a very steep (but smooth) density gradient as a contact discontinuity. When this happens, the gradient is usually turned into a series of contact discontinuities, producing a stair step appearance in one-dimensional flows or a series of parallel contact discontinuities in multi-dimensional flows. Under-resolving the flow in the vicinity of a steep gradient is a common cause of this problem. The directional splitting used in our implementation of PPM can also aggravate the situation. The contact steepening can be disabled at runtime by setting `use_steepening = .false.`.

The version of PPM in the FLASH code has an option to more closely couple the hydrodynamic solver with a gravitational source term. This can noticeably reduce spurious velocities caused by the operator splitting of the gravitational acceleration from the hydrodynamics. In our 'modified states' version of PPM, when calculating the left and right states for input to the Riemann solver, we locally subtract off from the pressure field the pressure that is locally supporting the atmosphere against gravity; this pressure is unavailable for generating waves. This can be enabled by setting `ppm_modifystates = .true.`.

The interpolation/monotonization procedure used in PPM is very nonlinear and can act differently on the different mass fractions carried by the code. This can lead to updated abundances that violate the constraint that the mass fractions sum to unity. Plewa and Müller (1999) (henceforth CMA) describe extensions to PPM that help prevent overshoots in the mass fractions as a result of the PPM advection. We implement two of the modifications they describe, the renormalization of the average mass fraction state as returned from the Riemann solvers (CMA eq. 13), and the (optional) additional flattening of the mass fractions to reduce overshoots (CMA eq. 14-16). The latter procedure is off by default and can be enabled by setting `use_cma_flattening = .true.`.

Finally, there is an odd-even instability that can occur with shocks that are aligned with the grid. This was first pointed out by Quirk (1997), who tested several different Riemann solvers on a problem designed to demonstrate this instability. The solution he proposed is to use a hybrid Riemann solver, using the regular solver in most regions but switching to an HLLE solver inside shocks. In the context of PPM, such a hybrid implementation was first used for simulations of Type II supernovae. We have implemented such a procedure, which can be enabled by setting `hybrid_riemann = .true.`.

14.1.3 The unsplit hydro solver

A directionally unsplit pure hydrodynamic solver (unsplit hydro) is an alternate gas dynamics solver to the split PPM scheme. The method basically adopts a predictor-corrector type formulation (zone-edge data-extrapolated method) that provides second-order solution accuracy for smooth flows and first-order accuracy for shock flows in both space and time. Recently, the order of spatial accuracy in data reconstruction for the normal direction has been extended to implement the 3rd order PPM and 5th order Weighted ENO (WENO) methods. This unsplit hydro solver can be considered as a reduced version of the Unsplit Staggered Mesh

(USM) MHD solver (see details in Section 14.3.3) that has been available in previous FLASH3 releases.

The unsplit hydro implementation can solve 1D, 2D and 3D problems with added capabilities of exploring various numerical implementations: different types of Riemann solvers; slope limiters; first, second, third and fifth reconstruction methods; a strong shock/rarefaction detection algorithm as well as two different entropy fix routines for Roe's linearized Riemann solver.

One of the notable features of the unsplit hydro scheme is that it particularly improves the preservation of flow symmetries as compared to the splitting formulation. Also, the scheme used in this unsplit algorithm can take a wide range of CFL stability limits (e.g., CFL < 1) for all three dimensions, which is based on using upwinded transverse flux formulations developed in the multidimensional USM MHD solver (Lee, 2006; Lee and Deane, 2009; Lee, 2013).

The above set of runtime parameters provide various types of different combinations that help in obtaining numerical accuracy, efficiency and stability. However, there are some important tips users should know before using them.

- [Extended stencil]: When `NGUARD=6` is used, users should also use `nxb, nyb`, and `nzb` larger than `2*NGUARD`. For example, specifying `-nxb=16` in the setup works well for 1D cases. Once setting up `NGUARD=6`, users still can use FOG, MH, PPM, or WENO without changing `NGUARD` back to 4.

- [`transOrder`]: The first order method `transOrder=1` is a default and only supported method that is stable according to the linear Fourier stability analysis. The choices for higher-order interpolations are no longer available in this release.

- [`EOSforRiemann`]: `EOSforRiemann = .true.` will call (expensive) EOS routines to compute consistent adiabatic indices (*i.e.*, `gamc, game`) according to the given left and right states in Riemann solvers. For the ideal gamma law, in which those adiabatic indices are constant, it is not required to call EOS at all and users can set it `.false.` to reduce computation time. On the other hand, for a degenerate gas, one can enable this switch to compute thermodynamically consistent `gamc, game`, which in turn are used to compute the sound speed and internal energy in Riemann flux calculations. When disabled, interpolations will be used instead to get approximations of `gamc, game`. This interpolation method has been tested and proven to gain significant computational efficiency and accuracy, giving reliable numerical solutions even for simulating a degenerate gas.

- [Gravity coupling with Unplit Hydro Solvers]: When gravity is included in a simulation using the unsplit hydro and MHD solvers, users can choose to include gravitational source terms in the Riemann state update at $n + 1/2$ time step (i.e., `use_gravHalfUpdate`=.true.). This will provide a second-order accuracy with respect to coupling gravitational accelerations to hydrodynamics. With `use_gravHalfUpdate`=.true., users can choose `use_gravConsv`=.true. to adopt conservative forms (expensive); although, an efficient primitive counterpart update should be accurate enough for most cases. Otherwise, if `use_gravHalfUpdate=.false.`, the gravitational source terms will only be included at the final update step (i.e., U^n to U^{n+1}), giving first order accuracy. We also have included a new approach to update gravity accelerations at $n + 1/2$ time step (i.e., `use_gravPotUpdate=.true.`) . In this new approach, the gravity potentials are calculated by calling a Poisson solver, giving more accurate values at cell-interfaces. The option `use_gravPotUpdate=.true.` only works with the primitive update, `use_gravConsv=.false.`. It should be noted that the new optimized unsplit hydro/MHD codes (i.e., `+uhd, +usm` in `source/physics/Hydro/HydroMain/unsplit`) do not support `use_gravPotUpdate=.true.` and `use_gravConsv=.true.` any more; however they are still supported in the old unsplit codes (i.e., `+uhdold, +usmold` in `source/physics/Hydro/HydroMain/unsplit_old`).

- [Reduced CTU vs. Full CTU for 3D in the unsplit hydro (UHD) and staggered mesh (USM) solvers]: `use_3dFullCTU` is a new switch that enhances a numerical stability for 3D simulations in the unsplit solvers using the corner transport upwind (CTU) algorithm by Colella. The unsplit solvers of FLASH are different from many other shock capturing codes, in that neither UHD nor USM solvers need intermediate Riemann solver solutions for updating transverse fluxes in multidimensional problems. This provides a computational efficiency because there is a reduced number of calls to Riemann solvers per cell per time step. The total number of required Riemann solver solutions are two for 2D and three for 3D (except for extra Riemann calls for constraint-transport (CT) update in USM). This is smaller

Table 14.3: Additional runtime parameters for *Interpolation Schemes* in the unsplit hydro solver (`physics/Hydro/HydroMain/unsplit/Hydro_Unsplit`)

Variable	Type	Default	Description
`order`	integer	2	Order of method in data reconstruction: 1st order Godunov (FOG), 2nd order MUSCL-Hancock (MH), 3rd order PPM, 5th order WENO.
`transOrder`	integer	1	Interpolation order of accuracy of taking upwind biased transverse flux derivatives in the unsplit data reconstruction: 1st, 2nd, 3rd. The choice of using `transOrder`=4 adopts a slope limiter between the 1st and 3rd order accurate methods to minimize oscillations in upwinding at discontinuities.
`slopeLimiter`	string	"vanLeer"	Slope limiter: "MINMOD", "MC", "VANLEER", "HYBRID", "LIMITED"
`LimitedSlopeBeta`	real	1.0	Slope parameter specific for the "LIMITED" slope by Toro
`charLimiting`	logical	.true.	Enable/disable limiting on characteristic variables (.false. will use limiting on primitive variables)
`use_steepening`	logical	.false.	Enable/disable contact discontinuity steepening for PPM and WENO
`use_flattening`	logical	.false.	Enable/disable flattening (or reducing) numerical oscillations for MH, PPM, and WENO
`use_avisc`	logical	.false.	Enable/disable artificial viscosity for FOG, MH, PPM, and WENO
`cvisc`	real	0.1	Artificial viscosity coefficient
`use_upwindTVD`	logical	.false.	Enable/disable upwinded TVD slope limiter PPM. NOTE: This requires NGUARD=6
`use_hybridOrder`	logical	.false.	Enable an adaptively varying reconstruction order scheme reducing its order from a high-order to first-order depending on monotonicity constraints
`use_gravHalfUpdate`	logical	.false.	On/off gravitational acceleration source terms at the half time Riemann state update
`use_gravConsv`	logical	.false.	Primitive/conservative update for including gravitational acceleration source terms at the half time Riemann state update
`use_gravPotUpdate`	logical	.false.	Use gravity source term update by calling Poisson solver. Note: this only can be used with `use_gravConsv=.false.`
`use_3dFullCTU`	logical	.true.	Enable a full CTU (e.g., similar to the standard 12-Riemann solve) algorithm that provides full CFL stability in 3D. If .false., then the theoretical CFL bound for 3D becomes less than 0.5 based on the linear Fourier analysis.

Table 14.4: Additional runtime parameters for *Riemann Solvers* in the unsplit hydro solver (`physics/Hydro/HydroMain/unsplit/Hydro_Unsplit`)

Variable	Type	Default	Description
`RiemannSolver`	string	"Roe"	Different choices for Riemann solver. "LLF (local Lax-Friedrichs)", "HLL", "HLLC", "HYBRID", "ROE", and "Marquina"
`shockDetect`	logical	.false.	On/off attempting to detect strong shocks/rarefactions (and saving flag in `"shok"` variable)
`shockLowerCFL`	logical	.false.	On/off lowering of CFL factor where strong shocks are detected, automatically sets `shockDetect` if on.
`EOSforRiemann`	logical	.false.	Enable/disable calling EOS in computing each Godunov flux
`entropy`	logical	.false.	On/off entropy fix algorithm for Roe solver
`entropyFixMethod`	string	`''HARTENHYMAN''`	Entropy fix method for the Roe solver. "HARTEN", "HARTENHYMAN"

than the usual stabilty requirement in many other codes which needs four for 2D and twelve for 3D in order to provide a full CFL limit (*i.e.*, CFL < 1).

In general for 3D, there is another computationally efficient approach that only uses six Riemann solutions (aka, 6-CTU) instead of solving twelve Riemann problems (aka, 12-CTU). In this efficient 6-CTU, however, the numerical stability limit becomes CFL< 0.5.

For solving 3D problems in UHD and USM, enabling the new switch `use_3dFullCTU=.true.` (i.e., full-CTU) will make the solution evolution scheme similar to 12-CTU while requiring to solve three Riemann problems only (again, except for the CT update in USM). On the other hand, `use_3dFullCTU=.false.` (i.e., reduced-CTU) will be similar to the 6-CTU integration algorithm with a reduced CFL limit (*i.e.*, CFL < 0.5).

Unsplit Hydro Solver vs. Unsplit Staggered MHD Mesh Solver

One major difference between the unsplit hydro solver and the USM MHD solver is the presence of magnetic and electric fields. The associated staggered mesh configuration required for the USM MHD solver is not needed in the unsplit hydro solver, and all hydrodynamic variables are stored at cell centers.

Stability Limits for both Unsplit Hydro Solver and Unsplit Staggered Mesh Solver

As mentioned above, the two unsplit solvers can take a wide range of CFL limits in all three dimensions (*i.e.*, CFL < 1). However, in some circumstances where there are strong shocks and rarefactions, `shockLowerCFL=.true.` could be useful to gain more numerical stability by lowering the CFL accordingly (e.g., default settings provide 0.45 for 2D and 0.25 for 3D for the Donor scheme). This approach will automatically revert such reduced stability conditions to any given original condition set by users when there are no significant shocks and rarefactions detected.

Setting up a simulation with the unsplit hydro solver

The default hydro implementation has changed from split to unsplit in FLASH4.4. One can still specify `+unsplitHydro` (or `+uhd` for short) in the setup line in order to explicitly request the unsplit hydro solver for a simulation. One needs to specify `+splitHydro` in the setup line if a split hydro solver is required instead. For instance, a setup call `./setup Sedov -2d -auto +splitHydro` will run a Sedov 2D problem using the split PPM hydro solver. Without specifying `+unsplitHydro`, the default unsplit hydro solver will be selected.

Diffusion terms

Non-ideal terms, such as viscosity and heat conduction, can be included in the unsplit hydro solver for simulating diffusive processes. Please see related descriptions in Section 14.3.5.

Non-Cartesian Grid Support

Grid support for non-Cartesian geometries has been revised in the unsplit hydro and MHD solvers in the current release. The supported geometries are (i) 1D spherical (ii) 2D cylindrical in r-z. Please see related descriptions in Section 8.11.

14.1.3.1 Implementation of Stationary Rigid Body in a Simulation Domain for Unsplit Hydro Solver

An approach to include a single or multiple stationary rigid body (bodies) in a simulation domain has been newly introduced in the unsplit hydro solver. Using this new feature it is possible to add any numbers of solid bodies that are of any shapes inside a computational domain, where a reflecting boundary condition is to be applied at each solid surface. Due to the nature of regualar box-like grid structure in FLASH, the surface of rigid body looks like stair steps at best rather than smooth or round shapes. High refinement levels are recommended at such stair shaped interfaces around the rigid body.

In order to add a rigid body in a simulation, users first need to add a variable called `BDRY_VAR` in a simulation `Config` file. The next step is to initialize `BDRY_VAR` in `Simulation_initBlock.F90` in such a way that a positive one is assigned to cells in a rigid body (i.e., `solnData(BDRY_VAR,i,j,k)=1.0`); otherwise a negative one for all other cells (i.e., `solnData(BDRY_VAR,i,j,k)=-1.0`).

Users can allow high resolutions around the rigid body by promoting `BDRY_VAR` to be one of the refinement variables (i.e., `refine_var_1=‘‘bdry’’` in `flash.par`).

The implementation automatically adapts `order` (a spatial reconstruction order; see Table 14.4) in fluid cells that are near the rigid body, reducing any `order` (> 1) to `order`=1 at those fluid cells adjacent to the body. This prohibits any high order (higher than 1) interpolation algorithms from reaching the rigid body data which should not be used when reconstructing high order Riemann states in the adjacent fluid cells.

For this reason there is one stability issue during simulations when `order` in the fluid cells becomes 1 and hence the local reconstruction scheme becomes a first order Godunov method. For these cells, the multidimensional local data reconstruction-evolution integration scheme reduces to a donor cell method (otherwise globally the corner-transport-upwind method by Colella) which requires a reduced CFL limit (*i.e.*, CFL $< 1/2$ for 2D; CFL $< 1/3$ for 3D). In FLASH4.3, a reduced CFL factor is automatically used in such cases; the theoretical reduced CFL limit of 1/`NDIM` is further adjusted by `hy_cflFallbackFactor`.

Two example simulations can be found in Section 30.1.12.1 and Section 30.1.12.2.

14.1.4 Multitemperature extension for Hydro

Chapter 13 described the new capabilities in FLASH for modeling High Energy Density Physics (HEDP) experiments and describes the basic theory. These experiments often require a 3T treatment of the plasma as described in Chapter 13. Equation (13.1) shows the full set of 3T equations solved by the current version of FLASH. A series of operator splits are used to isolate the hydrodynamic terms from the various source terms. The `Hydro` unit is responsible for solving the system of equations which includes the hydrodynamic terms, shown in (13.6). These terms describe advection and work. Note this system contains a redundant equation since the total energy equation, (13.6c), can be written as a sum which includes (13.6b), (13.6d), (13.6e), and (13.6f).

A significant challenge exists in solving (13.6) since (13.6d), (13.6e), and (13.6f) contain source terms that involve velocity divergences; these are the work terms. The quantity $\nabla \cdot \boldsymbol{v}$ is not defined at a shock, and thus directly evaluating this source term is not possible. Two techniques have been implemented in FLASH for solving (13.6) without evaluating the work terms directly. These will be referred to as the entropy advection approach and the RAGE-like approach. These approaches exploit the fact that the existing hydrodynamic solvers (the split and unsplit solvers) already solve the conservation equations for total mass, momentum, and energy. These equations retain the same form in the 3T case, however they are not complete and must be augmented with other equations to close the system since the total pressure is computed using an equation of state that requires knowledge of the properties of ions and electrons independently. For example, in many equations of state, we can write that $P_{\text{ele}} = P_{\text{ele}}(\rho, e_{\text{ele}})$ and $P_{\text{ion}} = P_{\text{ion}}(\rho, e_{\text{ion}})$. Thus $P = P_{\text{ele}} + P_{\text{ion}} = P(\rho, e_{\text{ele}}, e_{\text{ion}})$. In the 1T case, the system can be closed by assuming $T_{\text{ele}} = T_{\text{ion}}$.

14.1.4.1 The Entropy Advection Approach

The total entropy is not continuous at a shock. To conserve mass, momentum, and energy, shocks must irreversibly convert kinetic energy to internal energy. A good approximation that can be made is that the electron entropy is continuous across a shock. The entropy advection approach makes this assumption to solve for the state of the ions. The entropy advection approach has had limited testing. It has not been extended to incorporate radiation. Thus, there is no need to include (13.6f).

The entropy advection approach solves the first three equations of (13.6) for conservation of total mass, momentum, and energy. Now the system can be closed by solving either (13.6d) *or* (13.6e). However, this cannot be done, since those equations have terms that are divergent at shocks. The solution is to add an additional equation which states that electron entropy is advected with the fluid:

$$\frac{\partial}{\partial t}(\rho s_{\text{ele}}) + \nabla \cdot (\rho s_{\text{ele}} \boldsymbol{v}) = 0 \tag{14.10}$$

The electron internal energy, temperature and other properties are then computed using the EOS in a mode which accepts specific electron entropy s_{ele} in addition to specific combined internal energy Te_{tot} and ρ as inputs. Thus, the solution procedure for the entropy advection scheme is:

- Solve the system of equations defined by (13.6a), (13.6b), (13.6c), and (14.10)
- Compute the total specific internal energy, e_{tot}, by subtracting the kinetic energy from the total energy: $e_{\text{tot}} = E_{\text{tot}} - \boldsymbol{v} \cdot \boldsymbol{v}/2$
- Compute the electron specific internal energy using the 3T equation of state: $e_{\text{ele}} = \text{EOS}(\rho, s_{\text{ele}}, e_{\text{tot}})$
- Compute the ion specific internal energy from the total specific internal energy using the kinetic energy and the electron internal energy: $e_{\text{ion}} = e_{\text{tot}} - e_{\text{ele}}$

14.1.4.2 The RAGE-like Approach

The RAGE-like approach is so named because it is identical to the method implemented in the radiation hydrodynamics code RAGE (Gittings, 2008). Verification tests comparing the two codes have shown nearly identical behavior. The RAGE-like is physically accurate in smooth flow, but does not distribute internal energy correctly among the ions, electrons, and radiation field at shocks. This is in contrast to the entropy advection approach which does distribute energy correctly, but has its own limitations.

In general, let Δe_s be the change in the internal energy at a particular location over some short time, Δt. The subscript s refers to either ions, electrons, radiation, or the total specific internal energy. When considering only the hydrodynamic effects, $\Delta e_s = \Delta e_s^{\mathrm{adv}} + \Delta e_s^{\mathrm{work}} + \Delta e_s^{\mathrm{shock}}$, where:

1. $\Delta e_s^{\mathrm{adv}}$ refers to the change in internal energy due to the advection of internal energy with the fluid
2. $\Delta e_s^{\mathrm{work}}$ refers to the change in internal energy due to hydrodynamic work. This term is not well defined near shocks.
3. $\Delta e_s^{\mathrm{shock}}$ refers to changes in internal energy due to shock heating. Shock heating is the necessarily, irreversible conversion of kinetic energy to internal energy which occurs at shock as a consequence of conserving mass, momentum, and energy.

One physically accurate approximation is that $\Delta e_{\mathrm{ion}}^{\mathrm{shock}} = \Delta e_{\mathrm{tot}}^{\mathrm{shock}}$. The challenge of 3T hydrodynamics lies in dividing these components so that they can be correctly apportioned among the ions, electrons, and radiation field. The entropy advection approach avoids maintains the physically accurate result by solving an equation for electron entropy.

The RAGE-like approach does not apportion shock heating to only the ions. Rather it apportions the quantity $\Delta e_{\mathrm{tot}}^{\mathrm{work}} + \Delta e_{\mathrm{tot}}^{\mathrm{shock}}$ among the ions, electrons, and radiation field in proportion to the partial pressures of these components. This is consistent with (13.6) in smooth flow, but it not accurate near shocks where the shock heating should only contribute to the change in the ion internal energy. Note that it is possible to isolate internal energy changes due to advection by solving as set of advection equations for the ions, electrons, and radiation field.

Thus, the solution procedure for the RAGE-like approach is:

1. Solve the system of equations defined by (13.6a), (13.6b), and (13.6c) and simultaneously solve:

$$\frac{\partial}{\partial t}(\rho e_{\mathrm{ele}}) + \nabla \cdot (\rho e_{\mathrm{ele}} \boldsymbol{v}) = 0, \tag{14.11a}$$

$$\frac{\partial}{\partial t}(\rho e_{\mathrm{ion}}) + \nabla \cdot (\rho e_{\mathrm{ion}} \boldsymbol{v}) = 0, \tag{14.11b}$$

$$\frac{\partial}{\partial t}(\rho e_{\mathrm{rad}}) + \nabla \cdot (\rho e_{\mathrm{rad}} \boldsymbol{v}) = 0, \tag{14.11c}$$

   to update the internal energies by including only advection related changes.
2. Compute the change in total specific internal energy over the time step for each computational cell: $\Delta e_{\mathrm{tot}} = \Delta E_{\mathrm{tot}} - \boldsymbol{v} \cdot \boldsymbol{v}/2$
3. Compute $\Delta e_{\mathrm{tot}}^{\mathrm{work}} + \Delta e_{\mathrm{tot}}^{\mathrm{shock}}$ by subtracting the advected energy changes from the total change in internal energy
4. Divide $\Delta e_{\mathrm{tot}}^{\mathrm{work}} + \Delta e_{\mathrm{tot}}^{\mathrm{shock}}$ amongst the ions, electrons, and radiation field according to the ratio of pressures

14.1.4.3 Use, Implications, and Limitations of Multitemperature Hydro Approaches

Each approach has its own strengths and weaknesses. The entropy advection approach is more accurate in the sense that it correctly includes all shock heating in the ion internal energy. The RAGE-like approach is less accurate near shocks for this reason in terms of predicting the correct downstream ion temperature and electron temperature. In general, immediately downstream of a shock, the RAGE-like approach will predict an electron temperature that is too large and an ion temperature that is too small. However, the density and velocity in the vicinity of shocks will be accurate. Furthermore, ion/electron equilibration (see Chapter 13) will quickly act to equalize the ion and electron temperatures. Therefore, the RAGE-like approach is reasonable when the ion/electron equilibration time is small as is the case in many physical scenarios. The Shafranov Shock simulation (see Section 30.8.1) compares the temperatures produced by the RAGE-like approach through these two approaches.

Table 14.5: Aditional solution variables used with the hydrodynamics (`Hydro`) unit extended for multitemperature. Note that "specific" variables are understood as per mass unit of the *combined* fluid.

Variable	Corresponding 1T Variable	Type	Description
`tion`	`temp`	GENERIC	ion temperature
`tele`	`temp`	GENERIC	electron temperature
`trad`	`temp`	GENERIC	radiation temperature
`pion`	`pres`	GENERIC	ion pressure
`pele`	`pres`	GENERIC	electron pressure
`prad`	`pres`	GENERIC	radiation pressure
`eion`	`eint/ener`	PER_MASS	specific ion internal energy
`eele`	`eint/ener`	PER_MASS	specific electron internal energy
`erad`	`eint/ener`	PER_MASS	specific radiation energy
`sele`		PER_MASS (mass scalar)	specific electron entropy

The entropy advection approach has some practical limitations that prevent its use in FLASH for general problems. First, many of the 3T EOS models in FLASH do not support the calculation of electron entropy. The only EOS that does is the gamma-law model which is not appropriate modeling many HEDP experiments. Furthermore, oscillations in the electron and ion temperatures have been observed when using this approach. These oscillations can lead to negative ion temperatures. For these reasons, the entropy advection approach has not yet been used for production FLASH simulations of HEDP experiments.

Users can select which 3T hydro approach to use by setting the `hy_eosModeAfter` runtime parameter. When set to "dens_ie_gather" a RAGE-like approach is used. When set to "dens_ie_sele_gather", the entropy advection approach is used. Due to the limitations described above, the RAGE-like approach is currently the default option. The `+uhd3t` setup shortcut can be used to setup a simulation using the 3T extension of the unsplit hydrodynamics solver. The split solver is included by default whenever a multitemperature EOS is included in the simulation. The Shafranov Shock simulation (Section 30.8.1) and radiative shock (Section 30.8.2) simulations demonstrate the use of the split solver. The Laser Slab simulation (Section 30.7.5) demonstrates the use of the 3T unsplit hydrodynamics solver.

The multitemperature hydro extensions are implemented in several implementation directories named `multiTemp` within the normal hydrodynamic solvers. These contain source files that replace some of the source files of the same name that reside higher in the source tree, and related source and `Config` files. Together, these files add code functionality and solution variables that are appropriate for multitemperature simulations. The FLASH configuration mechanism automatically takes care of building with the right versions of source files when the `multiTemp` directories are included.

The `Hydro` unit thus adds variables that are used to describe the state of each of the three components. In the current version, these are maintained *in addition* to corresponding variables for the state of the fluid as a whole. There is thus redundancy in the state description. As a benefit of this redundancy, some code units that were written without multitemperature in mind may continue to function in a multitemperature context by referring to the usual 1T set of variables (like `temp`, `pres`, `ener`, `eint`). The set of variables may be optimized in future code revisions. Table 14.5 shows some of the additional variables.

`Hydro` needs a multitemperature implementation of `Eos` in oder to work for multitemperature setups. Thus when a simulation is configured to use the `multiTemp Hydro` code, it also needs to include one of the `Eos` implementations under `physics/Eos/EosMain/multiTemp`. The `Config` files under `multiTemp` in `Hydro` will take care of this, but the simulation may have to request a specific implementation under `physics/Eos/EosMain/multiTemp`. A simuation also needs to control which EOS modes to use during a simulation. Thus the runtime parameters `eosMode`, `eosModeInit`, and the new `hy_eosModeAfter` need to be set appropriately.

14.1.5 Chombo compatible Hydro

This is a slightly modified version of the split Hydro solver (Section Section 14.1.2) which must be used when including `Chombo Grid`. It is available at `physics/Hydro/HydroMain/split/PPM/chomboCompatible` and is automatically selected by the setup script whenever an application includes `Chombo Grid`.

It is required because the `Chombo` class `LevelFluxRegister` which performs flux correction at fine-coarse boundaries has a very different interface to the subroutines in Paramesh. A `LevelFluxRegister` conserves fluxes at fine-coarse boundaries and then corrects the coarse solution data. In contrast, the Paramesh subroutine `Grid_conserveFluxes` only conserves fluxes and then FLASH updates the solution data in `hy_ppm_updateSoln`.

This implementation has not been tested extensively and should not be used in a production simulation. We have encountered worse than expected mass and total energy conservation when it has been used with `Chombo Grid`. It is not yet known whether this is a problem with `Chombo` compatible Hydro or whether our AMR refinement is too aggressive and there is fine-coarse interpolation where there are sharp shock fronts. Aggressive AMR refinement could be the problem because the availability of cell-by-cell refinement in `Chombo` is very different to our prior experience with Paramesh which refines entire blocks at a time.

An example of bad mass and total energy conservation happens in a Sod problem that uses the included parameter file named `test_regular_fluxes_fbs_troublesome.par`. The boundary conditions are setup to be periodic, so that mass and total energy should be conserved. Integrated mass and total energy at the end of test problem change by order $1 \times 10^{-5}\%$. Increasing `lrefine_max` from 2 to 4 does not lead to worse conservation. We have found that we can eliminate the conservation problems in this test problem by setting `BRMeshRefineBlockFactor = 8` and `maxBlockSize = 8`, however, such a change has not fixed every test problem configuration which has shown poor conservation. In general, we get better conservation when using mesh parameter values `maxBlockSize >= 8`, `BRMeshRefineBlockFactor >= 8`, `refRatio = 2` and `tagRadius >= 2`, and so have added warning messages in the FLASH log file when these values are outside of the given range. We expect to learn more about the conservation issue soon after the FLASH4 release.

This Hydro implementation can be manually included in an application with Paramesh mesh package as follows:

```
./setup Sod -auto chomboCompatibleHydro=True -parfile=test_regular_fluxes_fbs_troublesome.par
```

The logical parameter chomboLikeUpdateSoln controls whether or not FLASH uses the standard `hy_ppm_updateSoln` for the solution update. A value of `.true.` indicates that it will not be used and is the only acceptable value for `Chombo` based applications. A value of `.false.` means it is used and is a possibility for Paramesh based applications.

Using Chombo Compatible Hydro

The runtime parameter eintSwitch should be set to 0.0 when using `physics/Hydro/-HydroMain/split/PPM/chomboCompatible`.

14.2 Relativistic hydrodynamics (RHD)

14.2.1 Overview

FLASH provides support for solving the equations of special relativistic hydrodynamics (RHD) in one, two and three spatial dimensions.

Relativistic fluids are characterized by at least one of the following two behaviors: (i) bulk velocities close to the speed of light (kinematically relativistic regime), (ii) internal energy greater than or comparable to the rest mass density (thermodynamically relativistic regime). As can be seen from the equations in Section 14.2.2, the two effects become coupled by the presence of the Lorentz factor; as a consequence, transverse velocities do not obey simple advection equations. Under these circumstances, Newtonian hydrodynamics is not adequate and a correct description of the flow must take relativistic effects into account.

14.2.2 Equations

The motion of an ideal fluid in special relativity is described by the system of conservation laws

$$\frac{\partial}{\partial t}\begin{pmatrix} D \\ \boldsymbol{m} \\ E \end{pmatrix} + \nabla\cdot\begin{pmatrix} D\boldsymbol{v} \\ \boldsymbol{m}\boldsymbol{v}+p\boldsymbol{I} \\ \boldsymbol{m} \end{pmatrix} = 0\,, \tag{14.12}$$

where D, $\boldsymbol{m}$, E, $\boldsymbol{v}$ and p define, respectively, the fluid density, momentum density, total energy density, three-velocity and pressure of the fluid. (14.12) is written in units of $c = 1$, where c is the speed of light. The same convention is also adopted in the FLASH code.

At present, only Cartesian (1, 2 and 3-D), 2-D cylindrical ($x = r$, $y = z$) and 1-D spherical (1-D, $x = r$) geometries are supported by FLASH. Gravity is not included, although it can be easily added with minor modifications.

An equation of state (Eos) provides an additional relation between thermodynamic quantities and closes the system of conservation laws ((14.12)). The current version of FLASH supports only the ideal equation of state, for which the specific enthalpy h may be expressed as

$$h = 1 + \frac{\Gamma}{\Gamma-1}\frac{p}{\rho} \tag{14.13}$$

where Γ (constant) is the specific heat ratio and ρ is the proper rest mass density. Causality ($c_s < c$) is preserved for $\Gamma < 2$. The specific heat ratio is specified as a runtime parameter (`"gamma"`).

As in classical hydrodynamics, relativistic fluids may be described in terms of a state vector of conservative, $\boldsymbol{U} = (D, \boldsymbol{m}, E)$, or primitive, $\boldsymbol{V} = (\rho, \boldsymbol{v}, p)$, variables. The connection between the two sets is given by

$$D = \gamma\rho\,, \quad \boldsymbol{m} = \rho h\gamma^2\boldsymbol{v}\,, \quad E = \rho h\gamma^2 - p\,, \tag{14.14}$$

where $\gamma = \left(1-\boldsymbol{v}^2\right)^{-1/2}$ is the Lorentz factor. Notice that the total energy density includes the rest mass contribution. The inverse relation, giving $\boldsymbol{V}$ in terms of $\boldsymbol{U}$, is

$$\rho = \frac{D}{\gamma}\,, \quad \boldsymbol{v} = \frac{\boldsymbol{m}}{E+p}\,, \quad p = Dh\gamma - E\,. \tag{14.15}$$

This inverse map is not trivial due to the non-linearity introduced by the Lorentz factor γ; it can be shown, in fact, that (14.15) can be combined together to obtain the following implicit expression for p:

$$p = Dh\big(p, \tau(p)\big)\gamma(p) - E\,. \tag{14.16}$$

(14.16) has to be solved at least once per time step in order to recover the pressure from a set of conservative variables $\boldsymbol{U}$. Notice that $\tau = \tau(p)$ depends on the pressure p through $\tau = \gamma(p)/D$ and that the specific enthalpy h is, in general, a function of both p and τ, $h = h(p, \tau(p))$. The conversion routines are implemented in the `rhd_conserveToPrimitive.F90` and `rhd_primitiveToConserve.F90` source files.

14.2.3 Relativistic Equation of State

A variant version of the ideal gamma law `Eos_wrapped.F90` routine is required by the `RHD` unit and is provided in `Eos/EosMain/Gamma/RHD`. In order to do so the unit requires a typical `Config` file which should look like this:

```
REQUIRES physics/Eos/EosMain/Gamma/RHD
```

For this specific purpose, the current `RHD` implementation supports `MODE_DENS_EI` (a default mode) and `MODE_DENS_PRES` only (but not `MODE_DENS_TEMP`) in making a `Eos_wrapped` call.

14.2.4 Additional Runtime Parameter

One additional runtime parameter used with the `RHD` unit is

Table 14.6: Additional parameters in the RHD unit.

Variable	Type	Default	Description
`rhd_reconType`	integer	1	Order of reconstruction scheme: 1 for piecewise liner; 2 for piecewise parabolic

14.3 Magnetohydrodynamics (MHD)

14.3.1 Description

The FLASH4 code includes two magnetohydrodynamic (MHD) units that represent two different algorithms. The first is the eight-wave model (`8Wave`) by Powell *et al.* (1999) that is already present in FLASH2. The second is a newly implemented unsplit staggered mesh algorithm (USM or `StaggeredMesh`). It should be noted that there are several major differences between the two MHD units. The first difference is how each algorithm enforces the solenoidal constraint of magnetic fields. The eight-wave model basically uses the truncation-error method, which effectively removes the effects of unphysical magnetic monopoles if they are generated during simulations. It does not, however, completely eliminate monopoles that are spurious in a strict physical law. To improve such unphysical effects in simulations, the unsplit staggered mesh algorithm uses the constrained transport method (Evans and Hawley, 1988) to enforce divergence-free constraints of magnetic fields. This method is shown to maintain magnitudes of $\nabla \cdot \mathbf{B}$ substantially low, e.g., to the orders of 10^{-12} or below, in most simulations. The second major difference is that the unsplit staggered mesh algorithm uses a directionally unsplit scheme to evolve the MHD governing equations, whereas the eight-wave method uses a directionally splitting method as in FLASH2. In general, the splitting method is shown to be robust, relatively straightforward to implement, and generally faster than the unsplit method. The splitting method, however, does generally introduce splitting errors when solving one-dimensional subproblems in each sweep direction for multidimensional MHD equations. This error gets introduced in simulations because (i) the linearized Jacobian flux matrices do not commute in most of the nonlinear multidimensional problems (LeVeque, 1992; LeVeque, 1998), and (ii) in MHD, dimensional-splitting based codes are not able to evolve the normal (to the sweep direction) magnetic field during each sweep direction (Gardiner and Stone, 2005).

Note that the eight-wave solver uses the same directionally splitting driver unit `Driver/DriverMain/split` as the `PPM` and `RHD` units do, while the unsplit staggered mesh solver (`StaggeredMesh`) has its own independent unsplit driver unit `Driver/DriverMain/unsplit`.

Both MHD units solve the equations of compressible ideal and non-ideal magnetohydrodynamics in one, two and three dimensions on a Cartesian system. Written in non-dimensional (hence without 4π or μ_0 coefficients) conservation form, these equations are

$$\frac{\partial \rho}{\partial t} + \nabla \cdot (\rho \mathbf{v}) = 0 \tag{14.17}$$

$$\frac{\partial \rho \mathbf{v}}{\partial t} + \nabla \cdot (\rho \mathbf{v}\mathbf{v} - \mathbf{B}\mathbf{B}) + \nabla p_* = \rho \mathbf{g} + \nabla \cdot \tau \tag{14.18}$$

$$\frac{\partial \rho E}{\partial t} + \nabla \cdot (\mathbf{v}(\rho E + p_*) - \mathbf{B}(\mathbf{v}\cdot\mathbf{B})) = \rho \mathbf{g}\cdot\mathbf{v} + \nabla \cdot (\mathbf{v}\cdot\tau + \sigma\nabla T) + \nabla \cdot (\mathbf{B} \times (\eta \nabla \times \mathbf{B})) \tag{14.19}$$

$$\frac{\partial \mathbf{B}}{\partial t} + \nabla \cdot (\mathbf{v}\mathbf{B} - \mathbf{B}\mathbf{v}) = -\nabla \times (\eta \nabla \times \mathbf{B}) \tag{14.20}$$

where

$$p_* = p + \frac{B^2}{2}, \tag{14.21}$$

$$E = \frac{1}{2}v^2 + \epsilon + \frac{1}{2}\frac{B^2}{\rho}, \tag{14.22}$$

$$\tau = \mu\left((\nabla \mathbf{v}) + (\nabla \mathbf{v})^{\mathrm{T}} - \frac{2}{3}(\nabla \cdot \mathbf{v})\mathbf{I}\right) \tag{14.23}$$

Table 14.7: Additional solution variables used in the MHD units.

Variable	Type	Description
`magx`	PER_VOLUME	x-component of magnetic field
`magy`	PER_VOLUME	y-component of magnetic field
`magz`	PER_VOLUME	z-component of magnetic field
`magp`	(GENERIC)	magnetic pressure
`divb`	(GENERIC)	divergence of magnetic field

are total pressure, specific total energy and viscous stress respectively. Also, ρ is the density of a magnetized fluid, $\mathbf{v}$ is the fluid velocity, p is the fluid thermal pressure, T is the temperature, ϵ is the specific internal energy, $\mathbf{B}$ is the magnetic field, $\mathbf{g}$ is the body force per unit mass, for example, due to gravity. τ is the viscosity tensor, μ is the coefficient of viscosity (dynamic viscosity), $\mathbf{I}$ is the unit (identity) tensor, σ is the heat conductivity, and η is the resistivity. The thermal pressure is a scalar quantity, so that the code is suitable for simulations of ideal plasmas in which magnetic fields are not so strong that they cause temperature anisotropies. As in regular hydrodynamics, the pressure is obtained from the internal energy and density using the equation of state. The two MHD units support general equations of state and multi-species fluids. Also, in order to prevent negative pressures and temperatures, a separate equation for internal energy is solved in a fashion described earlier in the hydrodynamics chapter.

The APIs of the MHD units are fairly minimal. The units honor all of hydrodynamics unit variables, interface functions and runtime parameters described in the above hydrodynamics unit chapter (see Chapter 15). In addition, both the eight-wave and the unsplit staggered mesh units declare additional plasma variables and runtime parameters, which are listed in Table 14.7 and Table 14.8.

14.3.2 Usage

In the current release, the eight-wave unit serves as a default MHD solver. In order to choose the unsplit staggered mesh unit for MHD simulations, users need to include `+usm` in a setup script. The default eight-wave unit will be automatically chosen if there is no such specification included.

A word of caution

The eight-wave solver is only compatible with native grid interpolation in AMR simulations. This is because the solver only uses two layers of guard cells in each coordinate direction. The choice `-gridinterpolation=native` is automatically adopted if `+8wave` is specified in setup, otherwise, `-gridinterpolation=native` should be explicitly included in order to use the eight-wave solver without specifying `+8wave`. For instance, running a script `./setup magnetoHD/BrioWu -1d -auto +8wave` will properly setup the `BrioWu` problem for the `8Wave` solver, and `./setup magnetoHD/BrioWu -1d -auto +usm` for the `StaggeredMesh` solver.

Supported configurations

Both MHD units currently support the uniform grid with `FIXEDBLOCKSIZE` and `NONFIXEDBLOCKSIZE` modes, and the adaptive grid with `PARAMESH` on Cartesian geometries, as well as 2D cylindrical (R-Z). When using AMR grids, the eight-wave unit supports both `PARAMESH` 2 and `PARAMESH` 4, while only `PARAMESH` 4 is supported in the unsplit staggered mesh solver because face-centered variables are only fully supported in `PARAMESH` 4.

Table 14.8: Additional runtime parameters used in the MHD units.

Variable	Type	Default	Description
`UnitSystem`	string	"none"	System of units in which MHD calculations are to be performed. Acceptable values are "none" "CGS" and "SI".
`killdivb`	logical	.true.	Enable/disable divergence cleaning.
`flux_correct`	logical	.true.	Enable/disable flux correction on AMR grid.

14.3.3 Algorithm: The Unsplit Staggered Mesh Solver

A directionally unsplit staggered mesh algorithm (USM), which solves ideal and non-ideal MHD governing equations (14.17) $\sim$ (14.20) in multiple dimensions, is a new MHD solver. Since FLASH4-beta, a full 3D implementation has been included as a new official release (Lee, submitted, 2012). The unsplit staggered mesh unit is based on a finite-volume, high-order Godunov method combined with a constrained transport (CT) type of scheme which ensures the solenoidal constraint of the magnetic fields on a staggered mesh geometry. In this approach, the cell-centered variables such as the plasma mass density ρ, plasma momentum density $\rho\mathbf{v}$ and total plasma energy ρE are updated via a second-order MUSCL-Hancock unsplit space-time integrator using the high-order Godunov fluxes. The rest of the cell face-centered (staggered) magnetic fields are updated using Stokes' Theorem as applied to a set of induction equations, enforcing the divergence-free constraint of the magnetic fields. Notice that this divergence-free constraint is automatically guaranteed and satisfied in pure one-dimensional MHD simulations, but special care must be taken in multidimensional problems.

The overall procedure of the unsplit staggered mesh scheme can be broken up into the following steps (Lee, 2006; Lee and Deane, 2009; Lee, submitted, 2012):

- *Quasi-linearization*: This step replaces the nonlinear system (14.17) $\sim$ (14.20) with an approximate, quasi-linearized system of equations.

- *Data Reconstruction-evolution*: This routine calculates and evolves cell interface values by half time step using a second-order MUSCL-Hancock TVD algorithm (Toro, 1999). The approach makes use of a new method of 'multidimensional characteristic analysis' that can be achieved in one single step, incorporating all flux contributions from both normal and transverse directions without requiring any need of solving a set of Riemann problems (that is usually adopted in transverse flux updates). In this step the USM scheme includes the multidimensional MHD terms in both normal and transverse directions, satisfying a perfect balance law for the terms proportional to $\nabla\cdot\mathbf{B}$ in the induction equations.

- *An intermediate Riemann problem*: An intermediate set of high-order Godunov fluxes is calculated using the cell interface values obtained from the data reconstruction-evolution step. The resulting fluxes are then used to evolve the normal fields by a half time step in the next procedure.

- *A half time step update for the normal fields*: The normal magnetic fields are evolved by a half time step using the flux-CT method at cell interfaces, ensuring the divergence-free property on a staggered grid. This intermediate update for the normal fields and the half time step data from the data reconstruction-evolution step together provide a second-order accurate MHD states at cell interfaces.

- *Riemann problem*: Using the second-order MHD states calculated from the above procedures, the scheme proceeds to solve the Riemann problem to obtain high-order Godunov fluxes at cell interfaces.

- *Unsplit update of cell-centered variables*: The unsplit time integrations are performed using the high-order Godunov fluxes to update the cell-centered variables for the next time step.

- *Construction of electric fields*: Using the high-order Godunov fluxes, the cell-cornered (edged in 3D) electric fields are constructed. The unsplit staggered mesh scheme computes a new modified electric field construction (MEC) scheme that includes first and second multidimensional derivative terms in Taylor expansions for high-order interpolations. This modified electric field construction provides enhanced accuracy by explicitly adding proper amounts of dissipation as well as spatial gradients in its interpolation scheme.

- *Flux-CT scheme*: The electric fields from the MEC scheme are used to evolve the cell face-centered magnetic fields by solving a set of discrete induction equations. The resulting magnetic fields satisfy the divergence-free constraint up to the accuracy of machine round-off errors.

- *Reconstruct cell-centered magnetic fields*: The cell-centered magnetic fields are reconstructed from the divergence free cell face-centered magnetic fields by taking arithmetic averages of the cell face-centered fields variables.

Note that the procedure required in solving one-dimensional MHD equations is much simpler than solving the multidimensional ones and only involves the first through third and the fifth steps in the above oulined scheme. The choices of TVD slope limiters available in the unsplit staggered mesh scheme (see Table 14.9) includes the `minmod` limiter as well as the compressible limiters such as `vanLeer` or `mc` limiter. Another choice, called `hybrid` limiter, can be used to provide a mixed type of limiters as described in Balsara (2004). In this choice, one uses a compressible limiter to produce a crisp representation for linearly degenerate waves (e.g., an entropy wave and left- and right-going Alfvén waves). To this end, a compressible limiter can be applied to the density and the magnetic fields variables, where these variables contribute much of the variations in such linearly degenerate waves. Other variables, the velocity field components and pressure, constitute four genuinely nonlinear wave families (*i.e.*, left- and right-going fast/slow magneto-sonic waves) in MHD. These genuinely nonlinear wave families inherently behave according to their self steepening mechanism and one can simply use a diffusive but robust `minmod` limiter. Another limiter, called `limited`, is also available (see details in Toro, 1999, 2nd Ed., section 13.8.4), and users need to specify a runtime parameter β (`LimitedSlopeBeta` in `flash.par`) if this limiter is chosen for a simulation.

The unsplit staggered mesh unit solves a set of discrete induction equations in multi-dimensional problems to proceed temporal evolutions of the staggered magnetic fields using electric fields. For instance, in a two-dimensional staggered grid, the unsplit staggered mesh unit solves a two-dimensional pair of discrete induction equations that were found originally by Yee (1966):

$$b^{n+1}_{x,i+1/2,j} = b^{n}_{x,i+1/2,j} - \frac{\Delta t}{\Delta y}\Big\{E^{n+1/2}_{z,i+1/2,j+1/2} - E^{n+1/2}_{z,i+1/2,j-1/2}\Big\}, \tag{14.24}$$

$$b^{n+1}_{y,i,j+1/2} = b^{n}_{y,i,j+1/2} - \frac{\Delta t}{\Delta x}\Big\{-E^{n+1/2}_{z,i+1/2,j+1/2} + E^{n+1/2}_{z,i-1/2,j+1/2}\Big\}. \tag{14.25}$$

The superindex $n + 1/2$ in the above equations simply indicates an intermediate timestep right after the temporal update of the cell-centered variables.

A three-dimensional schematic figure of the staggered grid geometry with collocations of edge-based values (electric fields E) and face based values (magnetic fields b) is shown in Figure 14.2.

One of the main advantages of using the CT-type of scheme is that the cell face-centered magnetic fields $b^{n+1}_{x,i+1/2,j}$ and $b^{n+1}_{y,i,j+1/2}$, which are updated via the above induction equations, satisfy the divergence-free constraint locally. The numerical divergence of the magnetic fields is defined as

$$(\nabla\cdot\mathbf{B})^{n+1}_{i,j} = \frac{b^{n+1}_{x,i+1/2,j} - b^{n+1}_{x,i-1/2,j}}{\Delta x} + \frac{b^{n+1}_{y,i,j+1/2} - b^{n+1}_{y,i,j-1/2}}{\Delta y} \tag{14.26}$$

and it remains zero to the accuracy of machine round-off errors, provided that $nabla \cdot \mathbf{B})^n_{i,j} = 0$.

On an AMR grid, the unsplit staggered mesh scheme uses a direct injection method as a default to preserve divergence-free prolongation to the cell face-centered fields variables. This method is one of the simplest approaches that is offered by `PARAMESH` 4 to maintain the divergence-free constraint in prolongation. This simple method ensures the solenoidal constraint well enough where the fields are varying smoothly, but can introduce oscillations in regions of steep field gradient. In such cases Balsara's prolongation algorithm can be useful. Both prolongation algorithms are supported and enabled using runtime parameters in the unsplit staggered mesh solver (see Table 14.9 below).

To solve the above induction equations (14.24) and (14.25) in a flux-CT type scheme, it is required to construct cell edge-based electric fields. The simplest choice is to use the cell face-centered high-order Godunov fluxes and take an arithmetic average to construct cell-cornered (edge-based in 3D) electric fields:

$$\begin{aligned} E^{n+1/2}_{z,i+1/2,j+1/2} &= \frac{1}{4}\Big\{ -F^{n+1/2}_{B_y,i+1/2,j} - F^{n+1/2}_{B_y,i+1/2,j+1} + G^{n+1/2}_{B_x,i,j+1/2} + G^{n+1/2}_{B_x,i+1,j+1/2} \Big\} \\ &= \frac{1}{4}\Big\{ E^{n+1/2}_{z,i+1/2,j} + E^{n+1/2}_{z,i+1/2,j+1} + E^{n+1/2}_{z,i,j+1/2} + E^{n+1/2}_{z,i+1,j+1/2} \Big\}, \end{aligned} \tag{14.27}$$

where F_{B_y} and G_{B_x} represent the x and y high-order Godunov flux components corresponding to the magnetic fields B_y and B_x, respectively (see details in Balsara and Spicer, 1999).

A high-order accurate version is also available by turning on a logical switch `E_modification` in the unsplit staggered mesh scheme, which takes Taylor series expansions of the cell-cornered electric field $E^{n+1/2}_{z,i+1/2,j+1/2}$ in all directions, followed by taking an arithmetic average of them (Lee, 2006; Lee and Deane, 2009).

The last step in the unsplit staggered mesh scheme is to reconstruct the cell-centered magnetic fields $B_{x,i,j}$ and $B_{y,i,j}$ from the divergence-free face-centered magnetic fields. The unsplit staggered mesh scheme takes arithmetic averages of the face-centered fields variables to obtain the cell-centered magnetic fields, which is sufficient for second order accuracy. After obtaining the new cell-centered magnetic fields, the total plasma energy may need to be corrected in order to preserve the positivity of the thermal temperature and pressure (Balsara and Spicer, 1999; Tóth, 2000). This energy correction is very useful especially in problems involving very low β plasma flows.

There are several choices available for calculating high order Godunov fluxes in the unsplit staggered mesh scheme. The default solver is Roe's linearized approximate solver, which takes into account all seven waves that arise in the MHD equations. The Roe solver can adopt one of the two entropy fix routines (Harten, 1983; Harten and Hyman, 1983) in ordetblrefr to avoid unphysical states near strong rarefaction regions. As all seven waves are considered in Roe's solver, high numerical resolutions can be achieved in most cases. However, Roe's solver still can fail to maintain positive states near very low densities even with the entropy fix. In this case, computationally efficient and positively conservative Riemann solvers such as HLL (Einfeldt *et al.*, 1991), HLLC (S. Li, 2005), or HLLD (Miyoshi and Kusano, 2005) can be used to maintain positive states in simulations. A hybrid type of Riemann solver which combines using the Roe solver for high accuracy and HLLD for stability is also available.

The USM solver has been recently extended also for 2D and 2.5D cylindrical (R-Z) geometries, both for uniform grids and AMR. In the cylindrical implementation, we followed the guidelines of Mignone et al. (2007) and Skinner & Ostriker (2010). Special care was also taken to ensure a divergence free interpolation of the staggered magnetic field components, when grid movements occur in AMR. This novel prolongation scheme is based on the methods described in Balsara (2001, 2004) and Li & Li (2004). More information regarding the cylindrical implementation can be found in Tzeferacos et al. (2012, in print) whereas new test problems, provided with this release, are available at Sections 30.2.3 and 30.2.4. Handling of different geometries will be available in future releases.

14.3.3.1 Slowly moving shock handling in PPM

A new dissipative mechanism is a hybridized slope limiter for PPM that combines a new upwind biased slope limiter with a conventional TVD slope limiter (Lee, D., Astronum Proc. 2010). This hybrid upwind limiter reduces spurious numerical oscillations near discontinuities, and therefore can compute sharp, monotonized profiles in compressible flows when using PPM, especially in Magnetohydrodynamics (MHD) slowly moving shock regions. (See more in Chapter 30.2.1.)

By the nature of very small numerical dissipations in PPM, unphysical oscillations in discontinuous MHD solutions can appear in a specific flow region, referred to as a *slowly moving shock* (SMS) relative to the grid. This new approach handles numerical non-oscillatory MHD solutions using PPM in SMS regions. The SMS should not be confused with so-called "slow MHD shock" which corresponds to two slow waves (i.e., $u \pm c_s$) in MHD, where c_s is the slow magneto-acoustic velocity.

The method first detects a local, slowly moving shock, and considers an upwind direction to compute a monotonicity-preserving slope limiter. This new approach, in addition to improving the numerical solutions in MHD to levels that reduce (or eliminate) such oscillatory behaviors while preserving sharp discontinuities

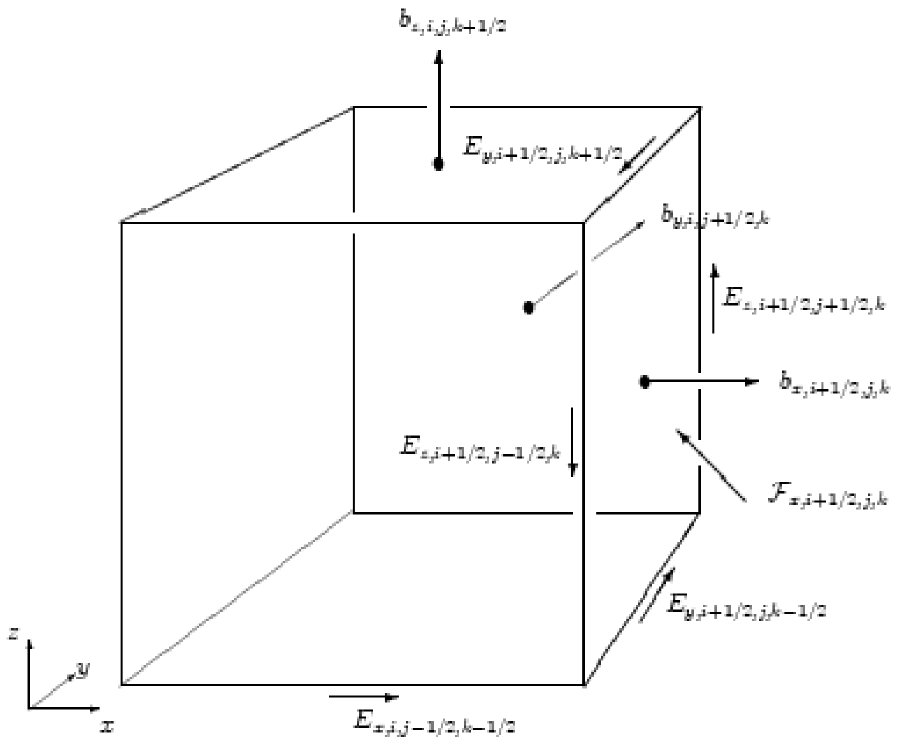

Figure 14.2: A 3D control volume on the staggered grid with the cell center at (i, j, k). The magnetic fields are collocated at the cell face centers and the electric fields at the cell edge centers. The line integral of the electric fields $\int\_\partial\mathcal{F}\_n\mathbf{E}\cdot\mathbf{T}dl$ along the four edges of the face $\mathcal{F}\_x, i+1/2, j, k$ gives rise to the negative of the rate of change of the magnetic field flux in x-direction through the area enclosed by the four edges (*i.e.*, the area of $\mathcal{F}\_x, i+1/2, j, k$).

in MHD, is also simple to implement. The method has been verified against the results from other high-resolution shock-capturing (HRSC) methods such as MUSCL and WENO schemes.

In order to enable the SMS treatment for PPM, users set a runtime parameter `upwindTVD=.true.` in `flash.par`. The SMS method does require to have an extended stencil, and users should specify `+supportPPMUpwind` in setup. See more in Section 14.1.3.

Stability limit

As described in the unsplit hydro solver unit (`physics/Hydro/HydroMain/unsplitHydro_Unsplit`), the USM MHD solver can take a wide range of CFL limits in all three dimensions (*i.e.*, CFL < 1). However, in some circumstances where there are strong shocks and rarefactions, `shockLowerCFL=.true.` could be useful to gain more numerical stability by using. It is also helpful to use (1) artificial viscosity and flattening, or (2) lower order reconstruction scheme (e.g., MH), or (2) diffusive Riemann solver such as HLL-type, or LLF solvers, or (3) a reduced CFL accordingly.

Table 14.9: Runtime parameters used in the unsplit staggered mesh MHD (`physics/Hydro/HydroMain/unsplit/MHD_StaggeredMesh`) solver additional to those described for the unsplit hydro solver (`physics/Hydro/HydroMain/unsplit/Hydro_Unsplit`).

Variable	Type	Default	Description
`killdivb`	logical	.true.	On/off $\nabla \cdot \mathbf{B} = 0$ handling on the staggered grid
`E_modification`	logical	.true.	Enable/disable high-order electric field construction
`E_upwind`	logical	.false.	Enable/disable an upwind update for induction equations
`energyFix`	logical	.true.	Enable/disable energy correction
`facevar2ndOrder`	logical	.true.	Turn on/off a second-order facevar update
`ForceHydroLimit`	logical	.false.	On/off pure Hydro mode
`prolMethod`	string	"INJECTION_PROL"	Use either direct injection method ("INJECTION_PROL") or Balsara's method ("BALSARA_PROL") in prolonging divergence-free magnetic fields stored in face-centered variables
`RiemannSolver`	string	"ROE"	"HLLD" is additionally available for MHD, "Hybrid" is also available for MHD.

Divergence-free prolongation of magnetic fields on AMR in the unsplit staggered mesh solver

It is of importance to preserve divergence-free evolutions of magnetic fields in MHD simulations. Moreover, some special cares are required in prolonging divergence-free magnetic fields on AMR grids. One simple straightforward way in this aspect is to prolong divergence-free fields to newly created children blocks using direct injection. This injection method therefore inherently preserves divergence-free properties on AMR block structures and works well in most cases. This method is a default in the unsplit staggered mesh solver and can also be enabled by setting a runtime parameter `prolMethod = "INJECTION_PROL"`. Another way, proposed by Balsara (2001), is also available in the unsplit staggered mesh solver and can be chosen by setting `prolMethod = "BALSARA_PROL"`. Both prolongation methods are supported in MHD's 2.5D and 3D simulations. In 2 and 2.5D cylindrical geometry however, since neither method takes into account geometrical factors, we use a modified prolongation algorithm based on Balsara (2004) and Li&Li (2004). This is the default option and is activated by choosing `prolMethod = "BALSARA_PROL"`. The need for this special refinement requires to have an MHD's own customized implementation of `Simulation_customizeProlong.F90` placed in the `source/Simulation/SimulationMain/magnetoHD/`.

14.3.4 Algorithm: The Eight-wave Solver

The eight-wave magnetohydrodynamic (MHD) unit is based on a finite-volume, cell-centered method that was proposed by Powell *et al.* (1999). The unit uses directional splitting to evolve the magnetohydrodynamics equations. Like the `PPM` and `RHD` units, this MHD unit makes one sweep in each spatial direction to advance physical variables from one time level to the next. In each sweep, the unit uses AMR functionality to fill in guard cells and impose boundary conditions. Then it reconstructs characteristic variables and uses these variables to compute time-averaged interface fluxes of conserved quantities. In order to enforce conservation at jumps in refinement, the unit makes flux conservation calls to AMR, which redistributes affected fluxes using the appropriate geometric area factors. Finally, the unit updates the solution and calls the EOS unit to ensure thermodynamical consistency.

After all sweeps are completed, the MHD unit enforces magnetic field divergence cleaning. In the current release only a diffusive divergence cleaning method (truncation-error method), which was the default method in FLASH2, is supported and the later release of the code will incorporate an elliptic projection cleaning method.

The ideal part of the MHD equations are solved using a high-resolution, finite-volume numerical scheme with MUSCL-type (van Leer, 1979) limited gradient reconstruction. In order to maximize the accuracy of the solver, the reconstruction procedure is applied to characteristic variables. Since this may cause certain variables, such as density and pressure, to fall outside of physically meaningful bounds, extra care is taken in the limiting step to prevent this from happening. All other variables are calculated in the unit from the interpolated characteristic variables.

In order to resolve discontinuous Riemann problems that occur at computational cell interfaces, the code by default employs a Roe-type solver derived in Powell *et al.* (1999). This solver provides full characteristic decomposition of the ideal MHD equations and is, therefore, particularly useful for plasma flow simulations that feature complex wave interaction patterns. An alternative Riemann solver of HLLE type, provided in FLASH2, has not been incorporated into FLASH4 yet.

Time integration in the MHD unit is done using a second-order, one-step method due to Hancock (Toro, 1999). For linear systems with unlimited gradient reconstruction, this method can be shown to coincide with the classic Lax-Wendroff scheme.

A difficulty particularly associated with solving the MHD equations numerically lies in the solenoidality of the magnetic field. The notorious $\nabla \cdot \mathbf{B} = 0$ condition, a strict physical law, is very hard to satisfy in discrete computations. Being only an initial condition of the MHD equations, it enters the equations indirectly and is not, therefore, guaranteed to be generally satisfied unless special algorithmic provisions are made. Without discussing this issue in much detail, which goes well beyond the scope of this user's guide (for example, see Tóth (2000) and references therein), we will remind the user that there are three commonly accepted methods to enforce the $\nabla \cdot \mathbf{B}$ condition: the elliptic projection method (Brackbill and Barnes, 1980), the constrained transport method (Evans and Hawley, 1988), and the truncation-level error method (Powell *et al.*, 1999). In the current release, the truncation-error cleaning methods is provided for the eight-wave MHD unit, and the constrained transport method is implemented for the unsplit staggered mesh MHD units (see Section 14.3.3 for details).

In the truncation-error method, the solenoidality of the magnetic field is enforced by including several terms proportional to $\nabla \cdot \mathbf{B}$. This removes the effects of unphysical magnetic tension forces parallel to the field and stimulates passive advection of magnetic monopoles, if they are spuriously created. In many applications, this method has been shown to be an efficient and sufficient way to generate solutions of high physical quality. However, it has also been shown (Tóth, 2000) that this method can sometimes, for example in strongly discontinuous and stagnated flows, lead to accumulation of magnetic monopoles, whose strength is sufficient to corrupt the physical quality of computed solutions. In order to eliminate this deficiency, the eight-wave MHD code also uses a simple yet very effective method originally due to Marder (1987) to destroy the magnetic monopoles on the scale on which they are generated. In this method, a diffusive operator proportional to $\nabla\nabla \cdot \mathbf{B}$ is added to the induction equation, so that the equation becomes

$$\frac{\partial \mathbf{B}}{\partial t} + \nabla \cdot (\mathbf{vB} - \mathbf{Bv}) = -\mathbf{v}\nabla \cdot \mathbf{B} + \eta_a \nabla\nabla \cdot \mathbf{B} \ , \tag{14.28}$$

with the artificial diffusion coefficient η_a chosen to match that of grid numerical diffusion. In the FLASH code, $\eta_a = \frac{\lambda}{2}(\frac{1}{\Delta x} + \frac{1}{\Delta y} + \frac{1}{\Delta z})^{-1}$, where λ is the largest characteristic speed in the flow. Since the grid magnetic diffusion Reynolds number is always on the order of unity, this operator locally destroys magnetic monopoles at the rate at which they are created. Recent numerical experiments (Powell *et al.*, 2001) indicate that this approach can very effectively bring the strength of spurious magnetic monopoles to levels that are sufficiently low, so that generated solutions remain physically consistent. The entire $\nabla \cdot \mathbf{B}$ control process is local and very inexpensive compared to other methods. Moreover, one can show that this process is asymptotically convergent (Munz *et al.*, 2000), and each of its applications is equivalent to one Jacobi iteration in solving the Poisson equation in the elliptic projection method. The caveat is that this method only suppresses but does not completely eliminate magnetic monopoles. Whether this is acceptable depends on the particular physical problem.

As an alternative way to eliminate magnetic monopoles completely, the FLASH2 code includes an elliptic projection method, in which the unphysical divergence of the magnetic field can be removed to any desired level down to machine precision. As yet, this method has not been made available in FLASH4 and will be supported in a later release.

14.3.5 Non-ideal MHD

Non-ideal terms (magnetic resistive, viscous and heat conduction terms) can be enabled or disabled in FLASH at run time via the `flash.par` file. For example, a typical `flash.par` file for non-ideal runtime parameters should look more or less like this:

```
# Magnetic Resistivity ---------
useMagneticResistivity  = .true.
resistivity             = 1.0E-0

# Viscosity --------------------
useViscosity            = .false.
diff_visc_nu            = 1.0E-2

# Conductivity -----------------
useConductivity         = .false.
diff_constant           = 1.0E-2
```

One way of simulating a diffusive process is to add those physics units in a simulation `Config` file. For example, a snippet of `Config` file can look like this:

```
# Magnetic Resistivity
REQUIRES physics/materialProperties/MagneticResistivity/MagneticResistivityMain

# Viscosity
REQUIRES physics/materialProperties/Viscosity/ViscosityMain

# Conduction
REQUIRES physics/materialProperties/Conductivity/ConductivityMain/Constant-diff

# Diffusive time step calculation
REQUIRES physics/sourceTerms/Diffuse/DiffuseMain
```

Including diffusive terms

New treatments has been made in including the non-ideal diffusive terms in the USM-MHD solver in the FLASH3.2 release and remain unchanged since then. In the previous releases before FLASH3.2, all the non-ideal diffusive terms had to be grouped together in the ”resistive MHD” part of the unit by turning the flag variable `useMagneticResistivity` on, and the non-ideal terms were included all together. In the FLASH3.2 release, each individual term can be separately included by turning each corresponding logical variables in run time. The Diffusion time step is computed using the `Diffuse_computeDt.F90` routine in `Driver_computeDt.F90` to provide a more consistent way of computing a non-ideal time step.

Chapter 15

Incompressible Navier-Stokes Unit

The IncompNS unit solves incompressible Navier-Stokes equations in two or three spatial dimensions. The currently released implementation assumes constant density throughout the simulation domain.

Multistep and Runge-Kutta explicit projection schemes are used for time integration. These methods are described in Armfield & Street 2002, Yang & Balaras 2006, and Vanella *et al.* 2010. Implementations using a staggered grid arrangement are provided for both uniform grid (UG) and PARAMESH adaptive mesh refinement Grid implementations. The MultigridMC and BiPCGStab Poisson solvers con be employed for AMR cases, whereas the homogeneous trigonometric solver + PFFT can be used in UG. Typical velocity boundary conditions for this problem are implemented.

More documentation to appear later.

As of FLASH4.4, Simulations that use the IncompNS unit should be configured to use a special implementation of Driver_evolveFlash located in Driver/DriverMain/INSfracstep. (Including IncompNS in the units of a simulation will automatically pull this directory into the configuration.) This requirement may change in the future.

Chapter 16

Equation of State Unit

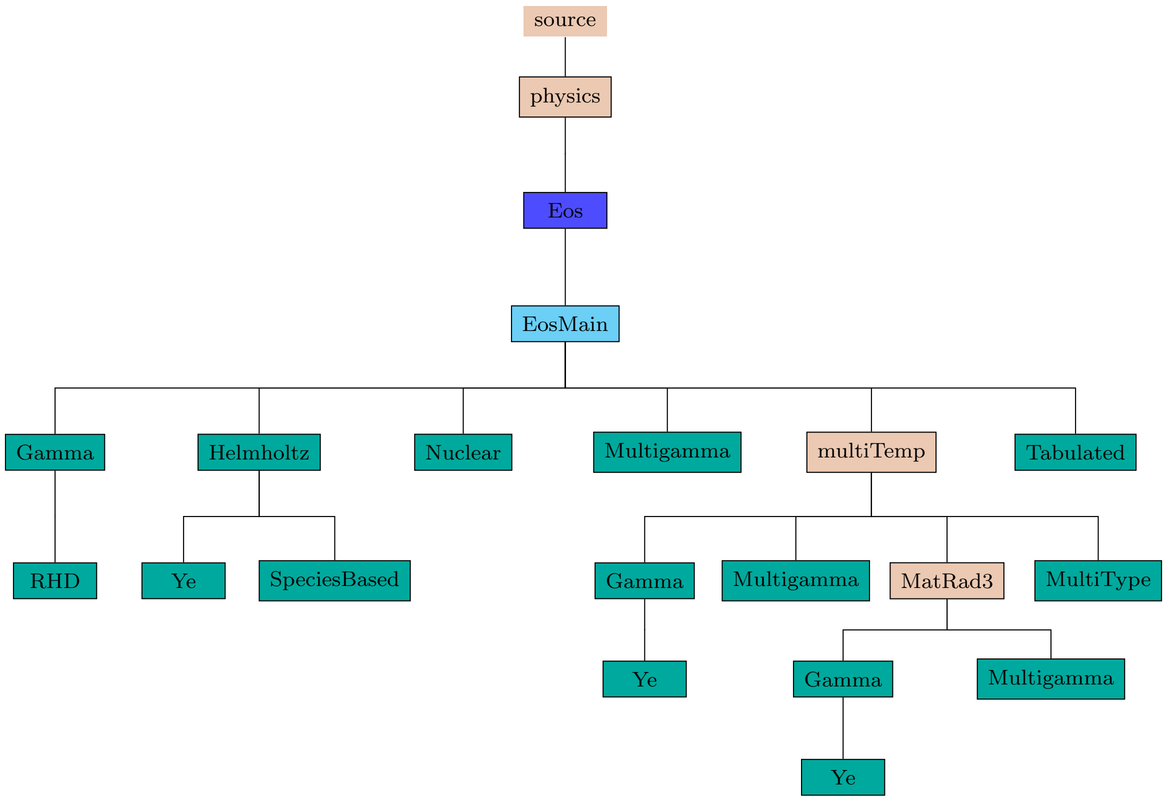

Figure 16.1: The `Eos` directory tree.

16.1 Introduction

The `Eos` unit implements the equation of state needed by the hydrodynamics and nuclear burning solvers. The function `Eos` provides the interface for operating on a one-dimensional vector. The same interface can be used for a single cell by reducing the vector size to 1. Additionally, this function can be used to find the thermodynamic quantities either from the density, temperature, and composition or from the density, internal energy, and composition. For user's convenience, a wrapper function (`Eos_wrapped`) is provided, which takes a section of a block and translates it into the data format required by the `Eos` function, then calls the function. Upon return from the Eos function, the wrapper translates the returned data back to the same section of the block.

Four implementations of the (Eos) unit are available in the current release of FLASH4: Gamma, which implements a perfect-gas equation of state; Gamma/RHD, which implements a perfect-gas equation taking relativistic effects into account; Multigamma, which implements a perfect-gas equation of state with multiple fluids, each of which can have its own adiabatic index (γ); and Helmholtz, which uses a fast Helmholtz free-energy table interpolation to handle degenerate/relativistic electrons/positrons and includes radiation pressure and ions (via the perfect gas approximation).

As described in previous sections, FLASH evolves the Euler equations for compressible, inviscid flow. This system of equations must be closed by an additional equation that provides a relation between the thermodynamic quantities of the gas. This relationship is known as the equation of state for the material, and its structure and properties depend on the composition of the gas.

It is common to call an equation of state (henceforth EOS) routine more than 10^9 times during a two-dimensional simulation and more than 10^{11} times during the course of a three-dimensional simulation of stellar phenomena. Thus, it is very desirable to have an EOS that is as efficient as possible, yet accurately represents the relevant physics. While FLASH is capable of using any general equation of state, we discuss here the three equation of state routines that are supplied: an ideal-gas or gamma-law EOS, an EOS for a fluid composed of multiple gamma-law gases, and a tabular Helmholtz free energy EOS appropriate for stellar interiors. The two gamma-law EOSs consist of simple analytic expressions that make for a very fast EOS routine both in the case of a single gas or for a mixture of gases. The Helmholtz EOS includes much more physics and relies on a table look-up scheme for performance.

16.2 Gamma Law and Multigamma

FLASH uses the method of Colella & Glaz (1985) to handle general equations of state. General equations of state contain 4 adiabatic indices (Chandrasekhar 1939), but the method of Colella & Glaz parameterizes the EOS and requires only two of the adiabatic indices. The first is necessary to calculate the adiabatic sound speed and is given by

$$\gamma_1 = \frac{\rho}{P}\frac{\partial P}{\partial \rho} \; . \tag{16.1}$$

The second relates the pressure to the energy and is given by

$$\gamma_4 = 1 + \frac{P}{\rho\epsilon} \; . \tag{16.2}$$

These two adiabatic indices are stored as the mesh-based variables GAMC_VAR and GAME_VAR. All EOS routines must return γ_1, and γ_4 is calculated from (16.2).

The gamma-law EOS models a simple ideal gas with a constant adiabatic index γ. Here we have dropped the subscript on γ, because for an ideal gas, all adiabatic indices are equal. The relationship between pressure P, density ρ, and specific internal energy ϵ is

$$P = (\gamma - 1)\,\rho\epsilon \; . \tag{16.3}$$

We also have an expression relating pressure to the temperature T

$$P = \frac{N_a k}{\bar{A}}\rho T \; , \tag{16.4}$$

where N_a is the Avogadro number, k is the Boltzmann constant, and $\bar{A}$ is the average atomic mass, defined as

$$\frac{1}{\bar{A}} = \sum_i \frac{X_i}{A_i} \; , \tag{16.5}$$

where X_i is the mass fraction of the ith element. Equating these expressions for pressure yields an expression for the specific internal energy as a function of temperature

$$\epsilon = \frac{1}{\gamma - 1}\frac{N_a k}{\bar{A}} T \; . \tag{16.6}$$

The relativistic variant of the ideal gas equation is explained in more detail in Section 14.2.

Simulations are not restricted to a single ideal gas; the multigamma EOS provides routines for simulations with several species of ideal gases each with its own value of γ. In this case the above expressions hold, but γ represents the weighted average adiabatic index calculated from

$$\frac{1}{(\gamma-1)} = \bar{A}\sum_i \frac{1}{(\gamma_i-1)}\frac{X_i}{A_i}\ . \tag{16.7}$$

We note that the analytic expressions apply to both the forward (internal energy as a function of density, temperature, and composition) and backward (temperature as a function of density, internal energy and composition) relations. Because the backward relation requires no iteration in order to obtain the temperature, this EOS is quite inexpensive to evaluate. Despite its fast performance, use of the gamma-law EOS is limited, due to its restricted range of applicability for astrophysical problems.

16.2.1 Ideal Gamma Law for Relativistic Hydrodynamics

The relativistic variant of the ideal gas equation is explained in more detail in Section 14.2.

16.3 Helmholtz

The Helmholtz EOS provided with the FLASH distribution contains more physics and is appropriate for addressing astrophysical phenomena in which electrons and positrons may be relativistic and/or degenerate and in which radiation may significantly contribute to the thermodynamic state. Full details of the Helmholtz equation of state are provided in Timmes & Swesty (1999). This EOS includes contributions from radiation, completely ionized nuclei, and degenerate/relativistic electrons and positrons. The pressure and internal energy are calculated as the sum over the components

$$P_{\rm tot} = P_{\rm rad} + P_{\rm ion} + P_{\rm ele} + P_{\rm pos} + P_{\rm coul} \tag{16.8}$$

$$\epsilon_{\rm tot} = \epsilon_{\rm rad} + \epsilon_{\rm ion} + \epsilon_{\rm ele} + \epsilon_{\rm pos} + \epsilon_{\rm coul}\ . \tag{16.9}$$

Here the subscripts "rad," "ion," "ele," "pos," and "coul" represent the contributions from radiation, nuclei, electrons, positrons, and corrections for Coulomb effects, respectively. The radiation portion assumes a blackbody in local thermodynamic equilibrium, the ion portion (nuclei) is treated as an ideal gas with $\gamma = 5/3$, and the electrons and positrons are treated as a non-interacting Fermi gas.

The blackbody pressure and energy are calculated as

$$P_{\rm rad} = \frac{aT^4}{3} \tag{16.10}$$

$$\epsilon_{\rm rad} = \frac{3P_{\rm rad}}{\rho} \tag{16.11}$$

where a is related to the Stephan-Boltzmann constant $\sigma_B = ac/4$, and c is the speed of light. The ion portion of each routine is the ideal gas of (Equations 16.3 – 16.4) with $\gamma = 5/3$. The number densities of free electrons $N_{\rm ele}$ and positrons $N_{\rm pos}$ in the noninteracting Fermi gas formalism are given by

$$N_{\rm ele} = \frac{8\pi\sqrt{2}}{h^3}\ m_{\rm e}^3\ c^3\ \beta^{3/2}\ \left[F_{1/2}(\eta,\beta)\ +\ F_{3/2}(\eta,\beta)\right] \tag{16.12}$$

$$N_{\rm pos} = \frac{8\pi\sqrt{2}}{h^3}\ m_{\rm e}^3\ c^3\ \beta^{3/2}\left[F_{1/2}\left(-\eta-2/\beta,\beta\right)\ +\ \beta\ F_{3/2}\left(-\eta-2/\beta,\beta\right)\right]\ , \tag{16.13}$$

where h is Planck's constant, m_e is the electron rest mass, $\beta = kT/(m_e c^2)$ is the relativity parameter, $\eta = \mu/kT$ is the normalized chemical potential energy μ for electrons, and $F_k(\eta, \beta)$ is the Fermi-Dirac integral

$$F_k(\eta, \beta) = \int_0^\infty \frac{x^k \ (1 + 0.5 \ \beta \ x)^{1/2} \ dx}{\exp(x - \eta) + 1} \ . \tag{16.14}$$

Because the electron rest mass is not included in the chemical potential, the positron chemical potential must have the form $\eta_{\rm pos} = -\eta - 2/\beta$. For complete ionization, the number density of free electrons in the matter is

$$N_{\rm ele,matter} = \frac{\bar{Z}}{\bar{A}} \ N_a \ \rho = \bar{Z} \ N_{\rm ion} \ , \tag{16.15}$$

and charge neutrality requires

$$N_{\rm ele,matter} = N_{\rm ele} - N_{\rm pos} \ . \tag{16.16}$$

Solving this equation with a standard one-dimensional root-finding algorithm determines η. Once η is known, the Fermi-Dirac integrals can be evaluated, giving the pressure, specific thermal energy, and entropy due to the free electrons and positrons. From these, other thermodynamic quantities such as γ_1 and γ_4 are found. Full details of this formalism may be found in Fryxell *et al.* (2000) and references therein.

The above formalism requires many complex calculations to evaluate the thermodynamic quantities, and routines for these calculations typically are designed for accuracy and thermodynamic consistency at the expense of speed. The Helmholtz EOS in FLASH provides a table of the Helmholtz free energy (hence the name) and makes use of a thermodynamically consistent interpolation scheme obviating the need to perform the complex calculations required of the above formalism during the course of a simulation. The interpolation scheme uses a bi-quintic Hermite interpolant resulting in an accurate EOS that performs reasonably well.

The Helmholtz free energy,

$$F = \epsilon - T \ S \tag{16.17}$$

$$dF = -S \ dT + \frac{P}{\rho^2} \ d\rho \ , \tag{16.18}$$

is the appropriate thermodynamic potential for use when the temperature and density are the natural thermodynamic variables. The free energy table distributed with FLASH was produced from the Timmes EOS (Timmes & Arnett 1999). The Timmes EOS evaluates the Fermi-Dirac integrals (16.14) and their partial derivatives with respect to η and β to machine precision with the efficient quadrature schemes of Aparicio (1998) and uses a Newton-Raphson iteration to obtain the chemical potential of (16.16). All partial derivatives of the pressure, entropy, and internal energy are formed analytically. Searches through the free energy table are avoided by computing hash indices from the values of any given $(T, \rho\bar{Z}/\bar{A})$ pair. No computationally expensive divisions are required in interpolating from the table; all of them can be computed and stored the first time the EOS routine is called.

We note that the Helmholtz free energy table is constructed for only the electron-positron plasma, and it is a 2-dimensional function of density and temperature, *i.e.* $F(\rho, {\rm T})$. It is made with $\bar{\rm A} = \bar{\rm Z} = 1$ (pure hydrogen), with an electron fraction $Y_{\rm e} = 1$. One reason for not including contributions from photons and ions in the table is that these components of the Helmholtz EOS are very simple (Equations 16.10 – 16.11), and one doesn't need fancy table look-up schemes to evaluate simple analytical functions. A more important reason for only constructing an electron-positron EOS table with $Y_{\rm e} = 1$ is that the 2-dimensional table is valid for *any* composition. Separate planes for each $Y_{\rm e}$ are not necessary (or desirable), since simple multiplication by $Y_{\rm e}$ in the appropriate places gives the desired composition scaling. If photons and ions were included in the table, then this valuable composition independence would be lost, and a 3-dimensional table would be necessary.

The Helmholtz EOS has been subjected to considerable analysis and testing (Timmes & Swesty 2000), and particular care was taken to reduce the numerical error introduced by the thermodynamical models below the formal accuracy of the hydrodynamics algorithm (Fryxell, et al. 2000; Timmes & Swesty 2000). The physical limits of the Helmholtz EOS are $10^{-10} < \rho < 10^{11}$ (g cm^{-3}) and $10^4 < T < 10^{11}$ (K). As with the gamma-law EOS, the Helmholtz EOS provides both forward and backward relations. In the case of the forward relation (ρ, T, given along with the composition) the table lookup scheme and analytic

Table 16.1: 1T and multitemperature Eos modes. The symbols are defined in `constants.h`. The column "1-T" indicates whether invoking `Eos` with this mode implies and/or ensures that the three components are in temperature equilibrium; a "yes" here implies that all temperatures provided as outputs are equal, and equal to T if T is listed as an input. For modes where component temperatures are allowed to stay different, the combined T has no physical meaning but indicates an "average" temperature to which the components would equilibrate if cells were held fixed without exchange of heat with neighboring cells. The columns RS indicates modes where, in the current multitemperature `Eos` implementations, a Newton-Raphson root search may be performed internally in order to compute some combined fluid quantities, in particular T. In this columnt "(y)" means the search is only necessary to get T and can otherwise be omitted. Subscripts i, e, and r stand for ions, electrons, and radiation, respectively, ϵ for specific internal energy, s for specific entropy. Note that combined density ρ is always assumed an input and omitted from the table. Material composition and ionization levels are currently also just inputs.

symbol	inputs	outputs		1-T	RS
`MODE_DENS_TEMP`	T	$\epsilon,\ P$		yes	no
`MODE_DENS_TEMP_EQUI`	T	$\epsilon,\ P,$	$T_\text{i}{=}T_\text{e}{=}T_\text{r},\ \epsilon_\text{i},\epsilon_\text{e},\epsilon_\text{r},s_\text{e},\ P_\text{i},P_\text{e},P_\text{r},\ \ldots$	yes	no
`MODE_DENS_TEMP_GATHER`	$T_\text{i},T_\text{e},T_\text{r}$	$T,\epsilon,P,$	$\epsilon_\text{i},\epsilon_\text{e},\epsilon_\text{r},s_\text{e},\ P_\text{i},P_\text{e},P_\text{r},\ \ldots$	no	(y)
`MODE_DENS_EI`	ϵ	$T,\ P$		yes	yes
`MODE_DENS_EI_SCATTER`	ϵ	$T,\ P,$	$T_\text{i}{=}T_\text{e}{=}T_\text{r},\ \epsilon_\text{i},\epsilon_\text{e},\epsilon_\text{r},s_\text{e},\ P_\text{i},P_\text{e},P_\text{r},\ \ldots$	yes	yes
`MODE_DENS_EI_GATHER`	$\epsilon_\text{i},\epsilon_\text{e},\epsilon_\text{r}$	$T,\epsilon,P,$	$T_\text{i},T_\text{e},T_\text{r},s_\text{e},\ P_\text{i},P_\text{e},P_\text{r},\ \ldots$	no	(y)
`MODE_DENS_EI_SELE_GATHER`	$\epsilon,s_\text{e},\epsilon_\text{r}$	$T,\ P,$	$T_\text{i},T_\text{e},T_\text{r},\epsilon_\text{i},\epsilon_\text{e},\ P_\text{i},P_\text{e},P_\text{r},\ \ldots$	no	(y)
`MODE_DENS_PRES`	P	$T,\ \epsilon$		yes	yes

formulae directly provide relevant thermodynamic quantities. In the case of the backward relation (ρ,ϵ, and composition given), the routine performs a Newton-Rhaphson iteration to determine temperature. It is possible for the input variables to be changed in the iterative modes since the solution is not exact. The returned quantities are thermodynamically consistent.

16.4 Multitemperature extension for Eos

Extended functionality is required of the `Eos` in order to work a multitemperature simulation. Such simulations need to use one of the implementations under the `multiTemp` directory. When the `Hydro multiTemp` code is used, as described in Section 14.1.4, one of the implementations under `physics/Eos/EosMain/multiTemp` *must* be used. Additional functionality includes

- Support for additional `Hydro` variables that describe the state for the fluid components (ions, electrons, radiation).
- Additional `Eos` modes. See Table 16.1.

16.4.1 Gamma

The multitemperature `Gamma` EOS implementation models the ion as well as the electron components as ideal gases, and the radiation component as black body thermal radiation (like the Helmholtz 1T implementation, see Section 16.3). It is a limitation of this implementation that the ionization state of ions is assumed to be fixed.

This `Eos` implementation has several runtime parameters, in part inherited from the 1T implementation, that can technically be changed but for which different values can lead to a nonsensical or inconsistent model. In particular, the values of `gamma`, `gammaIon`, `gammaEle`, and `gammaRad` should not be changed from their default values (5./3. for the first four and 4./3. for the latter). Other values have not been tested.

This EOS can include contributions from radiation, partially or completely ionized nuclei, and electrons. The desired (constant) ionization level $\bar{Z}$ of the nuclei should be specified with the `eos_singleSpeciesZ` runtime parameter. The eos_singleSpeciesA runtime parameter specifies the average atomic mass $\bar{A}$ and should be set to the mass of one atom of the material in atomic mass units. For example, for a plasma of fully ionized Carbon-12, one would set eos_singleSpeciesA $= 12.0$ and eos_singleSpeciesA $= 6.0$.

The combined pressure and internal energy are calculated as the sum over the components

$$P_{\text{tot}} = P_{\text{ion}} + P_{\text{ele}} + P_{\text{rad}} \tag{16.19}$$

$$\epsilon_{\text{tot}} = \epsilon_{\text{ion}} + \epsilon_{\text{ele}} + \epsilon_{\text{rad}} \ . \tag{16.20}$$

Here the subscripts "ion," "ele," and "rad" represent the contributions from nuclei, electrons, and radiation, respectively. The radiation portion assumes a black body in local thermodynamic equilibrium, the ion portion (nuclei) is treated as an ideal gas with $\gamma = 5/3$, and the electrons are treated as a classical ideal gas as well.

As for the 1T Helmholtz implementation, the black body pressure and energy relate to the radiation "temperature" by

$$P_{\text{rad}} = \frac{aT_{\text{rad}}^4}{3} \tag{16.21}$$

$$\epsilon_{\text{rad}} = \frac{3P_{\text{rad}}}{\rho} \tag{16.22}$$

where a is related to the Stephan-Boltzmann constant $\sigma_B = ac/4$, and c is the speed of light.

Like 1T implementations, all multitemperature implementations of Eos must return $\gamma = \gamma_1 = \frac{\rho}{P}\frac{\partial P}{\partial \rho}$, and γ_4 is calculated from (16.2). These two generalizations of adiabatic indices are usually stored as the mesh-based variables `GAMC_VAR` and `GAME_VAR` as a result of calling Eos_wrapped.

16.4.1.1 Gamma/Ye

The `Ye` variant of `Gamma` implementation is like the `Gamma` implementation, except that $\bar{A}$ and $\bar{Z}$ need not be constant throughout the domain but can vary in different parts of the fluid.

Typically, a simulation would implement a Simulation_initBlock that initializes mass scalar variables `sumy` and `ye` as desired. The initial values then get advected with the motion of the fluid. Eos interprets them as

$$\texttt{sumy} = \sum Y_i \tag{16.23}$$

and

$$\texttt{ye} = Y_e \tag{16.24}$$

and computes

$$\texttt{abar} = \bar{A} = \frac{1}{\sum Y_i} \tag{16.25}$$

and

$$\texttt{zbar} = \bar{Z} = Y_e \bar{A} \tag{16.26}$$

from them.

16.4.2 Multigamma

First a clarification, to avoid confusion: We will call ions, electrons, and radiation the three **components** of the fluid; and we designate different kinds of materials as different **species**. A fluid with several materials contributes its ions to the common ion component and its electrons to the common electron component. Currently, all adiabatic coefficients γ_i describing the electrons and the various kinds of ions should be 5/3 as for a monatomic ideal gas (despite the implementation's name!). Mixing of species in a cell results in a fluid whose matter components are described by average values $\bar{A}$ and $\bar{Z}$, which depends on the local composition as well as on the A_i and Z_i values of the various species.

In our multitemperature approximation, the three components may have different temperatures, but there is no notion of a per-species temperature.

The multitemperature `Multigamma` implementation is another variation on the multitemperature `Gamma` theme. Except for the different way of gettting $\bar{A}$ and $\bar{Z}$, all else goes as described for `Gamma`, above.

16.4.3 Tabulated

The Tabulated `Eos` implementation is currently only available for simulations configured in 3T mode. The currently supported table formats are IONMIX1 and IONMIX4. See the Opacity section Section 22.4.6 for a description of the IONMIX1 and IONMIX4 table file format.

Tables are read into memory at initialization. For IONMIX4, tables for $\bar{z}(T, Nion)$, $E_i(T, Nion)$, $E_e(T, Nion)$, $P_i(T, Nion)$, and $P_e(T, Nion)$ are used.

Eos modes like `MODE_DENS_TEMP`, `MODE_DENS_TEMP_`*component*, `MODE_DENS_TEMP_EQUI` compute Nion from dens and directly look up the output quantities in the appropriate tables. For other modes, root searches would be required.

However, the Tabulated Eos implementation is currently not being used on its own but only in connection with the Multitype implementation.

16.4.4 Multitype

Multitype implementation does Eos computations by combining Eos calls for different materials. A material is a species in the sense of the Multispecies unit. Properties of materials relevant to the Multitype Eos are thus kept in the Multispecies database.

The Multitype implementation can combine materials of different eos types. If can be used for 3T Eos modes. When used in this generally, we speak of MTMMMT Eos - multitemperature multimaterial multitype.

Currently, the Eos types that can be combined are:

- Gamma,
- Tabulated.

The Multitype implementation calls `eos_idealGamma` and `eos_tabIonmix` only in `MODE_DENS_TEMP_`*component* modes.

The prescription for combining results of such calls is currently simple: Make Eos calls for different materials separately, passing the material's partial density into the Eos as the density. Ther per-material calls are thus not aware of other materials in the same cell. Results are combined as appropriate: pressures are taken as partial pressures and are added up to give the total multimaterial pressure; specific energies are multiplied with partial densities to give energy densities, which are added up.

For 3T modes, the above is applied separately for ion and electron components, resulting in separate total energies, pressures, *etc.*, for ions and electrons. Newton-Raphson root search is done to implement Eos modes that take energies or pressures as inputs (like `MODE_DENS_EI`$*$, `MODE_DENS_PRES` [not completely implemented]), separately for ions and electrons if necessary. The blackbody radiation component is added.

To use MTMMMT, use the `+mtmmmt` setup shortcut. See the `LaserSlab` simulation for an example. See the `Multispecies` unit on initializing material properties.

16.5 Usage

16.5.1 Initialization

The initialization function of the Eos unit `Eos_init` is fairly simple for the two ideal gas gamma law implementations included. It gathers the runtime parameters and the physical constants needed by the equation of state and stores them in the data module. The Helmholtz EOS `Eos_init` routine is a little more complex. The `Helmholtz` EOS requires an input file `helm_table.dat` that contains the lookup table for the electron contributions. This table is currently stored in ASCII for portability purposes. When the table is first read in, a binary version called `helm_table.bdat` is created. This binary format can be used for faster subsequent restarts on the same machine but may not be portable across platforms. The `Eos_init` routine reads in the table data on processor 0 and broadcasts it to all other processors.

16.5.2 Runtime Parameters

Runtime parameters for the `Gamma` unit require the user to set the thermodynamic properties for the single gas. gamma, eos_singleSpeciesA, eos_singleSpeciesZ set the ratio of specific heats and the nucleon and proton numbers for the gas. In contrast, the `Multigamma` implementation does not set runtime parameters to define properties of the multiple species. Instead, the simulation `Config` file indicates the requested species, for example helium and oxygen can be defined as

```
SPECIES HE4
SPECIES O16
```

The properties of the gases are initialized in the file `Simulation_initSpecies.F90`, for example

```
subroutine Simulation_initSpecies()
  use Multispecies_interface, ONLY : Multispecies_setProperty
  implicit none
#include "Flash.h"
#include "Multispecies.h"
  call Multispecies_setProperty(HE4_SPEC, A, 4.)
  call Multispecies_setProperty(HE4_SPEC, Z, 2.)
  call Multispecies_setProperty(HE4_SPEC, GAMMA, 1.66666666667e0)
  call Multispecies_setProperty(O16_SPEC, A, 16.0)
  call Multispecies_setProperty(O16_SPEC, Z, 8.0)
  call Multispecies_setProperty(O16_SPEC, GAMMA, 1.4)
end subroutine Simulation_initSpecies
```

For the Helmholtz equation of state, the table-lookup algorithm requires a given temperature and density. When temperature or internal energy are supplied as the input parameter, an iterative solution is found. Therefore, no matter what mode is selected for `Helmholtz` input, the best initial value of temperature should be provided to speed convergence of the iterations. The iterative solver is controlled by two runtime parameters eos_maxNewton and eos_tolerance which define the maximum number of iterations and convergence tolerance. An additional runtime parameter for `Helmholtz`, eos_coulumbMult, indicates whether or not to apply Coulomb corrections. In some regions of the ρ-T plane, the approximations made in the Coulomb corrections may be invalid and result in negative pressures. When the parameter `eos_coulombMult` is set to zero, the Coulomb corrections are not applied.

16.5.3 Direct and Wrapped Calls

The primary function in the `Eos` unit, `Eos`, operates on a vector, taking density, composition, and either temperature, internal energy, or pressure as input, and returning γ_1, and either the pressure, temperature or internal energy (whichever was not used as input). This equation of state interface is useful for initializing a problem. The user is given direct control over the input and output, since everything is passed through the argument list. Also, the vector data format is more efficient than calling the equation of state routine directly on a point by point basis, since it permits pipelining and provides better cache performance. Certain optional quantities such electron pressure, degeneracy parameter, and thermodynamic derivatives can be calculated by the `Eos` function if needed. These quantities are selected for computation based upon a logical mask array provided as an input argument. A .true. value in the mask array results in the corresponding quantity being computed and reported back to the calling function. Examples of calling the basic implementation `Eos` are provided in the API description, see `Eos`.

The hydrodynamic and burning computations repeatedly call the Eos function to update pressure and temperature during the course of their calculation. Typically, values in all the cells of the block need of be updated in these calls. Since the primary Eos interface requires the data to be organized as a vector, using it directly could make the code in the calling unit very cumbersome and error prone. The wrapper interface, `Eos_wrapped` provides a means by which the details of translating the data from block to vector and back are hidden from the calling unit. The wrapper interface permits the caller to define a section of block by giving the limiting indices along each dimension. The `Eos_wrapped` routine translates the block section thus described into the vector format of the Eos interface, and upon return translates the vector format back to the block section. This wrapper routine cannot calculate the optional derivative quantities. If they are needed, call the `Eos` routine directly with the optional mask set to true and space allocated for the returned quantities.

16.6 Unit Test

The unit test of the Eos function can exercise all three implementations. Because the Gamma law allows only one species, the setup required for the three implementations is specific. To invoke any three-dimensional `Eos` unit test, the command is:

```
./setup unitTest/Eos/implementation -auto -3d
```

where *implementation* is one of `Gamma`, `Multigamma`, `Helmholtz`. The `Eos` unit test works on the assumption that if the four physical variables in question (density, pressure, energy and temperature) are in thermal equilibrium with one another, then applying the equation of state to any two of them should leave the other two completely unchanged. Hence, if we initialize density and temperature with some arbitrary values, and apply the equation of state to them in `MODE_DENS_TEMP`, then we should get pressure and energy values that are thermodynamically consistent with density and temperature. Now after saving the original temperature value, we apply the equation of state to density and newly calculated pressure. The new value of the temperature should be identical to the saved original value. This verifies that the `Eos` unit is computing correctly in `MODE_DENS_PRES` mode. By repeating this process for the remaining two modes, we can say with great confidence that the `Eos` unit is functioning normally.

In our implementation of the Eos unit test, the initial conditions applied to the domain create a gradient for density along the x axis and gradients for temperature and pressure along the y axis. If the test is being run for the Multigamma or Helmholtz implementations, then the species are initialized to have gradients along the z axis.

Chapter 17

Local Source Terms

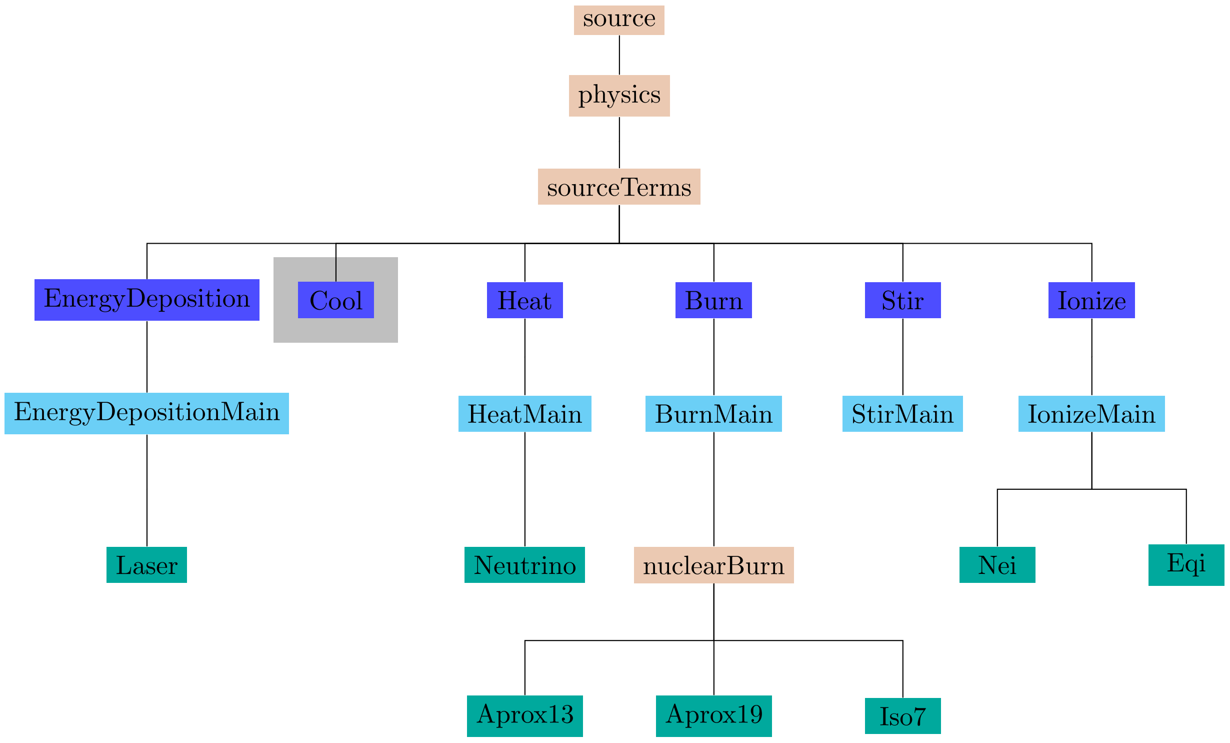

Figure 17.1: The organizational structure of physics source terms, which include units such as `Burn` and `Stir`. Shaded units include only stub implementations. Only a subset of units is shown.

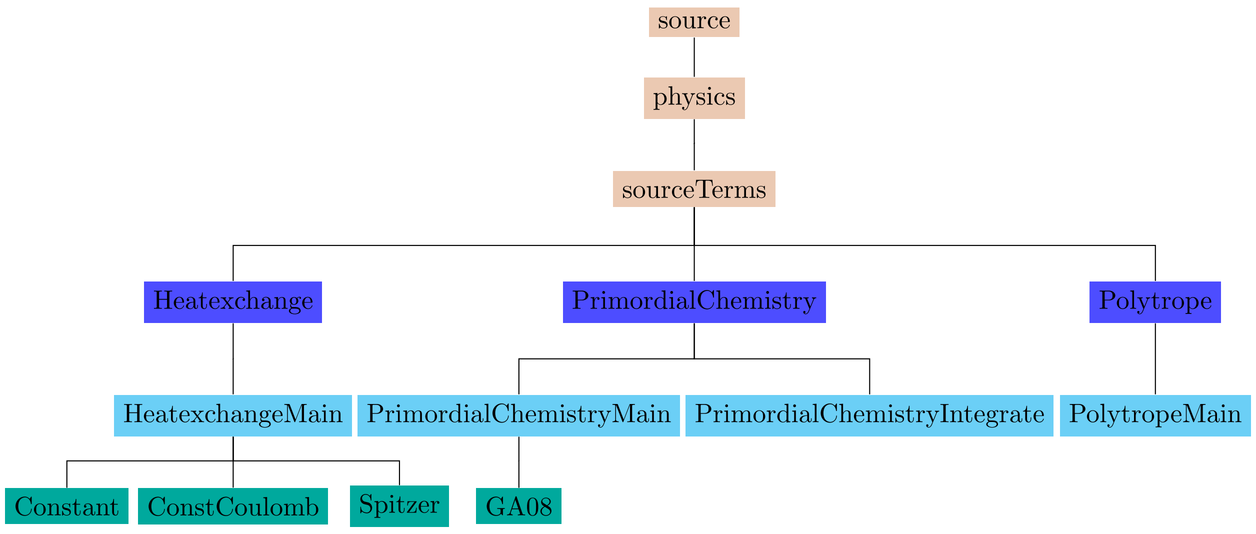

Figure 17.2: The organizational structure of physics source terms, with additional units, including `Heatexchange`.

The `physics/sourceTerms` organizational directory contains several units that implement forcing terms. The `Burn`, `Stir`, `Ionize`, and `Diffuse` units contain implementations in FLASH4. Two other units, `Cool` and `Heat`, contain only stub level routines in their API.

17.1 Burn Unit

The nuclear burning implementation of the `Burn` unit uses a sparse-matrix semi-implicit ordinary differential equation (ODE) solver to calculate the nuclear burning rate and to update the fluid variables accordingly (Timmes 1999). The primary interface routines for this unit are `Burn_init`, which sets up the nuclear isotope tables needed by the unit, and `Burn`, which calls the ODE solver and updates the hydrodynamical variables in a single row of a single block. The routine `Burn_computeDt` may limit the computational timestep because of burning considerations. There is also a helper routine `Simulation/SimulationComposition/-Simulation_initSpecies` (see `Simulation_initSpecies`) which provides the properties of ions included in the burning network.

17.1.1 Algorithms

Modeling thermonuclear flashes typically requires the energy generation rate due to nuclear burning over a large range of temperatures, densities and compositions. The average energy generated or lost over a period of time is found by integrating a system of ordinary differential equations (the nuclear reaction network) for the abundances of important nuclei and the total energy release. In some contexts, such as supernova models, the abundances themselves are also of interest. In either case, the coefficients that appear in the equations are typically extremely sensitive to temperature. The resulting stiffness of the system of equations requires the use of an implicit time integration scheme.

A user can choose between two implicit integration methods and two linear algebra packages in FLASH. The runtime parameter `odeStepper` controls which integration method is used in the simulation. The choice `odeStepper = 1` is the default and invokes a Bader-Deuflhard scheme. The choice `odeStepper = 2` invokes a Kaps-Rentrop or Rosenbrock scheme. The runtime parameter `algebra` controls which linear algebra package is used in the simulation. The choice `algebra = 1` is the default and invokes the sparse matrix MA28 package. The choice `algebra = 2` invokes the GIFT linear algebra routines. While any combination of the integration methods and linear algebra packages will produce correct answers, some combinations may execute more efficiently than others for certain types of simulations. No general rules have been found for best combination for a given simulation. The most efficient combination depends on the timestep being taken, the spatial resolution of the model, the values of the local thermodynamic variables, and the composition. Users are advised to experiment with the various combinations to determine the best one for their simulation. However, an extensive analysis was performed in the Timmes paper cited below.

Timmes (1999) reviewed several methods for solving stiff nuclear reaction networks, providing the basis for the reaction network solvers included with FLASH. The scaling properties and behavior of three semi-implicit time integration algorithms (a traditional first-order accurate Euler method, a fourth-order accurate Kaps-Rentrop / Rosenbrock method, and a variable order Bader-Deuflhard method) and eight linear algebra packages (LAPACK, LUDCMP, LEQS, GIFT, MA28, UMFPACK, and Y12M) were investigated by running each of these 24 combinations on seven different nuclear reaction networks (hard-wired 13- and 19-isotope networks and soft-wired networks of 47, 76, 127, 200, and 489 isotopes). Timmes' analysis suggested that the best balance of accuracy, overall efficiency, memory footprint, and ease-of-use was provided by the two integration methods (Bader-Deuflhard and Kaps-Rentrop) and the two linear algebra packages (MA28 and GIFT) that are provided with the FLASH code.

17.1.2 Reaction networks

We begin by describing the equations solved by the nuclear burning unit. We consider material that may be described by a density ρ and a single temperature T and contains a number of isotopes i, each of which has Z_i protons and A_i nucleons (protons + neutrons). Let n_i and ρ_i denote the number and mass density, respectively, of the ith isotope, and let X_i denote its mass fraction, so that

$$X_i = \rho_i/\rho = n_i A_i/(\rho N_A) \ , \tag{17.1}$$

where N_A is Avogadro's number. Let the molar abundance of the ith isotope be

$$Y_i = X_i/A_i = n_i/(\rho N_A) \ . \tag{17.2}$$

Mass conservation is then expressed by

$$\sum_{i=1}^{N} X_i = 1 \ . \tag{17.3}$$

At the end of each timestep, FLASH checks that the stored abundances satisfy (17.3) to machine precision in order to avoid the unphysical buildup (or decay) of the abundances or energy generation rate. Roundoff errors in this equation can lead to significant problems in some contexts (*e.g.*, classical nova envelopes), where trace abundances are important.

The general continuity equation for the ith isotope is given in Lagrangian formulation by

$$\frac{dY_i}{dt} + \nabla \cdot (Y_i \mathbf{V}_i) = \dot{R}_i \ . \tag{17.4}$$

In this equation $\dot{R}_i$ is the total reaction rate due to all binary reactions of the form *i(j,k)l*,

$$\dot{R}_i = \sum_{j,k} Y_l Y_k \lambda_{kj}(l) - Y_i Y_j \lambda_{jk}(i) \ , \tag{17.5}$$

where λ_{kj} and λ_{jk} are the reverse (creation) and forward (destruction) nuclear reaction rates, respectively. Contributions from three-body reactions, such as the triple-α reaction, are easy to append to (17.5). The mass diffusion velocities $\mathbf{V}_i$ in (17.4) are obtained from the solution of a multicomponent diffusion equation (Chapman & Cowling 1970; Burgers 1969; Williams 1988) and reflect the fact that mass diffusion processes arise from pressure, temperature, and/or abundance gradients as well as from external gravitational or electrical forces.

The case $\mathbf{V}_i \equiv 0$ is important for two reasons. First, mass diffusion is often unimportant when compared to other transport processes, such as thermal or viscous diffusion (*i.e.*, large Lewis numbers and/or small Prandtl numbers). Such a situation obtains, for example, in the study of laminar flame fronts propagating through the quiescent interior of a white dwarf. Second, this case permits the decoupling of the reaction network solver from the hydrodynamical solver through the use of operator splitting, greatly simplifying the algorithm. This is the method used by the default FLASH distribution. Setting $\mathbf{V}_i \equiv 0$ transforms (17.4) into

$$\frac{dY_i}{dt} = \dot{R}_i \ , \tag{17.6}$$

which may be written in the more compact, standard form

$$\dot{\mathbf{y}} = \mathbf{f}\ (\mathbf{y}) \ . \tag{17.7}$$

Stated another way, in the absence of mass diffusion or advection, any changes to the fluid composition are due to local processes.

Because of the highly nonlinear temperature dependence of the nuclear reaction rates and because the abundances themselves often range over several orders of magnitude in value, the values of the coefficients which appear in (17.6) and (17.7) can vary quite significantly. As a result, the nuclear reaction network equations are "stiff." A system of equations is stiff when the ratio of the maximum to the minimum eigenvalue of the Jacobian matrix $\tilde{\mathbf{J}} \equiv \partial \mathbf{f}/\partial \mathbf{y}$ is large and imaginary. This means that at least one of the isotopic abundances changes on a much shorter timescale than another. Implicit or semi-implicit time integration methods are generally necessary to avoid following this short-timescale behavior, requiring the calculation of the Jacobian matrix.

It is instructive at this point to look at an example of how (17.6) and the associated Jacobian matrix are formed. Consider the ^{12}C(α,γ)^{16}O reaction, which competes with the triple-α reaction during helium burning in stars. The rate R at which this reaction proceeds is critical for evolutionary models of massive stars, since it determines how much of the core is carbon and how much of the core is oxygen after the initial helium fuel is exhausted. This reaction sequence contributes to the right-hand side of (17.7) through the terms

$$\begin{aligned}
\dot{Y}(^4He) &= -Y(^4He)\, Y(^{12}C)\ R + \ldots \\
\dot{Y}(^{12}C) &= -Y(^4He)\, Y(^{12}C)\ R\ + \ldots \\
\dot{Y}(^{16}O) &= +Y(^4He)\, Y(^{12}C)\ R\ + \ldots ,
\end{aligned} \tag{17.8}$$

where the ellipses indicate additional terms coming from other reaction sequences. The minus signs indicate that helium and carbon are being destroyed, while the plus sign indicates that oxygen is being created. Each of these three expressions contributes two terms to the Jacobian matrix $\tilde{\mathbf{J}}$=$\partial \mathbf{f}/\partial \mathbf{y}$

$$\begin{aligned}
J(^4He,^4He) &= -Y(^{12}C)\ R\ + \ldots & J(^4He,^{12}C) &= -Y(^4He)\ R\ + \ldots \\
J(^{12}C,^4He) &= -Y(^{12}C)\ R\ + \ldots & J(^{12}C,^{12}C) &= -Y(^4He)\ R\ + \ldots \\
J(^{16}O,^4He) &= +Y(^{12}C)\ R\ + \ldots & J(^{16}O,^{12}C) &= +Y(^4He)\ R\ + \ldots .
\end{aligned} \tag{17.9}$$

Entries in the Jacobian matrix represent the flow, in number of nuclei per second, into (positive) or out of (negative) an isotope. All of the temperature and density dependence is included in the reaction rate R. The Jacobian matrices that arise from nuclear reaction networks are neither positive-definite nor symmetric, since the forward and reverse reaction rates are generally not equal. In addition, the magnitudes of the matrix entries change as the abundances, temperature, or density change with time.

This release of FLASH4 contains three reaction networks. A seven-isotope alpha-chain (`Iso7`) is useful for problems that do not have enough memory to carry a larger set of isotopes. The 13-isotope α-chain plus heavy-ion reaction network (`Aprox13`) is suitable for most multi-dimensional simulations of stellar phenomena, where having a reasonably accurate energy generation rate is of primary concern. The 19-isotope reaction network (`Aprox19`) has the same α-chain and heavy-ion reactions as the 13-isotope network, but it includes additional isotopes to accommodate some types of hydrogen burning (PP chains and steady-state CNO cycles), along with some aspects of photo-disintegration into ^{54}Fe. This 19 isotope reaction network is described in Weaver, Zimmerman, & Woosley (1978).

The networks supplied with FLASH are examples of a "hard-wired" reaction network, where each of the reaction sequences are carefully entered by hand. This approach is suitable for small networks, when minimizing the CPU time required to run the reaction network is a primary concern, although it suffers the disadvantage of inflexibility.

17.1.2.1 Two linear algebra packages: MA28 and GIFT

As mentioned in the previous section, the Jacobian matrices of nuclear reaction networks tend to be sparse, and they become more sparse as the number of isotopes increases. Since implicit or semi-implicit time integration schemes generally require solving systems of linear equations involving the Jacobian matrix, taking advantage of the sparsity can significantly reduce the CPU time required to solve the systems of linear equations.

The MA28 sparse matrix package used by FLASH is described by Duff, Erisman, & Reid (1986). This package, which has been described as the "Coke classic" of sparse linear algebra packages, uses a direct – as opposed to an iterative – method for solving linear systems. Direct methods typically divide the solution of $\tilde{\mathbf{A}} \cdot \mathbf{x} = \mathbf{b}$ into a symbolic LU decomposition, a numerical LU decomposition, and a backsubstitution phase. In the symbolic LU decomposition phase, the pivot order of a matrix is determined, and a sequence of decomposition operations that minimizes the amount of fill-in is recorded. Fill-in refers to zero matrix elements which become nonzero (*e.g.*, a sparse matrix times a sparse matrix is generally a denser matrix). The matrix is not decomposed; only the steps to do so are stored. Since the nonzero pattern of a chosen nuclear reaction network does not change, the symbolic LU decomposition is a one-time initialization cost for reaction networks. In the numerical LU decomposition phase, a matrix with the same pivot order and nonzero pattern as a previously factorized matrix is numerically decomposed into its lower-upper form. This phase must be done only once for each set of linear equations. In the backsubstitution phase, a set of linear equations is solved with the factors calculated from a previous numerical decomposition. The backsubstitution phase may be performed with as many right-hand sides as needed, and not all of the right-hand sides need to be known in advance.

MA28 uses a combination of nested dissection and frontal envelope decomposition to minimize fill-in during the factorization stage. An approximate degree update algorithm that is much faster (asymptotically and in practice) than computing the exact degrees is employed. One continuous real parameter sets the amount of searching done to locate the pivot element. When this parameter is set to zero, no searching is done and the diagonal element is the pivot, while when set to unity, partial pivoting is done. Since the matrices generated by reaction networks are usually diagonally dominant, the routine is set in FLASH to use the diagonal as the pivot element. Several test cases showed that using partial pivoting did not make a significant accuracy difference but was less efficient, since a search for an appropriate pivot element had to be performed. MA28 accepts the nonzero entries of the matrix in the $(i, j, a_{i,j})$ coordinate system and typically uses 70−90% less storage than storing the full dense matrix.

GIFT is a program which generates Fortran subroutines for solving a system of linear equations by Gaussian elimination (Gustafson, Liniger, & Willoughby 1970; Müller 1997). The full matrix $\tilde{\mathbf{A}}$ is reduced to upper triangular form, and backsubstitution with the right-hand side $\mathbf{b}$ yields the solution to $\tilde{\mathbf{A}} \cdot \mathbf{x} = \mathbf{b}$. GIFT generated routines skip all calculations with matrix elements that are zero; in this restricted sense, GIFT generated routines are sparse, but the storage of a full matrix is still required. It is assumed that the pivot element is located on the diagonal and no row or column interchanges are performed, so GIFT generated routines may become unstable if the matrices are not diagonally dominant. These routines must decompose the matrix for each right-hand side in a set of linear equations. GIFT writes out (in Fortran code) the sequence of Gaussian elimination and backsubstitution steps without any do loop constructions on the matrix $A(i, j)$. As a result, the routines generated by GIFT can be quite large. For the 489 isotope network discussed by Timmes (1999), GIFT generated $\sim 5.0\times10^7$ lines of code! Fortunately, for small reaction networks (less than about 30 isotopes), GIFT generated routines are much smaller and generally faster than other linear algebra packages.

The FLASH runtime parameter `algebra` controls which linear algebra package is used in the simulation. `algebra = 1` is the default choice and invokes the sparse matrix MA28 package. `algebra = 2` invokes the GIFT linear algebra routines.

17.1.2.2 Two time integration methods

One of the time integration methods used by FLASH for evolving the reaction networks is a 4th-order accurate Kaps-Rentrop, or Rosenbrock method. In essence, this method is an implicit Runge-Kutta algorithm. The reaction network is advanced over a timestep h according to

$$\mathbf{y}^{n+1} = \mathbf{y}^n + \sum_{i=1}^{4} b_i \Delta_i \ , \tag{17.10}$$

where the four vectors Δ^i are found from successively solving the four matrix equations

$$\begin{aligned}
(\tilde{\mathbf{1}}/\gamma h - \tilde{\mathbf{J}}) \cdot \Delta_1 &= \mathbf{f}(\mathbf{y}^n) && (17.11)\\
(\tilde{\mathbf{1}}/\gamma h - \tilde{\mathbf{J}}) \cdot \Delta_2 &= \mathbf{f}(\mathbf{y}^n + a_{21}\Delta_1) + c_{21}\Delta_1/h && (17.12)\\
(\tilde{\mathbf{1}}/\gamma h - \tilde{\mathbf{J}}) \cdot \Delta_3 &= \mathbf{f}(\mathbf{y}^n + a_{31}\Delta_1 + a_{32}\Delta_2) + (c_{31}\Delta_1 + c_{32}\Delta_2)/h && (17.13)\\
(\tilde{\mathbf{1}}^{\gamma} h - \tilde{\mathbf{J}}) \cdot \Delta_4 &= \mathbf{f}(\mathbf{y}^n + a_{31}\Delta_1 + a_{32}\Delta_2) + (c_{41}\Delta_1 + c_{42}\Delta_2 + c_{43}\Delta_3)/h \ . && (17.14)
\end{aligned}$$

b_i, γ, a_{ij}, and c_{ij} are fixed constants of the method. An estimate of the accuracy of the integration step is made by comparing a third-order solution with a fourth-order solution, which is a significant improvement over the basic Euler method. The minimum cost of this method $-$ which applies for a single timestep that meets or exceeds a specified integration accuracy $-$ is one Jacobian evaluation, three evaluations of the right-hand side, one matrix decomposition, and four backsubstitutions. Note that the four matrix equations represent a staged set of linear equations (Δ_4 depends on $\Delta_3 \ldots$ depends on Δ_1). Not all of the right-hand sides are known in advance. This general feature of higher-order integration methods impacts the optimal choice of a linear algebra package. The fourth-order Kaps-Rentrop routine in FLASH makes use of the routine GRK4T given by Kaps & Rentrop (1979).

Another time integration method used by FLASH for evolving the reaction networks is the variable order Bader-Deuflhard method (*e.g.*, Bader & Deuflhard 1983). The reaction network is advanced over a large timestep H from $\mathbf{y}^n$ to $\mathbf{y}^{n+1}$ by the following sequence of matrix equations. First,

$$\begin{aligned}
h &= H/m \\
(\tilde{\mathbf{1}} - \tilde{\mathbf{J}}) \cdot \Delta_0 &= h\mathbf{f}(\mathbf{y}^n) \\
\mathbf{y}_1 &= \mathbf{y}^n + \Delta_0 \ .
\end{aligned} \tag{17.15}$$

Then from $k = 1, 2, \ldots, m-1$

$$\begin{aligned}
(\tilde{\mathbf{1}} - \tilde{\mathbf{J}}) \cdot \mathbf{x} &= h\mathbf{f}(\mathbf{y}_k) - \Delta_{k-1} \\
\Delta_k &= \Delta_{k-1} + 2\mathbf{x} \\
\mathbf{y}_{k+1} &= \mathbf{y}_k + \Delta_k \ ,
\end{aligned} \tag{17.16}$$

and closure is obtained by the last stage

$$\begin{aligned}
(\tilde{\mathbf{1}} - \tilde{\mathbf{J}}) \cdot \Delta_m &= h[\mathbf{f}(\mathbf{y}_m) - \Delta_{m-1}] \\
\mathbf{y}^{n+1} &= \mathbf{y}_m + \Delta_m \ .
\end{aligned} \tag{17.17}$$

This staged sequence of matrix equations is executed at least twice with $m = 2$ and $m = 6$, yielding a fifth-order method. The sequence may be executed a maximum of seven times, which yields a fifteenth-order method. The exact number of times the staged sequence is executed depends on the accuracy requirements (set to one part in 10^6 in FLASH) and the smoothness of the solution. Estimates of the accuracy of an integration step are made by comparing the solutions derived from different orders. The minimum cost of this method — which applies for a single timestep that met or exceeded the specified integration accuracy — is one Jacobian evaluation, eight evaluations of the right-hand side, two matrix decompositions, and ten backsubstitutions. This minimum cost can be increased at a rate of one decomposition (the expensive part) and m backsubstitutions (the inexpensive part) for every increase in the order $2k+1$. The cost of increasing the order is compensated for, hopefully, by being able to take correspondingly larger (but accurate) timestep. The controls for order versus step size are a built-in part of the Bader-Deuflhard method. The cost per step of this integration method is at least twice as large as the cost per step of either a traditional first-order accurate Euler method or the fourth-order accurate Kaps-Rentrop discussed above. However, if the Bader-Deuflhard method can take accurate timesteps that are at least twice as large, then this method will be more efficient globally. Timmes (1999) shows that this is typically (but not always!) the case. Note that in Equations 17.15 – 17.17, not all of the right-hand sides are known in advance, since the sequence of linear equations is staged. This staging feature of the integration method may make some matrix packages, such as MA28, a more efficient choice.

The FLASH runtime parameter odeStepper controls which integration method is used in the simulation. The choice `odeStepper = 1` is the default and invokes the variable order Bader-Deuflhard scheme. The choice `odeStepper = 2` invokes the fourth order Kaps-Rentrop / Rosenbrock scheme.

17.1.3 Detecting shocks

For most astrophysical detonations, the shock structure is so thin that there is insufficient time for burning to take place within the shock. However, since numerical shock structures tend to be much wider than their physical counterparts, it is possible for a significant amount of burning to occur within the shock. Allowing this to happen can lead to unphysical results. The burner unit includes a multidimensional shock detection algorithm that can be used to prevent burning in shocks. If the useShockBurn parameter is set to `.false.`, this algorithm is used to detect shocks in the Burn unit and to switch off the burning in shocked cells.

Currently, the shock detection algorithm supports Cartesian and 2-dimensional cylindrical coordinates. The basic algorithm is to compare the jump in pressure in the direction of compression (determined by looking at the velocity field) with a shock parameter (typically 1/3). If the total velocity divergence is negative and the relative pressure jump across the compression front is larger than the shock parameter, then a cell is considered to be within a shock.

This computation is done on a block by block basis. It is important that the velocity and pressure variables have up-to-date guard cells, so a guard cell call is done for the burners only if we are detecting shocks (*i.e.* `useShockBurning = .false.`).

17.1.4 Energy generation rates and reaction rates

The instantaneous energy generation rate is given by the sum

$$\dot{\epsilon}_{\rm nuc} = N_A \sum_i \frac{dY_i}{dt} \ . \tag{17.18}$$

Note that a nuclear reaction network does not need to be evolved in order to obtain the instantaneous energy generation rate, since only the right hand sides of the ordinary differential equations need to be evaluated. It is more appropriate in the FLASH program to use the average nuclear energy generated over a timestep

$$\dot{\epsilon}_{\rm nuc} = N_A \sum_i \frac{\Delta Y_i}{\Delta t} \ . \tag{17.19}$$

In this case, the nuclear reaction network does need to be evolved. The energy generation rate, after subtraction of any neutrino losses, is returned to the FLASH program for use with the operator splitting technique.

The tabulation of Caughlan & Fowler (1988) is used in FLASH for most of the key nuclear reaction rates. Modern values for some of the reaction rates were taken from the reaction rate library of Hoffman (2001, priv. comm.). A user can choose between two reaction rate evaluations in FLASH. The runtime parameter useBurnTable controls which reaction rate evaluation method is used in the simulation. The choice `useBurnTable = 0` is the default and evaluates the reaction rates from analytical expressions. The choice `useBurnTable = 1` evaluates the reactions rates from table interpolation. The reaction rate tables are formed on-the-fly from the analytical expressions. Tests on one-dimensional detonations and hydrostatic burnings suggest that there are no major differences in the abundance levels if tables are used instead of the analytic expressions; we find less than 1% differences at the end of long timescale runs. Table interpolation is about 10 times faster than evaluating the analytic expressions, but the speedup to FLASH is more modest, a few percent at best, since reaction rate evaluation never dominates in a real production run.

Finally, nuclear reaction rate screening effects as formulated by Wallace *et al.* (1982) and decreases in the energy generation rate $\dot{\epsilon}_{\rm nuc}$ due to neutrino losses as given by Itoh *et al.* (1996) are included in FLASH.

17.1.5 Temperature-based timestep limiting

When using explicit hydrodynamics methods, a timestep limiter must be used to ensure the stability of the numerical solution. The standard CFL limiter is always used when an explicit hydrodynamics unit is included in FLASH. This constraint does not allow any information to travel more than one computational cell per timestep. When coupling burning with the hydrodynamics, the CFL timestep may be so large compared to the burning timescales that the nuclear energy release in a cell may exceed the existing internal energy in that cell. When this happens, the two operations (hydrodynamics and nuclear burning) become decoupled.

To limit the timestep when burning is performed, an additional constraint is imposed. The limiter tries to force the energy generation from burning to be smaller than the internal energy in a cell. The runtime parameter `enucDtFactor` controls this ratio. The timestep limiter is calculated as

$$\Delta t_{burn} = \texttt{enucDtFactor} \cdot \frac{E_{int}}{E_{nuc}} \tag{17.20}$$

where E_{nuc} is the nuclear energy, expressed as energy per volume per time, and E_{int} is the internal energy per volume. For good coupling between the hydrodynamics and burning, `enucDtFactor` should be < 1. The default value is kept artificially high so that in most simulations the time limiting due to burning is turned off. Care must be exercised in the use of this routine.

17.2 Ionization Unit

The analysis of UV and X-ray observations, and in particular of spectral lines, is a powerful diagnostic tool of the physical conditions in astrophysical plasmas (*e.g.*, the outer layers of the solar atmosphere, supernova remnants, *etc.*). Since deviation from equilibrium ionization may have a non-negligible effect on the UV and X-ray lines, it is crucial to take into account these effects in the modeling of plasmas and in the interpretation of the relevant observations.

In light of the above observations, FLASH contains the unit `Ionize`, in particular the implementation `physics/sourceTerms/Ionize/IonizeMain/Nei`, which is capable of computing the density of each ion species of a given element taking into account non-equilibrium ionization (NEI). This is accomplished by solving a system of equations consisting of the fluid equations of the whole plasma and the continuity equations of the ionization species of the elements considered. The densities of the twelve most abundant elements in astrophysical material (He, C, N, O, Ne, Mg, Si, S, Ar, Ca, Fe, and Ni) plus fully ionized hydrogen and electrons can be computed by this unit.

The Euler equations plus the set of advection equations for all the ion species take the following form

$$\begin{aligned} \frac{\partial \rho}{\partial t} + \nabla \cdot (\rho \mathbf{v}) &= 0 && (17.21)\\ \frac{\partial \rho \mathbf{v}}{\partial t} + \nabla \cdot (\rho \mathbf{v}\mathbf{v}) + \nabla P &= \rho \mathbf{g} && (17.22)\\ \frac{\partial \rho E}{\partial t} + \nabla \cdot [(\rho E + P)\,\mathbf{v}] &= \rho \mathbf{v} \cdot \mathbf{g}\ \ [+S\,] && (17.23)\\ \frac{\partial n_i^Z}{\partial t} + \nabla \cdot n_i^Z \mathbf{v} &= R_i^Z \quad (i = 0, \ldots, Z)\ , && (17.24) \end{aligned}$$

where ρ is the fluid density, t is the time, $\mathbf{v}$ is the fluid velocity, P is the pressure, E is the sum of the internal energy and kinetic energy per unit mass, $\mathbf{g}$ is the acceleration due to gravity, n_i^Z is the number density of ions of ionization level i of the element Z, and

$$R_i^Z = N_e [n_{i+1}^Z \alpha_{i+1}^Z + n_{i-1}^Z S_{i-1}^Z - n_i^Z(\alpha_i^Z + S_i^Z)]\ , \tag{17.25}$$

Table 17.1: Runtime parameters used with the `Ionize` unit.

Variable	Type	Default	Description
`tneimin`	real	1.0×10^4	Min nei temperature
`tneimax`	real	1.0×10^7	Max nei temperature
`dneimin`	real	1.0	Min nei electron number density
`dneimax`	real	1.0×10^{12}	Max nei electron number density

where N_e is the electron number density, $\alpha_i^Z \equiv \alpha(N_e, T)$ are the coefficients of collisional and dielectronic recombination, and $S_i^Z \equiv S(N_e, T)$ are the collisional ionization coefficients of Summers(1974). Note that `NSPECIES`, the total number of FLASH species, will be given by

$$N_{\rm spec} = 2 + \sum_Z (Z+1);$$

the sum ranges over all the elements from the list above that are included in the problem, and the additional 2 comes from the hydrogen and electron mass fractions which are automatically included by the `IonizeMain` subunit.

17.2.1 Algorithms

A fractional step method is required to integrate the equations and in particular to decouple the NEI solver from the hydro solver. For each timestep, the homogeneous hydrodynamic transport equations given by (17.21) are solved using the FLASH hydrodynamics solver with $R_i^Z = 0$. After each transport step, the "stiff" systems of ordinary differential equations (one system per element included in the simulation) for the NEI problem

$$\frac{\partial n_i^Z}{\partial t} = R_i^Z \ (i = 0, \ldots, Z) \tag{17.26}$$

are integrated. This step incorporates the reactive source terms. Within each grid cell, the above equations can be solved separately with a standard ODE method. Since this system is "stiff", it is solved using the Bader-Deuflhard time integration solver with the MA28 sparse matrix package. Timmes (1999) has shown that these two algorithms together provide the best balance of accuracy and overall efficiency for the similar problem of nuclear burning, see Section 17.1.

Note that in the present version, the contribution of the ionization and recombination to the energy equation (the bracketed term in (17.23)) is not accounted for. Also, it should be noted that the source term in the NEI unit implementation is adequate to solve the problem for optically thin plasma in the "coronal" approximation; just collisional ionization, auto-ionization, radiative recombination, and dielectronic recombination are considered.

17.2.2 Usage

In order to run a FLASH executable that uses the ionization unit, the ionization coefficients of Summers (1974) must be contained in a file named `summers_den_1e8.rates` in the same directory as the executable when the simulation is run. This file is copied into the `object/` directory with the `Config` keyword `DATAFILES` in the `physics/sourceTerms/Ionize/IonizeMain` implementation.

The `Ionize` unit supplies the runtime parameters described in Table 17.1. There are two implementations of `physics/sourceTerms/Ionize/IonizeMain`: the default implementation, `Nei` (tested using `Neitest` (see Section 30.7.1)), and `Eqi` (untested in FLASH4). The former computes ion species for non-equilibrium ionization, and the latter computes ion species in the approximation of ionization equilibrium.

The `Ionize` unit requires that the subunit implementation `Simulation/SimulationComposition/-Ionize` be used to set up the ion species of the fluid. The ions are defined in a file `Simulation/-SimulationComposition/Ionize/SpeciesList.txt`, however, the `Config` file in the simulation directory (e.g. `Simulation/SimulationMain/Neitest/Config`) defines which subset of these elements are to be used.

17.3 Stir Unit

The addition of driving terms in a hydrodynamical simulation can be a useful feature, for example, in generating turbulent flows or for simulating the addition of power on larger scales (*e.g.*, supernova feedback into the interstellar medium). The `Stir` unit comes in two implementations: 1) the `Generate` implementation, in which a divergence-free, random time-correlated 'stirring' velocity is directly added at selected modes in the simulation and 2) the `FromFile` implementation, in which a stirring field is set up from data residing on a file. The `FromFile` implementation allows to set up identical stirring fields on different platforms, and thus comparisons can be made between different codes.

Before FLASH 4.2, the implementation now called `Generate` was the only one provided. It is still the default that is being used if one specifies just REQUIRES physics/sourceTerms/Stir in a `Config` file or `-unit=physics/sourceTerms/Stir` on the `setup` command line.

17.3.1 Stir Unit: Generate Implementation

In the generate implementation, the Stir unit directly adds a divergence-free, time-correlated 'stirring' velocity at selected modes in the simulation.

The time-correlation is important for modeling realistic driving forces. Most large-scale driving forces are time-correlated, rather than white-noise; for instance, turbulent stirring from larger scales will be correlated on timescales related to the lifetime of an eddy on the scale of the simulation domain. This time correlation will lead to coherent structures in the simulation that will be absent with white-noise driving.

For each mode at each timestep, six separate phases (real and imaginary in each of the three spatial dimensions) are evolved by an Ornstein-Uhlenbeck (OU) random process (Uhlenbeck 1930). The OU process is a zero-mean, constant-rms process, which at each step 'decays' the previous value by an exponential $f = e^{(\frac{\Delta t}{\tau})}$ and then adds a Gaussian random variable with a given variance, weighted by a 'driving' factor $\sqrt{(}1 - f^2)$. Since the OU process represents a velocity, the variance is chosen to be the square root of the specific energy input rate (set by the runtime parameter `st_energy`) divided by the decay time τ (`st_decay`). In the limit that the timestep $\Delta t \to 0$, it is easily seen that the algorithm represents a linearly-weighted summation of the old state with the new Gaussian random variable.

By evolving the phases of the stirring modes in Fourier space, imposing a divergence-free condition is relatively straightforward. At each timestep, the solenoidal component of the velocities is projected out, leaving only the non-compressional modes to add to the velocities.

The velocities are then converted to physical space by a direct Fourier transform – *i.e.*, adding the sin and cos terms explicitly. Since most drivings involve a fairly small number of modes, this is more efficient than an FFT, since the FFT would need large numbers of modes (equal to six times the number of cells in the domain), the vast majority of which would have zero amplitude.

17.3.2 Stir Unit: FromFile Implementation

In the from file implementation, the Stir unit sets up a stirring field from data residing on a file. Here we summarize the method for driving turbulence used in Federrath et al. (2010, A&A, 512, A81). Please refer to that paper for further details.

Turbulence decays in about a crossing time, because the kinetic energy carried by the turbulence dissipates on small scales and turns into heat. In order to study the statistics of turbulence (e.g., the PDF, power spectrum, structure functions, etc.) over a significant time period thus requires continuous stirring (also called driving or forcing) with a turbulent acceleration field, which we call $\vec{f}(\vec{x}, t)$ in the following.

The stirring field $\vec{f}$ is often modeled with a spatially static pattern for which the amplitude is adjusted in time. This results in a roughly constant energy input on large scales, but has the disadvantage that the turbulence is not really random, because the large-scale pattern is fixed, which may introduce undesirable systematics. Other studies model $\vec{f}$ such that it can vary in time *and* space to achieve a smoothly varying pattern that resembles the flow of kinetic energy from scales larger than the simulation box scale. The most widely used method to achieve this is the Ornstein-Uhlenbeck (OU) process. The OU process is a well-defined stochastic process with a finite autocorrelation timescale. It can be used to excite turbulent motions in 3D, 2D, or 1D simulations as explained in Eswaran & Pope (1988, Computers & Fluids, 16, 257).

The OU process is a stochastic differential equation describing the evolution of $\widehat{\vec{f}}$ in Fourier space (k-space):

$$\mathrm{d}\widehat{\vec{f}}(\vec{k},t) = f_0(\vec{k})\,\underline{\mathcal{P}}^{\zeta}(\vec{k})\,\mathrm{d}\vec{\mathcal{W}}(t) \;-\; \widehat{\vec{f}}(\vec{k},t)\,\frac{\mathrm{d}t}{T}\;. \tag{17.27}$$

The first term on the right hand side is a diffusion term. This term is modeled by a Wiener process $\vec{\mathcal{W}}(t)$, which adds a Gaussian random increment to the vector field given in the previous time step $\mathrm{d}t$. Wiener processes are random processes, such that

$$\vec{\mathcal{W}}(t) - \vec{\mathcal{W}}(t-\mathrm{d}t) = \vec{\mathcal{N}}(0,\mathrm{d}t)\;, \tag{17.28}$$

where $\vec{\mathcal{N}}(0,\mathrm{d}t)$ denotes the 3D, 2D, or 1D version of a Gaussian distribution with zero mean and standard deviation $\mathrm{d}t$. This is combined with a projection using the projection tensor $\underline{\mathcal{P}}^{\zeta}(\vec{k})$ in Fourier space. In index notation, the projection operator reads

$$\mathcal{P}_{ij}^{\zeta}(\vec{k}) = \zeta\,\mathcal{P}_{ij}^{\perp}(\vec{k}) + (1-\zeta)\,\mathcal{P}_{ij}^{\parallel}(\vec{k}) = \zeta\,\delta_{ij} + (1-2\zeta)\,\frac{k_i k_j}{|k|^2}\;, \tag{17.29}$$

where δ_{ij} is the Kronecker symbol, and $\mathcal{P}_{ij}^{\perp} = \delta_{ij} - k_i k_j/k^2$ and $\mathcal{P}_{ij}^{\parallel} = k_i k_j/k^2$ are the solenoidal (divergence-free) and the compressive (curl-free) projection operators, respectively. The projection operator serves to construct a purely solenoidal stirring field by setting $\zeta = 1$. For $\zeta = 0$, a purely compressive stirring field is obtained. Any combination of solenoidal and compressive modes can be constructed by choosing $\zeta \in [0,1]$. By changing the parameter ζ, we can thus set the power of compressive modes with respect to the total power in the driving field. The analytical ratio of compressive power to total power can be derived from equation (17.29) by evaluating the norm of the compressive component of the projection tensor,

$$\left|(1-\zeta)\,\mathcal{P}_{ij}^{\parallel}\right|^2 = (1-\zeta)^2\;, \tag{17.30}$$

and by evaluating the norm of the full projection tensor

$$\left|\mathcal{P}_{ij}^{\zeta}\right|^2 = 1 - 2\zeta + D\zeta^2\;. \tag{17.31}$$

The result of the last equation depends on the dimensionality $D = 1,2,3$ of the simulation, because the norm of the Kronecker symbol $|\delta_{ij}| = 1$, 2 or 3 in one, two or three dimensions, respectively. The ratio of equations (17.30) and (17.31) gives the relative power in compressive modes, $F_{\mathrm{long}}/F_{\mathrm{tot}}$, as a function of ζ:

$$\frac{F_{\mathrm{long}}}{F_{\mathrm{tot}}} = \frac{(1-\zeta)^2}{1-2\zeta+D\zeta^2}\;. \tag{17.32}$$

Figure 17.3 provides a graphical representation of this ratio for the 1D, 2D, and 3D case. For comparison, we plot numerical values of the forcing ratio obtained in eleven 3D and 2D hydrodynamical simulations by Federrath et al. (2010, A&A, 512, A81), in which we varied the forcing parameter ζ from purely compressive stirring ($\zeta = 0$) to purely solenoidal stirring ($\zeta = 1$) in the range $\zeta = [0,1]$, separated by $\Delta\zeta = 0.1$. Note that a natural mixture of stirring modes is obtained for $\zeta = 0.5$, which leads to $F_{\mathrm{long}}/F_{\mathrm{tot}} = 1/3$ for 3D turbulence, and $F_{\mathrm{long}}/F_{\mathrm{tot}} = 1/2$ for 2D turbulence. A simple way to understand this natural ratio is to consider longitudinal and transverse waves. In 3D, the longitudinal waves occupy one of the three spatial dimensions, while the transverse waves occupy two of the three on average. Thus, the longitudinal (compressive) part has a relative power of 1/3, while the transverse (solenoidal) part has a relative power of 2/3 in 3D. In 2D, the natural ratio is 1/2, because longitudinal and transverse waves are evenly distributed in two dimensions.

The second term on the right-hand side of equation (17.27) is a drift term describing the exponential decay of the autocorrelation of $\vec{f}$. The usual procedure is to set the autocorrelation timescale equal to the turbulent crossing time, $T = L_{\mathrm{peak}}/V$, on the scale of energy injection, L_{peak}. This type of stirring models the kinetic energy input from large-scale turbulent fluctuations breaking up into smaller and smaller structures.

The runtime parameters associated with the `StirFromFile` unit are described in the 17.3.3 section.

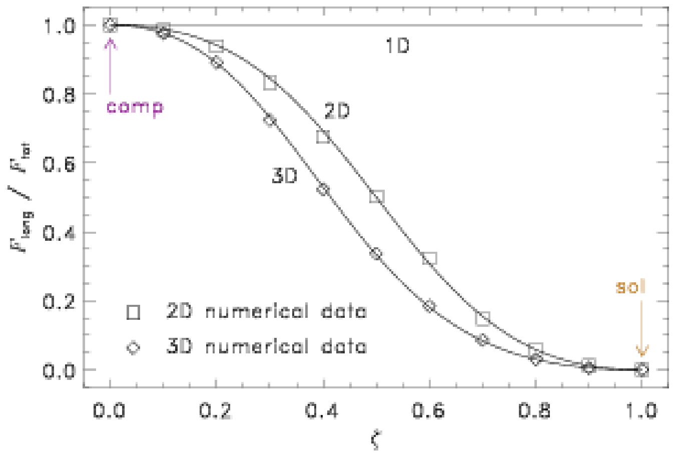

Figure 17.3: Ratio of compressive to total power of the turbulent stirring field, reprinted from Federrath et al. (2010, A&A, 512, A81) with permission by Astronomy & Astrophysics. The solid lines labelled with 1D, 2D, and 3D show the analytical expectation for this ratio, equation (17.32), as a function of the stirring parameter ζ for one-, two- and three-dimensional driving, respectively. The diamonds and squares show results of numerical simulations in 3D and 2D with $\zeta = [0, 1]$, separated by $\Delta\zeta = 0.1$. The two limiting cases of purely solenoidal stirring ($\zeta = 1$) and purely compressive stirring ($\zeta = 0$) are indicated as "sol" and "comp", respectively. Note that in any 1D model, all power is in the compressive component, and thus $F\_long/F\_tot = 1$, independent of ζ.

17.3.3 Using the StirFromFile Unit

17.3.3.1 Runtime Parameters

Table 17.2: Runtime parameters for the stirring module.

Variable	Type	Default	Description
`useStir`	boolean	.true.	switch stirring on/off
`st_computeDt`	boolean	.false.	restrict timestep based on stirring
`st_infilename`	string	"forcingfile.dat"	file containing the stirring time sequence

Table 17.2 lists the runtime parameters for the StirFromFile unit. This includes a switch for turning the stirring module on/off and a switch to restrict the timestep based on the acceleration field used for stirring (`st_computeDt` is switched off by default, because it is normally sufficient to restrict the timestep based on the gas velocity). Finally, `st_infilename` is the name of the input file containing the time and mode sequence used for stirring. This file must be prepared in advance with a separate Fortran program located in `SimulationMain/StirFromFile/forcing_generator/`. The reason for this structural splitting is to predetermine what the code is going to do. For instance, by preparing the time sequence of the stirring in advance, one can always reproduce exactly the full evolution of all driving patterns applied during a simulation. It also has the advantage that exactly identical stirring patterns can be applied in completely different codes, because they read the time and mode sequence from the same stirring file (Price & Federrath, 2010, MNRAS, 406, 1659).

The stirring module is compatible with any hydro or MHD solver and any grid implementation (uniform or AMR). Upon inclusion in a FLASH setup or module, the `StirFromFile` module defines three additional grid scalar fields, `accx`, `accy`, and `accz`, holding the three vector components of the stirring field $\vec{f}$.

17.3.3.2 Preparing the Stirring Sequence (`st_infilename`)

Table 17.3: Parameters in `forcing_generator.F90` to prepare a stirring sequence.

Variable	Type	Default	Description
`ndim`	integer	3	The dimensionality of the simulation (1, 2, or 3)
`xmin, xmax`	real	−0.5, 0.5	Domain boundary coordinates in x direction
`ymin, ymax`	real	−0.5, 0.5	Domain boundary coordinates in y direction
`zmin, zmax`	real	−0.5, 0.5	Domain boundary coordinates in z direction
`st_spectform`	integer	1	Spectral shape (0: band, 1: paraboloid)
`st_decay`	real	0.5	Autocorrelation time of the OU process, $T = L_{\mathrm{peak}}/V$
`st_energy`	real	2e-3	Determines the driving amplitude
`st_stirmin`	real	6.283	Minimum wavenumber stirred (e.g., $k_{\mathrm{min}} \lesssim 2\pi/L_{\mathrm{box}}$)
`st_stirmax`	real	18.95	Maximum wavenumber stirred (e.g., $k_{\mathrm{max}} \gtrsim 6\pi/L_{\mathrm{box}}$)
`st_solweight`	real	1.0	Mode mixture $\zeta = [0, 1]$ in Eq. (17.32). Typical values are 1.0: solenoidal; 0.0: compressive; 0.5: natural mixture.
`st_seed`	integer	140281	Random seed for stirring sequence
`end_time`	real	5.0	Final time in stirring sequence
`nsteps`	integer	100	Number of realizations between $t = 0$ and `end_time`
`outfilename`	string	"forcingfile.dat"	Output name (input file `st_infilename` for FLASH)

The code requires a time sequence of stirring modes at runtime, which have to be prepared with the standalone Fortran program `forcing_generator.F90` in `SimulationMain/StirFromFile/forcing_generator/`. A Makefile is provided in the same directory. This program prepares the time sequence of Fourier modes, which is then read by FLASH during runtime, to construct the physical acceleration fields used for stirring. It controls the spatial structure and the temporal correlation of the driving, its amplitude, the mode mixture, and the time separation between successive driving patterns. The user has to modify `forcing_generator.F90` to construct a requested driving sequence and to tailor it to the desired physical situation to be modeled.

Table 17.3 lists all the parameters that can be adjusted in the main routine of `forcing_generator.F90`. Most of them are straightforward to set (`ndim`, `xmin, xmax, ymin, ...`[1]), but others may require some explanation. For example, `st_spectform` determines the shape of the driving amplitude in Fourier space. Many colleagues drive a band (`st_spectform`=0), i.e., equal power injected between wavenumber modes k_{min} = `st_stirmin` and k_{max} = `st_stirmax`. This produces a sharp transition between stirred modes and modes that are not stirred. Here we set the default to a smooth function, a paraboloid (`st_spectform`=1), such that most power is injected on wavenumber $k_{\mathrm{peak}} = (k_{\mathrm{min}} + k_{\mathrm{max}})/2$ and falls off quadratically towards both wavenumber ends, normalized such that the injected power at k_{min} and k_{max} vanishes. This has the advantage of defining a characteristic peak injection scale k_{peak} and achieves a smooth transition between stirred and non-stirred wavenumbers.

`st_decay` and `st_energy` determine the autocorrelation time of the OU process and the total injected energy, which is simply a measure for the normalization of the acceleration field. These parameters must be adjusted according to the physical setup. For instance, for a given target velocity dispersion V on the injection scale $L_{\mathrm{peak}} = 2\pi/k_{\mathrm{peak}}$, the autocorrelation time should be set equal to the turbulent crossing time, $T = L_{\mathrm{peak}}/V$. In contrast, setting `st_decay` to a very small or a very large number results in white noise driving or in a static driving pattern, respectively.

The parameter `st_solweight` determines whether the acceleration field will be solenoidal (divergence-free) or compressive (curl-free) or any mixture, according to Equation (17.32). Incompressible gases should naturally be driven with a purely solenoidal field ($\zeta = 1$), while compressible turbulence in the interstellar medium may be driven primarily by a mixture of solenoidal and compressive modes. A detailed study of the influence of ζ is presented in Federrath et al. (2010, A&A, 512, A81).

[1]Note that we typically assume a cubic box with side length L_box = `xmax` − `xmin` = `ymax` − `ymin` = `zmax` − `zmin`

st_seed is the random seed for the OU sequence and determines the pseudo random number sequence for the integrated Box-Muller random number generator.

Finally, end_time and nsteps determine the final physical time for stirring and the number of driving patterns to be prepared within the time period from $t = 0$ to $t =$ end_time. This sets the number of equally-spaced times at which FLASH is going to read a new stirring pattern from the file. This allows the user to control how frequently a new driving pattern is constructed. A useful time separation of successive driving patterns is about 10% of a crossing time (or autocorrelation time), i.e., setting nsteps $= 10 \times$ end_time/st_decay. This will sample the smooth changes in the OU driving sequence sufficiently well for most applications.

17.3.4 Stirring Unit Test

An example setup using the StirFromFile unit is located in SimulationMain/StirFromFile/. The unit test can be invoked by

```
./setup StirFromFile -auto -3d -nxb=16 -nyb=16 -nzb=16 +ug -with-unit=physics/Hydro.
```

The FLASH executable must be copied into the run directory together with the standard flash.par for this setup, and together with the default forcing file (to be constructed using the standard parameters; see section 17.3.3.2). During runtime the code writes a file with the time evolution of spatially integrated quantities, amongst others, the rms Mach number and vorticity, which can used as basic code checks.

17.4 Energy Deposition Unit

The Energy Deposition unit calculates the energy deposited by one or more laser beams incident upon the simulation domain. The function EnergyDeposition is the main control driver of the Energy Deposition unit. The current implementation treats the laser beams in the geometric optics approximation. Beams are made of a number of rays whose paths are traced through the domain based on the local refractive index of each cell. The laser power deposited in a cell is calculated based on the inverse Bremsstrahlung power in the cell and depends on the local electron number density gradient and local electron temperature gradient. Currently there are two schemes implemented into FLASH: 1) a ray tracing algorithm based on cell average quantities and 2) a more refined ray tracing method based on cubic interpolation. Both schemes are discussed in the algorithmic implementation section 17.4.4 below.

17.4.1 Ray Tracing in the Geometric Optics Limit

In the geometric optics approach, the path of a laser wave can be described as the motion of a ray of unit-mass through the potential field

$$V(\mathbf{r}) \quad = \quad \frac{c^2}{2}\eta(\mathbf{r})^2, \tag{17.33}$$

where c is the speed of light in vacuum and η is the index of refraction of the medium, assumed to vary on a much longer spatial scale than the wavelength of the laser wave. Also $\eta(\mathbf{r})$ is considered constant during the time it takes for the ray to cross the domain (frozen medium). However $\eta(\mathbf{r})$ is allowed to vary from one time step to the next. For a non-relativistic unmagnetized plasma, the refractive index is given by

$$\eta(\mathbf{r})^2 \quad = \quad 1 - \frac{\omega_p^2(\mathbf{r})}{\omega^2} = 1 - \frac{n_e(\mathbf{r})}{n_c}, \tag{17.34}$$

where $\omega_p(\mathbf{r})$ is the plasma frequency, ω the laser frequency, $n_e(\mathbf{r})$ is the electron number density at location $\mathbf{r}$ and

$$n_c \quad = \quad \frac{m_e \pi \omega^2}{e^2} = \frac{m_e \pi c^2}{\lambda^2 e^2} \tag{17.35}$$

is the critical density at which the ray frequency and the plasma frequency are equal (m_e and e are the electron mass and charge, λ is the laser wavelength). The ray equation of motion is then

$$\frac{d^2\mathbf{r}}{dt^2} = \nabla\left(-\frac{c^2}{2}\frac{n_e(\mathbf{r})}{n_c}\right), \tag{17.36}$$

which constitutes the basic ray tracing 2nd order ODE equation. Splitting into two 1st order ODEs leads to

$$\frac{d\mathbf{r}}{dt} = \mathbf{v} \tag{17.37}$$

$$\frac{d\mathbf{v}}{dt} = -\frac{c^2\nabla n_e(\mathbf{r})}{2n_c}. \tag{17.38}$$

For short distances we can assume a first order Taylor expansion of the electron number density around a spcific location $\mathbf{r}_0$:

$$n_e(\mathbf{r}) \approx n_e(\mathbf{r}_0) + \nabla n_e(\mathbf{r}_0)\cdot(\mathbf{r}-\mathbf{r}_0), \tag{17.39}$$

where $\nabla n_e(\mathbf{r}_0)$ is the electron number density gradient vector at $\mathbf{r}_0$. Inserting equation 17.39 into 17.37 and 17.38 leads to equations for the ray velocity and position as a function of time

$$\mathbf{v}(t) = \mathbf{v}_0 - \frac{c^2}{2n_c}\nabla n_e(\mathbf{r}_0)t, \tag{17.40}$$

$$\mathbf{r}(t) = \mathbf{r}_0 + \mathbf{v}_0 t - \frac{c^2}{4n_c}\nabla n_e(\mathbf{r}_0)t^2, \tag{17.41}$$

where $\mathbf{r}_0$ and $\mathbf{v}_0$ are the initial ray position and velocity.

17.4.2 Laser Power Deposition

The power P of an electromagnetic wave is depleted by the inverse Bremsstrahlung (ib) process. The rate of power loss is governed by a 1st order ordinary differential equation (ODE):

$$\frac{dP}{dt} = -\nu_{ib}(t)P. \tag{17.42}$$

The inverse Bremsstrahlung frequency factor is given by the formula

$$\nu_{ib} = \frac{n_e}{n_c}\nu_{ei}, \tag{17.43}$$

where ν_{ei} is the electron-ion collision frequency

$$\nu_{ei} = \frac{4}{3}\left(\frac{2\pi}{m_e}\right)^{1/2}\frac{n_e Z e^4 \ln\Lambda}{(k_B T_e)^{3/2}}. \tag{17.44}$$

Here m_e is the electron mass, Z is the average ionization number of the plasma, e is the electron charge, $\ln\Lambda$ is the Coulomb logarithm, k_B is the Boltzmann constant and T_e is the electron temperature. The Coulomb logarithm is the natural logarithm of the Debye number Λ and is taken here as

$$\ln\Lambda = \ln\left[\frac{3}{2Ze^3}\left(\frac{k_B^3 T_e^3}{\pi n_e}\right)^{1/2}\right]. \tag{17.45}$$

The inverse Bremsstrahlung frequency depends thus on the electron number density and the electron temperature, both of which are functions of the position, and, since the position changes with time, it ultimately is also a function of time

$$\nu_{ib}(\mathbf{r}) = \nu_{ib}(t) = \frac{4}{3}\left(\frac{2\pi}{m_e}\right)^{1/2}\frac{Ze^4}{n_c k_B^{3/2}}\frac{n_e[\mathbf{r}(t)]^2\ln\Lambda[\mathbf{r}(t)]}{T_e[\mathbf{r}(t)]^{3/2}}. \tag{17.46}$$

Solution of the above ODE in Eq.(17.42) gives the attenuation of the ray's power from time zero to time t:

$$P_t \quad = \quad P_0 \exp\left\{-\int_0^t \nu_{ib}(t')\, dt'\right\}. \tag{17.47}$$

For a given small time step, the integral in Eq.(17.47) can be approximated in the following way. In order to remove the intermediate function $\mathbf{r}(t)$ from the expression in Eq.(17.46), we first assume that the Coulomb logarithm remains constant during the incremental time step

$$\ln\Lambda[\mathbf{r}(t)] \quad \approx \quad \ln\Lambda[\mathbf{r}_0] = \ln\left[\frac{3}{2Ze^3}\left(\frac{k^3T_e(\mathbf{r}_0)^3}{\pi n_e(\mathbf{r}_0)}\right)^{1/2}\right]. \tag{17.48}$$

Using first order Taylor expansions on both n_e and T_e similar to equation 17.39

$$n_e[\mathbf{r}(t)] \quad = \quad n_e(\mathbf{r}_0) + \nabla n_e(\mathbf{r}_0)\cdot(\mathbf{r}(t) - \mathbf{r}_0) \tag{17.49}$$
$$T_e[\mathbf{r}(t)] \quad = \quad T_e(\mathbf{r}_0) + \nabla T_e(\mathbf{r}_0)\cdot(\mathbf{r}(t) - \mathbf{r}_0) \tag{17.50}$$

and inserting the ray position equation 17.41, we get

$$n_e[\mathbf{r}(t)] \quad = \quad n_e(\mathbf{r}_0)\left[1 + \frac{\nabla n_e(\mathbf{r}_0)\cdot\mathbf{v}_0}{n_e(\mathbf{r}_0)}t - \frac{c^2\nabla n_e(\mathbf{r}_0)\cdot\nabla n_e(\mathbf{r}_0)}{4n_cn_e(\mathbf{r}_0)}t^2\right] \tag{17.51}$$
$$T_e[\mathbf{r}(t)] \quad = \quad T_e(\mathbf{r}_0)\left[1 + \frac{\nabla T_e(\mathbf{r}_0)\cdot\mathbf{v}_0}{T_e(\mathbf{r}_0)}t - \frac{c^2\nabla T_e(\mathbf{r}_0)\cdot\nabla n_e(\mathbf{r}_0)}{4n_cT_e(\mathbf{r}_0)}t^2\right]. \tag{17.52}$$

The inverse-Bremsstrahlung rate can thus be written as a rational polynomial expression

$$\nu_{ib}(t) \quad = \quad \nu_{ib}(0)\frac{(1+Ut+Rt^2)^2}{(1+Wt+St^2)^{3/2}}, \tag{17.53}$$

where $\nu_{ib,0}$ is the inverse-Bremsstrahlung rate at the initial point (zero time)

$$\nu_{ib}(0) \quad = \quad \frac{4}{3}\left(\frac{2\pi}{m_e}\right)^{1/2}\frac{Ze^4\ln\Lambda[\mathbf{r}_0]}{n_ck^{3/2}}\frac{n_e(\mathbf{r}_0)^2}{T_e(\mathbf{r}_0)^{3/2}} \tag{17.54}$$

and

$$U \quad = \quad \frac{\nabla n_e(\mathbf{r}_0)\cdot\mathbf{v}_0}{n_e(\mathbf{r}_0)} \tag{17.55}$$
$$W \quad = \quad \frac{\nabla T_e(\mathbf{r}_0)\cdot\mathbf{v}_0}{T_e(\mathbf{r}_0)} \tag{17.56}$$
$$R \quad = \quad -\frac{c^2\nabla n_e(\mathbf{r}_0)\cdot\nabla n_e(\mathbf{r}_0)}{4n_cn_e(\mathbf{r}_0)} \tag{17.57}$$
$$S \quad = \quad -\frac{c^2\nabla T_e(\mathbf{r}_0)\cdot\nabla n_e(\mathbf{r}_0)}{4n_cT_e(\mathbf{r}_0)}. \tag{17.58}$$

The integral in Eq.(17.47) can be solved by using a second order Gaussian quadrature

$$\int_0^t \nu_{ib}(t')\, dt' \quad = \quad \nu_{ib}(0)\frac{t}{2}\sum_{i=1}^{2} w_i\frac{(1+Ut_i+Rt_i^2)^2}{(1+Wt_i+St_i^2)^{3/2}}, \tag{17.59}$$

where $t_{1,2} = (1\pm 1/\sqrt{3})t/2$ and both weights are equal to 1. The rate of energy deposition (energy deposited per unit time) during this time is then $P_0 - P_t$.

17.4.3 Laser Energy Density

Experimentally implemented for only 3D Cartesian geometry in FLASH 4.4.

Light carries energy through space and therefore can be attributed an energy density (energy per volume). For example, light propagating at velocity c with power P through an area A has an energy density of $U_{light} = \frac{P}{Ac}$.

Splitting the laser's power across a finite number of rays is an abstraction with an interesting consequence. Because each ray's power is artificially confined to a 1D curvilinear axis, light rays in FLASH are naturally described by linear energy densities (energy per distance) rather than volumetric energy densities (energy per volume). Volumetric energy density is more physically relevant. Therefore, the contribution of each ray to volumetric laser energy density (a cell quantity, "lase", available as an output when using certain ray-tracing modules – see 17.4.10.5) is calculated by taking the linear energy density of each ray, integrating over the ray path within the cell, and dividing by the cell volume.

The details of the laser energy density calculation are as follows. Trading path length for parametrized time, ray power P_t changes along the ray path by Eq.(17.47). For light traveling at speed c (determined by frequency and medium), ray linear energy density E_t similarly varies along ray path:

$$E_t = \frac{P_t}{c} \tag{17.60}$$

Volumetric energy density U_{cell} is found by integrating linear energy density E_t over the ray's path within the cell (t_f is the parametrized time value for which the ray reaches edge of cell), then dividing by cell volume V_{cell}:

$$U_{cell} = \frac{\int_0^{t_f} E_t dt}{V_{cell}} = \frac{1}{cV_{cell}} \int_0^{t_f} P_t dt \tag{17.61}$$

For each cell, all contributions to volumetric laser energy density (all rays' U_{cell}) are summed to give a total laser energy density for that cell.

17.4.4 Algorithmic Implementations of the Ray Tracing

The current implementation of the laser energy deposition assumes that rays transit the entire domain in a single time step. This is equivalent of saying that the domain's reaction time (changes of its state variables) is much longer than the time it takes for each ray to either cross the domain or get absorbed by it. For each time step it is first checked, if at least one of the laser beams is still active. If this is the case, then for each active beam a collection of rays is generated possessing the right specifications according to the beam's direction of firing, its frequency, its pulse shape and its power. The Energy Deposition unit moves all rays across all blocks until every ray has either exited the domain or has been absorbed by the domain. The rays are moved on a block by block basis and for each block the rays are traced through the interior cells. The Energy Deposition unit utilizes the infrastructure from the Grid Particles unit 8.9 to move rays between blocks and processors. The code structure of the Energy Deposition unit during one time step is as follows:

```
Loop over all blocks containing rays
    Calculate needed block data for all cells.
    ———————- Start threading ——————————
    Loop over all rays in block
        Trace each ray through all cells in block
    End loop
    ———————- End threading ——————————
End loop
```

Reassign rays to blocks/processors and repeat (exit, if no more rays)

The inner loop over all rays in a block is conveniently handled in one subroutine to allow for compact (optional) threading. Currently there are three algorithmic options on how to trace the rays in FLASH: 1) Cell average algorithm, 2) Cubic interpolation with piecewise parabolic ray tracing and 3) Cubic interpolation using Runge Kutta integration schemes.

17.4.4.1 Cell Average (AVG) Algorithm

The AVG algorithm (Kaiser 2000) is based on tracing the rays on a cell-by-cell basis. Each cell has its own average center electron number density $\langle n_e \rangle$ and electron temperature $\langle T_e \rangle$ value at the center of the cell. The electron number density gradient vector $\langle \nabla n_e \rangle$ as well as the electron temperature gradient vector $\langle \nabla T_e \rangle$ are assumed to be constant within each cell. Rays will be transported through each cell between cell faces in one step. Electron number densities n_{e0} and electron temperatures T_{e0} on the entry cell face are calculated from the cell center values in accordance with equation 17.39 using first order Taylor expansions

$$\begin{aligned} n_{e0} &= \langle n_e \rangle + \langle \nabla n_e \rangle \cdot (\mathbf{r}_0 - \langle \mathbf{r} \rangle) && (17.62) \\ T_{e0} &= \langle T_e \rangle + \langle \nabla T_e \rangle \cdot (\mathbf{r}_0 - \langle \mathbf{r} \rangle), && (17.63) \end{aligned}$$

where $\mathbf{r}_0$ are the position coordinates of the ray at the cell's face and $\langle \mathbf{r} \rangle$ are the coordinates of the cell's center. The ray's cell crossing time t_{cross} is determined from the quadratic time equation 17.41 by inserting planar equations $A_x x + A_y y + A_z z + D = \mathbf{A} \cdot \mathbf{r}(t) + D = 0$ for all cell faces (in cartesian coordinates), leading to

$$-\frac{c^2 \mathbf{A} \cdot \langle \nabla n_e \rangle}{4n_c} t^2 + \mathbf{A} \cdot \mathbf{v}_0 t + \mathbf{A} \cdot \mathbf{r}_0 + D = 0, \tag{17.64}$$

and selecting the shortest time (excluding the zero time corresponding to the point of entry). In FLASH, the cartesian cell faces are coplanar with the xy-, xz- and the yz-plane, simplifying the quadratic time equation. A cell face located at x_{cell} and coplanar with the yz-plane has the plane equation $x = x_{cell}$ and thus $A_x = 1$, $A_y, A_z = 0$ and $D = -x_{cell}$. For this cell face, the quadratic time equation becomes

$$-\frac{c^2 \langle \nabla n_e \rangle_x}{4n_c} t^2 + v_{0x} t + r_{0x} - x_{cell} = 0 \tag{17.65}$$

and similar for the other cartesian components. In order to achieve a stable ray tracing algorithm and uniquely assign rays to cells and blocks while crossing through cell walls, a cell wall thickness is defined, which is shared between two adjacent cells. The code is set up such that rays are never to be found inside this wall. When crossing between two cells occurs (same block or different blocks), the rays positions are always adjusted (nudged) such that they will sit on this wall with finite thickness. The cell wall thickness is defined in the code as being a very tiny fraction (adjustable, with default value of 1:1,000,000) of the smallest cell dimension during a simulation.

The ray's rate of energy deposition between the cell entry face and the cell exit face is calculated using equations 17.47 to 17.59 with $\nabla n_e(\mathbf{r}_0)$ and $\nabla T_e(\mathbf{r}_0)$ replaced by their cell average values $\langle \nabla n_e \rangle$ and $\langle \nabla T_e \rangle$ and $n_e(\mathbf{r}_0)$ and $T_e(\mathbf{r}_0)$ replaced by their corresponding cell entry values n_{e0} and T_{e0}. The upper integration time limit is t_{cross}, the ray's cell crossing time.

The AVG algorithm, while conceptually simple, leads to discontinous change in n_e at the cell interfaces. To account for this, the ray undergoes refraction according to Snell's law. Refraction at cell interfaces causes a change in the ray's velocity normal to the interface surface while preserving the ray velocity component transverse to the interface normal. To derive the change in the ray normal velocity component, imagine the cell interface to have a small infinitesimal thickness s and the ray moving from left to right through the interface. On the left and right the normal velocity components are $v_\perp(\ell)$ and $v_\perp(r)$, respectively, while the corresponding n_e are $n_e(\ell)$ and $n_e(r)$. Since we are dealing with an interface of infinitesimal thickness, we can use the first order equation 17.40 to get

$$v_\perp(r) = v_\perp(\ell) - \frac{c^2}{2n_c} \frac{\Delta n_e}{s} t, \tag{17.66}$$

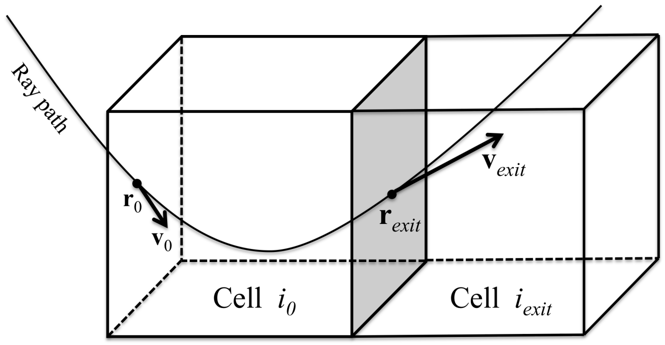

Figure 17.4: A single ray crossing a cell.

where $\Delta n_e = n_e(r) - n_e(\ell)$, and the electron number density gradient is $\nabla n_e = \Delta n_e/s$. But s/t is the average velocity of the ray passing through the interface and since we have constant acceleration we have $s/t = [v_\perp(r) + v_\perp(\ell)]/2$, which, when inserted into the last equation, gives

$$\begin{aligned} v_\perp(r) - v_\perp(\ell) &= -\frac{c^2}{n_c}\frac{\Delta n_e}{[v_\perp(r) + v_\perp(\ell)]} \\ v_\perp^2(r) - v_\perp^2(\ell) &= -\frac{c^2 \Delta n_e}{n_c} \\ \Delta v_\perp^2 &= -\frac{c^2 \Delta n_e}{n_c}. \end{aligned} \tag{17.67}$$

Clearly there is a limit as to how large Δn_e can be for refraction to occur. If $\Delta n_e > v_\perp^2(\ell) n_c/c^2$, we have $v_\perp^2(r) < 0$, which is impossible. The only way out is then for the ray to have $\Delta n_e = 0$, i.e. the ray stays in the same cell and reflects with $v_\perp(r) = -v_\perp(\ell)$.

The basic algorithmic steps for tracing a single ray through all cells in one block (see Figure 17.4) can be summarized as follows: The initial situation has the ray positioned on one of the block's faces with velocity components such that the ray's direction of movement is into the block.

- Identify ray entry cell i_0, entry position $\mathbf{r}_0$, entry velocity $\mathbf{v}_0$ and entry power P_0.
- Calculate n_{e0} and T_{e0} at the entry point using equations 17.62 and 17.63.
- Solve equation 17.41 for time for each possible cell face. Identify the cell crossing time t_{cross} as minimum of all solutions > 0.
- Using t_{cross} and equation 17.41 again, find the cell exit position $\mathbf{r}_{exit}$.
- Calculate $\ln \Lambda[\mathbf{r}_0]$, $\nu_{ib}(0)$, U, W, R, S and evaluate P_{exit} using equations 17.47 and 17.59.
- Using t_{cross} and equation 17.40, find the ray's exit velocity $\mathbf{v}_{exit}$.
- Based on $\mathbf{r}_{exit}$ and $\mathbf{v}_{exit}$ determine new entry cell i_{exit}.
- Calculate the electron number density jump Δn_e between both cells i_0 and i_{exit}, using equation 17.39.
- Check for reflection or refraction using Snell's law equation 17.67 and update $\mathbf{v}_{exit}$ and possibly new entry cell i_{exit}.
- If cell i_{exit} is still in block, set all exit variables equal to entry variables and repeat the steps.

17.4.4.2 Cubic Interpolation with Piecewise Parabolic Ray Tracing (CIPPRT)

The use of cubic interpolation schemes is an attempt at providing continuous n_e and T_e representations as well as continuous first derivatives ∇n_e and ∇T_e throughout the entire domain. This allows for the calculation of a more smoother path for each ray inside each cell when compared to the AVG algorithm. In effect, the cell-by-cell choppiness of the AVG algorithm can be avoided by taking many small ray steps inside each cell. Also, the troublesome n_e discontinuities at the cell boundaries and the application of Snell's law will disappear. The essential features of the cubic interpolation schemes are layed out in section 27.2. In what follows we show the piecewise parabolic ray tracing scheme.

The CIPPRT algorithm tries to map out the ray path inside each cell as a sequence of parabolic (i.e. constant acceleration) paths. It resembles the AVG algorithm and uses the same equations Eq.(17.40) and Eq.(17.41) for determination of velocity and position of each parabolic section of the path. The main difference between the AVG and the CIPPRT is that the latter uses the cubic interpolated ray acceleration field at each cell point, whereas the former assumes the same constant acceleration at each point throughout the cell. The CIPPRT can hence be viewed as a succession of AVG steps inside each cell. The energy deposition of each parabolic path section is also calculated like for the AVG algorithm, namely solving the exponential time integral in Eq.(17.47) using the second order Gaussian quadrature in Eq.(17.59). The required n_e and T_e at the Gaussian quadrature points are evaluated using the cubic interpolation equation Eq.(27.11). The following scheme illustrates the steps involved for tracing a ray through a cell, assuming the ray is somewhere located in the cell at $\mathbf{r}_0$ with velocity $\mathbf{v}_0$:

1. Calculate, using Eq.(27.13), the electron number density gradient $\nabla n_e(\mathbf{r}_0)$.

2. Determine the time t to reach the next cell face using the quadratic time equation Eq.(17.41) and determine the ray's position $\mathbf{r}(t)$ on the face.

3. Do two $t/2$ steps and calculate the $\mathbf{r}(2 \times t/2)$ position. The first $t/2$ step is guaranteed to stay inside the cell. Hence $\mathbf{r}(t/2) \in$ cell. However, despite $\mathbf{r}(2 \times t/2)$ having the potential to step outside the cell, we only need it for comparison with $\mathbf{r}(t)$.

4. Form the error vector $\mathbf{e} = \mathbf{r}(2 \times t/2) - \mathbf{r}(t)$. If $|\mathbf{e}| \leq$ target accuracy, accept the $\mathbf{r}(t)$ position. If not, set $t = t/2$ and repeat step 2).

5. Once a satisfactory stepping time has been determined, update the velocity using Eq.(17.40).

17.4.4.3 Cubic Interpolation with Runge Kutta Integration (CIRK)

Instead of using the piecewise parabolic ray tracing approach, the CIRK algorithm advances the ray through cells using Runge Kutta (RK) integration 29.2. An advantage of using the RK integrator is that the rate of power loss ODE 17.42 can be directly incorporated into the RK solution vector, thereby gaining access over its error control. The ray tracing RK vector has 7 entries

$$\frac{d}{dt}\begin{pmatrix}\mathbf{r}\\ \mathbf{v}\\ P\end{pmatrix} = \begin{pmatrix}\mathbf{v}\\ \mathbf{a}\\ -\nu_{ib}P\end{pmatrix} = \begin{pmatrix}\mathbf{v}\\ -c^2\nabla n_e(\mathbf{r})/2n_c\\ -\nu_{ib}(\mathbf{r})P\end{pmatrix}, \tag{17.68}$$

and the independent variable t does not appear on the rhs. Since each ray must be traced on a cell-by-cell basis, we have to make sure that each RK step either stays within the cell or hits one of its walls. The CIRK algorithm therefore has to use the confined RK stepping routine.

17.4.5 Setting up the Laser Pulse

The laser's pulse contains information about the laser's energy profile and can thus be characterized by a function of laser power in terms of time $P(t)$. The curve of $P(t)$ gives the power of the laser pulse at any given simulation time. In FLASH, the form of $P(t)$ is given by a series of points, which are connected via straight lines (see Figure 17.5). Each point denotes a power/time pair $P_i(t_i)$. The average laser power $\overline{P}$ of

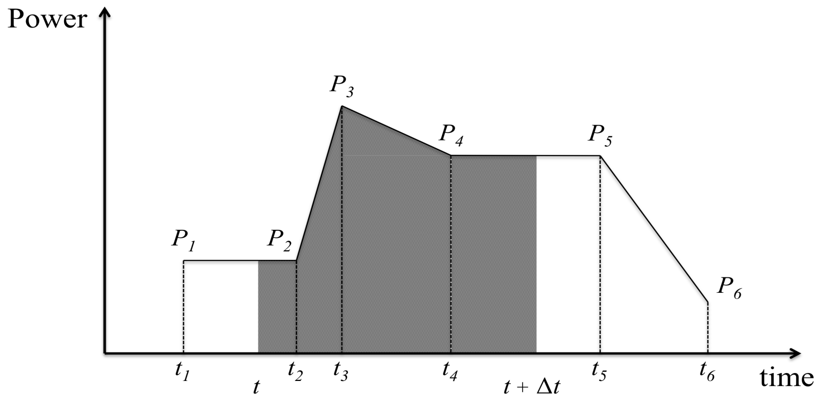

Figure 17.5: The structure of the laser pulse.

the pulse during a time step from $t \to t + \Delta t$ is then

$$\overline{P} \quad = \quad \frac{\int_t^{t+\Delta t} P(t)\ dt}{\Delta t}, \tag{17.69}$$

where the integration is performed piecewise between all the points $P_i(t_i)$ contained within the relevant time frame. The average laser power will be distributed among all the rays that will be created during that particular time step. Note, that t_1 is the time the laser first comes into existence. In Figure 17.5 there is therefore no line connecting the origin (zero power) with P_1. If the user wants a gradual buildup of laser power from zero, an explicit point $P_1 = 0$ must be given at time t_1. The same consideration applies for the other end of the timescale.

17.4.6 Setting up the Laser Beam

The laser's beam contains all the information about orientation and shape of the laser. The orientation is characterized by specifying lens and target coordinates. The shape of the laser is given by the size and shape of the lens and target cross section areas and the cross-sectional ray power distribution law. Figure 17.6 is helpful in visualizing the position of the vectors for the formulas below. The most important vectors for setting up the rays are the two local elliptical semiaxes unit vectors $\mathbf{u}_1$ and $\mathbf{u}_2$. These two unit vectors, together with the lens and target positions, are very convenient in calculating the rays lens and target coordinates. Note, that the unit vectors are the same for both the lens and the target, if defined from their corresponding local elliptical centers. In what follows, vectors in capital letters are defined in the global coordinate system and vectors in small letters are defined in the local target coordinate system.

17.4.6.1 The Local Elliptical Semiaxis Unit Vectors

The laser beam originates at the lens, whose center is located at $\mathbf{L}$, and hits the target, whose center is located at $\mathbf{T}$. In 3D geometries, the elliptical target area is defined as an ellipse perpendicular to the lens-target line and whose largest semiaxis $\mathbf{s}_1$ is positioned such that it makes a torsional angle ϕ_1 with the local target z-axis (see Figure 17.6). Let us define the beam vector $\mathbf{b} = \mathbf{L} - \mathbf{T}$ pointing from the target to the lens and connecting the two respective centers. We then have the defining equations for $\mathbf{s}_1$

$$s_{1x}b_x + s_{1y}b_y + s_{1z}b_z \quad = \quad 0 \tag{17.70}$$

$$s_{1x}^2 + s_{1y}^2 + s_{1z}^2 \quad = \quad \ell_1 \tag{17.71}$$

$$s_{1z} \quad = \quad \ell_1 \cos\phi_1 \cos(\theta - \pi/2), \tag{17.72}$$

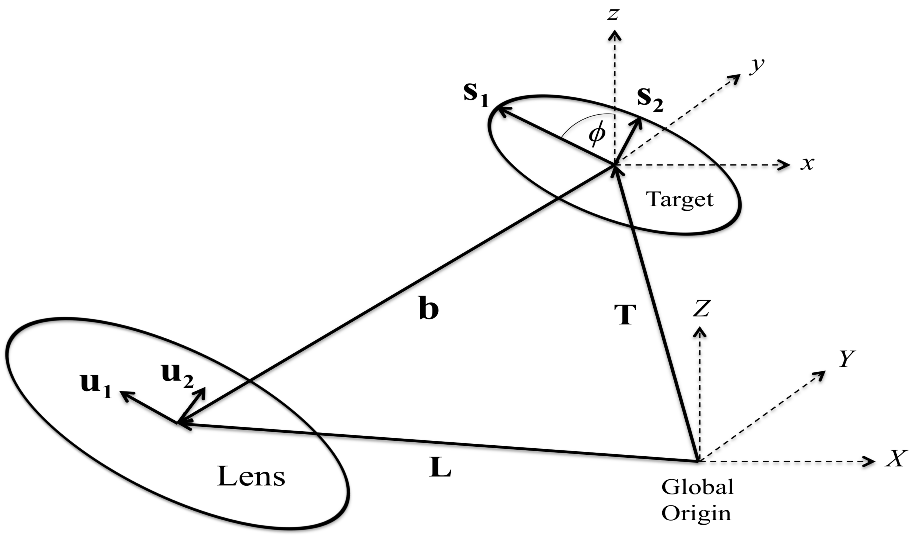

Figure 17.6: The laser beam.

where ℓ_1 is the length of $\mathbf{s}_1$ and θ is the angle that the beam vector $\mathbf{b}$ makes with the local z-axis. The first equation 17.70 says that $\mathbf{b}$ and $\mathbf{s}_1$ are orthogonal. The second one 17.71 defines the length of $\mathbf{s}_1$ and the third one 17.72 defines the local z-axis projection of $\mathbf{s}_1$. The last equation can be rewritten as

$$s_{1z} \quad = \quad \ell_1 \frac{\sqrt{b_x^2 + b_y^2}}{|\mathbf{b}|} \cos\phi_1. \tag{17.73}$$

Forming an expression for s_{1y}^2 from equation 17.70, an expression for s_{1z}^2 from equation 17.72 and inserting the results into equation 17.71, we obtain a quadratic equation in s_{1x}^2, from which we can obtain all three components. We get after some algebra and simplifications

$$s_{1x} \quad = \quad \frac{\ell_1}{\sqrt{b_x^2 + b_y^2}} \left[-\frac{b_x b_z}{|\mathbf{b}|} \cos\phi_1 \pm b_y \sin\phi_1 \right] \tag{17.74}$$

$$s_{1y} \quad = \quad \frac{\ell_1}{\sqrt{b_x^2 + b_y^2}} \left[-\frac{b_y b_z}{|\mathbf{b}|} \cos\phi_1 \mp b_x \sin\phi_1 \right] \tag{17.75}$$

$$s_{1z} \quad = \quad \ell_1 \frac{\sqrt{b_x^2 + b_y^2}}{|\mathbf{b}|} \cos\phi_1. \tag{17.76}$$

The two possible solutions for s_{1x} and s_{1y} correspond to the two possible definitions of the rotation angle ϕ_1 in either clockwise or counterclockwise rotation from the z-axis when looking along the beam vector $\mathbf{b}$ from the lens to the target. Let us henceforth define ϕ_1 to be the clockwise rotation. Then the lower signs in s_{1x} and s_{1y} apply and dividing each component by ℓ_1 we obtain for the unit vector components

$$u_{1x} \quad = \quad \frac{1}{\sqrt{b_x^2 + b_y^2}} \left[-\frac{b_x b_z}{|\mathbf{b}|} \cos\phi_1 - b_y \sin\phi_1 \right] \tag{17.77}$$

$$u_{1y} \quad = \quad \frac{1}{\sqrt{b_x^2 + b_y^2}} \left[-\frac{b_y b_z}{|\mathbf{b}|} \cos\phi_1 + b_x \sin\phi_1 \right] \tag{17.78}$$

$$u_{1z} \quad = \quad \frac{\sqrt{b_x^2 + b_y^2}}{|\mathbf{b}|} \cos\phi_1. \tag{17.79}$$

The second elliptical semiaxis $\mathbf{s}_2$ is perpendicular to the first and lays in the same elliptical target plane. If we define it to be at a right angle in clockwise direction from $\mathbf{s}_1$, the torsional angle it makes with the local z-axis is $\phi_2 = \phi_1 + \pi/2$. The formulas for its unit vector components are the same as for $\mathbf{s}_1$ but with ϕ_1 replaced by ϕ_2. From trigonometric sine and cosine relations we can re-express them in terms of ϕ_1

$$u_{2x} = \frac{1}{\sqrt{b_x^2 + b_y^2}} \left[\frac{b_x b_z}{|\mathbf{b}|} \sin\phi_1 - b_y \cos\phi_1 \right] \tag{17.80}$$

$$u_{2y} = \frac{1}{\sqrt{b_x^2 + b_y^2}} \left[\frac{b_y b_z}{|\mathbf{b}|} \sin\phi_1 + b_x \cos\phi_1 \right] \tag{17.81}$$

$$u_{2z} = -\frac{\sqrt{b_x^2 + b_y^2}}{|\mathbf{b}|} \sin\phi_1. \tag{17.82}$$

Note the importance of the $\sqrt{b_x^2 + b_y^2}$ term. If this term is equal to zero, then the unit vectors become undefined. This corresponds to the laser beam being parallel to the global z-axis (and thus coinciding with the local z-axis). Then both elliptical semiaxes are not defined uniquely through a z-axis torsional angle of zero. In this case the torsional angle must be defined through one of the other coordinate axis. The following coordinate index permutations in the above formulas apply:

$$\phi_1 \text{ defined through x-axis} = x \to y, y \to z, z \to x \tag{17.83}$$

$$\phi_1 \text{ defined through y-axis} = x \to z, y \to x, z \to y. \tag{17.84}$$

In 2D geometries, the beam's lens and target areas shrink to a line segment. All z-components are zero and the torsional angle is equal to $\pi/2$. The components of the unit vector can be deduced from the equations 17.77 and 17.78 as

$$u_x = -\frac{b_y}{|\mathbf{b}|} \tag{17.85}$$

$$u_y = \frac{b_x}{|\mathbf{b}|}. \tag{17.86}$$

17.4.6.2 Extremum Values for the Elliptical Target Zone

In 3D simulations, the planar elliptical target zone can be placed in any possible way inside the domain by specifying the lens $\mathbf{L}$ and target $\mathbf{T}$ positions, both elliptical target zone semiaxes lengths ℓ_1 and ℓ_2, the first semiaxis torsion angle ϕ_1 and the coordinate axis to which ϕ_1 refers to. We wish to enforce in the code a complete containment of the entire target plane inside the domain boundaries. To check this condition we need the extremum coordinate values of the elliptical boundary curve of the target. The collection of all points $\mathbf{e}$, based on the local target coordinate system, can be given in the following implicit form

$$\mathbf{e} = \ell_1 \mathbf{u}_1 \cos(\omega) + \ell_2 \mathbf{u}_2 \sin(\omega), \quad 0 \geq \omega \geq 2\pi. \tag{17.87}$$

Differentiating with respect to ω and equating to zero we get the minimax condition on all coordinate components as

$$\boldsymbol{\omega}_{min/max} = \arctan\left(\frac{\ell_2 \mathbf{u}_2}{\ell_1 \mathbf{u}_1}\right), \tag{17.88}$$

where $\boldsymbol{\omega}_{min/max}$ denotes the vector of the minimax angles for each cartesian component. The equation 17.88 has two possible answers for each ω component in the range $0 \geq \omega \geq 2\pi$, corresponding to the minimum and the maximum value. The ω_{min} and ω_{max} angles differ by π radians for each cartesian component. The corresponding minima and maxima on the elliptical boundary curve are obtained by inserting the ω_{min} and ω_{max} angles into equation 17.87.

In order to simplify things, we note that what we need are the sine and cosine values of ω_{min} and ω_{max}. From the definition of the trigonometric functions based on the length of the three sides of a right-angled

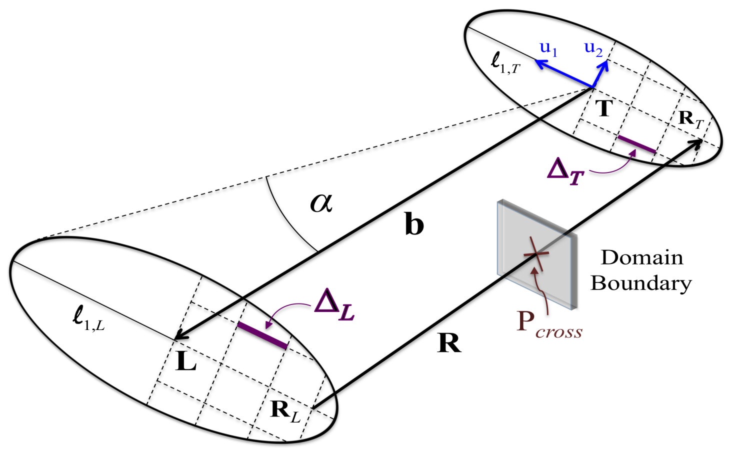

Figure 17.7: Setting up the rays between the beam's lens and target area using a square grid. Only half of the square elliptical grids are shown for clarity.

triangle (a = opposite side, b = adjacent side, c = hypotenuse for an angle ω), we have, using $\sin\omega = a/c$, $\cos\omega = b/c$, $\tan\omega = a/b$ and $c^2 = a^2 + b^2$

$$\sin(\arctan(a/b)) = \sin(\omega) = a/c = \frac{a}{\sqrt{a^2+b^2}} \quad (17.89)$$

$$\cos(\arctan(a/b)) = \cos(\omega) = b/c = \frac{b}{\sqrt{a^2+b^2}}. \quad (17.90)$$

When applied to equation 17.87, we obtain

$$\mathbf{e}_{min/max} = \pm\sqrt{(\ell_1\mathbf{u}_1)^2 + (\ell_2\mathbf{u}_2)^2}. \quad (17.91)$$

The corresponding minimax equation for the 2D geometries (ellipse $\rightarrow$ line segment) is

$$\mathbf{e}_{min/max} = \pm\ell\mathbf{u}, \quad (17.92)$$

with ℓ being half the length of the target line segment and $\mathbf{u}$ the line segment unit vector.

17.4.7 Setting up the Rays

For each Energy Deposition unit call, the code sets up the initial collection of rays, defined to be located on the domain boundary with specific velocity components such that they will hit the target area at precise locations if they would cross an empty domain. Key concepts in setting up the rays initial position, velocity and power are the elliptical local square, radial, delta or statistical grids and the beam cross section power function. Rays will be launched from the lens grid intersection points to the corresponding target grid intersection points. Using a square grid, a uniform beam cross-sectional ray density will be achieved, although this could be relaxed in the future to include the possibility of rectangular grids leading to different cross-sectional ray densities along the two elliptical semiaxes directions. A radial grid places the rays on concentrical ellipses.

17.4.7.1 The Elliptical Lens/Target Local Square Grid

In 3D geometries, both the lens and target areas are defined as two similar ellipses (different size, same shape). Given a specific elliptical shape by defining the lengths of both semiaxes $\ell_1 \geq \ell_2$, we can set up a square grid inside the ellipse, such that the number of grid intersection points matches closely the number of rays N_{rays} specified by the user. The grid is defined by the separation Δ between two grid points and the placement of the grid's origin at the center of the ellipse. Our goal is to find this Δ value.

Denote by $N_{rectangle}$ the number of grid intersection points for the circumscribing rectangle with sides $2\ell_1$ and $2\ell_2$. We then have

$$\begin{aligned} N_{rectangle} &= \text{Number of ellipse points}\frac{\text{Area rectangle}}{\text{Area ellipse}} \\ &= \frac{4N_{rays}}{\pi}, \end{aligned} \tag{17.93}$$

this relation holding only approximately due to the finite resolution of the grid. Let us denote by $r = \ell_1/\ell_2$ the ratio between the largest and smallest semiaxis. If n_1 is the number of tics along the ℓ_1-semiaxis starting at the grid origin (0,0), then the number of tics along the ℓ_2-semiaxis is approximately equal to n_1/r. Looking at the circumscribed rectangle area, the total number of grid intersection points laying on the grid's axes will be twice those on each semiaxis plus the grid's origin: $2n_1+2n_1/r+1$. The total number of grid intersection points not on any of the axes is $4(n_1)(n_1/r)$. Both numbers together should then equal to $N_{rectangle}$. Hence, from 17.93, we are lead to a quadratic equation in n_1

$$\frac{4}{r}n_1^2 + \left(2+\frac{2}{r}\right)n_1 - \left(\frac{4N_{rays}}{\pi} - 1\right) = 0, \tag{17.94}$$

whose solution is

$$n_1 = \frac{1}{4}\left[-(1+r) + \sqrt{(1-r)^2 + \frac{16rN_{rays}}{\pi}}\right]. \tag{17.95}$$

Always $n_1 > 0$, which can easily be seen from the lowest possible value that n_1 can attain for $N_{rays} = 1$ and the lowest possible ratio $r = 1$ (in this case $n_1 = 0.06418...$). Since n_1 has to be an integer we take the ceiling value of the solution 17.95. If the user specified $N_{rays} = 1$, the search for n_1 is bypassed and the ray is placed at the elliptical origin.

Having n_1, the next task is to find the optimum (or close to optimum) grid spacing Δ. This is done by defining a minimum and maximum grid spacing value

$$\Delta_{min} = \frac{\ell_1}{n_1+1} \tag{17.96}$$

$$\Delta_{max} = \frac{\ell_1}{n_1-1}. \tag{17.97}$$

A series of $\Delta_{min} \leq \Delta_k \leq \Delta_{max}$ grid spacings is then tested, and for each Δ_k the number of grid intersection points N_k inside the ellipse area is determined. Of all N_k obtained, a certain number of them will be closest to N_{rays}. The average over all these Δ_k will then be taken as the final Δ value. For this Δ we compute the final number of grid intersection points, which will then replace the user's specified N_{rays}.

Since the target ℓ_1 and ℓ_2 semiaxes are specified by the user, the Δ_T for the target square grid is evaluated using the above algorithm. The corresponding lens Δ_L value is set using the similarity in size between the lens and the target. Using the user's specified ℓ_1 for the lens, the preservation of length relations between similar objects leads to:

$$\frac{\Delta_L}{\ell_{1,L}} = \frac{\Delta_T}{\ell_{1,T}} \tag{17.98}$$

and hence

$$\Delta_L = \frac{\ell_{1,L}}{\ell_{1,T}}\Delta_T. \tag{17.99}$$

In 2D geometries the situation is much simpler. Due to the linear shape of the lens and target areas, it is very easy to calculate the Δ_T value of the linear target grid such that exactly N_{rays} grid points are obtained with the outer two grid points coinciding with the target end points. The corresponding Δ_L is evaluated using equation 17.99.

17.4.7.2 The Elliptical Lens/Target Local Radial Grid

In order to set up the radial lens and target grids, we use the implicit definition of the elliptical curve from 17.87. The grid will then be defined as the number of tics on the ℓ_1, ℓ_2 pair and the number of tics on the angle ω within the range $0 \geq \omega \geq 2\pi$. The number of tics on both of these 'axes' will be the same and will be denoted by n. The total number of radial grid points within the lens and target ellipses will be equal to $1 + n(n+1)$, leading to the quadratic equation

$$n^2 + n + 1 \quad = \quad N_{rays}, \tag{17.100}$$

whose relevant solution is

$$n \quad = \quad \frac{1}{2}\left[-1 + \sqrt{4N_{rays} - 3}\right]. \tag{17.101}$$

In order to reduce the error to N_{rays}, rounding to the nearest integer is applied for n. The individual grid points are calculated from

$$\mathbf{e}_{ij} \quad = \quad \frac{\ell_1 i}{n}\mathbf{u}_1 \cos\left(\frac{2\pi j}{n}\right) + \frac{\ell_2 i}{n}\mathbf{u}_2 \sin\left(\frac{2\pi j}{n}\right), \tag{17.102}$$

where the index ranges are

$$j \quad = \quad 0, 1, 2, \ldots, n \tag{17.103}$$
$$i \quad = \quad \min(1, j), \ldots, n. \tag{17.104}$$

In an effort to provide more control to the user, the default 'same number of tics on both radial and angular axes' has been extended, such that the user can enforce one or even both of these values. This is controlled by setting the requested number of radial and/or angular tics as runtime parameters for each beam. The resulting number of rays will then be recalculated and overwritten.

17.4.7.3 The Elliptical Lens/Target Local Delta Grid

One of the drawbacks of the local square grid is that the user has no direct control of the resulting tic separation. The main goal when setting up the local square grid is to have the number of rays match as closely as possible the number of rays requested by the user. The local delta grid is provided to give the user full control over the tic separations on both semiaxes, relaxing at the same time the number of rays constraint. The delta grid becomes useful if the user wants to enforce a more smooth energy deposition in the cells hit by the 3D laser beam. Rays can be forced to hit each cell well away from the cell boundary, thereby avoiding the initial uneven ray distributions due to some rays hitting the block walls with corresponding nudging to one block or the other. As a consequence the delta grids are most useful if the target area of the beam has or is known to have a uniform refinement level.

The setup of the delta grid is simple: the user has to provide the tic separation values as beam runtime parameters. The beam setup code then adheres strictly to these values and excludes any grid points laying outside the elliptical beam boundary. The number of rays requested initially by the user is completely ignored and replaced by the number of rays determined for the delta grid. The user must make sure that the supplied memory requirements for ray storage are ok. This can be done by estimating the number of rays resulting from the delta grid on the area of the circumscribed rectangle with sides $2\ell_1$ and $2\ell_2$ and rescaling by the ellipse/rectangle area factor. If we denote the user supplied tic separations corresponding to the ℓ_1 semiaxis and ℓ_2 semiaxis by Δ_1 and Δ_2, then the estmated number of rays would be:

$$\begin{aligned} N_{rays} &\approx 2\left(\frac{\ell_1}{\Delta_1}\right) \times 2\left(\frac{\ell_2}{\Delta_2}\right) \times \frac{\pi}{4} \\ &= \frac{\pi \ell_1 \ell_2}{\Delta_1 \Delta_2}. \end{aligned} \tag{17.105}$$

The first tics of the delta grid along each grid axis start at $\Delta_1/2$ and $\Delta_2/2$. The grid center $(0,0)$ is thus not part of the delta grid.

17.4.7.4 The Elliptical Lens/Target Local Statistical Grid

The local statistical grid is defined by a statistical collection of (x, y) pairs within the range $[-1, 1]$, where the x and y denote fractions of the ℓ_1 and ℓ_2 semiaxis. A random number generator for the range $[0, 1]$ is used and the numbers are shifted to the $[-1, 1]$ range by multiplying by 2 and adding -1. Every (x, y) pair is checked, if it actually lays within the ellipse and retained if it does. The random (x, y) pair generation stops, once the requested number of rays is reached. In order to use different statistical grids for each time step, the statistical grid is regenerated afresh for each time step using a different random seed value.

17.4.7.5 Beam Cross Section Power Function

The beam cross section power function describes the power distribution of the rays inside the beam at launching time. Currently there are two types of power distribution functions implemented in FLASH: 1) uniform (flat) distribution (equal power) and 2) gaussian decay from the center of the beam. The first one is trivial: every ray gets assigned an equal amount of power. The gaussian decay function assigns to each ray a relative weight according to the position inside the elliptical cross section of the beam. Using the local $\mathbf{s}_1$ and $\mathbf{s}_2$ target coordinate system located at the center of the beam, the gaussian weighting function for 2D target areas (3D geometries) reads

$$w = \exp^{-\left[\left(\frac{x}{R_x}\right)^2 + \left(\frac{y}{R_y}\right)^2\right]^\gamma}, \tag{17.106}$$

where x and y denote the local coordinates inside the ellipse along the $\mathbf{s}_1$ and $\mathbf{s}_2$ axes, respectively, R_x and R_y are user defined decay radii values and γ is the user defined gaussian super exponent. For 1D target areas (2D geometries) the weighting function is

$$w = \exp^{-\left[\left(\frac{x}{R_x}\right)^2\right]^\gamma}. \tag{17.107}$$

In order to determine the actual power assigned to each ray, we use the average laser power from equation 17.69

$$P_{ray} = \overline{P}\frac{w_{ray}}{\sum w_{ray}}. \tag{17.108}$$

The sum of the weights over all rays plays the role of a sort of partition function for the beam grid and can thus be precomputed and become part of the beam properties when setting up the beams.

17.4.7.6 The Rays Initial Position and Velocity

In 3D, after the local lens and target grids have been set up, each ray has associated with it a local lens elliptical coordinate pair (x_L, y_L) and a local target elliptical coordinate pair (x_T, y_T). The corresponding global coordinates can be obtained using the global lens and target center coordinates and the elliptical unit vectors (see Figure 17.7)

$$\mathbf{R}_L = x_L\mathbf{u}_1 + y_L\mathbf{u}_2 + \mathbf{L} \tag{17.109}$$

$$\mathbf{R}_T = x_T\mathbf{u}_1 + y_T\mathbf{u}_2 + \mathbf{T}. \tag{17.110}$$

Defining now the ray vector $\mathbf{R}$ pointing from the lens to the target

$$\mathbf{R} = \mathbf{R}_T - \mathbf{R}_L, \tag{17.111}$$

we can state the parametric ray line equation

$$\mathbf{P} = \mathbf{R}_L + w\mathbf{R}. \tag{17.112}$$

The ray line equation is used to determine where and which domain boundary surface the ray will hit. Consider a domain boundary surface contained within a plane given by the equation

$$\begin{aligned} A_x x + A_y y + A_z z + D &= 0 \\ \mathbf{A} \cdot (x\ y\ z) + D &= 0. \end{aligned} \tag{17.113}$$

The value of the real w parameter where the ray line meets this plane is obtained by inserting the ray line equation into the plane equation. It is

$$w = -\frac{\mathbf{A} \cdot \mathbf{R}_L + D}{\mathbf{A} \cdot \mathbf{R}}. \tag{17.114}$$

Inserting this w value into the ray line equation 17.112 we obtain the location $\mathbf{P}_{cross}$ of the crossing point on the plane. From Figure 17.7, for the ray vector to cross the plane, the value of w must be in the range $0 \leq w \leq 1$. A value of $w = 0$ or $w = 1$ indicates that the plane is crossing the lens or target area, respectively. If w is in proper range, it must next be checked if $\mathbf{P}_{cross}$ is located within the domain boundary surface. If yes, that w value is accepted. Note, that several proper w values can be obtained. A ray crossing near the corner of a rectangular domain gives three proper w values corresponding to crossing the three rectangular planes defining the corner. Since the rays originate from the lens, the relevant w is the one with minimum value and the corresponding $\mathbf{P}_{cross}$ will be taken as the rays initial position. The initial ray velocity components are determined from the unit vector of the ray vector

$$\mathbf{v} = v_0 \frac{\mathbf{R}}{|\mathbf{R}|}, \tag{17.115}$$

where v_0 is the initial magnitude of the velocity (in most simulations this is the speed of light). For 2D geometries all the above equations remain the same, except for the ray global coordinates, for which the terms in $\mathbf{u}_2$ are dropped and for the domain boundary planes, for which the terms involving the z-component in the defining equation 17.138 do not exist. The following steps summarize the determination of the initial ray positions and velocity components for each ray:

- Form the ray vector $\mathbf{R}$ using 17.111.
- Find the collection $\{w\}$ of all $0 \leq w \leq 1$ values using 17.114 for all domain surface planes $(\mathbf{A}, D)$.
- Using the ray line equation 17.112, remove all w values from $\{w\}$ which lead to plane crossing points $\mathbf{P}_{cross}$ not contained within the domain boundary surface.
- Take the minimum of the remaining w's in $\{w\}$ and calculate the corresponding $\mathbf{P}_{cross}$. This is the ray's initial position vector.
- Using the ray vector $\mathbf{R}$ again calculate the velocity components using 17.115.

17.4.8 3D Laser Ray Tracing in 2D Cylindrical Symmetry

Performing a pure 2D cylindrical ray tracing has an obvious disadvantage: each ray must also be treated as a 2D cylindrical symmetrical object. Each ray can only hit the R-disk of the cylindrical domain at precisely 90 degrees and no variation in this incident angle is possible. However, if one treats the cylinder as a true 3D object, then it is possible to trace each ray through this 3D cylinder. The advantage of retaining the 2D cylindrical description of the domain is obvious: only 2D storage is needed to describe the properties of the domain. 3D in 2D ray tracing is much more complicated than either the simple pure 3D or pure 2D counterparts. The interplay between the polar and the cartesian coordinates leads to ray tracing equations which can only be solved approximately via the use of elliptical integrals. Rather than approximating the integrals involved, a second approach decomposes the 3D cylinder into several identical cylindrical wedges with each wedge having planar boundaries. The larger the number of wedges the more accurate the 3D in 2D ray tracing will be. Both approaches (approximating the integrals and wedging the 3D cylinder) are entirely equivalent.

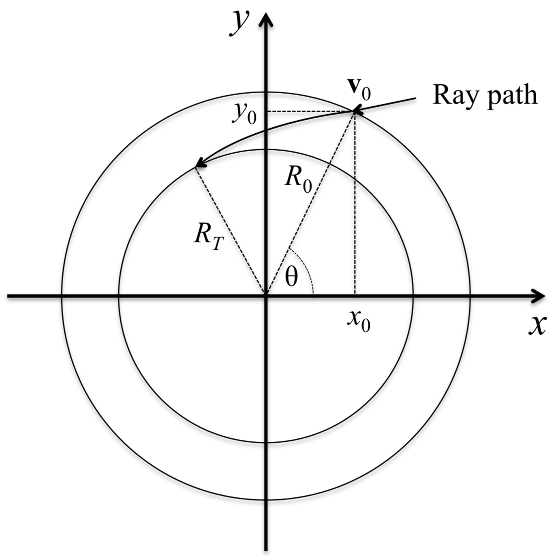

Figure 17.8: Tracing a ray in 3D in a 2D cylindrical domain. View onto the R-disk. The z-axis has been left out for clarity.

17.4.8.1 The Exact 3D in 2D Ray Tracing Solution

We will first state the exact time-radial solution of an object of mass m moving in a central force environment with no external forces acting on it. The motion of such an object is characterized by constant energy and angular momentum and is hence confined to a 2D plane. There are two ways to describe the position $\mathbf{r}$, velocity $\mathbf{v}$ and acceleration $\mathbf{a}$ vectors of a particle in a 2D plane: using cartesian $\hat{\mathbf{i}}, \hat{\mathbf{j}}$ or polar $\hat{\mathbf{R}}, \hat{\boldsymbol{\theta}}$ unit vectors. They are interrelated by

$$(\hat{\mathbf{R}}, \hat{\boldsymbol{\theta}}) = (\hat{\mathbf{i}}, \hat{\mathbf{j}}) \begin{pmatrix} \cos\theta & -\sin\theta \\ \sin\theta & \cos\theta \end{pmatrix} \tag{17.116}$$

Using these unit vectors and the differentiation chain rule we get

$$\mathbf{r} = x\hat{\mathbf{i}} + y\hat{\mathbf{j}} = R\hat{\mathbf{R}} \tag{17.117}$$
$$\mathbf{v} = \dot{x}\hat{\mathbf{i}} + \dot{y}\hat{\mathbf{j}} = \dot{R}\hat{\mathbf{R}} + R\dot{\theta}\hat{\boldsymbol{\theta}} \tag{17.118}$$
$$\mathbf{a} = \ddot{x}\hat{\mathbf{i}} + \ddot{y}\hat{\mathbf{j}} = (\ddot{R} - R\dot{\theta}^2)\hat{\mathbf{R}} + (R\ddot{\theta} + 2\dot{R}\dot{\theta})\hat{\boldsymbol{\theta}} \tag{17.119}$$

where each dot on the dotted variables stands for d/dt. The angular momentum of the object in polar coordinates is

$$\begin{aligned} \mathbf{L} &= \mathbf{r} \times m\mathbf{v} \\ &= R\hat{\mathbf{R}} \times m(\dot{R}\hat{\mathbf{R}} + R\dot{\theta}\hat{\boldsymbol{\theta}}) \\ &= mR^2\dot{\theta}(\hat{\mathbf{R}} \times \hat{\boldsymbol{\theta}}) \end{aligned} \tag{17.120}$$

and its magnitude

$$L = mR^2\dot{\theta} \tag{17.121}$$

Since only a central force component is present, this force depends only on the radial part

$$\mathbf{F}(R) = m\mathbf{a}_R = m(\ddot{R} - R\dot{\theta}^2)\hat{\mathbf{R}}. \tag{17.122}$$

We are now ready to state the equation of motion of the object in polar coordinates. Let's assume the object has initially at time t_0 the coordinates (R_0, θ_0), and let E be its constant energy. E is composed of two parts: kinetic and potential energy. Both parts will change as time passes by. The potential energy U can only change along a change in R, because the force has only a radial component. We have

$$\begin{aligned} E &= \frac{1}{2}mv^2 + U(R) \\ &= \frac{1}{2}m(\dot{R}^2 + R^2\dot{\theta}^2) + U(R) \\ &= \frac{1}{2}m\dot{R}^2 + \frac{1}{2}\frac{L^2}{mR^2} + U(R) \end{aligned} \tag{17.123}$$

where in the last step we have eliminated the angular dependence through the use of Eq. (17.121). The last equation for E is a first order differential equation allowing for separation of variables

$$\int_{R_0}^{R_T} \left[\frac{2}{m}(E - U(R)) - \frac{L^2}{m^2R^2}\right]^{-1/2} dR = \int_{t_0}^{t_T} dt \tag{17.124}$$

The potential energy can be obtained via integration

$$\begin{aligned} U(R) &= -\int_{R_0}^{R} F(R')dR' + U(R_0) \\ &= -m\int_{R_0}^{R} a_R(R')dR' + U(R_0). \end{aligned} \tag{17.125}$$

The value of the initial potential energy is arbitrary and is conveniently set to zero. Assuming further that $t_0 = 0$, we obtain

$$t_T = \int_{R_0}^{R_T} \left[\frac{2E}{m} - \frac{L^2}{m^2R^2} + 2\int_{R_0}^{R} a_R(R')dR'\right]^{-1/2} dR. \tag{17.126}$$

Given an initial radial R_0 and a final target radial R_T value, t_T is the time the object will take in travelling from R_0 to R_T under the specified initial conditions at R_0 (values of E and L). If the object will not reach R_T then t_T is either negative or complex. The time equation (17.126) can be solved analytically only for a small number of cases (like for example if $a_R = 0$). All other cases require numerical approximation to the radial integral. For our case, when the ray moves through one radial 2D cylindrical zone using the AVG approximation 17.4.4.1, the central force acceleration is constant, i.e $a_R = a$. For this case we have

$$t_T = \int_{R_0}^{R_T} \left[\frac{2E}{m} - \frac{L^2}{m^2R^2} + 2a(R - R_0)\right]^{-1/2} dR, \tag{17.127}$$

for which it is possible to give an analytical solution in terms of elliptical integrals. However, the analytical solution is far to complicated to be of practical use.

17.4.8.2 The Approximate 3D in 2D Ray Tracing Solution

The main reason for the complicated time equation has its roots in the θ polar variable describing the rotational symmetry. An approximate treatment can be formulated, in which each circle is treated as a linear polygon with n sides (n not necessarily integer), where the value of n determines the quality of the approximation. The exact 3D radial acceleration cylindrical problem in R, θ, z coordinates is transformed into an approximate 3D cartesian problem in x, y, z coordinates, where the z coordinate remains unaffected. Each torus cell is hence approximated as a collection of truncated wedge (TW) cells. The trapezoidal sides of these wedges are parallel to the x, y plane and the rectangular sides are perpendicular to this plane. Since all TW cells have exactly the same size and shape when coming from the same torus cell, it suffices to concentrate on just one of them. These representative TW cells will be placed inside the x, y plane, such that the positive x axis divides the trapezoidal sides into two equal areas. The collection of all representative TW cells has the shape of a wedge with opening angle Ω. In order to trace the rays through the TW cells,

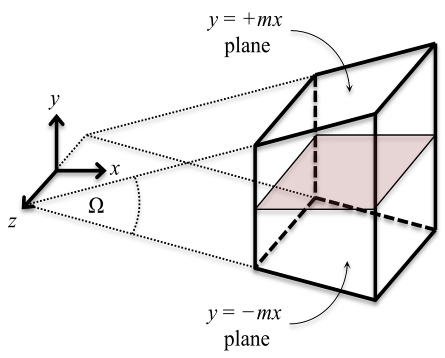

Figure 17.9: Shape and location of the TW cells.

we need the equation of all the cell boundary planes. The equations of the cell planes perpendicular to the z axis (containing the trapezoidal sides) are simply $z = z_{cell}$. The equations of the cell planes perpendicular to the x axis are similarly $x = x_{cell}$. The remaining cell plane equations corresponding to the non-coplanar cell faces are (see Figure 17.9)

$$\begin{aligned} y &= \pm \tan\left(\frac{\Omega}{2}\right) x \\ &= \pm m x. \end{aligned} \tag{17.128}$$

The quadratic time equations to be solved for the $x = x_{cell}$ and $z = z_{cell}$ plane equations are of the same form as equation 17.65. For the plane equations in 17.128 we obtain, after inserting the appropriate forms into the general cartesian quadratic time equation 17.64 and considering the zero gradient approximation in y direction

$$-\frac{c^2}{4n_c}\left[\mp m\langle\nabla n_e\rangle_x\right]t^2 + \left[\mp m v_{0x} + v_{0y}\right]t + \left[\mp m r_{0x} + r_{0y}\right] = 0 \tag{17.129}$$

We now describe the three main tasks for the 3D in 2D ray tracing: 1) proper setup of lenses and corresponding targets, 2) initial placement of the 3D rays on the 2D cylindrical domain and 3) tracing of the rays through the truncated wedges.

17.4.8.3 Extremum Global Radial 3D and 2D Distance Values for 3D Elliptical Lens and Target Zones

In curved domain setups (cylindrical and spherical), it becomes necessary to calculate extremum global radial distance values for a 3D elliptical curve from the domain origin in order to check proper placements of the lens and target zones. We start by stating the global equation of the elliptical target curve $\mathbf{E}$ (the treatment of the lens ellipse is analogous) in 3D in implicit form (see Figure 17.6):

$$\mathbf{E} = \mathbf{T} + \mathbf{s}_1\cos(\omega) + \mathbf{s}_2 sin(\omega), \quad 0 \geq \omega \geq 2\pi. \tag{17.130}$$

The 2D projections of this elliptical 3D curve in either the (x,y), (x,z) or (y,z) plane are themselves ellipses, however the 2D projections of $\mathbf{s}_1$ and $\mathbf{s}_2$ do no longer correspond to the 2D elliptical major and minor semi-axes. They generally are oblique to each other and their scalar product is non-zero. We will therefore develop general formulas taking the possible reduction of 3D to 2D into account. The square of the radial distance for any point on that curve from the global origin is

$$\begin{aligned} |\mathbf{E}|^2 &= |\mathbf{T}|^2 + 2\mathbf{s}_1\cdot\mathbf{T}\cos(\omega) + 2\mathbf{s}_2\cdot\mathbf{T}\sin(\omega) \\ &\quad + \mathbf{s}_1\cdot\mathbf{s}_1\cos^2(\omega) + \mathbf{s}_2\cdot\mathbf{s}_2\sin^2(\omega) + 2\mathbf{s}_1\cdot\mathbf{s}_2\cos(\omega)\sin(\omega). \end{aligned} \tag{17.131}$$

Table 17.4: Different cases arising in 3D, depending on values of A, B, C, D

D	C	A	B	Shape	$\|\mathbf{E}\|^2_{min}$	$\|\mathbf{E}\|^2_{max}$
0	0	0	0	Circle (radius $\|\mathbf{s}_1\|$)	$\|\mathbf{T}\|^2 + \|\mathbf{s}_1\|^2$	$\|\mathbf{T}\|^2 + \|\mathbf{s}_1\|^2$
0	0	0	$\neq 0$	Tilted circle	$\|\mathbf{T} - \mathbf{s}_2\|^2$	$\|\mathbf{T} + \mathbf{s}_2\|^2$
0	0	$\neq 0$	0	Tilted circle	$\|\mathbf{T} - \mathbf{s}_1\|^2$	$\|\mathbf{T} + \mathbf{s}_1\|^2$
0	0	$\neq 0$	$\neq 0$	Double-tilted circle	Solve quadratic	
0	$\neq 0$	0	0	Ellipse	$\|\mathbf{T} + \mathbf{s}_2\|^2$	$\|\mathbf{T} + \mathbf{s}_1\|^2$
0	$\neq 0$	0	$\neq 0$	Tilted ellipse	$\|\mathbf{T} - \mathbf{s}_2\|^2$	$\|\mathbf{T} + \mathbf{s}_1\|^2$
0	$\neq 0$	$\neq 0$	0	Tilted ellipse	Solve quadratic product	
0	$\neq 0$	$\neq 0$	$\neq 0$	Double-tilted ellipse	Solve quartic	

Differentiating with respect to ω and setting equal to zero leads to the minimax equation

$$B\cos(\omega) - A\sin(\omega) - C\sin(\omega)\cos(\omega) + D[\cos^2(\omega) - \sin^2(\omega)] = 0, \qquad (17.132)$$

where

$$A = \mathbf{s}_1 \cdot \mathbf{T} \qquad (17.133)$$
$$B = \mathbf{s}_2 \cdot \mathbf{T} \qquad (17.134)$$
$$C = \mathbf{s}_1 \cdot \mathbf{s}_1 - \mathbf{s}_2 \cdot \mathbf{s}_2 \qquad (17.135)$$
$$D = \mathbf{s}_1 \cdot \mathbf{s}_2. \qquad (17.136)$$

The minimax equation 17.132 contains a mixed trigonometric term and can only be solved by eliminating either the sine or the cosine function. This leads in general to a quartic equation

$$q_4x^4 + q_3x^3 + q_2x^2 + q_1x + q_0 = 0, \qquad (17.137)$$

whose coefficients are, depending on if x is either $\cos(\omega)$ or $\sin(\omega)$:

	$x = \cos(\omega)$	$x = \sin(\omega)$
q_4	$C^2 + 4D^2$	$C^2 + 4D^2$
q_3	$2AC + 4BD$	$-2BC + 4AD$
q_2	$A^2 + B^2 - C^2 - 4D^2$	$A^2 + B^2 - C^2 - 4D^2$
q_1	$-2AC - 2BD$	$2BC - 2AD$
q_0	$D^2 - A^2$	$D^2 - B^2$

All four A, B, C, D can have a value of zero. The coefficient of x^4 plays a special role. Note, that for this coefficient to be zero, both C and D must be zero, which corresponds to a circular curve in both 3D and 2D. For a circular target the quartic reduces to a quadratic. For the 3D cases we always have $D = 0$. The following table 17.4 shows the different cases that can arise for 3D, together with a description of the geometrical shapes of the target figures involved and the corresponding maximum and minimum radial distances: In this table we have used our convention $|\mathbf{s}_1| \geq |\mathbf{s}_2|$ and placement of the elliptical semi-axes in such a way that the angle they make with $\mathbf{T}$ is $\geq 90°$. The cases that arise for the 2D are summarized in the table 17.5: When solving the quartic or quadratic product equations, we must remember to eliminate the two non-valid extra solutions introduced due to squaring. All real solutions between -1 and $+1$ are inserted into 17.131 and the maximum and minimum of all four possible values are selected.

17.4.8.4 Initial Placement of the 3D Rays on the 2D Cylindrical Domain

There are two kinds of domain surfaces for a cylindrical domain. The first kind corresponds to the flat circular surface at both ends of the cylinder. These surfaces are planar and the determination of the ray

Table 17.5: Different cases arising in 2D, depending on values of $A, B, C, D, |\mathbf{s}_1|, |\mathbf{s}_2|$

D	C	A	B	$\|\mathbf{s}_1\|$	$\|\mathbf{s}_2\|$	Shape	$\|\mathbf{E}\|^2_{min}$	$\|\mathbf{E}\|^2_{max}$
0	0	0	0	0	0	Point	$\|\mathbf{T}\|^2$	$\|\mathbf{T}\|^2$
0	$\neq 0$	0	$0, \neq 0$	0	$\neq 0$	Line (length $\|\mathbf{s}_2\|$)	$\|\mathbf{T} - \mathbf{s}_2\|^2$	$\|\mathbf{T} + \mathbf{s}_2\|^2$
0	$\neq 0$	$0, \neq 0$	0	$\neq 0$	0	Line (length $\|\mathbf{s}_1\|$)	$\|\mathbf{T} - \mathbf{s}_1\|^2$	$\|\mathbf{T} + \mathbf{s}_1\|^2$
0	0	$0, \neq 0$	$0, \neq 0$	$\neq 0$	$\neq 0$	Circle (radius $\|\mathbf{s}_1\|$)	$(\|\mathbf{T}\| - \|\mathbf{s}_1\|)^2$	$(\|\mathbf{T}\| + \|\mathbf{s}_1\|)^2$
0	$\neq 0$	0	$\neq 0$	$\neq 0$	$\neq 0$	Ellipse ($\mathbf{s}_2 \| \mathbf{T}$)	Solve quadratic product	
0	$\neq 0$	$\neq 0$	0	$\neq 0$	$\neq 0$	Ellipse ($\mathbf{s}_1 \| \mathbf{T}$)	$(\|\mathbf{T}\| - \|\mathbf{s}_1\|)^2$	$(\|\mathbf{T}\| + \|\mathbf{s}_1\|)^2$
$0, \neq 0$	$\neq 0$	$\neq 0$	$\neq 0$	$\neq 0$	$\neq 0$	Tilted ellipse	Solve quartic	

intersection position on these surfaces proceeds along the same lines as shown in section 17.4.7.6. The second kind of surface is the cylinder mantle, whose geometrical equation is:

$$\begin{aligned} x^2 + y^2 - D &= 0 \\ (x\ y) \cdot (x\ y) - D &= 0. \end{aligned} \tag{17.138}$$

Inserting the parametric ray line equation 17.112, we obtain a quadratic equation in w:

$$(\mathbf{R} \cdot \mathbf{R})w^2 + (2\mathbf{R} \cdot \mathbf{R}_L)w + (\mathbf{R}_L \cdot \mathbf{R}_L - D) = 0, \tag{17.139}$$

where only the x and y components of the vectors are taken to form the scalar products. Having found the appropriate w for each ray and the corresponding crossing point $\mathbf{P}_{cross}$ on the domain cylindrical surface, we need to translate the ray 3D domain crossing coordinates P_x, P_y, P_z into the initial ray 2D cylindrical wedge coordinates W_R, W_y, W_z, where W_R and W_z correspond to the 2D cylindrical domain and W_y is the linearized angular coordinate from 17.128. Since the starting angular point is irrelevant (there is no preference of any point on the circle), we set this point equal to zero. Thus:

$$W_R = \sqrt{P_x^2 + P_y^2} \tag{17.140}$$

$$W_y = 0 \tag{17.141}$$

$$W_z = P_z \tag{17.142}$$

To determine the initial ray wedge velocities, we define two unit vectors of the 3D ray vector: 1) the unit vector in the (x,y)-plane and 2) the unit vector along the z-axis:

$$\mathbf{u}_{xy} = \mathbf{R}_{xy}/|\mathbf{R}| \tag{17.143}$$

$$\mathbf{u}_z = \mathbf{R}_z/|\mathbf{R}|, \tag{17.144}$$

where $\mathbf{R}_{xy}$ is the (x,y)-plane projection of the 3D ray vector. Likewise, the crossing point vector is also split into two components:

$$\mathbf{P}_{cross} = \mathbf{P}_{xy} + \mathbf{P}_z. \tag{17.145}$$

Since the origin of the cylindrical domain is located at $(x, y) = (0, 0)$, the vector $\mathbf{P}_{xy}$ is a radial vector in the (x,y)-plane. The ray vector component $\mathbf{R}_{xy}$ on the other hand is usually not radially oriented, because the ray's origin (on the lens) does not necessarily lay on the $(x, y) = (0, 0)$ line. Both vectors $\mathbf{P}_{xy}$ and $\mathbf{R}_{xy}$ are useful in order to determine the ray's initial wedge velocities (see Figure 17.10). Denote the angle between $\mathbf{R}_{xy}$ and $\mathbf{P}_{xy}$ by α. Then

$$\cos(\alpha) = \frac{\mathbf{R}_{xy} \cdot \mathbf{P}_{xy}}{|\mathbf{R}_{xy}||\mathbf{P}_{xy}|} \tag{17.146}$$

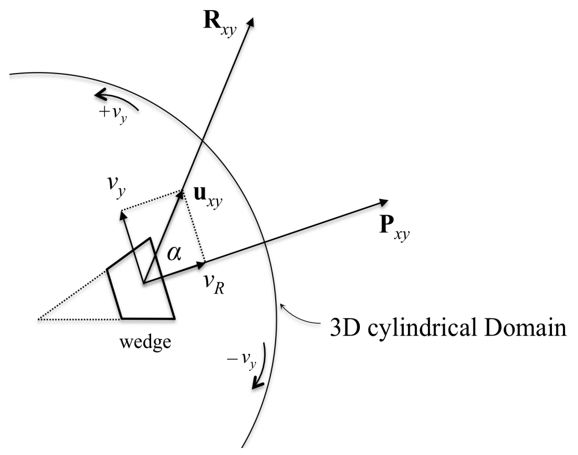

Figure 17.10: Initial radial (v_R) and angular (v_y) ray velocity components on the wedge from vectors $\mathbf{P}_{xy}$ and $\mathbf{R}_{xy}$.

and the initial ray wedge velocities are

$$\begin{aligned} v_R &= v_0 * \cos(\alpha)|\mathbf{u}_{xy}| && (17.147)\\ v_y &= v_0 * sign(\mathbf{R}_{xy} \times \mathbf{P}_{xy}) * \sin(\alpha)|\mathbf{u}_{xy}| && (17.148)\\ v_z &= v_0 * |\mathbf{u}_z|, && (17.149)\end{aligned}$$

where the sine and the cross product vector present in the expression for v_y are calculated as

$$\sin(\alpha) = +\sqrt{1 - \cos^2(\alpha)} \quad (17.150)$$

and

$$\mathbf{R}_{xy} \times \mathbf{P}_{xy} = \begin{vmatrix} \mathbf{i} & \mathbf{j} & \mathbf{k} \\ R_x & R_y & 0 \\ P_x & P_y & 0 \end{vmatrix} = (R_x P_y - R_y P_x)\mathbf{k}. \quad (17.151)$$

The sign of the cross product refers to the sign of the $\mathbf{k}$ component. Note, that the wedge's y-direction refers to the cylindrical θ-coordinate and the convention is that counterclockwise rotation along θ is considered positive.

17.4.8.5 Tracing the Rays through the Truncated Wedges

When a ray hits the R- or z-planes of a truncated wedge, the R- or z-components of the ray's position and velocity change the same way as for a pure 2D cylindrical simulation. The y-components stay the same. When the ray hits the y-planes of the truncated wedge, it will cross into a new rotated wedge and the y-position and the R- and y-components of the velocity must change to reflect that rotation. The change in y-position is simple: just invert its sign. For the velocity component changes we need the cosine and sine of the wedge's opening angle Ω. The new components are thus

$$\begin{aligned} W_y(\text{new}) &= -W_y && (17.152)\\ v_R(\text{new}) &= v_R * \cos(\Omega) \pm v_y * \sin(\Omega) && (17.153)\\ v_y(\text{new}) &= v_y * \cos(\Omega) \mp v_R * \sin(\Omega), && (17.154)\end{aligned}$$

where the sign options in v_R and v_y correspond to the two possible y-planes defined in 17.128 (see Figure 17.11). The change in direction of both velocity vector components is not a rotational effect on the ray due to

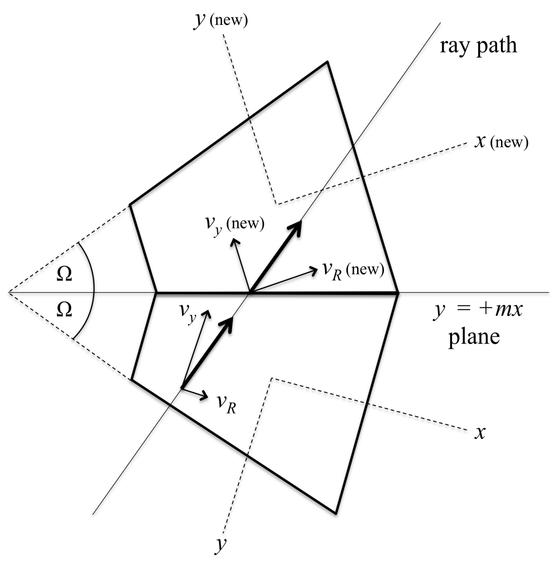

Figure 17.11: Change in position and velocity components when ray moves into a new wedge. For clarity, the velocity components in the original wedge are shifted from the boundary crossing point.

the medium through which it travels but rather a geometrical effect due to changing wedges. When crossing a common y-plane between two wedges, the ray is still on the same position in the (R,z) 2D cylindrical plane. Note, that Ω must not necessarily be a divisor of 360°. Since Ω is fixed through the entire simulation, cos(Ω) and sin(Ω) are conveniently computed only once during initialization.

17.4.9 Synchronous and Asynchronous Ray Tracing

The default laser implementation uses the Lagrangian particle framework to move rays (modeled as particles) across block and process boundaries. We generally find that particle movement consumes a relatively small portion of total runtime even in large-scale simulations with millions of particles (Dubey et al., 2012). This is not always case in laser-driven FLASH simulations, where realistic simulations can spend the majority of runtime moving rays between blocks. The reason for the discrepancy in performance is because a ray generally travels a much larger distance than a tracer particle in a single time-step. In the tracer particle case we only need one application of the communication subroutines in a single time-step because a particle never moves further than a nearest-neighbor block (see CFL limit). In contrast a ray can move to the other side of the domain in a single time-step which may involve visiting hundreds of intermediate blocks.

There are various implementations of particle exchange in the GridParticles sub-unit. In order to understand the performance bottlenecks, we describe the default implementation used in FLASH applications configured with Paramesh. The particle movement communication consists of an `MPI_Allreduce` to determine the number of particles and messages that each MPI rank will receive, followed by point to point messages which exchange the actual particles. In addition to the communication in the GridParticles unit, there is also an `MPI_Allreduce` in the laser unit which determines if all the rays have either left the domain or have been absorbed. This is the termination criteria and controls whether another round of particle exchange is needed.

Performance profiles of simulations using the laser indicate that most time is spent in `MPI_Allreduce` calls in a particle movement subroutine. The trace in Figure 17.12 shows that this happens because of load imbalance and not slowness of the underlying collective communication call. The two main colors in this trace are red and purple; red is time spent in a computational kernel named `ed_traceBlockRays2Dcyl3D` and purple is time spent in `MPI_Allreduce`. We see that the color map is dominated by purple which indicates most MPI ranks are waiting for the `MPI_Allreduce` to complete. The cascading red pattern shows the ray paths as rays move between blocks assigned to different MPI ranks. It is clear that there are many round of bulk synchronous particle exchange and that some MPI ranks must wait a long time before receiving any rays. The biggest impediment to good performance is the dependency between MPI ranks which happens

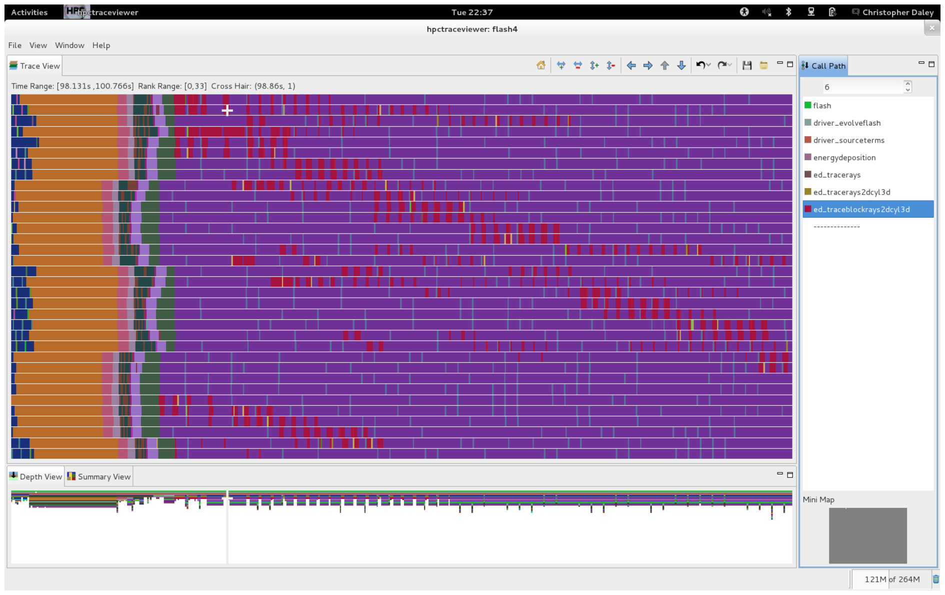

Figure 17.12: Performance trace of MPI ranks 0-33 in a laser simulation using synchronous communication and run with 2048 MPI ranks on Intrepid BG/P.

because ray paths are not known ahead of time. Performance quickly degrades at higher processor counts because increased domain decomposition means rays must cross more process boundaries. One approach to improve performance would be to use the mesh replication feature of FLASH to trivially parallelize over the rays, but this is not ideal because it introduces redundant computations of e.g. hydrodynamics in each mesh. The approach we take is to introduce pipelined parallelism to hide the dependency between MPI ranks; rays are sent to nearest-neighbor blocks on different MPI ranks as early as possible to minimize the time MPI ranks must wait for work. Computation and communication are overlapped, which is different to the current bulk synchronous approach where there are distinct computation and communication phases. The "asynchronous ray trace" is included in a FLASH application by setting up with the shortcut `+asyncLaser`. We describe the ray exchange and termination communication kernels in the asynchronous scheme below.

The ray exchange communication kernel requires all MPI ranks set up designated send and receive communication channels with only those MPI ranks which own nearest-neighbor blocks. This is a relatively small subset because of the block locality in Paramesh. We post one speculative non-blocking receive for each neighbor and then test all communication channels (at a rate determined by runtime parameter `ed_commRaysBetweenMsgTest`) for new rays. When an MPI rank receives a message we copy the rays and then post a new speculative non-blocking receive. This ensures that a message can be received from any nearest neighbor at any time. We send rays using non-blocking sends from source MPI ranks when send buffers (of size determined by runtime parameter `ed_commChannelSize`) are full. At idle phases, we also send rays before the send buffer is full to prevent deadlock and ensure good global progress. When exchange is complete all MPI ranks send a zero byte message to each neighboring MPI rank to match the remaining speculative receives.

The termination communication kernel must also be non-blocking to allow progress in the ray exchange communication kernel. This rules out using a blocking `MPI_Allreduce` as is used in the default synchronous scheme. We have multiple non-blocking implementations of the termination kernel which all have different library and MPI dependencies. The default implementation, which has no special dependencies, uses a master-slave approach to determine completion. It works by sending a count of local inactive rays from slaves to a master which maintains a count of global inactive rays. We send a notification message from the master to the slaves when the global number of inactive rays is equal to the initial count of active rays. Even though we have demonstrated that this implementation *can* work when using 8192 MPI ranks on Intrepid BG/P, there is a danger of exceeding internal MPI limits on the number of messages the master rank can receive. For this reason we have created another implementation which uses a non-blocking `MPI_Iallreduce` which is part of MPI-3. We recommend using this implementation because there is less danger of exceeding internal MPI limits. It can be used by setting up a FLASH application with the setup shortcut `+mpi3`. Given that the MPI-3 standard is still quite new, it is likely that some MPI implementations on today's production machines do not support non-blocking collectives. Therefore, we also support the non-blocking reduction in the Non Blocking Collectives (NBC) library `http://htor.inf.ethz.ch/research/nbcoll/libnbc/`. The necessary reduction name substitutions happen when a FLASH application is setup with `+libnbc`.

We repeat the experiment in Figure 17.12 with the asynchronous communication scheme and show results in Figure 17.13. The number of ranks on the y-axis and time scale on the x-axis are the same as before. The color map is much more chaotic than before because all MPI ranks are either computing or spinning in various subroutines looking for more work. As before, the red color indicates time spent in a computational kernel named `ed_traceBlockRays2Dcyl3D`. The red is now much more clustered on the left side of the figure indicating MPI ranks wait less time for rays than before. We see large segments of green for MPI rank 0 which indicates time spent testing for new messages. This is happening because we made use of the master-slave termination kernel in this test. A performance comparison of the synchronous and asynchronous communication schemes is shown in Figure 17.14. The parameters `ed_commChannelSize` and

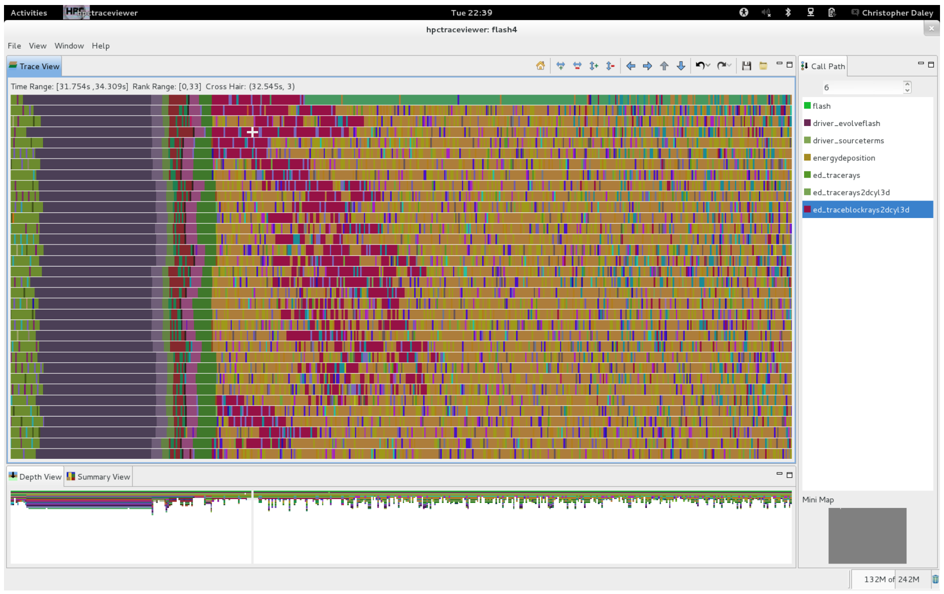

Time Range: [31.754s ,34.309s] Rank Range: [0,33] Cross Hair: (32.545s, 3)

6

- 🟩 flash
- 🟪 driver_evolveflash
- 🟩 driver_sourceterms
- 🟨 energydeposition
- 🟩 ed_tracerays
- 🟩 ed_tracerays2dcyl3d
- 🟥 ed_traceblockrays2dcyl3d

Figure 17.13: Performance trace of MPI ranks 0-33 in a laser simulation using asynchronous communication and run with 2048 MPI ranks on Intrepid BG/P.

`ed_commRaysBetweenMsgTest` give some control over the memory overhead and performance of the asynchronous scheme. The `ed_commChannelSize` parameter should be kept relatively small because it determines the amount of space available for rays in send and receive buffers. Large values lead to a very high memory footprint because there is a designated portion of space in the buffers for all communication channels (i.e. all possible pairs of communicating processors) and there can be 10-100s of communication channels. The parameter also determines the number of rays which are buffered before being sent from source processors to destination processors, and so smaller values will improve overall load balance. All messages are non-blocking and so the source processor returns immediately to computation and is free to send rays to different destination processors. However, the source processor will block (actually spin on various `MPI_Test` statements with no danger of deadlock) if a ray should be sent to the original processor and the original message is not yet delivered. This means it is important for the destination processor to frequently check for new messages not only to start work as soon as possible but also to enable the source processor to return to useful work. The

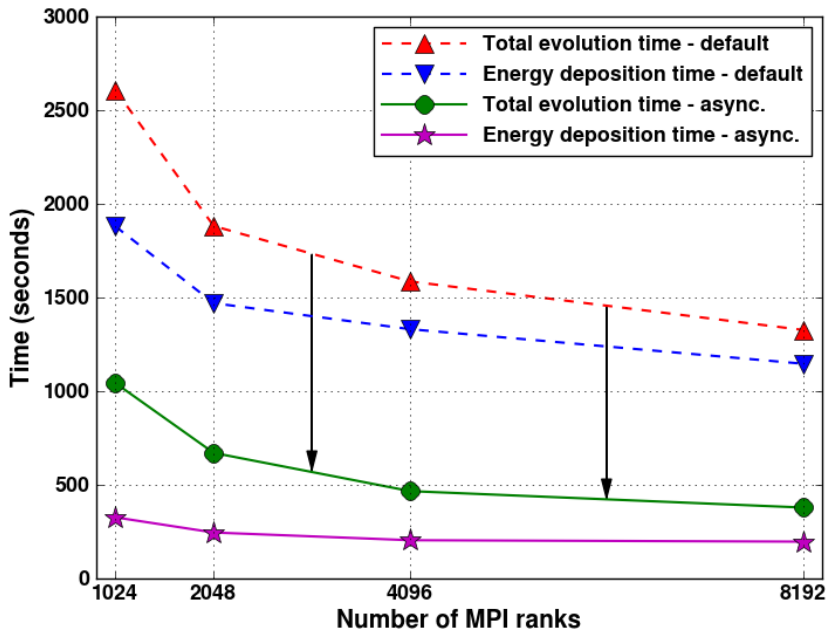

Figure 17.14: Strong scaling of a laser simulation run on Intrepid BG/P with the synchronous and asynchronous communication scheme.

parameter `ed_commRaysBetweenMsgTest` should therefore be kept relatively small so that the destination processor performs less computational work between message checks.

We set the default values of `ed_commRaysBetweenMsgTest`=50 and `ed_commChannelSize`=100. Very small values for both parameters improve load balance but introduce new overheads such as the cost of continually testing for new messages and the cost of preparing the laser computation routines for the newly received rays. The preparation work includes sorting the rays in block order and then scanning the ray array to find the start and end index for each block. Sorting improves the memory-access pattern and is a sensible optimization when computational time is large relative to the sort time (as always happens in the original synchronous communication scheme), however, it hurts performance when computational work is very fine-grained. Hence, we do not advise using parameter values much smaller than the default values. In future it would be interesting to see if removing the serial optimization improves the global time to solution. This could happen because more processors are doing useful work despite there being worse memory-access on each processor.

The asynchronous communication scheme conflicts with various capabilities in FLASH. It only works with Paramesh at the current time, although support for UG could probably be added without a huge amount of effort. We initially did not support UG because we did not know the MPI rank IDs of the corner neighboring blocks, although this is no longer the case. It also conflicts with the Laser I/O.

The asynchronous communication scheme is able to run without the GridParticles dependency by setting up with `useGridParticles=False`. This is generally a good idea because the GridParticles sub-unit has initialization code which allocates large send and receive buffers for bulk synchronous communication. These buffers are not needed in the asynchronous scheme and so removing the dependency significantly reduces the memory footprint. The only down-side is that a slower sorting subroutine will be used in place of Grid_SortParticles, which is able to achieve a fast sort by using the space in the bulk synchronous communication buffers.

The new asynchronous ray tracing implementation works and has been tested with several laser problems using multiple compilers and MPI implementations. However, since this is a rather new implementation, the asynchronous ray tracing mode should still be considered as being in its experimental stage. Both synschronous and asynchronous ray tracing modes are currently made available, with synchronous mode being the default. The asynchronous mode can be activated by using the appropriate setup parameter.

17.4.10 Usage

To include the use of the Energy Deposition unit, the following should be included into the setup line command:

```
+laser ed_maxPulses=<number> ed_maxPulseSections=<number> ed_maxBeams=<number>
```

The +laser is a shortcut that handles all the logistics for properly including the `EnergyDeposition` unit. By default, the ray tracing algorithm used is the AVG algorithm 17.4.4.1 in its synchronous communication mode 17.4.9. To activate the cubic interpolation ray tracing schemes, replace the +laser shortcut by the shortcut +laserCubicInterpolation. This automatically includes the relevant routines for cubic interpolation and bypasses the ones responsible for the AVG algorithm. The default ray tracing method for the cubic interpolation is the piecewise parabolic ray tracing method 17.4.4.2. To activate the cubic interpolation using the Runge Kutta integrator one has to set the shortcut +laserCubicInterpolationRK. To activate the asynchronous ray tracing communication mode, replace the +laser shortcut by the shortcut +asynchLaser. This enables the asynchronous communication routines and supresses the synchronous ones. Only the AVG ray tracing algorithm is currently implemented in asynchronous communication mode. The other three setup variables fix the dimensions needed for the pulses and beams:

- **ed_maxPulses**: The maximum number of different laser pulses for the simulation.
- **ed_maxPulseSections**: The maximum number of power/time pairs per pulse.
- **ed_maxBeams**: The maximum number laser beams for the simulation.

The Energy Deposition unit reads all the information it needs to construct the laser beams and pulses from runtime parameters specified in the flash.par file. Below is the list of runtime parameters that is needed to properly build the laser. For clarification and figuring out the input to a particular laser simulation, the reader is encouraged to have Figures 17.5, 17.6 and 17.7 at hand.

17.4.10.1 Laser Pulses Runtime Parameters

- `ed_numberOfPulses`: Controls the number of different laser pulses that are going to be used.
- `ed_numberOfSections_n`: Indicates the number of power/time pairs that are going to be used to set up the shape of the n-th laser pulse. There must be at least as many of these runtime parameters as there are number of laser pulses defined, i.e. n = 1,...,`ed_numberOfPulses`.
- `ed_power_n_i`: Sets the i-th power of the i-th power/time pair of the n-th laser pulse. The ranges of the indices must be at least: i = 1,...,`ed_numberOfSections_n` and n = 1,...,`ed_numberOfPulses`.
- `ed_time_n_i`: Sets the i-th time of the i-th power/time pair of the n-th laser pulse. The ranges of the indices must be at least: i = 1,...,`ed_numberOfSections_n` and n = 1,...,`ed_numberOfPulses`.

17.4.10.2 Laser Beams Runtime Parameters

- `ed_numberOfBeams`: The number of laser beams that are going to be used.
- `ed_lensX_n`: The x-component of the global lens center position vector **L** (n-th beam).
- `ed_lensY_n`: The y-component of the global lens center position vector **L** (n-th beam).
- `ed_lensZ_n`: The z-component of the global lens center position vector **L** (n-th beam).
- `ed_targetX_n`: The x-component of the global target center position vector **T** (n-th beam).
- `ed_targetY_n`: The y-component of the global target center position vector **T** (n-th beam).

- ed_targetZ_n: The z-component of the global target center position vector $\mathbf{T}$ (n-th beam).
- ed_targetSemiAxisMajor_n: The major (largest) semiaxis length ℓ_1 for the elliptical target area (n-th beam).
- ed_targetSemiAxisMinor_n: The minor (smallest) semiaxis length ℓ_2 for the elliptical target area (n-th beam).
- ed_lensSemiAxisMajor_n: The major (largest) semiaxis length ℓ_1 for the elliptical lens area (n-th beam).
- ed_semiAxisMajorTorsionAngle_n: The major elliptical semiaxis torsion angle ϕ_1 along the beam's lens target center line (n-th beam).
- ed_semiAxisMajorTorsionAxis_n: The major elliptical semiaxis torsion axis ('x','y' or 'z') from which the torsion angle ϕ_1 is defined (n-th beam).
- ed_pulseNumber_n: The pulse shape identification number (n-th beam).
- ed_wavelength_n: The wavelength of the laser (n-th beam).
- ed_initialRaySpeed_n: The initial speed of the rays when hitting the domain boundary, in units of the speed of light (n-th beam).
- ed_ignoreBoundaryCondition_n: Ignore the domain boundary conditions (reflective) when rays enter the domain (n-th beam)?
- ed_crossSectionFunctionType_n: Beam cross section power function (flat or gaussian decay) type. For a flat profile use 'uniform', for gaussian decay use 'gaussian1D' (two-dimensional beams) or 'gaussian2D' (three-dimensional beams) (n-th beam).
- ed_gaussianExponent_n: The Gaussian super exponent γ for the beam cross section power function in equation 17.106 (n-th beam).
- ed_gaussianRadiusMajor_n: The Gaussian radius (e-folding length) R_x along the major elliptical semiaxis in equation17.106 (n-th beam).
- ed_gaussianRadiusMinor_n: The Gaussian radius (e-folding length) R_y along the minor elliptical semiaxis in equation17.106 (n-th beam).
- ed_gaussianCenterMajor_n: The Gaussian center location along the major elliptical semiaxis (n-th beam).
- ed_gaussianCenterMinor_n: The Gaussian center location along the minor elliptical semiaxis (n-th beam).
- ed_numberOfRays_n: Number of rays to be created for the beam. Might be overwritten in 3D geometrical cases (n-th beam).
- ed_gridType_n: Specifies the grid type to be used for placing the rays inside the beam. For two-dimensional beams the options are 'regular1D' or 'statistical1D'. For three-dimensional beams the options are 'square2D', 'radial2D' or 'statistical2D'. (n-th beam).
- ed_gridnRadialTics_n: For radial grid types, the number of wanted grid positions along each radial spike can be specified (n-th beam).
- ed_gridnAngularTics_n: For radial grid types, the number of wanted angular slices can be specified (n-th beam).
- ed_gridDeltaSemiAxisMajor_n: For delta grid types, the tic separation along the major elliptical semiaxis (n-th beam).
- ed_gridDeltaSemiAxisMinor_n: For delta grid types, the tic separation along the minor elliptical semiaxis (n-th beam).

17.4.10.3 Laser General Runtime Parameters

- `ed_maxRayCount`: The maximum number of rays that can be created on one processor.
- `ed_gradOrder`: (AVG algorithm only) The order of approximation used for the electron number density n_e and the electron temperature T_e in a cell (equation 17.39). A value of 1 leads to linear and a value of 2 to parabolic (quadratic) ray trajectories inside the cell. The first case includes no gradients and only takes the cell's average value.
- `ed_computeGradNeleX`: (AVG algorithm 17.4.4.1 only) If false, the x-components of the gradients $\langle\nabla n_e\rangle$ are not computed, i.e. set to zero.
- `ed_computeGradNeleY`: (AVG algorithm 17.4.4.1 only) If false, the y-components of the gradients $\langle\nabla n_e\rangle$ are not computed, i.e. set to zero.
- `ed_computeGradNeleZ`: (AVG algorithm 17.4.4.1 only) If false, the z-components of the gradients $\langle\nabla n_e\rangle$ are not computed, i.e. set to zero.
- `ed_enforcePositiveNele`: (AVG algorithm 17.4.4.1 only) If true, the x-, y- and z-components of the gradients $\langle\nabla n_e\rangle$ will be rescaled such that they always deliver a positive (greater or equal zero) value for the number of electrons in a cell.
- `ed_enforcePositiveTele`: (AVG algorithm 17.4.4.1 only) If true, the x-, y- and z-components of the gradients $\langle\nabla T_e\rangle$ will be rescaled such that they always deliver a positive (greater or equal zero) value for the electron temperature in a cell.
- `ed_printMain`: If true, it prints general information regarding the laser setup to a file with name <basename>LaserMainDataPrint.txt, where <basename> is the base name of the simulation.
- `ed_printPulses`: If true, it prints detailed information about the laser pulses to a file with name <basename>LaserPulsesPrint.txt, where <basename> is the base name of the simulation.
- `ed_printBeams`: If true, it prints detailed information about the laser beams to a file with name <basename>LaserBeamsPrint.txt, where <basename> is the base name of the simulation.
- `ed_printRays`: If true, it prints detailed information about the all rays initially generated on each processor to a file(s) with name(s) <basename>LaserRaysPrint<PID>.txt, where <basename> is the base name of the simulation and PID is the processor rank number.
- `ed_laser3Din2D`: If true, 3D rays will be traced on a 2D cylindrical grid.
- `ed_laser3Din2DwedgeAngle`: The wedge opening angle Ω (in degrees) for a 3D in 2D laser ray trace simulation.
- `ed_rayZeroPower`: Below this value (erg/s), the ray is considered to have zero power.
- `ed_rayDeterminism`: If true, the Grid Unit will be forced to use the Sieve Algorithm to move the ray particle data. Forcing this algorithm will result in a slower movement of data, but will fix the order the processors pass data and eliminate round off differences in consecutive runs.
- `ed_cellWallThicknessFactor`: Controls the (imaginary) thickness of the cell walls to ensure computational stability of the laser code. The cell thickness is defined as this factor times the smallest cell dimension along all geometrical axes. The factor is currently set to 10^{-6} and should only very rarely be changed.
- `ed_cellStepTolerance`: (Cubic interpolation only) This factor times the smallest dimension of each cell is taken as the positional error tolerance for the CIPPRT 17.4.4.2 and the CIRK 17.4.4.3 ray tracing methods.
- `ed_powerStepTolerance`: (Cubic interpolation with Runge Kutta only) This factor denotes the fractional error (unit = current power) for a Runge Kutta step in the CIRK 17.4.4.3 ray tracing method.

- ed_RungeKuttaMethod: (Cubic interpolation with Runge Kutta only) Specifies which Runge Kutta method to use for the CIRK 17.4.4.3 ray tracing method. Current options are: 'CashKarp45' (order 4, default), 'EulerHeu12' (order 1), 'BogShamp23' (order 2), 'Fehlberg34' (order 3) and 'Fehlberg45' (order 4).
- ed_saveOutOfDomainRays: If true, the rays info will be stored into a separate saved ray array for those rays that exit the domain.
- useEnergyDeposition: If false, the energy deposition is not activated, even if the code was compiled to do so. Bypasses the need to rebuild the code.
- threadRayTrace: If true, the innermost ray loop, tracing all rays through a block, is threaded. This runtime parameter can only be set during setup of the code.

17.4.10.4 LaserIO Runtime Parameters and Usage

Often times it is useful to be able to visualize the paths of the individual rays in a simulation. This can be very helpful in ensuring that the laser beams are set up in the intended manner. The LaserIO directory in the source tree located at:

`source/physics/sourceTerms/EnergyDeposition/EnergyDepositionMain/Laser/LaserIO`

By default, this unit is requested by the Laser package (for example, when the `+laser` setup shortcut is specified).

The LaserIO package gives users the ability to write the trajectory of a certain number of rays to plot files when normal FLASH plot file writes occur. This feature is only compatible with parallel HDF5 IO implementations (for example, with `+parallelIO` or `+hdf5typeio`). Only three runtime parameter options need to be set to use LaserIO. These are:

- ed_useLaserIO: Set to `.true.` to activate LaserIO
- ed_laserIOMaxNumberOfRays: Sets the *approximate* maximum number of rays to write to the plot file. This number can be less than the total number of rays in the simulation. When greater than the maximum number of rays, every ray trajectory is written.
- ed_laserIOMaxNumberOfPositions: Sets the size of the LaserIO buffer. A good estimate of this value is 5 × NXB × NYB × NZB × ed_laserIOMaxNumberOfRays.

The ed_laserIOMaxNumberOfRays parameter sets the approximate maximum number of rays to write out. The exact number of rays that will be written is equal to:

$$\max\left[\text{int}\left(\frac{N_{\text{rays}}}{\text{ed\_laserIOMaxNumberOfRays}}\right), 1\right],$$

where N_{rays} is the sum of the number of rays to launch for each beam. The LaserIO ray information is written to the normal HDF5 plot files in the `RayData` dataset. The `extract_rays.py` script that is distributed with FLASH in the `tools/scripts` directory can be used to extract this data. This is a python script which requires the NumPy and PyTables python packages to operate. The script takes as arguments a list of plot files. For each plot file, the script will generate a corresponding VTK file which can be loaded into VisIt. The RayPower_Watts Pseudocolor in VisIt can be plotted to show the ray trajectories. The rays are colored based on their power (in watts). See the `LaserSlab` simulation Section 30.7.5 for an example which uses LaserIO.

17.4.10.5 Laser Energy Density Output

Laser energy density (energy per volume – see 17.4.3) is very useful for visualizing lasers in the simulation space and can be output to the variable "lase" in checkpoint and plot files. This is an experimental feature in FLASH 4.4 and is implemented **only for 3D Cartesian geometry**. To enable "lase" output, edit your simulation's Config file (*e.g.*, for the LaserSlab example, `Simulation/SimulationMain/LaserSlab/Config`) to include the line:

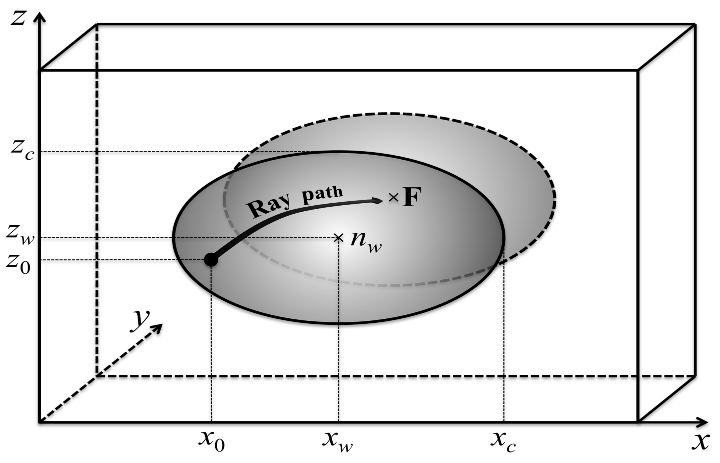

Figure 17.15: One ray moving through an ellipsoidal tube with a quadratic electron number density profile and reaching a focal point **F**.

```
VARIABLE lase TYPE: PER_VOLUME
```

Then setup and build FLASH to use 3D Cartesian ray tracing (otherwise, the added variable is ignored).

17.4.11 Unit Tests

The unit tests set up a series of beams that launch rays onto a domain with a particular electron number density and electron temperature distribution in such a way that an analytical solution is possible for the ray paths and their power deposited inside the domain. The tests are 3D cartesian extensions to the 2D analytical test solution for the quadratic trough as presented in the paper by Kaiser (2000). Figure 17.15 shows the basic structure. 2D cartesian versions of the tests is also available.

17.4.11.1 Analytic Path Solution for the Ellipsoidal Quadratic Potential Tube

Let us define a quadratic ellipsoidal electron number density profile in a 3D space along the xz-plane and having no variation along the y-axis:

$$n_e(\mathbf{r}) = n_w + A(x - x_w)^2 + B(z - z_w)^2, \tag{17.155}$$

Here x_w and z_w are the center coordinates of the ellipsoidal tube cross section, n_w is the value of the electron number density at the center of the ellipse and A, B are the scaling factors for the individual components. The values of A and B are determined by the boundary conditions of $n_e(\mathbf{r})$. For example, if one wants $n_e(\mathbf{r})$ to be equal to a critical value n_c at specific coordinates x_c and (separately) z_c, then we have:

$$A = (n_c - n_w)/(x_c - x_w)^2 \tag{17.156}$$

$$B = (n_c - n_w)/(z_c - z_w)^2. \tag{17.157}$$

Using the ray equation of motion

$$\frac{d^2\mathbf{r}}{dt^2} = \nabla\left(-\frac{c^2}{2}\frac{n_e(\mathbf{r})}{n_c}\right), \tag{17.158}$$

we can solve for the position vector $\mathbf{r}$ under several circumstances (boundary conditions). The first thing to note is that $n_e(\mathbf{r})$ does not contain mixed variable terms, hence the differential ray equation is separable into the individual components. Let us take the x-component. We have

$$\begin{aligned} \frac{d^2x}{dt^2} &= -\frac{c^2}{2n_c}\frac{d}{dx}A(x-x_w)^2 \\ &= -k(x-x_w), \end{aligned} \tag{17.159}$$

where $k = c^2A/n_c$. This is the differential equation for a simple harmonic oscillator around the point x_w. The boundary conditions are such that at time $t = 0$ the ray will be at an initial position x_0 and will posses a certain velocity component v_x

$$x = x_0 \text{ (at } t = 0) \tag{17.160}$$

$$\frac{dx}{dt} = v_x \text{ (at } t = 0). \tag{17.161}$$

To solve the simple harmonic oscillator equation, we make the ansatz

$$x(t) = x_w + (x_0 - x_w)\cos(\beta t) + b\sin(\beta t) \tag{17.162}$$

and find the expressions for b and β satisfying the boundary conditions. We have

$$\frac{dx}{dt} = -\beta(x_0 - x_w)\sin(\beta t) + b\beta\cos(\beta t) \tag{17.163}$$

$$\begin{aligned} \frac{d^2x}{dt^2} &= -\beta^2(x_0 - x_w)\cos(\beta t) - b\beta^2\sin(\beta t) \\ &= -\beta^2(x - x_w) \end{aligned} \tag{17.164}$$

from which we deduce that

$$\beta = \sqrt{k} \tag{17.165}$$

$$b = \frac{v_x}{\beta}. \tag{17.166}$$

The solution to the complete ray equation can thus be stated as

$$x(t) = x_w + (x_0 - x_w)\cos(\sqrt{k}t) + \frac{v_x}{\sqrt{k}}\sin(\sqrt{k}t) \tag{17.167}$$

$$y(t) = y_0 + v_y t \tag{17.168}$$

$$z(t) = z_w + (z_0 - z_w)\cos(\sqrt{k'}t) + \frac{v_z}{\sqrt{k'}}\sin(\sqrt{k'}t), \tag{17.169}$$

where $\mathbf{r}_0 = (x_0, y_0, z_0)$ is the ray's initial position, $\mathbf{v}_0 = (v_x, v_y, v_z)$ the initial velocity and

$$k = \frac{c^2A}{n_c} \tag{17.170}$$

$$k' = \frac{c^2B}{n_c}. \tag{17.171}$$

Let us now define a focal point $\mathbf{F}$, where all rays launched will meet. The obvious choice is a focal point along the tube's center line (x_w, z_w). Without specifying the y-coordinate of this point yet, we ask the question: at what times t and t' will $x(t) = x_w$ and $z(t') = z_w$ for the first time after launch? From the ray equation solutions we get

$$t = \frac{\arctan[-\sqrt{k}(x_0 - x_w)/v_x]}{\sqrt{k}} \tag{17.172}$$

$$t' = \frac{\arctan[-\sqrt{k'}(z_0 - z_w)/v_z]}{\sqrt{k'}}, \tag{17.173}$$

where the angular region of interest for the tangent is $0 \leq \theta \leq \pi$. It is interesting that there is both a lower and an upper limit to these times. While the lower limit of $t \rightarrow 0$ makes sense (if we shoot the ray with infinite velocity towards the tube's center) the upper limit of $t \rightarrow \pi/\sqrt{k}$ is less intuitive: there is no escape from the tube no matter what initial outward velocity we give the ray due to increasing pulling back force towards the center as the ray moves away from it. If the velocity component is zero we have $t = \pi/(2\sqrt{k})$.

In general, both times t and t' will be different. What this means is that the ray will not hit the focal point. For that to occur, both times must be equal, hence we must have

$$\frac{\arctan[-\sqrt{k}(x_0 - x_w)/v_x]}{\sqrt{k}} = \frac{\arctan[-\sqrt{k'}(z_0 - z_w)/v_z]}{\sqrt{k'}}. \tag{17.174}$$

Given A and B values (and thus k and k' values via equations 17.170 and 17.171) defining the tube's electron number density layout, this last relation imposes a condition among the variables x_0, z_0, v_x, v_z. Only if this condition is fulfilled will a focal point at $(x_w, y_\mathbf{F}, z_w)$ be reached. The y-coordinate $y_\mathbf{F}$ of the focal point is then obtained from the y-solution 17.168 of the ray equation by inserting the value of the time t obtained through either side of 17.174. For the unit test we must identify $y_\mathbf{F}$ to be sitting on the domain boundary. Hence when launching a series of ray's for the unit test, all $y_\mathbf{F}$ must be the same. A first scheme I thus emerges for setting up a very general unit test:

SCHEME I

- Fix the center (x_w, z_w) of the ellipsoidal tube cross section, set up the x- and z-dimensions of the domain, and assign a value to the electron number density n_w at the center.
- Set up the ellipsoidal tube parameters A and B, as shown in 17.156 and 17.157, and choose a constant v_y velocity component.
- For one trial ray, given the initial position and velocity x-components x_0 and v_x, determine the time t to reach the focal point **F** using equation 17.172.
- Using t and v_y, calculate $y_\mathbf{F}$ from 17.168, and set up the y-dimensions of the domain.
- Set up the initial x-component positions x_0 for the whole set of rays that are going to be launched.
- Using t, determine the corresponding x-component velocities v_x for all rays from equation 17.172.
- For each ray, choose a z_0 location and determine the needed velocity component v_z using the relation 17.174.
- Launch all rays and collect all the x- and z-components of the domain exit points (x_{exit}, z_{exit}).
- For each ray, check how close (x_{exit}, z_{exit}) is to the expected (x_w, z_w).

A second simplified scheme II (and the one that is currently implemented in FLASH) has all rays launched vertically onto the xz-face of the domain. This means that $v_x = v_z = 0$. By looking at the time condition 17.174, we see that the only possibility for a focal point in this case is if $k = k'$, and the time associated with it is equal to $t = \pi/(2\sqrt{k})$. This means that we must have $A = B$ (a circular tube). Scheme II is set up as follows:

SCHEME II

- Fix the center (x_w, z_w) of the circular tube cross section, set up the x- and z-dimensions of the domain, and assign a value to the electron number density n_w at the center.
- Set up the circular tube parameter A, as shown in 17.156, and choose a constant v_y velocity component.
- Calculate the time $t = (\pi/2c)\sqrt{n_c/A}$ to reach the focal point **F**.
- Using t and v_y, calculate $y_\mathbf{F}$ from 17.168, and set up the y-dimensions of the domain.

- Set up the initial positions (x_0, z_0) for the whole set of rays that are going to be launched.
- Launch all rays and collect all the x- and z-components of the domain exit points (x_{exit}, z_{exit}).
- For each ray, check how close (x_{exit}, z_{exit}) is to the expected (x_w, z_w).

Note, that for scheme II there is no restriction on the initial ray positions (x_0, z_0) like in scheme I. Rays launched vertically from anywhere onto the xz-plane with the same v_y velocity will reach the same focal point **F**. Their paths might be of different lengths, but the time it takes for them to reach **F** is always the same.

17.4.11.2 Analytic Power Deposition Solution for the Ellipsoidal Quadratic Potential Tube

According to equation 17.47, the power remaining after the ray exits the ellipsoidal tube is

$$P_{exit} = P_0 \exp\left\{-\int_0^{t_{cross}} \nu_{ib}[\mathbf{r}(t)]\; dt\right\}, \tag{17.175}$$

where P_0 and P_{exit} denote the ray's power at the tube's entry and exit point and t_{cross} is the time it takes for the ray to reach the focal point **F**. From 17.46, the inverse-Bremsstrahlung rate is

$$\nu_{ib}[\mathbf{r}(t)] = \frac{4}{3}\left(\frac{2\pi}{m_e}\right)^{1/2} \frac{e^4}{n_c k^{3/2}} \frac{Z[\mathbf{r}(t)] n_e[\mathbf{r}(t)]^2 \ln\Lambda[\mathbf{r}(t)]}{T_e[\mathbf{r}(t)]^{3/2}}. \tag{17.176}$$

Note the dependence of Z on position, since we are dealing with the entire domain and not with individual cells. In order to obtain an analytical integrand that is easy to integrate, the first assumption that we make is that both Z and Λ are independent of position. For convenience we chose:

$$Z[\mathbf{r}(t)] = 1 \tag{17.177}$$
$$\ln\Lambda[\mathbf{r}(t)] = 1. \tag{17.178}$$

To change the quadratic dependence on the electron number density to a linear dependency, we set the electron temperature as

$$T_e[\mathbf{r}(t)] = T_w \left[\frac{n_e[\mathbf{r}(t)]}{n_w}\right]^{2/3} \tag{17.179}$$

with a specific electron temperature T_w at the elliptical origin. Using these choices we obtain

$$\begin{aligned} \nu_{ib}[\mathbf{r}(t)] &= \frac{4}{3}\left(\frac{2\pi}{m_e}\right)^{1/2} \frac{n_w e^4}{n_c k^{3/2} {T_w}^{3/2}} n_e[\mathbf{r}(t)] \\ &= \nu_{ib,w} \frac{n_e[\mathbf{r}(t)]}{n_w}, \end{aligned} \tag{17.180}$$

where

$$\nu_{ib,w} = \frac{4}{3}\left(\frac{2\pi}{m_e}\right)^{1/2} \frac{n_w^2 e^4}{n_c k^{3/2} {T_w}^{3/2}} \tag{17.181}$$

is the inverse-Bremsstrahlung rate at the origin. The integral in the exponential becomes

$$\begin{aligned} \int_0^{t_{cross}} \nu_{ib}[\mathbf{r}(t)]\; dt &= \frac{\nu_{ib,w}}{n_w} \int_0^{t_{cross}} n_e[\mathbf{r}(t)]\; dt \\ &= \frac{\nu_{ib,w}}{n_w} \int_0^{t_{cross}} n_w + A(x[t]-x_w)^2 + B(z[t]-z_w)^2\; dt. \end{aligned} \tag{17.182}$$

Inserting the analytical path solutions 17.167 and 17.169, we can perform the integration. Let us concentrate on the x-component part only. We are lead to an integral of the form

$$\begin{aligned}\int_0^{t_{cross}} (x[t]-x_w)^2\; dt &= \int_0^{t_{cross}} \left[(x_0-x_w)\cos(\sqrt{k}t)+\frac{v_x}{\sqrt{k}}\sin(\sqrt{k}t)\right]^2 dt \\ &= \frac{v_x(x_0-x_w)}{2k}+\frac{v_x^2+k(x_0-x_w)^2}{2k}t_{cross}, \end{aligned} \tag{17.183}$$

where t_{cross} is given by the expression in 17.172. For this integration, known sine and cosine integration rules have been used as well as the fact that $\sin(\arctan a)=a/\sqrt{1+a^2}$ and $\cos(\arctan a)=1/\sqrt{1+a^2}$. The z-component integration is similar. Collecting everything together and using the expressions for k,k',A and B from 17.170, 17.171, 17.156 and 17.157 we obtain

$$\begin{aligned}\int_0^{t_{cross}} \nu_{ib}[\mathbf{r}(t)]\; dt &= \nu_{ib,w}\left[t_{cross}+\frac{n_c}{2c^2n_w}\left\{v_x(x_0-x_w)+v_z(z_0-z_w)+(v_x^2+v_z^2)t_{cross}\right\}\right. \\ &\quad \left. +\frac{n_c-n_w}{2n_w}\left\{\frac{(x_0-x_w)^2}{(x_c-x_w)^2}+\frac{(z_0-z_w)^2}{(z_c-z_w)^2}\right\}t_{cross}\right]. \end{aligned} \tag{17.184}$$

This is the general expression of the exponent integral for evaluating the power deposition of the rays for scheme I. For the circular tube of scheme II we have $v_x=v_z=0$, $t_{cross}=(\pi/2c)\sqrt{n_c/A}$, $A=B$, and the exponent integral simplifies to

$$\int_0^{t_{cross}} \nu_{ib}[\mathbf{r}(t)]\; dt = \nu_{ib,w}t_{cross}\left[1+\frac{A}{2n_w}\left\{(x_0-x_w)^2+(z_0-z_w)^2\right\}\right]. \tag{17.185}$$

If all rays start with the same power and imposing equal power deposition for all rays, then the term inside the curly brackets must be equal to a constant value

$$(x_0-x_w)^2+(z_0-z_w)^2 = R^2. \tag{17.186}$$

This condition implies that the rays have to be launched on a circle with radius R around the tube origin (x_w,z_w). This ensures equal path lengths for all rays and hence equal power deposition.

17.4.11.3 Unit Tests Parameters and Results

The current Energy Deposition unit test coded into FLASH is based on the analytic solutions for scheme II. The circular quadratic potential tube is defined through the following parameters and constants:

Parameters	Constants in FLASH
$x_c, z_c = 10$ cm	$m_e = 9.10938215\times10^{-28}$ g
$x_w, z_w = 5$ cm	$e = 4.80320427\times10^{-10}$ esu
$R = 3$ cm	$k = 1.3806504\times10^{-16}$ erg/K
$\lambda = 1\times10^{-4}$ cm	$c = 2.99792458\times10^{10}$ cm/sec
$v_y = c$	
$T_w = 10$ keV	
$P_0 = 1$ erg/sec	

With these values we obtain the following additional variable values (in parenthesis are the equations used), completing the picture:

n_c	$= 1.1148542\ldots\times10^{21}$ cm^{-3}	(17.35)
n_w	$= n_c/2$	
t_{cross}	$= 5\pi/c\sqrt{2}$ sec	(17.172 with $v_x=0$)
$y_\mathbf{F}$	$= 5\pi/\sqrt{2}$ cm	(17.168)
$\nu_{ib,w}$	$= 8.1002987\ldots\times10^8$ sec^{-1}	(17.181)
P_{exit}	$= 0.7017811\ldots$ erg/sec	(17.185 and 17.175)

Evaluation of each cell's average electron number density is done by integrating equation 17.155 over the entire cell xz-area

$$\begin{aligned}
\langle n_e \rangle &= \frac{\displaystyle\int_{z_1}^{z_2} \int_{x_1}^{x_2} n_e(x,y)\; dx\; dz}{(x_2 - x_1)(z_2 - z_1)} \\
&= n_w + A(\overline{x} - x_w)^2 + A(\overline{z} - z_w)^2 + \frac{A}{3}(\Delta x^2 + \Delta z^2), \qquad (17.187)
\end{aligned}$$

where x_1, z_1 are the lower and x_2, z_2 the upper corresponding cell edge coordinates and

$$\overline{x} = \frac{x_1 + x_2}{2} \qquad (17.188)$$

$$\Delta x = \frac{x_1 - x_2}{2} \qquad (17.189)$$

with corresponding equations for the z-part. The average cell's electron temperature is evaluated directly from the average electron number density using 17.179

$$\langle T_e \rangle = T_w \left[\frac{\langle n_e \rangle}{n_w} \right]^{2/3}. \qquad (17.190)$$

The gradients are obtained from the cell average values using the symmetrized derivative formula (shown here for the i-th cell x-component of the electron number density gradient)

$$\frac{\partial}{\partial x} n_e(i) = \frac{\langle n_e \rangle_{i+1} - \langle n_e \rangle_{i-1}}{d_{i-1,i+1}}, \qquad (17.191)$$

where $d_{i-1,i+1}$ is twice the distance between neighboring cells on the x-axis.

TEST I

For test I, a series of 8 rays (from 8 beams with 1 ray each) with radial distances of $3cm$ from $(x_w, z_w) = (5cm, 5cm)$ are launched with the following initial (x_0, z_0) coordinates (all in cm):

Ray	x_0	z_0
1	8	5
2	5	8
3	2	5
4	5	2
5	$5 + 3/\sqrt{2}$	$5 + 3/\sqrt{2}$
6	$5 + 3/\sqrt{2}$	$5 - 3/\sqrt{2}$
7	$5 - 3/\sqrt{2}$	$5 + 3/\sqrt{2}$
8	$5 - 3/\sqrt{2}$	$5 - 3/\sqrt{2}$

Results are shown only for the ray 1 and ray 5, the other ones are related to these two by symmetry. Also z_{exit} is not given, because for ray 1 we have $z_{exit} = 5cm$ and for ray 5 we have $z_{exit} = x_{exit}$. The percentage errors were calculated as $|x_{exit} - x_w|/x_w$ and likewise for the power deposition.

Refinement Level	x_{exit}	% error	P_{exit}	% error
Ray 1				
1	5.04894	0.98	0.69487	0.98
2	5.16343	3.27	0.69864	0.45
3	5.02737	0.55	0.70107	0.10
4	4.98971	0.21	0.70185	0.01
5	5.00004	0.00	0.70176	0.00
6	5.00234	0.05	0.70174	0.00
Ray 5				
1	5.35171	7.03	0.69283	1.23
2	4.77272	4.55	0.70200	0.03
3	4.96221	0.76	0.70115	0.09
4	4.94433	1.11	0.70204	0.04
5	4.95092	0.98	0.70235	0.08
6	4.97987	0.40	0.70198	0.02
Analytical				
∞	5.00000		0.70178	

TEST II

The second test is also based on scheme II and aims at launching a large number of rays using only one beam centered along the tube's origin with a specific cross section power function, such that all rays reaching the focal point have an equal exit power. Since the power deposited depends on the ray path length, the cross section power function must be such that each ray gets the appropriate initial power to account for the differences in path lengths. For a specific ray we have for the exit power

$$P_{exit,ray} = \overline{P}\frac{w_{ray}}{\sum w_{ray}} \exp\left\{-\nu_{ib,w}\; t_{cross}\left[1+\frac{AR_{ray}}{2n_w}\right]\right\}, \tag{17.192}$$

where equations 17.185, 17.175 and 17.108 have been used and $R_{ray} = (x_0 - x_w)^2 + (z_0 - z_w)^2$ is the ray's radial distance from the tube origin. If we set the ray weighting function equal to the inverse gaussian function

$$w_{ray} = e^{+\dfrac{A\nu_{ib,w}t_{cross}}{2n_w}R_{ray}^2}, \tag{17.193}$$

we obtain

$$P_{exit,ray} = \frac{\overline{P}}{Z}e^{-\nu_{ib,w}\; t_{cross}}, \tag{17.194}$$

where we have used Z for the power partition function $\sum w_{ray}$. For a particular number of rays per beam, Z is constant and therefore the exit power of all rays are equal. To get independent of the number of rays, the unit test records the partition scaled exit power $P_{exit,ray}Z$ for each ray as well as their focal (x_{exit}, z_{exit}) coordinates. A maximum square radial deviation

$$\Delta R_{focal}^2 = \max\left\{(x_{exit} - x_w)^2 + (z_{exit} - z_w)^2\right\} \tag{17.195}$$

from the focal point is then defined and recorded. The maximum absolute deviation in the partition scaled power is registered as

$$\Delta P_{focal} = \max|P_{exit,ray}Z - \overline{P}e^{-\nu_{ib,w}\; t_{cross}}|. \tag{17.196}$$

Both quantities are then checked against tolerance values.

17.5 Heatexchange

The `Heatexchange` unit implements coupling among the different components (Ion, Electron, Radiation) as a simple relaxation law.

$$\frac{\partial \rho E_{Ele}}{\partial t} = \kappa_{i,e}(T_{Ion} - T_{Ele}) + \kappa_{e,r}(T_{Rad} - T_{Ele}) \tag{17.197}$$

$$\frac{\partial E_{Rad}}{\partial t} = -\kappa_{e,r}(T_{Rad} - T_{Ele}) \tag{17.198}$$

$$\frac{\partial \rho E_{Ion}}{\partial t} = -\kappa_{i,e}(T_{Ion} - T_{Ele}) \tag{17.199}$$

This unit is required because FLASH operator splits the ion/electron equilibration term from the rest of the calculations. All realistic 3T HEDP simulations should include the `Heatexchange` unit since it is responsible for equilibrating the ion/electron temperatures over time. The radiation terms in (17.197) are *only* included when the legacy gray radiation diffusion unit is used. The more sophisticated multigroup radiation diffusion unit, described in Chapter 24, includes the emission and absorption internally.

There are several different implementations residing under Heatexchange unit,

- **Immediate:** Instantaneous complete equilibration.
- **Constant:** `hx_couplingConst12`, `hx_couplingConst13` and `hx_couplingConst23` can be used for setting the constant coupling terms.
- **ConstCoulomb:** Uses a constant coulomb logarithm to compute ion-electron equilibration. `hx_coulombLog` can be used to set this value.
- **Spitzer:** Uses a Spitzer ion-electron equilibration timescale.
- **LeeMore:** Uses a Spitzer-like ion-electron equilibration timescale but with the Coulomb logarithm from Lee & More 1984.

The `Constant` and `ConstCoulomb` implementations are really designed to be used for testing purposes. The `Spitzer` and `LeeMore` implementation should be used for simulations of actual HEDP experiments since it is more accurate and physically realistic. This is described in detail in Section 17.5.1 and Section 17.5.2.

hx_relTol runtime parameter affects the time step computed by Heatexchange_computeDt. Basically, if the max (abs) temperature adjustment that would be introduced in any nonzero component in any cell is less than hx_relTol, then the time step limit is relaxed. Set to a negative value to inherite the value of runtime parameter eos_tolerance.

Usage: To use any implementation of Heatexchange unit, a simulation should include the Heatexchange using an option like `-with-unit=physics/sourceTerms/Heatexchange/HeatexchangeMain/ConstCoulomb` on the setup line, or add
`REQUIRES physics/sourceTerms/Heatexchange/HeatexchangeMain/ConstCoulomb` in the Config file. The same process can be repeated for other implementations.Constant implementation is
set as the default.

17.5.1 Spitzer Heat Exchange

The `Spitzer` implementation described here and `LeeMore` implementation described later in Section 17.5.2 should be used to model ion-electron equilibration in realistic HEDP simulations. See Section 30.7.5 for an example of how to use the `Spizter Heatexchange` implementation in an HEDP simulation. Note, that this implementation only models ion-electron equilibration, and does not include any radiation related physics. In that sense it is designed to be used in conjunction with the multigroup radiation unit described in diffusion

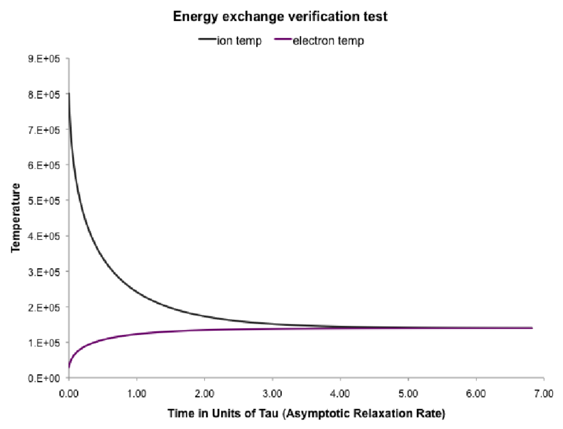

Figure 17.16: .Verication test for heat exchange code units, showing electrons and ions at different temperatures coming into mutual equilibrium, as expected from the form of the electron-ion coupling. The time axis unit is equal to the asymptotic value of the exponential decay time.

Chapter 24, since this unit includes the emission and absorption terms internally. Thus the equations solved by the `Spitzer` implementation are:

$$\frac{de_{\text{ion}}}{dt} = \frac{c_{v,\text{ele}}}{\tau_{ei}}(T_{\text{ele}} - T_{\text{ion}}) \tag{17.200a}$$

$$\frac{de_{\text{ele}}}{dt} = \frac{c_{v,\text{ele}}}{\tau_{ei}}(T_{\text{ion}} - T_{\text{ele}}) \tag{17.200b}$$

where:

- T_{ele} is the electron temperature
- T_{ion} is the ion temperature
- e_{ele} is the electron specific internal energy
- e_{ion} is the ion specific internal energy
- $c_{v,\text{ele}}$ is the electron specific internal energy
- τ_{ei} is the ion/electron equilibration time

We then replace de with $c_v dT$ for the ions and electrons to obtain:

$$\frac{dT_{\text{ion}}}{dt} = \frac{m}{\tau_{ei}}(T_{\text{ele}} - T_{\text{ion}}) \tag{17.201a}$$

$$\frac{dT_{\text{ele}}}{dt} = \frac{1}{\tau_{ei}}(T_{\text{ion}} - T_{\text{ele}}) \tag{17.201b}$$

where $m = c_{v,\text{ele}}/c_{v,\text{ion}}$ is the ratio of specific heats. (17.201) can be solved by assuming that the specific heats and ion/electron equilibration times are constant over a time step, Δt. The result is that the ion/electron temperatures equilibrate exponentially over a time step. This is shown in (17.202).

$$T_{\text{ion}}^{n+1} = \left(\frac{T_{\text{ion}}^n + mT_{\text{ele}}^n}{1+m}\right) - m\left(\frac{T_{\text{ele}}^n - T_{\text{ion}}^n}{1+m}\right)\exp\left[-(1+m)\frac{\Delta t}{\tau_{ei}}\right] \tag{17.202a}$$

$$T_{\text{ele}}^{n+1} = \left(\frac{T_{\text{ion}}^n + mT_{\text{ele}}^n}{1+m}\right) + \left(\frac{T_{\text{ele}}^n - T_{\text{ion}}^n}{1+m}\right)\exp\left[-(1+m)\frac{\Delta t}{\tau_{ei}}\right] \tag{17.202b}$$

The `Spitzer` implementation does not directly update the temperatures, however, since this would lead to energy conservation errors. Rather, the specific internal energies are directly updated according to:

$$e_{\text{ele}}^{n+1} = e_{\text{ele}}^{n} + c_{v,\text{ele}}^{n}(T_{\text{ele}}^{n+1} - T_{\text{ele}}^{n}) \tag{17.203a}$$

$$e_{\text{ion}}^{n+1} = e_{\text{ion}}^{n} + c_{v,\text{ion}}^{n}(T_{\text{ion}}^{n+1} - T_{\text{ion}}^{n}) \tag{17.203b}$$

The final temperatures are then computed using a call to the equation of state.

The subroutine `hx_ieEquilTime` is responsible for computing the ion/electron equilibration time, τ_{ei}. Currently, the formula used is consistent with that given in (Atzeni, 2004) and the NRL Plasma Formulary (Huba, 2011). The value of τ_{ei} is shown in (17.204).

$$\tau_{ei} = \frac{3k_B^{3/2}}{8\sqrt{2\pi}e^4}\frac{(m_{\text{ion}}T_{\text{ele}} + m_{\text{ele}}T_{\text{ion}})^{3/2}}{(m_{\text{ele}}m_{\text{ion}})^{1/2}\,\bar{z}^2 n_{\text{ion}}\ln\Lambda_{ei}}. \tag{17.204}$$

where:

- k_B is the Boltzmann constant
- e is the electron charge
- m_{ion} is the average mass of an ion
- m_{ele} is the mass of an electron
- $\bar{z}$ is the average ionization as computed by the EOS
- n_{ion} is the ion number density in the plasma
- $\ln\Lambda_{ei}$ is the Coulomb Logarithm associated with ion/electron collision, further description below.

The Coulomb logarithm is the logarithmic ratio of the maximum impactor parameter, $b_{\max}$, to minimum impact parameter, $b_{\min}$, for ion-electron collisions, i.e.,

$$\ln\Lambda_{ei} = \ln\left[\frac{b_{\max}}{b_{\min}}\right] \tag{17.205}$$

In general, the scales of $b_{\min}$ and $b_{\max}$ should be well separated and therefore the Coulomb logarithm should always be a dimensionless, positive number with a value of a few or greater. The expressions for $b_{\max}$ and $b_{\min}$ used in the `Spitzer` heat exchange are given by (Brysk, 1974),

$$b_{\max} = \frac{k_B T_{\text{ele}}}{4\pi e^2 n_{\text{ele}}} \tag{17.206}$$

and

$$b_{\min} = \max\left(\frac{\bar{z}e^2}{3k_B T_{\text{ele}}}\,,\,\frac{\hbar}{2\sqrt{3k_B T_{\text{ele}} m_{\text{ele}}}}\right). \tag{17.207}$$

where n_{ele} is the electron number density and $\hbar$ is Planck's constant.

Note that in HED plasmas, there are situations where $b_{\max} \sim b_{\min}$ and the Coulomb logarithm given by the above expressions can become very small or negative. To avoid this, the Coulomb logarithm used in the `Spitzer` heat exchange is hard coded to be greater or equal to the value of 1.0 (as in Brysk, 1974).

Finally, note that the runtime parameter `hx_ieTimeCoef` multiplies τ_{ei} and can be used to scale τ_{ei}.

17.5.2 LeeMore Heat Exchange

The `LeeMore` heat exchange uses (17.204), but with a different expression for the Coulomb logarithm, $\ln\Lambda_{ei}$. The expression for $\ln\Lambda_{ei}$ comes from Sec. III.B. of Lee & More 1984,

$$\ln\Lambda_{ei} = \frac{1}{2}\ln\left[1 + \left(\frac{b_{\max}}{b_{\min}}\right)^2\right] \tag{17.208}$$

where b_{max} is equal to the Debeye-Huckel screening length, $\lambda_{\rm DH}$, in an expression that includes the ion temperature and mean ionization state,

$$\frac{1}{\lambda^2_{\rm D\mathit{H}}} = \frac{4\pi n_{\rm ele} e^2}{kT_{\rm ele}} + \frac{4\pi n_{\rm ion}(e\bar{z})^2}{kT_{\rm ion}} \tag{17.209}$$

and $b_{\rm m\mathit{in}}$ is the same as used in the `Spitzer` heat exchange model, i.e. (17.207).

Like the `Spitzer` heat exchange model, the Coulomb logarithm in the `LeeMore` heat exchange is hard coded to be greater or equal to some positive value. Lee & More 1984 cite numerical results that conclude that the floor on the Columb logarithm should be 2.0 (instead of 1.0 as in the `Spitzer` heat exchange model).

It should be reiterated that the `LeeMore` heat exchange model just described only differs from the `Spitzer` heat exchange in the calculation of the Coulomb logarithm. The expression in Lee & More 1984 for the electron relaxation time (their Eq. 24) also contains fermi-dirac factors that we neglect here for simplicity. These factors may be incorporated into the `LeeMore` heat exchange model at a later date. Regardless, the `LeeMore` heat exchange module should be more accurate than the `Spitzer` heat exchange because of the improvement to the Coulomb logarithm.

17.6 Flame

The `Flame` unit implements an artificial reaction front model based on a simplified single-variable reaction-diffusion model. This is intended to be used to model the behavior of under-resolved reaction fronts propagated spatially by thermal diffusion, commonly called flames or deflagration fronts. As the reaction-diffusion front is also carried with the fluid, this model is sometimes termed an advection-diffusion-reaction (ADR) model. The principal usage to date of this model has been during the deflagration phase of models of Type Ia Supernovae. See Townsley et al. (2007), from which some text in this section has been adapted, and works that reference it for examples.

17.6.1 Reaction-Diffusion Forms

Generally, an ADR scheme characterizes the location of a flame front using a reaction progress variable, ϕ, which increases monotonically across the front from 0 (fuel) to 1 (ash). Evolution of this progress variable is accomplished via an advection-diffusion-reaction equation of the form

$$\frac{\partial\phi}{\partial t} + \vec{v}\cdot\nabla\phi = \kappa\nabla^2\phi + \frac{1}{\tau}R(\phi) \ , \tag{17.210}$$

where $\vec{v}$ is the local fluid velocity, and the reaction term, $R(\phi)$, timescale, τ, and the diffusion constant, κ, are chosen so that the front propagates at the desired speed. Vladimirova et al. (2006) showed that the step-function reaction rate leads to a substantial amount of unwanted acoustic noise. They studied a suitable alternative, the Kolmogorov Petrovski Piskunov (KPP) reaction term which has an extensive history in the study of reaction-diffusion equations. In the KPP model the reaction term is given by

$$R(\phi) = \frac{1}{4}\phi(1-\phi) \ . \tag{17.211}$$

The symmetric and low-order character of this function gives it very nice numerical properties, leading to amazingly little acoustic noise. Following Vladimirova et al. (2006), we adopt $\kappa \equiv sb\Delta x/16$ and $\tau \equiv b\Delta x/16s$, where Δx is the grid spacing, s is the desired propagation speed, and b sets the desired front width scaled to represent approximately the number of zones.

The KPP reaction term, however, has two serious drawbacks. Formally, the flame speed is only single valued for initial conditions that are precisely zero (and stay that way) outside the burned region (Xin 2000), which cannot really be effected in a hydrodynamics simulation. This can lead to an unbounded increase of the propagation speed, which is precisely the property we wish to have under good control. Secondly, the progress variable ϕ takes an infinite amount of time to actually reach 1 (complete consumption of fuel). While not a fatal flaw like the flame speed problem, this is a problem for our simulations in which we would like to have a localized flame front so that fully-burned ash can be treated as pure NSE material.

Both of these drawbacks can be ameliorated by a slight modification of the reaction term (S. Asida, private communication) to

$$R(\phi) = \frac{f}{4}(\phi - \epsilon_0)(1 - \phi + \epsilon_1) \ , \tag{17.212}$$

where $0 < \epsilon_0, \epsilon_1 \ll 1$ and f is an additional factor that depends on ϵ_0 and ϵ_1 and the flame width so that the flame speed is preserved with the same constants as for KPP above. This "sharpened" KPP (sKPP) has truncated tails in both directions (thus being sharpened), making the flame front fully localized, and is a bi-stable reaction rate and thus gives a unique flame speed (Xin 2000). The price paid is that since $R(\phi) = 0$ for $\phi \le 0$ and $\phi \ge 1$, (17.212) is discontinuous, adding some noise to the solution. Since the suppression of the tails is stronger for higher ϵ_0 and ϵ_1, we adjusted ϵ_0 and ϵ_1 so that for a particular flame width we could meet noise goals (Townsley et al. 2007). The parameter the default parameter values obtained are $\epsilon_0 = \epsilon_1 = 10^{-3}$, $f = 1.309$, and $b = 3.2$. The noise properties of these choices are discussed in Townsley et al. (2007).

Diffusive flames are known to be subject to a curvature effect that affects the flame speed when the radius of curvature is similar to the flame thickness, a frequent circumstance with modestly-resolved flame front structure. In testing, the curvature effect of the step-function reaction rate proved surprisingly strong, likely due to the exponential "nose" that the flame front possesses (Vladimirova et al. 2006). Both KPP and sKPP show significantly better curvature properties.

17.6.2 Unit Structure

The unit is divided into several subunits to allow flexibility in how the propagation speed is determined and how the enery release of the reaction front takes place. The main subunit `FlameMain` just implements the actual the reaction and diffusion terms defined above. There is currently only one implementation, `RDSplit5point`, that uses operator-split steps for the reaction and diffusion, and a 5 point stencil for the Laplacian operator.

The order of operations occurs as follows, for each block of the mesh in sequence: The progress variable, ϕ, stored in `FLAM_MSCALAR` is extracted, the Unit-internal function `fl_flameSpeed()` is called to fill a temporary array with the flame speed evaluated for each cell in the current block. The mesh scalar `FLAM_MSCALAR` is then updated based on this flame speed while saving temporarily the effective $\dot{\phi}$ for this time step. This information is then passed on to the internal function `fl_effects()` which performs any energy release or other desired side effects of the propagation of the RD front. Note both the temporary arrays storing the flame speed and the $\dot{\phi}$ for the current block are destroyed before processing the next block. However some implementations of `fl_flameSpeed()` may save this information in the main grid arrays for informational or other purposes.

17.6.2.1 Flame Speed

The flame speed is generally determined by various physical quantities on the grid. However, since the flame is generally an artificial reaction front, many aspects other than the composition may influence the speed. The simplest alternative implementation for determining the flame speed, which is the default one, is `Flame/FlameSpeed/Constant`. This simply sets a constant flame speed everywhere on the grid.

The flame speed can also include a turbulence-flame interaction (TFI). The implemented options are discussed in Jackson, Townsley, & Calder (2014, submitted). This is accomplished by including one of the implementations under, for example `Flame/FlameSpeed/Constant/TFI`. Since the TFI always modifies some base flame speed, it is generally included as a implementation of that type of flame speed, in this case a constant flame speed. In order to facilitate sharing of the TFI components, they are stored in their own implementation directories under `Flame/FlameSpeed/turbulent` and included as needed. All of the TFI options require the inclusion of the `Turb` unit which provides a measurement of the local turbulence strength.

17.6.2.2 Flame Effects

The flame effects subunit performs functions related to the actual energy deposition or changes in abundances caused by advance of the reaction front being modeled by the reaction-diffusion progress variable ϕ. The simplest implementation, included under `Flame/FlameEffects/EIP`, implements fixed energy input and change in $\bar{A}$ and $\bar{Z}$ across the reaction front. This is constructed to utilize the fully ionized electron-ion plasma EOS called the ”Helmholtz” EOS in Flash.

17.7 Turbulence Measurement

The `Turb` unit implements a method to measure the local turbulence strength at the grid scale. The implementation is based on the operator OP_2 in Colin et al. (2000),

$$v' = OP_2(\vec{v}) = c_2 \Delta_x^3 \nabla^2 (\nabla \times \vec{v}) \ . \tag{17.213}$$

Here c_2 is a calibration constant, set with the `turb_c2` runtime variable. The default value, 0.9, was determined for the PPM hydodynamics method by Jackson et al. (2014, submitted) based on simulations of stirred turbulence. Δ_x is the grid spacing and v is the velocity field on the grid. Two options are implemented for sampling the velocity field, each of which uses a 5-point stencil for the Laplacian operator. If `turb_stepSize` is set to 1, the stencil samples adjacent cells, if set to 2 every other cell is sampled, for an effective stencil size of 9 points. The latter option requeres a guardcell fill between the curl and Laplacian operators. The result of equation 17.213 is stored in the `TURB` mesh variable.

Chapter 18

Diffusive Terms

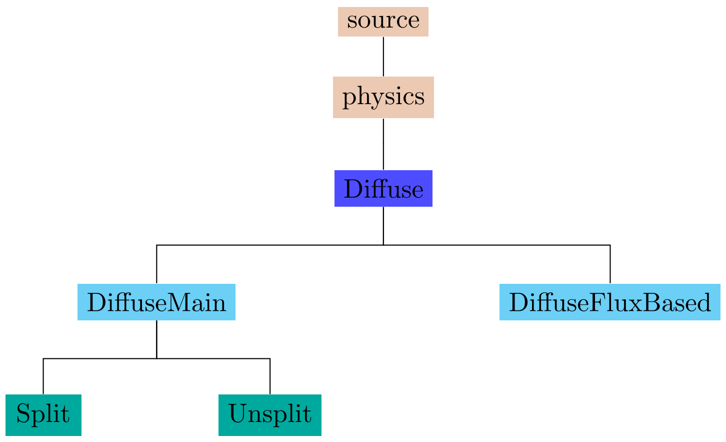

Figure 18.1: The organizational structure of the `Diffuse` unit.

The `physics/Diffuse` unit implements diffusive effects, such as heat conduction, viscosity, and mass diffusivity.

18.1 Diffuse Unit

The `Diffuse` unit contains four things:

1. Flux-Based Diffusion Solvers: These are *explicit* diffusion solvers used to compute fluxes for *specific processes*, such as thermal conduction or magnetic resistivity. These fluxes can then be added to the total fluxes in the hydrodynamic solvers (see Section 18.1.1).

2. General Implicit Diffusion Solvers: The `Diffuse` unit also contains *explicit* diffusion solvers that are *general purpose*. These subroutines can be used to implicitly solve scalar diffusion problems in FLASH (see Section 18.1.2).

3. Flux Limiters: The `Diffuse` unit contains a general purpose subroutine which modifies diffusion coefficients to incorporate a flux limiters (see Section 18.1.3).

4. Electron Thermal Conduction: The `Diffuse` unit contains code which uses the general purpose implicit diffusion solver to solve an equation which models electron thermal conduction in a 3T plasma (see Section 18.1.4)

18.1.1 Diffuse Flux-Based implementations

There are some important differences between other physics units and the flux-based `Diffuse` implementations:

- `DiffuseFluxBased` does not operate by modifying solution data arrays (like `UNK`, *etc.*) directly. `DiffuseFluxBased` modifies **flux arrays** instead.
- `DiffuseFluxBased` therefore depends on another physics unit to
  1. define and initialize the flux arrays (before `DiffuseFluxBased` calls add to them), and to
  2. apply the fluxes to actually update the solution data in `UNK`.
- `DiffuseFluxBased` calls that implement the diffusive effects are not made from `Driver_evolveFlash` as for other physics units and the `DiffuseMain` subunit. Rather, those `DiffuseFluxBased` calls need to be made from cooperating code unit that defines, initializes, and applies the flux arrays. As of FLASH4, among the provided unit implementations only the `PPM` implementation of the `Hydro` unit does this (by calls in the `hy_ppm_sweep` routine).
- The `DiffuseFluxBased` routines that implement the diffusive effects are called separately for each flux direction for each block of cells.

Other `Hydro` implementations, in particular the MHD implementations, currently implement some diffusive effects in their own flux-based way that does not use the `DiffuseFluxBased` unit.

To use `DiffuseFluxBased` routines of the `Diffuse` unit, a simulation should

- include the `Diffuse` unit using an option like `-with-unit=physics/Diffuse/DiffuseFluxBased` on the setup line, or `REQUIRES physics/Diffuse/DiffuseFluxBased` in a Config file;
- include a unit that makes `Diffuse` calls, currently the PPM implementation of `Hydro`;
- set `useXXX` runtimes parameters appropriately (see below).

The appropriate calls to `DiffuseFluxBased` routines will then be made by the following `Hydro` code (which can be found in `hy_ppm_sweep.F90`):

```
     call Diffuse_therm(sweepDir, igeom, blockList(blk), numCells,&
                        blkLimits, blkLimitsGC, primaryLeftCoord, &
                        primaryRghtCoord, tempFlx, tempAreaLeft)

     call Diffuse_visc (sweepDir, igeom, blockList(blk), numCells,&
                        blkLimits, blkLimitsGC, primaryLeftCoord,primaryRghtCoord,&
                        tempFlx, tempAreaLeft,secondCoord,thirdCoord)

!!      call Diffuse_species(sweepDir, igeom, blockList(blk), numCells,&
!!                           blkLimits, blkLimitsGC, primaryLeftCoord,primaryRghtCoord,&
!!                           tempFlx, tempFly, tempFlz)
```

To use the `Diffuse` unit for heat conduction in a simulation, the runtime parameters `useDiffuse` and `useDiffuseTherm` must be set to `.true.`; and to use the `Diffuse` unit for viscosity effects in a simulation, the runtime parameters `useDiffuse` and `useDiffuseVisc` must be set to `.true.`.

18.1.2 General Implicit Diffusion Solver

FLASH contains a general purpose implicit diffusion solver that can be used to include physics such as electron thermal conduction and multigroup diffusion. The actual code for these solvers is located in `GridSolvers`. Two implementations of these solvers exist in the `Diffuse` unit. An older and less useful version lies under the `Split` directory. A newer solver which uses the HYPRE library is contained in the `Unsplit` directory. As the name suggests, the split solver is directionally split (default: Strang) to interact with the pencil grid infrastructure of the `GridSolvers/Pfft` implementation of the `Grid` unit. The runtime parameter `useDiffuse` must be set to `.true.` to activate the general purpose implicit solver.

The typical diffusion equation that can be solved by this unit takes the form,

$$A\frac{\partial f}{\partial t} + Cf = \nabla \cdot B\nabla f + D, \tag{18.1}$$

where f is the variable to be diffused in time, and A, B, C, D are parameters with spatial variation. The infrastructure is provided for a general diffusion equation and can be customized to solve specific equations. The API function `Diffuse_solveScalar` provides a comprehensive interface to solve different types of equations.

In the unsplit solver the equation is implicitly advanced as follows,

$$A^n\frac{f^{n+1} - f^n}{\delta t} + C^n f^{n+1} = \theta(\nabla \cdot B^n\nabla f^{n+1}) + (1-\theta)(\nabla \cdot B^n\nabla f^n) + D, \tag{18.2}$$

In the split solver, the solution is advanced along each direction separately. i.e,

$$A^n\frac{f^{n+\frac{1}{3}} - f^n}{\delta t} + \frac{1}{3}C^n f^{n+\frac{1}{3}} = \theta\frac{\partial}{\partial x}(B^n\frac{\partial}{\partial x}f^{n+\frac{1}{3}}) + (1-\theta)\frac{\partial}{\partial x}(B^n\frac{\partial}{\partial x}f^n) + \frac{1}{3}D \tag{18.3}$$

$$A^n\frac{f^{n+\frac{2}{3}} - f^{n+\frac{1}{3}}}{\delta t} + \frac{1}{3}C^n f^{n+\frac{2}{3}} = \theta\frac{\partial}{\partial y}(B^n\frac{\partial}{\partial y}f^{n+\frac{2}{3}}) + (1-\theta)\frac{\partial}{\partial y}(B^n\frac{\partial}{\partial y}f^{n+\frac{1}{3}}) + \frac{1}{3}D \tag{18.4}$$

$$A^n\frac{f^{n+1} - f^{n+\frac{2}{3}}}{\delta t} + \frac{1}{3}C^n f^{n+1} = \theta\frac{\partial}{\partial z}(B^n\frac{\partial}{\partial z}f^{n+1}) + (1-\theta)\frac{\partial}{\partial z}(B^n\frac{\partial}{\partial z}f^{n+\frac{2}{3}}) + \frac{1}{3}D \tag{18.5}$$

θ	Scheme
0.0	Explicit
0.5	Crank Nicholson
1.0	Backward Euler

Implicitness: It should be noted that the parameters A, B, C are time lagged and evaluated at t^n. Whereas keeping with the spirit of the implicit scheme these should have been evaluated at t^{n+1}. Evaluating them at t^{n+1} makes the problem non-linear for non-constant values of A, B and C. These equations are much more complicated to solve. Although time lagged coefficient essentially linearized the non-linear problem, the trade off is the scheme is no longer completely implicit. The scheme is fully implicit only in the constant case. This could possibly impact the overall stability characteristics of the scheme.

The Laplacian term is discretized using a central difference scheme as follows,

$$\begin{aligned}\nabla \cdot B\nabla f \quad &= \frac{B_{i+\frac{1}{2},j,k}(f_{i+1,j,k}-f_{i,j,k}) - B_{i-\frac{1}{2},j,k}(f_{i,j,k}-f_{i-1,j,k})}{\delta x^2} \\ &+ \frac{B_{i,j+\frac{1}{2},k}(f_{i,j+1,k}-f_{i,j,k}) - B_{i,j-\frac{1}{2},k}(f_{i,j,k}-f_{i,j-1,k})}{\delta y^2} \\ &+ \frac{B_{i,j,k+\frac{1}{2}}(f_{i,j,k+1}-f_{i,j,k}) - B_{i,j,k-\frac{1}{2}}(f_{i,j,k}-f_{i,j,k-1})}{\delta z^2}\end{aligned} \tag{18.6}$$

Where, f and B are cell centered variables, and

$$B_{i+\frac{1}{2},j,k} = \frac{B_{i+1,j,k} + B_{i,j,k}}{2}, \tag{18.7}$$

$$B_{i+\frac{1}{2},j,k} = \frac{B_{i-1,j,k} + B_{i,j,k}}{2}, \tag{18.8}$$

$$B_{i,j+\frac{1}{2},k} = \frac{B_{i,j+1,k} + B_{i,j,k}}{2}, \tag{18.9}$$

$$B_{i,j-\frac{1}{2},k} = \frac{B_{i,j-1,k} + B_{i,j,k}}{2}, \tag{18.10}$$

$$B_{i,j,k+\frac{1}{2}} = \frac{B_{i,j,k+1} + B_{i,j,k}}{2}, \tag{18.11}$$

$$B_{i,j,k-\frac{1}{2}} = \frac{B_{i,j,k-1} + B_{i,j,k}}{2} \tag{18.12}$$

Paramesh: In coming up with a numerical scheme in AMR, it is important to ensure that fluxes are conserved at fine-coarse boundary. This is typically done in FLASH using `Grid_consvervefluxes` routine. However this is an option which is not available to the implicit solver. Since it uses HYPRE to solve the linear system, the flux conversation should be embedded in the system being solved by HYPRE.

Looking at standard diffusion equation mentioned earlier, for simplicity we set $C = D = 0$.

So,

$$A\frac{\partial f}{\partial t} = \nabla \cdot B\nabla f, \tag{18.13}$$

We introduce a new variable $\vec{F}$ defined as,

$$\vec{F} = B\nabla f, \text{and} \tag{18.14}$$

$$A\frac{\partial f}{\partial t} = \nabla \cdot \vec{F}, \tag{18.15}$$

We discretize the equation as follows,

$$A^n \frac{f^{n+1} - f^n}{\delta t} \partial v = \theta(\vec{F}^{n+1} \cdot \partial\vec{s}) + (1-\theta)(\vec{F}^n \cdot \partial\vec{s}) \tag{18.16}$$

$$\tag{18.17}$$

The idea is then to compute $\vec{F} \cdot \partial\vec{s}$ on the fine coarse boundary so as to conserve flux.In a 1D problem the $\vec{F} \cdot \partial\vec{s}$ on a fine-coarse boundary is computed as,

$$(F^L)_{i+\frac{1}{2}} = (F^R)_{i+\frac{1}{2}} = B_{i+\frac{1}{2}} \frac{f_{i+1} - f_i}{\frac{\delta x_{i+1} + \delta x_i}{2}} \tag{18.18}$$

$$(F^L)_{i-\frac{1}{2}} = (F^R)_{i-\frac{1}{2}} = B_{i-\frac{1}{2}} \frac{f_i - f_{i-1}}{\frac{\delta x_{i-1} + \delta x_i}{2}} \tag{18.19}$$

$$\tag{18.20}$$

The idea is similarly extended to 2D where coarse cell flux is set to sum of computed fine cell fluxes of its neighbors.

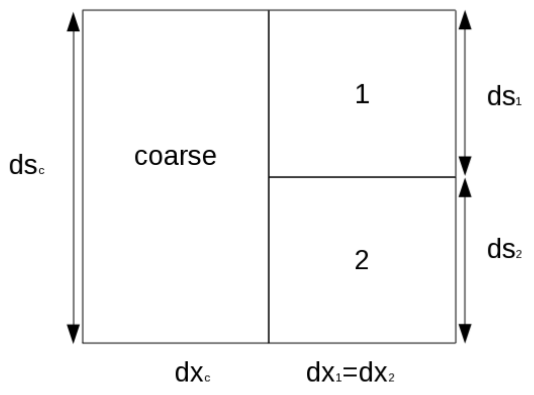

$$F_c ds_c = F_1 ds_1 + F_2 ds_2 \tag{18.21}$$

Table 18.2: General Implicit Diffusion Solver Boundary Conditions

Name	**Integer**	**Effect**
Neumann	`GRID_PDE_BND_NEUMANN`	$\nabla f \cdot \boldsymbol{n} = 0$
Dirichlet	`GRID_PDE_BND_DIRICHLET`	$f = c$
Vacuum	`VACUUM`	something like $\frac{1}{2}f + \frac{1}{4}\nabla f \cdot \boldsymbol{n} = 0$
Outstream	`OUTSTREAM`	free streaming radiation at outer boundary (1D spherical only)

Where,

$$F_1 = B_{face}\frac{f_1 - f_c}{\frac{\delta x_1 + \delta x_c}{2}} \tag{18.22}$$

$$F_2 = B_{face}\frac{f_2 - f_c}{\frac{\delta x_2 + \delta x_c}{2}} \tag{18.23}$$

The value of B_{face} can then be evaluated from surrounding cells using paramesh interpolation.

Usage: To use the "Split" implementation of the `Diffuse` unit, a simulation should include the `Diffuse` unit using an option like `-with-unit=source/physics/Diffuse/DiffuseMain/Split` on the setup line, or add `REQUIRES physics/Diffuse/DiffuseMain/Split` in the `Config` file. To get the "Unsplit" implementation, replace `Split` with `Unsplit`. Split and Unsplit solver are mutually exclusive implementations and cannot exist in the same simulation.

Table 18.1: comparison of capabilities of Split and Unsplit diffusion.

Capability	Split	Unsplit
Paramesh	no	yes
Uniform grid	yes	yes
Cartesian 1D, 2D	yes	yes
Cartesian 3D	yes	yes
Cylindrical 1D	yes	yes
Cylindrical 2D (R-Z)	yes	yes
Spherical 1D	yes	yes

18.1.2.1 Boundary Conditions

Unlike much of the rest of FLASH, the general purpose implicit diffusion solver does not implement boundary conditions explicitly through guard cell fills. Instead the diffusion matrix is modified to directly include boundary conditions. The `bcTypes` and `bcValues` arguments to `Diffuse_solveScalar` are used to indicate the boundary condition to use. Each of these arguments is an array of length six corresponding to the six faces of the domain: `imin`, `imax`, `jmin`, `imax`, `kmin`, `kmax` in that order. The `bcTypes` argument is used to set the type of boundary condition to use. Several integer values are acceptable that are defined in the "constants.h" header file. The allowed integer values and the mathematical effect are shown in Table 18.2. When a Dirichlet (constant value) boundary conditions is required, `bcTypes` stores the value to use.

18.1.3 Flux Limiters

The `Diffuse` unit contains the subroutine `Diffuse_fluxLimiter` which modifies a mesh variable representing a diffusion coefficient over the entire mesh to include a flux-limit. The subroutine modifies the

Table 18.3: String and Integer Representations of Flux-Limiter Modes

Mode	Integer Constant	String Representation
None	`FL_NONE`	“fl_none”
Harmonic	`FL_HARMONIC`	“fl_harmonic”
Min/Max	`FL_MINMAX`	“fl_minmax”
Larsen	`FL_LARSEN`	“fl_larsen”
Levermore-Pomraning	`FL_LEVPOM`	“fl_levermorepomraning1981”

diffusion coefficient to smoothly transition to some maximum flux, $q_{\max}$. The subroutine takes the following arguments:

```
subroutine Diffuse_fluxLimiter(idcoef, ifunc, ifl, mode, blkcnt, blklst)
```

where:

- `idcoef` [integer,input] Mesh variable representing the diffusion coefficient (e.g. `COND_VAR` for electron thermal conduction)
- `ifunc` [integer,input] Mesh variable representing the function being diffused (e.g. `TELE_VAR` for thermal conduction)
- `ifl` [integer,input] Mesh variable representing the flux limit (e.g. `FLLM_VAR` for electron thermal conduction)
- `mode` [integer,input] The type of flux-limiter to apply
- `blkcnt` [integer,input] Number of blocks
- `blklst` [integer array, input] List of blocks

The subroutine modifies the mesh variable whose index is given by `idcoef` by applying a flux-limit. Many methods of incorporating flux-limits into the diffusion coefficient exist. `Diffuse_fluxLimiter` currently supports three of these: “harmonic”, “min/max”, “Larsen”, and “none”. The `mode` argument selects the specific method to use. The modes are integers defined in the “constants.h” header file. String representations also exist and can be converted to the integer values using the `RuntimeParameters_mapStrToInt` subroutine. The string representations can be used to create runtime parameters which represent a flux-limiter mode. Table 18.3 shows the integer constants used as arguments for `Diffuse_fluxLimiter` as well as the string representations of these constants.

Each flux limiter mode modifies the existing diffusion coefficient to incorporate the flux limiter in a different way. If D is the original diffusion coefficient and D_{fl} is the flux-limited diffusion coefficient then:

- the “none” flux limiter sets:
$$D_{fl} = D \tag{18.24}$$
- the “harmonic” flux limiter sets:
$$D_{fl} = \frac{1}{\frac{1}{D} + \frac{|\nabla f|}{q_{\max}}} \tag{18.25}$$
- the “Larsen” flux limiter sets:
$$D_{fl} = \frac{1}{\left[\left(\frac{1}{D}\right)^2 + \left(\frac{|\nabla f|}{q_{\max}}\right)^2\right]^{1/2}} \tag{18.26}$$
- the “min/max” flux limiter sets:
$$D_{fl} = \min\left(D, \frac{q_{\max}}{|\nabla f|}\right) \tag{18.27}$$

where f is the value of the function being diffused. The gradient of f is computed using a second order central difference.

18.1.4 Stand-Alone Electron Thermal Conduction

The `Diffuse` unit also contains a subroutine which solves the diffusion equation for the case of electron thermal conduction. This code is in the `diff_advanceTherm` subroutine that is called by `Diffuse`. The diffusion equation has the form:

$$\rho c_{v,\mathrm{ele}} \frac{\partial T_{\mathrm{ele}}}{\partial t} = \nabla \cdot K_{\mathrm{ele}} \nabla T_{\mathrm{ele}} \tag{18.28}$$

where ρ is the mass density, $c_{v,\mathrm{ele}}$ is the electron specific heat, and K_{ele} is the electron thermal conductivity. The conductivity is computed by the `Conductivity` unit (see Section 22.1 for more information). This equation is solved implicitly over a time step to avoid overly restricted time step constraints. In many cases a flux-limiter is needed in situations where overly large temperature gradients are present. The flux-limit used for electron thermal conduction, $q_{\max,\mathrm{ele}}$, is defined as:

$$q_{\max,\mathrm{ele}} = \alpha_{\mathrm{ele}} n_{\mathrm{ele}} k_B T_{\mathrm{ele}} \sqrt{\frac{k_B T_{\mathrm{ele}}}{m_{\mathrm{ele}}}} \tag{18.29}$$

where:

- α_{ele} is the electron conductivity flux-limiter coefficient
- n_{ele} is the electron number density
- k_B is the Boltzmann constant
- m_{ele} is the electron mass

The `Diffuse_solveScalar` subroutine is used for the implicit solve. The use of the electron thermal conduction solver is demonstrated in several simulations. See Section 30.8.1 and Section 30.7.5 for examples. For electron thermal conduction to function, the `useConductivity` and `useDiffuse` runtime parameters must be set to `.true.`. The following runtime parameters control the behavior of the electron thermal conduction package:

- `diff_useEleCond`: Set to `.true.` to activate electron thermal conduction
- `diff_eleFlMode`: String indicating which flux-limiter mode to use for electron conduction. Valid values are described in Section 18.1.3.
- `diff_eleFlCoef`: Sets the value of α_{ele}
- `diff_thetaImplct`: A number between 0 and 1. When set to 0, an explicit treatment is used for the diffusion solve. When set to 1, a fully implicit solve is used.

The runtime parameters:

```
diff_eleXlBoundaryType
diff_eleXrBoundaryType
diff_eleYlBoundaryType
diff_eleYrBoundaryType
diff_eleZlBoundaryType
diff_eleZrBoundaryType
```

are strings which are used to set the boundary conditions for electron conduction on each of the six faces of the domain. Acceptable values are:

- "DIRICHLET", "Dirichlet", or "dirichlet" to indicate a Dirichlet boundary condition where T_{ele} is set to zero on the boundary
- "OUTFLOW", "neumann", "zero-gradient", "outflow" to indicate a Neumann boundary condition

Chapter 19

Gravity Unit

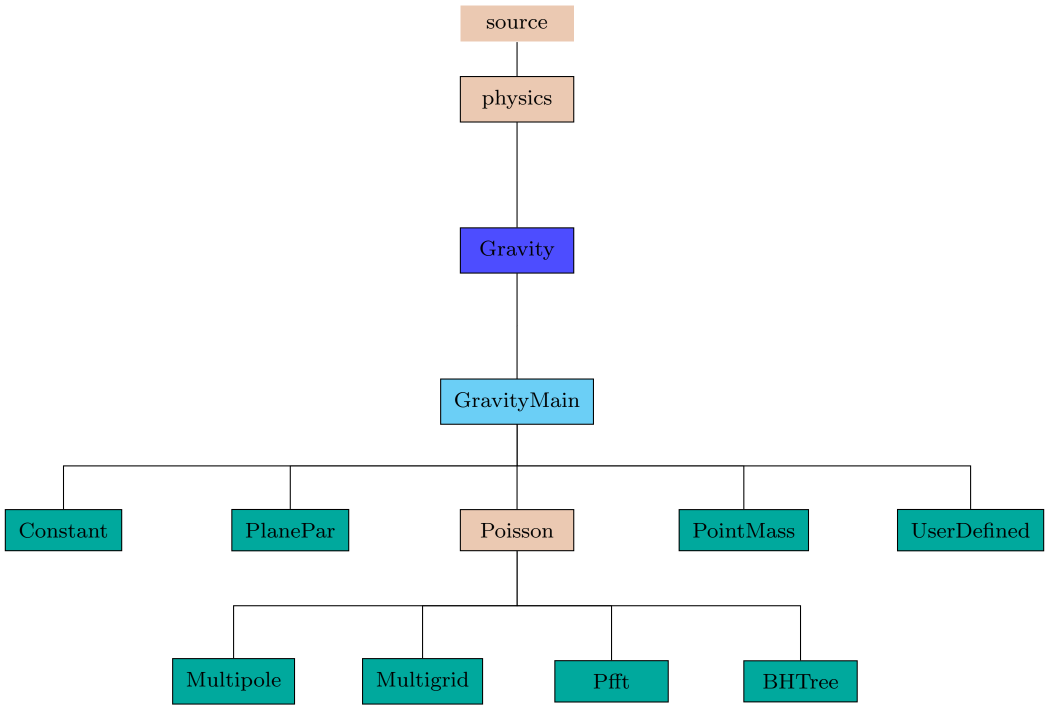

Figure 19.1: The `Gravity` unit directory tree.

19.1 Introduction

The `Gravity` unit supplied with FLASH4 computes gravitational source terms for the code. These source terms can take the form of the gravitational potential $\phi(\mathbf{x})$ or the gravitational acceleration $\mathbf{g}(\mathbf{x})$,

$$\mathbf{g}(\mathbf{x}) = -\nabla\phi(\mathbf{x}) \ . \tag{19.1}$$

The gravitational field can be externally imposed or self-consistently computed from the gas density via the Poisson equation,

$$\nabla^2\phi(\mathbf{x}) = 4\pi G\rho(\mathbf{x}) \ , \tag{19.2}$$

where G is Newton's gravitational constant. In the latter case, either periodic or isolated boundary conditions can be applied.

19.2 Externally Applied Fields

The FLASH distribution includes three externally applied gravitational fields, along with a placeholder module for you to create your own. Each provides the acceleration vector $\mathbf{g}(\mathbf{x})$ directly, without using the gravitational potential $\phi(\mathbf{x})$ (with the exception of `UserDefined`, see below).

When building an application that uses an external, time-independent `Gravity` implementation, no additional storage in `unk` for holding gravitational potential or accelerations is needed or defined.

19.2.1 Constant Gravitational Field

This implementation creates a spatially and temporally constant field parallel to one of the coordinate axes. The magnitude and direction of the field can be set at runtime. This unit is called `Gravity/GravityMain/-Constant`.

19.2.2 Plane-parallel Gravitational field

This `PlanePar` version implements a time-constant gravitational field that is parallel to one of the coordinate axes and falls off with the square of the distance from a fixed location. The field is assumed to be generated by a point mass or by a spherically symmetric mass distribution. A finite softening length may optionally be applied.

This type of gravitational field is useful when the computational domain is large enough in the direction radial to the field source that the field is not approximately constant, but the domain's dimension perpendicular to the radial direction is small compared to the distance to the source. In this case the angular variation of the field direction may be ignored. The `PlanePar` field is cheaper to compute than the `PointMass` field described below, since no fractional powers of the distance are required. The acceleration vector is parallel to one of the coordinate axes, and its magnitude drops off with distance along that axis as the inverse distance squared. Its magnitude and direction are independent of the other two coordinates.

19.2.3 Gravitational Field of a Point Mass

This `PointMass` implementation describes the gravitational field due to a point mass at a fixed location. A finite softening length may optionally be applied. The acceleration falls off with the square of the distance from a given point. The acceleration vector is everywhere directed toward this point.

19.2.4 User-Defined Gravitational Field

The `UserDefined` implementation is a placeholder module for the user to create their own external gravitational field. All of the subroutines in this module are stubs, and the user may copy these stubs to their setup directory to write their own implementation, either by specifying the gravitational acceleration directly or by specifying the gravitational potential and taking its gradient. If your user-defined gravitational field is time-varying, you may also want to set `PPDEFINE FLASH_GRAVITY_TIMEDEP` in your setup's Config file.

19.3 Self-gravity

The self-consistent gravity algorithm supplied with FLASH computes the Newtonian gravitational field produced by the matter. The produced potential function satisfies Poisson's equation (19.2). This unit's implementation can also return the acceleration field $\mathbf{g}(\mathbf{x})$ computed by finite-differencing the potential using the expressions

$$
\begin{aligned}
g_{x;ijk} &= \frac{1}{2\Delta x}\left(\phi_{i-1,j,k} - \phi_{i+1,j,k}\right) + \mathcal{O}(\Delta x^2) \\
g_{y;ijk} &= \frac{1}{2\Delta y}\left(\phi_{i,j-1,k} - \phi_{i,j+1,k}\right) + \mathcal{O}(\Delta y^2) \\
g_{z;ijk} &= \frac{1}{2\Delta z}\left(\phi_{i,j,k-1} - \phi_{i,j,k+1}\right) + \mathcal{O}(\Delta z^2)\ .
\end{aligned}
\tag{19.3}
$$

In order to preserve the second-order accuracy of these expressions at jumps in grid refinement, it is important to use quadratic interpolants when filling guard cells at such locations. Otherwise, the truncation error of the interpolants will produce unphysical forces at these block boundaries.

Two algorithms are available for solving the Poisson equations: `Gravity/GravityMain/Multipole` and `Gravity/GravityMain/Multigrid`. The initialization routines for these algorithms are contained in the `Gravity` unit, but the actual implementations are contained below the `Grid` unit due to code architecture constraints.

The multipole-based solver described in Section 8.10.2.1 for self gravity is appropriate for spherical or nearly-spherical mass distributions with isolated boundary conditions. For non-spherical mass distributions higher order moments of the solver must be used. Note that storage and CPU costs scale roughly as the square of number of moments used, so it is best to use this solver only for nearly spherical matter distributions.

The multigrid solver described in Section 8.10.2.6 is appropriate for general mass distributions and can solve problems with more general boundary conditions.

The tree solver described in 8.10.2.4 is appropriate for general mass distributions and can solve problems with both isolated and periodic boundary conditions set independently in individual directions.

19.3.1 Coupling Gravity with Hydrodynamics

The gravitational field couples to the Euler equations only through the momentum and energy equations. If we define the total energy density as

$$\rho E \equiv \frac{1}{2}\rho v^2 + \rho\epsilon \ , \tag{19.4}$$

where ϵ is the specific internal energy, then the gravitational source terms for the momentum and energy equations are $\rho\mathbf{g}$ and $\rho\mathbf{v}\cdot\mathbf{g}$, respectively. Because of the variety of ways in which different hydrodynamics schemes treat these source terms, the gravity module only supplies the potential ϕ and acceleration $\mathbf{g}$, leaving the implementation of the fluid coupling to the hydrodynamics module. Finite-difference and finite-volume hydrodynamic schemes apply the source terms in their advection steps, sometimes at multiple intermediate timesteps and sometimes using staggered meshes for vector quantities like $\mathbf{v}$ and $\mathbf{g}$.

For example, the PPM algorithm supplied with FLASH uses the following update steps to obtain the momentum and energy in cell i at timestep $n+1$

$$\begin{aligned} (\rho v)_i^{n+1} &= (\rho v)_i^n + \tfrac{\Delta t}{2} g_i^{n+1}\left(\rho_i^n + \rho_i^{n+1}\right) \\ (\rho E)_i^{n+1} &= (\rho E)_i^n + \tfrac{\Delta t}{4} g_i^{n+1}\left(\rho_i^n + \rho_i^{n+1}\right)\left(v_i^n + v_i^{n+1}\right) \ . \end{aligned} \tag{19.5}$$

Here g_i^{n+1} is obtained by extrapolation from ϕ_i^{n-1} and ϕ_i^n. The `Poisson` gravity implementation supplies a mesh variable to contain the potential from the previous timestep; future releases of FLASH may permit the storage of several time levels of this quantity for hydrodynamics algorithms that require more steps. Currently, $\mathbf{g}$ is computed at cell centers.

Note that finite-volume schemes do not retain explicit conservation of momentum and energy when gravity source terms are added. Godunov schemes such as PPM, require an additional step in order to preserve second-order time accuracy. The gravitational acceleration component g_i is fitted by interpolants along with the other state variables, and these interpolants are used to construct characteristic-averaged values of $\mathbf{g}$ in each cell. The velocity states $v_{L,i+1/2}$ and $v_{R,i+1/2}$, which are used as inputs to the Riemann problem solver, are then corrected to account for the acceleration using the following expressions

$$\begin{aligned} v_{L,i+1/2} &\rightarrow v_{L,i+1/2} + \frac{\Delta t}{4}\left(g^+_{L,i+1/2} + g^-_{L,i+1/2}\right) \\ v_{R,i+1/2} &\rightarrow v_{R,i+1/2} + \frac{\Delta t}{4}\left(g^+_{R,i+1/2} + g^-_{R,i+1/2}\right) \ . \end{aligned} \tag{19.6}$$

Here $g^{\pm}_{X,i+1/2}$ is the acceleration averaged using the interpolant on the X side of the interface $(X = L, R)$ for $v \pm c$ characteristics, which bring material to the interface between cells i and $i+1$ during the timestep.

19.3.2 Tree Gravity

The `Tree` implementation of the gravity unit in `physics/Gravity/GravityMain/Poisson/BHTree` is meant to be used together with the tree solver implementation `Grid/GridSolvers/BHTree/Wunsch`. It either calculates the gravitational potential field which is subsequently differentiated in subroutine `Gravity_accelOneRow` to obtain the gravitational acceleration, or it calculates the gravitational acceleration directly. The latter approach is more accurate, because the error due to numerical differentiation is avoided, however, it consumes more memory for storing three components of the gravitational acceleration. The direct acceleration calculation can be switched on by specifying `bhtreeAcc=1` as a command line argument of the setup script.

The gravity unit provides subroutines for building and walking the tree called by the tree solver. In this version, only monopole moments (node masses) are used for the potential/acceleration calculation. It also defines new multipole acceptance criteria (MACs) that estimate the error in gravitational acceleration of a contribution of a single node to the potential (hereafter partial error) much better than purely geometrical MAC defined in the tree solver. They are: (1) the approximate partial error (APE), and (2) the maximum partial error (MPE). The first one is based on an assumption that the partial error is proportional to the multipole moment of the node. The node is accepted for calculation of the potential if

$$D^{m+2} > \frac{GMS^m_{\mathrm{node}}}{\Delta a_{\mathrm{p,APE}}} \tag{19.7}$$

where D is distance between the *point-of-calculation* and the node, M is the node mass, S_{node} is the node size, m is a degree of the multipole approximation and $\Delta a_{\mathrm{p,APE}}$ is the requested maximum error in acceleration (controlled by runtime parameter `grv_bhAccErr`). Since only monopole moments are used for the potential calculation, the most reasonable choice of m seems to be $m = 2$. This MAC is similar to the one used in Gadget2 (see Springel, 2005, MNRAS, 364, 1105).

The second MAC (maximum partial error, MPE) calculates the error in acceleration of a single node contribution $\Delta a_{\mathrm{p,MPE}}$ according to formula 9 from Salmon&Warren (1994; see this paper for details):

$$\Delta a_{\mathrm{p,MPE}} \leq \frac{1}{D^2}\frac{1}{(1-S_{\mathrm{node}}/D)^2}\left(\frac{3\lceil B_2\rceil}{D^2} - \frac{2\lfloor B_3\rfloor}{D^3}\right) \tag{19.8}$$

where $B_n = \Sigma_i m_i|\mathbf{r}_i - \mathbf{r}_0|^n$ where m_i and $\mathbf{r}_i$ are masses and positions of individual grid cells within the node and $\mathbf{r}_0$ is the node mass center position. Moment B_2 can be easily determined during the tree build, moment B_3 can be estimated as $B_3^2 \geq B_2^3/M$. The maximum allowed partial error in gravitational acceleration is controlled by runtime parameters `grv_bhAccErr` and `grv_bhUseRelAccErr` (see 19.4.1).

During the tree walk, subroutine `Gravity_bhNodeContrib` adds contributions of tree nodes to the gravitational potential or acceleration fields. In case of the potential, the contribution is

$$\Phi = -\frac{GM}{|\vec{r}|} \tag{19.9}$$

if `isolated` boundary conditions are used, or

$$\Phi = -GMf_{\mathrm{EF},\Phi}(\vec{r}) \tag{19.10}$$

if periodic `periodic` or `mixed` boundary conditions are used. In case of the acceleration, the contributions are

$$\vec{a}_g = \frac{GM\vec{r}}{|\vec{r}|^3} \tag{19.11}$$

for `isolated` boundary conditions, or

$$\vec{a}_g = GMf_{\mathrm{EF,a}}(\vec{r}) \tag{19.12}$$

for `periodic` or `mixed` boundary conditions. In In the above formulae, G is the constant of gravity, M is the node mass, $\vec{r}$ is the position vector between *point-of-calculation* and the node mass center and $f_{\mathrm{EF},\Phi}$ and $f_{\mathrm{EF,a}}$ are the Ewald fields for the potential and the acceleration (see below).

Boundary conditions can be isolated or periodic, set independently for each direction. If they are periodic at least in one direction, the Ewald method is used for the potential calculation (Ewald, P. P., 1921, Ann. Phys. 64, 253). The original Ewald method is an efficient method for computing gravitational field for problems with periodic boundary conditions in three directions. Ewald speeded up evaluation of the gravitational potential by splitting it into two parts, $Gm/r = Gm\,\mathrm{erf}(\alpha r)/r + Gm\,\mathrm{erfc}(\alpha r)/r$ (α is an arbitrary constant) and then by applying Poisson summation formula on erfc terms, gravitational field at position $\vec{r}$ can be written in the form

$$\phi(\vec{r}) = -G\sum_{a=1}^{N} m_a \left(\sum_{i_1,i_2,i_3} A_S(\vec{r},\vec{r}_a,\vec{l}_{i_1,i_2,i_3}) + A_L(\vec{r},\vec{r}_a,\vec{l}_{i_1,i_2,i_3}) \right) = -G\sum_{a=1}^{N} m_a f_{\mathrm{EF},\Phi}(\vec{r}_a - \vec{r}) \ , \qquad (19.13)$$

the first sum runs over whole computational domain, where at position $\vec{r}_a$ is mass m_a. Second sum runs over all neigbouring computational domains, which are at positions $\vec{l}_{i_1,i_2,i_3}$ and $A_S(\vec{r},\vec{r}_a,\vec{l}_{i_1,i_2,i_3})$ and $A_L(\vec{r},\vec{r}_a,\vec{l}_{i_1,i_2,i_3})$ are short and long–range contributions, respectively. It is sufficient to take into account only few terms in eq. 19.13. The Ewald field for the acceleration, $f_{\mathrm{EF,a}}$, is obtained using a similar decomposition. We modified Ewald method for problems with periodic boundary conditions in two directions and isolated boundary conditions in the third direction and for problems with periodic boundary conditions in one direction and isolated in two directions.

The gravity unit allows also to use a static external gravitational field read from file. In this version, the field can be either spherically symmetric or planar being only a function of the z-coordinate. The external field file is a text file containing three columns of numbers representing the coordinate, the potential and the acceleration. The coordinate is the radial distance or z-distance from the center of the external field given by runtime parameters. The external field if mapped to a grid using a linear interpolation each time the gravitational acceleration is calculated (in subroutine `Gravity_accelOneRow`).

19.4 Usage

To include the effects of gravity in your FLASH executable, include the option

-with-unit=physics/Gravity

on your command line when you configure the code with `setup`. The default implementation is `Constant`, which can be overridden by including the entire path to the specific implementation in the command line or `Config` file. The other available implementations are `Gravity/GravityMain/Planepar`, `Gravity/-GravityMain/Pointmass` and `Gravity/GravityMain/Poisson`. The `Gravity` unit provides accessor functions to get gravitational acceleration and potential. However, none of the external field implementations of Section Section 19.2 explicitly compute the potential, hence they inherit the null implementation from the API for accessing potential. The gravitation acceleration can be obtained either on the whole domain, a single block or a single row at a time.

When building an application that solves the Possion equation for the gravitational potential, additional storage is needed in `unk` for holding the last, as well as (usually) the previous, gravitational potential field; and, depending on the Poisson solver used, additional variables may be needed. The variables `GPOT_VAR` and `GPOT_VAR`, and others as needed, will be automatically defined in `Flash.h` in those cases. See `Gravity_potentialListOfBlocks` for more information.

19.4.1 Tree Gravity Unit Usage

Calculation of gravitational potential can be enabled by compiling in this unit and setting the runtime parameter `useGravity` true. The constant of gravity can be set independently by runtime parameter `grv_bhNewton`; if it is not positive, the constant `Newton` from the FLASH `PhysicalConstants` database is used. If parameters `gr_bhPhysMACTW` or `gr_bhPhysMACComm` are set, the gravity unit MAC is used and it can be chosen by setting `grv_bhMAC` to either `ApproxPartialErr` or `MaxPartialErr`. If the first one is used, the order of the multipole approximation is given by `grv_bhMPDegree`.

The maximum allowed partial error in gravitational acceleration is set with the runtime parameter `grv_bhAccErr`. It has either the meaning of an error in absolute acceleration or in relative acceleration normalized by the acceleration from the previous time-step. The latter is used if `grv_bhUseRelAccErr` is set to True, and in this case the first call of the tree solver calculates the potential using purely geometrical MAC (because the acceleration from the previous time-step does not exist).

Boundary conditions are set by the runtime parameter grav_boundary_type and they can be isolated, periodic or mixed. In the case of mixed boundary conditions, runtime parameters grav_boundary_type_x, grav_boundary_type_y and grav_boundary_type_z specify along which coordinate boundary conditions are periodic and isolated (possible values are periodic or isolated). Arbitrary combination of these values is permitted, thus suitable for problems with planar resp. linear symmetry. It should work for computational domain with arbitrary dimensions. The highest accuracy is reached with blocks of cubic physical dimensions.

If runtime parameter grav_boundary_type is periodic or mixed, then the Ewald field for appropriate symmetry is calculated at the beginning of the simulation. Parameter grv_bhEwaldSeriesN controls the range of indices i_1, i_2, i_3 in (eq. 19.13). There are two implementations of the Ewald method: the new one (default) requires less memory and it should be faster and of comparable accuracy as the old one. The default implementation computes Ewald field minus the singular $1/r$ term and its partial derivatives on a single cubic grid, and the Ewald field is then approximated by the first order Taylor formula. Parameter grv_bhEwaldNPer controls number of grid points in the x direction in the case of periodic or in periodic direction(s) in the case of mixed boundary conditions. Since an elongated computational domain is often desired when grav_boundary_type is mixed, the cubic grid would lead to a huge field of data. In this case, the amount of necessary grid points is reduced by using an analytical estimate to the Ewald field sufficiently far away of the symmetry plane or axis.

The old implementation (from Flash4.2) is still present and is enabled by adding bhtreeEwaldV42=1 on the setup command line. The Ewald field is then stored in a nested set of grids, the first of them corresponds in size to full computational domain, and each following grid is half the size (in each direction) of the previous grid. Number of nested grids is controlled by runtime parameter grv_bhEwaldNRefV42. If grv_bhEwaldNRefV42 is too low to cover origin (where is the Ewald field discontinuous), then the run is terminated. Each grid is composed of grv_bhEwaldFieldNxV42 × grv_bhEwaldFieldNyV42 × grv_bhEwaldFieldNzV42 points. When evaluation of the Ewald Field at particular point is needed at any time during a run, the field value is found by interpolation in a suitable level of the grid. Linear or semi-quadratic interpolation can be chosen by runtime parameter grv_bhLinearInterpolOnlyV42 (option true corresponds to linear interpolation). Semi-quadratic interpolation is recommended only in the case when there are periodic boundary conditions in two directions.

The external gravitational field can be switched on by setting grv_useExternalPotential true. The parameter grv_bhExtrnPotFile gives the name of the file with the external potential and grv_bhExtrnPotType specifies the field symmetry: spherical for the spherical symmetry and planez for the planar symmetry with field being a function of the z-coordinate. Parameters grv_bhExtrnPotCenterY, grv_bhExtrnPotCenterX and grv_bhExtrnPotCenterZ specify the position (in the simulation coordinate system) of the external field origin (the point where the radial or z-coordinate is zero).

Table 19.1: Tree gravity unit parameters controlling the accuracy of calculation.

Variable	Type	Default	Description
grv_bhNewton	real	-1.0	constant of gravity; if < 0, it is obtained from internal physical constants database
grv_bhMAC	string	"ApproxPartialErr"	MAC, other option: "MaxPartialErr"
grv_bhMPDegree	integer	2	degree of multipole in error estimate in APE MAC
grv_bhUseRelAccErr	logical	.false.	if .true., grv_bhAccErr has meaning of relative error, otherwise absolute
grv_bhAccErr	real	0.1	maximum allowed error in gravitational acceleration

Tree gravity unit parameters controlling the external gravitational field.

Table 19.2: Tree gravity unit parameters controlling the boundary conditions.

Variable	Type	Default	Description
grav_boundary_type	string	"isolated"	or "periodic" or "mixed"
grav_boundary_type_x	string	"isolated"	or "periodic"
grav_boundary_type_y	string	"isolated"	or "periodic"
grav_boundary_type_z	string	"isolated"	or "periodic"
grv_bhEwaldAlwaysGenerate	boolean	true	whether Ewald field should be regenerated
grv_bhEwaldSeriesN	integer	10	number of terms in the Ewald series
grv_bhEwaldNPer	integer	32	number of points+1 of the Taylor expansion
grv_bhEwaldFName	string	"ewald_coeffs"	file with coefficients of the Ewald field Taylor expansion
grv_bhEwaldFieldNxV42	integer	32	size of the Ewald field grid in x-direction
grv_bhEwaldFieldNyV42	integer	32	size of the Ewald field grid in y-direction
grv_bhEwaldFieldNzV42	integer	32	size of the Ewald field grid in z-direction
grv_bhEwaldNRefV42	integer	-1	number of refinement levels (nested grids) for the Ewald field; if < 0, determined automatically
grv_bhLinearInterpolOnlyV42	logical	.true.	if .false., semi-quadratic interpolation is used for interpolation in the Ewald field
grv_bhEwaldFNameAccV42	string	"ewald_field_acc"	file with the Ewald field for acceleration
grv_bhEwaldFNamePotV42	string	"ewald_field_pot"	file with coefficients of the Ewald field for potential

Variable	Type	Default	Description
grv_bhUseExternalPotential	logical	.false.	whether to use external field
grv_bhUsePoissonPotential	logical	.true.	whether to use gravitational field calculated by the tree solver
grv_bhExtrnPotFile	string	"external_potential.dat"	file containing the external gravitational field
grv_bhExtrnPotType	string	"planez"	type of the external field: planar or spherical symmetry
grv_bhExtrnPotCenterX	real	0.0	x-coordinate of the center of the external field
grv_bhExtrnPotCenterY	real	0.0	y-coordinate of the center of the external field
grv_bhExtrnPotCenterZ	real	0.0	z-coordinate of the center of the external field

19.5 Unit Tests

There are two unit tests for the gravity unit. `Poisson3` is essentially the Maclaurin spheroid problem described in Section 30.3.4. Because an analytical solution exists, the accuracy of the gravitational solver can be quantified. The second test, `Poisson3_active` is a modification of `Poisson3` to test the mapping of particles in `Grid_mapParticlesToMesh`. Some of the mesh density is redistributed onto particles, and the particles are then mapped back to the mesh, using the analytical solution to verify completeness. This test is similar to the simulation `PoisParticles` discussed in Section 30.4.3. `PoisParticles` is based on the Huang-Greengard Poisson gravity test described in Section 30.3.3.

Chapter 20

Particles Unit

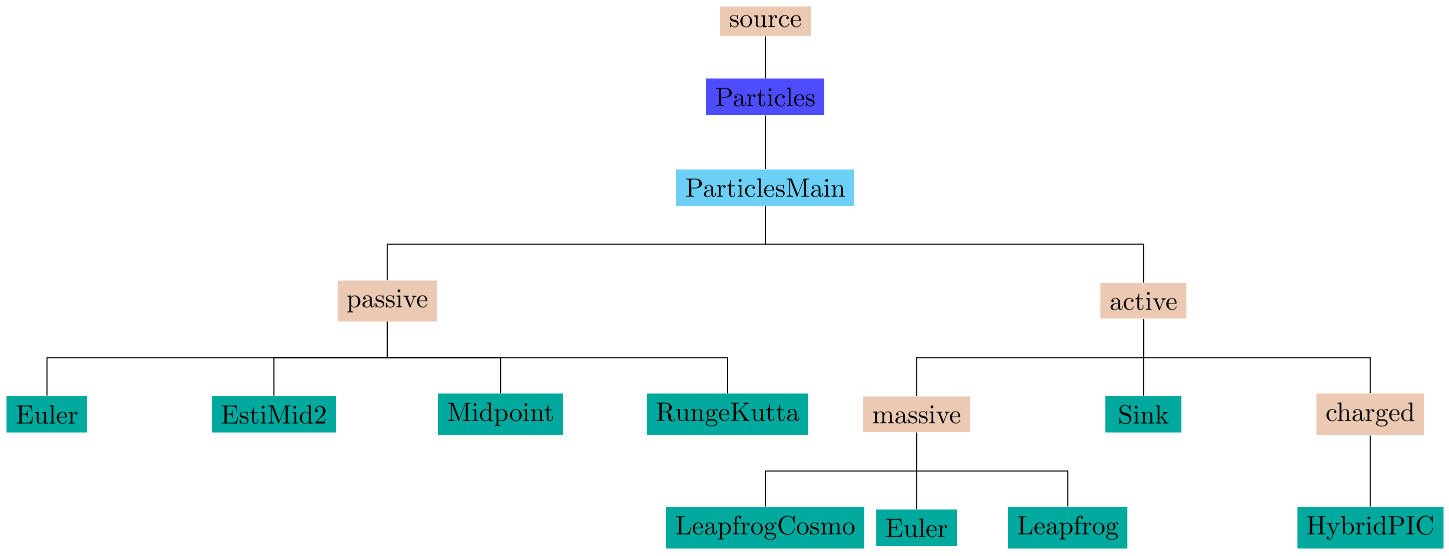

Figure 20.1: The `Particles` unit main subunit.

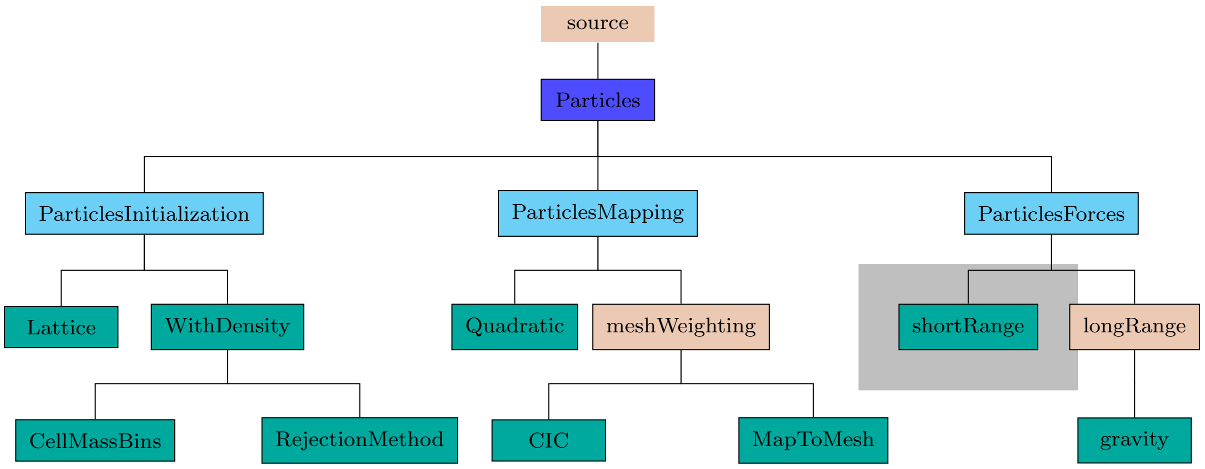

Figure 20.2: The `Particles` unit with ParticlesInitialization and ParticlesMapping subunits.

The support for particles in FLASH4 comes in two flavors, *active* and *passive*. Active particles are further classified into two categories; *massive* and *charged*. The active particles contribute to the dynamics of the simulation, while passive particles follow the motion of Lagrangian tracers and make no contribution to the dynamics. Particles are dimensionless objects characterized by positions $\mathbf{x}_i$, velocities $\mathbf{v}_i$, and sometimes other quantities such as mass m_i or charge q_i . Their characteristic quantities are considered to be defined at their positions and may be set by interpolation from the mesh or may be used to define mesh quantities by extrapolation. They move relative to the mesh and can travel from block to block, requiring communication patterns different from those used to transfer boundary information between processors for mesh-based data.

Passive particles acquire their kinematic information (velocities) directly from the mesh. They are meant to be used as passive flow tracers and do not make sense outside of a hydrodynamical context. The governing equation for the ith passive particle is particularly simple and requires only the time integration of interpolated mesh velocities.

$$\frac{d\mathbf{x}_i}{dt} = \mathbf{v}_i \tag{20.1}$$

Active particles experience forces and may themselves contribute to the problem dynamics (*e.g.*, through long-range forces or through collisions). They may additionally have their own motion independent of the grid, so an additional motion equation of

$$\mathbf{v}_i^{n+1} = \mathbf{v}_i^n + \mathbf{a}_i^n \Delta t^n \ . \tag{20.2}$$

may come into play. Here $\mathbf{a}_i$ is the particle acceleration. Solving for the motion of active particles is also referred to as solving the N-body problem. The equations of motion for the ith active particle include the equation (20.1) and another describing the effects of forces.

$$m_i \frac{d\mathbf{v}_i}{dt} = \mathbf{F}_{\mathrm{lr},i} + \mathbf{F}_{\mathrm{sr},i} \ , \tag{20.3}$$

Here, $\mathbf{F}_{\mathrm{lr},i}$ represents the sum of all long-range forces (coupling all particles, except possibly those handled by the short-range term) acting on the ith particle and $\mathbf{F}_{\mathrm{sr},i}$ represents the sum of all short-range forces (coupling only neighboring particles) acting on the particle.

For both types of particles, the primary challenge is to integrate (20.1) forward through time. Many alternative integration methods are described in Section Section 20.1 below. Additional information about the mesh to particle mapping is described in Section 20.2. An introduction to the particle techniques used in FLASH is given by R. W. Hockney and J. W. Eastwood in *Computer Simulation using Particles* (Taylor and Francis, 1988).

FLASH Transition

Please note that the particles routines have not been thoroughly tested with non-Cartesian coordinates; use them at your own risk!

New since FLASH3.1

Since release 3.1 of FLASH, a single simulation can have both active and passive particles defined. FLASH3 and FLASH2 allowed only active *or* passive particles in a simulation. Because of the added complexity, new `Config` syntax and new `setup` script syntax is necessary for Particles. See Section 5.2 for command line options, Section 6.6 for `Config` sytax, and Section 20.3 below for more details.

FLASH4 includes support for **sink particles**. These are a special kind of (massive) active particles, with special rules for creation, mass accretion, and interaction with fluid variables and other particles. See Section 20.4 below for information specific to sink particles.

20.1 Time Integration

The active and passive particles have many different time integration schemes available. The subroutine `Particles_advance` handles the movement of particles through space and time. Because FLASH4 has support for including different types of both active and passive particles in a single simulation, the implementation of `Particles_advance` may call several helper routines of the form `pt_advance`*METHOD* (*e.g.*, `pt_advanceLeapfrog`, `pt_advanceEuler_active`, `pt_advanceCustom`), each acting on an appropriate subset of existing particles. The *METHOD* here is determined by the `ADVMETHOD` part of the `PARTICLETYPE` `Config` statement (or the `ADV` par of a `-particlemethods setup` option) for the type of particle. See the `Particles_advance` source code for the mapping from `ADVMETHOD` keyword to `pt_advance`*METHOD* subroutine call.

20.1.1 Active Particles (Massive)

The `active` particles implementation includes different time integration schemes, long-range force laws (coupling all particles), and short-range force laws (coupling nearby particles). The attributes listed in Table 20.1 are provided by this subunit. A specific implementation of the active portion of `Particles_advance` is selected by a setup option such as `-with-unit=Particles/ParticlesMain/active/massive/Leapfrog`, or by specifying something like `REQUIRES Particles/ParticlesMain/active/massive/Leapfrog` in a simulation's `Config` file (or by listing the path in the `Units` file if not using the `-auto` configuration option). Further details are given is Section 20.3 below.

Available time integration schemes for active particles include

- **Forward Euler.** Particles are advanced in time from t^n to $t^{n+1} = t^n + \Delta t^n$ using the following difference equations:

$$\begin{aligned} \mathbf{x}_i^{n+1} &= \mathbf{x}_i^n + \mathbf{v}_i^n \Delta t^n \\ \mathbf{v}_i^{n+1} &= \mathbf{v}_i^n + \mathbf{a}_i^n \Delta t^n \ . \end{aligned} \qquad (20.4)$$

  Here $\mathbf{a}_i$ is the particle acceleration. Within FLASH4, this scheme is implemented in `Particles/-ParticlesMain/active/massive/Euler`. This Euler scheme (as well as the Euler scheme for the passive particles) is first-order accurate and is included for testing purposes only. It should not be used in a production run.

- **Variable-timestep leapfrog.** Particles are advanced using the following difference equations

$$\begin{aligned} \mathbf{x}_i^1 &= \mathbf{x}_i^0 + \mathbf{v}_i^0 \Delta t^0 \\ \mathbf{v}_i^{1/2} &= \mathbf{v}_i^0 + \tfrac{1}{2}\mathbf{a}_i^0 \Delta t^0 \\ \mathbf{v}_i^{n+1/2} &= \mathbf{v}_i^{n-1/2} + C_n \mathbf{a}_i^n + D_n \mathbf{a}_i^{n-1} \\ \mathbf{x}_i^{n+1} &= \mathbf{x}_i^n + \mathbf{v}_i^{n+1/2} \Delta t^n \ . \end{aligned} \tag{20.5}$$

  The coefficients C_n and D_n are given by

$$\begin{aligned} C_n &= \tfrac{1}{2}\Delta t^n + \tfrac{1}{3}\Delta t^{n-1} + \tfrac{1}{6}\left(\tfrac{\Delta t^{n2}}{\Delta t^{n-1}}\right) \\ D_n &= \tfrac{1}{6}\left(\Delta t^{n-1} - \tfrac{\Delta t^{n2}}{\Delta t^{n-1}}\right) \ . \end{aligned} \tag{20.6}$$

  By using time-centered velocities and stored accelerations, this method achieves second-order time accuracy even with variable timesteps. Within FLASH4, this scheme is implemented in `Particles/-ParticlesMain/active/massive/Leapfrog`

- **Cosmological variable-timestep leapfrog.** (`Particles/ParticlesMain/active/massive/LeapfrogCosmo`) The coefficients in the leapfrog update are modified to take into account the effect of cosmological red-shift on the particles. The particle positions $\mathbf{x}$ are interpreted as comoving positions, and the particle velocities $\mathbf{v}$ are interpreted as comoving peculiar velocities ($\mathbf{v} = \dot{\mathbf{x}}$). The resulting update steps are

$$\begin{aligned} \mathbf{x}_i^1 &= \mathbf{x}_i^0 + \mathbf{v}_i^0 \Delta t^0 \\ \mathbf{v}_i^{1/2} &= \mathbf{v}_i^0 + \frac{1}{2}\mathbf{a}_i^0 \Delta t^0 \\ \mathbf{v}_i^{n+1/2} &= \mathbf{v}_i^{n-1/2}\left[1 - \frac{A^n}{2}\Delta t^n + \frac{1}{3!}\Delta t^{n2}\left(A^{n2} - \dot{A}^n\right)\right]\left[1 - \Delta t^{n-1}\frac{A^n}{2} + \Delta t^{n-1\,2}\frac{A^{n2} + 2\dot{A}^n}{12}\right] \\ &\quad + \mathbf{a}_i^n\left[\frac{\Delta t^{n-1}}{2} + \frac{\Delta t^{n2}}{6\Delta t^{n-1}} + \frac{\Delta t^{n-1}}{3} - \frac{A^n \Delta t^n}{6}\left(\Delta t^n + \Delta t^{n-1}\right)\right] \\ &\quad + \mathbf{a}_i^{n-1}\left[\frac{\Delta t^{n-1\,2} - \Delta t^{n2}}{6\Delta t^{n-1}} - \frac{A^n \Delta t^{n-1}}{12}(\Delta t^n + \Delta t^{n-1})\right] \\ \mathbf{x}_i^{n+1} &= \mathbf{x}_i^n + \mathbf{v}_i^{n+1/2}\Delta t^n \ . \end{aligned}$$

  Here we define $A \equiv -2\dot{a}/a$, where a is the scale factor. Note that the acceleration $\mathbf{a}_i^{n-1}$ from the previous timestep must be retained in order to obtain second order accuracy. Using the `Particles/-ParticlesMain/passive/LeapfrogCosmo` time integration scheme only makes sense if the `Cosmology` module is also used, since otherwise $a \equiv 1$ and $\dot{a} \equiv 0$.

- **Sink particles** have their own implementation of several advancement methods (with time subcycling), implemented under `Particles/ParticlesMain/active/Sink`, see description below in Section 20.4.

The leapfrog-based integrators implemented under `Particles/ParticlesMain/active/massive` supply the additional particle attributes listed in Table 20.2.

Table 20.1: Particle attributes provided by active particles.

Attribute	Type	Description
`MASS_PART_PROP`	REAL	Particle mass
`ACCX_PART_PROP`	REAL	x-component of particle acceleration
`ACCY_PART_PROP`	REAL	y-component of particle acceleration
`ACCZ_PART_PROP`	REAL	z-component of particle acceleration

Table 20.2: Particle attributes provided by leapfrog time integration.

Attribute	Type	Description
`OACX_PART_PROP`	REAL	x-component of particle acceleration at previous timestep
`OACY_PART_PROP`	REAL	y-component of particle acceleration at previous timestep
`OACZ_PART_PROP`	REAL	z-component of particle acceleration at previous timestep

20.1.2 Charged Particles - Hybrid PIC

Collisionless plasmas are often modeled using fluid magnetohydrodynamics (MHD) models. However, the MHD fluid approximation is questionable when the gyroradius of the ions is large compared to the spatial region that is studied. On the other hand, kinetic models that discretize the full velocity space, or full particle in cell (PIC) models that treat ions and electrons as particles, are computationally very expensive. For problems where the time scales and spatial scales of the ions are of interest, hybrid models provide a compromise. In such models, the ions are treated as discrete particles, while the electrons are treated as a (often massless) fluid. This mean that the time scales and spatial scales of the electrons do not need to be resolved, and enables applications such as modeling of the solar wind interaction with planets. For a detailed discussion of different plasma models, see Ledvina et al. (2008).

20.1.2.1 The hybrid equations

In the hybrid approximation, ions are treated as particles, and electrons as a massless fluid. In what follows we use SI units. We have N_I ions at positions $\mathbf{r}_i(t)$ [m] with velocities $\mathbf{v}_i(t)$ [m/s], mass m_i [kg] and charge q_i [C], $i = 1, \ldots, N_I$. By spatial averaging we can define the charge density $\rho_I(\mathbf{r}, t)$ [Cm^{-3}] of the ions, their average velocity $\mathbf{u}_I(\mathbf{r}, t)$ [m/s], and the corresponding current density $\mathbf{J}_I(\mathbf{r}, t) = \rho_I \mathbf{u}_I$ [Cm^{-2}s^{-1}]. Electrons are modelled as a fluid with charge density $\rho_e(\mathbf{r}, t)$, average velocity $\mathbf{u}_e(\mathbf{r}, t)$, and current density $\mathbf{J}_e(\mathbf{r}, t) = \rho_e \mathbf{u}_e$. The electron number density is $n_e = -\rho_e/e$, where e is the elementary charge. If we assume that the electrons are an ideal gas, then $p_e = n_e k T_e$, so the pressure is directly related to temperature (k is Boltzmann's constant).

The trajectories of the ions are computed from the Lorentz force,

$$\frac{d\mathbf{r}_i}{dt} = \mathbf{v}_i, \quad \frac{d\mathbf{v}_i}{dt} = \frac{q_i}{m_i}\left(\mathbf{E} + \mathbf{v}_i \times \mathbf{B}\right), \quad i = 1, \ldots, N_I$$

where $\mathbf{E} = \mathbf{E}(\mathbf{r}, t)$ is the electric field, and $\mathbf{B} = \mathbf{B}(\mathbf{r}, t)$ is the magnetic field. The electric field is given by

$$\mathbf{E} = \frac{1}{\rho_I}\left(-\mathbf{J}_I \times \mathbf{B} + \mu_0^{-1}\left(\nabla \times \mathbf{B}\right) \times \mathbf{B} - \nabla p_e\right) + \eta \mathbf{J} - \eta_h \nabla^2 \mathbf{J},$$

where ρ_I is the ion charge density, $\mathbf{J}_I$ is the ion current, p_e is the electron pressure, $\mu_0 = 4\pi \cdot 10^{-7}$ is the magnetic constant, $\mathbf{J} = \mu_0^{-1} \nabla \times \mathbf{B}$ is the current, and η_h is a hyperresistivity. Here we assume that p_e is adiabatic. Then the relative change in electron pressure is related to the relative change in electron density by

$$\frac{p_e}{p_{e0}} = \left(\frac{n_e}{n_{e0}}\right)^{\gamma},$$

where the zero subscript denote reference values (here the initial values at $t = 0$). Then Faraday's law is used to advance the magnetic field in time,

$$\frac{\partial \mathbf{B}}{\partial t} = -\nabla \times \mathbf{E}.$$

20.1.2.2 A cell-centered finite difference hybrid PIC solver

We use a cell-centered representation of the magnetic field on a uniform grid. All spatial derivatives are discretized using standard second order finite difference stencils. Time advancement is done by a predictor-corrector leapfrog method with subcycling of the field update, denoted cyclic leapfrog (CL) by Matthew (1994). An advantage of the discretization is that the divergence of the magnetic field is zero, down to round off errors. The ion macroparticles (each representing a large number of real particles) are deposited on the grid by a cloud-in-cell method (linear weighting), and interpolation of the fields to the particle positions are done by the corresponding linear interpolation. Initial particle positions are drawn from a uniform distribution, and initial particle velocities from a Maxwellian distribution. Further details of the algorithm can be found in Holmström, M. (2012,2013) and references therein, where an extension of the solver that include inflow and outflow boundary conditions was used to model the interaction between the solar wind and the Moon. In what follows we describe the FLASH implementation of the hybrid solver with periodic boundary conditions.

20.1.2.3 Hybrid solver implementation

The two basic operations needed for a PIC code are provided as standard operations in FLASH:

- Deposit charges and currents onto the grid: `call Grid_mapParticlesToMesh()`
- Interpolate fields to particle positions: `call Grid_mapMeshToParticles()`

At present the solver is restricted to a Cartesian uniform grid, since running an electromagnetic particle code on an adaptive grid is not straightforward. Grid refinement/coarsening must be accompanied by particle split/join operations. Also, jumps in the cell size can lead to reflected electromagnetic waves.

The equations are stated in SI units, so all parameters should be given in SI units, and all output will be in SI units. The initial configuration is a spatial uniform plasma consisting of two species. The first species, named `pt_picPname_1` consists of particles of mass `pt_picPmass_1` and charge `pt_picPcharge_1`. The initial (at $t = 0$) uniform number density is `pt_picPdensity_1`, and the velocity distribution is Maxwellian with a drift velocity of (`pt_picPvelx_1`, `pt_picPvely_1`, `pt_picPvelz_1`), and a temperature of `pt_picPtemp_1`. Each model macro-particle represents many real particles. The number of macro-particles per grid cell at the start of the simulation is set by `pt_picPpc_1`. So this parameter will control the total number of macro-particles of species 1 in the simulation.

All the above parameters are also available for a second species, e.g., `pt_picPmass_2`, which is initialized in the same way as the first species. The grid is initialized with the uniform magnetic field (`sim_bx`, `sim_by`, `sim_bz`).

Now for grid quantities. The cell averaged mass density is stored in `pden`, and the charge density in `cden`. The magnetic field is represented by (`grbx`, `grby`, `grbz`). A background field can be set during initialization in (`gbx1`, `gby1`, `gbz1`). We then solve for the deviation from this background field. Care must be take so that the background field is divergence free, using the discrete divergence operator. The easiest way to ensure this is to compute the background field as the rotation of a potential. The electric field is stored in (`grex`, `grey`, `grez`), the current density in (`grjx`, `grjy`, `grjz`) , and the ion current density in (`gjix`, `gjiy`, `gjiz`). A resistivity is stored in `gres`, thus it is possible to have a non-uniform resistivity in the simulation domain, but the default is to set the resistivity to the constant value of `sim_resistivity` everywhere. For post processing, separate fields are stored for charge density and ion current density for species 1 and 2.

Regarding particle properties. Each computational meta-particles is labeled by a positive integer, `specie` and has a `mass` and `charge`. As all FLASH particles they also each have a position $\mathbf{r}_i$=(`posx`, `posy`, `posz`) and a velocity $\mathbf{v}_i$=(`velx`, `vely`, `velz`). To be able to deposit currents onto the grid, each particle stores the current density corresponding to the particle, $\mathbf{J}_{Ii}$. For the movement of the particles by the Lorentz force, we also need the electric and magnetic fields at the particle positions, $\mathbf{E}(\mathbf{r}_i)$ and $\mathbf{B}(\mathbf{r}_i)$, respectivly.

Table 20.3: Runtime parameters for the hybrid solver. Initial values are at $t = 0$. For each parameter for species 1, there is a corresponding parameter for species 2 (named with 2 instead of 1), e.g., `pt_picPvelx_2`.

Variable	Type	Default	Description
`pt_picPname_1`	STRING	"H+"	Species 1 name
`pt_picPmass_1`	REAL	1.0	Species 1 mass, m_i [amu]
`pt_picPcharge_1`	REAL	1.0	Species 1 charge, q_i [e]
`pt_picPdensity_1`	REAL	1.0	Initial n_I species 1 [m^{-3}]
`pt_picPtemp_1`	REAL	1.5e5	Initial T_I species 1 [K]
`pt_picPvelx_1`	REAL	0.0	Initial $\mathbf{u}_I$ species 1 [m/s]
`pt_picPvely_1`	REAL	0.0	
`pt_picPvelz_1`	REAL	0.0	
`pt_picPpc_1`	REAL	1.0	Number of macro-particle of species 1 per cell
`sim_bx`	REAL	0.0	Initial $\mathbf{B}$ (at $t = 0$) [T]
`sim_by`	REAL	0.0	
`sim_bz`	REAL	0.0	
`sim_te`	REAL	0.0	Initial T_e [K]
`pt_picResistivity`	REAL	0.0	Resistivity, η [Ω m]
`pt_picResistivityHyper`	REAL	0.0	Hyperresistivity, η_h
`sim_gam`	REAL	-1.0	Adiabatic exponent for electrons
`sim_nsub`	INTEGER	3	Number of CL B-field update subcycles (must be odd)
`sim_rng_seed`	INTEGER	0	Seed the random number generator (if > 0)

Regarding the choice of time step. The timestep must be constant, $\Delta t =$`dtinit = dtmin = dtmax`, since the leap frog solver requires this. For the solution to be stable the time step, Δt, must be small enough. We will try and quantify this, and here we asume that the grid cells are cubes, $\Delta x = \Delta y = \Delta z$, and that we have a single species plasma.

First of all, since the time advancement is explicit, there is the standard CFL condition that no particle should travel more than one grid cell in one time step, i.e. $\Delta t \max_i(|\mathbf{v}_i|) < \Delta x$. This time step is printed to standard output by FLASH (as `dt_Part`), and can thus be monitored.

Secondly, we also have an upper limit on the time step due to Whistler waves (Pritchett 2000),

$$\Delta t < \frac{\Omega_i^{-1}}{\pi}\left(\frac{\Delta x}{\delta_i}\right)^2 \sim \frac{n}{B}\left(\Delta x\right)^2, \qquad \delta_i = \frac{1}{|q_i|}\sqrt{\frac{m_i}{\mu_0\, n}},$$

where δ_i is the ion inertial length, and $\Omega_i = |q_i|B/m_i$ is the ion gyrofrequency.

Finally, we also want to resolve the ion gyro motion by having several time steps per gyration. This will only put a limit on the time step if, approximately, $\Delta x > 5\,\delta_i$, and we then have that $\Delta t < \Omega_i^{-1}$.

All this are only estimates that does not take into account, *e.g.*, the initial functions, or the subcycling of the magnetic field update. In practice one can just reduce the time step until the solution is stable. Then for runs with different density and/or magnetic field strength, the time step will need to be scaled by the change in n_I/B, *e.g.*, if n_I is doubled, Δt can be doubled. The factor $(\Delta x)^2$ implies that reducing the cell size by a factor of two will require a reduction in the time step by a factor of four.

20.1.3 Passive Particles

Passive particles may be moved using one of several different methods available in FLASH4. With the exception of **Midpoint**, they are all single-step schemes. The methods are either first-order or second-order accurate, and all are explicit, as described below. In all implementations, particle velocities are obtained by mapping grid-based velocities onto particle positions as described in Section 20.2.

Table 20.4: The grid variables for the hybrid solver that are most important for a user. For each property for species 1, there is a corresponding variable for species 2 (named with 2 instead of 1), e.g., `cde2`.

Variable	Type	Description
`cden`	PER_VOLUME	Total charge density, ρ [C/m^3]
`grbx`	GENERIC	Magnetic field, $\mathbf{B}$ [T]
`grby`	GENERIC	
`grbz`	GENERIC	
`grex`	GENERIC	Electric field, $\mathbf{E}$ [V/m]
`grey`	GENERIC	
`grez`	GENERIC	
`grjx`	PER_VOLUME	Current density, $\mathbf{J}$ [A/m^2]
`grjy`	PER_VOLUME	
`grjz`	PER_VOLUME	
`gjix`	PER_VOLUME	Ion current density, $\mathbf{J}_I$ [A/m^2]
`gjiy`	PER_VOLUME	
`gjiz`	PER_VOLUME	
`cde1`	PER_VOLUME	Species 1 charge density, ρ_I [C/m^3]
`jix1`	PER_VOLUME	Species 1 ion current density, $\mathbf{J}_I$ [A/m^2]
`jiy1`	PER_VOLUME	
`jiz1`	PER_VOLUME	

Numerically solving Equation (20.1) for passive particles means solving a set of simple ODE initial value problems, separately for each particle, where the velocities $\mathbf{v}_i$ are given at certain discrete points in time by the state of the hydrodynamic velocity field at those times. The time step is thus externally given and cannot be arbitrarily chosen by a particle motion ODE solver[1]. Statements about the order of a method in this context should be understood as referring to the same method if it were applied in a hypothetical simulation where evaluations of velocities $\mathbf{v}_i$ could be performed at arbitrary times (and with unlimited accuracy). Note that FLASH4 does not attempt to provide a particle motion ODE solver of higher accuracy than second order, since it makes little sense to integrate particle motion to a higher order than the fluid dynamics that provide its inputs.

In all cases, particles are advanced in time from t^n (or, in the case of `Midpoint`, from t^{n-1}) to $t^{n+1} = t^n + \Delta t^n$ using one of the difference equations described below. The implementations assume that at the time when `Particles_advance` is called, the fluid fields have already been updated to t^{n+1}, as is the case with the `Driver_evolveFlash` implementations provided with FLASH4. A specific implementation of the passive portion of `Particles_advance` is selected by a setup option such as `-with-unit=Particles/ParticlesMain/-passive/Euler`, or by specifying something like `REQUIRES Particles/ParticlesMain/passive/Euler` in a simulation's `Config` file (or by listing the path in the `Units` file if not using the `-auto` configuration option). Further details are given is Section 20.3 below.

- **Forward Euler (`Particles/ParticlesMain/passive/Euler`).** Particles are advanced in time from t^n to $t^{n+1} = t^n + \Delta t^n$ using the following difference equation:

$$\mathbf{x}_i^{n+1} = \mathbf{x}_i^n + \mathbf{v}_i^n \Delta t^n \quad . \tag{20.7}$$

  Here $\mathbf{v}_i^n$ is the velocity of the particle, which is obtained using particle-mesh interpolation from the grid at $t = t^n$.

  Note that this evaluation of $\mathbf{v}_i^n$ cannot be deferred until the time when it is needed at $t = t^{n+1}$, since at that point the fluid variables have been updated and the velocity fields at $t = t^n$ are not available any more. Particle velocities are therefore interpolated from the mesh at $t = t^n$ and stored as particle

[1]Even though it is possible to do so, see `Particles_computeDt`, one does not in general wish to let particles integration dictate the time step of the simulation.

Table 20.5: Important particle properties for the hybrid solver. Note that this is for the computational macro-particles.

Variable	Type	Description
`specie`	REAL	Particle type (an integer number 1,2,3,...)
`mass`	REAL	Mass of the particle, m_i [kg]
`charge`	REAL	Charge of the particle, q_i [C]
`jx`	REAL	Particle ion current, $\mathbf{J}_{Ii} = q_i\mathbf{v}_i$ [A m]
`jy`	REAL	
`jz`	REAL	
`bx`	REAL	Magnetic field at particle, $\mathbf{B}(\mathbf{r}_i)$ [T]
`by`	REAL	
`bz`	REAL	
`ex`	REAL	Electric field at particle, $\mathbf{E}(\mathbf{r}_i)$ [V/m]
`ey`	REAL	
`ez`	REAL	

attributes. Similar concerns apply to the remaining methods but will not be explicitly mentioned every time.

- **Two-Stage Runge-Kutta (`Particles/ParticlesMain/passive/RungeKutta`).** This 2-stage Runge-Kutta scheme is the preferred choice in FLASH4. It is also the default which is compiled in if particles are included in the setup but no specific alternative implementation is requested. The scheme is also known as Heun's Method:

$$\begin{aligned} \mathbf{x}_i^{n+1} &= \mathbf{x}_i^n + \frac{\Delta t^n}{2}\left[\mathbf{v}_i^n + \mathbf{v}_i^{*,n+1}\right] , \qquad (20.8)\\ \text{where}\quad \mathbf{v}_i^{*,n+1} &= \mathbf{v}(\mathbf{x}_i^{*,n+1}, t^{n+1}) ,\\ \mathbf{x}_i^{*,n+1} &= \mathbf{x}_i^n + \Delta t^n \mathbf{v}_i^n \quad . \end{aligned}$$

  Here $\mathbf{v}(\mathbf{x}, t)$ denotes evaluation (interpolation) of the fluid velocity field at position $\mathbf{x}$ and time t; $\mathbf{v}_i^{*,n+1}$ and $\mathbf{x}_i^{*,n+1}$ are intermediate results [2]; and $\mathbf{v}_i^n = \mathbf{v}(\mathbf{x}_i^n, t^n)$ is the velocity of the particle, obtained using particle-mesh interpolation from the grid at $t = t^n$ as usual.

- **Midpoint (`Particles/ParticlesMain/passive/Midpoint`).** This Midpoint scheme is a two-step scheme. Here, the particles are advanced from time t^{n-1} to $t^{n+1} = t^{n-1} + \Delta t^{n-1} + \Delta t^n$ by the equation

$$\mathbf{x}_i^{n+1} = \mathbf{x}_i^{n-1} + \mathbf{v}_i^n(\Delta t^{n-1} + \Delta t^n) \quad . \qquad (20.9)$$

  The scheme is second order if $\Delta t^n = \Delta t^{n-1}$.

  To get the scheme started, an Euler step (as described for `passive/Euler`) is taken the first time `Particles/ParticlesMain/passive/Midpoint/pt_advancePassive` is called.

  The `Midpoint` alternative implementation uses the following additional particle attributes:

```
PARTICLEPROP pos2PrevX REAL          # two previous x-coordinate
PARTICLEPROP pos2PrevY REAL          # two previous y-coordinate
PARTICLEPROP pos2PrevZ REAL          # two previous z-coordinate
```

- **Estimated Midpoint with Correction (`Particles/ParticlesMain/passive/EstiMidpoint2`).** The scheme is second order even if $\Delta t^n = \Delta t^{n+1}$ is not assumed. It is essentially the `EstiMidpoint` or "Predictor-Corrector" method of previous releases, with a correction for non-constant time steps by

[2] They can be considered "predicted" positions and velocities.

using additional evaluations (at times and positions that are easily available, without requiring more particle attributes).

Particle advancement follows the equation

$$\mathbf{x}_i^{n+1} = \mathbf{x}_i^n + \Delta t^n \, \mathbf{v}_i^{\text{comb}} \; , \tag{20.10}$$

where

$$\mathbf{v}_i^{\text{comb}} = c_1 \, \mathbf{v}(\mathbf{x}_i^{*,n+\frac{1}{2}}, t^n) + c_2 \, \mathbf{v}(\mathbf{x}_i^{*,n+\frac{1}{2}}, t^{n+1}) + c_3 \, \mathbf{v}(\mathbf{x}_i^n, t^n) + c_4 \, \mathbf{v}(\mathbf{x}_i^n, t^{n+1}) \tag{20.11}$$

is a combination of four evaluations (two each at the previous and the current time),

$$\mathbf{x}_i^{*,n+\frac{1}{2}} = \mathbf{x}_i^n + \frac{1}{2}\Delta t^{n-1}\mathbf{v}_i^n$$

are estimated midpoint positions as before in the Estimated Midpoint scheme, and the coefficients

$$\begin{aligned} c_1 &= c_1(\Delta t^{n-1}, \Delta t^n) \; , \\ c_2 &= c_2(\Delta t^{n-1}, \Delta t^n) \; , \\ c_3 &= c_3(\Delta t^{n-1}, \Delta t^n) \; , \\ c_4 &= c_4(\Delta t^{n-1}, \Delta t^n) \end{aligned}$$

are chosen dependent on the change in time step so that the method stays second order when $\Delta t^{n-1} \neq \Delta t^n$.

Conditions for the correction can be derived as follows: Let $\Delta t_*^n = \frac{1}{2}\Delta t^{n-1}$ the estimated half time step used in the scheme, let $t_*^{n+\frac{1}{2}} = t^n + \Delta t_*^n$ the estimated midpoint time, and $t^{n+\frac{1}{2}} = t^n + \frac{1}{2}\Delta t^n$ the actual midpoint of the $[t^n, t^{n+1}]$ interval. Also write $\mathbf{x}_i^{\text{E},n+\frac{1}{2}} = \mathbf{x}_i^n + \frac{1}{2}\Delta t^n \mathbf{v}_i^n$ for first-order (Euler) approximate positions at the actual midpoint time $t^{n+\frac{1}{2}}$, and we continue to denote with $\mathbf{x}_i^{*,n+\frac{1}{2}}$ the estimated positions reached at the estimated mipoint time $t_*^{n+\frac{1}{2}}$.

Assuming reasonably smooth functions $\mathbf{v}(\mathbf{x}, t)$, we can then write for the exact value of the velocity field at the approximate positions evaluated at the actual midpoint time

$$\mathbf{v}(\mathbf{x}_i^{\text{E},n+\frac{1}{2}}, t^{n+\frac{1}{2}}) = \mathbf{v}(\mathbf{x}_i^n, t^n) + \mathbf{v}_t(\mathbf{x}_i^n, t^n)\frac{1}{2}\Delta t^n + (\mathbf{v}_i^n \cdot \frac{\partial}{\partial \mathbf{x}})\mathbf{v}(\mathbf{x}_i^n, t^n)\frac{1}{2}\Delta t^n + O((\frac{1}{2}\Delta t^n)^2) \tag{20.12}$$

by Taylor expansion. It is known that the propagation scheme $\tilde{\mathbf{x}}_i^{n+1} = \mathbf{x}_i^n + \mathbf{v}(\mathbf{x}_i^{\text{E},n+\frac{1}{2}}, t^{n+\frac{1}{2}})\Delta t$ using these velocities is second order (this is known as the modified Euler method).

On the other hand, expansion of (20.11) gives

$$\begin{aligned} \mathbf{v}_i^{\text{comb}} &= (c_1 + c_2 + c_3 + c_4)\mathbf{v}(\mathbf{x}_i^n, t^n) \\ &\quad + (c_2 + c_4)\mathbf{v}_t(\mathbf{x}_i^n, t^n)\Delta t \; + \; (c_1 + c_2)(\mathbf{v}_i^n \cdot \frac{\partial}{\partial \mathbf{x}})\mathbf{v}(\mathbf{x}_i^n, t^n)\Delta t_*^n \\ &\qquad + \quad \text{higher order terms in } \Delta t \text{ and } \Delta t_*^n. \end{aligned}$$

After introducing a time step factor f defined by $\Delta t_*^n = f \, \Delta t^n$, this becomes

$$\begin{aligned} \mathbf{v}_i^{\text{comb}} &= (c_1 + c_2 + c_3 + c_4)\mathbf{v}(\mathbf{x}_i^n, t^n) \\ &\quad + (c_2 + c_4)\mathbf{v}_t(\mathbf{x}_i^n, t^n)\Delta t \; + \; (c_1 + c_2)(\mathbf{v}_i^n \cdot \frac{\partial}{\partial \mathbf{x}})\mathbf{v}(\mathbf{x}_i^n, t^n) \, f \, \Delta t \\ &\qquad + O((\Delta t)^2) \quad . \end{aligned} \tag{20.13}$$

One can derive conditions for second order accuracy by comparing (20.13) with (20.12) and requiring that

$$\mathbf{v}_i^{\text{comb}} = \mathbf{v}(\mathbf{x}_i^{\text{E},n+\frac{1}{2}}, t^{n+\frac{1}{2}}) + O((\Delta t)^2) \quad . \tag{20.14}$$

It turns out that the coefficients have to satisfy three conditions in order to eliminate from the theoretical difference between numerical and exact solution all $O(\Delta t^{n-1})$ and $O(\Delta t^n)$ error terms:

$$\begin{aligned} c_1 + c_2 + c_3 + c_4 &= 1 \quad \text{(otherwise the scheme will not even be of first order)}\ , \\ c_2 + c_4 &= \frac{1}{2} \quad \text{(and thus also } c_1 + c_3 = \tfrac{1}{2})\ , \\ c_1 + c_2 &= \frac{\Delta t^n}{\Delta t^{n-1}} \quad . \end{aligned}$$

The provided implementation chooses $c_4 = 0$ (this can be easily changed if desired by editing in the code). All four coefficients are then determined:

$$\begin{aligned} c_1 &= \frac{\Delta t^n}{\Delta t^{n-1}} - \frac{1}{2}\ , \\ c_2 &= \frac{1}{2}\ , \\ c_3 &= 1 - \frac{\Delta t^n}{\Delta t^{n-1}}\ , \\ c_4 &= 0 \quad . \end{aligned}$$

Note that when the time step remains unchanged we have $c_1 = c_2 = \frac{1}{2}$ and $c_3 = c_4 = 0$, and so (20.10) simplifies significantly.

An Euler step, as described for `passive/Euler` in (20.7), is taken the first time when `Particles/-ParticlesMain/passive/EstiMidpoint2/pt_advancePassive` is called and when the time step has changed too much. Since the integration scheme is tolerant of time step changes, it should usually not be necessary to apply the second criterion; even when it is to be employed, the criteria should be less strict than for an uncorrected `EstiMidpoint` scheme. For `EstiMidPoint2` the timestep is considered to have changed too much if either of the following is true:

$$\Delta t^n > \Delta t^{n-1} \quad \text{and} \quad \left|\Delta t^n - \Delta t^{n-1}\right| \geq \texttt{pt\_dtChangeToleranceUp} \times \Delta t^{n-1}$$

or

$$\Delta t^n < \Delta t^{n-1} \quad \text{and} \quad \left|\Delta t^n - \Delta t^{n-1}\right| \geq \texttt{pt\_dtChangeToleranceDown} \times \Delta t^{n-1},$$

where `pt_dtChangeToleranceUp` and `pt_dtChangeToleranceDown` are runtime parameter specific to the `EstiMidPoint2` alternative implementation.

The `EstiMidpoint2` alternative implementation uses the following additional particle attributes for storing the values of $\mathbf{x}_i^{*,n+\frac{1}{2}}$ and $\mathbf{v}_i^{*,n+\frac{1}{2}}$ between the `Particles_advance` calls at t^n and t^{n+1}:

```
PARTICLEPROP velPredX REAL
PARTICLEPROP velPredY REAL
PARTICLEPROP velPredZ REAL
PARTICLEPROP posPredX REAL
PARTICLEPROP posPredY REAL
PARTICLEPROP posPredZ REAL
```

The time integration of passive particles is tested in the `ParticlesAdvance` unit test, which can be used to examine the convergence behavior, see Section 20.3.4.

20.2 Mesh/Particle Mapping

Particles behave in a fundamentally different way than grid-based quantities. Lagrangian, or passive particles are essentially independent of the grid mesh and move along with the velocity field. Active particles may be located independently of mesh refinement. In either case, there is a need to convert grid-based quantities into similar attributes defined on particles, or vice versa. The method for interpolating mesh quantities to tracer particle positions must be consistent with the numerical method to avoid introducing systematic error. In the case of a finite-volume methods such as those used in FLASH4, the mesh quantities have cell-averaged rather than point values, which requires that the interpolation function for the particles also represent cell-averaged values. Cell averaged quantities are defined as

$$f_i\left(x\right) \equiv \frac{1}{\Delta x}\int_{x_{i-1/2}}^{x_{i-1/2}} f\left(x'\right)dx' \tag{20.15}$$

where i is the cell index and Δx is the spatial resolution. The mapping back and forth from the mesh to the particle properties are defined in the routines `Particles_mapFromMesh` and `Particles_mapToMeshOneBlk`.

Specifying the desired mapping method is accomplished by designating the `MAPMETHOD` in the Simulation `Config` file for each type of particle. See Section 6.6.1 for more details.

20.2.1 Quadratic Mesh Mapping

The quadratic mapping package defines an interpolation back and forth to the mesh which is second order. This implementation is primarily meant to be used with passive tracer particles.

To derive it, first consider a second-order interpolation function of the form

$$f\left(x\right) = A + B\left(x - x_i\right) + C\left(x - x_i\right)^2 \ . \tag{20.16}$$

Then integrating gives

$$\begin{aligned} f_{i-1} &= \frac{1}{\Delta x}\left[A + \frac{1}{2}B\left(x - x_i\right)^2\Big|_{x_{i-3/2}}^{x_{i-1/2}} + \frac{1}{3}C\left(x - x_i\right)^3\Big|_{x_{i-3/2}}^{x_{i-1/2}}\right] \\ &= A - B\Delta x + \frac{13}{12}C\Delta x^2 \ , \end{aligned} \tag{20.17}$$

$$\begin{aligned} f_{i} &= \frac{1}{\Delta x}\left[A + \frac{1}{2}B\left(x - x_i\right)^2\Big|_{x_{i-1/2}}^{x_{i+1/2}} + \frac{1}{3}C\left(x - x_i\right)^3\Big|_{x_{i-1/2}}^{x_{i+1/2}}\right] \\ &= A + \frac{1}{12}C\Delta x^2 \ , \end{aligned} \tag{20.18}$$

and

$$\begin{aligned} f_{i+1} &= \frac{1}{\Delta x}\left[A + \frac{1}{2}B\left(x - x_i\right)^2\Big|_{x_{i+1/2}}^{x_{i+3/2}} . + \frac{1}{3}C\left(x - x_i\right)^3\Big|_{x_{i-3/2}}^{x_{i-1/2}}\right] \\ &= A - B\Delta x + \frac{13}{12}C\Delta x^2 \ , \end{aligned} \tag{20.19}$$

We may write these as

$$\left[\begin{array}{c} f_{i+1} \\ f_i \\ f_{i-1} \end{array}\right] = \left[\begin{array}{ccc} 1 & -1 & \frac{13}{12} \\ 1 & 0 & \frac{1}{12} \\ 1 & 1 & \frac{13}{12} \end{array}\right]\left[\begin{array}{c} A \\ B\Delta x \\ C\Delta x^2 \end{array}\right] . \tag{20.20}$$

Inverting this gives expressions for A, B, and C,

$$\left[\begin{array}{c} A \\ B\Delta x \\ C\Delta x^2 \end{array}\right] = \left[\begin{array}{ccc} -\frac{1}{24} & \frac{13}{12} & -\frac{1}{24} \\ -\frac{1}{2} & 0 & \frac{1}{2} \\ \frac{1}{2} & -1 & \frac{1}{2} \end{array}\right]\left[\begin{array}{c} f_{i+1} \\ f_i \\ f_{i-1} \end{array}\right] . \tag{20.21}$$

In two dimensions, we want a second-order interpolation function of the form

$$f\left(x,y\right) = A + B\left(x - x_i\right) + C\left(x - x_i\right)^2 + D\left(y - y_j\right) + E\left(y - y_j\right)^2 + F\left(x - x_i\right)\left(y - y_j\right) \ . \tag{20.22}$$

In this case, the cell averaged quantities are given by

$$f_{i,j}(x,y) \equiv \frac{1}{\Delta y}\Delta x \int_{x_{i-1/2}}^{x_{i+1/2}} dx' \int_{y_{j-1/2}}^{x_{j-1/2}} dy' f(x',y') \ . \tag{20.23}$$

Integrating the 9 possible cell averages gives, after some algebra,

$$\begin{bmatrix} f_{i-1,j-1} \\ f_{i,j-1} \\ f_{i+1,j-1} \\ f_{i-1,j} \\ f_{i,j} \\ f_{i+1,j} \\ f_{i-1,j+1} \\ f_{i,j+1} \\ f_{i+1,j+1} \end{bmatrix} = \begin{bmatrix} 1 & -1 & \frac{13}{12} & -1 & \frac{13}{12} & 1 \\ 1 & 0 & \frac{1}{12} & -1 & \frac{13}{12} & 0 \\ 1 & 1 & \frac{13}{12} & -1 & \frac{13}{12} & -1 \\ 1 & -1 & \frac{13}{12} & 0 & \frac{1}{12} & 0 \\ 1 & 0 & \frac{1}{12} & 0 & \frac{1}{12} & 0 \\ 1 & 1 & \frac{13}{12} & 0 & \frac{1}{12} & 0 \\ 1 & -1 & \frac{13}{12} & 1 & \frac{13}{12} & -1 \\ 1 & 0 & \frac{1}{12} & 1 & \frac{13}{12} & 0 \\ 1 & 1 & \frac{13}{12} & 1 & \frac{13}{12} & 1 \end{bmatrix} \begin{bmatrix} A \\ B\Delta x \\ C\Delta x^2 \\ D\Delta y \\ E\Delta y^2 \\ F\Delta x\Delta y \end{bmatrix} . \tag{20.24}$$

At this point we note that there are more constraints than unknowns, and we must make a choice of the constraints. We chose to ignore the cross terms and take only the face-centered cells next to the cell containing the particle, giving

$$\begin{bmatrix} f_{i,j-1} \\ f_{i-1,j} \\ f_{i,j} \\ f_{i+1,j} \\ f_{i,j+1} \end{bmatrix} = \begin{bmatrix} 1 & 0 & \frac{1}{12} & -1 & \frac{13}{12} \\ 1 & -1 & \frac{13}{12} & 0 & \frac{1}{12} \\ 1 & 0 & \frac{1}{12} & 0 & \frac{1}{12} \\ 1 & 1 & \frac{13}{12} & 0 & \frac{1}{12} \\ 1 & 0 & \frac{1}{12} & 1 & \frac{13}{12} \end{bmatrix} \begin{bmatrix} A \\ B\Delta x \\ C\Delta x^2 \\ D\Delta y \\ E\Delta y^2 \end{bmatrix} . \tag{20.25}$$

Inverting gives

$$\begin{bmatrix} A \\ B\Delta x \\ C\Delta x^2 \\ D\Delta y \\ E\Delta y^2 \end{bmatrix} = \begin{bmatrix} -\frac{1}{24} & -\frac{1}{24} & \frac{7}{6} & -\frac{1}{24} & -\frac{1}{24} \\ 0 & -\frac{1}{2} & 0 & \frac{1}{2} & 0 \\ 0 & \frac{1}{2} & -1 & \frac{1}{2} & 0 \\ -\frac{1}{2} & 0 & 0 & 0 & \frac{1}{2} \\ \frac{1}{2} & 0 & -1 & 0 & \frac{1}{2} \end{bmatrix} \begin{bmatrix} f_{i,j-1} \\ f_{i-1,j} \\ f_{i,j} \\ f_{i+1,j} \\ f_{i,j+1} \end{bmatrix} . \tag{20.26}$$

Similarly, in three dimensions, the interpolation function is

$$f(x,y,z) = A + B(x-x_i) + C(x-x_i)^2 + D(y-y_j) + E(y-y_j)^2 + F(z-z_k) + G(z-z_k)^2 \ . \tag{20.27}$$

and we have

$$\begin{bmatrix} A \\ B\Delta x \\ C\Delta x^2 \\ D\Delta y \\ E\Delta y^2 \\ F\Delta z \\ G\Delta z^2 \end{bmatrix} = \begin{bmatrix} -\frac{1}{24} & -\frac{1}{24} & -\frac{1}{24} & \frac{5}{4} & -\frac{1}{24} & -\frac{1}{24} & -\frac{1}{24} \\ 0 & 0 & -\frac{1}{2} & 0 & \frac{1}{2} & 0 & 0 \\ 0 & 0 & \frac{1}{2} & -1 & \frac{1}{2} & 0 & 0 \\ 0 & -\frac{1}{2} & 0 & 0 & 0 & \frac{1}{2} & 0 \\ 0 & \frac{1}{2} & 0 & -1 & 0 & \frac{1}{2} & 0 \\ -\frac{1}{2} & 0 & 0 & 0 & 0 & 0 & \frac{1}{2} \\ \frac{1}{2} & 0 & 0 & -1 & 0 & 0 & \frac{1}{2} \end{bmatrix} \begin{bmatrix} f_{i,j,k-1} \\ f_{i,j-1,k} \\ f_{-i,j,k} \\ f_{i,j,k} \\ f_{i+1,j,k} \\ f_{i,j+1,k} \\ f_{i,j,k+1} \end{bmatrix} . \tag{20.28}$$

Finally, the above expressions apply only to Cartesian coordinates. In the case of cylindrical (r,z) coordinates, we have

$$\begin{aligned} f(r,z) = & \\ & A + B(r-r_i) + C(r-r_i)^2 + D(z-z_j) \\ & +E(z-z_j)^2 + F(r-r_i)(z-z_j) \ . \end{aligned} \tag{20.29}$$

and

$$\begin{bmatrix} A \\ B\Delta r \\ C\Delta r^{\frac{2}{6}} \\ D\Delta z \\ E\Delta z^2 \end{bmatrix} =$$

$$\begin{bmatrix} -\frac{1}{24} & -\frac{h_1-1}{24h_1} & \frac{7}{6} & -\frac{h_1-1}{24h1} & -\frac{1}{24} \\ 0 & -\frac{(7+6h_1)(h_1-1)}{3h_2} & \frac{2h_1}{3h2} & \frac{(7+6h_1)(h_1-1)}{3h_2} & 0 \\ 0 & \frac{\left(12h_1^2+12h_1-1\right)(h_1-1)}{h_1h_2} & -2\frac{12h_1^2-13}{h_2} & -\frac{\left(12h_1^2+12h_1-1\right)(h_1-1)}{h_1h_2} & 0 \\ -\frac{1}{2} & 0 & 0 & \frac{1}{2} & 0 \\ 0 & \frac{1}{2} & -1 & \frac{1}{2} & 0 \end{bmatrix} \begin{bmatrix} f_{i,j-1} \\ f_{i-1,j} \\ f_{i,j} \\ f_{i+1,j} \\ f_{i,j+1} \end{bmatrix} . \qquad (20.30)$$

20.2.2 Cloud in Cell Mapping

Other interpolation routines can be defined that take into account the actual quantities defined on the grid. These "mesh-based" algorithms are represented in FLASH4 by the Cloud-in-Cell mapping, where the interpolation to/from the particles is defined as a simple linear weighting from nearby grid points. The weights are defined by considering only the region of one "cell" size around each particle location; the proportional volume of the particle "cloud" corresponds to the amount allocated to/from the mesh. The `CIC` method can be used with both types of particles. When using it with active particles the MapToMesh methods should also be selected. In order to include the CIC method with passive particles, the `setup` command line option is `-with-unit=Particles/ParticlesMapping/CIC`. Two additional command line option `-with-unit=Particles/ParticlesMapping/MapToMesh` and `-with-unit=Grid/GridParticles/MapToMesh` are necessary when using the active particles. All of these command line options can be replaced by placing the appropriate `REQUIRES/REQUESTS` directives in the Simulation `Config` file.

20.3 Using the Particles Unit

The Particles unit encompasses nearly all aspects of Lagrangian particles. The exceptions are input/output the movement of related data structures between different blocks as the particles move from one block to another, and mapping the particle attributes to and from the grid.

Beginning with release of version 4 it is possible to add particles to a simulation during evolution, a new function `Particles_addNew` has been added to the unit's API for this purpose. It has been possible to include multiple different types of particles in the same simulation since release FLASH3.1. Particle types must be specified in the `Config` file of the Simulations unit setup directory for the application, and the syntax is explained in Section 6.6. At configuration time, the setup script parses the `PARTICLETYPE` specifications in the Config files, and generates an F90 file `Particles_specifyMethods.F90` that populates a data structure `gr_ptTypeInfo`. This data structure contains information about the method of initialization and interpolation methods for mapping the particle attributes to and from the grid for each included particle type. Different time integration schemes are applied to active and passive particles. However, in one simulation, all active particles are integrated using the same scheme, regardless of how many active types exists. Similarly, only one passive integration scheme is used. The added complexity of multiple particle types allows different methods to be used for initialization of particles positions and their mapping to and from the grid quantities. Because several different implementations of each type of functionality can co-exist in one simulation, there are no defaults in the `Particles` unit `Config` files. These various functionalities are organized into different subunits; a brief description of each subunit is included below and further expanded in subsections in this chapter.

- The `ParticlesInitialization` subunit distributes a given set of particles through the spatial domain at the simulation startup. Some type of spatial initialization is always required; the functionality is provided by `Particles_initPositions`. The users of active particles typically have their own custom initialization. The following two implementations of initialization techniques are included in the FLASH4 distribution (they are more likely to used with the passive tracer particles):

`Lattice` distributes particles regularly along the axes directions throughout a subsection of the physical grid.

`WithDensity` distributes particles randomly, with particle density being proportional to the grid gas density.

Users have two options for implementing custom initialization methods. The two files involved in the process are: `Particles_initPositions` and pt_initPositions. The former does some housekeeping such as allowing for inclusion of one of the available methods along with the user specified one, and assigning tags at the end. A user wishing to add one custom method with no constraints on tags etc is advised to implement a custom version of the latter. This approach allows the user to focus the implementation on the placement of particles only. Users desirous of refining the grid based on particles count during initialiation should see the setup `PoisParticles` for an example implementation of the Particles_initPositions routine. If more than one implementation of pt_initPositions is desired in the same simulation then it is necessary to implement each one separately with different names (as we do for tracer particles: pt_initPositionsLattice and pt_initPositionsWithDensity) in their simulation setup directory. In addition, a modified copy of Particles_initPostions, which calls these new routines in the loop over types, must also be placed in the same directory.

- The `ParticlesMain` subunit contains the various time-integration options for both active and passive particles. A detailed overview of the different schemes is given in Section 20.1.

- The `ParticlesMapping` subunit controls the mapping of particle properties to and from the grid. FLASH currently supplies the following mapping schemes:

  `Cloud-in-cell` (`ParticlesMapping/meshWeighting/CIC`), which weights values at nearby grid cells; and

  `Quadratic` (`ParticlesMapping/Quadratic`), which performs quadratic interpolation.

  Some form of mapping must always be included when running a simulation with particles. As mentioned in Section 20.2 the quadratic mapping scheme is only available to map *from* the grid quantities to the corresponding particle attributes. Since active particles require the same mapping scheme to be used in mapping to and from the mesh, they cannot use the quadratic mapping scheme as currently implemented in FLASH4. The CIC scheme may be used by both the active and passive particles.

  For active particles, we use the mapping routines to assign particles' mass to the particle density grid-based solution variable (`PDEN_VAR`). This mapping is the initial step in the particle-mesh (PM) technique for evaluating the long range gravitational force between all particles. Here, we use the particle mapping routine `Particles_mapToMeshOneBlk` to "smear" the particles' attribute over the cells of a temporary array. The temporary array is an input argument which is passed from the grid mapping routine `Grid_mapParticlesToMesh`. This encapsulation means that the particle mapping routine is independent of the current state of the grid, and is not tied to a particular `Grid` implementation. For details about the task of mapping the temporary array values to the cells of the appropriate block(s), please see Section 8.9.2. New schemes can be created that "smear" the particle across many more cells to give a more accurate `PDEN_VAR` distribution, and thus a higher quality force approximation between particles. Any new scheme should implement a customized version of the `pt_assignWeights` routine, so that it can be used by the `Particles_mapToMeshOneBlk` routine during the map.

- The `ParticlesForces` subunit implements the long and short range forces described in Equation (20.3) in the following directories:

  – `longRange` collects different long-range force laws (requiring elliptic solvers or the like and dependent upon all other particles);

  – `shortRange` collects different short-range force laws (directly summed or dependent upon nearest neighbors only).

Currently, only one long-range force law (gravitation) with one force method (particle-mesh) is included with FLASH. Long-range force laws are contained in the `Particles/ParticlesForces/longRange`, which requires that the `Gravity` unit be included in the code. In the current release, no `shortRange` implementation of `ParticlesForces` is supplied with FLASH. However, note that the sink particle implementation described below in Section 20.4 includes directly computed particle–particle forces.

After particles are moved during time integration or by forces, they may end up on other blocks within or without the current processor. The redistribution of particles among processors is handled by the `GridParticles` subunit, as the algorithms required vary considerably between the grid implementations. The boundary conditions are also implemented by the GridParticles unit. See Section 8.9 for more details of these redistribution algorithms. The user should include the option `-with-unit=Grid/GridParticles` on the setup line, or `REQUIRES Grid/GridParticles` in the Config file.

In addition, the input-output routines for the Particles unit are contained in a subunit `IOParticles`. Particles are written to the main checkpoint files. If the user desires, a separate output file can be created which contains only the particle information. See Section 20.3.3 below as well as Section 9.2.3 for more details. The user should include the option `-with-unit=IO/IOParticles` on the setup line, or `REQUIRES IO/IOParticles` in the Config file.

In FLASH4, the initial particle positions can be used to construct an appropriately refined grid, i.e. more refined in places where there is a clustering of particles. To use this feature the `flash.par` file must include: `refine_on_particle_count=.true.` and `max_particles_per_blk=[some value]`. Please be aware that FLASH will abort if the criterion is too demanding. To overcome the abort, specify a less demanding criterion, or increase the value of `lrefine_max`.

20.3.1 Particles Runtime Parameters

There are several general runtime parameters applicable to the `Particles` unit, which affect every implementation. The variable `useParticles` obviously must be set equal to `.true.` to utilize the Particles unit. The time stepping is controlled with `pt_dtFactor`; a value less than one ensures that particles will not step farther than one entire cell in any given time interval. The `Lattice` initialization routines have additional parameters. The number of evenly spaced particles is controlled in each direction by `pt_numX` and similar variables in Y and Z. The physical range of initialization is controlled by `pt_initialXMin` and the like. Finally, note that the output of particle properties to special particle files is controlled by runtime parameters found in the `IO` unit. See Section 9.2.3 for more details.

20.3.2 Particle Attributes

By default, particles are defined to have eight real properties or attributes: 3 positions in x,y,z; 3 velocities in x,y,z; the current block identification number; and a tag which uniquely identifies the particle. Additional properties can be defined for each particle. For example, active particles usually have the additional properties of mass and acceleration (needed for the integration routines, see Table Table 20.1). Depending upon the simulation, the user can define particle properties in a manner similar to that used for mesh-based solution variables. To define a particle attribute, add to a `Config` file a line of the form

`PARTICLEPROP` *property-name*

For attributes that are meant to merely sample and record the state of certain mesh variables along trajectories, FLASH can automatically invoke interpolation (or, in general, some map method) to generate attribute values from the appropriate grid quantities. (For passive tracer particles, these are typically the only attributes beyond the default set of eight mentioned above.) The routine `Particles_updateAttributes` is invoked by FLASH at appropriate times to effect this mapping, namely before writing particle data to checkpoint and particle plot files. To direct the default implementation of `Particles_updateAttributes` to act as desired for tracer attributes, the user must define the association of the particle attribute with the appropriate mesh variable by including the following line in the `Config` file:

`PARTICLEMAP TO` *property-name* `FROM VARIABLE` *variable-name*

These particle attributes are carried along in the simulation and output in the checkpoint files. At runtime, the user can specify the attributes to output through runtime parameters `particle_attribute_1`, `particle_attribute_2`, etc. These specified attributes are collected in an array by the `Particles_init` routine. This array in turn is used by `Particles_updateAttributes` to calculate the values of the specified attributes from the corresponding mesh quantities before they are output.

20.3.3 Particle I/O

Particle data are written to and read from checkpoint files by the I/O modules (Section 9.1). For more information on the format of particle data written to output files, see Section 9.9.1 and Section 9.9.2.

Particle data can also be written out to the `flash.dat` file. The user should include a local copy of `IO_writeIntegralQuantities` in their Simulation directory. The `Orbit` test problem supplies an example `IO_writeIntegralQuantities` routine that is useful for writing individual particle trajectories to disk at every timestep.

There is also a utility routine `Particles_dump` which can be used to dump particle output to a plain text file. An example of usage can be found in `Particles_unitTest`. Output from this routine can be read using the fidlr routine `particles_dump.pro`.

20.3.4 Unit Tests

The unit tests provided for `Particles` exercise the `Particles_advance` methods for tracer particles. Tests under `Simulation/SimulationMain/unitTest/ParticlesAdvance` can be used to examine and compare convergence behavior of various time integration schemes. The tests compare numerical and analytic solutions for a problem (with a given velocity field) where analytic solutions can be computed.

Currently only one `ParticlesAdvance` test is provided. It is designed to be easily modified by replacing a few source files that contain implementations of the equation and the analytic solution. The use the test, configure it with a command like

```
./setup -auto -1d unitTest/ParticlesAdvance/HomologousPassive \
                  -unit=Particles/ParticlesMain/passive/EstiMidpoint2
```

and replace `EstiMidpoint2` with one of the other available methods (or omit the option to get the default method), see Section 20.1.3. Add other options as desired.

For `unitTest/ParticlesAdvance/HomologousPassive`,

```
./setup -auto -1d unitTest/ParticlesAdvance/HomologousPassive +ug -nxb=80
```

is recommended to get started.

When varying the test, the following runtime parameters defined for `Simulation/SimulationMain/unitTest/ParticlesAdvance` will probably need to be adjusted:

`PARAMETER` `sim_schemeOrder` `INTEGER 2` — The order of the integration scheme. This should probably always be either 1 or 2.

`PARAMETER` `sim_maxTolCoeff0` `REAL 1.0e-8` — Zero-th order error coefficient C_0, used for convergence criterion if `sim_schemeOrder`= 0.

`PARAMETER` `sim_maxTolCoeff1` `REAL 0.0001` — First order error coefficient C_1, used for convergence criterion if `sim_schemeOrder`= 1.

`PARAMETER` `sim_maxTolCoeff2` `REAL 0.01` — Second order error coefficient C_2, used for convergence criterion if `sim_schemeOrder`= 2.

A test for order k is considered successful if the following criterion is satisfied:

$$\texttt{maxError} \leq C_k \times \texttt{maxActualDt}^k ,$$

where `maxError` is the maximum absolute error between numerical and analytic solution for any particle that was encountered during a simulation run, and `maxActualDt` is the maximum time step Δt used in the run.

The appropriate runtime parameters of various units, in particular `Driver`, `Particles`, and `Grid`, should be used to control the desired simulation run. In particular, it is recommended to vary `dtmax` by several orders of magnitude (over a range where it directly determines `maxActualDt`) for a given test in order to examine convergence behavior.

20.4 Sink Particles

20.4.1 Basics of Sink Particles

Sink particles are required in collapse simulations to model dense core, star, or black hole formation and accretion. Using sink particles solves two main problems in collapse calculations:

1. The physical length scale associated with the collapse, the Jeans length,

$$\lambda_{\mathrm{J}} = \sqrt{\frac{\pi c_{\mathrm{s}}^2}{G\rho}} \tag{20.31}$$

   decreases with increasing gas density ρ (here, G is the gravitational constant and c_{s} the sound speed). To avoid artificial fragmentation, the Jeans length must be resolved with at least 4 grid cells (Truelove et al. 1997, ApJ 489, L179). More recent calculations show that a minimum of 32 grid cells is required to resolve the kinetic energy in rotational motions inside the Jeans volume and to resolve minimum turbulent MHD dynamo action (Sur et al. 2010, ApJ 721, L134; Federrath et al. 2011, ApJ 731, 62). The FLASH sink particle module automatically refines the AMR grid based on the Jeans length (controlled by runtime parameters `refineOnJeansLength`, `jeans_ncells_ref`, and `jeans_ncells_deref`). However, once the highest level of the AMR hierarchy is reached, sink particles must be created to avoid artificial fragmentation when the Jeans length drops further during the collapse.

2. The typical timescale for collapsing objects is the freefall time, $t_{\mathrm{ff}} = \sqrt{3\pi/(32G\rho)}$. With increasing gas density, this timescale becomes shorter and shorter, which means that the code will literally grind to a halt during runaway collapse, as time steps become shorter and shorter. The first object going into freefall collapse thus determines the time step of the whole calculation, such that following the formation of a star cluster would be impossible. To avoid these problems, the gas in regions that are in a state of runaway collapse are replaced by sink particles.

20.4.2 Using the Sink Particle Unit

To include sink particles, specify `REQUIRES Particles/ParticlesMain/active/Sink` in the simulation `Config` file. This automatically includes all required subunits for the sink particles. Currently, sink particles require a Paramesh 4 `Grid` implementation and Poisson gravity. Currently, various subunits and implementation directories of the `Particles` unit and are also included automatically. Table 20.6 lists all runtime parameters of the sink particle module. The default values of these parameters should be ok in most simulations, except `sink_density_thresh`, `sink_accretion_radius`, and `sink_softening_radius`. Those three parameters have to be adopted to the resolution and physics of a given simulation.

First, the sink particle accretion radius, r_{acc} (`sink_accretion_radius`) should be calculated, based on the minimum cell size Δx for a given simulation. The recommended value is $r_{\mathrm{acc}} = 2.5\Delta x$. If sink particles are included, the code will print a message to the standard output, stating the number of cells that a chosen sink accretion radius corresponds to. The recommended value for the sink particle softening radius (`sink_softening_radius`) is to set it equal to the accretion radius.

In order to avoid artificial fragmentation, the gas density on the AMR grid must not exceed a critical density ρ_{thresh} in regions of gravitational collapse (Truelove et al. 1997). This density is related to the smallest resolvable Jeans length λ_{J} on the highest level of the AMR hierarchy. The density threshold ρ_{thresh} (`sink_density_thresh`) is obtained by solving the definition of the Jeans length, Equation (20.31) for ρ,

$$\rho_{\mathrm{thresh}} = \frac{\pi c_{\mathrm{s}}^2}{G\lambda_{\mathrm{J}}^2} = \frac{\pi c_{\mathrm{s}}^2}{4Gr_{\mathrm{acc}}^2}\ . \tag{20.32}$$

This equation relates the sink particle accretion radius to the sink particle density threshold and depends on the thermodynamics (sound speed) of a given simulation. Since the Jeans length should be resolved with at least 4 grid cells (Truelove et al. 1997), the sink particle accretion radius r_{acc} must not be smaller than 2 grid cells. The accretion radius is thus determined by the smallest linear cell size Δx of the AMR grid. As recommended above, setting $r_{\mathrm{acc}} \simeq 2.5\Delta x$ satisfies the Truelove criterion, because the Jeans length $\lambda_{\mathrm{J}} = 2r_{\mathrm{acc}}$ is thus resolved with 5 grid cells on the top level of the AMR hierarchy.

Please cite Federrath et al. (2010, ApJ 713, 269) if you are using this unit.

20.4.3 The Sink Particle Method

For technical details and tests of the FLASH sink particle unit, see Federrath et al. (2010, ApJ 713, 269) and Federrath et al. (2011, IAUS 270, 425). We only summarize here the most important aspects of the implementation.

Before a sink particle is created, we define a spherical control volume with the accretion radius r_{acc} around each cell that exceeds the resolution-dependent density threshold, ρ_{thresh} given by Equation (20.32), and check whether the gas in this control volume

- is on the highest level of refinement,
- is converging ($\nabla \cdot \mathbf{v} < 0$; i.e., has negative radial velocity),
- has a central gravitational potential minimum,
- is gravitationally bound ($|E_{\mathrm{grav}}| > E_{\mathrm{int}} + E_{\mathrm{kin}} + E_{\mathrm{mag}}$),
- is gravitationally unstable (Jeans-unstable),
- and is not within the accretion radius of an existing sink particle.

These checks are designed to avoid spurious sink particle formation and to trace only truly collapsing and star-forming gas. As soon as a sink particle is created, it can gain further mass by accretion from the AMR grid, if this gas is inside the sink particle accretion radius and is bound and collapsing towards the sink particle. If the accretion radii of multiple sink particles overlap, the gas of a given cell is accreted onto the sink particle to which the gas is most strongly bound.

We take all contributions to the gravitational interactions between the gas on the grid and the sink particles into account. Those interactions are

1. GAS–GAS (handled by either the multigrid or the tree Poisson solver)
2. GAS–SINKS (computed by direct summation over all particles and grid cells)
3. SINKS–GAS (computed by direct summation over all particles and grid cells)
4. SINKS–SINKS (computed by direct N-body summation over all sink particles).

We note that all interactions including sink particles (GAS–SINKS, SINKS–GAS, SINKS–SINKS) do not require the Poisson solver or any particle–grid mapping procedure. Since these are all computed by direct summation, computational costs can become quite expensive once the number of sink particles reaches thousands and more, but is significantly more accurate than mapping procedures. In fact, a previous implementation used interpolation of sink particle masses back onto the grid and employing the Poisson solver to compute all interactions. This resulted in very smooth gravitational interactions that made it impossible to follow close orbits and highly eccentric encounters of multiple (two and more) sink particles, in particular for the sink–sink interactions. Thus, the current implementation of sink particles is designed to follow a maximum of a few thousand particles. Linear and spline softening of the gravitational forces for extremely close encounters of multiple sink particles are implemented. By default, linear softening is used for gas–sinks and sinks–gas interactions (`sink_softening_type_gas`), motivated by an almost uniform gas density inside the sink particle radius. Spline softening is used for sink–sink interactions (`sink_softening_type_sinks`), as it is more suitable to follow N-body dynamics. Softening is only applied inside the sink softening radius (`sink_softening_radius`). A second-order accurate leapfrog integrator is used to advance the sink

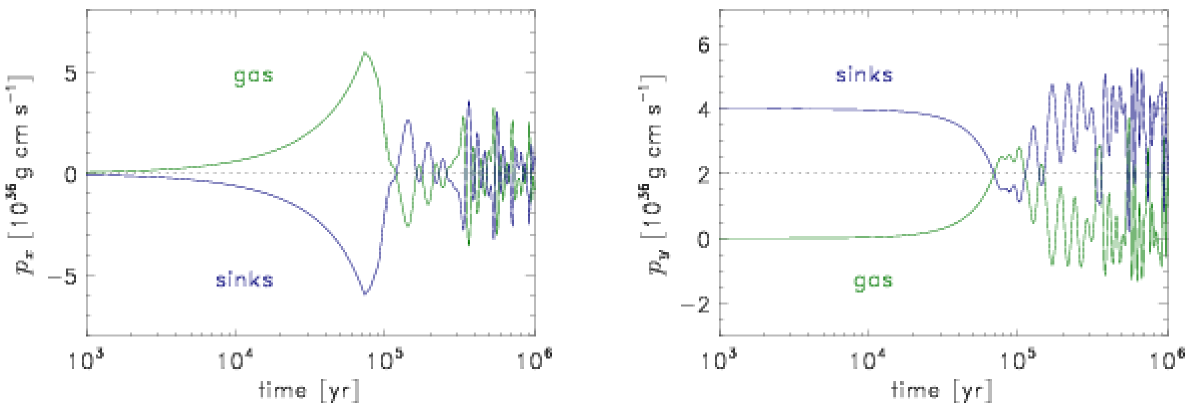

Figure 20.3: Sink particle unit test to check momentum conservation during sink particle creation, accretion, and eccentric orbits.

particles. For cosmological simulations, a cosmological version of the leapfrog integrator is available (see `sink_integrator`). The sink particles are fully integrated into the MPI parallelization of the FLASH code. Any split or unsplit solver for hydro or MHD (in which case the bound state check includes the contribution of the magnetic energy) is supported.

20.4.4 Sink Particle Unit Test

To invoke the sink particle unit test, use `./setup unitTest/SinkMomTest -auto -3d`. This initializes a momentum conservation test. An initially uniform cloud with radius 0.025 pc and density $10^{-18}\,\mathrm{g\,cm^{-3}}$ at rest starts collapsing and forms a sink particle. An initial sink particle with $0.1\,M_\odot$ and initial momentum $p_y = 4 \times 10^{36}\,\mathrm{g\,cm\,s^{-1}}$ in positive y-direction is also present. The purpose of this test is to see how well the total x-momentum p_x and the total y-momentum p_y are conserved. This test is particularly suitable, because it involves gas collapse, sink particle creation, accretion, more than one sink particle, and thus all gravitational interactions (gas–gas, gas–sinks, sinks–gas, sinks–sinks), as well as close eccentric orbits of the two sink particles. Figure 20.3 shows p_x and p_y as a function of time for both sink particles and gas separately. The symmetry between sink and gas momenta shows that momentum is well conserved for several orbits. Figure 20.3 can be reproduced with the IDL and Python tools in `/source/Simulation/SimulationMain/unitTest/SinkMomTest/utils/` by running the IDL script `plot_mom_sinks.pro`.

Table 20.6: Runtime parameters for the sink particle module.

Variable	Type	Default	Description
`useSinkParticles`	BOOLEAN	.false.	switch sinks on/off
`sink_density_thresh`	REAL	1.0e-14	density threshold for sink creation and accretion
`sink_accretion_radius`	REAL	1.0e14	creation and accretion radius
`sink_softening_radius`	REAL	1.0e14	gravitational softening radius
`sink_softening_type_gas`	STRING	"linear"	sink–gas softening type (options: "linear", "spline")
`sink_softening_type_sinks`	STRING	"spline"	sink–sink softening type (options: "linear", "spline")
`sink_integrator`	STRING	"leapfrog"	sink particle time integrator (options: "euler", "leapfrog", "leapfrog_cosmo")
`sink_dt_factor`	REAL	0.5	time step safety factor (≤ 0.5)
`sink_subdt_factor`	REAL	0.01	time step safety factor for sink–sink subcycling (≤ 0.5)
`sink_convergingFlowCheck`	BOOLEAN	.true.	creation check for converging gas flow
`sink_potentialMinCheck`	BOOLEAN	.true.	creation check for gravitational potential minimum
`sink_jeansCheck`	BOOLEAN	.true.	creation check for Jeans instability
`sink_negativeEtotCheck`	BOOLEAN	.true.	creation check for gravitationally bound gas
`sink_GasAccretionChecks`	BOOLEAN	.true.	check for bound and converging state before gas accretion
`sink_merging`	BOOLEAN	.false.	switch for sink particle merging
`sink_offDomainSupport`	BOOLEAN	.false.	support for sink particles to remain active when leaving the grid domain (in case of outflow boundary conditions)
`sink_AdvanceSerialComputation`	BOOLEAN	.true.	use the global sink particle array for time advancement (to greatly speed up computation of sink–sink interaction)
`pt_maxSinksPerProc`	INTEGER	100	number of sinks per processor
`refineOnSinkParticles`	BOOLEAN	.true.	sinks must be on highest AMR level
`refineOnJeansLength`	BOOLEAN	.true.	switch for refinement on Jeans length
`jeans_ncells_ref`	REAL	32.0	number of cells for Jeans length refinement
`jeans_ncells_deref`	REAL	64.0	number of cells for Jeans length de-refinement

Chapter 21

Cosmology Unit

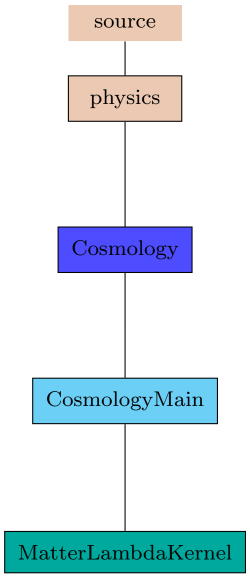

Figure 21.1: The `Cosmology` unit tree.

The `Cosmology` unit solves the Friedmann equation for the scale factor in an expanding universe, applies a cosmological redshift to the hydrodynamical quantities, and supplies library functions for various routine cosmological calculations needed by the rest of the code for initializing, performing, and analyzing cosmological simulations.

21.1 Algorithms and Equations

The `Cosmology` unit makes several assumptions about the interpretation of physical quantities that enable any hydrodynamics or materials units written for a non-expanding universe to work unmodified in a cosmological context. All calculations are assumed to take place in comoving coordinates $\mathbf{x} = \mathbf{r}/a$, where $\mathbf{r}$ is a proper position vector and $a(t)$ is the time-dependent cosmological scale factor. The present epoch is defined to correspond to $a = 1$; in the following discussion we use $t = t_0$ to refer to the age of the Universe at the present epoch. The gas velocity $\mathbf{v}$ is taken to be the comoving peculiar velocity $\dot{\mathbf{x}}$. The comoving gas density, pressure, temperature, and internal energy are defined to be

$$\begin{aligned} \rho &\equiv a^3\tilde{\rho} \\ p &\equiv a\tilde{p} \\ T &\equiv \frac{\tilde{T}}{a^2} \\ \rho\epsilon &\equiv a\tilde{\rho}\tilde{\epsilon}\ . \end{aligned} \tag{21.1}$$

The quantities marked with a tilde, such as $\tilde{\rho}$, are the corresponding "proper" or physical quantities. Note that, in terms of comoving quantities, the equation of state has the same form as for the proper quantities in noncomoving coordinates. For example, the perfect-gas equation of state is

$$\rho\epsilon = \frac{p}{\gamma - 1} = \frac{\rho k T}{(\gamma - 1)\mu}\ . \tag{21.2}$$

With these definitions, the Euler equations of hydrodynamics can be written in the form

$$\frac{\partial \rho}{\partial t} + \nabla \cdot (\rho \mathbf{v}) = 0 \tag{21.3}$$

$$\frac{\partial \rho \mathbf{v}}{\partial t} + \nabla \cdot (\rho \mathbf{v}\mathbf{v}) + \nabla p + 2\frac{\dot{a}}{a}\rho\mathbf{v} + \rho\nabla\phi = 0 \tag{21.4}$$

$$\frac{\partial \rho E}{\partial t} + \nabla \cdot [(\rho E + p)\mathbf{v}] + \frac{\dot{a}}{a}[(3\gamma - 1)\rho\epsilon + 2\rho v^2] + \rho\mathbf{v}\cdot\nabla\phi = 0 \tag{21.5}$$

$$\frac{\partial \rho\epsilon}{\partial t} + \nabla \cdot [(\rho\epsilon + p)\mathbf{v}] - \mathbf{v}\cdot\nabla p + \frac{\dot{a}}{a}(3\gamma - 1)\rho\epsilon = 0\ . \tag{21.6}$$

Here E is the specific total energy, $\epsilon + \frac{1}{2}v^2$, and γ is the effective ratio of specific heats. The `Cosmology` unit applies the terms involving $\dot{a}$ via the `Cosmology_redshiftHydro` routine.

The comoving potential ϕ in the above equations is the solution to the Poisson equation in the form

$$\nabla^2\phi = \frac{4\pi G}{a^3}(\rho - \bar{\rho})\ , \tag{21.7}$$

where $\bar{\rho}$ is the comoving mean matter density. Note that, because of the presence of a in (21.7), the gravity units must explicitly divide their source terms by a^3.

Units like the `Gravity` unit, which require the scale factor or the redshift z ($a = (1 + z)^{-1}$), can obtain the redshift via `Cosmology_getRedshift`, and use the previous relation to obtain the scaling factor. The time represented by a cosmological redshift can be obtained by a call to `Cosmology_redshiftToTime` and passing it a cosmological redshift. Note also that if a collisionless matter component (*e.g.*particles) is also present, its density must be added to the gas density on the right-hand side of (21.7). Accounting for particle masses in density is handled by the `Gravity` unit.

The comoving mean matter density is defined in terms of the critical density $\rho_{\rm crit}$ by

$$\begin{aligned} \bar{\rho} &\equiv \Omega_m\rho_{\rm crit} \\ \rho_{\rm crit} &\equiv \frac{3H^2}{8\pi G}\ . \end{aligned} \tag{21.8}$$

The Hubble parameter $H(t)$ [to be distinguished from the Hubble "constant" $H_0 \equiv H(t_0)$] is given by the Friedman equation

$$H^2(t) \equiv \left(\frac{\dot{a}}{a}\right)^2 = H_0^2\left(\frac{\Omega_m}{a^3} + \frac{\Omega_r}{a^4} + \Omega_\Lambda - \frac{\Omega_c}{a^2}\right)\ . \tag{21.9}$$

Here Ω_m, Ω_r, and Ω_Λ are the present-day densities, respectively, of matter, radiation, and cosmological constant, divided by $\rho_{\rm crit}$. The contribution of the overall spatial curvature of the universe is given by

$$\Omega_c \equiv \Omega_m + \Omega_r + \Omega_\Lambda - 1\ . \tag{21.10}$$

The Cosmology_solveFriedmannEqn routine numerically solves the Friedmann equation to obtain the scale factor and its rate of change as functions of time. In principle, any good ODE integrator can be used; the `csm_integrateFriedman` subroutine uses a fourth-order Runge-Kutta method to integrate the Friedmann equation under the assumption that $\Omega_r = 0$. Subunits can also use analytic solutions where appropriate.

Redshift terms for particles are handled separately by the appropriate time integration subunits of the `Particles` unit. For an example, see the `LeapfrogCosmo` implementation of the ParticlesMain subunit in Section 20.1.1.

21.2 Using the Cosmology unit

To include cosmological expansion in your FLASH executable, include the line

```
REQUESTS physics/Cosmology/
```

in your setup's `Config` file. At present the Cosmology unit in FLASH4 is built around the `MatterLambda-Kernel`. This kernel assumes the contribution of radiation to be negligible in comparison with those of matter and the cosmological constant.

The runtime parameters available with the `Cosmology` unit are described in Table 21.1. Note that the total effective mass density is not explicitly specified but is inferred from the sum of the `OmegaMatter`, `OmegaRadiation`, and `CosmologicalConstant` parameters. The `MaxScaleChange` parameter sets the maximum allowed fractional change in the scale factor a during a single timestep. This behavior is enforced by the Cosmology_computeDt routine. The default value is set to the system's `HUGE` value for a double precision real floating point value to avoid interfering with non-cosmological simulations.

Table 21.1: Runtime parameters used with the `Cosmology` unit.

Parameter	Type	Default	Description
`useCosmology`	BOOLEAN	.true.	True if cosmology is to be used in this simulation
`OmegaMatter`	REAL	0.3	Ratio of total mass density to critical density at the present epoch (Ω_m)
`OmegaBaryon`	REAL	0.05	Ratio of baryonic (gas) mass density to critical density at the present epoch; must be $\leq$ `OmegaMatter` (Ω_b)
`CosmologicalConstant`	REAL	0.7	Ratio of the mass density equivalent in the cosmological constant to the critical density at the present epoch (Ω_Λ)
`OmegaRadiation`	REAL	5×10^{-5}	Ratio of the mass density equivalent in radiation to the critical density at the present epoch (Ω_r)
`HubbleConstant`	REAL	2.1065×10^{-18}	Value of the Hubble constant H_0 in sec^{-1}
`MaxScaleChange`	REAL	`HUGE(1.)`	Maximum permitted fractional change in the scale factor during each timestep

The `MatterLambdaKernel` supplies a number of functions and routines that are helpful in initializing, performing, and analyzing cosmological simulations. They should be accessed through the wrapper functions shown below.

- Cosmology_cdmPowerSpectrum
  Return the present-day cold dark matter power spectrum as a function of a given wavenumber. The `MatterLambdaKernel` provides a fit to this power spectrum from Bardeen *et al.* (1986), which assumes baryons do not make a significant contribution to the mass density. Other fits are available; see *e.g.*, Hu and Sugiyama (1996) or Bunn and White (1997).

- `Cosmology_computeVariance`
  Given an array of comoving length scales and a processed power spectrum, compute the linear variance $(\delta M/M)^2$ at the present epoch. A top-hat filter is applied in Fourier-space as a smoothing kernel.

- `Cosmology_computeDeltaCrit`
  This subroutine computes the linear overdensity at turnaround in the spherical collapse model. For more information, see the appendix of Lacey and Cole (1993).

- `Cosmology_redshiftToTime`
  Compute the age of the Universe corresponding to a cosmological redshift .

- `Cosmology_massToLength`
  Given a mass scale, return the corresponding comoving diameter of a sphere containing the given amount of mass.

21.3 Unit Test

FLASH provides a unit test for checking the basic functionality of the Cosmology module. It tests the unit's generated cosmological scaling factor, cosmological redshift, and the time calculated from that redshift against an analytical solution of these quantities.

The test is run with the following parameters:

`OmegaMatter` = 1.0
`OmegaLambda` = 0.0
`OmegaBaryon` = 1.0
`OmegaRadiation` = 0.0
`HubbleConstant` = $1.62038 \times 10^{-18}\text{sec}^{-1}$ (50 km/s/Mpc)

The Cosmological scaling factor is related to time by the equation:

$a(t) = \left(\frac{t}{t_0}\right)^{2/3}$

where $t_0 = \frac{2}{3H_0}$, H_0 is the HubbleConstant and is related to the cosmological redshift by the equation $z(t) = \frac{1}{a(t)} - 1$. The change in time is a uniform step, and by comparing the analytical and code results at time t, we can see if the Friedmann equations are correctly integrated by the `Cosmology` unit, and that the results fall within a tolerance set in `Cosmology_unitTest`.

Chapter 22

Material Properties Units

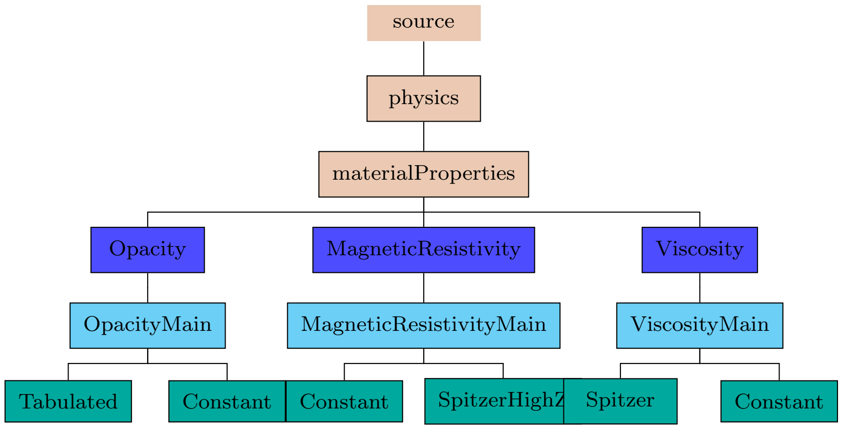

Figure 22.1: The `materialProperties` directory with Opacity, MagneticResistivity and Viscosity subunits.

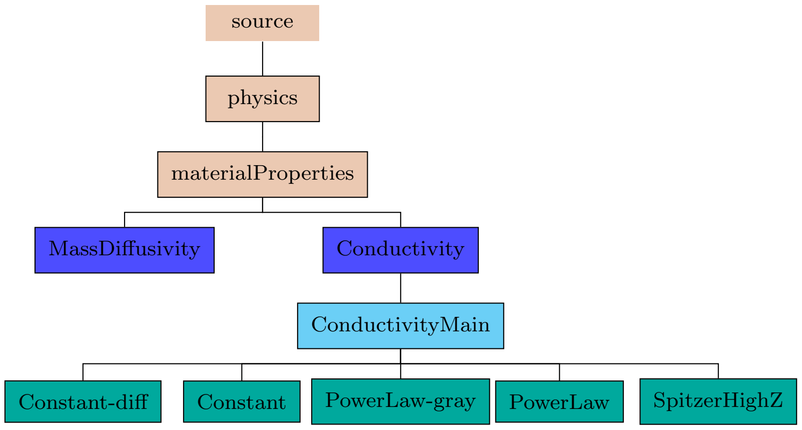

Figure 22.2: The `materialProperties` directory with MassDiffusivity and Conductivity subunits.

FLASH Transition

The set of implementations of the material properties units provided with FLASH is not comprehensive. For Heat Conductivity and Viscosity, we provide implementations for effects with constant coefficients; these can be used as models for implementing effects that follow other laws. For MassDiffusivity, only no-operation stubs are provided. A routine that calculates constant magnetic resistivity and viscosity is provided in the MagneticResistivity unit and can be used in non-ideal magnetohydrodynamics simulations. Several add-on capabilities are being made available to the users from the Download Page on Flash Website.

22.1 Thermal Conductivity

The Conductivity unit implements a prescription for computing thermal conductivity coefficients used by the Hydro PPM, the unsplit hydro and MHD solvers. The FLASH4 release provides three implementations:

- Constant for heat conduction with a constant isochoric conductivity;
- Constant-diff for heat conduction with a constant coefficient of diffusion.
- SpitzerHighZ which is used for electron thermal conduction. Note that this model can be used with any material.
- LeeMore is another model for electron thermal conduction. Like SpitzerHighZ, it can also be used with any material. The LeeMore model is based on Lee & More (Phys. Fluids, 1984) and should be more accurate than SpitzerHighZ.

To use thermal conductivity in a FLASH4 simulation, the runtime parameter useConductivity must be set to .true. SpitzerHighZ and LeeMore are the most useful options for realistic HEDP simulations. See Section 30.7.5 for an example of how the SpitzerHighZ implementation is used in a realistic simulation.

The Spitzer conductivity implemented here is shown in (22.1). It is consistent with the value given in (Atzeni, 2004).

$$K_{\text{ele}} = \left(\frac{8}{\pi}\right)^{3/2} \frac{k_B^{7/2}}{e^4\sqrt{m_{\text{ele}}}} \left(\frac{1}{1+3.3/\bar{z}}\right) \frac{T_{\text{ele}}^{5/2}}{\bar{z}\ln\Lambda_{ei}} \tag{22.1}$$

where:

- K_{ele} is the electron conductivity
- k_B is the Boltzmann constant
- e is the electron charge
- m_{ele} is the mass of an electron
- $\bar{z}$ is the average ionization as computed by the EOS
- T_{ele} is the electron temperature
- $\ln\Lambda_{ei}$ is the Coulomb logarithm associated with electron-ion collisions and is discussed in Section 17.5.

At high temperatures, LeeMore and SpitzerHighZ are nearly identical aside from differences in the treatments of the Coulomb logarithm (Section 17.5.2). At lower temperatures there can be substantial differences between LeeMore and SpitzerHighZ and generally the LeeMore model should be much more accurate. This is because SpitzerHighZ incorrectly assumes that the material remains a classical plasma even at low temperatures. In practice, however, it is often the case in HEDP simulations that the laser heating will rapidly bring the material to the temperatures where the classical plasma approximation is valid and the differences between `SpitzerHighZ` and `LeeMore` will be minimal.

Users are encouraged to experiment with using both the `SpitzerHighZ` and `LeeMore` models in HEDP simulations in order to determine the sensitivity of the results to the electron thermal conductivity model. Although `LeeMore` should always be much more accurate than `SpitzerHighZ`, there may be cases where the `LeeMore` model may still not be accurate enough for a specific application. It is well known that some materials do not agree well with the `LeeMore` prediction in certain density-temperature regimes (e.g. Desjarlais et al. 2002).

22.2 Magnetic Resistivity

The magnetic resistivity unit `source/physics/materialProperties/MagneticResistivity` provides routines that computes magnetic resistivity η (and thus viscosity ν_m) for a mixture of fully ionized gases used by the MHD solvers. The relationship between magnetic resistivity and viscosity is $\nu_m = \frac{c^2}{4\pi}\eta$ in CGS and $\nu_m = \frac{1}{\mu_0}\eta$ in SI. The default top level routines return zero values for resistivity (a stub functionality). Specific routines for constant and variable resistivity are provided in the low level subdirectories `/MagneticResistivityMain/Constant` and `/MagneticResistivityMain/SpitzerHighZ`. By default, all routines return results in non-dimensional units (hence without 4π or μ_0 coefficients). However they provide an option to return results either in CGS or SI unit.

22.2.1 Constant resistivity

This subunit returns constant magnetic resistivity. The unit declares a runtime parameter, `resistivity`, that is the constant resistivity. The default value is zero. The magnetic resistivity routine reads in `resistivity` (η) and returns it to the calling routine with proper scalings depending on unit system. For example, $\frac{c^2}{4\pi}\eta$ is returned in CGS unit, $\frac{1}{\mu_0}\eta$ in SI, and simply η in non-dimensional unit.

FLASH Transition

In previous implementations, there used to be two runtime parameters: magnetic resistivity and magnetic viscosity. They respectively refer η and $\frac{c^2}{4\pi}\eta$ in CGS (or $\frac{1}{\mu_0}\eta$ in SI, where $\mu_0 = 4\pi \times 10^{-7}$ henry/meter). What it was done in the old way was to initialize magnetic viscosity (e.g., $\frac{c^2}{4\pi}\eta$) using the magnetic resistivity, η. As of FLASH3.1, such distinctions between the magnetic resistivity and magnetic viscosity has been removed and we only use magnetic resistivity with proper scalings depending on unit system.

22.2.2 Spitzer HighZ resistivity

This subunit returns the Spitzer resistivity for the induction equation and is the most useful option for HEDP simulations. The implementation follows the prescription of Braginskii (1965), defining a perpendicular and parallel magnetic resistivity, with respect to the field line, as

$$\eta_{perp} = \frac{m_{ele}}{e^2\, n_{ele}\, \tau_{ele}}\,, \tag{22.2}$$

$$\eta_{par} = \eta_{perp}/1.96\,. \tag{22.3}$$

Here we denote with m_{ele}, e, n_{ele}, τ_{ele} the mass, charge, number density and the collision time of electrons, respectively. In its current form, the implementation `/MagneticResistivityMain/SpitzerHighZ/-MagneticResistivity` returns only the parallel component when calculating the resistive fluxes. This can be modified by calling the `/MagneticResistivityMain/SpitzerHighZ/MagneticResistivity_fullState` implementation and requesting the optional perpendicular component. To activate the Spitzer HighZ resistivity implementation, simply add the appropriate path in the `Config` file of your simulation directory.

22.3 Viscosity

The `Viscosity` unit implements a prescription for computing viscosity coefficients used by the Hydro PPM, the unsplit hydro and MHD solvers. In this release the unit provides support for either constant dynamic viscosity or constant kinematic viscosity, where the choice between the two is made with the runtime parameter `visc_whichCoefficientIsConst`.

To use viscosity in a FLASH4 simulation, the runtime parameter `useViscosity` must be set to `.true.`

22.4 Opacity

The `Opacity` unit, which resides in `physics/materialProperties/Opacity`, exists to provide opacities for multigroup radiation diffusion to the `RadTrans` unit. Thus, the `Opacity` unit does not have an API for providing continuous opacities. The group structure is specified using parameters which are described in Chapter 24. Opacities are accessed by the `RadTrans` unit using the `Opacity` subroutine.

```
call Opacity(soln, ngrp, opacityAbsorption, opacityEmission, opacityTransport)
```

The first argument is an input and provides the complete state within a cell as provided by the routine `Grid_getBlPtr`. The second input argument is the group number. The last three arguments are outputs which return the absorption, emission, and transport opacities in units of $1/cm$ using the conditions provided by the `soln` argument. See Chapter 24 for a description of these three opacities. There are currently two `Opacity` implementations: Constant and Multispecies which are described below.

22.4.1 Constant Implementation

The Constant implementation is very simple and is useful for running test problems. It sets the absorption, emission, and transport opacities to constant values that are specified using the runtime parameters `op_absorbConst`, `op_emissConst`, and `op_transConst`. Users can provide custom implementations of the Constant `Opacity` subroutine to test different formulas for opacities in FLASH.

The Constant opacity implementation can be included with the following setup option:

```
-with-unit=physics/materialProperties/Opacity/OpacityMain/Constant
```

22.4.2 Constcm2g Implementation

The Constcm2g implementation is also very simple and is useful for running test problems. It sets the absorption, emission, and transport opacities, in units of cm^2/g, to constant values that are specified using the runtime parameters `op_absorbConst`, `op_emissConst`, and `op_transConst`. Users can provide custom implementations of the `Constcm2g Opacity` subroutine to test different formulas for opacities in FLASH.

The Constcm2g opacity implementation can be included with the following setup option:

```
-with-unit=physics/materialProperties/Opacity/OpacityMain/Constcm2g
```

22.4.3 BremsstrahlungAndThomson Implementation

The `BremsstrahlungAndThomson` Opacity implementation assumes that the free-free Bremsstrahlung process is responsible for the coupling between radiation and matter (the `emit_opac` and `absorb_opac` terms) and that simple Thomson scattering dominates the diffusion of radiation through matter (the `trans_opac` term). Therefore, the emission and absorption opacities are given by the following formula, in units of cm^{-1}:

$$\kappa_{emit,absorb} = 3.68 \times 10^{22} g_{ff}(1-Z)(1+X)T^{-3.5}\rho^2, \tag{22.4}$$

where g_{ff} is the Gaunt factor ($\simeq 1$), Z the fractional abundance of elements heavier than hydrogen, X the fractional abundance of hydrogen, T the temperature and ρ the temperature.

For the transport opacity, dominated by Thompson scattering, we have, in units of cm^{-1}:

$$\kappa_{trans} = 0.2(1+X)\rho. \tag{22.5}$$

The parameters op_absorbScale, op_emitScale, op_transScale are also introduced allowing the user to scale the three opacities accordingly.

This is a gray opacity implementation. The ngrp argument in Opacity calls has to be supplied but will be ignored.

The BremsstrahlungAndThomson opacity implementation can be included with the following setup option:

```
-with-unit=physics/materialProperties/Opacity/OpacityMain/BremsstrahlungAndThomson
```

22.4.4 OPAL Implementation

The OPAL Opacity implementation reads opacities from OPAL tables. *Documentation to be added; see* README *in the source tree.*

This is a gray opacity implementation. The ngrp argument in Opacity calls has to be supplied but will be ignored.

22.4.5 Multispecies Implementation

In general, the opacity is a strong function of the material (or species in FLASH parlance), frequency (or group number), and state of the fluid. The Multispecies Opacity unit implementation provides the flexibility to specify different opacities to use as a function of species and opacity *type* (either absorption, emission, or transport). It can be included in the simulation using the following setup option:

```
-with-unit=physics/materialProperties/Opacity/OpacityMain/Multispecies
```

The opacities for each species are averaged together based on the relative number densities to produce an average opacity of each type for a given cell. For each species and type, the Multispecies implementation allows the user must specify an opacity model to use. There are currently three commonly used opacity models in FLASH:

- constant: This model simply returns a constant value for the opacity in units of 1/cm
- constcm2g: This model also returns a constant opacity but uses units of cm^2/g
- tabulated: This model allows the user to specify the names of files which store opacity tables. These tables store opacities as functions electron temperature and density

The first two opacity models, constant and constcm2g, are fairly self-explanatory. The tabulated opacity model is useful for modeling realistic opacities in a general way. Each table is tabulates an opacity at N_D discrete density points and N_T discreet electron temperature points. The table for each species and opacity type can have different a temperature/density grid. However, each table must use the same energy group structure which is consistent with the group structure used by the RadTrans unit.

Extraction (interpolation) of opacities from the stored tables is currently done using the bilinear form. For a temperature/density pair (t,d) inside the grid, the code determines the quadrant corners $T_1 \le t \le T_2$ and $D_1 \le d \le D_2$ and the corresponding four opacities $\kappa_{xy} = \kappa(T_x, D_y); x, y = 1, 2$ and performs the bilinear interpolation:

$$\tau_1 = \frac{T_2 - t}{T_2 - T_1} \tag{22.6}$$

$$\tau_2 = \frac{t - T_1}{T_2 - T_1} \tag{22.7}$$

$$\delta_1 = \frac{D_2 - d}{D_2 - D_1} \tag{22.8}$$

$$\delta_2 = \frac{d - D_1}{D_2 - D_1} \tag{22.9}$$

$$\kappa(t,d) = \sum_{i=1}^{2}\sum_{j=1}^{2} \tau_i \delta_j \kappa_{ij}. \tag{22.10}$$

Table 22.1: Multispecies Opacity Runtime Parameters

Runtime Parameter	**Description**
`op_<spec>Absorb`	Model to use for the absorption opacity
`op_<spec>Emiss`	Model to use for the emission opacity
`op_<spec>Trans`	Model to use for the transport opacity
`op_<spec>AbsorbConstant`	Constant value to use for absorption opacity
`op_<spec>EmissConstant`	Constant value to use for emission opacity
`op_<spec>TransConstant`	Constant value to use for transport opacity
`op_<spec>FileName`	Name of IONMIX file for tabulated opacity
`op_<spec>FileType`	Tabulated opacity file type, either "IONMIX" or "IONMIX4"

In case the target (t, d) lays outside the grid boundaries, the corresponding boundary value(s) is(are) taken. This is a temporary solution and will be supplemented with options for calculating more accurate opacities, especially for lower cell temperatures. Two possible options are provided for performing the interpolation: i) on the original tabulated opacities or ii) on the logarthmically (base 10) transformed tabulated opacities.

Currently, the tables must be stored in either the IONMIX or IONMIX4 formats. The exact specification of this format can be found in Section 22.4.6. The IONMIX4 format is the most general since it allows for arbitrary temperature/density points. Users who wish to use their own tabulated opacities may convert their files into the IONMIX4 format for use in FLASH. As Section 22.4.6 describes, IONMIX4 files contain group opacities in units of cm^2/g. Each file contains three different group opacities: a Planck Absorption, a Planck Emission, and a Rosseland opacity. The user must specify which of these opacities to use for each species/opacity type in FLASH.

22.4.5.1 Runtime Parameters for the Multispecies Opacity

Use of the Multispecies opacity implementation requires the `Multispecies` unit. At least one species must be defined in the simulation to use the Multispecies opacity. Furthermore, the species must all be specified using the `species` setup variable and cannot be defined using the `SPECIES` keyword in a `Config` file. Please see Section 11.4 for more details.

Once the species are specified, the Multispecies opacity implementation will automatically create a set of runtime parameters to allow users to control how the opacity is computed for each species and opacity type. These runtime parameters are shown in Table 22.1. The symbol `<spec>` in the table should be replaced by the species names as specified using the species setup variable.

The opacity models for each species are specified using the `op_<spec>[Absorb,Emiss,Trans]` runtime parameters. These parameters can be set to the following string values:

- "op_constant" Use a constant opacity in units of $1/cm$. The constant values are specified using the appropriate `op_<spec><type>Constant` runtime parameter.

- "op_constcm2g" Use a constant opacity in units of cm^2/g. The constant values are specified using the appropriate `op_<spec><type>Constant` runtime parameter.

- "op_tabpa" Use the tabulated Planck Absorption opacity from the IONMIX or IONMIX4 file with name `op_<spec>FileName`.

- "op_tabpe" Use the tabulated Planck Emission opacity from the IONMIX or IONMIX4 file with name `op_<spec>FileName`.

- "op_tabro" Use the tabulated Rosseland opacity from the IONMIX or IONMIX4 file with name `op_<spec>FileName`.

When any of the models for a species is set to "op_tabpa", "op_tabpe", or "op_tabro", FLASH will attempt to read a file which contains the tabulated opacities. The file name, for each species, is given by the runtime parameter `op_<spec>FileName`. The type of the file is set using the parameter `op_<spec>FileType`.

Currently, FLASH only supports reading opacity files in the IONMIX or IONMIX4 format, but this will likely change in the future.

The code segment below shows an example of how one would specify the runtime parameters for the Multispecies opacity in a simulation with two species named `cham` and `targ` (this simulation would have been set up using the `species=cham,targ` setup argument):

```
# Specify opacity models for the species cham:
op_chamAbsorb   = "op_tabpa"       # Use tabulated Planck Absorption opacity for
                                   # the absorption term
op_chamEmiss    = "op_tabpe"       # Use the Planck Emission opacity for the emission
                                   # term
op_chamTrans    = "op_tabro"       # Use the Rosseland opacity for the transport term
op_chamFileName = "he-imx-005.cn4" # Specify tabulated opacity file name
op_chamFileType = "ionmix4"        # Set tabulated opacity file type to IONMIX4

# Specify opacity models for the species targ:
op_targAbsorb      = "op_constcm2g" # Use a constant opacity for the absorption term
op_targEmiss       = "op_constcm2g" # Use a constant opacity for the emission term
op_targTrans       = "op_constcm2g" # Use a constant opacity for the transport term
op_targAbsorbConst = 10.0           # Set targ species absorption opacity to 10 cm^2/g
op_targEmissConst  =  0.0           # Set targ species absorption opacity to zero
                                    # This species won't emit radiation
op_targTransConst  = 1.0e+06        # Set targ species transport opacity to a large
                                    # value Radiation will diffuse very slowly through
                                    # this material
```

In this example species `cham` uses a tabulated opacity while species `targ` uses constant opacities. The opacities for `targ` are chosen so that the material will not emit any radiation, and to suppress the transport of radiation. The `LaserSlab` simulation shows a comprehensive example of how the Multispecies opacity is used in a realistic HEDP simulation.

22.4.6 The IONMIX EOS/Opacity Format

FLASH reads tabulated opacity and Equation Of State (EOS) files in the IONMIX, IONMIX4, and IONMIX6 formats. The IONMIX4 and IONMIX6 formats are very similar and are more flexible than the IONMIX format. Thus, only the IONMIX4 and IONMIX6 formats will be documented here. These three formats are not particularly user friendly and future FLASH releases will likely include support for EOS and opacity file formats which are easier to handle. Nevertheless, by manipulating their data into the IONMIX4 or IONMIX6 formats, users can use their own EOS/opacity data in FLASH simulations. Each file contains information for a single material. All EOS/opacity information is defined on a temperature/density grid. The densities are actually ion number densities.

Below, the IONMIX4 and IONMIX6 formats are defined. They are very similar: the latter is identical to the former but also includes electron specific entropy information. Certain information is ignored by FLASH, meaning that it is read in, but not used for any calculations (right now). Other information is used by the EOS unit alone, or by the opacity unit alone.

1. Number of temperature points
2. Number of ion number density points
3. Line containing information about the atomic number of each element in this material (ignored by FLASH)
4. Line containing information about the relative fraction of each element in this material (ignored by FLASH)
5. Number of radiation energy groups

6. List of temperatures
7. List of ion number densities
8. Average ionization ($\bar{z}$) for each temperature/density (only used for tabulated EOS in FLASH)
9. $d\bar{z}/dT_e$ $[1/eV]$ for each temperature/density (ignored by FLASH)
10. Ion pressure (P_i) $[J/cm^3]$ for each temperature/density (only used for tabulated EOS in FLASH)
11. Electron pressure (P_e) $[J/cm^3]$ for each temperature/density (only used for tabulated EOS in FLASH)
12. dP_i/dT_i $[J/cm^3/eV]$ for each temperature/density (ignored by FLASH)
13. dP_e/dT_e $[J/cm^3/eV]$ for each temperature/density (ignored by FLASH)
14. Ion specific internal energy e_i $[J/g]$ for each temperature/density (only used for tabulated EOS in FLASH)
15. Electron specific internal energy e_e $[J/g]$ for each temperature/density (only used for tabulated EOS in FLASH)
16. de_i/dT_i $[J/g/eV]$ for each temperature/density point (ignored by FLASH)
17. de_e/dT_e $[J/g/eV]$ for each temperature/density point (ignored by FLASH)
18. de_i/dn_i $[J/g/cm^3]$ for each temperature/density point (ignored by FLASH)
19. de_e/dn_i $[J/g/cm^3]$ for each temperature/density point (ignored by FLASH)
20. **ONLY INCLUDE FOR IONMIX6 FORMAT**
    Electron specific entropy $[J/g/eV]$ for each temperature/density point.
21. Each energy group boundary [eV]. There are $g + 1$ boundaries for a simulation with g groups.
22. Rosseland opacity $[cm^2/g]$ for each density/temperature/energy group (only used for tabulated opacity in FLASH)
23. Planck absorption opacity $[cm^2/g]$ for each density/temperature/energy group (only used for tabulated opacity in FLASH)
24. Planck emission opacity $[cm^2/g]$ for each density/temperature/energy group (only used for tabulated opacity in FLASH)

Below, the exact format of the IONMIX4 file is defined. This is done by providing code listing which shows how the data can be read in using FORTRAN read statements. Users can use this information to convert their own data into the IONMIX4 format so that it can be used by FLASH.

```
! *** Write the header ***
! Write the number of temperature and density points:
write (header,923)  ntemp, ndens

! Write the atomic number of each element in this material:
write (headr2,921) (izgas(l),l=1,ngases)

! Write the fraction (by number of ions) of each element in this material:
write (headr3,922) (fracsp(l),l=1,ngases)

write (10,980) header
write (10,980) headr2
write (10,980) headr3

! Write the number of radiation energy groups:
```

```
write (10,982) ngrups

! Write the temperature points (in eV):
write (10,991) (tplsma(it),it=1,ntemp)

! Write the number density points (in cm^-3):
write (10,991) (densnn(id),id=1,ndens)

! Write out the zbar at each temperature/density point (nele/nion):
write (10,991) ((densne(it,id)/densnn(id),it=1,ntemp),id=1,ndens)

! Write d(zbar)/dT:
write (10,991) ((dzdt(it,id),it=1,ntemp),id=1,ndens)

! Write the ion pressure (in Joules/cm^3):
write (10,991) ((densnn(id)*tplsma(it)*1.602E-19_idk,it=1,ntemp),id=1,ndens)

! Write the electron pressure (in Joules/cm^3):
write (10,991) ((tplsma(it)*densne(it,id)*1.602E-19_idk,it=1,ntemp),id=1,ndens)

! Write out d(pion)/dT (in Joules/cm^3/eV):
write (10,991) ((densnn(id)*1.602E-19_idk,it=1,ntemp),id=1,ndens)

! Write out d(pele)/dT (in Joules/cm^3/eV):
write (10,991) &
  (((tplsma(it)*densnn(id)*dzdt(it,id) + densne(it,id))*1.602E-19_idk,it=1,ntemp),id=1,ndens)

! Write out the ion specific internal energy (in Joules/gram):
write (10,991) ((enrgyion(it,id),it=1,ntemp),id=1,ndens)

! Write out the electron specific internal energy (in Joules/gram):
write (10,991) ((enrgy(it,id)-enrgyion(it,id),it=1,ntemp),id=1,ndens)

! Write out the ion specific heat (in Joules/gram/eV):
write (10,991) ((heatcpion(it,id),it=1,ntemp),id=1,ndens)

! Write out the electron specific heat (in Joules/gram/eV):
write (10,991) ((heatcp(it,id)-heatcpion(it,id),it=1,ntemp),id=1,ndens)

! Write out d(eion)/d(nion) (I think, but I'm not sure...)
write (10,991) ((dedden_ion(it,id)*condd*densnn(id)/tplsma(it)**2, it=1,ntemp),id=1,ndens)

! Write out d(eele)/d(nele) (I think, but I'm not sure...)
write (10,991) &
  (((dedden(it,id)-dedden_ion(it,id))*condd*densnn(id)/tplsma(it)**2, it=1,ntemp),id=1,ndens)

! ONLY FOR IONMIX6 FORMAT, IONMIX4 FORMAT DOES NOT INCLUDE ELECTRON
! SPECIFIC ENTROPY:
!
! Write out electron specific entropy
write (10,991) ((entrele(it,id),it=1,ntemp),id=1,ndens)

! Write out the energy group boundaries (in eV):
write (10,991) (engrup(ig),ig=1,ngrups+1)

! Write the Rosseland group opacities
write (10,991) (((orgp(it,id,ig),it=1,ntemp),id=1,ndens),ig=1,ngrups)

! Write the Planck absorption opacities
```

```
write (10,991) (((opgpa(it,id,ig),it=1,ntemp),id=1,ndens),ig=1,ngrups)

! Write the Planck emission opacities
write (10,991) (((opgpe(it,id,ig),it=1,ntemp),id=1,ndens),ig=1,ngrups)

921 format (' atomic #s of gases: ',5i10)
922 format (' relative fractions: ',1p5e10.2)
923 format (2i10)
980 format (a80)
981 format (4e12.6,i12)
982 format (i12)
991 format (4e12.6)
```

22.5 Mass Diffusivity

The `MassDiffusivity` unit implements a prescription for calculating a generic mass diffusivity that can be used by the Hydro PPM, and MHD solvers. In this release the unit only provides non-operational stub functionalities.

Chapter 23

Physics Utilities

23.1 PlasmaState

The `PlasmaState` unit was introduced in FLASH4.4 as a place to implement auxiliary routines that have knowledge of the behavior of plasmas. These should eventually include routines to compute quantities like collision frequencies that are used by various `materialProperties` units.

The interfaces provided by `PlasmaState` are intended to be used n the context of zimulations of strongly ionized plasmas, but should also return "something useful" in other domains of application where this makes sense.

Currently, the only useful routine provided is `PlasmaState_getComposition`, for computing the elemantal composition of the mixture of materials in a cell (expressed as number fractions of elements). It is intended to be used with the `Multispecies` unit. Note that to get correct results, a simulation has to define the elemental compositions of the different species (materials) that may be present.

Chapter 24

Radiative Transfer Unit

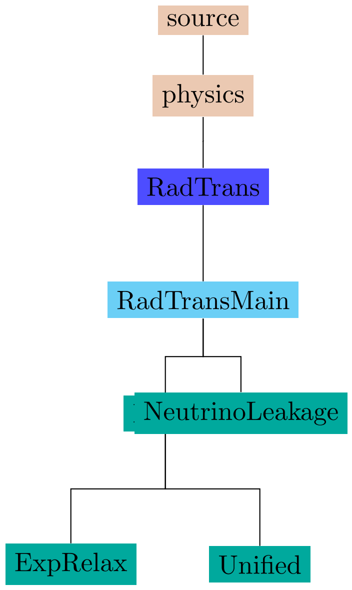

Figure 24.1: The organizational structure of the `RadTrans` unit.

The `RadTrans` unit is responsible for solving the radiative transfer equation

$$\frac{1}{c}\frac{\partial I}{\partial t} + \hat{\mathbf{\Omega}} \cdot \nabla I + \rho\kappa I = \eta, \tag{24.1}$$

where, $I(\mathbf{x}, \hat{\mathbf{\Omega}}, \nu, t)$ is the radiation intensity, c is the speed of light, ρ is the mass density, $\kappa(\mathbf{x}, \nu, t)$ is the opacity in units of cm^2/g, $\eta(\mathbf{x}, \nu, t)$ is the emissivity, ν is the radiation frequency, and $\hat{\mathbf{\Omega}}$ is the unit direction vector. This equation is coupled to the electron internal energy through

$$\frac{\partial u_e}{\partial t} = \int_0^\infty \mathrm{d}\nu \int_{4\pi} \mathrm{d}\hat{\mathbf{\Omega}} (\rho\kappa I - \eta), \tag{24.2}$$

where u_e is the electron internal energy density.

The `RadTrans` unit is responsible for solving the radiative transfer equation and updating the electron energy using (24.2) over a single time step. This ensures that the total system energy is conserved. Radiation-hydrodynamics effects, such as work, are operator-split and handled by the hydrodynamics unit. Currently, there is only a single `RadTrans` solver, `MGD`, which uses a simple multigroup diffusion approximation and is described in Section 24.1.

24.1 Multigroup Diffusion

The radiative transfer (24.1) and electron energy (24.2) equations can be simplified using a multigroup diffusion approximation. The frequency space is divided into N_g groups with N_{g+1}. Group g is defined by the frequency range from ν_g to ν_{g+1}. The plasma is assumed to emit radiation in a Planck spectrum with a given emission opacity. The multigroup diffusion equations solved by FLASH are

$$\frac{1}{c}\frac{\partial u_g}{\partial t} - \nabla\cdot\left(\frac{1}{3\sigma_{t,g}}\nabla u_g\right) + \sigma_{a,g}u_g = \sigma_{e,g}aT_e^4\frac{15}{\pi^4}\left[P(x_{g+1}) - P(x_g)\right] \tag{24.3}$$

$$\frac{\partial u_e}{\partial t} = \sum_g\left\{\sigma_{a,g}u_g - \sigma_{e,g}aT_e^4\frac{15}{\pi^4}\left[P(x_{g+1}) - P(x_g)\right]\right\} \tag{24.4}$$

where u_g is the radiation energy density, $\sigma_{t,g}$ is the transport opacity, $\sigma_{a,g}$ is the absorption opacity, $\sigma_{e,g}$ is the emission opacity, a is the radiation constant, T_e is the electron temperature, and $P(x)$ is the Planck integral, defined below. The argument to the Planck integral, is $x = h\nu/k_BT_e$ where h is Planck's constant and k_B is the Boltzmann constant. The opacities in (24.3) and (24.4) are in units of 1/cm and $\sigma = \rho\kappa$. The Planck integral, $P(x)$ is defined as

$$P(x) = \int_0^x \mathrm{d}x'\frac{(x')^3}{\exp(x') - 1} \tag{24.5}$$

The multigroup diffusion equation and electron internal energy equation are operator-split using an explicit treatment. Thus, on each time step (24.4) is solved for each energy group using coefficients evaluated at time level n using an implicit treatment for the diffusion solution itself. The equation below shows how the multigroup equations are discretized in time

$$\frac{1}{c}\frac{u_g^{n+1} - u_g^n}{\Delta t} - \nabla\cdot\left(D_g^n\nabla u_g^{n+1}\right) + \sigma_{a,g}^n u_g^{n+1} = \sigma_{e,g}^n a(T_e^n)^4\frac{15}{\pi^4}\left[P(x_{g+1}^n) - P(x_g^n)\right] \tag{24.6}$$

$$\frac{u_e^{n+1} - u_e^n}{\Delta t} = \sum_g\left\{\sigma_{a,g}^n u_g^{n+1} - \sigma_{e,g}^n a(T_e^n)^4\frac{15}{\pi^4}\left[P(x_{g+1}^n) - P(x_g^n)\right]\right\} \tag{24.7}$$

where the n superscript denotes the time level, and Δt is the time step length. These equations are solved on each time step. The diffusion coefficient, D_g^n, has been introduced. When no flux-limiter is employed, $D_g^n = 1/3\sigma_{t,g}^n$. The flux-limiter limits the radiation flux in each group to the free streaming limit, cu_g^n. Several flux limiter options are available in FLASH. These are described in section 18.1.3. The string runtime parameter rt_mgdFlMode controls the flux limiter mode. The maximum flux is set to $q_{\max} = \alpha_r cu_g^n$ for each energy group. The coefficient α_r is set to one by default, which is what is physically most realistic. However, it can be controlled using the runtime parameter rt_mgdFlCoef.

The diffusion equation, (24.6), is an implicit equation and is solved using the general implicit diffusion solver described in section 18.1.2. It is recommended that users familiarize themselves with the general implicit diffusion solver to learn more about using MGD in FLASH.

24.1.1 Using Multigroup Radiation Diffusion

This section describes how to use MGD in FLASH. Section 30.7.5 shows an example of how to use MGD in a realistic HEDP simulation and is extremely informative.

Several setup options are needed to use MGD. The `+mgd` setup shortcut will include the `MGD` unit in the simulation. In addition, storage needs to be created for storing the specific energy for each group. This is done using the `mgd_meshgroups` setup variable. The user must set `mgd_meshgroups` such that:

$$(\text{mgd\_meshgroups})N_{\text{mesh}} \geq N_g \tag{24.8}$$

where N_{mesh} represents the number of meshes (please see section 24.1.2 for more information). If you don't know what this is, you can assume that $N_{\text{mesh}} = 1$. In this case, the constraint is that the `mgd_meshgroups` setup variable must be greater than or equal to the number of energy groups. The actual number of energy groups, N_g, is set at run time using the runtime parameter rt_mgdNumGroups. Thus, as an example, the setup options for a 4-group simulation could be:

```
  +mgd mgd_meshgroups=6
```

and the runtime parameter file must contain rt_mgdNumGroups = 4. No changes are needed to the Config file of the simulation.

The FLASH checkpoint files will contain the specific energy in each radiation energy group for each cell. The variables are named r### where ### is a three digit number from one to N_g. Users can also add these variables to the list of plot variables so they will be included in plot files.

Several runtime parameters are used to control the MGD unit. The runtime parameter rt_useMGD must be set to .true. for MGD simulations. The energy group structure (values of the group boundaries) are specified, manually, using runtime parameters. A simulation with N_g groups will have $N_g + 1$ energy group boundaries. These are set using the rt_mgdBounds_### runtime parameters, where ### is a number between 1 and $N_g + 1$. By default, enough runtime parameters exist for specifying 101 energy group boundaries. In the case that more groups are needed, the mgd_maxgroups setup variable sets the number of group boundary runtime parameters. For example, if 200 energy groups are needed, then mgd_maxgroups=200 should be specified on the setup line. If $N_g \leq 100$, no action is needed.

When MGD is in use, the Opacity unit provides opacities for each cell. Thus, the useOpacity runtime parameter must be set to true and the appropriate opacity model must be specified. Please see section 22.4 for a detailed description on how to use the Opacity unit in FLASH.

Finally, the radiation boundary conditions must be specified using runtime parameters. The parameters:

```
rt_mgdXlBoundaryType
rt_mgdXrBoundaryType
rt_mgdYlBoundaryType
rt_mgdYrBoundaryType
rt_mgdZlBoundaryType
rt_mgdZrBoundaryType
```

control the boundary condition on each logical face of the domain. The allowed values are:

- reflecting, neumann: This is a zero-flux, or Neumann boundary condition and should be used to model reflecting boundaries
- dirichlet: This (poorly named) value represents a fixed radiation temperature boundary condition
- vacuum: This represents a vacuum boundary condition

Please see section 18.1.2.1 for more information on boundary conditions for the diffusion solver.

As was mentioned earlier, FLASH uses the generalized implicit diffusion solver, described in section 18.1.2, to solve (24.6) for each energy group. Thus, users must make sure to include an appropriate diffusion solver in their simulation.

24.1.2 Using Mesh Replication with MGD

When many energy groups are needed, domain decomposition alone is not an effective method for speeding up calculations. The computation time scales roughly linearly with the number of energy groups. As the number of groups increases, users can divide the mesh among larger number of processors to compensate. This is an effective strategy until the strong scaling limit for the simulation is reached. At this point, mesh replication becomes the only way to speed up the simulation further.

Mesh replication allows FLASH to perform the diffusion solves for each energy group in parallel. By default, mesh replication is deactivated and each diffusion equation is solved serially. When mesh replication is in use the total pool of N_p processes is divided among N_m identical copies of the computational mesh. The radiation solver uses these copies of the mesh to perform N_m parallel radiation solves. The runtime parameter meshCopyCount is used to set N_m and has a value of 1 by default.

This is best illustrated with an example. Suppose N_g, the total number of energy groups, is set to 100, and there are $N_p = 6$ processes available to run the simulation. If meshCopyCount=1, then $N_m = 1$ and the computational mesh will not be replicated. This is FLASH's normal mode of operation: the mesh will be divided into six pieces and each process will be responsible for one of these pieces. Each process will also be involved in the solution of the diffusion equation for all 100 energy groups. If `meshCopyCount=2`, then the computational domain will be divided into three pieces. Two processes will be assigned to each piece. In other words two groups of three processes will be created. The first set of three processes will be responsible for solving the diffusion equations for the odd numbered energy groups. The second set of processes will solve the diffusion equations for the even numbered energy groups. Each process only knows about 50 of the 100 groups. In some cases, this may be substantially faster than the `meshCopyCount=1` approach.

Another benefit of mesh replication is that it reduces the amount of memory needed per process. In the example above, when `meshCopyCount=1`, each process must store the energy density for all 100 energy groups. Thus, storage must exist for 100 cell centered variables on each process. When `meshCopyCount=2`, storage is only needed for 50 cell centered variables. The setup variable `mgd_meshgroups` controls the number of cell centered variables created on process. Thus, when `meshCopyCount=2`, we can set `mgd_meshgroups` to 50 instead of 100. As a result, far less memory is used per block.

Whether or not mesh replication is helpful for a particular simulation can only be determined through extensive testing. It depends on the particular simulation and the hardware.

24.1.3 Specifying Initial Conditions

The initial conditions must be specified throughout the domain for each radiation energy group. This involves setting the specific energy, $e_g = u_g/\rho$, in units of erg/g for each group. Because of the mesh replication capability, the user is discouraged from manually setting the value of the underlying radiation mass scalars. Instead, several routines have been added to the `RadTrans` unit to simplify this process dramatically. Specifying the initial conditions involves two steps. First, the value of e_g must be set for each group in each cell. Second, either the total specific radiation energy, $e_r = \sum_g e_g$, or the radiation temperature, $T_r = (u_r/a)^{1/4}$, must be set - depending on the value of `eosModeInit`. Below, two use cases are described.

24.1.3.1 Initializing using a Radiation Temperature

The easiest way to set the initial condition is to use a radiation temperature in each cell and to assume that the radiation field is described by a Planck spectrum. The subroutine:

```
RadTrans_mgdEFromT(blockId, axis, trad, tradActual)
```

will automatically set the value of e_g for each group using a given radiation temperature and assuming a black body spectrum. The arguments are:

1. `blockId`: The block ID
2. `axis`: A 3 dimensional array of integers indicating the cell within the block
3. `trad`: An input, the desired radiation temperature
4. `tradActual`: An output, The actual radiation temperature (described further below)

When the simulation is initialized, it is important that $T_r = (\sum_g u_g/a)^{1/4}$. This will not always be the case. The reason is that a black body spectrum has a non zero energy density for all frequencies. But FLASH simulations require finite energy group boundaries. For example, if `trad` is set to 11604 K (this corresponds to 1 eV), but the upper energy group boundary is only set to 10 eV, then we are effectively cutting off the part of the spectrum above 10 eV. The *actual* radiation temperature, which is consistent with the sum of the energies in each group, will be slightly less than 1 eV. The argument `tradActual` contains this new radiation temperature.

Once `RadTrans_mgdEFromT` has been used to initialize e_g, either the total radiation specific energy, e_r, must be set or the radiation temperature for the cell must be specified. When the runtime parameter `eosModeInit` is set to “dens_temp_gather”, the initial radiation temperature must be specified in the variable `TRAD_VAR`. When `eosModeInit` is set to “dens_ie_gather”, e_r must be specified in the variable `ERAD_VAR`.

The example below shows a segment from a `Simulation_initBlock` routine from a typical simulation which uses MGD:

```
do k = blkLimits(LOW,KAXIS),blkLimits(HIGH,KAXIS)
   do j = blkLimits(LOW,JAXIS),blkLimits(HIGH,JAXIS)
      do i = blkLimits(LOW,IAXIS),blkLimits(HIGH,IAXIS)

         axis(IAXIS) = i
         axis(JAXIS) = j
         axis(KAXIS) = k

         ...

         ! Set the secific energy in each radiation group using a
         ! radiation temperature of 1~eV (11604.55~K):
         call RadTrans_mgdEFromT(blockId, axis, 11604.55, tradActual)

         ! Set the radiation temperature:
         call Grid_putPointData(blockId, CENTER, TRAD_VAR, EXTERIOR, axis, tradActual)

         ! Alternatively, we could have set ERAD_VAR using a*(tradActual)**4

      enddo
   enddo
enddo
```

Note that `tradActual` is used to specify the value of `TRAD_VAR`.

24.1.3.2 Manually setting the radiation spectrum

Specifying the radiation temperature is sufficient for many cases. Alternatively, users can manually specify the radiation spectrum. The subroutine

```
RadTrans_mgdSetEnergy(blockId, axis, group, eg)
```

has been created for this purpose. The arguments are:

- `blockId`: The block ID
- `axis`: A 3 dimensional array of integers indicating the cell within the block
- `group`: The group number, between 1 and N_g
- `eg`: The specific radiation energy (erg/g) for the group

This subroutine sets the value of e_g for a particular cell and should be called from the `Simulation_initBlock` subroutine.

The example below assumes that the user would like to initialize the radiation field so that $e_1 = aT_r^4/\rho$ and all other groups are initialized to zero energy. Note, that for this example, the user should obtain the value of a, the radiation constant, from the `PhysicalConstants` unit. This simulations used $N_g = 4$.

```
do k = blkLimits(LOW,KAXIS),blkLimits(HIGH,KAXIS)
   do j = blkLimits(LOW,JAXIS),blkLimits(HIGH,JAXIS)
      do i = blkLimits(LOW,IAXIS),blkLimits(HIGH,IAXIS)

         axis(IAXIS) = i
         axis(JAXIS) = j
         axis(KAXIS) = k

         ...
         ! Set the secific energy in each radiation group:
         call RadTrans_mgdSetEnergy(blockId, axis, 1, a*sim_trad**4/sim_rho)
         call RadTrans_mgdSetEnergy(blockId, axis, 2, 0.0)
         call RadTrans_mgdSetEnergy(blockId, axis, 3, 0.0)
         call RadTrans_mgdSetEnergy(blockId, axis, 4, 0.0)

         ! Set the radiation temperature:
         call Grid_putPointData(blockId, CENTER, TRAD_VAR, EXTERIOR, axis, sim_trad)

         ! Alternatively, we could have set ERAD_VAR using a*sim_trad**4/sim_rho

      enddo
   enddo
enddo
```

24.1.4 Altering the Radiation Spectrum

In some cases, it is necessary to alter the radiation spectrum manually, for example, to add a radiation energy source. In these cases, it is useful to manually alter the mesh variables which store the *specific* radiation energy within each group: $e_g = u_g/\rho$. However, because of mesh replication, altering these variables requires a different procedure than modifying other mesh variables (such as the density) in FLASH. The reason is that each process does not, in general, have access to each e_g. The procedure for modifying e_g directly is as follows:

1. Loop over the energy groups that each process sees
2. Modify e_g
3. Modify the total specific radiation energy, e_{rad}, so that it stores the sum over all e_g

Note, that in step 1, looping over the energy groups does not simply involve looping from 1 to N_g. The reason is that each process must loop over only those groups that it is responsible for. Again, because of mesh replication, this may be less than N_g. Below, an example is shown where the specific energy in each group is manually set to 10^{12} erg/g. An ideal place for this type of code to exist is in the `Simulation_adjustEvolution` subroutine which gets called every time step.

```
! Loop over all cells, set the specific radiation energy to zero:
do lb = 1, nblk
  call Grid_getBlkIndexLimits(blklst(lb),blkLimits,blkLimitsGC)
  call Grid_getBlkPtr(blklst(lb), blkPtr)

  do k = blkLimits(LOW,KAXIS), blkLimits(HIGH,KAXIS)
    do j = blkLimits(LOW,JAXIS), blkLimits(HIGH,JAXIS)
      do i = blkLimits(LOW,IAXIS), blkLimits(HIGH,IAXIS)
        blkPtr(ERAD_VAR,i,j,k) = 0.0
      end do
    end do
  end do
  call Grid_releaseBlkPtr(blklst(lb), blkPtr)
end do

! Loop over radiation energy groups:
do gloc = 1, NONREP_NLOCS(rt_acrossMe, rt_meshCopyCount, rt_mgdNumGroups)

  ! g represents the global energy group number:
```

```
  g = NONREP_LOC2GLOB(gloc, rt_acrossMe, rt_meshCopyCount)

  ! gvar represents the index in the block pointer for group g:
  gvar = MGDR_NONREP_LOC2UNK(gloc)

  ! Loop over blocks and set the energy density in each group:
  do lb = 1, nblk
    call Grid_getBlkIndexLimits(blklst(lb),blkLimits,blkLimitsGC)
    call Grid_getBlkPtr(blklst(lb), blkPtr)

    do k = blkLimits(LOW,KAXIS), blkLimits(HIGH,KAXIS)
      do j = blkLimits(LOW,JAXIS), blkLimits(HIGH,JAXIS)
        do i = blkLimits(LOW,IAXIS), blkLimits(HIGH,IAXIS)

          ! Set the specific energy in group g:
          blkPtr(gvar,i,j,k) = 1.0e+12

          ! Make sure to track the total radiation energy in the cell:
          blkPtr(ERAD_VAR,i,j,k) = blkPtr(ERAD_VAR,i,j,k) + &
                                   blkPtr(gvar,i,j,k)
        end do
      end do
    end do
    call Grid_releaseBlkPtr(blklst(lb), blkPtr)
  end do
end do

! Finally, every process needs to know the total specific radiation
! energy. RadTrans_sumEnergy adds up ERAD_VAR across all of the
! meshes:
call RadTrans_sumEnergy(ERAD_VAR, nblk, blklst)

! Call EOS to get a consistent state:
do lb = 1, nblk
  call Grid_getBlkIndexLimits(blklst(lb),blkLimits,blkLimitsGC)
  call Eos_wrapped(MODE_DENS_EI_GATHER,blkLimits,blklst(lb))
end do
```

In the first part of the example, the value of ERAD_VAR is set to zero. ERAD_VAR simply stores the total specific radiation energy in each cell. After we are done modifying the energy for each group, it is important that ERAD_VAR be updated to contain the total specific radiation energy.

The second part of the example loops over the groups. Notice the strange loop ending index. The NONREP_NLOCS macro computes the number of groups represented on a given process. To find the actual group number, g, a call is made to NONREP_LOC2GLOB. Next, MGDR_NONREP_LOC2UNK is called to get the actual index into the block pointer which corresponds to group g. Following this is a fairly standard loop over blocks and cells where the block pointer is used to modify the specific energy in each group. Notice that we are keeping a running total of the total specific energy in the cell which is stored in ERAD_VAR.

Finally, we must call RadTrans_sumEnergy to add up ERAD_VAR across all of the meshes. After this call, every process will contain the same total specific energy in each cell. This is followed by a call to the equation of state. This is needed to update the radiation temperature and pressure, TRAD_VAR and ERAD_VAR, respectively.

Part VI

Monitor Units

Chapter 25

Logfile Unit

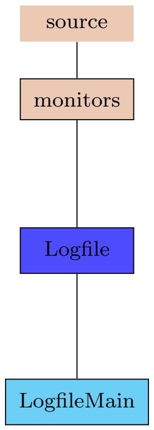

Figure 25.1: The `Logfile` unit directory structure.

FLASH supplies the `Logfile` unit to manage an output log during a FLASH simulation. The logfile contains various types of useful information, warnings, and error messages produced by a FLASH run. Other units can add information to the logfile through the `Logfile` unit interface. The `Logfile` routines enable a program to open and close a log file, write time or date stamps to the file, and write arbitrary messages to the file. The file is kept closed and is only opened for appending when information is to be written, thus avoiding problems with unflushed buffers. For this reason, `Logfile` routines should not be called within time-sensitive loops, as system calls are generated. Even when starting from scratch, the logfile is opened in append mode to avoid deleting important logfiles. Two kinds of Logfiles are supported. The first kind is similar to that in FLASH2 and early releases of FLASH3, where the master processor has exclusive access to the logfile and writes global information to it. The newer kind gives all processors access to their own private logfiles if they need to have one. Similar to the traditional logfile, the private logfiles are opened in append mode, and they are created the first time a processor writes to one. The private logfiles are extremely useful to gather information about failures causes by a small fraction of processors; something that cannot be done in the traditional logfile.

The `Logfile` unit is included by default in all the provided FLASH simulations because it is required by the `Driver/DriverMain Config`. As with all the other units in FLASH, the data specific to the Logfile unit is stored in the module `Logfile_data.F90`. Logfile unit scope data variables begin with the prefix `log_variableName` and they are initialized in the routine `Logfile_init`.

By default, the logfile is named `flash.log` and found in the output directory. The user may change the name of the logfile by altering the runtime parameter `log_file` in the `flash.par`.

```
# names of files
```

```
basenm   = "cellular_"
log_file = "cellular.log"
```

25.1 Meta Data

The `logfile` stores meta data about a given run including the time and date of the run, the number of MPI tasks, dimensionality, compiler flags and other information about the run. The snippet below is an example from a `logfile` showing the basic setup and compilation information:

```
================================================================================
 Number of MPI tasks:                 2
 MPI version:                         1
 MPI subversion:                      2
 Dimensionality:                      2
 Max Number of Blocks/Proc:        1000
 Number x zones:                      8
 Number y zones:                      8
 Number z zones:                      1
 Setup stamp:     Wed Apr 19 13:49:36 2006
 Build stamp:     Wed Apr 19 16:35:57 2006
 System info:
 Linux zingiber.uchicago.edu 2.6.12-1.1376_FC3smp #1 SMP Fri Aug 26 23:50:33 EDT
 Version:         FLASH 3.0.
 Build directory: /home/kantypas/FLASH3/trunk/Sod
 Setup syntax:
 /home/kantypas/FLASH3/trunk/bin/setup.py Sod -2d -auto -unit=IO/IOMain/hdf5/parallel/PM
                   -objdir=Sod
 f compiler flags:
 /usr/local/pgi6/bin/pgf90 -I/usr/local/mpich-pg/include -c -r8 -i4 -fast -g
                   -DMAXBLOCKS=1000 -DNXB=8 -DNYB=8 -DNZB=1 -DN_DIM=2
 c compiler flags:
 /usr/local/pgi6/bin/pgcc -I/usr/local/hdf5-pg/include -I/usr/local/mpich-pg/include
                   -c -O2 -DMAXBLOCKS=1000 -DNXB=8 -DNYB=8 -DNZB=1 -DN_DIM=2
===============================================================================
```

25.2 Runtime Parameters, Physical Constants, and Multispecies Data

The `logfile` also records which units were included in a simulation, the runtime parameters, physical constants, and any species and their properties from the `Multispecies` unit. The FLASH3 logfile keeps track of whether a runtime parameter is a default value or whether its value has been redefined in the `flash.par` file. The `[CHANGED]` symbol will occur next to a runtime parameter if its value has been redefined in the `flash.par`. Note that the runtime parameters are output in alphabetical order within the Fortran datatype – so integer parameters are shown first, then real, then string, then Boolean. The snippet below shows the this portion of the `logfile`; omitted sections are indicated with "...".

```
 ==============================================================================
  FLASH Units used:
   Driver
   Driver/DriverMain
   Driver/DriverMain/TimeDep
   Grid
   Grid/GridMain
   Grid/GridMain/paramesh
   Grid/GridMain/paramesh/paramesh4
   ...
   Multispecies
   Particles
   PhysicalConstants
   PhysicalConstants/PhysicalConstantsMain
   RuntimeParameters
   RuntimeParameters/RuntimeParametersMain
   ...
   physics/utilities/solvers/LinearAlgebra
 ==============================================================================
 RuntimeParameters:

 ==============================================================================
algebra                    =          2 [CHANGED]
bndpriorityone             =          1
bndprioritythree           =          3
...
cfl                        =                 0.800E+00
checkpointfileintervaltime  =                 0.100E-08 [CHANGED]
cvisc                      =                 0.100E+00
derefine_cutoff_1          =                 0.200E+00
derefine_cutoff_2          =                 0.200E+00
...
zmax                       =                 0.128E+02 [CHANGED]
zmin                       =                 0.000E+00
basenm                     = cellular_                        [CHANGED]
eosmode                    = dens_ie
eosmodeinit                = dens_ie
geometry                   = cartesian
log_file                   = cellular.log                     [CHANGED]
output_directory           =
pc_unitsbase               = CGS
plot_grid_var_1            = none
plot_grid_var_10           = none
plot_grid_var_11           = none
plot_grid_var_12           = none
plot_grid_var_2            = none
...
yr_boundary_type           = periodic
zl_boundary_type           = periodic
zr_boundary_type           = periodic
bytepack                   =  F
chkguardcells              =  F
converttoconsvdformeshcalls =  F
converttoconsvdinmeshinterp =  F
...
useburn                    =  T [CHANGED]
useburntable               =  F

 ==============================================================================

 Known units of measurement:
```

```
             Unit                          CGS Value              Base Unit
  1                 cm                     1.0000                        cm
  2                  s                     1.0000                         s
  3                  K                     1.0000                         K
  4                  g                     1.0000                         g
  5                esu                     1.0000                       esu
  6                  m                     100.00                        cm
  7                 km                    0.10000E+06                    cm
  8                 pc                    0.30857E+19                    cm
  ...
 Known physical constants:

   Constant Name       Constant Value   cm        s         g         K         esu
  1             Newton    0.66726E-07   3.00     -2.00     -1.00      0.00      0.00
  2      speed of light   0.29979E+11   1.00     -1.00      0.00      0.00      0.00
 ...
 15              Euler    0.57722       0.00      0.00      0.00      0.00      0.00
 ==============================================================================

 Multifluid database contents:

Initially defined values of species:
Name     Index          Total   Positive  Neutral   Negative  bind Ener Gamma
ar36        12       3.60E+01  1.80E+01 -9.99E+02 -9.99E+02  3.07E+02 -9.99E+02
c12         13       1.20E+01  6.00E+00 -9.99E+02 -9.99E+02  9.22E+01 -9.99E+02
ca40        14       4.00E+01  2.00E+01 -9.99E+02 -9.99E+02  3.42E+02 -9.99E+02
...
ti44        24       4.40E+01  2.20E+01 -9.99E+02 -9.99E+02  3.75E+02 -9.99E+02
 ==============================================================================
```

25.3 Accessor Functions and Timestep Data

Other units within FLASH may make calls to write information, or stamp, the logfile. For example, the `Driver` unit calls the API routine `Logfile_stamp` after each timestep. The `Grid` unit calls `Logfile_stamp` whenever refinement occurs in an adaptive grid simulation. If there is an error that is caught in the code the API routine `Driver_abortFlash` stamps the `logfile` before aborting the code. Any unit can stamp the logfile with one of two routines `Logfile_stamp` which includes a data and time stamp along with a logfile message, or `Logfile_stampMessage` which simply writes a string to the `logfile`.

The routine `Logfile_stamp` is overloaded so the user must use the interface file `Logfile_interface.F90` in the calling routine. The next snippit shows logfile output during the evolution loop of a FLASH run.

```
 ==============================================================================
 [ 04-19-2006  16:40.43 ] [Simulation_init]: initializing Sod problem
 [GRID amr_refine_derefine]             initiating refinement
 [GRID amr_refine_derefine] min blks 0    max blks 1    tot blks 1
 [GRID amr_refine_derefine] min leaf blks 0    max leaf blks 1    tot leaf blks 1
 [GRID amr_refine_derefine]             refinement complete
 [ 04-19-2006  16:40.43 ] [GRID gr_expandDomain]: create level=2
 ...
 [GRID amr_refine_derefine]             initiating refinement
 [GRID amr_refine_derefine] min blks 250    max blks 251    tot blks 501
 [GRID amr_refine_derefine] min leaf blks 188    max leaf blks 188    tot leaf blks 376
 [GRID amr_refine_derefine]             refinement complete
```

```
[ 04-19-2006  16:40.44 ] [GRID gr_expandDomain]: create level=7
[ 04-19-2006  16:40.44 ] [GRID gr_expandDomain]: create level=7
[ 04-19-2006  16:40.44 ] [GRID gr_expandDomain]: create level=7
[ 04-19-2006  16:40.44 ] [IO_writeCheckpoint] open: type=checkpoint name=sod_hdf5_chk_0000
[ 04-19-2006  16:40.44 ] [io_writeData]: wrote     501          blocks
[ 04-19-2006  16:40.44 ] [IO_writeCheckpoint] close: type=checkpoint name=sod_hdf5_chk_0000
[ 04-19-2006  16:40.44 ] [IO writePlotfile] open: type=plotfile name=sod_hdf5_plt_cnt_0000
[ 04-19-2006  16:40.44 ] [io_writeData]: wrote     501          blocks
[ 04-19-2006  16:40.44 ] [IO_writePlotfile] close: type=plotfile name=sod_hdf5_plt_cnt_0000
[ 04-19-2006  16:40.44 ] [Driver_evolveFlash]: Entering evolution loop
[ 04-19-2006  16:40.44 ] step: n=1 t=0.000000E+00 dt=1.000000E-10
...
[ 04-19-2006  16:41.06 ] [io_writeData]: wrote     501          blocks
[ 04-19-2006  16:41.06 ] [IO_writePlotfile] close: type=plotfile name=sod_hdf5_plt_cnt_0002
[ 04-19-2006  16:41.06 ] [Driver_evolveFlash]: Exiting evolution loop
==============================================================================
```

25.4 Performance Data

Finally, the `logfile` records performance data for the simulation. The `Timers` unit (see Section 26.1) is responsible for storing, collecting and interpreting the performance data. The `Timers` unit calls the API routine `Logfile_writeSummary` to format the performance data and write it to the logfile. The snippet below shows the performance data section of a logfile.

```
==============================================================================
perf_summary: code performance summary
                     beginning : 04-19-2006  16:40.43
                        ending : 04-19-2006  16:41.06
  seconds in monitoring period :             23.188
        number of subintervals :                 21
       number of evolved zones :              16064
              zones per second :            692.758
------------------------------------------------------------------------------
accounting unit                       time sec  num calls   secs avg  time pct
------------------------------------------------------------------------------
initialization                           1.012       1         1.012     4.366
 guardcell internal                      0.155      17         0.009     0.669
 writeCheckpoint                         0.085       1         0.085     0.365
 writePlotfile                           0.061       1         0.061     0.264
evolution                               22.176       1        22.176    95.633
 hydro                                  18.214      40         0.455    78.549
  guardcell internal                     2.603      80         0.033    11.227
 sourceTerms                             0.000      40         0.000     0.002
 particles                               0.000      40         0.000     0.001
 Grid_updateRefinement                   1.238      20         0.062     5.340
  tree                                   1.126      10         0.113     4.856
   guardcell tree                        0.338      10         0.034     1.459
    guardcell internal                   0.338      10         0.034     1.458
   markRefineDerefine                    0.339      10         0.034     1.460
    guardcell internal                   0.053      10         0.005     0.230
   amr_refine_derefine                   0.003      10         0.000     0.011
   updateData                            0.002      10         0.000     0.009
   guardcell                             0.337      10         0.034     1.453
    guardcell internal                   0.337      10         0.034     1.452
  eos                                   0.111     10          0.011     0.481
  update particle refinemen             0.000     10          0.000     0.000
 io                                     2.668     20          0.133    11.507
  writeCheckpoint                       0.201      2          0.101     0.868
  writePlotfile                         0.079      2          0.039     0.340
  diagnostics                           0.040     20          0.002     0.173
==============================================================================
[ 04-19-2006  16:41.06 ] LOGFILE_END: FLASH run complete.
```

25.5 Example Usage

An example program using the Logfile unit might appear as follows:

```
program testLogfile

    use Logfile_interface, ONLY: Logfile_init, Logfile_stamp, Logfile_open, Logfile_close
    use Driver_interface, ONLY: Driver_initParallel
    use RuntimeParameters_interface, ONLY: RuntimeParameters_init
    use PhysicalConstants_interface, ONLY: PhysicalConstants_init

    implicit none

    integer :: i
    integer :: log_lun
    integer :: myPE, numProcs
    logical :: restart, localWrite

    call Driver_initParallel(myPE, numProcs) !will initialize MPI
    call RuntimeParameters_init(myPE, restart) ! Logfile_init needs runtime parameters
    call PhysicalConstants_init(myPE) ! PhysicalConstants information adds to logfile
    call Logfile_init(myPE, numProcs) ! will end with Logfile_create(myPE, numProcs)

    call Logfile_stamp (myPE, "beginning log file test...", "[programtestLogfile]")
    localWrite=.true.
    call Logfile_open(log_lun,localWrite) !! open the local logfile
    do i = 1, 10
      write (log_lun,*) 'i = ', i
    enddo
    call Logfile_stamp (myPE, "finished logfile test", "[program testLogfile]")
    call Logfile_close(myPE, log_lun)


end program testLogfile
```

Chapter 26

Timer and Profiler Units

26.1 Timers

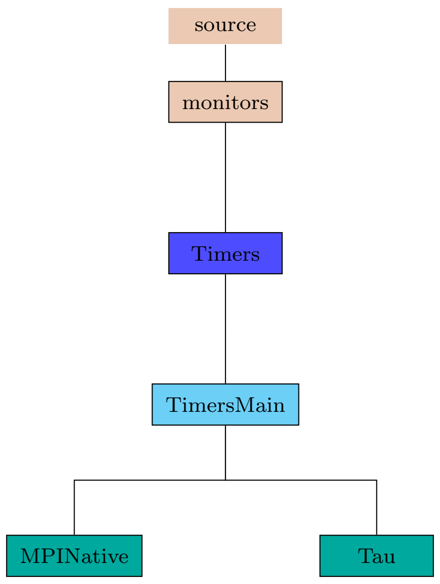

Figure 26.1: The `Timers` unit directory tree.

26.1.1 MPINative

FLASH includes an interface to a set of stopwatch-like timing routines for monitoring performance. The interface is defined in the `monitors/Timers` unit, and an implementation that uses the timing functionality provided by MPI is provided in `monitors/Timers/TimersMain/MPINative`. Future implementations might use the PAPI framework to track hardware counter details.

The performance routines start or stop a timer at the beginning or end of a section of code to be monitored, and accumulate performance information in dynamically assigned accounting segments. The code also has an interface to write the timing summary to the FLASH logfile. These routines are not recommended for timing very short segments of code due to the overhead in accounting.

There are two ways of using the `Timers` routines in your code. One mode is to simply pass timer names as strings to the start and stop routines. In this first way, a timer with the given name will be created if it doesn't exist, or otherwise reference the one already in existence. The second mode of using the timers references them not by name but by an integer key. This technique offers potentially faster access if a timer is to be started and stopped many times (although still not recommended because of the overhead). The integer key is obtained by calling with a string name `Timers_create` which will only create the timer if it doesn't exist and will return the integer key. This key can then be passed to the start and stop routines.

The typical usage pattern for the timers is implemented in the default `Driver` implementation. This pattern is: call `Timers_init` once at the beginning of a run, call `Timers_start` and `Timers_stop` around sections of code, and call `Timers_getSummary` at the end of the run to report the timing summary at the end of the logfile. However, it is possible to call `Timers_reset` in the middle of a run to reset all timing information. This could be done along with writing the summary once per-timestep to report code times on a per-timestep basis, which might be relevant, for instance, for certain non-fixed operation count solvers. Since `Timers_reset` does not reset the integer key mappings, it is safe to obtain a key through `Timers_create` once in a saved variable, and continue to use it after calling `Timers_reset`.

Two runtime parameters control the `Timer` unit and are described below.

Table 26.1: Timer Unit runtime parameters.

Parameter	Type	Default value	Description
`eachProcWritesSummary`	`LOGICAL`	`TRUE`	Should each process write its summary to its own file? If true, each process will write its summary to a file named timer_summary_<process id>
`writeStatSummary`	`LOGICAL`	`TRUE`	Should timers write the max/min/avg values for timers to the logfile?

`monitors/Timers/TimersMain/MPINative` writes two summaries to the logfile: the first gives the timer execution of the master processor, and the second gives the statistics of max, min, and avg times for timers on all processors. The secondary max, min, and avg times will not be written if some process executed timers differently than another. For example, this anomaly happens if not all processors contain at least one block. In this case, the `Hydro` timers only execute on the processors that possess blocks. See Section 25.4 for an example of this type of output. The max, min, and avg summary can be disabled by setting the runtime parameter `writeStatSummary` to false. In addition, each process can write its summary to its own file named `timer_summary_<process id>`. To prohibit each process from writing its summary to its own file, set the runtime parameter `eachProcWritesSummary` to false.

26.1.2 Tau

In `FLASH3.1` we add an alternative `Timers` implementation which is designed to be used with the `Tau` framework (`http://acts.nersc.gov/tau/`). Here, we use `Tau` API calls to time the `FLASH` labeled code sections (marked by `Timers_start` and `Timers_stop`). After running the simulation, the `Tau` profile contains timing information for both `FLASH` labeled code sections and all individual subroutines / functions. This is useful because fine grained subroutine / function level data can be overwhelming in a huge code like `FLASH`. Also, the callpaths are preserved, meaning we can see how long is spent in individual subroutines / functions when they are called from within a particular `FLASH` labeled code section. Another reason to use the `Tau` version is that the `MPINative` version (See Section 26.1.1) is implemented using recursion, and so incurs significant overhead for fine grain measurements.

To use this implementation we must compile the `FLASH` source code with the `Tau` compiler wrapper scripts. These are set as the default compilers automatically whenever we specify the `-tau` option (see Section 5.2) to the setup script. In addition to the `-tau` option we must specify `--with-unit=monitors/Timers/Timers-Main/Tau` as this `Timers` implementation is not the default.

26.2 Profiler

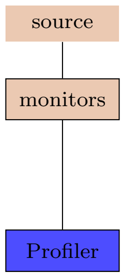

Figure 26.2: The `Profiler` unit directory tree.

In addition to an interface for simple timers, FLASH includes a generic interface for third-party profiling or tracing libraries. This interface is defined in the `monitors/Profiler` unit.

In FLASH4 we created an interface to the IBM profiling libraries libmpihpm.a and libmpihpm_smp.a and also to HPCToolkit `http://hpctoolkit.org/` (Rice University). We make use of this interface to profile FLASH evolution only, i.e. not initialization. To use this style of profiling add `-unit=monitors/-Profiler/ProfilerMain/mpihpm` or `-unit=monitors/Profiler/ProfilerMain/hpctoolkit` to your setup line and also set the FLASH runtime parameter `profileEvolutionOnly` = .true.

For the IBM profiling library (mpihpm) you need to add LIB_MPIHPM and LIB_MPIHPM_SMP macros to your Makefile.h to link FLASH to the profiling libraries. The actual macro used in the link line depends on whether you setup FLASH with multithreading support (LIB_MPIHPM for MPI-only FLASH and LIB_MPIHPM_SMP for multithreaded FLASH). Example values from sites/miralac1/Makefile.h follow

```
LIB_MPI =
HPM_COUNTERS = /bgsys/drivers/ppcfloor/bgpm/lib/libbgpm.a
LIB_MPIHPM = -L/soft/perftools/hpctw -lmpihpm $(HPM_COUNTERS) $(LIB_MPI)
LIB_MPIHPM_SMP = -L/soft/perftools/hpctw -lmpihpm_smp $(HPM_COUNTERS) $(LIB_MPI)
```

For HPCToolkit you need to set the environmental variable HPCRUN_DELAY_SAMPLING=1 at job launch to enable selective profiling (see the HPCToolkit user guide).

Part VII

Diagnostic Units

26.3 Proton Imaging Unit

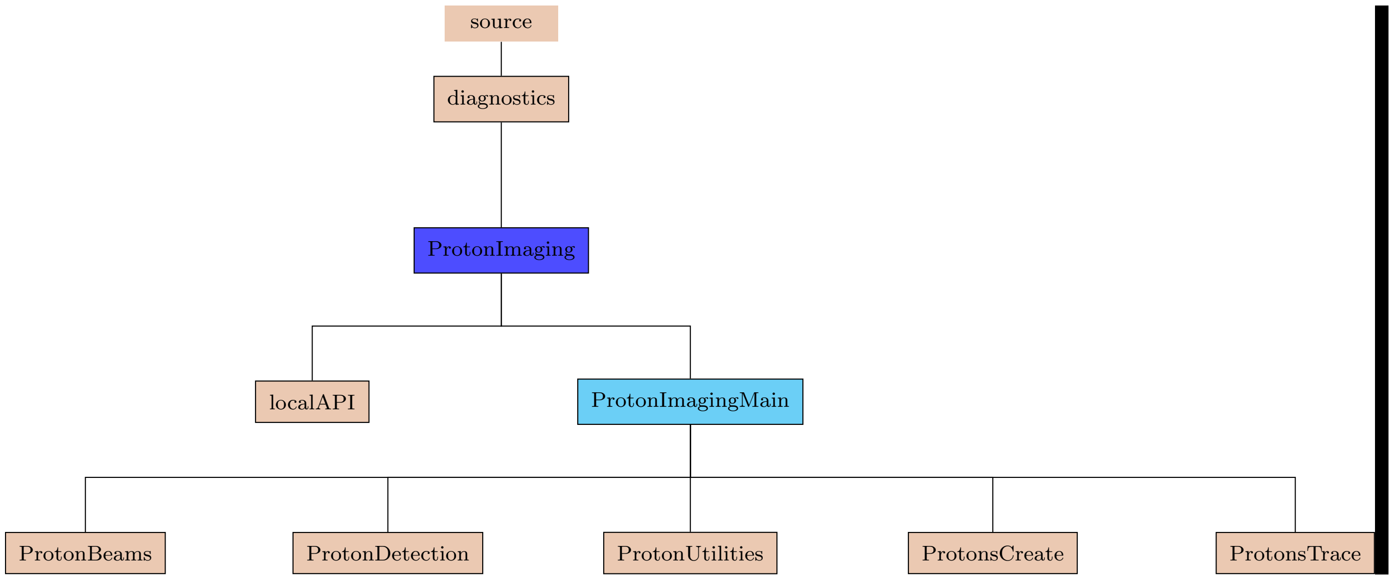

Figure 26.3: The `Proton Imaging` unit directory tree.

The `Proton Imaging` unit fires proton beams onto the simulation domain and records their deflection due to electric and magnetic fields on detector screens. The function `ProtonImaging` is the main driver that orchestrates the proton imaging execution. The deflection of the protons are calculated using the Lorentz force. For each cell in the domain the average electric and magnetic fields are used and the electric and magnetic components do not change within each cell. The code allows for setting up several proton beams with possibly different activation times and several detector screens. Each beam is associated with only one detector, but a detector is allowed to record the protons coming from more than one beam. This way one can simulate multienergetic proton beams by splitting them into several computational beams with identical spacial specifications and identical detector target but using different proton energies. The mapping 'beam → many detectors' is currently not allowed.

Tracing of the protons through the domain can be done in two ways: 1) crossing the domain during one time step or 2) allowing for time resolved proton tracing, i.e. tracing the protons through the domain during many time steps, if the velocities of the protons are sufficiently small. Although the proton imaging driver can be called during an entire simulation with proton beams being activated at certain simulation times, it is highly recommended to apply the proton imaging diagnostic as a post processing application on existing checkpoint files. Screen protons can be appended to existing detector files, but the proton imaging code does not write currently any data to the checkpoint files. Restarting a FLASH application from a previous proton imaging run is hence not recommended, especially if the time resolved proton imaging version is used. Old disk protons waiting to be transported though the domain may be out of sync when restarting a previous run.

26.3.1 Proton Deflection by Lorentz Force

In the presence of an electric and magnetic field, the (relativistic and non-relativistic) Lorentz force in CGS units on a proton in motion is:

$$\mathbf{F} = Q(\mathbf{E} + \mathbf{v}/c \times \mathbf{B}), \tag{26.1}$$

where Q is the charge of the proton in esu (g$^{1/2}$ cm$^{3/2}$ s^{-1}), $\mathbf{F}$ the force in dyne (g cm s^{-2}), $\mathbf{v}$ the proton velocity (cm s^{-1}), c the speed of light (2.998×10^{10} cm s^{-1}) and $\mathbf{E}$ and $\mathbf{B}$ are the electric and magnetic fields in Gauss ($g^{1/2}$ cm$^{-1/2}$ s^{-1}). The non-relativistic acceleration the proton experiences is:

$$\mathbf{a} \;=\; Q_m(\mathbf{E}+\mathbf{v}/c\times\mathbf{B}), \tag{26.2}$$

where Q_m is the mass rescaled charge Q/m of the proton. For uniform fields in each cell (constant (E_x, E_y, E_z) and (B_x, B_y, B_z)), this leads to a set of 1st order coupled differential equations in time

$$\begin{aligned}
\dot{v}_x(t) &= Q_m[E_x + v_y(t)B_z/c - v_z(t)B_y/c] && (26.3)\\
\dot{v}_y(t) &= Q_m[E_y + v_z(t)B_x/c - v_x(t)B_z/c] && (26.4)\\
\dot{v}_z(t) &= Q_m[E_z + v_x(t)B_y/c - v_y(t)B_x/c] && (26.5)
\end{aligned}$$

for the velocity components $v_x(t)$, $v_y(t)$ and $v_z(t)$. Given the initial proton velocity components (v_{0x}, v_{0y}, v_{0z}) at time $t = 0$, the analytical solution to this system of coupled differential equations becomes:

$$\begin{aligned}
v_x(t) &= (b_x^2E_x + b_xb_yE_y + b_xb_zE_z)Q_mt\\
&\quad +(b_x^2 + b_y^2\cos[BQ_mt/c] + b_z^2\cos[BQ_mt/c])v_{0x}\\
&\quad +b_ze_y(1-\cos[BQ_mt/c])c + b_ye_z(\cos[BQ_mt/c]-1)c\\
&\quad +b_xb_y(1-\cos[BQ_mt/c])v_{0y} + b_xb_z(1-\cos[BQ_mt/c])v_{0z}\\
&\quad +(b_y^2e_x + b_z^2e_x - b_xb_ye_y - b_xb_ze_z)\sin[BQ_mt/c]c\\
&\quad +(b_x^2b_z + b_y^2b_z + b_z^3)\sin[BQ_mt/c]v_{0y}\\
&\quad -(b_x^2b_y + b_z^2b_y + b_y^3)\sin[BQ_mt/c]v_{0z} && (26.6)\\
v_y(t) &= [x\to y, y\to z, z\to x]\ v_x(t) && (26.7)\\
v_z(t) &= [x\to z, y\to x, z\to y]\ v_x(t) && (26.8)
\end{aligned}$$

where B is the magnitude of the magnetic field vector and $b_x = B_x/B$ and $e_x = E_x/B$ are the magnetic field magnitude rescaled magnetic and electric field components. The operator $[x\to y, y\to z, z\to x]$ stands for 'replace x with y, y with z and z with x' in the formula for $v_x(t)$. Q_m is the mass rescaled charge of the proton. Note that the units of E_xQ_mt are the same as velocity. The quantities b_x, e_x and BQ_mt/c are dimensionless. Integrating $v_x(t)$, $v_y(t)$ and $v_z(t)$ over t, we get expressions for the positions $r_x(t)$, $r_y(t)$ and $r_z(t)$ as a function of time. The resulting equations have terms involving t, t^2, $\cos[BQ_mt/c]$ and $\sin[BQ_mt/c]$, and cannot be solved analytically. We therefore resort to a Runge-Kutta integration approach with the 6-dimensional ODE vector:

$$\frac{d}{dt}\begin{pmatrix}\mathbf{r}\\ \mathbf{v}\end{pmatrix} \;=\; \begin{pmatrix}\mathbf{v}\\ \mathbf{a}\end{pmatrix} = \begin{pmatrix}\mathbf{v}\\ Q_m(\mathbf{E}+\mathbf{v}/c\times\mathbf{B})\end{pmatrix}, \tag{26.9}$$

For certain orientations of **E** and **B**, however, analytical solutions for **r** and **v** are possible (see the unit test section).

26.3.1.1 Relativistic Proton Equation of Motion

Although not (yet) implemented into FLASH, we state here briefly the relativistic proton equation of motion. Starting from the Lorentz equation 26.1, the force **F** is the time derivative of the relativistic momentum **p**:

$$\mathbf{F} \;=\; \frac{d\mathbf{p}}{dt} = \frac{d[\gamma(\mathbf{v})m\mathbf{v}]}{dt}, \tag{26.10}$$

where m is the rest mass of the proton and $\gamma(\mathbf{v})$ is the Lorentz factor:

$$\gamma(\mathbf{v}) \;=\; 1/\sqrt{1-(\mathbf{v}\cdot\mathbf{v}/c)^2} = 1/\sqrt{1-(v/c)^2}. \tag{26.11}$$

Performing the differentiation on the r.h.s. of Eq.(26.10) using the chain rule (since both **v** and thus γ depend on time), we arrive at:

$$\mathbf{F} \;=\; \gamma(\mathbf{v})m\mathbf{a}_\perp + \gamma(\mathbf{v})^3m\mathbf{a}_\parallel, \tag{26.12}$$

where $\mathbf{a}_{\|}$ and $\mathbf{a}_{\perp}$ are the parallel and perpendicular components of the acceleration $\mathbf{a} = d\mathbf{v}/dt$ with respect to the velocity vector:

$$\mathbf{a} = \mathbf{a}_{\|} + \mathbf{a}_{\perp} \quad , \quad \mathbf{v}\cdot\mathbf{a}_{\perp} = 0 \quad , \quad \mathbf{v}\cdot\mathbf{a} = \mathbf{v}\cdot\mathbf{a}_{\|}. \tag{26.13}$$

Inverting Eq.(26.12) to find the acceleration from the force on a moving proton leads to:

$$\mathbf{a} \;=\; \frac{1}{\gamma(\mathbf{v})m}\left(\mathbf{F} - \frac{[\mathbf{v}\cdot\mathbf{F}]\mathbf{v}}{c^2}\right) \tag{26.14}$$

with magnitude:

$$a \;=\; \frac{1}{\gamma(\mathbf{v})m}\sqrt{F^2 - \frac{1+\gamma(\mathbf{v})^2}{c^2\gamma(\mathbf{v})^2}[\mathbf{v}\cdot\mathbf{F}]^2}, \tag{26.15}$$

and inserting the Lorentz force equation 26.1 we get the relativistic expression for the acceleration:

$$\mathbf{a} \;=\; Q_{m\gamma}\left(\mathbf{E} + \mathbf{v}/c\times\mathbf{B} - [\mathbf{v}/c\cdot\mathbf{E}]\;\mathbf{v}/c\right), \tag{26.16}$$

where $Q_{m\gamma}$ is the relativistic mass rescaled charge $Q/m\gamma(\mathbf{v})$ of the proton. Comparing this expression with its non-relativistic version from Eq.(26.2), the main difference is not only the relativistic increase in mass ($m\gamma(\mathbf{v})$) but also an extra term of order c^{-2} involving the electric field.

26.3.1.2 Approximate Solutions to the Non-Relativistic Proton Equation of Motion

Since Runge-Kutta integration with constraints (due to the cell boundaries) is expensive, we wish to derive conditions under which the proton path through a cell approximates a parabola, for which quadratic solutions to the path positions become available. To this end we expand $\mathbf{v}(t)$ in terms of t around the cell entry point $t = 0$. We get:

$$\mathbf{v}(t) \;=\; \mathbf{v}_0 + \left|\frac{d\mathbf{v}(t)}{dt}\right|_{t=0} t + \frac{1}{2}\left|\frac{d^2\mathbf{v}(t)}{dt^2}\right|_{t=0} t^2 + O[t^3] \tag{26.17}$$

$$\;=\; \mathbf{v}_0 + \mathbf{a}_0 t + \frac{\mathbf{j}_0}{2}t^2 + O[t^3], \tag{26.18}$$

where

$$\mathbf{a}_0 \;=\; Q_m(\mathbf{E} + \mathbf{v}_0/c\times\mathbf{B}) \tag{26.19}$$

$$\mathbf{j}_0 \;=\; Q_m(\mathbf{a}_0/c\times\mathbf{B}) \tag{26.20}$$

are the acceleration and jerk vectors at the cell entry point. Integration of Eq.(26.18) yields the path equation:

$$\mathbf{r}(t) \;=\; \mathbf{r}_0 + \mathbf{v}_0 t + \frac{\mathbf{a}_0}{2}t^2 + \frac{\mathbf{j}_0}{6}t^3 + O[t^4]. \tag{26.21}$$

The leading parabolic error term is hence the term involving the jerk vector. The largest parabolic error term ϵ can be estimated by:

$$\epsilon \;=\; \frac{\max \mathbf{j}_0}{6}t^3. \tag{26.22}$$

If ϵ is less than the allowed positional error of the computation, the parabolic approximation is used. To get also the velocity components with the same accuracy, the jerk terms are used to compute the velocities. If the jerk terms are omitted from the velocity calculations, the velocity components would only be accurate to first order in t and considerable error in velocity directions can accumulate during a proton imaging application.

In order to get a feeling for the conditions under which the parabolic approximation is applied in FLASH, let us first state the expression for the jerk vector $\mathbf{j}_0$, which is obtained by noting that $\mathbf{j}_0 = d\mathbf{a}_0/dt$ and using the acceleration vector expression twice:

$$\mathbf{j}_0 = (Q_m^2/c)\mathbf{E}\times\mathbf{B} + (Q_m^2/c^2)(\mathbf{v}_0\times\mathbf{B})\times\mathbf{B}. \tag{26.23}$$

The maximum magnitude that the $\mathbf{j}_0$ vector can achieve is given by the situation in which the pairs $\mathbf{B},\mathbf{v}_0$ and $\mathbf{E},\mathbf{B}$ are perpendicular and $\mathbf{E}\times\mathbf{B}$ is opposite to $\mathbf{v}_0$. This leads to

$$|\mathbf{j}_0| \leq (Q_m^2/c)EB + (Q_m^2/c^2)B^2v_0 \tag{26.24}$$

and the inequality will also hold for the individual components of $\mathbf{j}_0$. Assuming no electric field, we can estimate the magnitude of B for which the parabolic approximation should be valid. In FLASH, the positional error is defined as a fraction f times the minimum cell side size. For a cubic cell with sides Δ we can set up the parabolic condition on B as follows:

$$\frac{Q_m^2B^2v_0}{6c^2}t^3 \leq \Delta f. \tag{26.25}$$

The time it takes to cross the cubic cell is of the order of $t=\Delta/v_0$ and we conservatively extend this time by the factor of $\sqrt[3]{6}$ to get rid of the 6 in the denominator. The parabolic condition on B becomes

$$B \leq \frac{cv_0}{Q_m\Delta}\sqrt{f}. \tag{26.26}$$

For typical FLASH runs, we have for 20MeV protons $v\approx c/5$ and Δ is of the order of microns (10^{-4}cm) for typical simulations. The accuracy fraction f is typically 10^{-6}. We also have $Q_m \approx 2.9\times10^{14}$ and $c = 2.99\times10^{10}$. Hence under these conditions we have:

$$B \leq \approx 10^7\text{Gauss}, \tag{26.27}$$

i.e., all magnetic fields under 10^7 Gauss in a cell can be treated parabolically.

26.3.1.3 Approximate Solutions to the Relativistic Proton Equation of Motion

This follows along the lines of the previous section (26.3.1.2). Eq.(26.19) must be replaced by the relativistic expression from Eq.(26.16), replacing $\mathbf{v}$ by $\mathbf{v}_0$, and Eq.(26.20) must be replaced by the time derivative of Eq.(26.16), replacing in the final expression $\mathbf{v}$ by $\mathbf{v}_0$ and $\mathbf{a}$ by $\mathbf{a}_0$:

$$\mathbf{a}_0 = Q_{m\gamma}\left(\mathbf{E}+\mathbf{v}_0/c\times\mathbf{B} - [\mathbf{v}_0/c\cdot\mathbf{E}]\,\mathbf{v}_0/c\right), \tag{26.28}$$

$$\mathbf{j}_0 = Q_{m\gamma}\left(\mathbf{a}_0/c\times\mathbf{B} - [\mathbf{a}_0/c\cdot\mathbf{E}]\,\mathbf{v}_0/c - 2[\mathbf{v}_0/c\cdot\mathbf{E}]\,\mathbf{a}_0/c\right), \tag{26.29}$$

where $Q_{m\gamma}$ is equal to $Q/m\gamma(\mathbf{v}_0)$. Note the extra terms of order c^{-2} when compared with Eqs.(26.19) and (26.20). The largest parabolic error expression in Eq.(26.22) remains the same. Assuming again no electric field, the same steps leading to the non-relativistic parabolic B condition in Eq.(26.26), leads to:

$$B \leq \frac{cv_0}{Q_{m\gamma}\Delta}\sqrt{f}, \tag{26.30}$$

the only difference being in using the relativistic mass rescaled proton charge. For the 20MeV protons $v\approx c/5$ this would lead to a factor of ≈ 1.02 larger B than in Eq.(26.27), due to the relativistically reduced magnitude of $\mathbf{j}_0$.

26.3.2 Setting up the Proton Beam

The setup of each proton beam follows closely the setup of the laser beams in 17.4.6. The major difference is that the proton imaging beams originate from 3D capsules instead of 2D planar crossection areas. This allows for simulating proton capsule aberrations in the proton beams. The radius of the capsule as well as its center location is specified for each beam at runtime, as well as each beams full conical aperture angle. Target coordinates are only needed for directional purposes and the target area is circular and perpendicular to the beam's direction. Additional runtime parameters needed for each beam are: 1) the launching time (the beam fires once the simulation time exceeds the launching time), 2) its target detector screen and 3) the number of protons to be launched and their energies. Once each beam has been set up, it is checked, if its capsule volume is completely outside of the computational domain. A beam capsule (partially) inside the domain is not allowed. A local set of 3D rectangular grid unit vectors $\mathbf{u}_1$,$\mathbf{u}_2$,$\mathbf{u}_3$ is constructed for each beam, such that $\mathbf{u}_3$ points from the capsule center to the target center and $\mathbf{u}_1 \times \mathbf{u}_2 = \mathbf{u}_3$. The 3D grid unit vectors serve for generating statistical 3D points inside the spherical capsule as well as statistical 2D points inside the circular target area.

26.3.3 Creating the Protons

The protons inside each beam are created by connecting one-to-one the statistical 3D grid points inside the capsule with the statistical 2D grid points inside the circular target area. The proton directions inside each beam are therefore not conically collinear and are allowed to cross. The proton initial positions and velocities on the domain surface are calculated using the same strategy as presented in 17.4.7.6. Protons missing the domain can either be simply ignored or directly recorded on the detector screen.

26.3.3.1 Moving Protons throught the Domain

As the total number of protons generated can be very large, special techniques have to be used to overcome the computational memory constraints. The Proton Imaging unit has been designed to work with a proton batch and screen proton bucket combination. Both the batch and the bucket are of much smaller size than the total protons and screen protons generated and can be seen as temporary storage devices for both entities. During a time step, the active proton beams start filling the generated protons into the beam proton batch. Once filled, the beam protons in the batch are sent through the domain, where they are either collected as disk protons into the disk proton batch (if time resolved proton imaging was requested) or as screen protons into the screen proton bucket. If the screen proton bucket is full, its contents (screen protons) are written to the corresponding detector files and emptied. The refilling of both the beam/disk proton batch and the screen bucket are independent of each other and both batch and bucket can be of different sizes. The main function `ProtonImaging` processes beam/disk proton batch after batch until no more active beam/disk protons are present. As an example, if at a time step we have 3 active beams with $1,000,000$ protons each and the dimension of the proton batch is set to $100,000$, a total of 30 beam proton batches will be generated and sent through the domain.

26.3.3.2 Proton Specifications

Each beam/disk proton needs to know its position x, y, z and velocity v_x, v_y, v_z as it traverses the domain. In addition to these 6 components it needs to know: 1) the time spent travelling in domain, 2) the current block and processor numbers, 3) a global identification tag, 4) the originating beam and target detector numbers. Screen protons on the other hand are only defined on the detector screen and hence need no specific information for domain travelling. Their information is reduced to a screen position coordinate pair x, y and a detector number to which detector they are associated with.

Additionally, upon request, the proton imaging code is able to calculate extra magnetic diagnostic quantities $\mathbf{k}$ and J for each beam/disk and screen proton:

$$\mathbf{k} = \int \mathbf{B}\, d\ell, \tag{26.31}$$

$$J = \int \mathbf{v}_n \cdot (\nabla \times \mathbf{B})\, d\ell, \tag{26.32}$$

where $\int d\ell$ denotes path integration, $\mathbf{B}$ is the magnetic field vector and $\mathbf{v}_n$ is the unit normal velocity vector along the proton path. Transforming the path integrals into time integrals using the relation $d\ell = |\mathbf{v}(t)|dt$, we get the differentials:

$$\frac{d\mathbf{k}}{dt} = \mathbf{B}|\mathbf{v}(t)|, \tag{26.33}$$

$$\frac{dJ}{dt} = \mathbf{v}(t) \cdot (\nabla \times \mathbf{B}). \tag{26.34}$$

leading to extra 4 entries in the Runge-Kutta vector in Eq.(26.9):

$$\frac{d}{dt}\begin{pmatrix} \mathbf{r} \\ \mathbf{v} \\ \mathbf{k} \\ J \end{pmatrix} = \begin{pmatrix} \mathbf{v} \\ Q_m(\mathbf{E} + \mathbf{v}/c \times \mathbf{B}) \\ \mathbf{B}v \\ \mathbf{v} \cdot (\nabla \times \mathbf{B}) \end{pmatrix}, \tag{26.35}$$

If the parabolic path approximation is used for a cell, then $\mathbf{v}(t) = \mathbf{v}_0 + \mathbf{a}_0 t$, where $\mathbf{v}_0$ and $\mathbf{a}_0$ are the velocity and acceleration at cell entry. For a J cell contribution we have (note this is a general result not depending on the parabolic approximation):

$$J = \int_0^T \mathbf{v}(t) \cdot (\nabla \times \mathbf{B}) dt = \int_0^T d\mathbf{r}(t) \cdot (\nabla \times \mathbf{B}) = [\mathbf{r}(T) - \mathbf{r}_0] \cdot (\nabla \times \mathbf{B}) \tag{26.36}$$

where T is the cell crossing time and $\mathbf{r}_0$,$\mathbf{r}(T)$ are the cell entry and exit locations of the proton. For the parabolic $\mathbf{k}$ cell contribution we have;

$$\mathbf{k} = \mathbf{B} \int_0^T |\mathbf{v}_0 + \mathbf{a}_0 t| dt. \tag{26.37}$$

The parabolic path length integral can be solved exactly. Using the following two dimensionless quantities:

$$X = \frac{|\mathbf{a}_0|}{|\mathbf{v}_0|} T \tag{26.38}$$

$$\cos\theta = \frac{\mathbf{a}_0 \cdot \mathbf{v}_0}{|\mathbf{a}_0||\mathbf{v}_0|} \tag{26.39}$$

we get

$$\begin{aligned} \int_0^T |\mathbf{v}_0 + \mathbf{a}_0 t| dt &= \frac{1}{2}|\mathbf{v}_0| T \Big[1 + \left(X^{-1}\cos\theta + 1\right)\left(\sqrt{X^2 + 2X\cos\theta + 1} - 1\right) \\ &\quad + X^{-1}(1 - \cos^2\theta) \ln\left(\frac{\cos\theta + X + \sqrt{X^2 + 2X\cos\theta + 1}}{\cos\theta + 1}\right)\Big]. \end{aligned} \tag{26.40}$$

Computational application of this formula must be done with some care to avoid loss of accuracy.

26.3.4 Setting up the Detector Screens

Each detector screen is defined as a square planar area with a specific side length s and an optional circular pinhole. The orientation of the screen in 3D space is specified by three components: 1) the center location of the screen $\mathbf{C}$, 2) the normal vector of the screen plane $\mathbf{n}$ and 3) the orthogonal unit vector pair $\mathbf{u}_x$,$\mathbf{u}_y$ with origin at the center and oriented in such a way that each unit vector is parallel to two opposite sides of the detector screen. Location of the pinhole $\mathbf{H}$ is fixed by giving the distance between the two pinhole and detector centers and is always located on the detector side opposite to $\mathbf{n}$. The circular pinhole area is coplanar to the detector screen area. While $\mathbf{C}$ and $\mathbf{n}$ are sufficient to characterize the screen plane, the exact location of the detector square area is only specified once the orientation of $\mathbf{u}_y$ (or $\mathbf{u}_x$) is fixed. For that purpose we define a tilting angle α of $\mathbf{u}_y$ wrt one of the global 3D axes along the normal vector $\mathbf{n}$. A tilting angle of $\alpha = 0$ would thus mean that the chosen global axis and $\mathbf{u}_y$ are coplanar.

26.3.4.1 Recording Protons on the Detector Screen

After each proton leaves the domain, it is located on the domain surface at a position $\mathbf{P}$ and with (outward from domain) velocity $\mathbf{v}$. The goal is to see, if the proton actually hits the screen plane and to record the local coordinates (x, y) on the screen plane with coordinate basis $[\mathbf{u}_x, \mathbf{u}_y]$. After some algebra we arrive at the following conditions

$$\mathbf{v} \cdot \mathbf{n} = 0 \qquad \text{proton moves parallel to screen plane} \tag{26.41}$$

$$\frac{(\mathbf{C} - \mathbf{P}) \cdot \mathbf{n}}{\mathbf{v} \cdot \mathbf{n}} > 0 \qquad \text{proton hits screen plane} \tag{26.42}$$

and the following expressions for the local coordinates

$$\begin{aligned} x &= \frac{\mathbf{u}_y \cdot [\mathbf{v} \times (\mathbf{C} - \mathbf{P})]}{\mathbf{v} \cdot \mathbf{n}} \\ y &= \frac{\mathbf{u}_x \cdot [(\mathbf{C} - \mathbf{P}) \times \mathbf{v}]}{\mathbf{v} \cdot \mathbf{n}}. \end{aligned} \tag{26.43}$$

For better handling of the screen output data, the local coordinates are shifted and rescaled such that $(x, y) \in [0, 1]$ when the proton is on the detector screen. Using the detectors side length s, we achieve this by the following local coordinate transformation:

$$x \longrightarrow (x + s/2)/s \tag{26.44}$$

$$y \longrightarrow (y + s/2)/s. \tag{26.45}$$

If a pinhole is present, the code has to check, if the proton makes it through the hole. Since the detector screen area and the circular pinhole area are coplaner, we can use the local coordinate basis $[\mathbf{u}_x, \mathbf{u}_y]$ located at the pinhole center $\mathbf{H}$ to calculate a local pinhole coordinate for each proton, in analogy to Eq.(26.43):

$$h_x = \frac{\mathbf{u}_y \cdot [\mathbf{v} \times (\mathbf{H} - \mathbf{P})]}{\mathbf{v} \cdot \mathbf{n}} \tag{26.46}$$

$$h_y = \frac{\mathbf{u}_x \cdot [(\mathbf{H} - \mathbf{P}) \times \mathbf{v}]}{\mathbf{v} \cdot \mathbf{n}}. \tag{26.47}$$

The proton makes it through the pinhole, if $h_x^2 + h_y^2 \leq r_h^2$, where r_h is the radius of the pinhole.

The user is able to specify via a runtime parameter, if he wants only the detector screen protons $(x, y) \in [0, 1]$ to be written to the detector file or if he also wants to record the offscreen protons $(x, y) \notin [0, 1]$. Each detector file is currently an ascii file (formatted) and named:

$$\text{<basename>ProtonDetectorFile<detectorID>\_<timestamp>} \tag{26.48}$$

where <basename> is the name of the simulation, <detectorID> is the detector number (currently limited to the range [01-99]) and (optionally) <timestamp> is the simulation time when the file was created. Only the (x, y) pairs are written (first x followed by y on each line) without any headers. Thus the file can be directly incorporated and read by other software for graphical output (see for example the proton imaging ASCII $- >$ PGM greyscale converter). Additionally, if requested, the detector file will contain in columns 3 to 6 the proton magnetic diagnostic quantities k_x, k_y, k_z, J from Eqs.(26.31) and (26.32), in that order.

26.3.5 Time Resolved Proton Imaging

For some applications (slow moving protons, fast domain changing) it is desireable to adjust the domain environment as the protons move through it. The proton imaging unit has been given this capability by monitoring the time each proton spends in the domain and compare it to the computational time step. When the proton time exceeds the time step value, it is stored as a disk proton which will be written to disk. All disk protons from a previous time step must be first processed during a new time step before any new beam protons are generated. During a time step, the main driver `ProtonImaging` calls the following two tasks, each of which does the following operations:

Transport disk protons:

- Read all disk protons from old disk proton file
- Trace all disk protons through domain:
  - To new disk proton file (if proton time > time step)
  - To screen detector
- Rename new disk proton file ⟶ old disk proton file

Transport beam protons:

- Create all beam protons
- Trace all beam protons through domain:
  - To new disk proton file (if proton time > time step)
  - To screen detector
- Append new disk proton file ⟶ old disk proton file

The time resolved application requires extra memory and disk storage due to the presence of disk protons as well as extra reading/writing time from/to disk. If only a non-time resolved proton imaging run is requested, the code skips all array allocations and operations associated with the disk protons, and only the underlined actions of the transport beam protons task get activated.

26.3.6 Usage

To include the use of the Proton Imaging unit, the following should be included into the setup line command:

```
+protonImaging [pi_maxBeams=<number> pi_maxDetectors=<number> threadProtonTrace=True]
```

The +protonImaging shortcut handles all the logistics for properly including the `ProtonImaging` unit. The default settings are: maximum number of beams = 1, maximum number of detectors = 1 and no use of threading during tracing of protons through the domain, which can be changed by the following three setup variables:

- **pi_maxBeams**: The maximum number proton beams for the simulation.
- **pi_maxDetectors**: The maximum number of proton imaging detectors for the simulation.
- **threadProtonTrace**: Enables threading during proton domain tracing.

Using proton imaging runtime parameters in the flash.par file, the user can set up the proper proton imaging configuration for his specific needs. The following list of runtime parameters is currently available for the user.

26.3.6.1 Proton Imaging Beams Runtime Parameters

The following are the runtime parameters for the proton imaging beams. The _n at the end of each runtime parameter characterizes the beam number, hence replace _n by _1 for the first beam, _n by _2 for the second beam, etc.

- `pi_numberOfBeams`: The number of proton imaging beams that are going to be used.
- `pi_beamCapsule[X,Y,Z]_n`: The global 3D components of the capsule center position vector **C**.
- `pi_beamCapsuleRadius_n`: The radius of the spherical capsule.
- `pi_beamTarget[X,Y,Z]_n`: The global 3D components of the target position vector **T** for directional purpose.

- `pi_beamApertureAngle_n`: The conical full aperture angle.
- `pi_beamProtonEnergy_n`: The energy (in MeV) of the protons in the beam.
- `pi_beamTime2Launch_n`: The time during the simulation, when the beam should be fired.
- `pi_beamDetector_n`: The detector number, where the protons of the beam should be recorded.
- `pi_beamNumberOfProtons_n`: Number of protons to be launched from the beam.
- `pi_beamNoBoundaryCondition_n`: Ignore domain boundary conditions (reflective) when protons enter the domain?

26.3.6.2 Proton Imaging Detectors Runtime Parameters

The following are the runtime parameters for the proton imaging detectors. As for the beams, the _n at the end of each runtime parameter characterizes the detector number.

- `pi_numberOfDetectors`: The number of proton imaging detectors that are going to be used.
- `pi_detectorCenter[X,Y,Z]_n`: The global 3D components of the detector center position vector $\mathbf{C}$.
- `pi_detectorNormal[X,Y,Z]_n`: The local 3D components of the detector normal vector $\mathbf{n}$.
- `pi_detectorSideLength_n`: The side length (cm) of the detector square screen.
- `pi_detectorSideTiltingAngle_n`: The tilting angle (degrees) of two sides parallel to the detector screen unit axis $\mathbf{u}_y$] with respect to the tilting axis.
- `pi_detectorSideTiltingAxis_n`: The global tilting axis ('x','y' or 'z') for the detector screen.
- `pi_detectorAlignWRTbeamNr_n`: A useful shortcut to place the detector screen right along a beam path with the screen surface orthogonal to the beam path. This, together with the specified detector distance from the beam capsule center, automatically calculates the center vector $\mathbf{C}$ and the normal vector $\mathbf{n}$. If a beam number ≤ 0 is specified, no alignment is performed and the user has to supply center vector and normal vector coordinates.
- `pi_detectorDistance2BeamCapsule_n`: The detector distance from the beam capsule center, used only if the detector is alligned with respect to a beam.
- `pi_detectorPinholeRadius_n`: The radius of the pinhole. If ≤ 0 no pinhole is used.
- `pi_detectorPinholeDist2Det_n`: The pinhole center distance from the detector center, useful only if a pinhole radius > 0 was specified.

26.3.6.3 Proton Imaging General Runtime Parameters

- `pi_cellStepTolerance`: This factor times the smallest dimension of each cell is taken as the positional error tolerance for the protons during their path (parabolic or Runge-Kutta) tracing through each cell.
- `pi_cellWallThicknessFactor`: Controls the (imaginary) thickness of the cell walls to ensure computational stability of the proton imaging code. The cell thickness is defined as this factor times the smallest cell dimension along all geometrical axes. The factor is currently set to 10^{-6} and should only very rarely be changed.
- `pi_detectorFileNameTimeStamp`: If set to true, a time stamp will be added to each detector file name. This allows for time splitting of detectors.
- `pi_detectorXYwriteFormat`: Controls formatted ascii output of the proton (x, y) pairs on the detector screens (default 'es20.10').

- pi_detectorDGwriteFormat: Controls formatted ascii output of the magnetic diagnostic quantities k_x, k_y, k_z, J on the detector screens (default 'es15.5').
- pi_flagDomainMissingProtons: If true, any proton missing the domain will abort the program. If false, protons missing the domain will be recorded directly on the detector screen.
- pi_ignoreElectricalField: If true, the electrical field in each cell is ignored and the proton movement is only governed by the magnetic field (deflection only).
- pi_IOaddDetectorScreens: If true, the square frame of each detector will be added to the plotfile.
- pi_IOaddProtonsCapsule2Domain: If true, the proton paths from the capsule to the domain entry point will be added to the plotfile.
- pi_IOaddProtonsDomain2Screen: If true, the proton paths from the domain exit point to the detector screen will be added to the plotfile.
- pi_IOmaxBlockCrossingNumber: This is an estimate of the maximum proton path length while travelling through the block. This estimate is given as an integer number in units of block sides (default 5). Only in extremely rare cases, when the magnetic and electric fields are strong and sufficiently warped inside a block and the protons start to circulate inside the block, does one have to increase this number.
- pi_IOnumberOfProtons2Plot: The number of protons that are to be plotted and written to the plotfile.
- pi_maxProtonCount: The maximum number of beam/disk protons that can be created/read-in on one processor per batch in the domain.
- pi_opaqueBoundaries: If true, the protons do not go through cells marked as opaque boundaries.
- pi_printBeams: If true, it prints detailed information about the proton beams to a file with name <basename>ProtonBeamsPrint.txt, where <basename> is the base name of the simulation.
- pi_printDetectors: If true, it prints detailed information about the proton detectors to a file with name <basename>ProtonImagingDetectors.txt, where <basename> is the base name of the simulation.
- pi_printMain: If true, it prints general information regarding the proton imaging setup to a file with name <basename>ProtonImagingMainPrint.txt, where <basename> is the base name of the simulation.
- pi_printProtons: If true, it prints detailed information about the all protons generated during the simulation. Protons are 'generated' on the domain surface and the info is written to several files labeled by batch number BID, processor rank number PID and a time stamp. Each processor writes its own file(s) with name(s): <basename>printProtonsBatch<BID>Proc<PID>.txt, where <basename> is the base name of the simulation. Use of this feature is reserved ONLY for debugging purposes and is currently limited to 10 batches and 100 processors per time stamp. Usage of a larger number of batches/processors during a simulation does not abort the run, but protons on batches with BID > 10 and processors with PID > 99 are simply ignored and not printed. Users other than code developers should not activate this feature.
- pi_protonDeterminism: If true, the Grid Unit will be forced to use the sieve algorithm to move the proton particle data. Forcing this algorithm will result in a slower movement of data, but will fix the order the processors pass data and eliminate round off differences in consecutive runs.
- pi_recordOffScreenProtons: If true, protons not hitting their target detector screen are also recorded on the detector files. These protons will have screen coordinate pairs $(x, y) \notin [0, 1]$.
- pi_RungeKuttaMethod: Specifies which Runge Kutta method to use for proton tracing. Current options are: 'CashKarp45' (order 4, default), 'EulerHeu12' (order 1), 'BogShamp23' (order 2), 'Fehlberg34' (order 3) and 'Fehlberg45' (order 4).

- `pi_screenProtonBucketSize`: Sets the bucket size for flushing screen protons out to disk.
- `pi_screenProtonDiagnostics`: If true, the magnetic diagnostic quantities k_x, k_y, k_z, J are evaluated for each proton and recorded on the detector screens.
- `pi_timeResolvedProtonImaging`: If true, it activates the time resolved proton imaging part of the code. Protons might need several time steps to cross the domain.
- `pi_useIOprotonPlot`: If true, protons are plotted to the plotfile for visualization pusposes.
- `pi_useParabolicApproximation`: If true, the code traces protons parabolically through cells for low B / high v combinations (section 26.3.1.2).
- `useProtonImaging`: If false, no proton imaging will be performed, even if the code was compiled to do so. Bypasses the need to rebuild the code.
- `threadProtonTrace`: If true, proton tracing through a block is threaded. This runtime parameter can only be set during setup of the code.

26.3.7 Unit Test

The unit test for the proton imaging unit consists in sending a ring of protons perpendicular onto a uniform circular B field and measuring the deflection (radial increase) of the ring. Due to the circular B field and the velocity direction of the protons, each proton experiences a radial outward force and the radial increase of the protons can be calculated analytically.

26.3.7.1 Deflection of a Proton Ring by a Uniform Circular Magnetic Field

Consider the case of a uniform circular magnetic field with constant magnetic flux density B pointing tangentially in clock- or anticlock-wise orientation around an axis, which we chose to be the y axis. If a proton has only a y component velocity $v_{0y} \neq 0$ initially, then it will be deflected radially outward or inward, depending on the clock- or anticlockwise orientation of $\mathbf{B}$. To simplify the calculations, we assume that the proton is located such that at this point we have only a z magnetic component, that is $B_z = \pm B$ and $B_x, B_y = 0$. Since also no electric field is present, we have that:

$$E_x, E_y, E_z, e_x, e_y, e_z, b_x, b_y = 0 \tag{26.49}$$
$$b_z = B_z/B = \pm 1 \tag{26.50}$$
$$v_{0x}, v_{0z} = 0. \tag{26.51}$$

Putting these values into Eqs.26.6, 26.7 and 26.8, the proton velocities become:

$$v_x(t) = \pm v_{0y} \sin[BQ_m t/c] \tag{26.52}$$
$$v_y(t) = v_{0y} \cos[BQ_m t/c] \tag{26.53}$$
$$v_z(t) = 0 \tag{26.54}$$

showing that the proton moves within the same z-plane. The $+$ sign in $v_x(t)$ applies, if $B_z = +B$ (anti-clockwise orientation) and the $-$ sign, if $B_z = -B$ (clockwise orientation). Integration over time gives the position equations:

$$r_x(t) = r_{0x} \pm \frac{cv_{0y}}{BQ_m}(1 - \cos[BQ_m t/c]) \tag{26.55}$$
$$r_y(t) = r_{0y} + \frac{cv_{0y}}{BQ_m} \sin[BQ_m t/c] \tag{26.56}$$
$$r_z(t) = r_{0z} \tag{26.57}$$

Taking the anticlockwise orientation of B, looking from above onto the fized z-plane, the proton will perform a half-circle of radius cv_{0y}/BQ_m. We are interested in the (radial) deflection along the x axis. The proton will travel through the domain in the y direction, where on exit the detector screen is placed. If we place the detector right at the exit of the y direction, then we can calculate from the $r_y(t)$ equation the time it takes for the proton to travel through (exit) the domain:

$$t_{exit} \quad = \quad \frac{c}{BQ_m} \arcsin\left(\frac{D_y BQ_m}{cv_{0y}}\right), \tag{26.58}$$

where D_y is the length of the domain in y direction. If $D_y BQ_m / cv_{0y} > 1$, then the proton will not exit the domain but rather curve back inside the domain. This happens if either D_y is too large (the domain extends too far into the y direction), B is too large or the initial velocity v_{0y} is too low. For a given D_y and v_{0y}, the limiting B would be:

$$B_{limit} \quad = \quad \frac{cv_{0y}}{D_y Q_m}. \tag{26.59}$$

Inserting the t_{exit} expression into the $r_x(t)$ equation, we get:

$$r_x(t_{exit}) \quad = \quad r_{0x} + \frac{cv_{0y}}{BQ_m}\left(1 - \sqrt{1 - \left(\frac{D_y BQ_m}{cv_{0y}}\right)^2}\right). \tag{26.60}$$

The radial deflection Δr of the proton on the detector screen will be equal to $r_x(t_{exit}) - r_{0x}$ and therefore:

$$\Delta r \quad = \quad \frac{cv_{0y}}{BQ_m}\left(1 - \sqrt{1 - \left(\frac{D_y BQ_m}{cv_{0y}}\right)^2}\right). \tag{26.61}$$

The limiting radial deflection (i.e., the maximal radial deflection) that can be detected by the screen at the domains exit is obtained by inserting the expression of B_{limit} into the last equation, which gets:

$$\Delta r_{limit} \quad = \quad D_y, \tag{26.62}$$

and is hence equal to the domains extension in y direction.

26.3.7.2 FLASH Setup of the Unit Test and Results of some Test Runs

We set up a 3D cartesian domain consisting of a rectangular box with dimensions (in cm): x axis $[0, 3]$, y axis $[0, 1]$ and z axis $[0, 3]$. A circular beam of 10000 protons with radius 0.5cm is shot along the y axis perpendicular to the xy plane and centered on the xz plane at (1.5,1.5). The square detector screen was placed extremely close to the domain exit in y direction and was of the same size as the domain's xz plane, i.e., of side length 3cm and centered at (1.5,1.5).

The variable parameters used were: 1) the proton energies (3 and 20MeV), 2) the uniform refinement levels (3,4,5) and the magnetic field flux B (in Gauss). The following radial deflections Δr were recorded: 1) the theoretical Δr_{thr}, 2) the maximum Δr_{max}, 3) the minimum Δr_{min} and 4) the average Δr_{avg}. The results are presented in the following tables.

Table 26.2: Maximum Δr_{max}, minimum Δr_{min}, average Δr_{avg} and theoretical Δr_{thr} outward radial deflections on a ring of 3 MeV protons for uniform domain refinement levels 3,4,5. Subscript numbers indicate multiplication by negative exponents: n_e means $n \times 10^{-e}$.

Proton energy 3 MeV (0.080 c), Refinement Levels = 3,4,5				
B	Δr_{max}	Δr_{min}	Δr_{avg}	Δr_{thr}
$1,000$	2.00259_3	2.00116_3	2.00230_3	
	2.00259_3	2.00220_3	2.00251_3	2.00259_3
	2.00259_3	2.00250_3	2.00257_3	
$10,000$	2.00339_2	2.00230_2	2.00309_2	
	2.00339_2	2.00314_2	2.00331_2	2.00339_2
	2.00339_2	2.00333_2	2.00337_2	
$100,000$	2.09006_1	2.08924_1	2.08977_1	
	2.09006_1	2.08986_1	2.08998_1	2.09006_1
	2.09006_1	2.09001_1	2.09004_1	
$249,677$	9.97589_1	9.80670_1	9.86783_1	
	9.97589_1	9.90126_1	9.92832_1	9.97588_1
	9.97589_1	9.94638_1	9.95797_1	

Table 26.3: Idem like for Table 26.2, but for 20 MeV protons.

Proton energy 20 MeV (0.203 c), Refinement Levels = 3,4,5				
B	Δr_{max}	Δr_{min}	Δr_{avg}	Δr_{thr}
$1,000$	7.86058_4	7.85494_4	7.85946_4	
	7.86058_4	7.85885_4	7.86025_4	7.86058_4
	7.86058_4	7.86018_4	7.86050_4	
$10,000$	7.86106_3	7.85565_3	7.85991_3	
	7.86106_3	7.85995_3	7.86075_3	7.86106_3
	7.86106_3	7.86081_3	7.86098_3	
$100,000$	7.90975_2	7.90635_2	7.90862_2	
	7.90975_2	7.90891_2	7.90946_2	7.90975_2
	7.90975_2	7.90956_2	7.90968_2	
$636,085$	9.98376_1	9.80750_1	9.86908_1	
	9.98376_1	9.90287_1	9.93061_1	9.98375_1
	9.98376_1	9.94942_1	9.96196_1	

Table 26.4: Idem like for Table 26.2, but for 200 MeV protons.

Proton energy 200 MeV (0.566 c), Refinement Levels = 3,4,5				
B	Δr_{max}	Δr_{min}	Δr_{avg}	Δr_{thr}
$10,000$	2.82180_3	2.81978_3	2.82139_3	
	2.82180_3	2.82128_3	2.82168_3	2.82180_3
	2.82180_3	2.82168_3	2.82177_3	
$100,000$	2.82403_2	2.82268_2	2.82361_2	
	2.82403_2	2.82370_2	2.82392_2	2.82403_2
	2.82403_2	2.82395_2	2.82400_2	
$1,000,000$	3.09146_1	3.09026_1	3.09100_1	
	3.09146_1	3.09116_1	3.09133_1	3.09145_1
	3.09146_1	3.09138_1	3.09142_1	
$1,771,934$	9.99584_1	9.80813_1	9.87006_1	
	9.99584_1	9.90413_1	9.93244_1	9.99581_1
	9.99584_1	9.95191_1	9.96538_1	

Part VIII

Numerical Tools Units

Chapter 27

Interpolate Unit

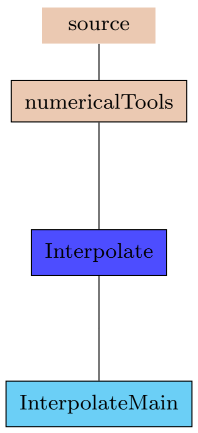

Figure 27.1: The `Interpolate` unit directory tree.

27.1 Introduction

The `Interpolate` unit supplied with FLASH4 contains a collection of interpolation utilities that can be applied to interpolate quantities on specific grids. It currently contains only cubic interpolation routines for 1D, 2D and 3D rectangular grids, based on piecewise (Hermite) cubic interpolation techniques.

27.2 Piecewise Cubic Interpolation

Piecewise cubic interpolation is a technique that can be used to create functional C^1 surfaces (1st derivative continuous) throughout a grid domain by using functional and derivative information at each vertex of a grid cell. The domain function F and its derivatives dF are assumed to be known or at least calculable at each vertex. In order to show the essential features of the piecewise cubic interpolation method and to keep the formulas and matrix sizes manageable, we present the method for 2D domain geometries.

Consider a particular rectangular 2D cell. We wish to calculate a domain function F as a piecewise cubic polynomial in terms of $[0,1]$ rescaled variables x, y inside each cell:

$$F(x,y) = \sum_{i,j=0}^{3} a_{ij} x^i y^j. \tag{27.1}$$

The $[0,1]$ rescaled variable x is obtained from the domain global variable X and the cell's lower X_ℓ and upper X_u dimension as

$$x = \frac{X - X_\ell}{X_u - X_\ell}, \tag{27.2}$$

with a similar expression for y. From the expansion in 27.1, there are 16 expansion coefficients which need to be determined (fitted) to an appropriate set of data for specific points on the cell, which, in order to assure continuous representation of F over the entire domain, have to sit on the cell's boundaries. The most obvious choice for these points are the cell vertices, each vertex belonging to four cells. The data needed for each vertex are F, dF/dx, dF/dy and $d^2F/dxdy$. This leads to a linearly independent and rotationally invariant set of 16 data values, from which the 16 expansion coefficients can be uniquely determined. It can also be shown that for other dimensions only the inclusion of all mixed simple higher order derivatives leads to a linearly independent and rotationally invariant set of data values. For example, for rectangular 3D geometries the data needed at each of the 8 vertices of a cubic cell is F, dF/dx, dF/dy, dF/dz, $d^2F/dxdy$, $d^2F/dxdz$, $d^2F/dydyz$ and $d^3F/dxdydz$.

Let us now organize the 16 expansion coefficients a_{ij} into a vector $\mathbf{a}$, such that each element $a(k)$ of $\mathbf{a}$ is associated with the following expansion coefficient:

$$a(k) = a_{ij} \quad ; \quad k = 1 + i + 4j. \tag{27.3}$$

Likewise, we stack the data values of the four vertices $v = 1,2,3,4$ into a vector $\mathbf{b}$ as follows:

$$\mathbf{b} = \left\{ \begin{array}{l} F_v \\ (dF/dx)_v \\ (dF/dy)_v \\ (d^2F/dxdy)_v \end{array} \right. \quad ; \quad F_v = \left\{ \begin{array}{l} F_1 \\ F_2 \\ F_3 \\ F_4 \end{array} \right. \quad ; \quad (dF/dx)_v = \left\{ \begin{array}{l} (dF/dx)_1 \\ (dF/dx)_2 \\ (dF/dx)_3 \\ (dF/dx)_4 \end{array} \right. \quad ; \quad \text{etc...} \tag{27.4}$$

Let us associate the four vertex indices with the following four $[0,1]$ rescaled variables of the cell:

$$\begin{array}{lcl} v = 1 & \longrightarrow & (x,y) = (0,0) \\ v = 2 & \longrightarrow & (x,y) = (1,0) \\ v = 3 & \longrightarrow & (x,y) = (0,1) \\ v = 4 & \longrightarrow & (x,y) = (1,1) \end{array} . \tag{27.5}$$

Substituting these values for x and y into equation 27.1 and its derivatives, we can establish a connection between the expansion coefficient vector and the data vector in the form

$$\mathbf{b} = \mathbf{Ba}, \tag{27.6}$$

where the 16 x 16 matrix $\mathbf{B}$ has the following structure

$$\mathbf{B} = \begin{pmatrix} 1&0&0&0&0&0&0&0&0&0&0&0&0&0&0&0 \\ 1&1&1&1&0&0&0&0&0&0&0&0&0&0&0&0 \\ 1&0&0&0&1&0&0&0&1&0&0&0&1&0&0&0 \\ 1&1&1&1&1&1&1&1&1&1&1&1&1&1&1&1 \\ 0&1&0&0&0&0&0&0&0&0&0&0&0&0&0&0 \\ 0&1&2&3&0&0&0&0&0&0&0&0&0&0&0&0 \\ 0&1&0&0&0&1&0&0&0&1&0&0&0&1&0&0 \\ 0&1&2&3&0&1&2&3&0&1&2&3&0&1&2&3 \\ 0&0&0&0&1&0&0&0&0&0&0&0&0&0&0&0 \\ 0&0&0&0&1&1&1&1&0&0&0&0&0&0&0&0 \\ 0&0&0&0&1&0&0&0&2&0&0&0&3&0&0&0 \\ 0&0&0&0&1&1&1&1&2&2&2&2&3&3&3&3 \\ 0&0&0&0&0&1&0&0&0&0&0&0&0&0&0&0 \\ 0&0&0&0&0&1&2&3&0&0&0&0&0&0&0&0 \\ 0&0&0&0&0&1&0&0&0&2&0&0&0&3&0&0 \\ 0&0&0&0&0&1&2&3&0&2&4&6&0&3&6&9 \end{pmatrix}, \tag{27.7}$$

containing only positive integers and many zeros (175 out of 256 elements). Since we are ultimately interested in the expansion coefficients for the cell, we invert equation 27.6 and get

$$\mathbf{a} \;=\; \mathbf{B}^{-1}\mathbf{b}. \tag{27.8}$$

The inverse $\mathbf{B}^{-1}$ is also an integer matrix and again contains many zero elements, although not as many as $\mathbf{B}$ itself (156 out of 256 elements):

$$\mathbf{B}^{-1} \;=\; \begin{pmatrix}
1 & 0 & 0 & 0 & 0 & 0 & 0 & 0 & 0 & 0 & 0 & 0 & 0 & 0 & 0 & 0 \\
0 & 0 & 0 & 0 & 1 & 0 & 0 & 0 & 0 & 0 & 0 & 0 & 0 & 0 & 0 & 0 \\
-3 & 3 & 0 & 0 & -2 & -1 & 0 & 0 & 0 & 0 & 0 & 0 & 0 & 0 & 0 & 0 \\
2 & -2 & 0 & 0 & 1 & 1 & 0 & 0 & 0 & 0 & 0 & 0 & 0 & 0 & 0 & 0 \\
0 & 0 & 0 & 0 & 0 & 0 & 0 & 0 & 1 & 0 & 0 & 0 & 0 & 0 & 0 & 0 \\
0 & 0 & 0 & 0 & 0 & 0 & 0 & 0 & 0 & 0 & 0 & 0 & 1 & 0 & 0 & 0 \\
0 & 0 & 0 & 0 & 0 & 0 & 0 & 0 & -3 & 3 & 0 & 0 & -2 & -1 & 0 & 0 \\
0 & 0 & 0 & 0 & 0 & 0 & 0 & 0 & 2 & -2 & 0 & 0 & 1 & 1 & 0 & 0 \\
-3 & 0 & 3 & 0 & 0 & 0 & 0 & 0 & -2 & 0 & -1 & 0 & 0 & 0 & 0 & 0 \\
0 & 0 & 0 & 0 & -3 & 0 & 3 & 0 & 0 & 0 & 0 & 0 & -2 & 0 & -1 & 0 \\
9 & -9 & -9 & 9 & 6 & 3 & -6 & -3 & 6 & -6 & 3 & -3 & 4 & 2 & 2 & 1 \\
-6 & 6 & 6 & -6 & -3 & -3 & 3 & 3 & -4 & 4 & -2 & 2 & -2 & -2 & -1 & -1 \\
2 & 0 & -2 & 0 & 0 & 0 & 0 & 0 & 1 & 0 & 1 & 0 & 0 & 0 & 0 & 0 \\
0 & 0 & 0 & 0 & 2 & 0 & -2 & 0 & 0 & 0 & 0 & 0 & 1 & 0 & 1 & 0 \\
-6 & 6 & 6 & -6 & -4 & -2 & 4 & 2 & -3 & 3 & -3 & 3 & -2 & -1 & -2 & -1 \\
4 & -4 & -4 & 4 & 2 & 2 & -2 & -2 & 2 & -2 & 2 & -2 & 1 & 1 & 1 & 1
\end{pmatrix} \tag{27.9}$$

The matrix $\mathbf{B}^{-1}$ is universal for all 2D cells. Each cell has its specific data vector $\mathbf{b}$ from which its expansion coefficient vector $\mathbf{a}$ can be established via 27.8. Rather than storing $\mathbf{B}^{-1}$ in matrix form and performing a direct matrix times vector operation for each cell, $\mathbf{B}^{-1}$ is used implicitly when converting $\mathbf{b}$ to $\mathbf{a}$. This avoids the redundant zero multiplications and is thus much more efficient. In fact, by using cleverly arranged reusable intermediates, this $\mathbf{b}$ to $\mathbf{a}$ transformation can be coded using only additions and subtractions and no multiplications at all.

Once the expansion coefficient vector $\mathbf{a}$ for a cell has been established, equation 27.1 can be used to obtain the function value F at any point inside the cell, provided the $[0,1]$ rescaled coordinates of that point are given. The function values are given by Eq.(27.1), which can be computed efficiently using a double Horner scheme:

$$\tilde{a}_j \;=\; ((a_{3j}x + a_{2j})x + a_{1j})x + a_{0j} \tag{27.10}$$
$$F(x,y) \;=\; ((\tilde{a}_3 y + \tilde{a}_2)y + \tilde{a}_1)y + \tilde{a}_0 \tag{27.11}$$

The evaluation of the global coordinate differentials is done using the chain rule and leads to:

$$\frac{d^{m+n}F(X,Y)}{dX^m dY^n} \;=\; (X_u - X_\ell)^{-m}(Y_u - Y_\ell)^{-n}\frac{d^{m+n}F(x,y)}{dx^m dy^n} \tag{27.12}$$
$$\frac{d^{m+n}F(x,y)}{dx^m dy^n} \;=\; \sum_{i=m}^{3}\sum_{j=n}^{3}(i)_m (j)_n a_{ij} x^{i-m} y^{j-n}, \tag{27.13}$$

where the Pochhammer symbol $(i)_m$ is defined as $(i)_m = i(i-1)...(i-m+1)$.

27.3 Usage

To include the cubic interpolation tool into your FLASH development, add the line

```
REQUIRES numericalTools/Interpolate
```

into the Config file of the directory where the global API's of the interpolation unit will be used. Another way would be to include the option

-with-unit=numericalTools/Interpolate

into your command line when you configure the code with `setup`. Both ways will give you access to the following cubic interpolation tools in order of their application, where XX stand for the 3 rectangular domain geometries 1D,2D and 3D:

- **Interpolate_cubicXXmonoDerv**: Handles the logistics for producing optimum sets of mixed vertex derivatives for a (sub)grid from vertex functional values to ensure monotonicity of the generated C^1 cubic interpolation surfaces. Note that in oder to generate these mixed derivatives the user needs to provide the vertex function values on a larger (sub)grid than the target (sub)grid: 1,2,3 extra vertex layers for 1D,2D,3D rectangular geometries.

- **Interpolate_cubicXXcoeffs**: Calculate the cubic expansion coefficients a_{ij} in equation 27.1 from user provided sets of vertex data **b**, arranged as shown in 27.4. The calculation is performed in situ, i.e. the input vector **b** is overwritten by the cubic expansion coefficient vector **a** using equation 27.8. The routine accepts a collection of different **b** vectors and processes them all at once. For XX = 2D or 3D, the code allows for multithreading.

- **Interpolate_cubicXXF(d1)(d2)**: For a specific cubic expansion coefficient vector **a** and a set of up to three $[0, 1]$ rescaled coordinates x, y, z, these function routines calculate the functional value F using equation 27.1 and additionally the complete set of 1st (dx,dy,dz) and 2nd (d^2x,d^2y,d^2z,$dxdy$,$dxdz$,$dydz$) order $[0, 1]$ rescaled coordinate derivatives using equation 27.13. Transformation to global coordinate derivatives via equation 27.12 is not done here and has to be done by the user in his specific application.

Chapter 28

Roots Unit

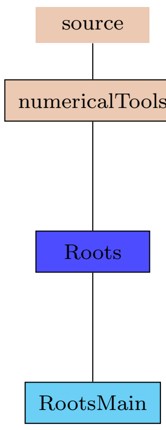

Figure 28.1: The `Roots` unit directory tree.

28.1 Introduction

The `Roots` unit supplied with FLASH4 aims at collecting all those utilities that find solutions (roots) to equations of the form $f(x) = 0$. Currently the `Roots` unit only contains routines to find all the roots of quadratic, cubic and quartic polynomials with real coefficients. Particular emphasis has been put on speed and stability of root evaluation.

28.2 Roots of Quadratic Polynomials

Here we solve

$$x^2 + a_1 x + a_0 \quad = \quad 0, \tag{28.1}$$

where a_1 and a_0 are real. Well known techniques (larger magnitude root x_1 computed by quadratic formula, smaller magnitude root computed by applying Vieta's rule: $x_2 = a_0/x_1$) are used to ensure numerical accuracy of the roots. Additionally the code is equipped to deal with extremely large coefficients, such that computational overflow will not occur. A coefficient rescaling technique is applied if during evaluation of the quadratic formula either the term $(a_1/2)^2$ or the discriminant $(a_1/2)^2 - a_0$ become larger than the largest positive number on the machine.

28.3 Roots of Cubic Polynomials

This solves the cubic polynomial equation

$$x^3 + a_2x^2 + a_1x + a_0 \quad = \quad 0, \tag{28.2}$$

where a_2,a_1 and a_0 are real. Rather than calculating the roots by the analytical formulas, a special technique has been devised to pinpoint down one of the real roots by iteration. After rescaling the cubic polynomial coefficients such that $-1 \leq a_2, a_1, a_0 \leq +1$ and classifying the rescaled cubic polynomials into 6 classes, an analysis of the real root(s) surfaces for each class enables one to find an optimum starting point for a fast convergent Newton-Raphson iteration. In rare cases when the Newton-Raphson iterations start oscillating around the root due to numerical rounding errors, a bisection iteration follows to get the root to within machine accuracy. Details of this procedure can be found in Flocke 2015. After one of the real roots has been found, the remaining roots (real or complex) are found by solving the residual quadratic, which is obtained by composite (forward/backward) deflation.

28.4 Roots of Quartic Polynomials

Solutions to the quartic polynomial equation

$$x^4 + a_3x^3 + a_2x^2 + a_1x + a_0 \quad = \quad 0, \tag{28.3}$$

where a_3,a_2,a_1 and a_0 are all real, are found again by Newton-Raphson and bisection iterations techniques, even for quartics possessing only complex roots. Please consult Flocke 2015 for the theoretical and computational details.

28.5 Usage

To include the root tools into your FLASH development, add the line

    REQUIRES numericalTools/Roots

into the Config file of the directory where the global API's of the interpolation unit will be used. Another way would be to include the option

    -with-unit=numericalTools/Roots

into your command line when you configure the code with `setup`. Both ways will give you access to the following root tools:

- **Roots_x2Polynomial**: Finds all roots of a quadratic polynomial. The coefficient of the leading quadratic term must be equal to 1. For ordering of the roots, please consult the info in the header of this routine.
- **Roots_x3Polynomial**: Finds all roots of a cubic polynomial. The coefficient of the leading cubic term must be equal to 1. For ordering of the roots, please consult the info in the header of this routine.
- **Roots_x4Polynomial**: Finds all roots of a quartic polynomial. The coefficient of the leading quartic term must be equal to 1. For ordering of the roots, please consult the info in the header of this routine.

28.6 Unit Tests

There is currently a unit test for each kind of polynomial. They are all based on setting up the polynomial coefficients for known roots and checking the obtained root accuracies from the respective root solvers. The unit tests try to stress test the root solvers by setting up polynomials which are hard to solve. Two measures are used for judging accuracy of the roots obtained. The relative accuracy of a root is defined as

$$\text{Relative root accuracy} \quad = \quad |(x_e - x_c)/x_e|, \tag{28.4}$$

where x_e is the exact analytical root and x_c the computational root. The absolute accuracy of a computational root x_c is

$$\text{Absolute root accuracy} \quad = \quad |x_c|. \tag{28.5}$$

For the unit tests we will use the relative root accuracy if $x_e \neq 0$ and the absolute root accuracy otherwise.

28.6.1 Quadratic Polynomials Root Test

This test solves quadratic polynomials with extreme coefficients involving the largest positive number L and the smallest postive number S representable on the machine under the working precision (for double precision we would have $L \approx 1.797... \times 10^{308}$ and $S \approx 2.225... \times 10^{-308}$). All possible combinations are tested. We examine only the LL combination in detail. The four quadratic LL polynomials are:

$$x^2 \pm Lx \pm L \quad = \quad 0 \tag{28.6}$$

with the two roots:

$$x_1 \quad = \quad \mp L/2 + \sqrt{(L/2)^2 \mp L} \tag{28.7}$$
$$x_2 \quad = \quad \mp L/2 - \sqrt{(L/2)^2 \mp L}. \tag{28.8}$$

Since $(L/2)^2$ is much larger than L, we can expand the square root in a Taylor series

$$\sqrt{(L/2)^2 \mp L} \quad \approx \quad L/2 \mp 1 + O[L^{-1}]. \tag{28.9}$$

The roots are approximated as

$$x_1 \quad = \quad \mp L/2 + L/2 \mp 1 + O[L^{-1}] \tag{28.10}$$
$$x_2 \quad = \quad \mp L/2 - L/2 \mp 1 + O[L^{-1}]. \tag{28.11}$$

However, a quantity like $L+1$ cannot be accurately represented on a machine due to limited mantissa space and will get converted to L. The following table shows the computational roots to be expected for the quadratic LL polynomials

a_1	a_0	x_1	x_2
$+L$	$+L$	-1	$-L$
$+L$	$-L$	$+1$	$-L$
$-L$	$+L$	$+L$	$+1$
$-L$	$-L$	$+L$	-1

Likewise, after going throught the same kind of analysis for the remaining LS, SL and SS polynomials, we can establish their computational roots. For the four SS polynomials we get (since $\sqrt{S} \gg S$):

a_1	a_0	x_1	x_2
$+S$	$+S$	$+i\sqrt{S}$	$-i\sqrt{S}$
$+S$	$-S$	$+\sqrt{S}$	$-\sqrt{S}$
$-S$	$+S$	$+i\sqrt{S}$	$-i\sqrt{S}$
$-S$	$-S$	$+\sqrt{S}$	$-\sqrt{S}$

The four LS polynomials give (since S/L is not representable and hence equal to zero)

Table 28.1: Coefficients of the cubics I-IX used for the cubic polynomial root test.

Cubic	a_2	a_1	a_0
I	$-1.00000010000001e{+}14$	$+1.00000010000001e{+}21$	$-1.e{+}21$
II	-3.000003	$+3.000006000002$	-1.000003000002
III	$+8.999e{+}80$	$-1.0009e{+}161$	$+1.e{+}238$
IV	$+1.e{+}24$	-1.0	$-1.e{+}24$
V	$-1.99999999999999e{+}14$	$+0.99999999999998e{+}28$	$+1.e{+}28$
VI	$-3.e{+}5$	$+3.0000000001e{+}10$	$-1.0000000001e{+}15$
VII	-3.0	$+1.00000000000003e{+}14$	$-1.00000000000001e{+}14$
VIII	$-2.0000001e{+}7$	$+1.00000020000001e{+}14$	$-1.00000000000001e{+}14$
IX	$+0.99999999999998e{+}14$	$-1.99999999999998e{+}14$	$+2.e{+}14$

Table 28.2: Analytical roots and FLASH4 cubic solver accuracy performance of the cubics I-IX used for the cubic polynomial root test.

Cubic	Roots	Comments on Roots	Accuracy
I	$+10^{+14}, +10^{+7}, +1$	3 widely spaced real	$< 1.e{-}15$
II	$+1.000002, +1.000001, +1$	3 closely spaced real	$< 1.e{-}9$
III	$-10^{+81}, +10^{+80}, +10^{+77}$	3 large real	$< 1.e{-}15$
IV	$-10^{+24}, +1, -1$	1 large, 2 small real	$< 1.e{-}15$
V	$+10^{+14}, +10^{+14}, -1$	2 degenerate large, 1 small real	$< 1.e{-}15$
VI	$+10^{+5}, +10^{+5} \pm i$	3 closely spaced, small imag parts	$< 1.e{-}15$
VII	$+1, +1 \pm 10^{+7}i$	1 small real, 2 large complex, large imag parts	$< 1.e{-}15$
VIII	$+1, +10^{+7} \pm i$	1 small real, 2 large complex, small imag parts	$< 1.e{-}15$
IX	$-10^{+14}, +1 \pm i$	1 large real, 2 small complex	$< 1.e{-}15$

a_1	a_0	x_1	x_2
$+L$	$+S$	0	$-L$
$+L$	$-S$	0	$-L$
$-L$	$+S$	$+L$	0
$-L$	$-S$	$+L$	0

and the four SL polynomials have computational roots

a_1	a_0	x_1	x_2
$+S$	$+L$	$+i\sqrt{L}$	$-i\sqrt{L}$
$+S$	$-L$	$+\sqrt{L}$	$-\sqrt{L}$
$-S$	$+L$	$+i\sqrt{L}$	$-i\sqrt{L}$
$-S$	$-L$	$+\sqrt{L}$	$-\sqrt{L}$

The quadratic solver implemented in FLASH4 obtains all the above roots to within machine epsilon accuracy.

28.6.2 Cubic Polynomials Root Test

The following set of cubic polynomials I-IX is used for the test. It corresponds to the set used in xxx and represents difficult to solve cases that stress test the cubic solver. In Tables 28.1 and 28.2 we list all the coefficients, analytical roots and FLASH4 cubic solver accuracy performance of these polynomials. The polynomials were designed to be tested with double precision machine working precision.

Table 28.3: Coefficients of the quartics I-XIII used for the quartic polynomial root test.

Quartic	a_3	a_2	a_1	a_0
I	$-1.001001001e{+}9$	$+1.001002001001e{+}15$	$-1.001001001e{+}18$	$+1.e{+}18$
II	-4.006	$+6.018011$	-4.018022006	$+1.006011006$
III	$-9.98899e{+}79$	$-1.1008989e{+}157$	$-1.010999e{+}233$	$-1.e{+}307$
IV	$-1.00000000000002e{+}14$	$+1.99999999999999e{+}14$	$+1.00000000000002e{+}14$	$-2.e{+}14$
V	$+1.e{+}7$	$-2.00000000000001e{+}14$	$-1.e{+}7$	$+2.e{+}14$
VI	$-9.000002e{+}6$	$-0.9999981999998e{+}13$	$+1.9999982e{+}13$	$-2.e{+}13$
VII	$+2.000011e{+}6$	$+1.010022000028e{+}12$	$+1.1110056e{+}13$	$+2.828e{+}13$
VIII	$-1.00002011e{+}8$	$+2.01101022001e{+}11$	$-1.02200111000011e{+}14$	$+1.1000011e{+}15$
IX	$-2.0000002e{+}7$	$+1.01000040000005e{+}14$	$-2.020001e{+}14$	$+5.05e{+}14$
X	$-1.9986e{+}4$	$+1.00720058e{+}8$	$-1.8600979874e{+}10$	$+1.00004909000441e{+}14$
XI	-4.006	$+5.6008018e{+}1$	$-1.04148036024e{+}2$	$+6.75896068064016e{+}2$
XII	$-4.0e{+}3$	$+6.00001e{+}6$	$-4.00002e{+}9$	$+1.000010000009e{+}12$
XIII	-6.0	$+1.01000013e{+}8$	$-2.04000012e{+}8$	$+1.00000104000004e{+}14$

Table 28.4: Analytical roots and FLASH4 quartic solver accuracy performance of the quartics I-XIII used for the quartic polynomial root test.

Quartic	Roots	Comments on Roots	Accuracy
I	$+10^{+9}$, $+10^{+6}$, $+10^{+3}$, $+1$	4 widely spaced real	$< 1.e{-}15$
II	$+1.003$, $+1.002$, $+1.001$, $+1$	4 closely spaced real	$< 1.e{-}7$
III	$+10^{+80}$, -10^{+77}, -10^{+76}, -10^{+74}	4 large real	$< 1.e{-}15$
IV	$+10^{+14}$, $+2$, $+1$, -1	1 large, 3 small real	$< 1.e{-}15$
V	$-2 \times 10^{+7}$, $+10^{+7}$, $+1$, -1	2 large, 2 small real	$< 1.e{-}15$
VI	$+10^{+7}$, -10^{+6}, $+1 \pm i$	2 large real, 2 small complex	$< 1.e{-}15$
VII	-7, -4, $-10^{+6} \pm 10^{+5}i$	2 small real, 2 large complex	$< 1.e{-}15$
VIII	$+10^{+8}$, $+11$, $+10^{+3} \pm i$	1 large and small real, 2 medium complex	$< 1.e{-}15$
IX	$+10^{+7} \pm 10^{+6}i$, $+1 \pm 2i$	2 large, 2 small complex	$< 1.e{-}15$
X	$+10^{+4} \pm 3i$, $-7 \pm 10^{+3}i$	4 complex, mixed size real and imag parts	$< 1.e{-}14$
XI	$+1.002 \pm 4.998\, i$, $+1.001 \pm 5.001\, i$	4 closely spaced complex	$< 1.e{-}12$
XII	$+10^{+3} \pm 3i$, $+10^{+3} \pm i$	4 complex, equal real, small imag parts	$< 1.e{-}15$
XIII	$+2 \pm 10^{+4}i$, $+1 \pm 10^{+3}i$	4 complex, small real, large imag parts	$< 1.e{-}15$

28.6.3 Quartic Polynomials Root Test

Again the set of quartic polynomials I-XIII have been taken from xxx. Tables 28.3 and 28.4 list all the coefficients, analytical roots and FLASH4 quartic solver accuracy performance of these polynomials. The polynomials were designed to be tested with double precision machine working precision.

Chapter 29

RungeKutta Unit

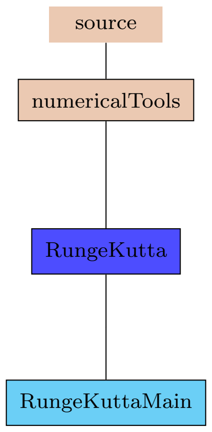

Figure 29.1: The `RungeKutta` unit directory tree.

29.1 Introduction

The `RungeKutta` unit in FLASH4 provides users with the tools to perform various kinds of (embedded) Runge Kutta (RK) iterations. The RK iterations are characterized by their implemented Butcher tableaus of various sizes and orders. The specific ODE to be solved must be transmitted via argument to the individual RK stepping routines. The RK routines contain no specifics of the ODE equations to be solved. This clean separation between the ODE function and the details of the RK iterations gives a universally applicable RK tool, which can be called from any FLASH4 application.

29.2 Runge Kutta Integration

The RK integration scheme starts from an initial set of first order ODE dependent variable values $\mathbf{y}_0$ and advances the ODE solution $\mathbf{y}$ through well defined steps in the independent variable x. Control of the dependent variable errors allows for optimum step size control. We describe here the embedded RK schemes, which use the same intermediate vectors $\mathbf{k}$ to get an estimate of the error vector $\mathbf{e}$. An embedded RK step can be represented by the following equations:

$$\frac{d}{dx}\mathbf{y}(x) = f(\mathbf{y}(x), x) \tag{29.1}$$

$$\mathbf{k}_i = hf(\mathbf{y}(x) + \sum_{j=1}^{s} a_{ij}\mathbf{k}_j, x + c_i h) \tag{29.2}$$

$$\mathbf{y}(x+h) = \mathbf{y}(x) + \sum_{i=1}^{s} b_i\mathbf{k}_i + O[h^{p+2}] \tag{29.3}$$

$$\mathbf{y}(x+h) = \mathbf{y}(x) + \sum_{i=1}^{s} b_i^*\mathbf{k}_i + O[h^{p+1}] \tag{29.4}$$

$$\mathbf{e} = \sum_{i=1}^{s} (b_i - b_i^*)\mathbf{k}_i + O[h^{p+1}] \tag{29.5}$$

Here h denotes the step size and s is the size of the embedded RK scheme. Each particular embedded RK scheme is characterized by the four sets of coefficients a_{ij}, b_i, b_i^*, c_i, which can be arranged into a table known as a Butcher tableau:

$$\begin{array}{c|cccc} c_1 & a_{11} & a_{12} & \cdots & a_{1s} \\ c_2 & a_{21} & a_{22} & \cdots & a_{2s} \\ \vdots & \vdots & \vdots & \ddots & \vdots \\ c_s & a_{s1} & a_{s2} & \cdots & a_{ss} \\ \hline & b_1 & b_2 & \cdots & b_s \\ & b_1^* & b_2^* & \cdots & b_s^* \end{array}$$

The coefficients b and b^* correspond to RK methods of order $p+1$ and p, from which the error vector is constructed via equation 29.5. If only the strict lower triangle of the a_{ij} values are non-zero, then the embedded RK scheme is explicit. Otherwise we have an implicit scheme. Explicit RK schemes are much easier to solve, because all intermediate $\mathbf{k}$ vectors can be evaluated one after another using previously evaluated $\mathbf{k}$ vectors. Implicit RK schemes on the other hand have to be solved in an iteratively fashion and are much more expensive. FLASH4 currently has only explicit RK schemes implemented. Error control on each RK step is done by passing a maximum allowed absolute error vector $\mathbf{e}_{max}$ corresponding to each of the dependent variables in $\mathbf{y}$. Step size control is currently implemented using information from the obtained error vector $\mathbf{e}$ after the RK step and the maximum error vector $\mathbf{e}_{max}$. Using the fact that the error scales as $\mathbf{O}[h^{p+1}]$ due to the lower p order embedded RK method, the new step size h_{new} is adjusted from the old step size h_{old} as follows

$$h_{new} = h_{old}S\left(max\left|\frac{\mathbf{e}_{max}}{\mathbf{e}}\right|\right)^{1/(p+1)} \tag{29.6}$$

and used as the next trial step size. A safety factor (typically $S = 0.9$) is used to account for the fact that only the leading h^{p+1} term from $\mathbf{O}[h^{p+1}]$ was used in deriving this formula.

In some situations one needs an initial guess for the very first initial trial step size. This can be done from the supplied ODE vector $\mathbf{y}$ and the maximum allowed error vector $\mathbf{e}_{max}$ as follows. Consider the Taylor expansion of $\mathbf{y}(x+h)$ around x:

$$\mathbf{y}(x+h) = \mathbf{y}(x) + h\mathbf{y}^{(1)}(x) + h^2\mathbf{y}^{(2)}(x)/2 + \cdots + h^p\mathbf{y}^{(p)}(x)/p! + \mathbf{O}[h^{p+1}], \tag{29.7}$$

where $\mathbf{y}^{(p)}$ denotes the p-th derivative of $\mathbf{y}$ with respect to x. The expansion error $\mathbf{O}[h^{p+1}]$ can be directly related to the $\mathbf{O}[h^{p+1}]$ error of a RK method of order p (cf. equation 29.4). As an approximation one can equate the absolute value of the Taylor remainder term with the error goal of the RK method (i.e. plugging in formulas for both $\mathbf{O}[h^{p+1}]$ terms):

$$h^{p+1}|\mathbf{y}^{(p+1)}(x^*)|/(p+1)! = |\mathbf{e}_{max}|, \tag{29.8}$$

where $x \leq x^* \leq x+h$. Since we are dealing with an approximation, we further set $x^* = x$ (this in effect approximates $\mathbf{O}[h^{p+1}]$ by its leading term and ignores the $> p+1$ terms), leading to

$$h = min\left((p+1)!\left|\frac{\mathbf{e}_{max}}{\mathbf{y}^{(p+1)}(x)}\right|\right)^{1/p+1}. \tag{29.9}$$

We then solve for h and take the minimum to satisfy all components. To use this formula we need to evaluate the derivative. The following are second order central difference formulas based on equal spacing h (not to be confused with the RK step size) between functions:

$$\mathbf{y}^{(m+2k+\delta)}(x) = \frac{1}{h^{2k+\delta}}\sum_{n=-(k+\delta)}^{k+\delta}(-1)^{k+n-\delta}\frac{n^\delta(2k+\delta)!}{(k+n+\delta)!(k-n+\delta)!}\mathbf{y}^{(m)}(x+nh)+\mathbf{R}[h^2], \tag{29.10}$$

where the remainder term is equal to

$$\mathbf{R}[h^2] = -\frac{k+2\delta}{12}h^2\mathbf{y}^{(m+2k+2+\delta)}(x^*) \tag{29.11}$$

with $x-(k+\delta)h \leq x^* \leq x+(k+\delta)h$ and $\delta = 0,1$, depending on if one wants even or odd higher order derivatives. For $m=0$ the derivatives are given in terms of the original functions $\mathbf{y}(x+ih)$, whereas for $m>0$ we get higher order derivatives from lower order derivatives. These formulas can be derived by setting up a system of derivative linear equations from the Taylor expansions of all the (derivative) functions $\mathbf{y}^{(m)}(x \pm nh)$ for a certain range of n integers and solving these equations for the lowest derivatives (the technique is discribed in J. Mathews, Computer Derivations of Numerical Differentiation Formulae, International Journal of Mathematics Education in Science and Technology, Volume 34 No 2, pp.280-287). The functions $\mathbf{y}(x \pm nh)$ could in principle be obtained using the RK equation 29.3, but a much more economical approach would be to use the 1st derivatives (i.e. using $m=1$ in equation 29.10). We have from equation 29.1:

$$\begin{aligned}\mathbf{y}^{(1)}(x+nh) &= f(\mathbf{y}(x+nh), x+nh) & (29.12)\\ &\approx f(\mathbf{y}(x)+nh\mathbf{y}^{(1)}(x), x+nh) & (29.13)\\ &\approx f(\mathbf{y}(x)+nhf(\mathbf{y}(x),x), x+nh), & (29.14)\end{aligned}$$

where, since the nh are small, the first order expansion of $\mathbf{y}(x+nh)$ has been used. Note the nested use of the derivative ODE function f in equation 29.14. Since the goal is to estimate $\mathbf{y}^{(p+1)}(x)$ via equation 29.10, we set $p = 2k+\delta$, from which k and δ are uniquely determined.

In practice it turns out that equation 29.10 is numerically very unstable for higher order derivatives. We will use it only for estimating low order derivatives. This leaves us with the problem of estimating higher order derivatives in equation 29.9. We follow ideas presented in J. Comp. Appl. Math. **18**, 176-192 (1987). To this end we first split the maximum error vector into an error base vector and an error fraction scalar

$$\mathbf{e}_{max} = e_{frac}\cdot\mathbf{e}_{base} \tag{29.15}$$

and have the user supplied both quantities. The purpose of this splitting is that we separate the maximum error vector into an accuracy part (the e_{frac}, typically of the order of 10^{-6} to 10^{-12}) and a part which relates to the magnitude of the vectors involved in the ODE (the $\mathbf{e}_{base}$). We further assume that the user has sufficient knowledge about his ODE problem, such that he can construct these two quantities obeying roughly the following inequalities:

$$\begin{aligned}e_{frac} &< 1 & (29.16)\\ \mathbf{e}_{base} &\neq \mathbf{0} & (29.17)\\ |\mathbf{e}_{base}| &\geq max\left\{|h^n\mathbf{y}^{(n)}(x)/n!|; n=0,1,\ldots\infty\right\}. & (29.18)\end{aligned}$$

With this choice of $\mathbf{e}_{base}$, all terms in equation 29.7 can be divided by $\mathbf{e}_{base}$. If we now assume a smooth convergence of the Taylor series and further postulate an exponential type decay between the individual

$\mathbf{e}_{base}$-rescaled Taylor terms (which all must be ≤ 1 due to the assumptions in equation 29.18)

$$\left|\frac{h^n \mathbf{y}^{(n)}(x)}{n!\,\mathbf{e}_{base}}\right| = \left|\frac{h^m \mathbf{y}^{(m)}(x)}{m!\,\mathbf{e}_{base}}\right|^{n/m} \qquad n \geq m, \tag{29.19}$$

we can replace the higher order derivatives in equation 29.9 by lower order ones and obtain:

$$h = e_{frac}^{1/p+1} \cdot min\left(m!\left|\frac{\mathbf{e}_{base}}{\mathbf{y}^{(m)}(x)}\right|\right)^{1/m}. \tag{29.20}$$

Note the similar structure to equation 29.9. The higher order contribution has been relegated to e_{frac}, which, due to the condition in equation 29.16, leads to larger initial step size estimates for higher order RK schemes. In practice we calculate step size estimates using only $m = 2$ and $m = 1$. In rare cases when all 1st and 2nd order derivatives of $\mathbf{y}(x)$ vanish, the (user supplied) default maximum step size estimate is used. This maximum step size estimate can be given for example as a cell/domain size measure, when it is clear that the RK stepper should not step beyond a cell or outside of the domain.

A separate RK stepping routine exists in FLASH4, which performs confined RK steps, which will be explained next. Looking at equation 29.2, we see that for an RK step the ODE function f has to be evaluated repeatedly for several intermediate $\mathbf{y}_i$ vectors

$$\mathbf{y}_i = \mathbf{y}(x) + \sum_{j=1}^{s} a_{ij}\mathbf{k}_j. \tag{29.21}$$

For certain applications it may not be possible to evaluate the ODE function at some of these intermediate vectors due to lack of sufficient data. An example would be tracing the (classical) path of a particle through a cell. Only the acceleration vector field of that particular cell is available. If one of the position variables in $\mathbf{y}_i$ steps outside of the cell boundaries, the acceleration vector at that point cannot be evaluated and the step size h must be reduced. The confined RK stepping routine needs extra boundary vectors corresponding to the variables in the $\mathbf{y}$ vectors. The boundary vectors can be only a subset of all the $\mathbf{y}$ vector variables. Those variables which have no corresponding boundary vector entries are assumed to be unbound. Since the boundaries might itself depend on the variables in $\mathbf{y}$, the boundary vectors are transmitted to the confined RK stepper as functions, which have to be designed by the user.

29.3 Usage

To include the RK integration tool into your FLASH development, add the line

REQUIRES numericalTools/RungeKutta

into the Config file of the directory where the global API's of the interpolation unit will be used. Another way would be to include the option

-with-unit=numericalTools/RungeKutta

into your command line when you configure the code with `setup`. This gives you access to the following RK tools:

- **RungeKutta_step**: Performs one unconfined RK step. Optimum stepping size is calculated internally by using equation 29.6 and readjusted until target accuracy is met. The routine requires as input an initial step size to start the RK stepping process.
- **RungeKutta_stepConfined**: Performs one confined RK step. Same underlaying machinery as for the unconfined RK stepper, except stepping size is additionally readjusted to comply with the supplied boundaries of the confined dependent variables.
- **RungeKutta_stepSizeEstimate**: Returns an estimate for initial step sizes in situations where no good initial guess of step size is available. The code is based on equations 29.10, 29.14 and 29.20.

29.4 Unit Tests

29.4.1 Runge Kutta FLASH Test for a 2D Elliptical Path

29.4.1.1 Derivation of the 2D elliptical path ODE

Consider the following ODE in 2D, operating on a 2D vector $\mathbf{r}$:

$$\frac{d\mathbf{r}}{dt} = \begin{pmatrix} \lambda_1 & \omega \\ -\omega & \lambda_2 \end{pmatrix} \mathbf{r} = \mathbf{A}\mathbf{r}. \tag{29.22}$$

This ODE describes a rotational (ω) and sheer (λ_1, λ_2) force on a particle located at $\mathbf{r}$. If $\lambda_1, \lambda_2 = 0$, then the ODE describes a particle revolving in a circle of radius $\mathbf{r}(0)$, the initial radius of the particle. The general solution to the above ODE is:

$$\mathbf{r}(t) = e^{\mathbf{A}t}\mathbf{r}(0). \tag{29.23}$$

The matrix exponential is given by:

$$e^{\mathbf{A}t} = \frac{1}{\Delta}\begin{pmatrix} (e^{\mathbf{A}t})_{11} & (e^{\mathbf{A}t})_{12} \\ (e^{\mathbf{A}t})_{21} & (e^{\mathbf{A}t})_{22} \end{pmatrix}, \tag{29.24}$$

where

$$(e^{\mathbf{A}t})_{11} = \frac{1}{2}e^{t(\lambda_1+\lambda_2+\Delta)/2}(\lambda_1 - \lambda_2 + \Delta) + \frac{1}{2}e^{t(\lambda_1+\lambda_2-\Delta)/2}(-\lambda_1 + \lambda_2 + \Delta) \tag{29.25}$$

$$(e^{\mathbf{A}t})_{12} = \omega(e^{t(\lambda_1+\lambda_2+\Delta)/2} - e^{t(\lambda_1+\lambda_2-\Delta)/2} \tag{29.26}$$

$$(e^{\mathbf{A}t})_{21} = -(e^{\mathbf{A}t})_{12} \tag{29.27}$$

$$(e^{\mathbf{A}t})_{22} = \frac{1}{2}e^{t(\lambda_1+\lambda_2+\Delta)/2}(-\lambda_1 + \lambda_2 + \Delta) + \frac{1}{2}e^{t(\lambda_1+\lambda_2-\Delta)/2}(\lambda_1 - \lambda_2 + \Delta) \tag{29.28}$$

and

$$\Delta = \sqrt{(\lambda_1 - \lambda_2)^2 - 4\omega^2}. \tag{29.29}$$

For general values of $\lambda_1, \lambda_2, \omega$, the path of the particle is a spiral around the origin. Closed paths are possible, if at certain times $t \neq 0$ we have $e^{\mathbf{A}t} = \mathbf{I}$. A necessary condition is thus that the offdiagonal elements of $e^{\mathbf{A}t}$ have to become zero for certain $t \neq 0$. Since each of these elements has a factor of the structure $e^B - e^C$, then either both B and C are real and equal or B and C are imaginary with oposite sign. Both situations can only happen, if $\lambda_2 = -\lambda_1$. The first case (B, C real and equal) is only possible if $\Delta = 0$ and the second case (B, C imaginary and of opposite sign) only if Δ is imaginary. Hence, necessary conditions for a closed path are:

$$\lambda_2 = -\lambda_1 \tag{29.30}$$

$$\omega^2 \geq \lambda_1^2. \tag{29.31}$$

Let us now introduce the parameter $|k| > 1$ such that:

$$\omega = k\lambda_1. \tag{29.32}$$

Then our closed path ODE becomes:

$$\frac{d\mathbf{r}}{dt} = \lambda_1\begin{pmatrix} 1 & k \\ -k & -1 \end{pmatrix}\mathbf{r} \tag{29.33}$$

and, since λ_1 is now just merely a scaling factor, we can further condense the closed path ODE to:

$$\frac{d\mathbf{r}}{dt} = \begin{pmatrix} 1 & k \\ -k & -1 \end{pmatrix}\mathbf{r}. \tag{29.34}$$

This is the 2D ellipse ODE we are going to use for our Runge Kutta test. Inserting $\lambda_1 = 1$, $\lambda_2 = -1$ and $\omega = k$ into the above general solution, we obtain, after inserting the identity $e^{i\phi} = \cos(\phi) + i\sin(\phi)$, the following real path solution:

$$\begin{pmatrix} x(t) \\ y(t) \end{pmatrix} = \begin{pmatrix} \dfrac{\sin(\phi)}{\sqrt{k^2-1}} + \cos(\phi) & \dfrac{k\sin(\phi)}{\sqrt{k^2-1}} \\ -\dfrac{k\sin(\phi)}{\sqrt{k^2-1}} & -\dfrac{\sin(\phi)}{\sqrt{k^2-1}} + \cos(\phi) \end{pmatrix} \begin{pmatrix} x_0 \\ y_0 \end{pmatrix}, \tag{29.35}$$

where

$$\phi = t\sqrt{k^2-1}. \tag{29.36}$$

For $\phi = n\pi; n = 1, 3, 5, \ldots$, the 2x2 matrix is equal to $-\mathbf{I}$, i.e. the particle made a half revolution. For $\phi = n\pi; n = 2, 4, 6, \ldots$, the 2x2 matrix is equal to $\mathbf{I}$ and the particle made a complete revolution. The time T it takes for the particle to make one complete revolution (its time period) is thus:

$$T = \frac{2\pi}{\sqrt{k^2-1}}. \tag{29.37}$$

The square of the distance $d^2 = [x(t)]^2 + [y(t)]^2$ the particle is found from the origin has a minimum and a maximum at the following angles:

$$\phi_{max}(k>1) = \arctan\left[\sqrt{\frac{k+1}{k-1}}\frac{x_0+y_0}{x_0-y_0}\right] \tag{29.38}$$

$$\phi_{min}(k>1) = -\arctan\left[\sqrt{\frac{k-1}{k+1}}\frac{x_0-y_0}{x_0+y_0}\right] \tag{29.39}$$

$$\phi_{max}(k<1) = -\phi_{min}(k>1) \tag{29.40}$$

$$\phi_{min}(k<1) = -\phi_{max}(k>1). \tag{29.41}$$

These angles (range $[-\pi/2, +\pi/2]$) give only the angles to the nearest maximum/minimum point from the original position (x_0, y_0). The other two angles corresponding to the remaining maximum/minimum distance points are obtained by adding π. The corresponding times are:

$$t_{max} = \phi_{max}/\sqrt{k^2-1} \tag{29.42}$$

$$t_{min} = \phi_{min}/\sqrt{k^2-1}. \tag{29.43}$$

The corresponding minimum and maximum square distances are:

$$d^2_{min} = \frac{k(x_0^2+y_0^2)+2x_0y_0}{k+\mathrm{sgn}[k]} \tag{29.44}$$

$$d^2_{max} = \frac{k(x_0^2+y_0^2)+2x_0y_0}{k-\mathrm{sgn}[k]}, \tag{29.45}$$

where the signum function sgn is:

$$k > 0 \longrightarrow \mathrm{sgn}[k] = +1 \tag{29.46}$$

$$k < 0 \longrightarrow \mathrm{sgn}[k] = -1. \tag{29.47}$$

From these formulas we see that

- if $x_0 = y_0$ and $k > 1$, then the first t_{min} is equal to zero, i.e. the particle is at its minimum distance $\sqrt{2}|x_0|$ from the origin.
- if $x_0 = y_0$ and $k < -1$, then the first t_{max} is equal to zero, i.e. the particle is at its maximum distance $\sqrt{2}|x_0|$ from the origin.

- if $x_0 = -y_0$ and $k > 1$, then the first t_{max} is equal to zero, i.e. the particle is at its maximum distance $\sqrt{2}|x_0|$ from the origin.
- if $x_0 = -y_0$ and $k < -1$, then the first t_{min} is equal to zero, i.e. the particle is at its minimum distance $\sqrt{2}|x_0|$ from the origin.
- the aspect ratio A of the elliptical path is equal to $A = \sqrt{(k + \mathrm{sgn}[k])/(k - \mathrm{sgn}[k])}$.

We next develop the approach and formulas to find the minimum/maximum distance from a general point in a 2D domain to a general ellipse inside this 2D domain.

29.4.1.2 Minimum and maximum distance from a point to a general ellipse in a 2D cartesian domain

We will first get the general parametric equation of an ellipse in 2D cartesian space. We start by placing a 2D ellipse with its center at the cartesian origin and with its minor/major axis aligned along the cartesian y/x axis. Let the semi-major axis have length a and the semi-minor axis have length b. The parametric equation for this ellipse is:

$$\begin{pmatrix} x \\ y \end{pmatrix} = \begin{pmatrix} a\sin\theta \\ b\cos\theta \end{pmatrix}, \tag{29.48}$$

where the angle parameter is in the range $0 \le \theta \le 2\pi$. Next we clockwise rotate the entire ellipse such that the minor axis makes an angle α with the cartesian y-axis. The range of this rotation angle is $0 \le \alpha \le \pi$. The parametric equation for the rotated ellipse becomes

$$\begin{pmatrix} x \\ y \end{pmatrix} = \mathbf{R}\begin{pmatrix} a\sin\theta \\ b\cos\theta \end{pmatrix} = \begin{pmatrix} \cos\alpha & \sin\alpha \\ -\sin\alpha & \cos\alpha \end{pmatrix}\begin{pmatrix} a\sin\theta \\ b\cos\theta \end{pmatrix}, \tag{29.49}$$

where $\mathbf{R}$ is the rotation matrix that sends every point to its new rotated point. Finally we add the center translation vector $\mathbf{T} = (T_x, T_y)$ to the equation for ellipses that are not located at the cartesian origin:

$$\begin{pmatrix} x \\ y \end{pmatrix} = \begin{pmatrix} \cos\alpha & \sin\alpha \\ -\sin\alpha & \cos\alpha \end{pmatrix}\begin{pmatrix} a\sin\theta \\ b\cos\theta \end{pmatrix} + \begin{pmatrix} T_x \\ T_y \end{pmatrix}. \tag{29.50}$$

This is the general parametric equation of any ellipse in 2D cartesian space. Consider a specific point (x, y) on the ellipse. The tangent line at this ellipse point contains the tiny derivative vector

$$\mathbf{v} = \begin{pmatrix} dx/d\theta \\ dy/d\theta \end{pmatrix} = \begin{pmatrix} a\cos\alpha\cos\theta - b\sin\alpha\sin\theta \\ -a\sin\alpha\cos\theta - b\cos\alpha\sin\theta \end{pmatrix}, \tag{29.51}$$

with its origin at the ellipse point (x, y). The other vector we consider is the vector

$$\mathbf{w} = \begin{pmatrix} x_p - x \\ y_p - y \end{pmatrix} = \begin{pmatrix} x_p - a\cos\alpha\sin\theta - b\sin\alpha\cos\theta - T_x \\ y_p + a\sin\alpha\sin\theta - b\cos\alpha\cos\theta - T_y \end{pmatrix}, \tag{29.52}$$

which also has its origin at the ellipse point (x, y). The minimum distance occurs for those θ for which $\mathbf{v}\cdot\mathbf{w} = 0$ (perpendicular vectors). This gives the following equation for θ:

$$R\cos\theta + S\sin\theta + U\cos\theta\sin\theta = 0, \tag{29.53}$$

where

$$R = a[(y_p - T_y)\sin\alpha - (x_p - T_x)\cos\alpha] \tag{29.54}$$
$$S = b[(x_p - T_x)\sin\alpha + (y_p - T_y)\cos\alpha] \tag{29.55}$$
$$U = a^2 - b^2. \tag{29.56}$$

Note, that $U \neq 0$, whenever $a \neq b$. For $a = b$ (a circle) we will have $U = 0$ and the equation becomes easily solvable. The elliptical U term makes the equation much harder to solve. Eliminating the $\sin\theta$ term, we arrive at the following quartic equation in $\cos\theta$:

$$\cos^4\theta + 2\left(\frac{S}{U}\right)\cos^3\theta + \left[\left(\frac{R}{U}\right)^2 + \left(\frac{S}{U}\right)^2 - 1\right]\cos^2\theta - 2\left(\frac{S}{U}\right)\cos\theta - \left(\frac{S}{U}\right)^2 = 0.$$

Its solutions give us up to 4 different possible angles θ. However, to each $\cos\theta$ solution there correspond two $\sin\theta$ solutions via $\sin\theta = \pm\sqrt{1-\cos^2\theta}$, increasing the total possible solutions to 8. Each of these 8 solutions must be checked for the minimum and maximum distance given by $|\mathbf{w}|$. As far as the number of real solutions for the above quartic is concerned, when the point is inside or close to the ellipse, we can visualize that there are 4 possible directions from the point to the ellipse for which we have $\mathbf{v}\cdot\mathbf{w} = 0$ (i.e. we hit the ellipse curve at right angles). Hence for this point location we expect 4 real quartic solutions. On the other hand, if we are far away from the ellipse, only 2 such points on the elliptical curve will exist and we expect 2 real and 2 complex solutions. We should never get 4 complex solutions of the above quartic.

29.4.1.3 The FLASH test problem for the Runge Kutta 2D ellipse test

We will now set up the unit test for the Runge Kutta 2D ellipse test. We start by stating the initial conditions and the requested shape of the ellipse:

1. The particle is initially at position $(x_0, y_0) = (1, 1)$.
2. We want the particle to follow an elliptical path with given aspect ratio A.

From this requested aspect ratio we calculate our needed k as:

$$k = \frac{A^2+1}{A^2-1} \tag{29.57}$$

and we take k to be positive from now on. This means that the particle will start moving along the elliptical curve in the clockwise direction. By looking at the general formulas derived in the previous sections, we can state the following properties and equations for the ellipse. The square distance extrema and locations will be:

$$d^2_{min} = 2 \qquad \text{(located at } (1,1) \text{ and } (-1,-1)) \tag{29.58}$$

$$d^2_{max} = 2A^2 \qquad \text{(located at } (A,-A) \text{ and } (-A,A)). \tag{29.59}$$

From this we see that the major and minor semi-axis will have lengths:

$$a = \sqrt{2}A \tag{29.60}$$

$$b = \sqrt{2}. \tag{29.61}$$

From the particle's initial position at $(1,1)$, the minor and major semi-axis will be reached at the following times $(n = 0, 1, 2, \ldots)$:

$$t_{minor} = \frac{(A^2-1)}{2A}\pi n \tag{29.62}$$

$$t_{major} = \frac{(A^2-1)}{2A}\pi(n+1/2). \tag{29.63}$$

Hence the period of one complete revolution (returning to $(1,1)$) is given by:

$$T = \frac{(A^2-1)}{A}\pi. \tag{29.64}$$

The ellipse is represented by the following two (equivalent) forms:

$$\frac{(x-y)^2}{4A^2} + \frac{(x+y)^2}{4} = 1 \tag{29.65}$$

and the parametric time equations:

$$x(t) = A\sin\left(\frac{2A}{A^2-1}t\right) + \cos\left(\frac{2A}{A^2-1}t\right) \tag{29.66}$$

$$y(t) = -A\sin\left(\frac{2A}{A^2-1}t\right) + \cos\left(\frac{2A}{A^2-1}t\right). \tag{29.67}$$

We will show 4 kinds of errors during a Runge Kutta run:

$$e_x = \text{Runge Kutta error in x-coordinate} \tag{29.68}$$

$$e_y = \text{Runge Kutta error in y-coordinate} \tag{29.69}$$

$$e_r = \text{Minimum distance from Runge Kutta point to ellipse curve} \tag{29.70}$$

$$e_t = \text{Time distance error: } e_t = \sqrt{[x-x(t)]^2 + [y-y(t)]^2} \tag{29.71}$$

Part IX

Simulation Units

Chapter 30

The Supplied Test Problems

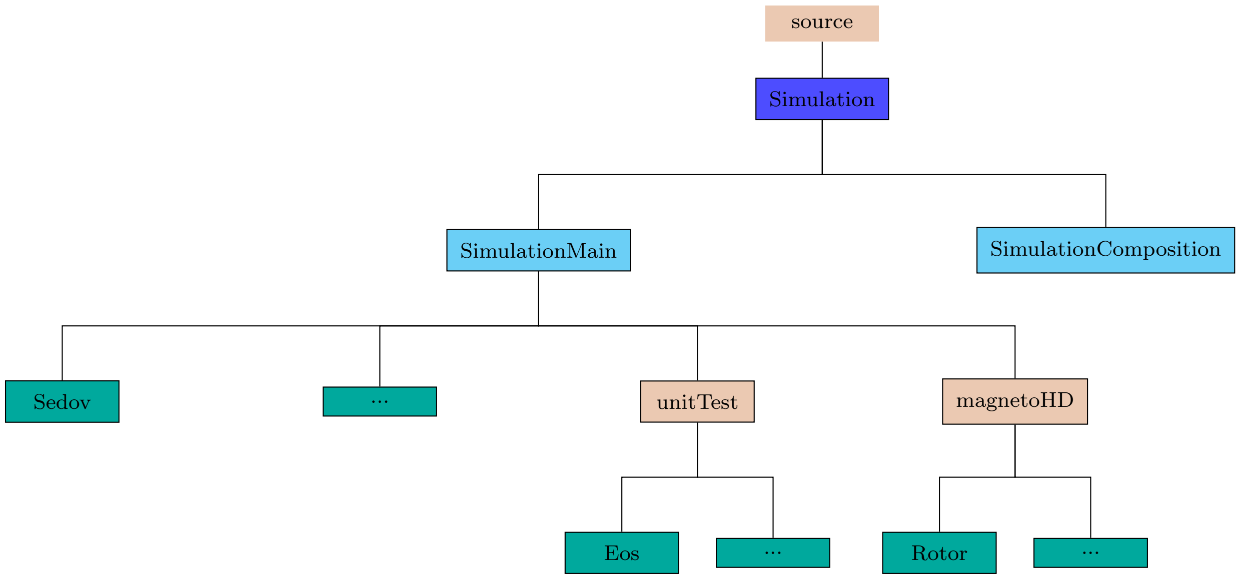

Figure 30.1: The `Simulation` unit directory tree. Only some of the provided simulation implementations are shown. Users are expected to add their own simulations to the tree.

To verify that FLASH works as expected and to debug changes in the code, we have created a suite of standard test problems. Many of these problems have analytical solutions that can be used to test the accuracy of the code. Most of the problems that do not have analytical solutions produce well-defined flow features that have been verified by experiments and are stringent tests of the code. For the remaining problems, converged solutions, which can be used to test the accuracy of lower resolution simulations, are easy to obtain. The test suite configuration code is included with the FLASH source tree (in the `Simulation/` directory), so it is easy to configure and run FLASH with any of these problems 'out of the box.' Sample runtime parameter files are also included. All the test problems reside in the `Simulations` unit. The unit provides some general interfaces most of which do not have general implementations. Each application provides its own implementation for these interfaces, for example, `Simulation_initBlock`. The exception is `Simulation_initSpecies`, which provides general implementations for different classes of problems.

30.1 Hydrodynamics Test Problems

These problems are primarily designed to test the functioning of the hydrodynamics solvers within FLASH4.

30.1.1 Sod Shock-Tube

The Sod problem (Sod 1978) is a one-dimensional flow discontinuity problem that provides a good test of a compressible code's ability to capture shocks and contact discontinuities with a small number of cells and to produce the correct profile in a rarefaction. It also tests a code's ability to correctly satisfy the Rankine-Hugoniot shock jump conditions. When implemented at an angle to a multidimensional grid, it can be used to detect irregularities in planar discontinuities produced by grid geometry or operator splitting effects.

We construct the initial conditions for the Sod problem by establishing a planar interface at some angle to the x- and y-axes. The fluid is initially at rest on either side of the interface, and the density and pressure jumps are chosen so that all three types of nonlinear, hydrodynamic waves (shock, contact, and rarefaction) develop. To the "left" and "right" of the interface we have

$$\begin{array}{lllllll} \rho_{\rm L} & = & 1.0 & \qquad & \rho_{\rm R} & = & 0.125 \\ p_{\rm L} & = & 1.0 & \qquad & p_{\rm R} & = & 0.1 \end{array} \tag{30.1}$$

The ratio of specific heats γ is chosen to be 1.4 on both sides of the interface.

In FLASH, the Sod problem (`Sod`) uses the runtime parameters listed in Table 30.1 in addition to those supplied by default with the code. For this problem we use the `Gamma` equation of state alternative implementation and set `gamma` to 1.4. The default values listed in Table 30.1 are appropriate to a shock with normal parallel to the x-axis that initially intersects that axis at $x = 0.5$ (halfway across a box with unit dimensions).

Table 30.1: Runtime parameters used with the `Sod` test problem.

Variable	Type	Default	Description
`sim_rhoLeft`	real	1	Initial density to the left of the interface ($\rho_{\rm L}$)
`sim_rhoRight`	real	0.125	Initial density to the right ($\rho_{\rm R}$)
`sim_pLeft`	real	1	Initial pressure to the left ($p_{\rm L}$)
`sim_pRight`	real	0.1	Initial pressure to the right ($p_{\rm R}$)
`sim_uLeft`	real	0	Initial velocity (perpendicular to interface) to the left ($u_{\rm L}$)
`sim_uRight`	real	0	Initial velocity (perpendicular to interface) to the right ($u_{\rm R}$)
`sim_xangle`	real	0	Angle made by interface normal with the x-axis (degrees)
`sim_yangle`	real	90	Angle made by interface normal with the y-axis (degrees)
`sim_posn`	real	0.5	Point of intersection between the interface plane and the x-axis

Figure 30.2 shows the result of running the Sod problem with FLASH on a two-dimensional grid with the analytical solution shown for comparison. The hydrodynamical algorithm used here is the directionally split piecewise-parabolic method (PPM) included with FLASH. In this run the shock normal is chosen to be parallel to the x-axis. With six levels of refinement, the effective grid size at the finest level is 256^2, so the finest cells have width 0.00390625. At $t = 0.2$, three different nonlinear waves are present: a rarefaction between $x = 0.263$ and $x = 0.486$, a contact discontinuity at $x = 0.685$, and a shock at $x = 0.850$. The two discontinuities are resolved with approximately two to three cells each at the highest level of refinement, demonstrating the ability of PPM to handle sharp flow features well. Near the contact discontinuity and in the rarefaction, we find small errors of about $1 - 2\%$ in the density and specific internal energy, with similar errors in the velocity inside the rarefaction. Elsewhere, the numerical solution is close to exact; no oscillations are present.

Figure 30.3 shows the result of running the Sod problem on the same two-dimensional grid with different shock normals: parallel to the x-axis ($\theta = 0°$) and along the box diagonal ($\theta = 45°$). For the diagonal solution, we have interpolated values of density, specific internal energy, and velocity to a set of 256 points

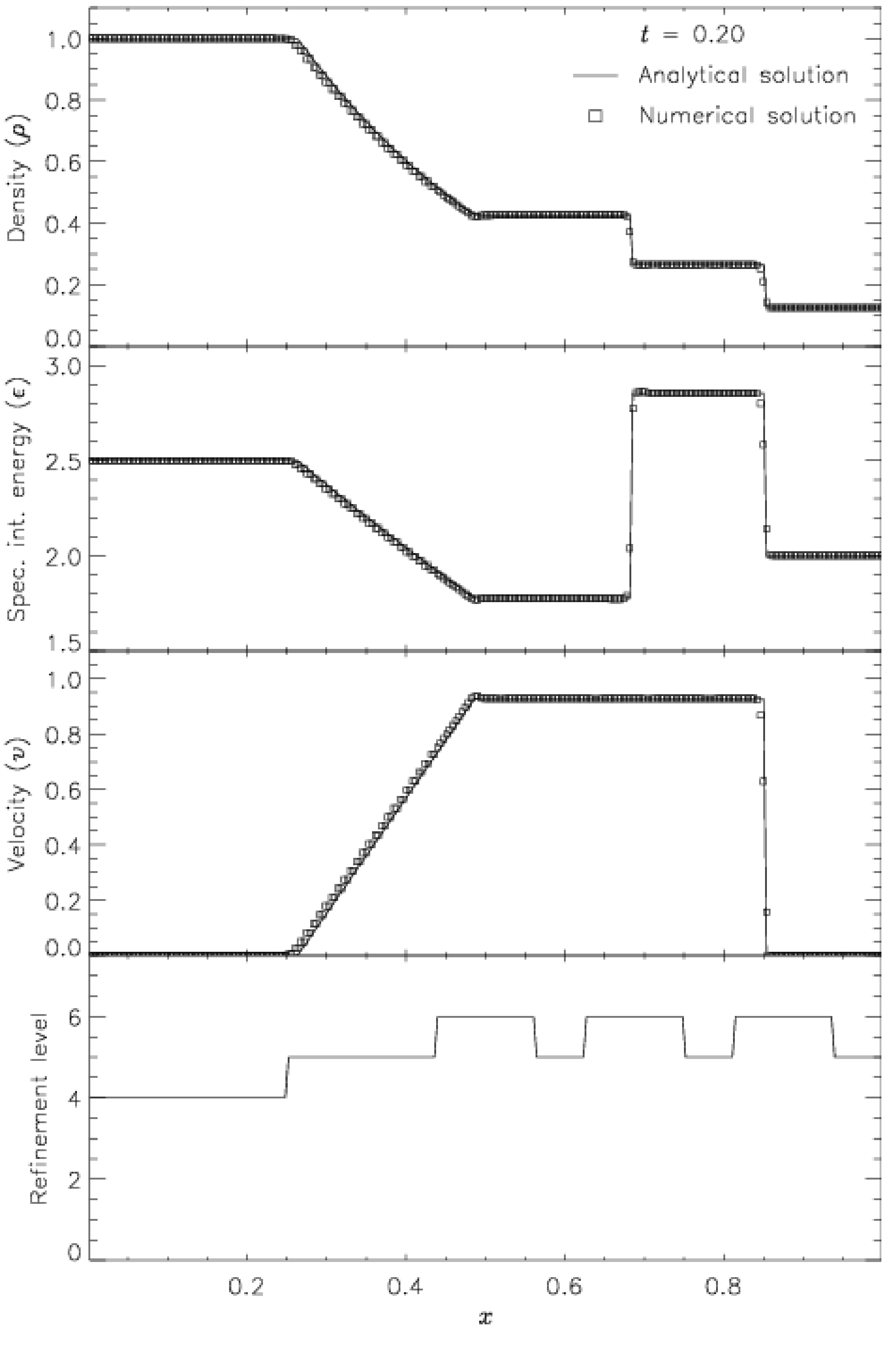

Figure 30.2: Comparison of numerical and analytical solutions to the Sod problem. A 2D grid with six levels of refinement is used. The shock normal is parallel to the x-axis.

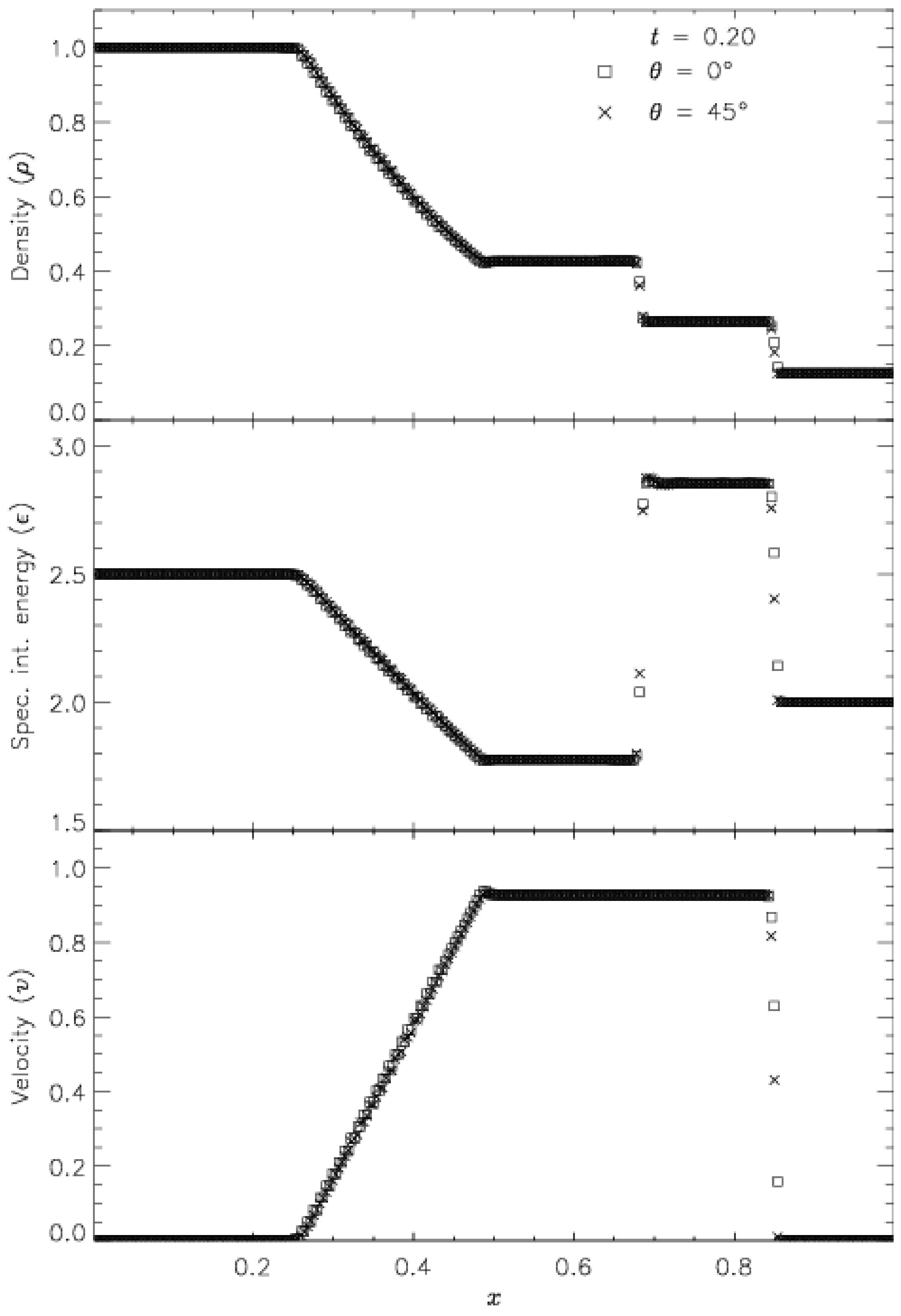

Figure 30.3: Comparison of numerical solutions to the Sod problem for two different angles (θ) of the shock normal relative to the x-axis. A 2D grid with six levels of refinement is used.

spaced exactly as in the x-axis solution. This comparison shows the effects of the second-order directional splitting used with FLASH on the resolution of shocks. At the right side of the rarefaction and at the contact discontinuity, the diagonal solution undergoes slightly larger oscillations (on the order of a few percent) than the x-axis solution. Also, the value of each variable inside the discontinuity regions differs between the two solutions by up to 10%. However, the location and thickness of the discontinuities is the same for the two solutions. In general, shocks at an angle to the grid are resolved with approximately the same number of cells as shocks parallel to a coordinate axis.

Figure 30.4 presents a colormap plot of the density at $t = 0.2$ in the diagonal solution together with the block structure of the AMR grid. Note that regions surrounding the discontinuities are maximally refined, while behind the shock and contact discontinuity, the grid has de-refined, because the second derivative of the density has decreased in magnitude. Because zero-gradient outflow boundaries were used for this test, some reflections are present at the upper left and lower right corners, but at $t = 0.2$ these have not yet propagated to the center of the grid.

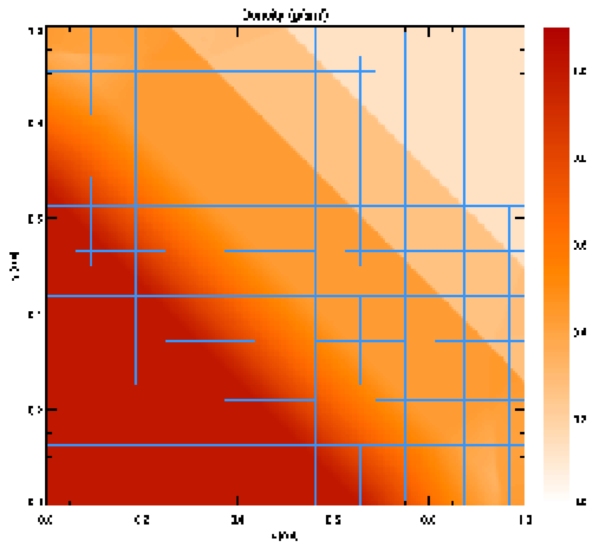

Figure 30.4: Density in the diagonal 2D Sod problem with six levels of refinement at $t = 0.2$. The outlines of AMR blocks are shown (each block contains 8×8 cells).

SodStep Example

FLASH4 also contains under the name SodStep a variant of the Sod problem. This setup is provided as an example for setting up simulations on domains with steps and obstacles. See the files in the SodStep simulation directory and the Simulation_defineDomain description for more information on how to use this feature.

30.1.2 Variants of the Sod Problem in Curvilinear Geometries

Variants of the Sod problems can be set up in in various geometries in order to test the handling of non-Cartesion geometries.

- An axisymmetric variant of the Sod problem can be configured by setting up the regular Sod simulation with `./setup Sod -auto -2d -geometry=cylindrical` and using runtime parameters that include `geometry = "cylindrical"`. Use `sim_xangle = 0` to configure an initial shock front that is shaped like a cylinder. Results as in those discussed in Toro 1999 can be obtained.

- A spherically symmetric variant of the Sod problem can be configured by setting up the regular `Sod` simulation with `./setup Sod -auto -1d -geometry=spherical` and using runtime parameters that include `geometry = "spherical"`. Again results as in those discussed in Toro 1999 can be obtained.
- To test the behavior of FLASH solutions when the physical symmetry of the problem does not match the geometry of the simulation, a separate simulation is provided under the name `SodSpherical`. To use this, configure with `./setup SodSpherical -auto -2d -geometry=spherical` and using runtime parameters that include `geometry = "spherical"`. As a 2D setup, `SodSpherical` represents physically axisymmetric initial conditions in spherical coordinates. The physical problem can be chosen to be the same as in the previous case with cylindrical `Sod`. Again results as in those discussed in Toro 1999 can be obtained.
- The `SodSpherical` setup can also configured in 1D and will act like the 1D `Sod` setup in that case.

30.1.3 Interacting Blast-Wave `Blast2`

This `Blast2` problem was originally used by Woodward and Colella (1984) to compare the performance of several different hydrodynamical methods on problems involving strong shocks and narrow features. It has no analytical solution (except at very early times), but since it is one-dimensional, it is easy to produce a converged solution by running the code with a very large number of cells, permitting an estimate of the self-convergence rate. For FLASH, it also provides a good test of the adaptive mesh refinement scheme.

The initial conditions consist of two parallel, planar flow discontinuities. Reflecting boundary conditions are used. The density is unity and the velocity is zero everywhere. The pressure is large at the left and right and small in the center

$$p_{\mathrm{L}} = 1000, \qquad p_{\mathrm{M}} = 0.01, \qquad p_{\mathrm{R}} = 100\,. \tag{30.2}$$

The equation of state is that of a perfect gas with $\gamma = 1.4$.

Figure 30.5 shows the density and velocity profiles at several different times in the converged solution, demonstrating the complexity inherent in this problem. The initial pressure discontinuities drive shocks into the middle part of the grid; behind them, rarefactions form and propagate toward the outer boundaries, where they are reflected back into the grid. By the time the shocks collide at $t = 0.028$, the reflected rarefactions have caught up to them, weakening them and making their post-shock structure more complex. Because the right-hand shock is initially weaker, the rarefaction on that side reflects from the wall later, so the resulting shock structures going into the collision from the left and right are quite different. Behind each shock is a contact discontinuity left over from the initial conditions (at $x \approx 0.50$ and 0.73). The shock collision produces an extremely high and narrow density peak. The peak density should be slightly less than 30. However, the peak density shown in Figure 30.5 is only about 18, since the maximum value of the density does not occur at exactly $t = 0.028$. Reflected shocks travel back into the colliding material, leaving a complex series of contact discontinuities and rarefactions between them. A new contact discontinuity has formed at the point of the collision ($x \approx 0.69$). By $t = 0.032$, the right-hand reflected shock has met the original right-hand contact discontinuity, producing a strong rarefaction, which meets the central contact discontinuity at $t = 0.034$. Between $t = 0.034$ and $t = 0.038$, the slope of the density behind the left-hand shock changes as the shock moves into a region of constant entropy near the left-hand contact discontinuity.

Figure 30.6 shows the self-convergence of density and pressure when FLASH is run on this problem. We compare the density, pressure, and total specific energy at $t = 0.038$ obtained using FLASH with ten levels of refinement to solutions using several different maximum refinement levels. This figure plots the L1 error norm for each variable u, defined using

$$\mathcal{E}(N_{\mathrm{ref}}; u) \equiv \frac{1}{N(N_{\mathrm{ref}})} \sum_{i=1}^{N(N_{\mathrm{ref}})} \left| \frac{u_i(N_{\mathrm{ref}}) - Au_i(10)}{u_i(10)} \right|\,, \tag{30.3}$$

against the effective number of cells ($N(N_{\mathrm{ref}})$). In computing this norm, both the 'converged' solution $u(10)$ and the test solution $u(N_{\mathrm{ref}})$ are interpolated onto a uniform mesh having $N(N_{\mathrm{ref}})$ cells. Values of N_{ref} between 2 (corresponding to cell size $\Delta x = 1/16$) and 9 ($\Delta x = 1/2048$) are shown.

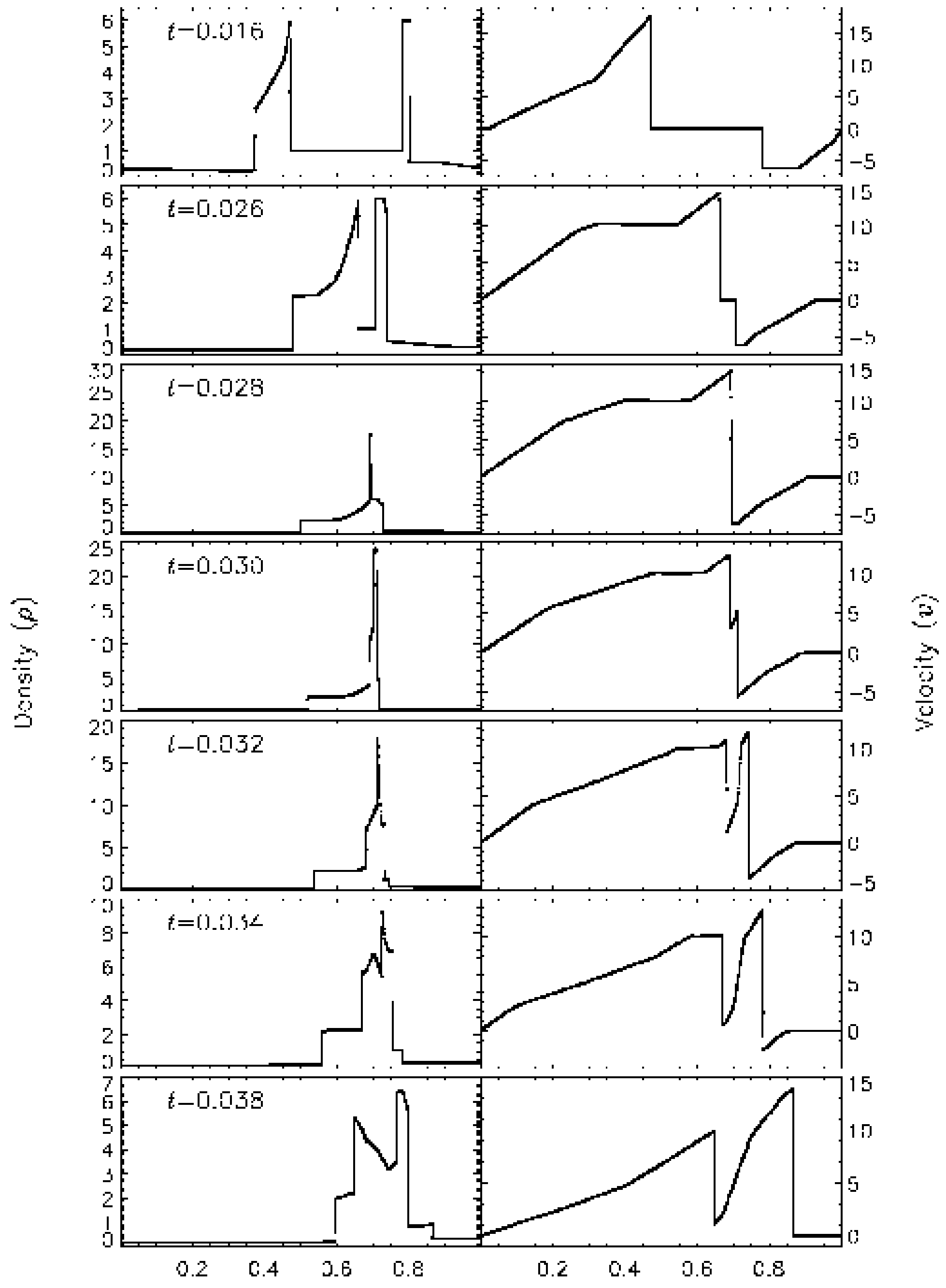

Figure 30.5: Density and velocity profiles in the Woodward-Colella interacting blast-wave problem `Blast2` as computed by FLASH using ten levels of refinement.

Although PPM is formally a second-order method, the convergence rate is only linear. This is not surprising, since the order of accuracy of a method applies only to smooth flow and not to flows containing discontinuities. In fact, all shock capturing schemes are only first-order accurate in the vicinity of discontinuities. Indeed, in their comparison of the performance of seven nominally second-order hydrodynamic methods on this problem, Woodward and Colella found that only PPM achieved even linear convergence; the other methods were worse. The error norm is very sensitive to the correct position and shape of the strong, narrow shocks generated in this problem.

The additional runtime parameters supplied with the `2blast` problem are listed in Table 30.2. This problem is configured to use the perfect-gas equation of state (`gamma`) with `gamma` set to 1.4 and is run in a two-dimensional unit box. Boundary conditions in the y-direction (transverse to the shock normals) are taken to be periodic.

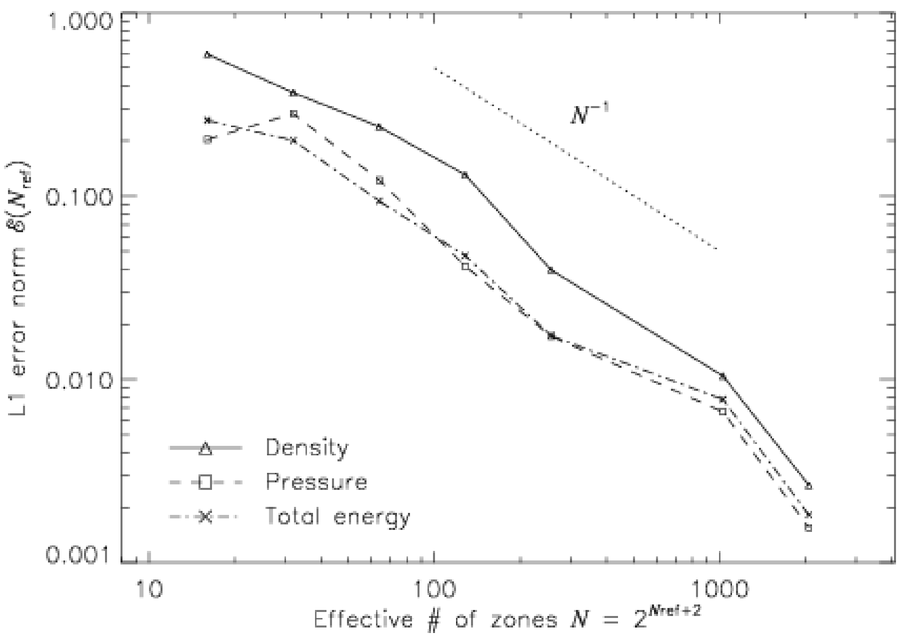

Figure 30.6: Self-convergence of the density, pressure, and total specific energy in the `Blast2` test problem.

Table 30.2: Runtime parameters used with the `2blast` test problem.

Variable	Type	Default	Description
`rho_left`	real	1	Initial density to the left of the left interface ($\rho_{\rm L}$)
`rho_mid`	real	1	Initial density between the two interfaces ($\rho_{\rm M}$)
`rho_right`	real	1	Initial density to the right of the right interface ($\rho_{\rm R}$)
`p_left`	real	1000	Initial pressure to the left ($p_{\rm L}$)
`p_mid`	real	0.01	Initial pressure in the middle ($p_{\rm M}$)
`p_right`	real	100	Initial pressure to the right ($p_{\rm R}$)
`u_left`	real	0	Initial velocity (perpendicular to interface) to the left ($u_{\rm L}$)
`u_mid`	real	0	Initial velocity (perpendicular to interface) in the middle ($u_{\rm M}$)
`u_right`	real	0	Initial velocity (perpendicular to interface) to the right ($u_{\rm R}$)
`xangle`	real	0	Angle made by interface normal with the x-axis (degrees)
`yangle`	real	90	Angle made by interface normal with the y-axis (degrees)
`posnL`	real	0.1	Point of intersection between the left interface plane and the x-axis
`posnR`	real	0.9	Point of intersection between the right interface plane and the x-axis

30.1.4 Sedov Explosion

The Sedov explosion problem (Sedov 1959) is another purely hydrodynamical test in which we check the code's ability to deal with strong shocks and non-planar symmetry. The problem involves the self-similar evolution of a cylindrical or spherical blast wave from a delta-function initial pressure perturbation in an otherwise homogeneous medium. To initialize the code, we deposit a quantity of energy $E = 1$ into a small region of radius δr at the center of the grid. The pressure inside this volume p_0' is given by

$$p_0' = \frac{3(\gamma - 1)E}{(\nu + 1)\pi\, \delta r^\nu} \ , \tag{30.4}$$

where $\nu = 2$ for cylindrical geometry and $\nu = 3$ for spherical geometry. We set the ratio of specific heats $\gamma = 1.4$. In running this problem we choose δr to be 3.5 times as large as the finest adaptive mesh resolution in order to minimize effects due to the Cartesian geometry of our grid. The density is set equal to $\rho_0 = 1$ everywhere, and the pressure is set to a small value $p_0 = 10^{-5}$ everywhere but in the center of the grid. The fluid is initially at rest. In the self-similar blast wave that develops for $t > 0$, the density, pressure, and radial velocity are all functions of $\xi \equiv r/R(t)$, where

$$R(t) = C_\nu(\gamma)\left(\frac{Et^2}{\rho_0}\right)^{1/(\nu+2)} \ . \tag{30.5}$$

Here C_ν is a dimensionless constant depending only on ν and γ; for $\gamma = 1.4$, $C_2 \approx C_3 \approx 1$ to within a few percent. Just behind the shock front at $\xi = 1$ the analytical solution is

$$\begin{aligned} \rho = \quad \rho_1 &\equiv \frac{\gamma+1}{\gamma-1}\rho_0 \\ p = \quad p_1 &\equiv \frac{2}{\gamma+1}\rho_0 u^2 \\ v = \quad v_1 &\equiv \frac{2}{\gamma+1} u \ , \end{aligned} \tag{30.6}$$

where $u \equiv dR/dt$ is the speed of the shock wave. Near the center of the grid,

$$\begin{aligned} \rho(\xi)/\rho_1 &\propto \xi^{\nu/(\gamma-1)} \\ p(\xi)/p_1 &= \text{constant} \\ v(\xi)/v_1 &\propto \xi \ . \end{aligned} \tag{30.7}$$

Figure 30.7 shows density, pressure, and velocity profiles in the two-dimensional, cylindrical Sedov problem at $t = 0.05$. Solutions obtained with FLASH on grids with 2, 4, 6, and 8 levels of refinement are shown in comparison with the analytical solution. In this figure we have computed average radial profiles in the following way. We interpolated solution values from the adaptively gridded mesh used by FLASH onto a uniform mesh having the same resolution as the finest AMR blocks in each run. Then, using radial bins with the same width as the cells in the uniform mesh, we binned the interpolated solution values, computing the average value in each bin. At low resolutions, errors show up as density and velocity overestimates behind the shock, underestimates of each variable within the shock, and a very broad shock structure. However, the central pressure is accurately determined, even for two levels of refinement. Because the density goes to a finite value rather than to its correct limit of zero, this corresponds to a finite truncation of the temperature (which should go to infinity as $r \to 0$). This error results from depositing the initial energy into a finite-width region rather than starting from a delta function. As the resolution improves and the value of δr decreases, the artificial finite density limit also decreases; by $N_{\rm ref} = 6$ it is less than 0.2% of the peak density. Except for the $N_{\rm ref} = 2$ case, which does not show a well-defined peak in any variable, the shock itself is always captured with about two cells. The region behind the shock containing 90% of the swept-up material is represented by four cells in the $N_{\rm ref} = 4$ case, 17 cells in the $N_{\rm ref} = 6$ case, and 69 cells for $N_{\rm ref} = 8$. However, because the solution is self-similar, for any given maximum refinement level, the structure will be four cells wide at a sufficiently early time. The behavior when the shock is under-resolved is to underestimate the peak value of each variable, particularly the density and pressure.

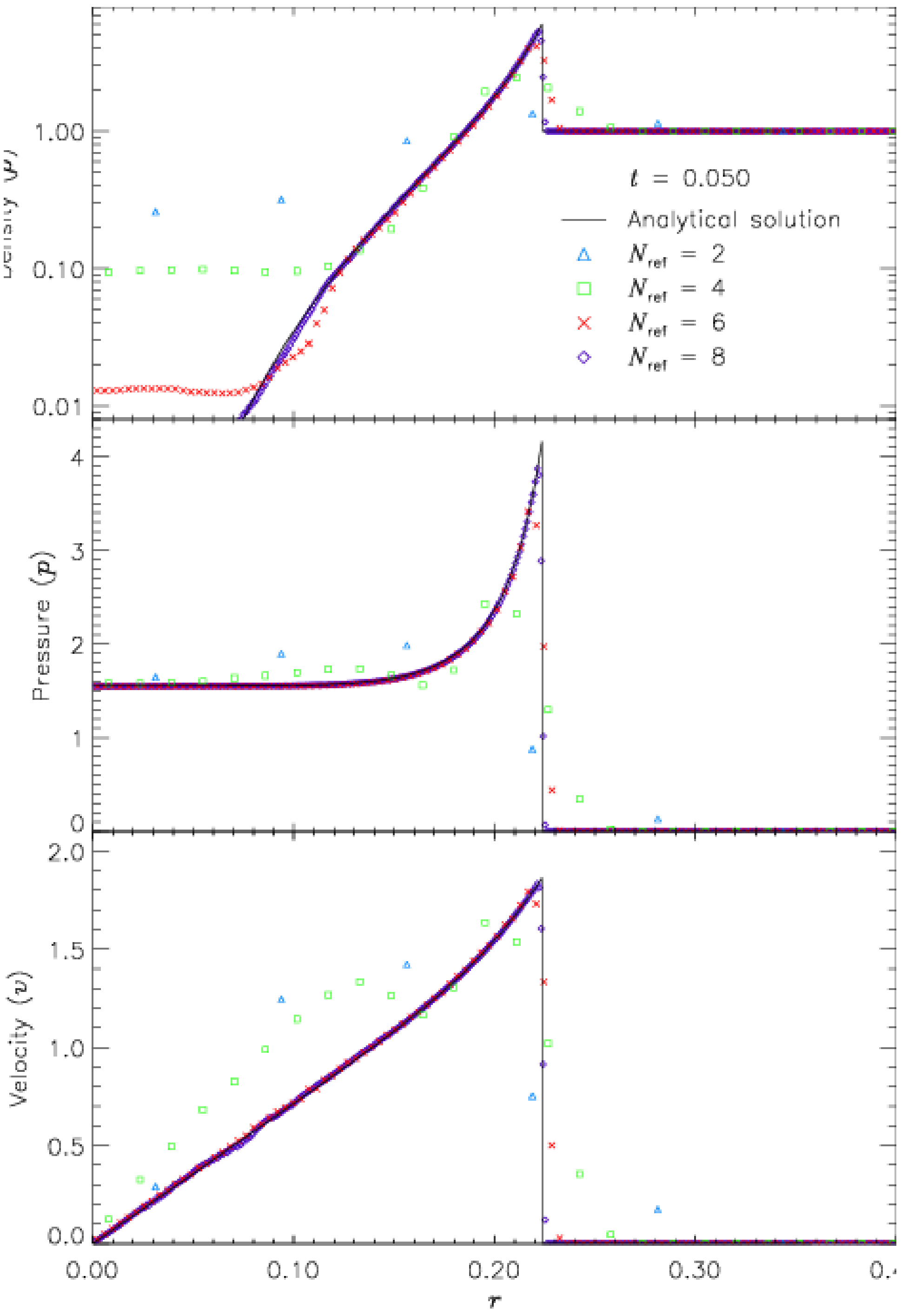

Figure 30.7: Comparison of numerical and analytical solutions to the Sedov problem in two dimensions. Numerical solution values are averages in radial bins at the finest AMR grid resolution N_ref in each run.

Figure 30.8 shows the pressure field in the 8-level calculation at $t = 0.05$ together with the block refinement pattern. Note that a relatively small fraction of the grid is maximally refined in this problem. Although the pressure gradient at the center of the grid is small, this region is refined because of the large temperature gradient there. This illustrates the ability of `PARAMESH` to refine grids using several different variables at once.

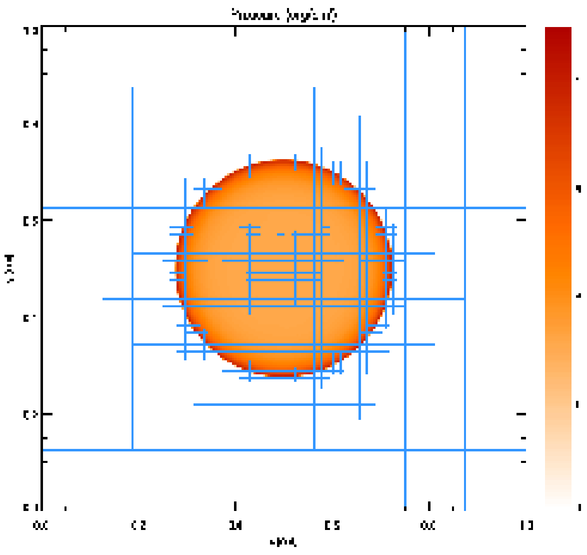

Figure 30.8: Pressure field in the 2D Sedov explosion problem with 8 levels of refinement at $t = 0.05$. The outlines of the AMR blocks are overlaid on the pressure colormap.

We have also run FLASH on the spherically symmetric Sedov problem in order to verify the code's performance in three dimensions. The results at $t = 0.05$ using five levels of grid refinement are shown in Figure 30.9. In this figure we have plotted the average values as well as the root-mean-square (RMS) deviations from the averages. As in the two-dimensional runs, the shock is spread over about two cells at the finest AMR resolution in this run. The width of the pressure peak in the analytical solution is about 1 1/2 cells at this time, so the maximum pressure is not captured in the numerical solution. Behind the shock the numerical solution average tracks the analytical solution quite well, although the Cartesian grid geometry produces RMS deviations of up to 40% in the density and velocity in the de-refined region well behind the shock. This behavior is similar to that exhibited in the two-dimensional problem at comparable resolution.

The additional runtime parameters supplied with the `Sedov` problem are listed in Table 30.3. This problem is configured to use the perfect-gas equation of state (`Gamma`) with `gamma` set to 1.4. It is simulated in a unit-sized box.

30.1.4.1 Sedov Self-Gravity

Another variant of the Sedov problem is included in the release which runs with spherical coordinates in one dimension. The `Sedov Self-Gravity` problem also allows the effects of gravitational acceleration where the gravitational potential is calculated using the multipole solver. Figure 30.10 and 30.11 show the snapshots of the density profile and the gravitational potential at two different times during the evolution. The first snapshot is at $t = 0.5$ sec, when evolution is halfway through, while the second snapshot is at the end of the evolution, where $t = 1.0$ sec.

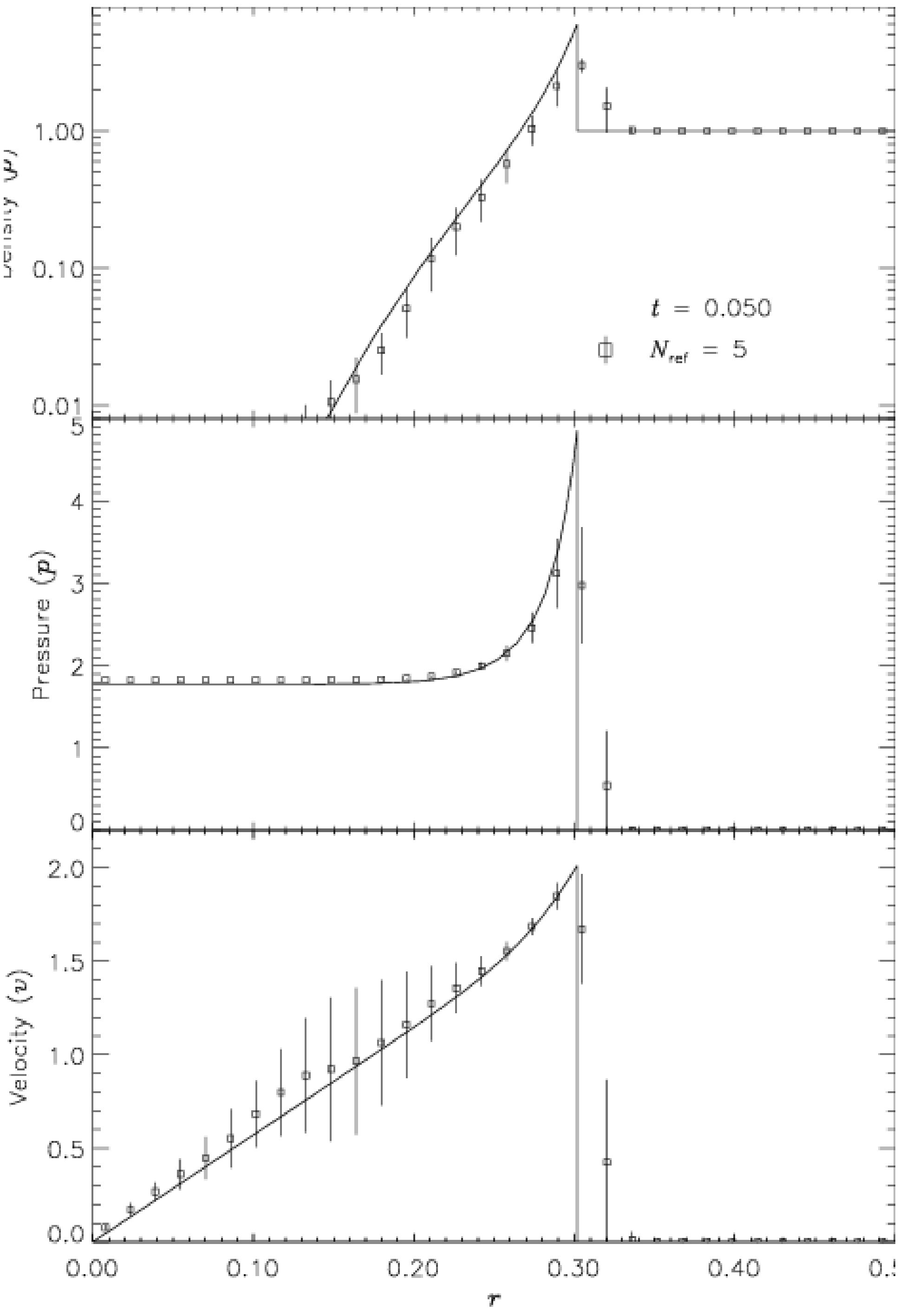

Figure 30.9: Comparison of numerical and analytical solutions versus radius r to the spherically symmetric Sedov problem. A 3D grid with five levels of refinement is used.

Table 30.3: Runtime parameters used with the `Sedov` test problem.

Variable	Type	Default	Description
`sim_pAmbient`	real	10^{-5}	Initial ambient pressure (p_0)
`sim_rhoAmbient`	real	1	Initial ambient density (ρ_0)
`sim_expEnergy`	real	1	Explosion energy (E)
`sim_rInit`	real	0.05	Radius of initial pressure perturbation (δr)
`sim_xctr`	real	0.5	x-coordinate of explosion center
`ssim_yctr`	real	0.5	y-coordinate of explosion center
`sim_zctr`	real	0.5	z-coordinate of explosion center
`sim_nSubZones`	integer	7	Number of sub-cells in cells for applying the 1D profile

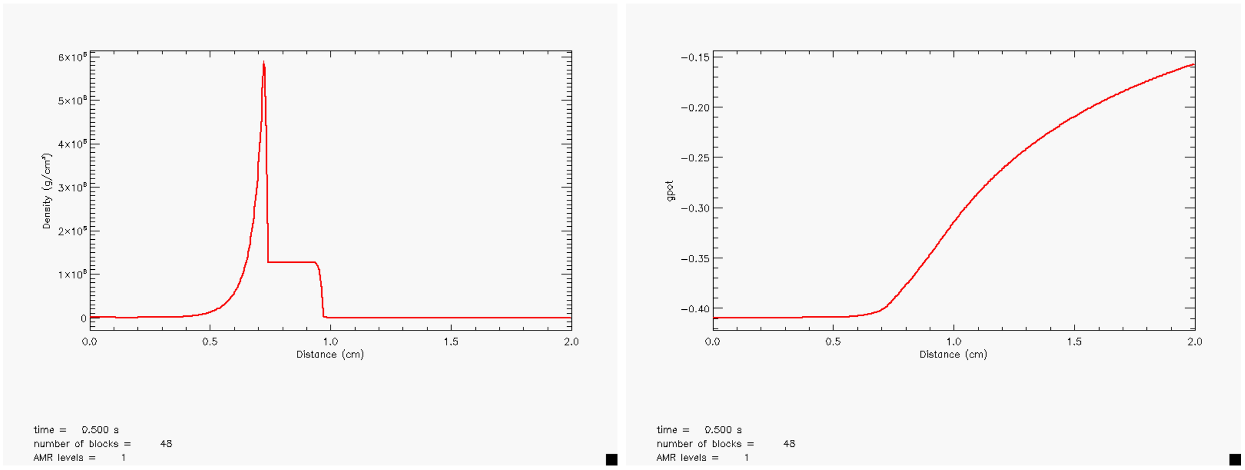

Figure 30.10: Snapshots of Sedov Self-gravity density profile and gravitational potential at time t=0.5 sec.

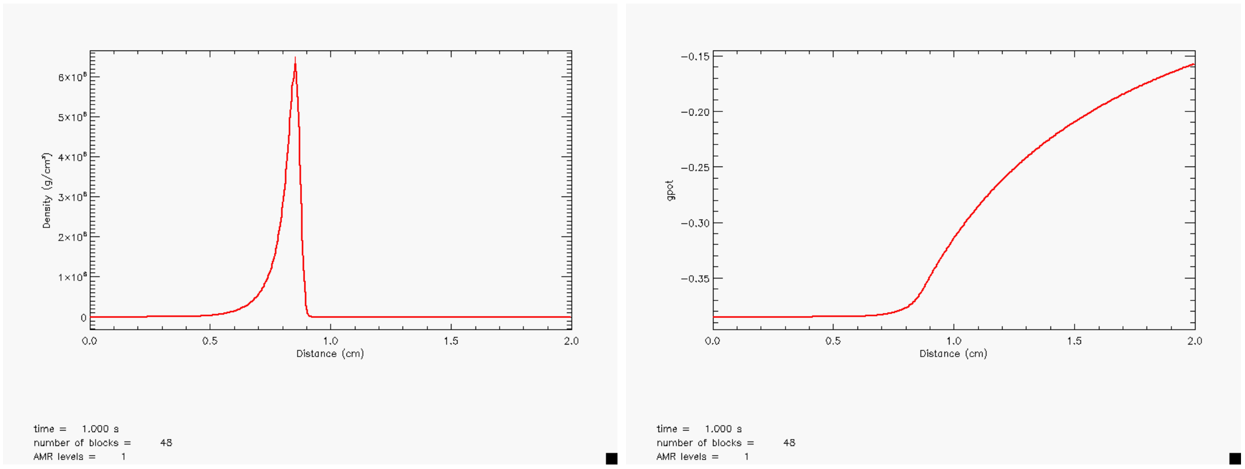

Figure 30.11: Snapshots of Sedov Self-gravity density profile and gravitational potential at time t=1.0 sec.

30.1.5 Isentropic Vortex

The two-dimensional isentropic vortex problem is often used as a benchmark for comparing numerical methods for fluid dynamics. The flow-field is smooth (there are no shocks or contact discontinuities) and contains no steep gradients, and the exact solution is known. It was studied by Yee, Vinokur, and Djomehri (2000) and by Shu (1998). In this subsection the problem is described, the FLASH control parameters are explained, and some results demonstrating how the problem can be used are presented.

The simulation domain is a square, and the center of the vortex is located at (x_{ctr}, y_{ctr}). The flow-field is defined in coordinates centered on the vortex center ($x' = x - x_{ctr}, y' = y - y_{ctr}$) with $r^2 = x'^2 + y'^2$. The domain is periodic, but it is assumed that off-domain vortexes do not interact with the primary; practically, this assumption can be satisfied by ensuring that the simulation domain is large enough for a particular vortex strength. We find that a domain size of 10×10 (specified through the `Grid` runtime parameters `xmin`, `xmax`, `ymin`, and `ymax`) is sufficiently large for a vortex strength (defined below) of 5.0. In the initialization below, x' and y' are the coordinates with respect to the nearest vortex in the periodic sense.

The ambient conditions are given by ρ_∞, u_∞, v_∞, and p_∞, and the non-dimensional ambient temperature is $T^*_\infty = 1.0$. Using the equation of state, the (dimensional) T_∞ is computed from p_∞ and ρ_∞. Perturbations are added to the velocity and nondimensionalized temperature, $u = u_\infty + \delta u$, $v = v_\infty + \delta v$, and $T^* = T^*_\infty + \delta T^*$ according to

$$\delta u = -y' \frac{\beta}{2\pi} \exp\left(\frac{1-r^2}{2}\right) \tag{30.8}$$

$$\delta v = x' \frac{\beta}{2\pi} \exp\left(\frac{1-r^2}{2}\right) \tag{30.9}$$

$$\delta T^* = -\frac{(\gamma-1)\beta}{8\gamma\pi^2} \exp\left(1-r^2\right) , \tag{30.10}$$

where $\gamma = 1.4$ is the ratio of specific heats and $\beta = 5.0$ is a measure of the vortex strength. The temperature and density are then given by

$$T = \frac{T_\infty}{T^*_\infty} T^* \tag{30.11}$$

$$\rho = \rho_\infty \left(\frac{T}{T_\infty}\right)^{\frac{1}{\gamma-1}} . \tag{30.12}$$

At any location in space, the conserved variables (density, x- and y-momentum, and total energy) can be computed from the above quantities. The flow-field is initialized by computing cell averages of the conserved variables; in each cell, the average is approximated by averaging over `nx_subint` $\times$ `ny_subint` subintervals. The runtime parameters for the isentropic vortex problem are listed in Table 30.4.

Table 30.4: Parameters for the `IsentropicVortex` problem.

Variable	Type	Default	Description
`p_ambient`	real	1.0	Initial ambient pressure (p_∞)
`rho_ambient`	real	1.0	Initial ambient density (ρ_∞)
`u_ambient`	real	1.0	Initial ambient x-velocity (u_∞)
`v_ambient`	real	1.0	Initial ambient y-velocity (v_∞)
`vortex_strength`	real	5.0	Non-dimensional vortex strength
`xctr`	real	0.0	x-coordinate of vortex center
`yctr`	real	0.0	y-coordinate of vortex center
`nx_subint`	integer	10	number of subintervals in x-direction
`ny_subint`	integer	10	number of subintervals in y-direction

Figure 30.12 shows the exact density distribution represented on a 40×40 uniform grid with $-5.0 \leq x, y \leq 5.0$. The borders of each grid block (8×8 cells) are superimposed. In addition to the shaded representation, contour lines are shown for $\rho = 0.95$, 0.85, 0.75, and 0.65. The density distribution is radially symmetric, and the minimum density is $\rho_{min} = 0.510287$. Because the exact solution of the isentropic vortex problem is the initial solution shifted by $(u_\infty t, v_\infty t)$, numerical phase (dispersion) and amplitude (dissipation) errors are easy to identify. Dispersive errors distort the shape of the vortex, breaking its symmetry. Dissipative errors smooth the solution and flatten extrema; for the vortex, the minimum in density at the vortex core will increase.

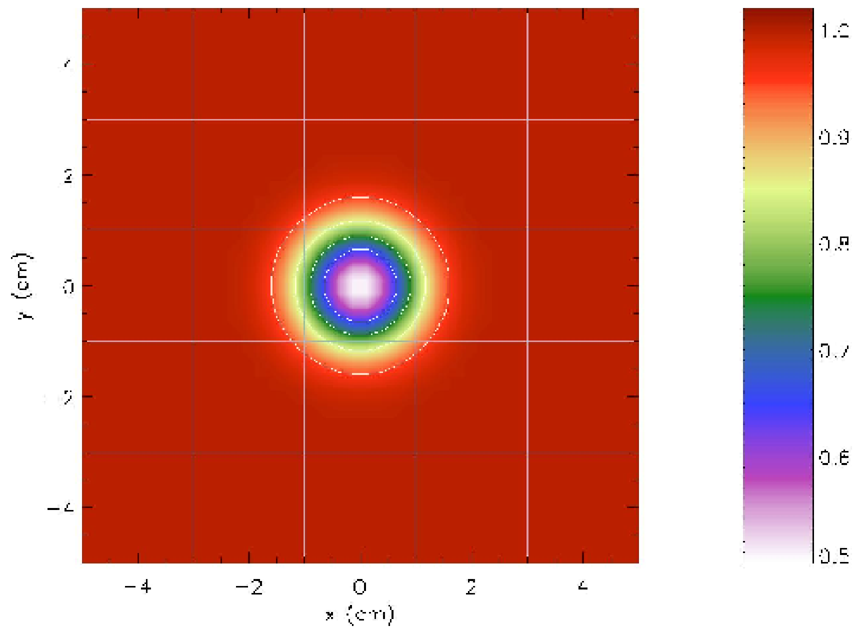

Figure 30.12: Density at $t = 0.0$ for the isentropic vortex problem. Shown are the initial condition and the exact solution at $t = 10.0, 20.0, \ldots$.

A numerical simulation using the PPM scheme was run to illustrate such errors. The simulation used the same grid shown in Figure 30.12 with the same contour levels and color values. The grid is intentionally coarse and the evolution time long to make numerical errors visible. The vortex is represented by approximately 8 grid points in each coordinate direction and is advected diagonally with respect to the grid. At solution times of $t = 10, 20, \ldots$, *etc.*, the vortex should be back at its initial location.

Figure 30.13 shows the solution at $t = 50.0$; only slight differences are observed. The density distribution is almost radially symmetric, although the minimum density has risen to 0.0537360. Accumulating dispersion error is clearly visible at $t = 100.0$ (Figure 30.14), and the minimum density is now 0.601786.

Figure 30.15 shows the density near $y = 0.0$ at three simulation times. The black line shows the initial condition. The red line corresponds to $t = 50.0$ and the blue line to $t = 100.0$. For the later two times, the density is not radially symmetric. The lines plotted are just representative profiles for those times, which give an idea of the magnitude and character of the errors.

30.1.6 The double Mach reflection problem

This numerical planar shock test problem introduced by Woodward and Colella (1984) simulates an evolution of an unsteady planar shock that is incident on an oblique surface. Initially, the incident planar shock begins to propagate to the bottom surface at a 30° angle with the shock Mach number of 10. Later, the solution to this problem produces a self-similar wave pattern that corresponds to the double Mach reflection. Following

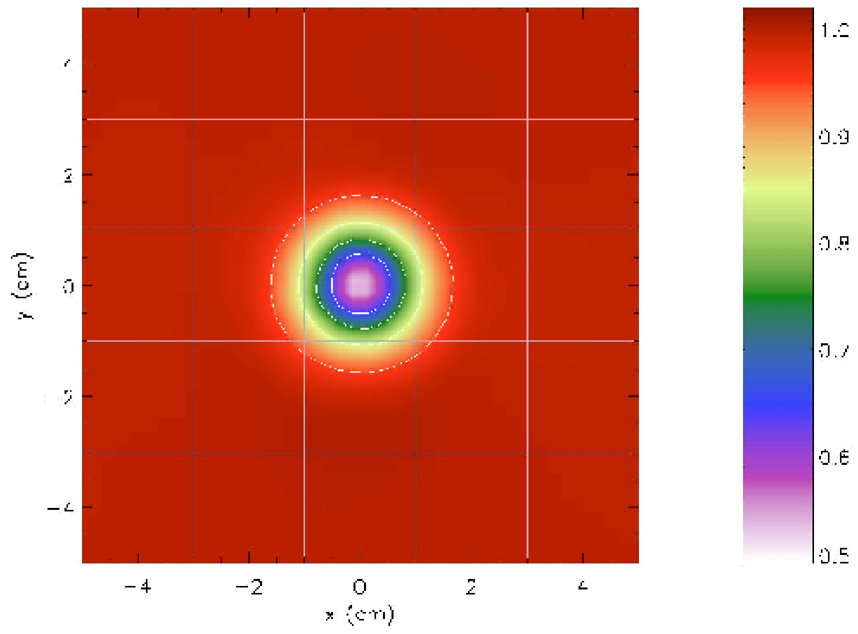

Figure 30.13: Density at $t = 50.0$ for the isentropic vortex problem.

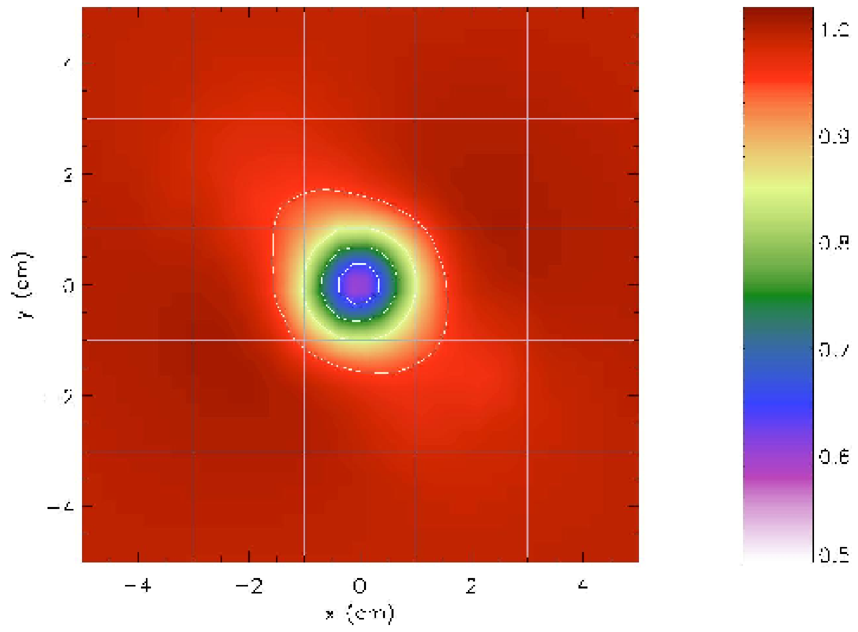

Figure 30.14: Density at $t = 100.0$ for the isentropic vortex problem.

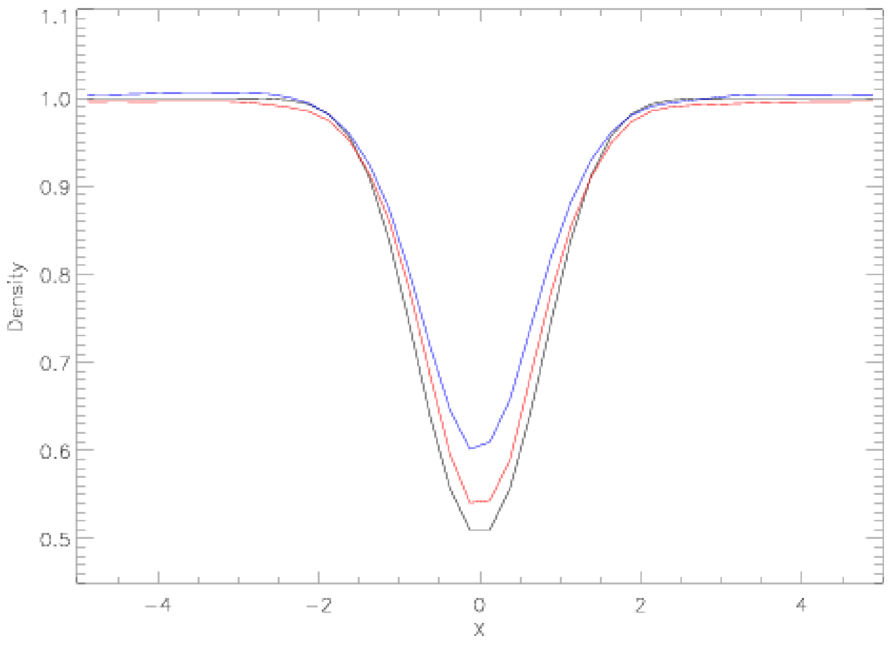

Figure 30.15: Representative density profiles for the isentropic vortex near $y = 0.0$ at $t = 0.0$ (black), $t = 50.0$ (red), and $t = 100.0$ (blue).

many other numerical setups of this problem, we tilt the incident shock rather than the reflecting wall so as to avoid numerical complications in modeling an oblique physical boundary.

The initial setup involves a Mach 10 shock in air, $\gamma = 1.4$, on a rectangular 2D domain of size $[0, 4] \times [0, 1]$. The reflecting wall is represented as the bottom surface of the domain, beginning at $x = 1/6$. The velocity normal to the incident shock in the post-shock region is 8.25, and the flow is at rest in the pre-shock region. The undisturbed air ahead of the shock has a density of 1.4 and a pressure of 1. See the initial density profile in Figure 30.16 resolved on 6 refinement AMR levels using 16^2-cell block size.

The boundary condition on $0 \leq x \leq 1/6$ at $y = 0$ is fixed in time with the initial values so that the reflected shock is attached to the bottom surface. We impose reflecting boundary condition (i.e., negating the y velocity field v) on the rest of the bottom surface. On the top surface of $y = 1$, we allow the initial Mach 10 shock proceeds exactly as a function of time in order that the numerical evolution follows the oblique shock propagation without any planar distortion. At $x = 0$, we impose a supersonic inflow boundary condition, and the outflow condition at $x = 4$.

In later time, the solution develops to form two Mach stems and two contact discontinuities, as shown in Figure 30.17 the density at $t = 2.5$ sec. Also shown in Figure 30.18 are 30 levels of contour lines of pressure, illustrating the evolved flow discontinuities at $t = 2.5$ sec. We can also see that the numerical solution is smooth and non-oscillatory in the region bounded by the curved reflected shock, the bottom surface and the second Mach stem (see more discussion in Woodward and Colella, 1984).

The 5th order WENO method in the unsplit hydrodynamics solver is used with a choice of hybrid Riemann solver which selectively adopts HLL only at strong shocks and HLLC otherwise.

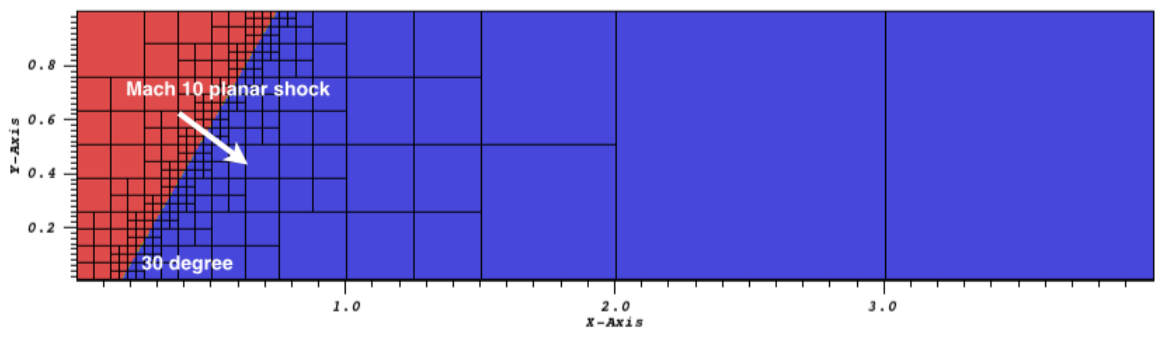

Figure 30.16: The initial density at $t = 0$ visualized with 6 levels of AMR block structures.

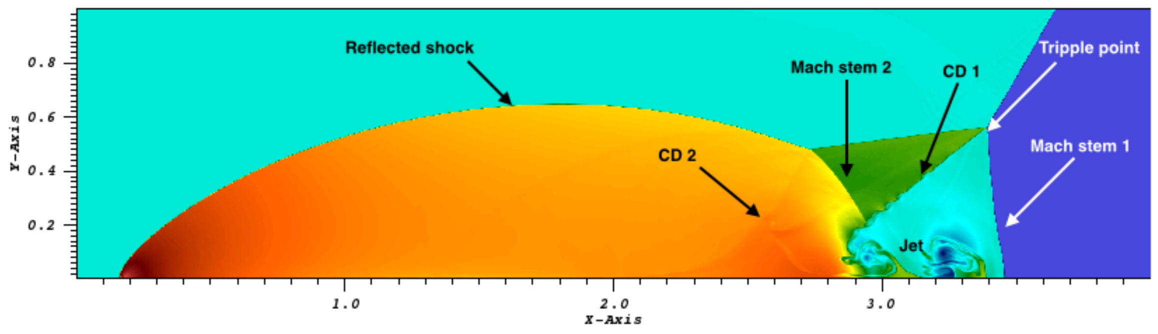

Figure 30.17: Density profile at $t = 2.5$. Two contact discontinuities are denoted as ”CD”, along with two Mach stems, a curved reflected shock, and a jet formulation of the denser fluid along the bottom surface.

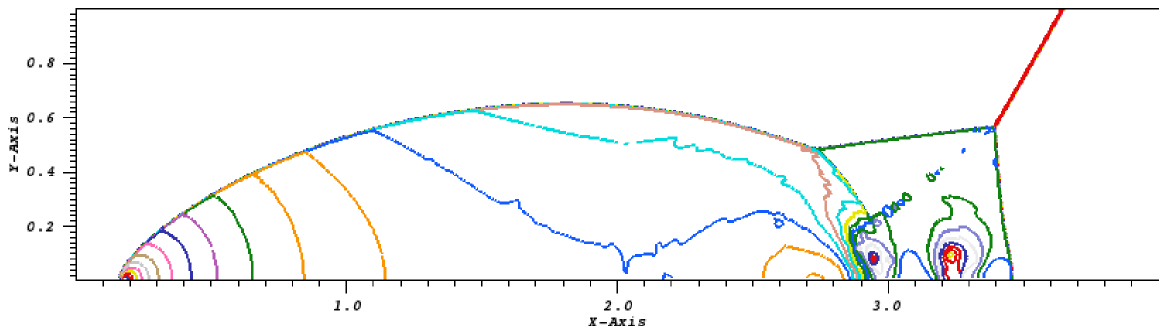

Figure 30.18: The 30 levels of contour lines of pressure at $t = 2.5$.

Table 30.5: Runtime parameters used with the `double Mach reflection` test problem.

Variable	Type	Default	Description
`sim_rhoLeft`	real	8	Initial density to the left of the shock ($\rho_{\rm L}$)
`sim_rhoRight`	real	1.4	Initial density to the right ($\rho_{\rm R}$)
`sim_pLeft`	real	116.5	Initial pressure to the left ($p_{\rm L}$)
`sim_pRight`	real	1	Initial pressure to the right ($p_{\rm R}$)
`sim_uLeft`	real	7.1447096	Initial x-velocity to the left ($u_{\rm L}$)
`sim_uRight`	real	0	Initial x-velocity to the right ($u_{\rm R}$)
`sim_vLeft`	real	-4.125	Initial y-velocity to the left ($v_{\rm L}$)
`sim_vRight`	real	0	Initial y-velocity to the right ($v_{\rm R}$)
`sim_xangle`	real	-30	Angle made by shock normal with the x-axis (degrees)
`sim_yangle`	real	90	Angle made by shock normal with the y-axis (degrees)
`sim_posn`	real	1/6	Point of intersection between the shock plane and the x-axis

30.1.7 Wind Tunnel With a Step

The problem of a wind tunnel containing a step, `WindTunnel` was first described by Emery (1968), who used it to compare several hydrodynamical methods. Woodward and Colella (1984) later used it to compare several more advanced methods, including PPM. Although it has no analytical solution, this problem is useful because it exercises a code's ability to handle unsteady shock interactions in multiple dimensions. It also provides an example of the use of FLASH to solve problems with irregular boundaries.

The problem uses a two-dimensional rectangular domain three units wide and one unit high. Between $x = 0.6$ and $x = 3$ along the x-axis is a step 0.2 units high. The step is treated as a reflecting boundary, as are the lower and upper boundaries in the y-direction. For the right-hand x-boundary, we use an outflow (zero gradient) boundary condition, while on the left-hand side we use an inflow boundary. In the inflow boundary cells, we set the density to ρ_0, the pressure to p_0, and the velocity to u_0, with the latter directed parallel to the x-axis. The domain itself is also initialized with these values. We use

$$\rho_0 = 1.4, \qquad p_0 = 1, \qquad u_0 = 3\ , \qquad \gamma = 1.4, \tag{30.13}$$

which corresponds to a Mach 3 flow. Because the outflow is supersonic throughout the calculation, we do not expect reflections from the right-hand boundary.

The additional runtime parameters supplied with the `WindTunnel` problem are listed in Table 30.6. This problem is configured to use the perfect-gas equation of state (`Gamma`) with `gamma` set to 1.4. We also set `xmax` = 3, `ymax` = 1, `Nblockx` = 15, and `Nblocky` = 5 in order to create a grid with the correct dimensions. The version of `Simulation_defineDomain` supplied with this problem removes all but the first three top-level blocks along the lower edge of the grid to generate the step, and gives `REFLECTING` boundaries to the obstacle blocks. Finally, we use `xl_boundary_type = "user"` (`USER_DEFINED` condition) and `xr_boundary_type = "outflow"` (`OUTFLOW` boundary) to instruct FLASH to use the correct boundary conditions in the x-direction. Boundaries in the y-direction are reflecting (`REFLECTING`).

Until $t = 12$, the flow is unsteady, exhibiting multiple shock reflections and interactions between different types of discontinuities. Figure 30.19 shows the evolution of density and velocity between $t = 0$ and $t = 4$ (the period considered by Woodward and Colella). Immediately, a shock forms directly in front of the step and begins to move slowly away from it. Simultaneously, the shock curves around the corner of the step, extending farther downstream and growing in size until it strikes the upper boundary just after $t = 0.5$. The corner of the step becomes a singular point, with a rarefaction fan connecting the still gas just above the step to the shocked gas in front of it. Entropy errors generated in the vicinity of this singular point produce a numerical boundary layer about one cell thick along the surface of the step. Woodward and Colella reduce this effect by resetting the cells immediately behind the corner to conserve entropy and the sum of enthalpy

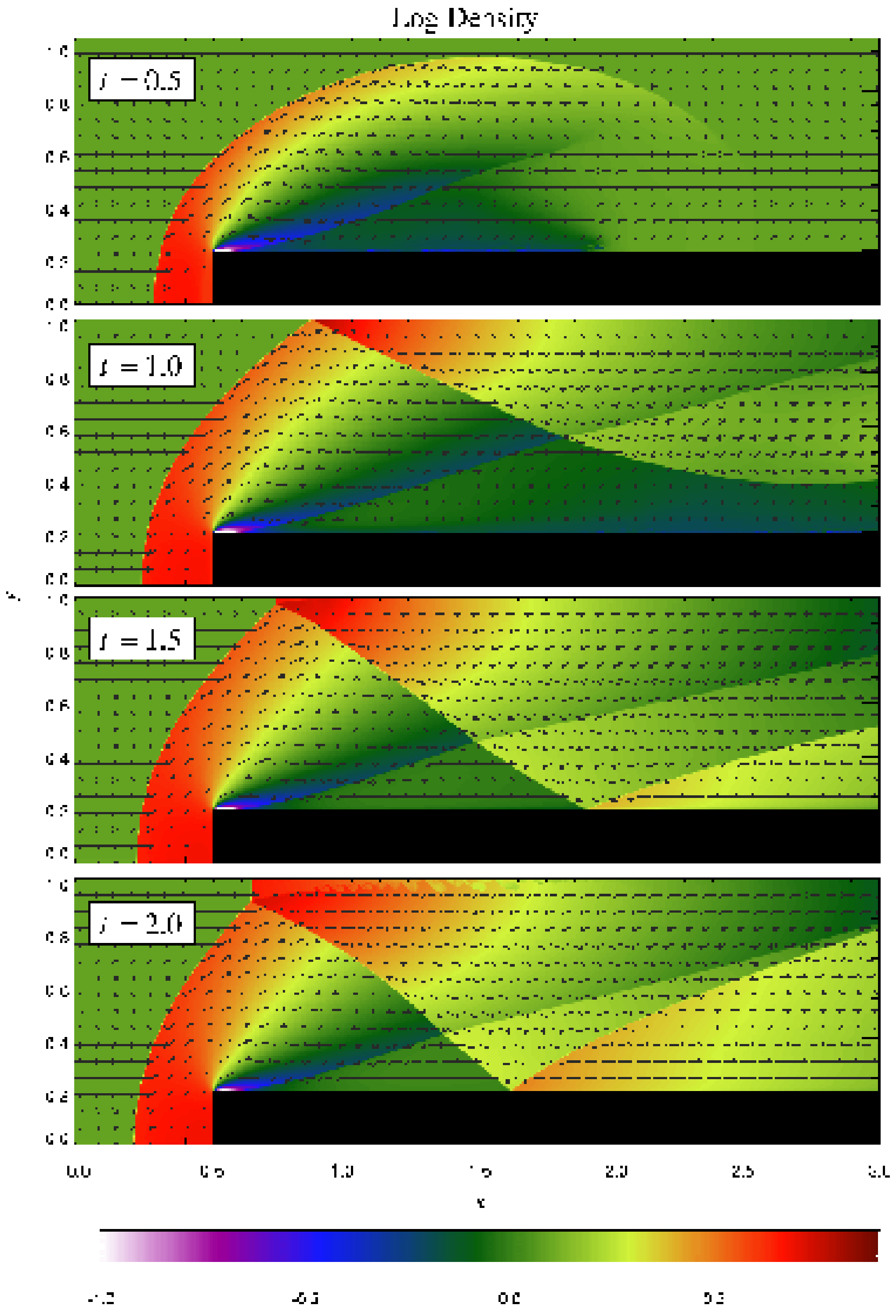

Figure 30.19: Density and velocity in the Emery wind tunnel test problem, as computed with FLASH. A 2D grid with five levels of refinement is used.

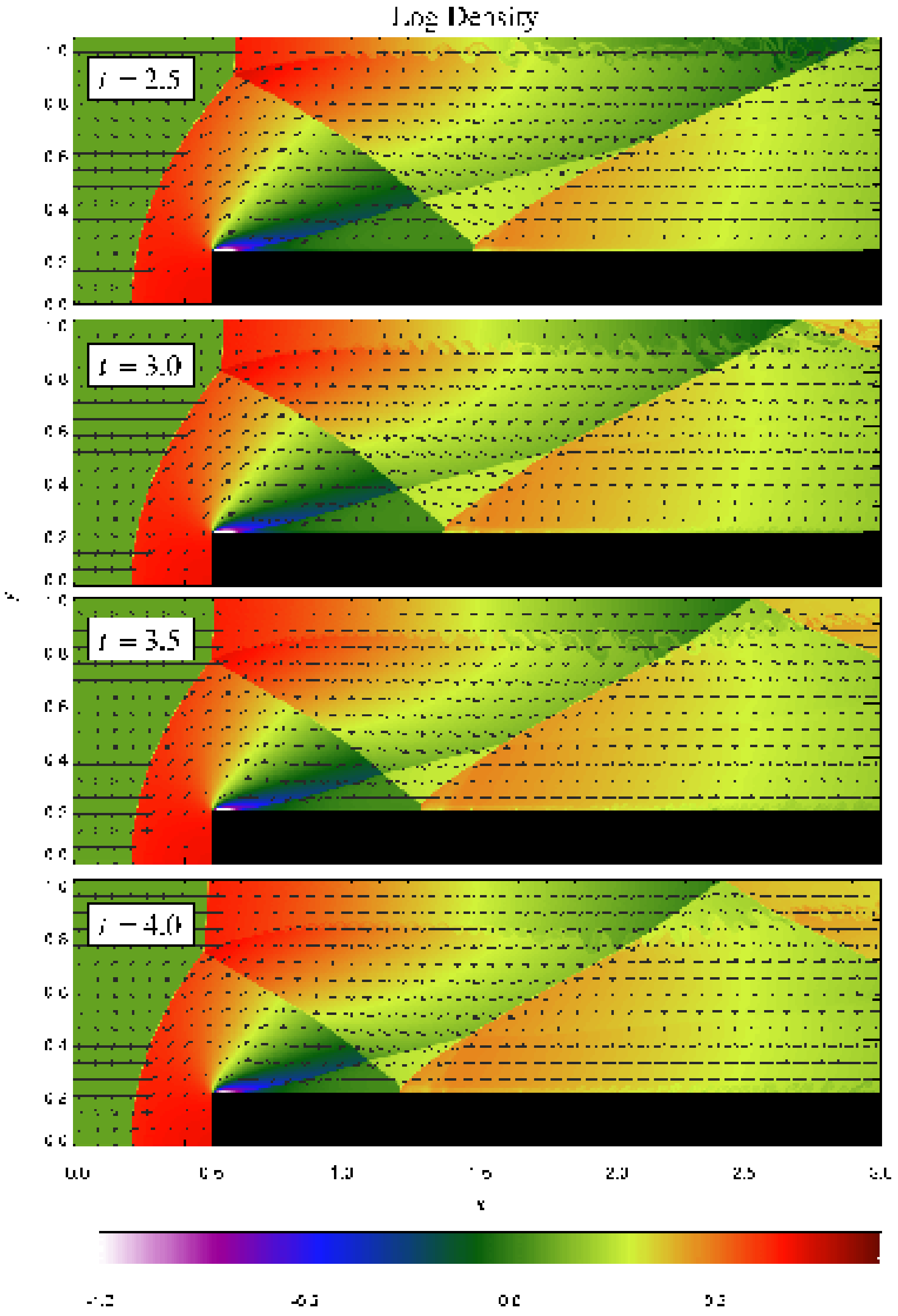

Figure 30.19: Density and velocity in the Emery wind tunnel test problem (continued).

Table 30.6: Runtime parameters used with the `WindTunnel` test problem.

Variable	Type	Default	Description
`sim_pAmbient`	real	1	Ambient pressure (p_0)
`sim_rhoAmbient`	real	1.4	Ambient density (ρ_0)
`sim_windVel`	real	3	Inflow velocity (u_0)

and specific kinetic energy through the rarefaction. However, we are less interested here in reproducing the exact solution than in verifying the code and examining the behavior of such numerical effects as resolution is increased, so we do not apply this additional boundary condition. The errors near the corner result in a slight over-expansion of the gas there and a weak oblique shock where this gas flows back toward the step. At all resolutions we also see interactions between the numerical boundary layer and the reflected shocks that appear later in the calculation.

The shock reaches the top wall at $t \approx 0.65$. The point of reflection begins at $x \approx 1.45$ and then moves to the left, reaching $x \approx 0.95$ at $t = 1$. As it moves, the angle between the incident shock and the wall increases until $t = 1.5$, at which point it exceeds the maximum angle for regular reflection (40° for $\gamma = 1.4$) and begins to form a Mach stem. Meanwhile the reflected shock has itself reflected from the top of the step, and here too the point of intersection moves leftward, reaching $x \approx 1.65$ by $t = 2$. The second reflection propagates back toward the top of the grid, reaching it at $t = 2.5$ and forming a third reflection. By this time in low-resolution runs, we see a second Mach stem forming at the shock reflection from the top of the step; this results from the interaction of the shock with the numerical boundary layer, which causes the angle of incidence to increase faster than in the converged solution. Figure 30.20 compares the density field at $t = 4$ as computed by FLASH using several different maximum levels of refinement. Note that the size of the artificial Mach reflection diminishes as resolution improves.

The shear cell behind the first ("real") Mach stem produces another interesting numerical effect, visible at $t \geq 3$ — Kelvin-Helmholtz amplification of numerical errors generated at the shock intersection. The waves thus generated propagate downstream and are refracted by the second and third reflected shocks. This effect is also seen in the calculations of Woodward and Colella, although their resolution was too low to capture the detailed eddy structure we see. Figure 30.21 shows the detail of this structure at $t = 3$ on grids with several different levels of refinement. The effect does not disappear with increasing resolution, for three reasons. First, the instability amplifies numerical errors generated at the shock intersection, no matter how small. Second, PPM captures the slowly moving, nearly vertical Mach stem with only 1–2 cells on any grid, so as it moves from one column of cells to the next, artificial kinks form near the intersection, providing the seed perturbation for the instability. Third, the effect of numerical viscosity, which can diffuse away instabilities on course grids, is greatly reduced at high resolution. This effect can be reduced by using a small amount of extra dissipation to smear out the shock, as discussed by Colella and Woodward (1984). This tendency of physical instabilities to amplify numerical noise vividly demonstrates the need to exercise caution when interpreting features in supposedly converged calculations.

Finally, we note that in high-resolution runs with FLASH, we also see some Kelvin-Helmholtz roll up at the numerical boundary layer along the top of the step. This is not present in Woodward and Colella's calculation, presumably because their grid resolution was lower (corresponding to two levels of refinement for us) and because of their special treatment of the singular point.

30.1.8 The Shu-Osher problem

The Shu-Osher problem (Shu and Osher, 1989) tests a shock-capturing scheme's ability to resolve small-scale flow features. It gives a good indication of the numerical (artificial) viscosity of a method. Since it is designed to test shock-capturing schemes, the equations of interest are the one-dimensional Euler equations for a single-species perfect gas.

In this problem, a (nominally) Mach 3 shock wave propagates into a sinusoidal density field. As the shock advances, two sets of density features appear behind the shock. One set has the same spatial frequency as the unshocked perturbations, but for the second set, the frequency is doubled. Furthermore, the second set

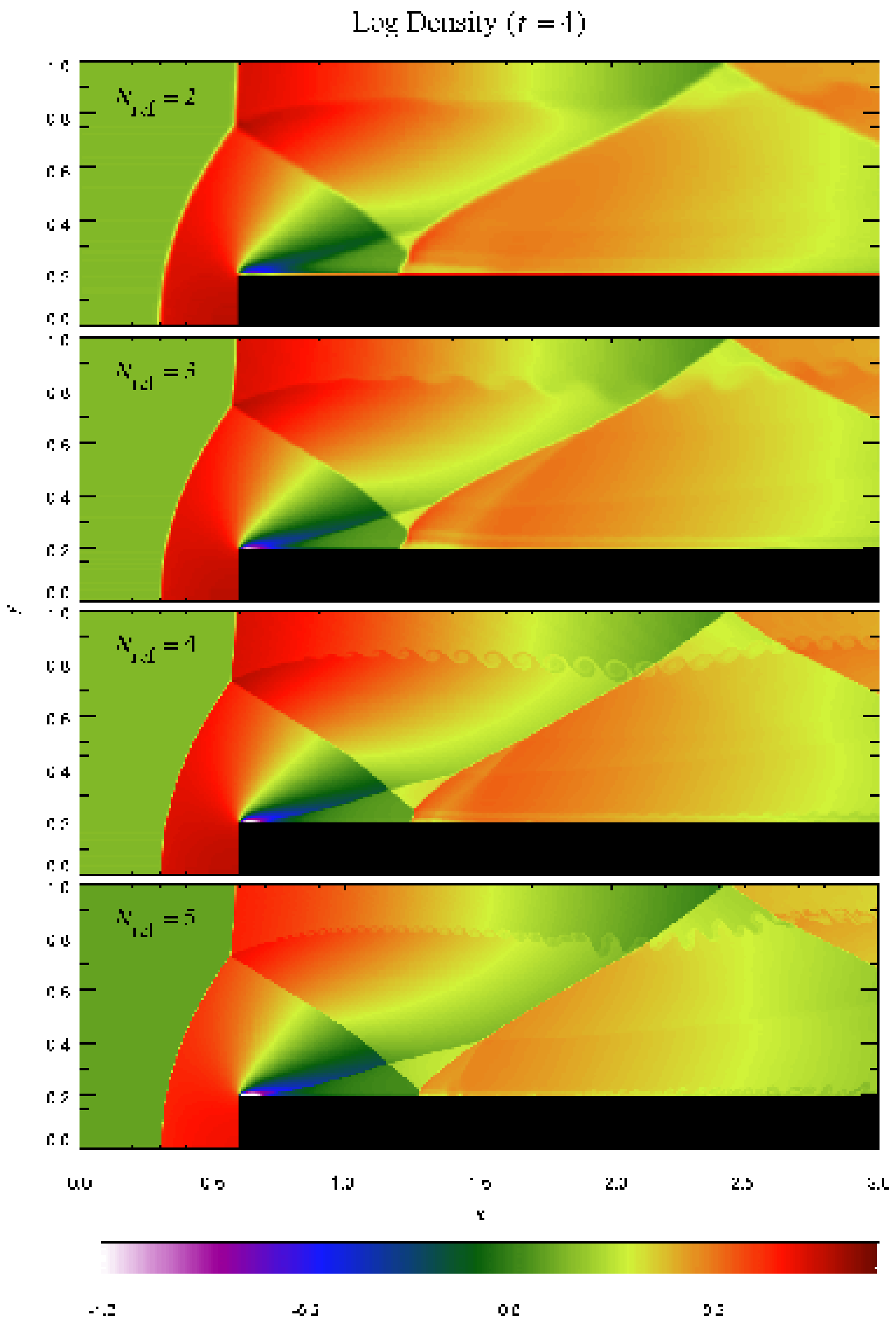

Figure 30.20: Density at t = 4 in the Emery wind tunnel test problem, as computed with FLASH using several different levels of refinement.

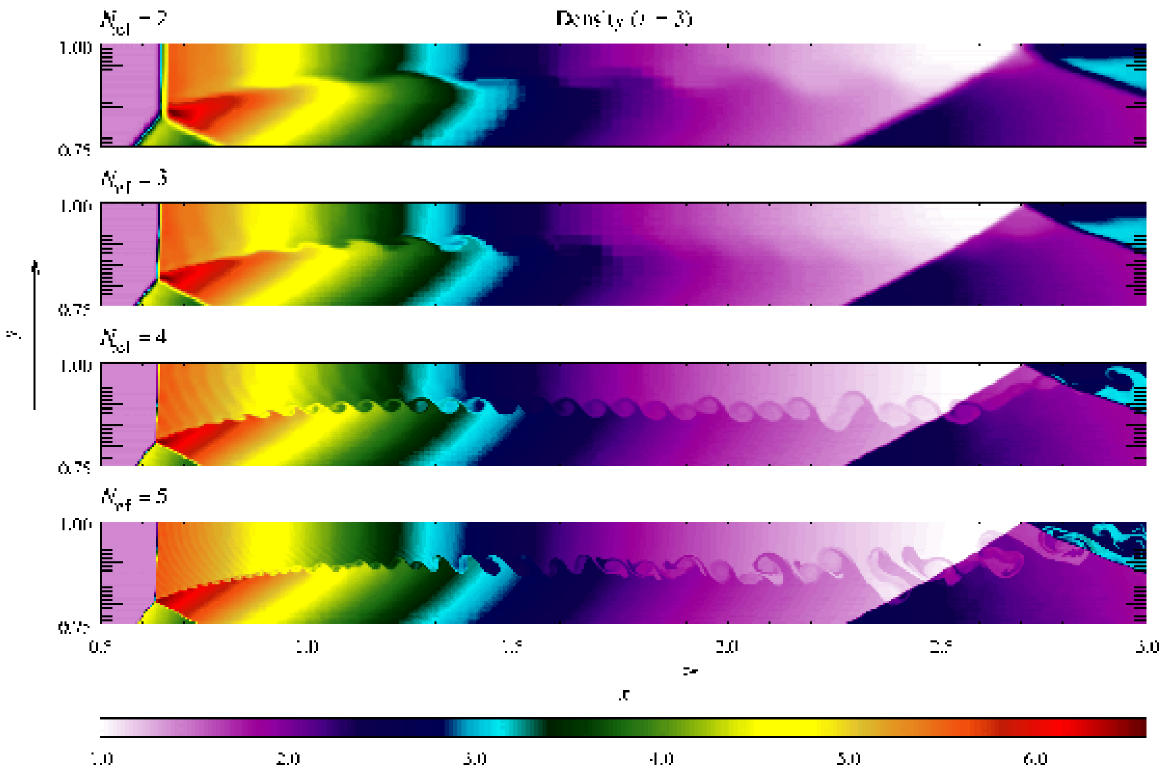

Figure 30.21: Detail of the Kelvin-Helmholtz instability seen at $t = 3$ in the Emery wind tunnel test problem for several different levels of refinement.

follows more closely behind the shock. None of these features is spurious. The test of the numerical method is to accurately resolve the dynamics and strengths of the oscillations behind the shock.

The `shu_osher` problem is initialized as follows. On the domain $-4.5 \le x \le 4.5$, the shock is at $x = x_s$ at $t = 0.0$. On either side of the shock,

$$\begin{array}{ccc} & x \le x_s & x > x_s \\ \rho(x) & \rho_L & \rho_R\,(1.0 + a_\rho \sin(f_\rho x)) \\ p(x) & p_L & p_R \\ u(x) & u_L & u_R \end{array} \tag{30.14}$$

where a_ρ is the amplitude and f_ρ is the frequency of the density perturbations. The `gamma` equation of state alternative implementation is used with `gamma` set to 1.4. The runtime parameters and their default values are listed in Table 30.7. The initial density, x-velocity, and pressure distributions are shown in Figure 30.22.

Table 30.7: Runtime parameters used with the `shu_osher` test problem.

Variable	Type	Default	Description
`posn`	real	-4.0	Initial shock location (x_s)
`rho_left`	real	3.857143	Initial density to the left of the shock (ρ_L)
`rho_right`	real	1.0	Nominal initial density to the right (ρ_R)
`p_left`	real	10.33333	Initial pressure to the left (p_L)
`p_right`	real	1.0	Initial pressure to the right (p_R)
`u_left`	real	2.629369	Initial velocity to the left (u_L)
`u_right`	real	0.0	Initial velocity to the right (u_R)
`a_rho`	real	0.2	Amplitude of the density perturbations

`f_rho`	real	5.0	Frequency of the density perturbations

The problem is strictly one-dimensional; building 2-d or 3-d executables should give the same results along each x-direction grid line. For this problem, special boundary conditions are applied. The initial conditions should not change at the boundaries; if they do, errors at the boundaries can contaminate the results. To avoid this possibility, a boundary condition subroutine was written to set the boundary values to their initial values.

The purpose of the tests is to determine how much resolution, in terms of mesh cells per feature, a particular method requires to accurately represent small scale flow features. Therefore, all computations are carried out on equispaced meshes *without* adaptive refinement. Solutions are obtained at $t = 1.8$. The reference solution, using 3200 mesh cells, is shown in Figure 30.23. This solution was computed using PPM at a CFL number of 0.8. Note the shock located at $x \simeq 2.4$, and the high frequency density oscillations just to the left of the shock. When the grid resolution is insufficient, shock-capturing schemes underpredict the amplitude of these oscillations and may distort their shape.

Figure 30.24 shows the density field for the same scheme at 400 mesh cells and at 200 mesh cells. With 400 cells, the amplitudes are only slightly reduced compared to the reference solution; however, the shapes of the oscillations have been distorted. The slopes are steeper and the peaks and troughs are broader, which is the result of overcompression from the contact-steepening part of the PPM algorithm. For the solution on 200 mesh cells, the amplitudes of the high-frequency oscillations are significantly underpredicted.

30.1.9 Driven Turbulence `StirTurb`

The driven turbulence problem `StirTurb` simulates homogeneous, isotropic and weakly-compressible turbulence. Because theories of turbulence generally assume a steady state, and because turbulence is inherently a dissipative phenomenon, the fluid must be driven to sustain a steady-state. This driving must be done carefully in order to avoid introducing artifacts into the turbulent flow. We use a relatively sophisticated stochastic driving method originally introduced by Eswaran & Pope (1988). The initial conditions sets up a homogeneous background. The resolution used for this test run was 32^3, and the boundary conditions were periodic. The Table 30.8 shows values the runtime parameters values to control the amount of driving, and the Figures Figure 30.25 and Figure 30.26 show the density and x velocity profile of an xy plane in the center of the domain.

30.1.10 Relativistic Sod Shock-Tube

The relativistic version of the shock tube problem (`RHD_Sod`) is a simple one-dimensional setup that involves the decay of an initially discontinuous two fluids into three elementary wave structures: a shock, a contact, and a rarefaction wave. As in Newtonian hydrodynamics case, this type of problem is useful in addressing the ability of the Riemann solver to check the code correctness in evolving such simple elementary waves.

We construct the initial conditions for the relativistic shock tube problem as found in Martí & Müller (2003). We use an ideal equation of state with $\Gamma = 5/3$ for this problem and the left and right states are

Table 30.8: Runtime parameters used with the `Driven Turbulence` test problem.

Variable	Type	Value	Description
`st_stirmax`	real	25.1327	maximum stirring wavenumber
`st_stirmin`	real	6.2832	minimum stirring wavenumber
`st_energy`	real	5.E-6	energy input per mode
`st_decay`	real	0.5	correlation time for driving
`st_freq`	integer	1	frequency of stirring

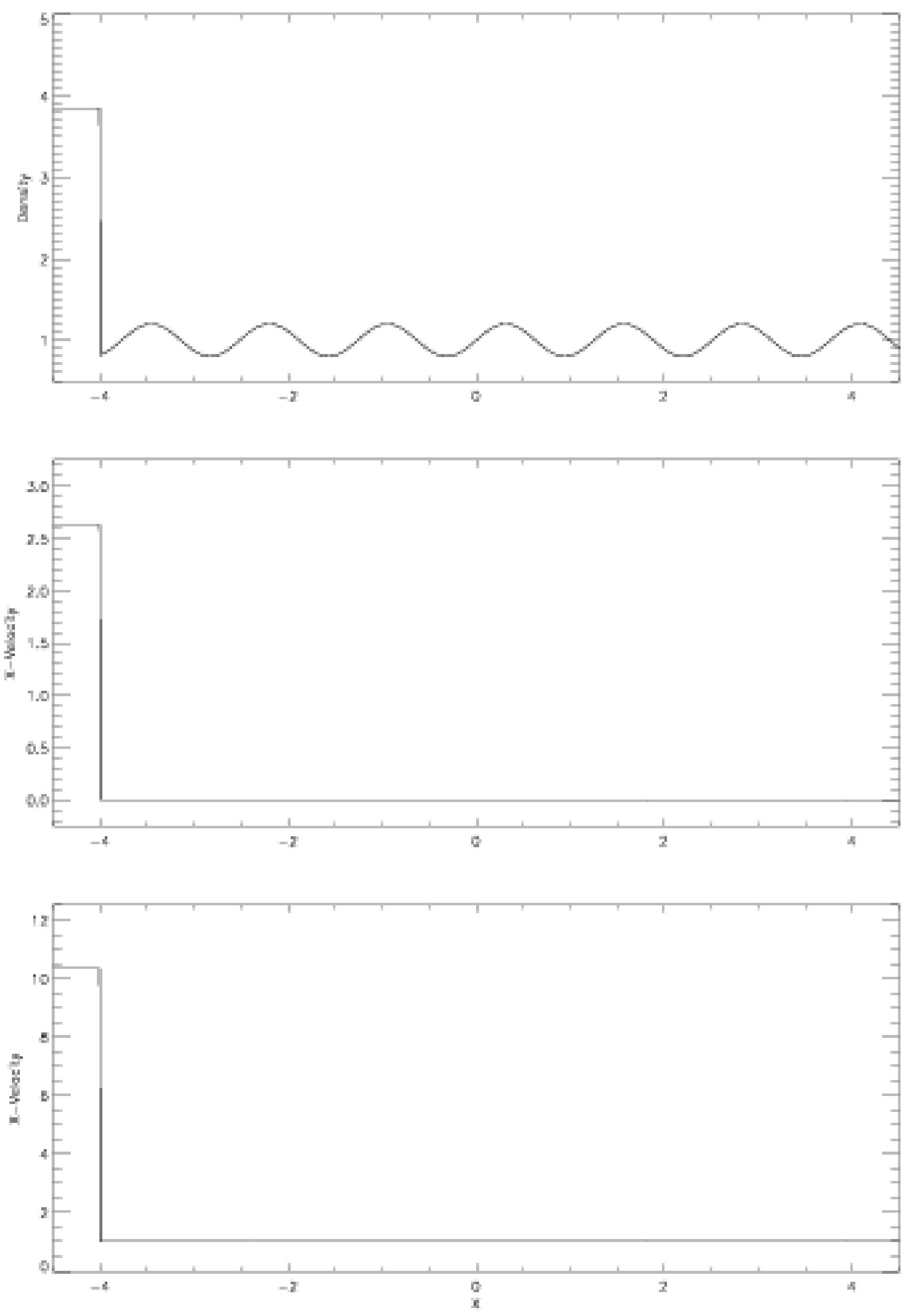

Figure 30.22: Initial density, x-velocity, and pressure for the Shu-Osher problem.

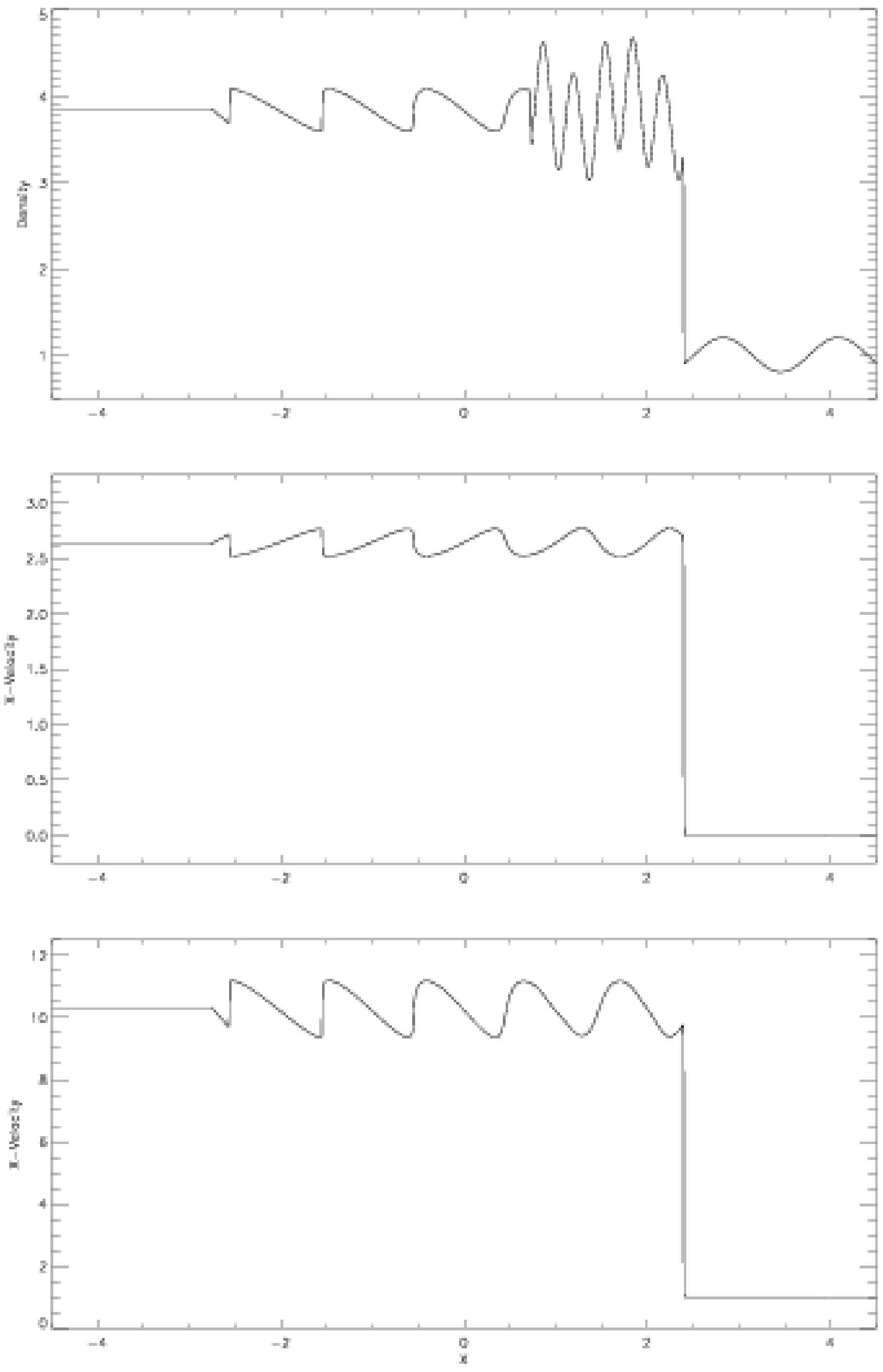

Figure 30.23: Density, x-velocity, and pressure for the reference solution at $t = 1.8$.

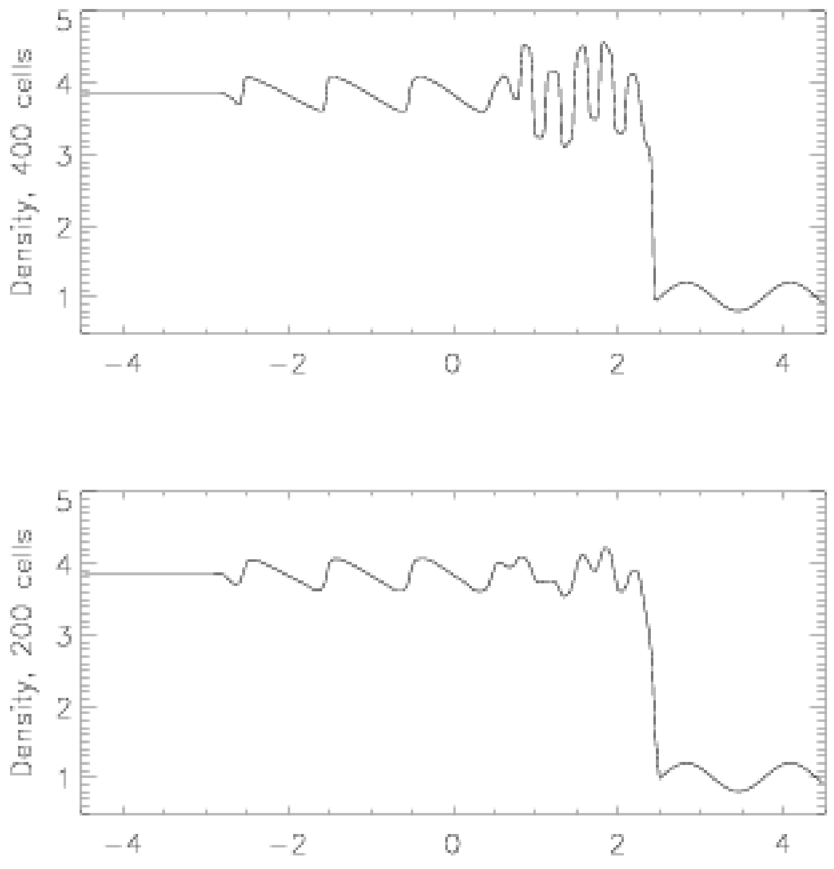

Figure 30.24: Density fields on 400 and 200 mesh cells from the PPM scheme.

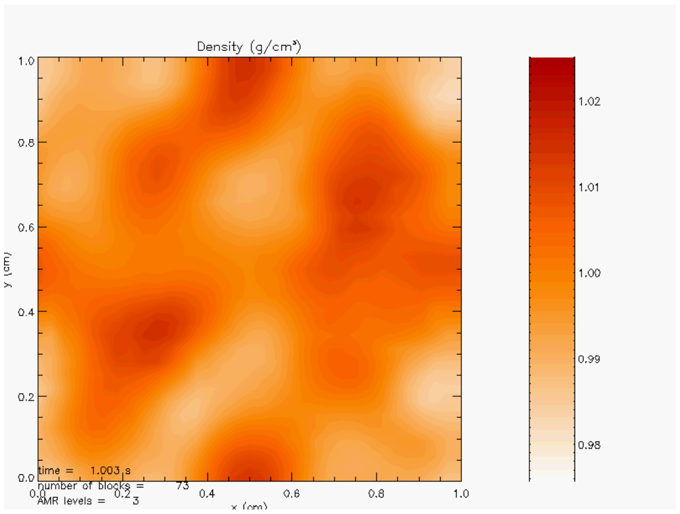

Figure 30.25: Density profile for the `StirTurb` driven turbulence problem.

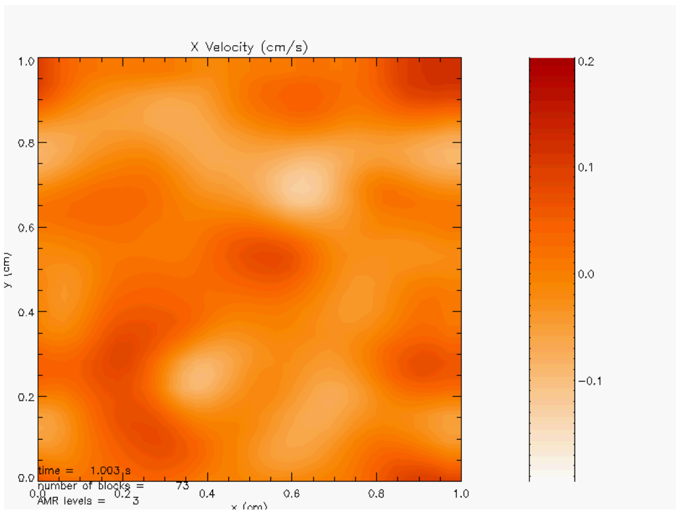

Figure 30.26: velocity along X dimension for the `StirTurb` driven turbulence problem.

given:

$$\begin{aligned} \rho_{\rm L} &= 10 & \rho_{\rm R} &= 1.0 \\ p_{\rm L} &= 40/3 & p_{\rm R} &= 2/3 \times 10^{-6} \end{aligned} \quad (30.15)$$

and the computational domain is $0 \leq x \leq 1$. The initial shock location is at $x = 0.5$ (halfway across a box with unit dimensions).

In FLASH, the RHD Sod problem (`RHD_Sod`) uses the runtime parameters listed in Table 30.9:

Table 30.9: Runtime parameters used with the `RHD_Sod` test problem.

Variable	Type	Default	Description
`sim_rhoLeft`	real	10	Initial density to the left of the interface ($\rho_{\rm L}$)
`sim_rhoRight`	real	1.0	Initial density to the right ($\rho_{\rm R}$)
`sim_pLeft`	real	40/3	Initial pressure to the left ($p_{\rm L}$)
`sim_pRight`	real	$2/3 \times 10^{-6}$	Initial pressure to the right ($p_{\rm R}$)
`sim_uLeft`	real	0	Initial velocity (perpendicular to interface) to the left ($u_{\rm L}$)
`sim_uRight`	real	0	Initial velocity (perpendicular to interface) to the right ($u_{\rm R}$)
`sim_xangle`	real	0	Angle made by interface normal with the x-axis (degrees)
`sim_yangle`	real	90	Angle made by interface normal with the y-axis (degrees)
`sim_posn`	real	0.5	Point of intersection between the interface plane and the x-axis

Figure 30.27, Figure 30.28, and Figure 30.29 show the results of running the RHD Sod problem on a one-dimensional uniform grid of size 400 at simulation time $t = 0.36$. In this run the left-going wave is the rarefaction wave, while two right-going waves are the contact discontinuity and the shock wave. This configuration results in mildly relativistic effects that are mainly thermodynamical in nature.

The differences in the relativistic regime, as compared to Newtonian hydrodynamics, can be seen in a curved velocity profile for the rarefaction wave and the narrow constant state (density shell) in between

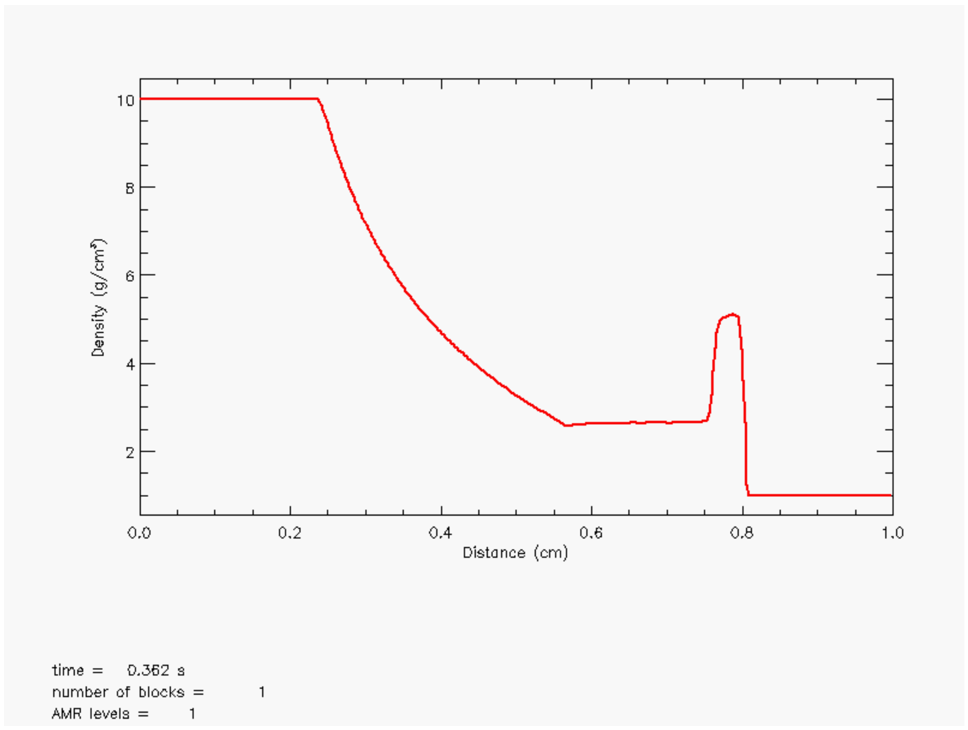

Figure 30.27: Density of numerical solution to the relativistic Sod problem at time $t = 0.36$.

the shock wave and contact discontinuity. Numerically, it is particularly challenging to resolve the thin narrow density plateau, which is bounded by a leading shock front and a trailing contact discontinuity (see Figure 30.27).

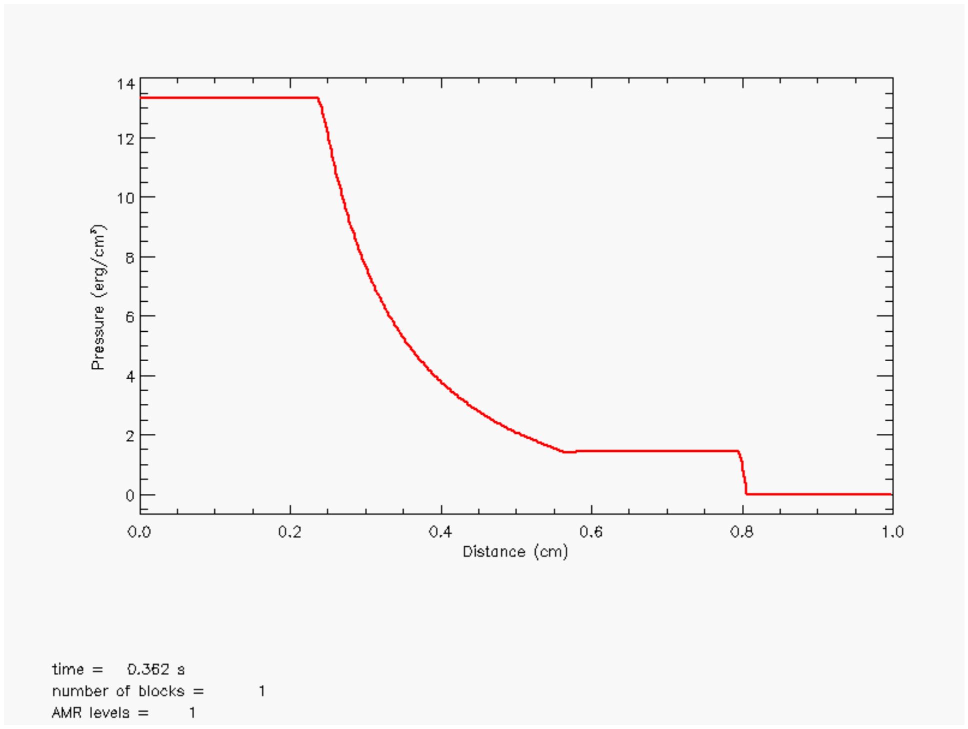

Figure 30.28: Pressure of numerical solution to the relativistic Sod problem at time $t = 0.36$.

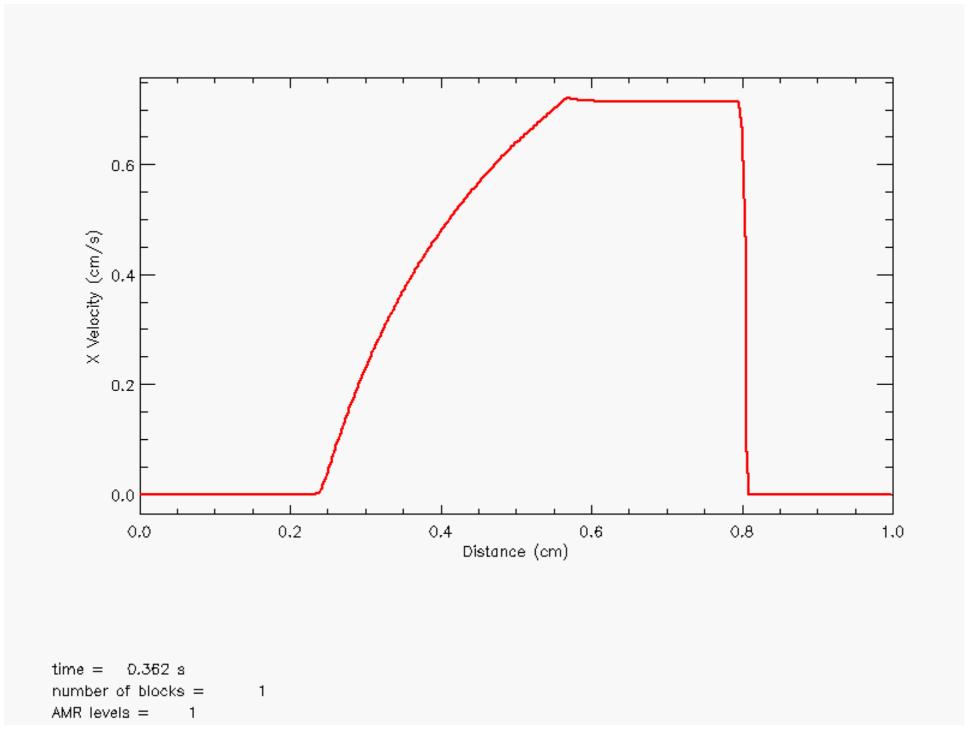

Figure 30.29: Normal velocity of numerical solution to the relativistic Sod problem at time $t = 0.36$.

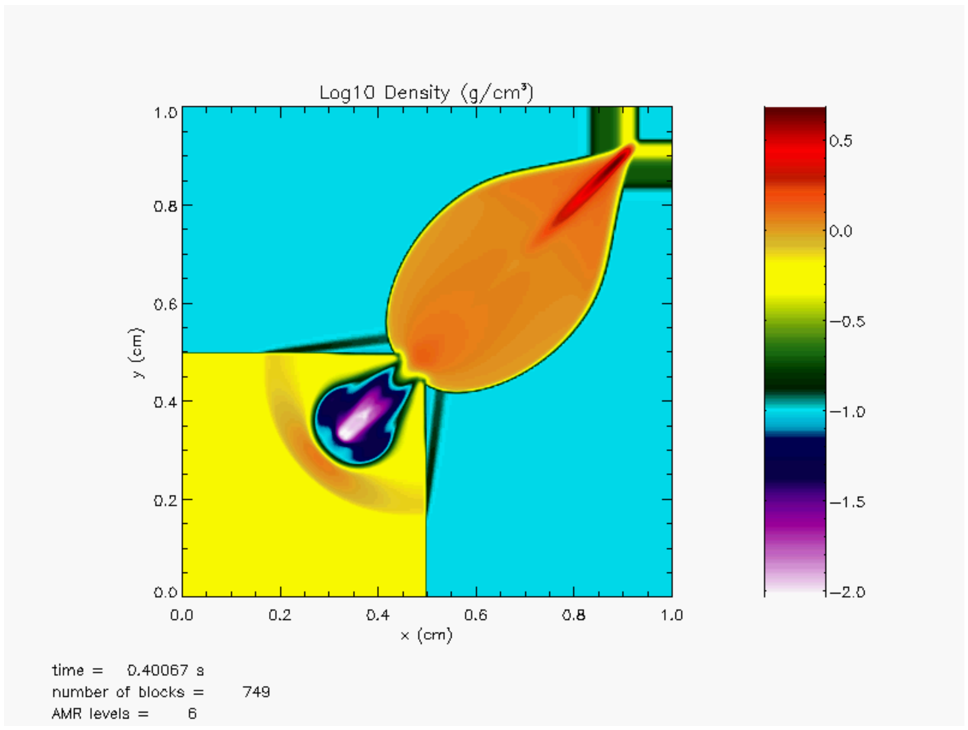

Figure 30.30: Log of density of numerical solution to the relativistic 2D Riemann problem at time $t = 0.8$. The solution was resolved on AMR grid with 6 levels of refinements

30.1.11 Relativistic Two-dimensional Riemann

The two-dimensional Riemann problem (`RHD_Riemann2D`), originally proposed by Schulz et al. (1993), involves studying interactions of four basic waves that consist of shocks, rarefactions, and contact discontinuities. The initial condition provided here is based on Migone et al. (2005) producing these elementary waves at every interface. The setup of the problem is given on a rectangular domain of size $[-1, 1] \times [-1, 1]$, which is divided into four constant state subregions as:

$$(\rho, p, v_x, v_y) = \begin{cases} (0.5, 1.0, 0.0, 0.0) & -1.0 \le x < 0.0, \quad -1.0 \le y < 0.0 \\ (0.1, 1.0, 0.0, 0.99) & 0.0 \le x \le 1.0, \quad -1.0 \le y < 0.0 \\ (0.1, 1.0, 0.99, 0.0) & -1.0 \le x < 0.0, \quad 0.0 \le y \le 1.0 \\ (\rho_1, p_1, 0.0, 0.0) & 0.0 \le x \le 1.0, \quad 0.0 \le y \le 1.0 \end{cases}, \tag{30.16}$$

where $\rho_1 = 5.477875 \times 10^{-3}$ and $p_1 = 2.762987 \times 10^{-3}$. An ideal EOS is used with the specific heat ratio $\Gamma = 5/3$.

The solution obtained at $t = 0.8$ in Figure 30.30 shows that the symmetry of the problem is well maintained. The two shocks are propagated from the upper left and the lower right regions to the upper right region, yielding continuous collisions of shocks at the upper right corner.The curved shock fronts are transmitted and formed in the diagonal region of the domain. The lower left region is bounded by contact discontinuities. By the time $t = 0.8$ most of regions are filled with shocked gas, whereas there are still two unperturbed regions in the lower left and upper right regions.

30.1.12 Flow Interactions with Stationary Rigid Body

The stationary rigid body is only implemented and tested in the unsplit hydro solver Section 14.1.3. It is possible that the unsplit staggered mesh MHD solver Section 14.3.3 can support the rigid body but we have not tested yet.

30.1.12.1 NACA Airfoil

Flow simulations over a series of NACA airfoils (or a simple flat plate) can be obtained using the implementation of a stationary rigid body in the unsplit hydro solver described in Section 14.1.3.1. In this example, the cambered NACA2412 airfoil is initialized with positive unity values indicating the part of the domain that belongs to a stationary rigid body. The rest of the domain is assigned negative unity values to indicate it as a flow region for the unsplit hydro solver. At the surface of the rigid body, a reflecting boundary condition is applied in order to represent the fact that there is no flow penetrating the rigid object.

Plots in 30.31(a) – 30.33(b) illusrate Mach number and pressure plots over the airfoil with the three different initial Mach numbers, 0.65, 0.95 and 1.2 at $t = 1.8$. By this time, the flow conditions have reached their steady states. For Mach number = 0.65, the critical Mach number has not yet been obtained and the flow over the airfoil is all subsonic as shown in 30.31(a). Since the airfoil is asymmetric and cambered, we see there are pressure gradients across the top and bottom surfaces even at zero angle of attack in 30.31(b). These pressure gradients (higher pressure at the bottom than the top) generate a lift force by which an airplane can fly defying gravity.

At Mach number reaching 0.95 as shown in 30.32(a) there are local points that are supersonic. This indicates that the critical Mach number for the airfoil is between 0.65 and 0.95. In fact, one can show that the critical Mach number is around 0.7 for the NACA2412 airfoil. We see that there is a development of a bow shock formation in front of the airfoil. A formation of a subsonic region between the bow shock and the nose of the airfoil is visible in the Mach number plot. Inside the bow shock, a sonic line at which the local flow speed becomes the sound speed makes an oval shape together with the bow shock. In both the Mach number and pressure plots, a strong wake forms starting from the top and bottom of the surfaces near the trailing edge. The wake is hardly visible for Mach number 0.65 in 30.31(a) and 30.31(b). Normal shock waves have formed steming from the trailing edge as seen in 30.32(a) and 30.32(b).

At Mach number 1.2 the flow becomes supersonic everywhere. In this case, the shape of the bow shock becomes narrower and there are much larger supersonic pockets developed on the top and bottom surfaces with a smaller subsonic region between the bow shock and the nose region.

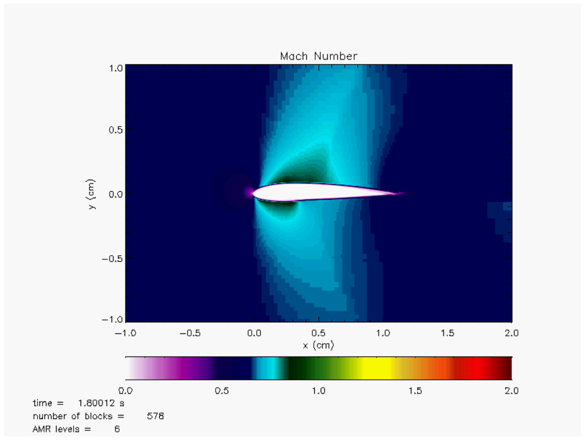

(a) a

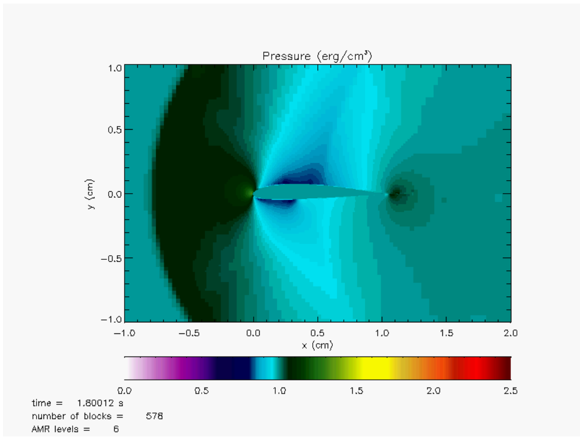

(b) b

Figure 30.31: NACA2412 in Mach number 0.65 flow at 0 degree angle of attack problem at $t = 1.8$ (a) Mach number (b) Pressure

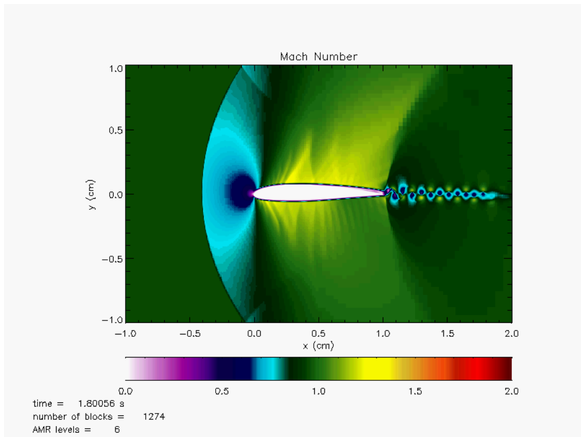

(a) a

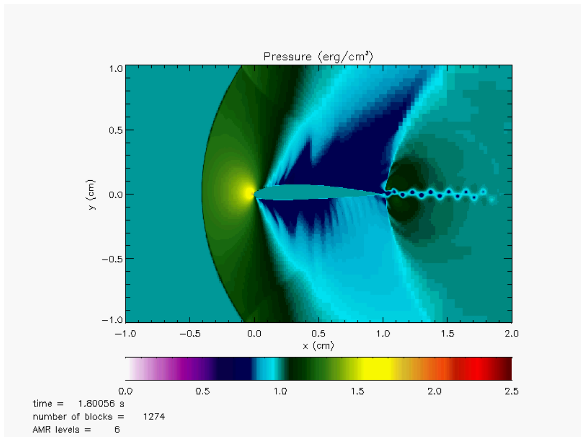

(b) b

Figure 30.32: NACA2412 in Mach number 0.95 flow at 0 degree angle of attack problem at $t = 1.8$ (a) Mach number (b) Pressure

30.1.12.2 Solid Objects in Sedov Explosion

Another problem for testing a stationary rigid body in a simulation is to consider the Sedov-like explosion in a chamber surrounded by a solid wall with holes The wall is shown as red blocks with white boundry in 30.34(a) and 30.34(b). The simulation was done on a uniform Cartesian grid with 300 cells on each direction. Three holes in the wall subdivide it into four different stationary solid bodies in a square computational domain $[0, 1.5] \times [0, 1.5]$. The explosion goes off at the origin and generate shock waves inside the chamber. In later time, when the shock waves pass though the three holes in the wall, turbulence effects are triggered from the interaction between the fluid and the wall and enhance vortical fluid motions.

One important thing in this problem is to keep the given symmetry throughout the simulation. The flow symmetry across the diagonal direction is well preseved in 30.34(a) and 30.34(b).

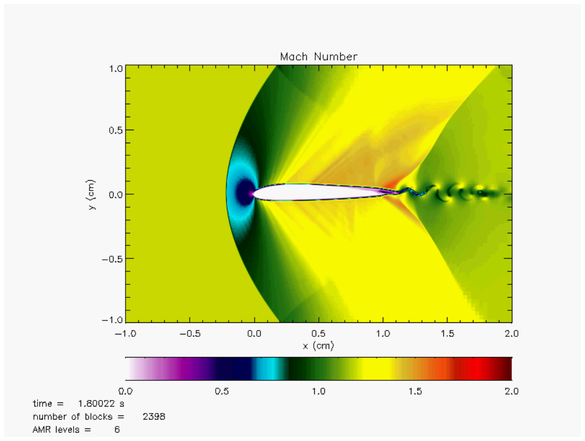

(a) a

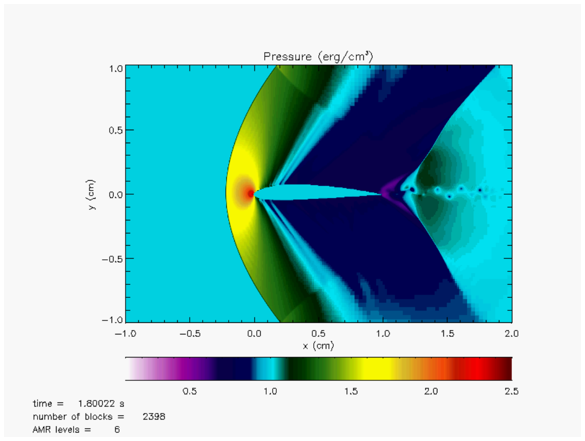

(b) b

Figure 30.33: NACA2412 in Mach number 1.2 flow at 0 degree angle of attack problem at $t = 1.8$ (a) Mach number (b) Pressure

30.2 Magnetohydrodynamics Test Problems

The magnetohydrodynamics (MHD) test problems provided in this release can be found in `source/-Simulation/SimulationMain/magnetoHD/`. In order to set up an MHD problem, users need to specify the `magnetoHD` path in a setup script. For instance, the `BrioWu` problem can be configured by typing `./setup magnetoHD/BrioWu -auto -1d`.

30.2.1 Brio-Wu MHD Shock Tube

The Brio-Wu MHD shock tube problem (Brio and Wu, 1988), `magnetoHD/BrioWu`, is a coplanar magnetohydrodynamic counterpart of the hydrodynamic Sod problem (Section 30.1.1). The initial left and right states are given by $\rho_l = 1$, $u_l = v_l = 0$, $p_l = 1$, $(B_y)_l = 1$; and $\rho_r = 0.125$, $u_r = v_r = 0$, $p_r = 0.1$, $(B_y)_r = -1$. In addition, $B_x = 0.75$ and $\gamma = 2$. This is a good problem to test wave properties of a particular MHD solver, because it involves two fast rarefaction waves, a slow compound wave, a contact discontinuity and a slow shock wave.

The conventional 800 point solution to this problem computed with FLASH is presented in Figure 30.35, Figure 30.36, Figure 30.37, Figure 30.38, and Figure 30.39 . The figures show the distribution of density, normal and tangential velocity components, tangential magnetic field component and pressure at $t = 0.1$ (in non-dimensional units). As can be seen, the code accurately and sharply resolves all waves present in the solution. There is a small undershoot in the solution at $x \approx 0.44$, which results from a discontinuity-enhancing monotonized centered gradient limiting function (LeVeque 1997). This undershoot can be easily removed if a less aggressive limiter, *e.g.* a minmod or a van Leer limiter, is used instead. This, however, will degrade the sharp resolution of other discontinuities.

The directionally splitting `8Wave` MHD solver with a second-order MUSCL-Hancock scheme (setup with `+8wave`) was used for the results shown in this simulation. The `StaggeredMesh` MHD solver (setup with `+usm`) can also be used for this Brio-Wu problem in one- and two-dimensions. However, in the latter case, the `StaggeredMesh` solver only supports non-rotated setups for which a shock normal is parallel to the x-axis that initially intersects that axis at $x = 0.5$ (halfway across a box with unit dimensions). This limitation occurs in the `StaggeredMesh` scheme because the currently released version of the FLASH code does not truly support physically correct boundary conditions for this rotated shock geometry.

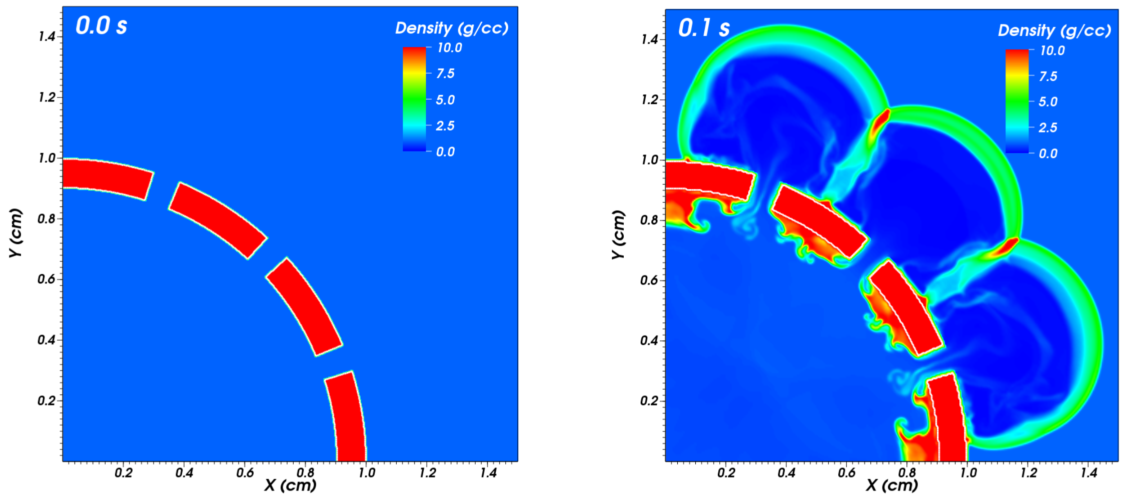

(a) a

(b) b

Figure 30.34: The Sedov explosion in a chamber surrounded by a wall with holes. (a) Density plot at $t = 0.0$ sec. (b) Denstiy plot at $t = 0.1$ sec.

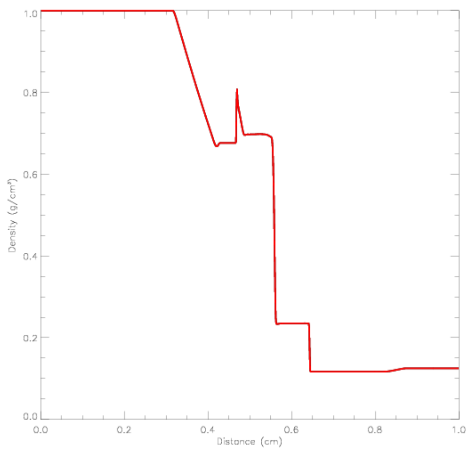

Figure 30.35: Density profile for the Brio-Wu shock tube problem.

30.2.1.1 Slowly moving shocks (SMS) issues in the Brio-Wu problem

Figure 30.40 clearly demonstrates that the conventional PPM reconstruction method fails to preserve monotonicities, shedding oscillations especially in the plateau near strong discontinuities such as the contact and right going slow MHD shock. In Fig. 30.41, Mach numbers are plotted with varying strengths of the transverse field B_y. The oscillations increase with an increase of B_y; the reason being that stronger B_y introduces more transverse effect that resists shock propagation in the x direction causing the shock to move slowly. This effect is clearly seen in the locations of the shock fronts (right going slow MHD shocks in this case), which remain closer to the initial location $x = 0.5$ when B_y is stronger.

Results from using the upwind biased slope limiter for PPM are illustrated in Figures 30.42 – 30.45 . The oscillation shedding found in the conventional PPM (e.g., Fig. 30.40) are significantly reduced in both density, and Mach number profiles. The overall qualitative solution behavior of using the upwind PPM

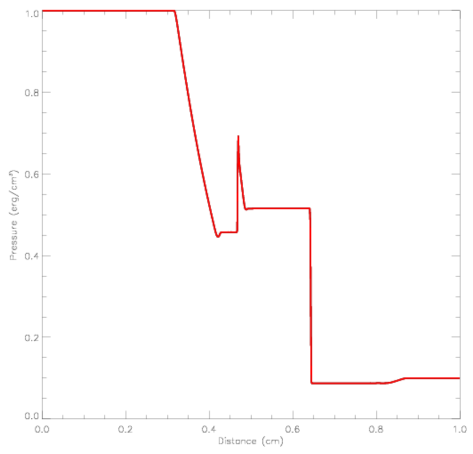

Figure 30.36: Pressure profile for the Brio-Wu shock tube problem.

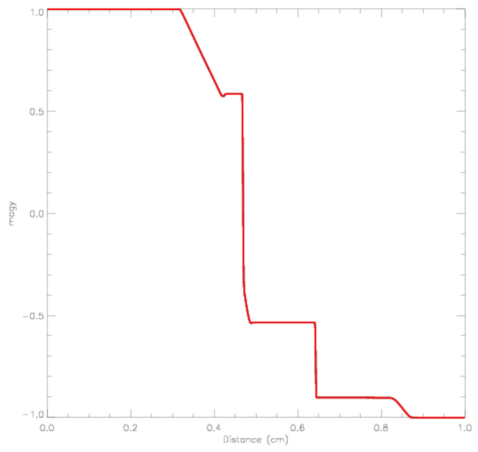

Figure 30.37: Tangential magnetic field profile for the Brio-Wu shock tube problem.

approach, shown in Fig. 30.42, is very much similar to those from the 5th order WENO method as illustrated in Fig. 30.43. As shown in the closeup views in Fig. 30.44 and 30.45, the solutions with the upwind PPM slope limiter (blue curves) outperforms the conventional PPM method (red curves), and compares well with the WENO scheme (green curves). In fact, the upwind approach shows the most flat density plateau of all methods. Note that the SMS issue can be observed regardless of the choice of Riemann solvers and the dissipation mechanism in PPM (e.g., even with flattening on). 400 grid points were used.

30.2.2 Orszag-Tang MHD Vortex

The Orszag-Tang MHD vortex problem (Orszag and Tang, 1979), `magnetoHD/OrszagTang`, is a simple two-dimensional problem that has become a classic test for MHD codes. In this problem a simple, non-random initial condition is imposed at time $t = 0$

$$\mathbf{V} = V_0\left(-\sin(2\pi y), \sin(2\pi x), 0\right), \quad \mathbf{B} = B_0\left(-\sin(2\pi y), \sin(4\pi x), 0\right), \quad (x, y) = \in [0, 1]^2, \tag{30.17}$$

where B_0 is chosen so that the ratio of the gas pressure to the RMS magnetic pressure is equal to 2γ. In this setup the initial density, the speed of sound and V_0 are set to unity; therefore, the initial pressure $p_0 = 1/\gamma$

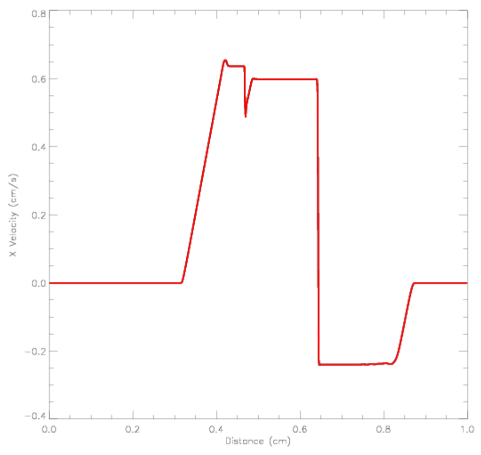

Figure 30.38: Normal velocity profile for the Brio-Wu shock tube problem.

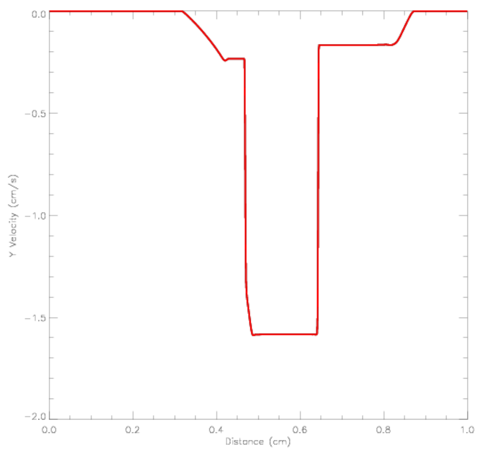

Figure 30.39: Tangential velocity profile for the Brio-Wu shock tube problem.

and $B_0 = 1/\gamma$.

As the evolution time increases, the vortex flow pattern becomes increasingly complicated due to the nonlinear interactions of waves. A highly resolved simulation of this problem should produce two-dimensional MHD turbulence. Figure 30.46 and Figure 30.47 shows density and magnetic field contours at $t = 0.5$. As one can observe, the flow pattern at this time is already quite complicated. A number of strong waves have formed and passed through each other, creating turbulent flow features at all spatial scales.

The results were obtained using the directionally splitting `8Wave` MHD solver for this Orszag-Tang problem.

The 3D version are also shown in the below solved using the unsplit staggered mesh MHD solver.

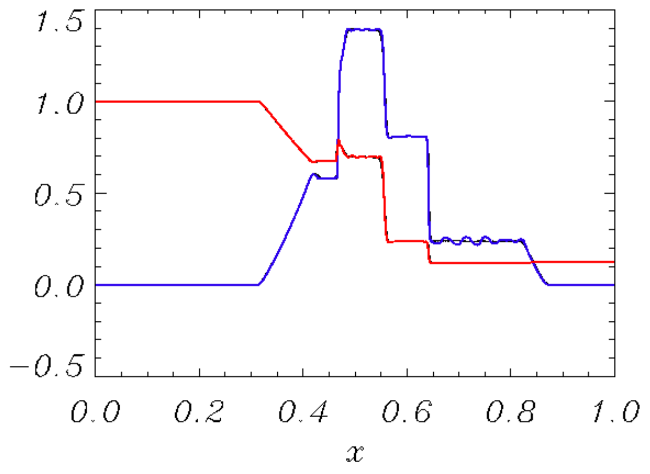

Figure 30.40: Density (thick red) and Mach number (thick blue) at $t = 0.1$ of the Brio-Wu test with the conventional PPM's MC limiter. Thin black curves represent reference solutions using the PLM of MUSCL-Hancock scheme. Severe numerical oscillations are evident in the solution using the conventional PPM reconstruction on 400 grid points.

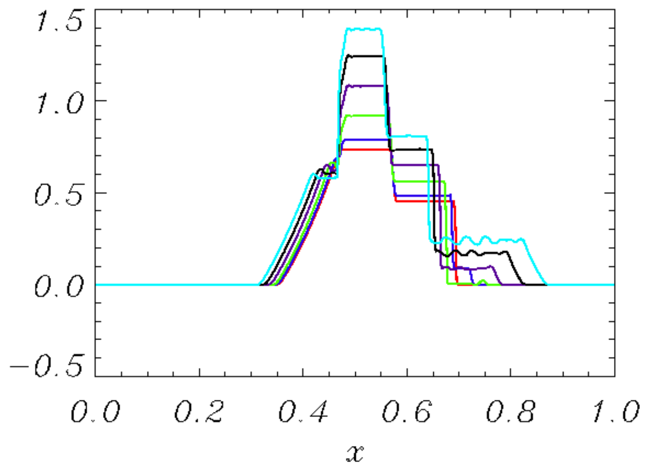

Figure 30.41: Mach numbers at $t = 0.1$ with varying B_y from 0 to 1 with the conventional PPM's MC limiter. Curves in red, blue, green, purple, black, and cyan represent $B_y = 0, 0.2, 0.4, 0.6, 0.8$, and 1, respectively. Severe numerical oscillations are evident in the solution using the conventional PPM reconstruction on 400 grid points.

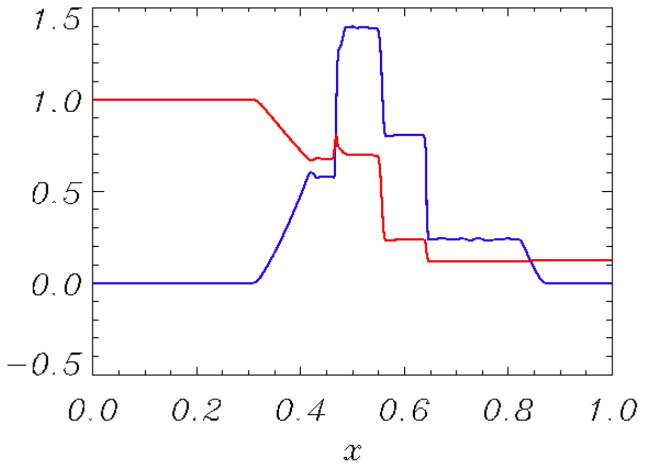

Figure 30.42: Density (red) and Mach number (blue) at $t = 0.1$ of the Brio-Wu test using the upwind biased PPM limiter.

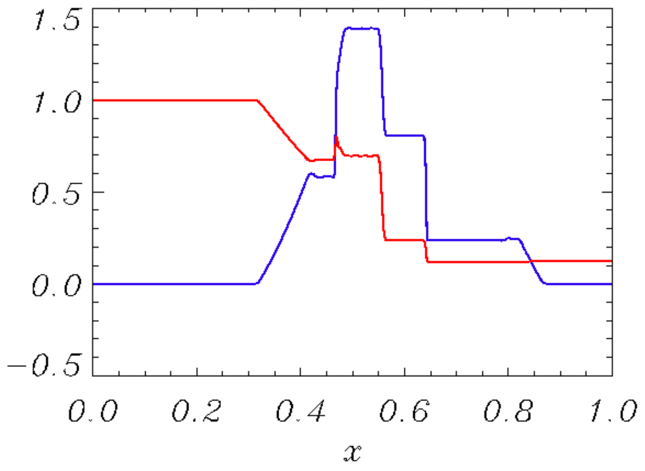

Figure 30.43: Density (red) and Mach number (blue) at $t = 0.1$ of the Brio-Wu test using the 5th order WENO scheme.

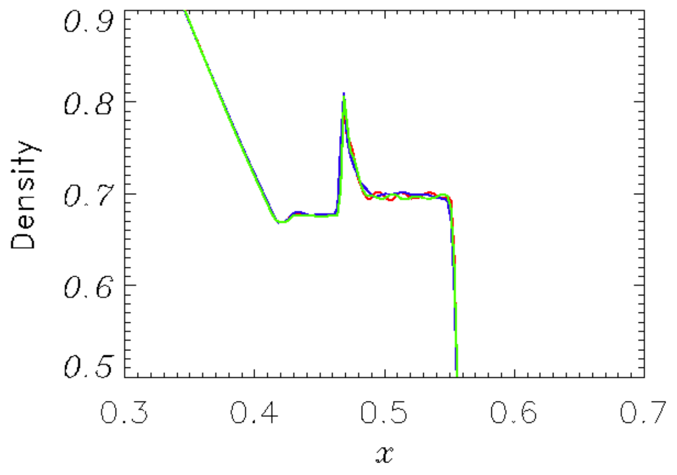

Figure 30.44: Density closeup at $t = 0.1$ of the Brio-Wu test. The conventional PPM in red curve, the upwind PPM in blue curve, and the WENO scheme in green curve.

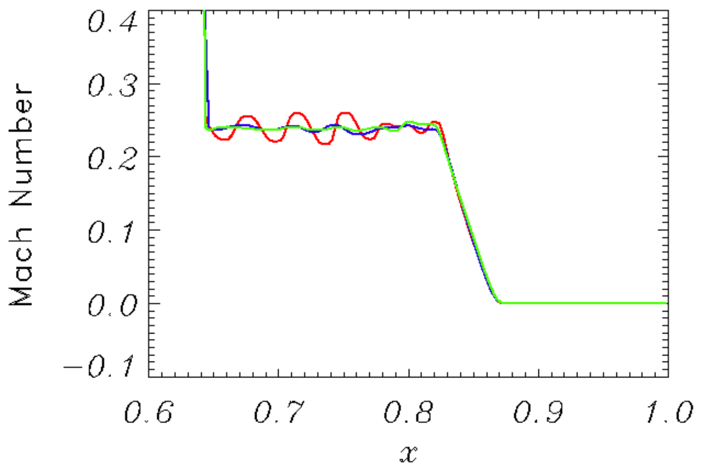

Figure 30.45: Mach number closeup at $t = 0.1$ of the Brio-Wu test. The conventional PPM in red curve, the upwind PPM in blue curve, and the WENO scheme in green curve.

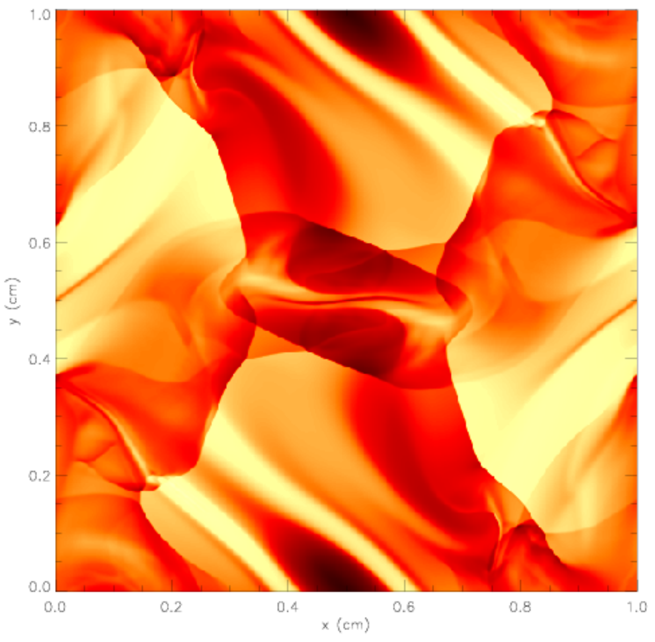

Figure 30.46: Density contours in the Oszag-Tang MHD vortex problem at $t = 0.5$.

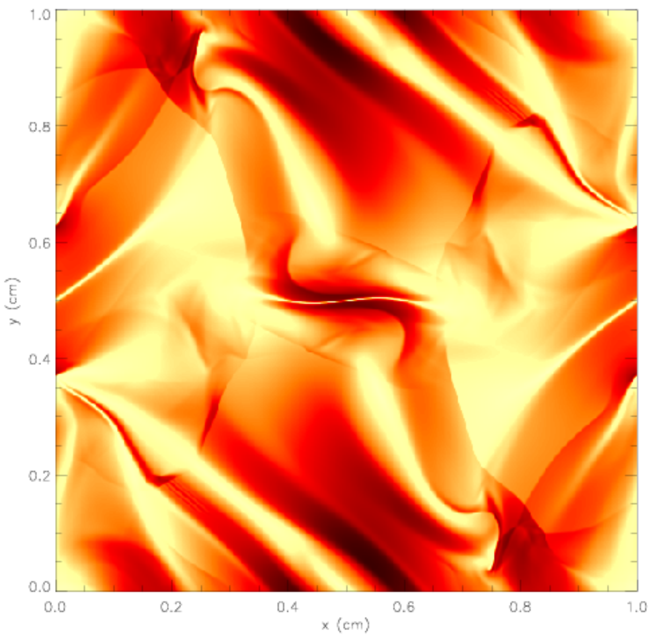

Figure 30.47: Magnetic field contours in the Oszag-Tang MHD vortex problem at $t = 0.5$.

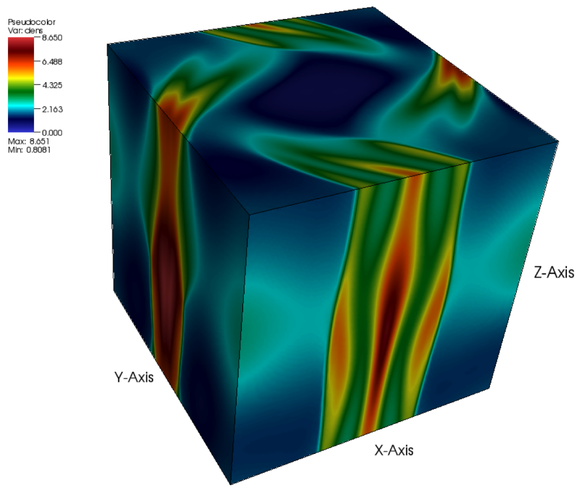

(a) a

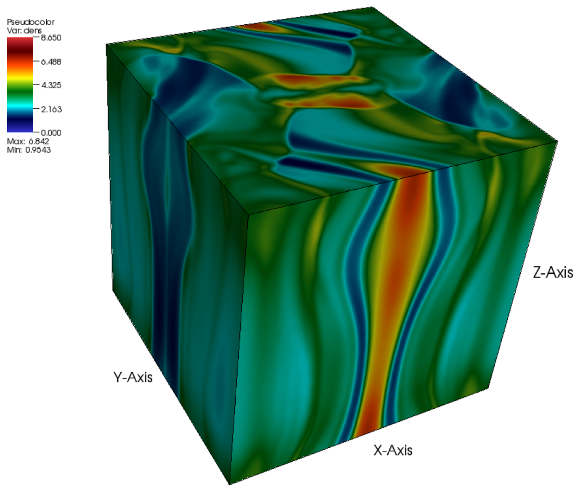

(b) b

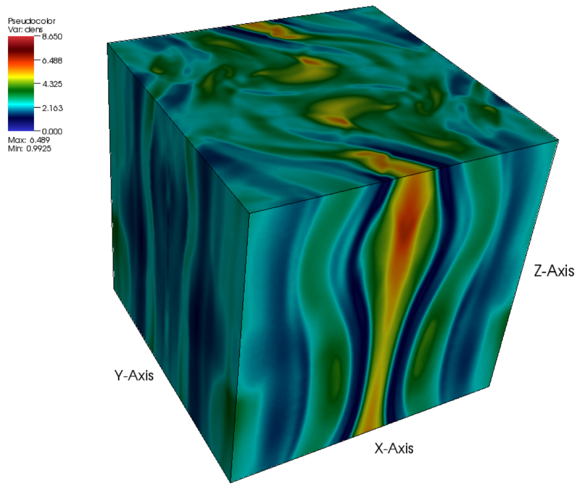

(c) c

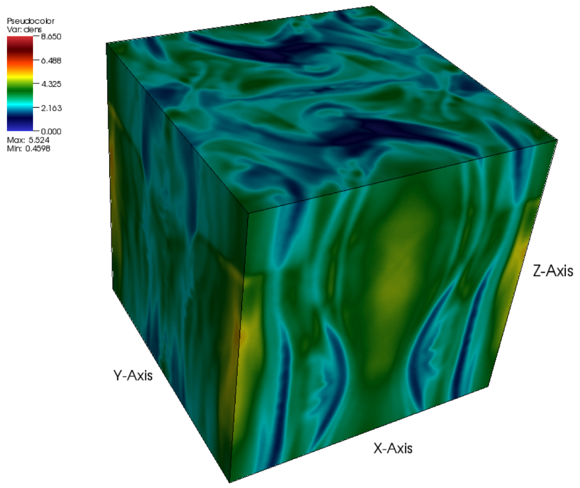

(d) d

Figure 30.48: Density plots of a 3D version of the Orszag-Tang problem on a 128^3 uniform grid resolution. (a) Density at $t = 0.2$ (b) Density at $t = 0.5$ (c) Density at $t = 0.7$ (d) Density at $t = 1.0$.

30.2.3 Magnetized Accretion Torus

The magnetized accretion torus problem is based on the global magneto-rotational instability (MRI) simulations of Hawley (2000). It can be found under `magnetoHD/Torus`. We consider a magnetized torus of constant angular momentum ($\Omega \propto r^{-2}$), inside a normalized Paczyńsky-Wiita pseudo-Newtonean gravitational potential (Paczyńsky&Wiita, 1980) of the form $\Phi = -1/(R-1)$, where $R = \sqrt{r^2+z^2}$.

The cylindrical computational domain, with lengths normalized at r_0, extends from 1.5 r_0 to 15.5 r_0 in the radial direction and from -7 r_0 to 7 r_0 in the z direction. For this specific simulation we use seven levels of refinement, linear reconstruction with vanLeer limiter and the HLLC Riemann solver. The boundary conditions are set to outflow, except for the leftmost side where a diode-like condition is applied.

Assuming an adiabatic equation of state, the initial density profile of the torus is given by

$$\frac{\Gamma P}{(\Gamma-1)\rho} = C - \Phi - \frac{l_K^2}{2r^2}, \tag{30.18}$$

where the specific heats ratio is $\Gamma = 5/3$, l_K is the Keplerian angular momentum at the pressure maximum ($r_{Pmax} = 4.7 r_0$) and C is an integration constant that specifies the outer surface of the torus, given its inner radius ($r_{in} = 3\,r_0$). The initial poloidal magnetic field is computed using the ϕ component of the vector potential, $A_\phi \propto \max(\rho - 5,\, 0)$, and normalized so as the initial minimum value of the plasma $\beta = 2P/\mathbf{B}^2$ is equal to 10^2. The resulting field follows the contours of density, i.e. torus-like nested loops, and is embedded well within the torus.

We allow the system to evolve for $t = 150\,t_0$. The torus is MRI unstable and after approximately one revolution accretion sets in. The strong shear generates an azimuthal field component and the angular momentum is redistributed. Due to the instability, fillamentary structures form at the torus surface that account for its rich morphology (Figure 30.49). These results can be promtly compared to those in Hawley (2000) and Mignone et al. (2007).

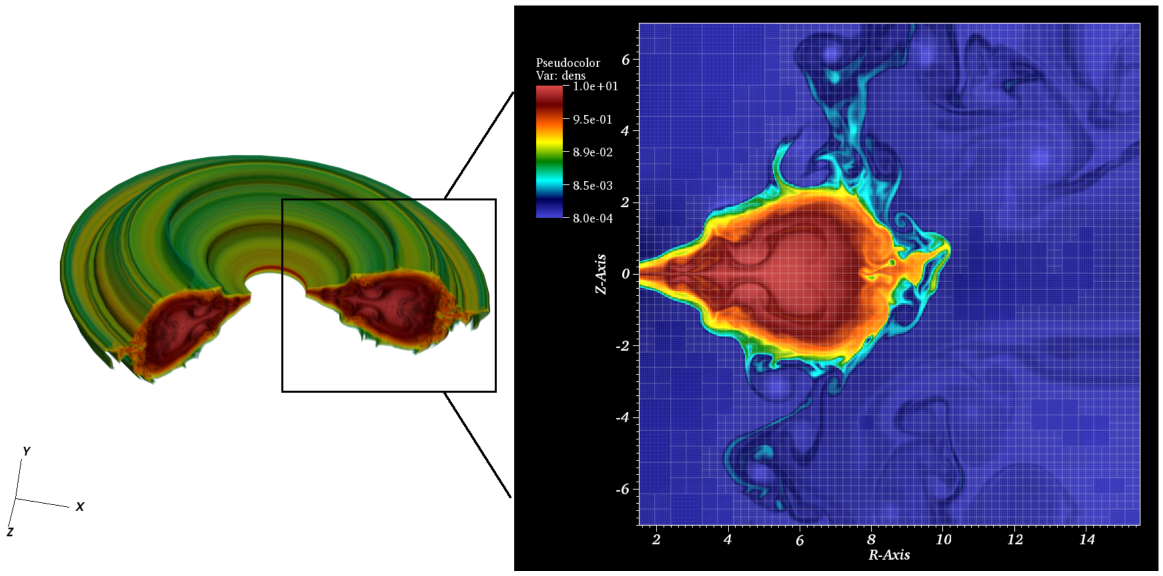

Figure 30.49: Left: 3D rendering of the axisymmetric torus evolution. Right: Density logarithm of the magnetized accretion torus after 150 t_0. Superposed are the AMR levels and the mesh.

30.2.4 Magnetized Noh Z-pinch

In this test we consider the magnetized version of the classical Noh problem (Noh, 1987). It consists of a cylindrically symmetric implosion of a pressure-less gas: the gas stagnates at the symmetry axis and creates an outward moving accretion shock which propagates at a constant velocity. The self-similar analytic solution of this problem has been widely used as benchmark test for hydrodynamic codes, especially those targeting implosion.

Recently, Velikovich et al. (2012) have extended the original test problem to include an embedded azimuthal magnetic field, in accordance with the Z-pinch physics. In their study, they present a family of exact analytic solutions for which the values of primitive variables are finite everywhere, providing an excellent benchmark for Z-pinch and general MHD codes.

We perform this test in both cartesian and cylindrical geometries. The tests can be found respectively in `magnetoHD/Noh` and `magnetoHD/NohCylindrical`. For brevity we describe only the cylindrical initialization. The cartesian can be easily recovered by projecting the solution onto the X-Y plane. A 3T MHD version of this test can also be found under `magnetoHD/unitTest/NohCylindricalRagelike`.

The simulation is initialized in a computational box that spans [0, 3] cm in the r and z directions, in cylindrical $(r-z)$ geometry. The leftmost boundary condition is set to axisymmetry, whereas the remaining boundaries are set to outflow (zero gradient). The initial condition in primitive variables is defined as

$$\begin{aligned} \rho &= 3.1831 \times 10^{-5}\, r^2\, g/cm^3, \\ \mathbf{v} &= (-3.24101 \times 10^7,\ 0,\ 0)\,\mathrm{cm/s}, \\ \mathbf{B} &= (0,\ 6.35584 \times 10^5\, r,\ 0)\,\mathrm{gauss}, \\ P &= C\,\mathbf{B}^2. \end{aligned} \tag{30.19}$$

Since Godunov-type codes cannot run with zero pressure, we initialize P by choosing $C = P/\mathbf{B}^2 = 10^{-6}$, ensuring a magnetically dominated plasma.

The simulations are evolved for 30 ns, utilizing the unsplit solver and a Courant number of 0.8. We use 6 levels of refinement, corresponding to an equivalent resolution of 256×256 zones. The reconstruction is piecewise-linear (second order) with characteristic limiting, whereas the Riemann solvers employed are the HLLD and Roe.

The resulting density profile is shown in Figure 30.50. The refinement closely follows the propagation of the discontinuity which reaches the analytically predicted location ($r = 0.3$ cm) at $t = 30$ ns. The lineouts for HLLD (green dots) and Roe (blue dots) shown on the right, display good agreement with the analytic solution (red line) and the discontinuity is sharply captured (resolved on two points). Our Figure 30.50 can be directly compared to Figures 2a and 3a of Velikovich et al. (2012).

30.2.5 MHD Rotor

The two-dimensional MHD rotor problem (Balsara and Spicer, 1999), `magnetoHD/Rotor`, is designed to study the onset and propagation of strong torsional Alfvén waves, which is thereby relevant for star formation. The computational domain is a unit square $[0,1] \times [0,1]$ with non-reflecting boundary conditions on all four sides. The initial conditions are given by

$$\rho(x,y) = \begin{cases} 10 & r \le r_0 \\ 1 + 9f(r) & r_0 < r < r_1 \\ 1 & r \ge r_1 \end{cases} \tag{30.20}$$

$$u(x,y) = \begin{cases} -f(r)u_0(y-0.5)/r_0 & r \le r_0 \\ -f(r)u_0(y-0.5)/r & r_0 < r < r_1 \\ 0 & r \ge r_1 \end{cases} \tag{30.21}$$

$$v(x,y) = \begin{cases} f(r)u_0(x-0.5)/r_0 & r \le r_0 \\ f(r)u_0(x-0.5)/r & r_0 < r < r_1 \\ 0 & r \ge r_1 \end{cases} \tag{30.22}$$

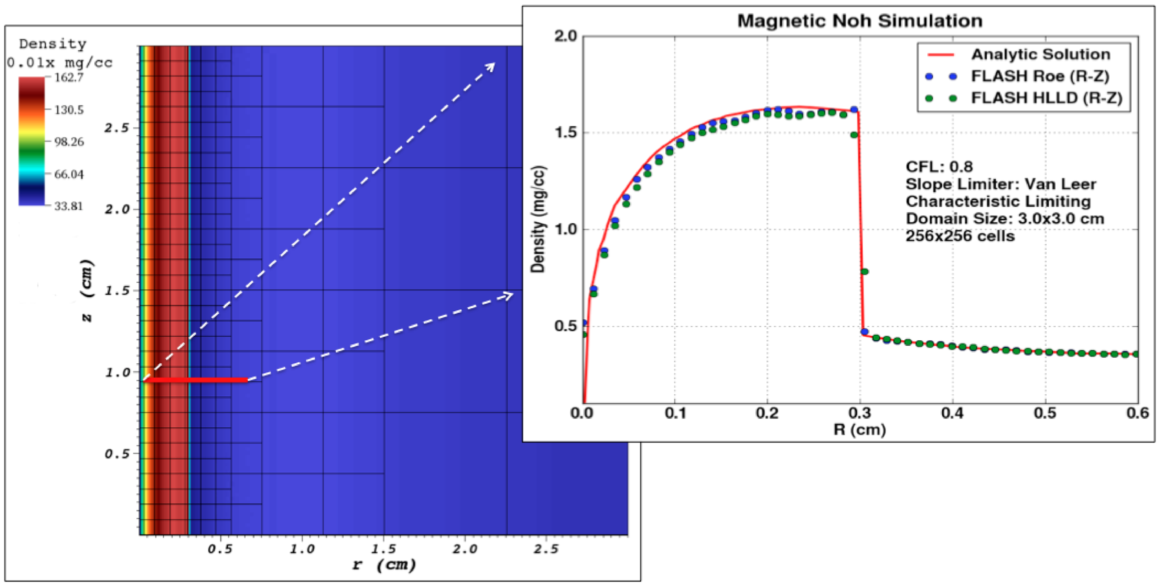

Figure 30.50: Magnetized Noh problem in cylindrical coordinates. Left: density snapshot along with AMR levels after 30 ns for the HLLD Riemann solver. Right: Lineouts of density close to the origin, $r = [0, 0.6]$ cm, for HLLD and Roe, superposed on the analytic solution.

$$p(x, y) = 1 \tag{30.23}$$
$$B_x(x, y) = \frac{5}{\sqrt{4\pi}} \tag{30.24}$$
$$B_y(x, y) = 0, \tag{30.25}$$

where $r_0 = 0.1, r_1 = 0.115, r = \sqrt{(x-0.5)^2 + (y-0.5)^2}, w = B_z = 0$ and a taper function $f(r) = \big(r_1 - r\big)/\big(r - r_0\big)$. The value $\gamma = 1.4$ is used. The initial set-up is occupied by a dense rotating disk at the center of the domain, surrounded by the ambient flow at rest with uniform density and pressure. The rapidly spinning rotor is not in an equilibrium state due to the centrifugal forces. As the rotor spins with the given initial rotating velocity, the initially uniform magnetic field in x-direction will wind up the rotor. The rotor will be wrapped around by the magnetic field, and hence start launching torsional Alfvén waves into the ambient fluid. The angular momentum of the rotor will be diminished in later times as the evolution time increases. The circular rotor will be progressively compressed into an oval shape by the build-up of the magnetic pressure around the rotor. The results shown in Figure 30.51 were obtained using the `StaggeredMesh` MHD solver using 6 refinement levels. The divergence free evolution of the magnetic fields are well preserved as illustrated in Figure 30.52.

30.2.6 MHD Current Sheet

The two-dimensional current sheet problem, `magnetoHD/CurrentSheet`, has recently been studied by Gardiner and Stone (2005) in ideal MHD regime. The two current sheets are initialized and therefore magnetic reconnections are inevitably driven. In the regions the magnetic reconnection takes place the magnetic flux approaches vanishingly small values, and the loss in the magnetic energy is converted into heat (thermal energy). This phenomenon changes the overall topology of the magnetic fields and hence affects the global magnetic configuration.

The square computational domain is given as $[0, 2] \times [0, 2]$ with periodic boundary conditions on all four

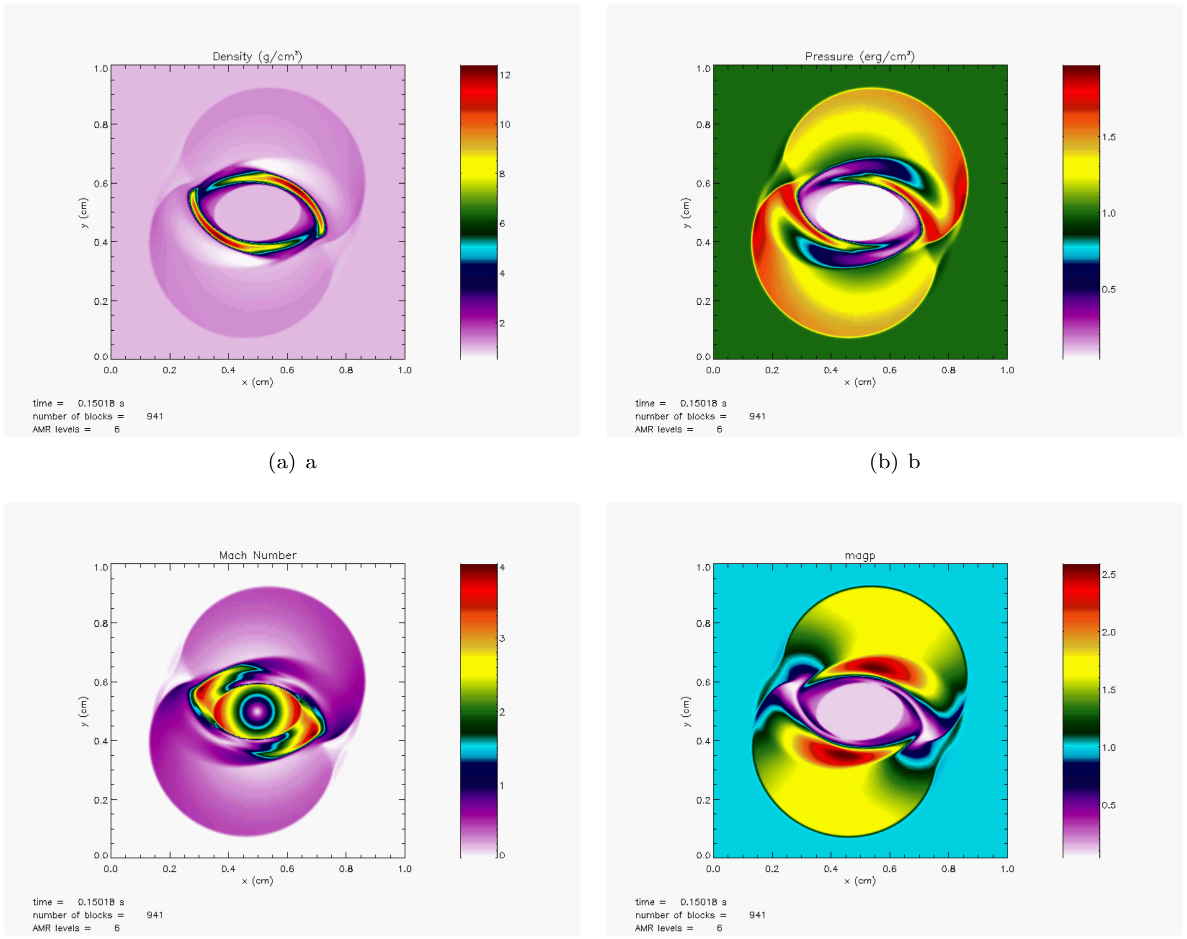

(a) a (b) b (c) c (d) d

Figure 30.51: The Rotor problem at $t = 0.15$ (a) Density (b) Pressure (c) Mach number (d) Magnetic pressure.

sides. We initialize two current sheets in the following:

$$B_y = \begin{cases} B_0 & 0.0 \le x < 0.5 \\ -B_0 & 0.5 \le x < 1.5 \\ B_0 & 1.5 \le x \le 2.0 \end{cases}, \tag{30.26}$$

where $B_0 = 1$. The other magnetic field components B_x, B_z are set to be zeros. The x component of the velocity is given by $u = u_0 \sin 2\pi y$ with $u_0 = 0.1$, and all the other velocity components are initialized with zeros. The density is unity and the gas pressure $p = 0.1$.

The changes of the magnetic fields seed the magnetic reconnection and develop formations of magnetic islands along the two current sheets. The small islands are then merged into the bigger islands by continuously shifting up and down along the current sheets until there is one big island left in each current sheet.

The temporal evolution of the magnetic field lines from $t = 0.0$ to $t = 5.0$ are shown in 30.53(a) – 30.53(f) on a 256×256 uniform grid. In Figure 30.54 the same problem is resolved on an AMR grid with 6 refinement levels, showing the current density j_z along with the AMR block structures at $t = 4.0$. The `StaggeredMesh` solver was used for this problem.

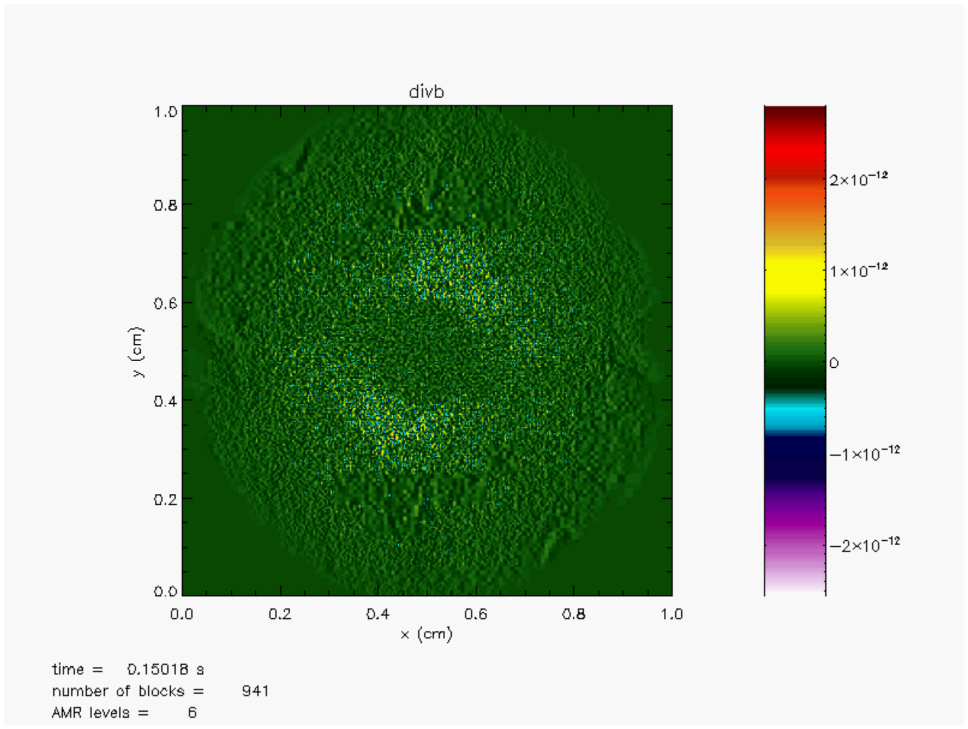

Figure 30.52: Divergence of magnetic fields using the `StaggeredMesh` solver at $t = 0.15$ for the Rotor problem.

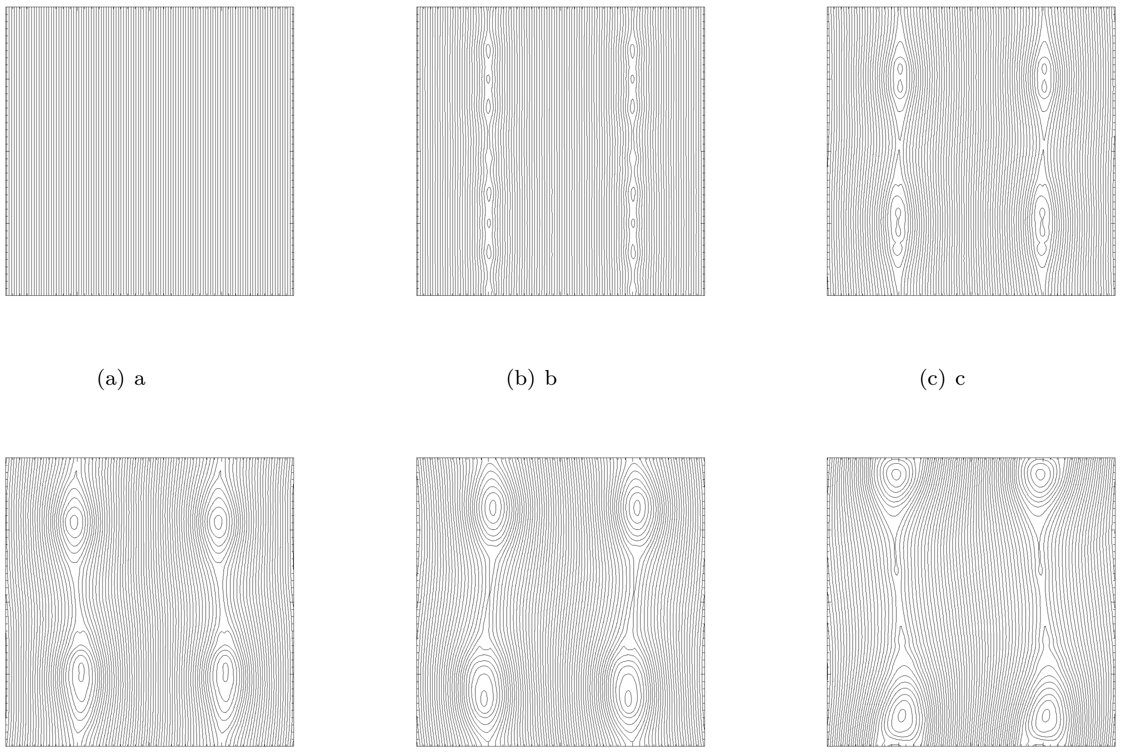

(a) a (b) b (c) c

(d) d (e) e (f) f

Figure 30.53: The temporal evolutions of field lines for the MHD `CurrentSheet` problem. Equally spaced 60 contour lines are shown at time (a) $t = 0.0$ (b) $t = 1.0$ (c) $t = 2.0$ (d) $t = 3.0$ (e) $t = 4.0$ (f) $t = 5.0$.

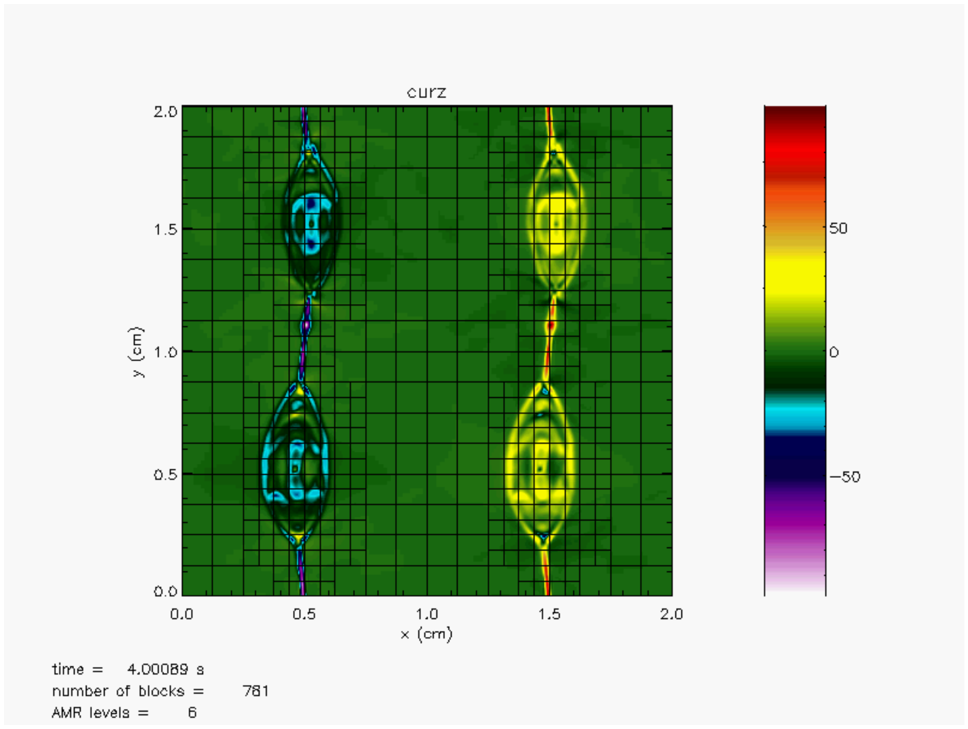

Figure 30.54: Current density at $t = 4.0$ using the `StaggeredMesh` solver for the MHD `CurrentSheet` problem.

30.2.7 Field Loop

The 2D and 3D field loop advection problems (`magnetoHD/FieldLoop`) are known to be stringent test cases in multidimensional MHD. In this test problem we consider a 2D advection of a weakly magnetized field loop traversing the computational domain diagonally. Details of the problem has been described in Gardiner and Stone (2005).

The computational domain is $[-1, 1] \times [-0.5, 0.5]$, with a grid resolution 256×148, and doubly-periodic boundary conditions. With this rectangular grid cell, the flow is not symmetric in x and y directions because the field loop does not advect across each *grid cell* diagonally and hence the resulting fluxes are different in x and y directions. The density and pressure are unity everywhere and $\gamma = 5/3$. The velocity fields are defined as,

$$\mathbf{U} = u_0(\cos\theta, \sin\theta, 1) \tag{30.27}$$

with the advection angle θ, given by $\theta = \tan^{-1}(0.5) \approx 26.57°$. For the choice of the initial advection velocity we set $u_0 = \sqrt{5}$. The size of domain and other parameters were chosen such that the weakly magnetized field loop makes one complete cycle by $t = 1$. It is important to initialize the magnetic fields to satisfy $\nabla \cdot \mathbf{B} = 0$ numerically in order to avoid any initial nonzero error in $\nabla \cdot \mathbf{B}$. As suggested in Gardiner and Stone (2005), the magnetic field components are initialized by taking the numerical curl of the z-component of the magnetic vector potential A_z,

$$B_x = \frac{\partial A_z}{\partial y}, \quad B_y = -\frac{\partial A_z}{\partial x}, \tag{30.28}$$

where

$$A_z = \begin{cases} A_0(R - r) & r \le R \\ 0 & \text{otherwise.} \end{cases}, \tag{30.29}$$

By using this initialization process, divergence-free magnetic fields are constructed with a maximum value of $\nabla \cdot \mathbf{B}$ in the order of 10^{-16} at the chosen resolution. The parameters in (30.29) are $A_0 = 10^{-3}$ and a field loop radius $R = 0.3$. This initial condition results in a very high plasma beta $\beta = p/B_p = 2 \times 10^6$ for the inner region of the field loop. Inside the loop the magnetic field strength is very weak and the flow dynamics is dominated by the gas pressure.

The field loop advection is integrated to a final time $t = 2$. The advection test is found to truly require the full multidimensional MHD approach (Gardiner and Stone, 2005, 2008; Lee and Deane, 2008). Since the field loop is advected at an oblique angle to the x-axis of the computational domain, the values of $\partial B_x/\partial x$ and $\partial B_y/\partial y$ are non-zero in general and their roles are crucial in multidimensional MHD flows. These terms, together with the multidimensional MHD terms $\mathbf{A}_{B_x}$ and $\mathbf{A}_{B_y}$, are explicitly included in the data reconstruction-evolution algorithm in the USM scheme (see Lee and Deane, 2008). During the advection a good numerical scheme should maintain: (a) the circular symmetry of the loop at all time: a numerical scheme that lacks proper numerical dissipation results in spurious oscillations at the loop, breaking the circular symmetry; (b) $B_z = 0$ during the simulation: B_z will grow proportional to $w\nabla \cdot \mathbf{B}\Delta t$ if a numerical scheme does not properly include multidimensional MHD terms.

From the results in Figure 30.55, the USM scheme maintains the circular shape of the loop extremely well to the final time step. The scheme successfully retains the initial circular symmetry and does not develop severe oscillations.

A variant 3D version of this problem (Gardiner and Stone, 2008) is also available, and is illustrated in in Fig. 30.56. This problem is considered to be a particularly challenging test because the correct solution requires inclusion of the multidimensional MHD terms to preserve the in-plane dynamics. Otherwise, the failure in preserving the in-plane dynamics (i.e., growth in the out-of-plane component) results in erroneous behavior of the field loop. As shown in Fig. 30.56, the USM solver successfully maintains the circular shape of the field loop and maintains the out-of-plane component of the magnetic field to very small values over the domain. This figure compares very well with Fig. 2 in Gardiner and Stone, 2008.

30.2.8 3D MHD Blast

A 2D version of the MHD blast problem was studied by Zachary *et al.* (Zachary, Malagoli, and Colella, 1994) and we consider a variant 3D version of the MHD spherical blast wave problem here. This problem

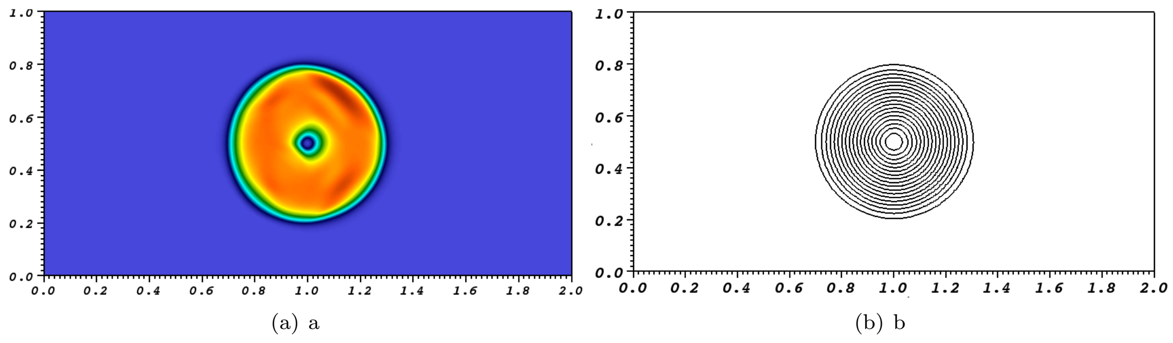
(a) a (b) b

Figure 30.55: The field loop advection problem using the `StaggeredMesh` solver at time $t = 2$ with the Roe Riemann solver. (a)B_p with the MEC at $t = 2$. The color scheme between 2.32×10^{-25} and 7.16×10^{-7} was used. (b)Magnetic field lines with the MEC at $t = 2$. 20 contour lines of A_z between -2.16×10^{-6} and 2.7×10^{-4} are shown.

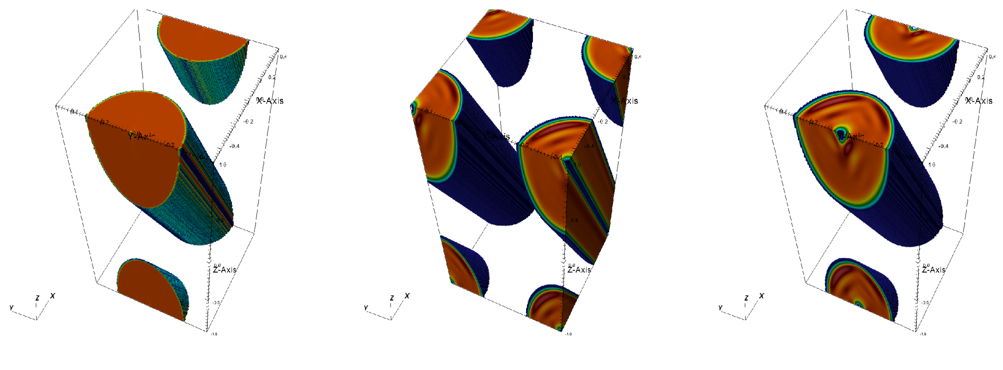
(a) B_p at $t = 0.0$ (b) B_p at $t = 1.5$ (c) B_p at $t = 2.0$

Figure 30.56: Thresholded images of the field loop advection problem at times $t = 0.0, 1.5$, and 2.0 using a uniform grid size $128 \times 128 \times 256$.

leads to the formation and propagation of strong MHD discontinuities, relevant to astrophysical phenomena where the magnetic field energy has strong dynamical effects. With a numerical scheme that fails to preserve the divergence-free constraint, unphysical states could be obtained involving negative gas pressure because the background magnetic pressure increases the strength of magnetic monopoles.

This problem can be computed in various magnetized flow regimes by considering different magnetic field strengths. The computational domain is a square $[-0.5, 0.5] \times [-0.5, 0.5] \times [-0.5, 0.5]$ with a maximum refinement level 4. The explosion is driven by an over-pressurized circular region at the center of the domain with a radius $r = 0.1$. The initial density is unity everywhere, and the pressure of the ambient gas is 0.1, whereas the pressure of the inner region is 1000. The strength of a uniform magnetic field in the x-direction are 0, $50/\sqrt{4\pi}$ and $100/\sqrt{4\pi}$. This initial condition results in a very low-β ambient plasma state, $\beta = 2.513 \times 10^{-4}$. Through this low-$\beta$ ambient state, the explosion emits almost spherical fast magneto-sonic shocks that propagate with the fastest wave speed. The flow has $\gamma = 1.4$.

With this strong magnetic field strength, $B_x = 100/\sqrt{4\pi}$, shown in Figure 30.57, the explosion now becomes highly anisotropic as shown in the pressure plot in Figure 30.57. The Figure shows that the displacement of gas in the transverse y-direction is increasingly inhibited and hydrodynamical shocks propagate in both positive and negative x-directions parallel to B_x. This process continues until total pressure equilibrium is reached in the central region. This problem is also available in 2D setup.

30.3 Gravity Test Problems

30.3.1 Jeans Instability

The linear instability of self-gravitating fluids was first explored by Jeans (1902) in connection with the problem of star formation. The nonlinear phase of the instability is currently of great astrophysical interest, but the linear instability still provides a very useful test of the coupling of gravity to hydrodynamics in FLASH.

The `Jeans` problem allows one to examine the behavior of sinusoidal, adiabatic density perturbations in both the pressure-dominated and gravity-dominated limits. This problem uses periodic boundary conditions. The equation of state is that of a perfect gas. The initial conditions at $t = 0$ are

$$\begin{aligned} \rho(\mathbf{x}) &= \rho_0 \left[1 + \delta \cos(\mathbf{k} \cdot \mathbf{x})\right] \\ p(\mathbf{x}) &= p_0 \left[1 + \gamma\delta \cos(\mathbf{k} \cdot \mathbf{x})\right] \\ \mathbf{v}(\mathbf{x}) &= 0 \ , \end{aligned} \tag{30.30}$$

where the perturbation amplitude $\delta \ll 1$. The stability of the perturbation is determined by the relationship between the wavenumber $k \equiv |\mathbf{k}|$ and the Jeans wavenumber k_J, where k_J is given by

$$k_J \equiv \frac{\sqrt{4\pi G \rho_0}}{c_0} \ , \tag{30.31}$$

and where c_0 is the unperturbed adiabatic sound speed

$$c_0 = \sqrt{\frac{\gamma p_0}{\rho_0}} \tag{30.32}$$

(Chandrasekhar 1961). If $k > k_J$, the perturbation is stable and oscillates with frequency

$$\omega = \sqrt{c_0^2 k^2 - 4\pi G \rho_0} \ ; \tag{30.33}$$

otherwise, it grows exponentially, with a characteristic timescale given by $\tau = (i\omega)^{-1}$.

We checked the dispersion relation (30.33) for stable perturbations with $\gamma = 5/3$ by fixing ρ_0 and p_0 and performing several runs with different k. We followed each case for roughly five oscillation periods using a uniform grid in the box $[0, L]^2$. We used $\rho_0 = 1.5 \times 10^7$ g cm^{-3} and $p_0 = 1.5 \times 10^7$ dyn cm^{-2}, yielding

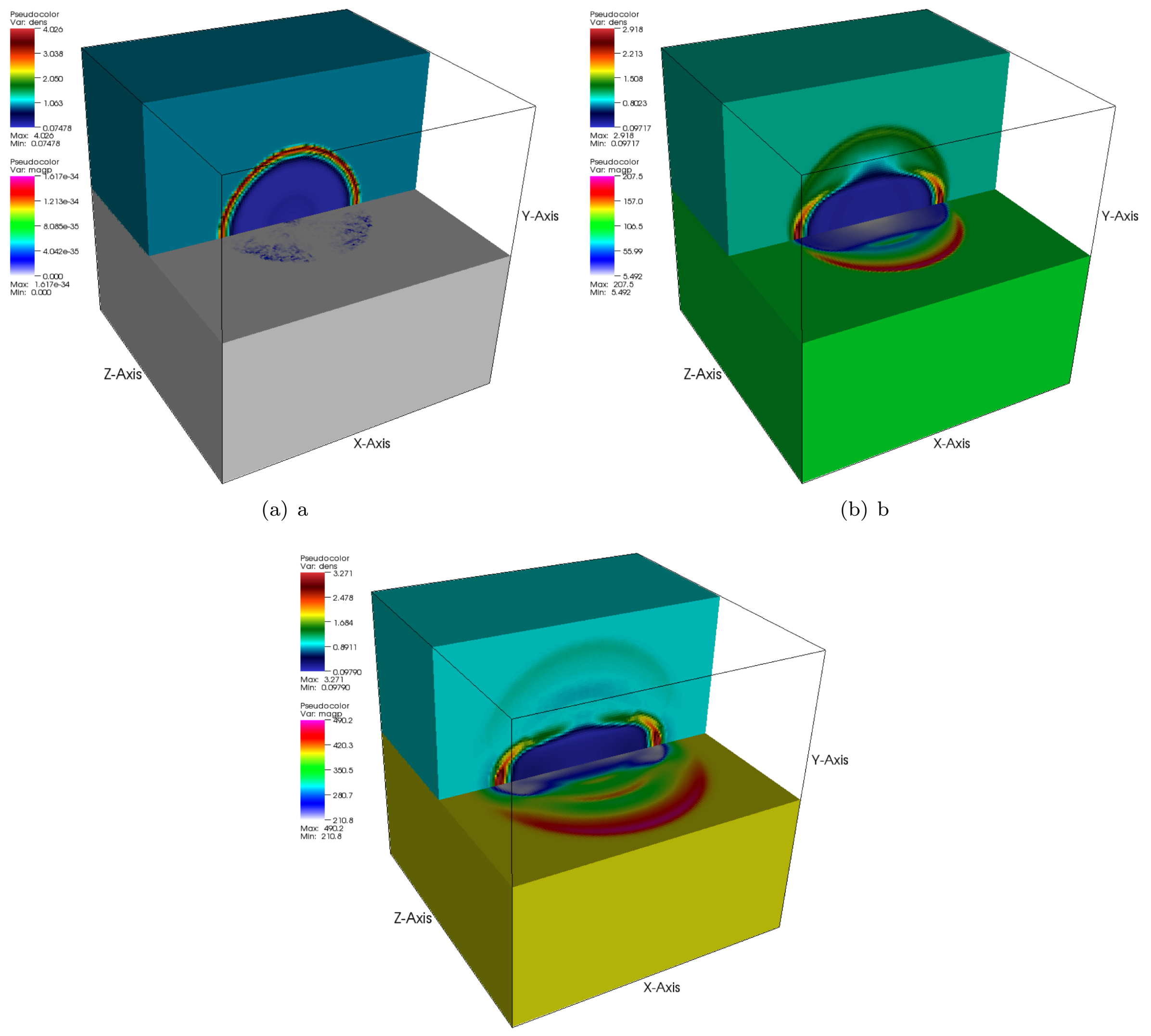

(a) a (b) b (c) c

Figure 30.57: The MHD blast test at time $t = 0.01$ using the unsplit staggered mesh MHD solver. Density (top half) and magnetic pressure (bottom half) plots for three different strengths of B_x. (a) $B\_x = 0$ (b) $B\_x = 50/\sqrt{4\pi}$ (c) $B\_x = 100/\sqrt{4\pi}$.

$k_J = 2.747$ cm^{-1}. The perturbation amplitude δ was fixed at 10^{-3}. The box size L is chosen so that k_J is smaller than the smallest nonzero wavenumber that can be resolved on the grid

$$L = \frac{1}{2}\sqrt{\frac{\pi\gamma p_0}{G\rho_0^2}} \ . \tag{30.34}$$

This prevents roundoff errors at wavenumbers less than k_J from being amplified by the physical Jeans instability. We used wavevectors $\mathbf{k}$ parallel to and at 45 degrees to the x-axis. Each test calculation used the multigrid Poisson solver together with its default settings.

The resulting kinetic, thermal, and potential energies as functions of time for one choice of $\mathbf{k}$ are shown in Figure 30.58 together with the analytic solution, which is given in two dimensions by

$$\begin{aligned} T(t) &= \frac{\rho_0 \delta^2 |\omega|^2 L^2}{8k^2} \left[1 - \cos(2\omega t)\right] \\ U(t) - U(0) &= -\frac{1}{8}\rho_0 c_0^2 \delta^2 L^2 \left[1 - \cos(2\omega t)\right] \\ W(t) &= -\frac{\pi G \rho_0^2 \delta^2 L^2}{2k^2} \left[1 + \cos(2\omega t)\right] \ . \end{aligned} \qquad (30.35)$$

The figure shows that FLASH obtains the correct amplitude and frequency of oscillation. We computed the average oscillation frequency for each run by measuring the time interval required for the kinetic energy to undergo exactly ten oscillations. Figure 30.59 compares the resulting dispersion relation to (30.33). It can be seen from this plot that FLASH correctly reproduces (30.33). At the highest wave number ($k = 100$), each wavelength is resolved using only about 14 cells on a six-level uniform grid, and the average timestep (which depends on c_0, Δx, and Δy, and has nothing to do with k) turns out to be comparable to the oscillation period. Hence the frequency determined from the numerical solution for this value of k is somewhat more poorly determined than for the other runs. At lower wavenumbers, however, the frequencies are correct to less than 1%.

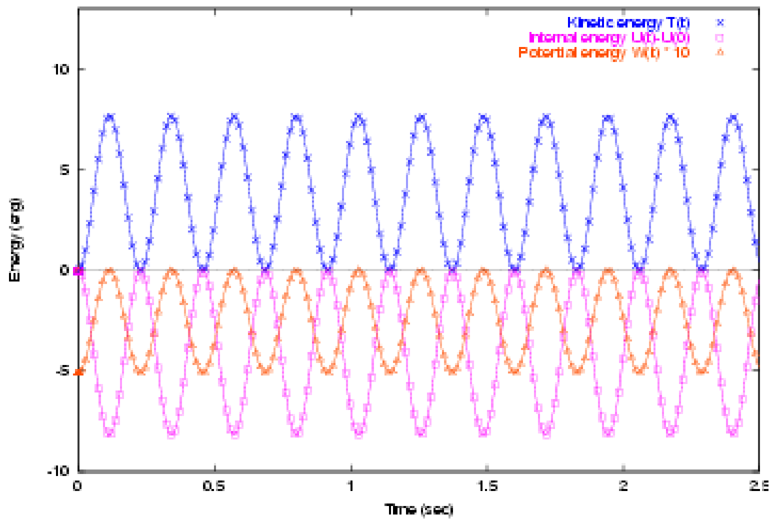

Figure 30.58: Kinetic, internal, and potential energy versus time for a stable Jeans mode with $k = 10.984$. Points indicate numerical values found using FLASH 3.0 with a fixed four-level adaptive grid. The analytic solution for each form of energy is shown using a solid line.

The additional runtime parameters supplied with the `Jeans` problem are listed in Table 30.10. This problem is configured to use the perfect-gas equation of state (`gamma`) with `gamma` set to 1.67 and is run in a two-dimensional unit box. The refinement marking routine (`Grid_markRefineDerefine.F90`) supplied with this problem refines blocks whose mean density exceeds a given threshold. Since the problem is not spherically symmetric, the multigrid Poisson solver should be used.

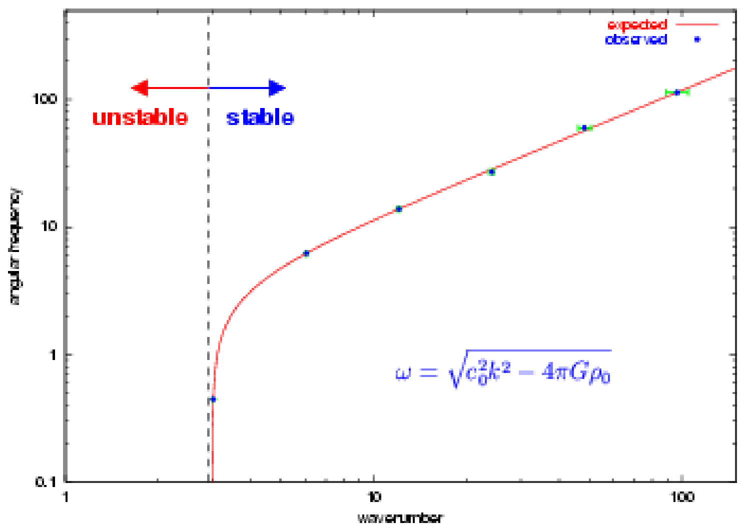

Figure 30.59: Computed versus expected Jeans dispersion relation (for stable modes) found using FLASH 1.62 with a six-level uniform grid.

Table 30.10: Runtime parameters used with the `Jeans` test problem.

Variable	Type	Default	Description
`rho0`	real	1.5×10^7	Initial unperturbed density (ρ_0)
`p0`	real	1.5×10^7	Initial unperturbed pressure (p_0)
`amplitude`	real	0.001	Perturbation amplitude (δ)
`lambdax`	real	0.572055	Perturbation wavelength in x direction ($\lambda_x = 2\pi/k_x$)
`lambday`	real	1.0×10^{10}	Perturbation wavelength in y direction ($\lambda_y = 2\pi/k_y$)
`lambdaz`	real	1.0×10^{10}	Perturbation wavelength in z direction ($\lambda_z = 2\pi/k_z$)
`delta_ref`	real	0.01	Refine a block if the maximum density contrast relative to ρ_{ref} is greater than this
`delta_deref`	real	-0.01	Derefine a block if the maximum density contrast relative to ρ_{ref} is less than this
`reference_density`	real	1.5×10^7	Reference density for grid refinement (ρ_{ref}). Density contrast is used to determine which blocks to refine; it is defined as $$\max_{\text{block}} \left\{ \left| \frac{\rho_{ijk}}{\rho_{\text{ref}}} - 1 \right| \right\}$$

30.3.2 Homologous Dust Collapse

The homologous dust collapse problem `DustCollapse` is used to test the ability of the code to solve self-gravitating problems in which the flow geometry is spherical and gas pressure is negligible. The problem was first described by Colgate and White (1966) and has been used by Mönchmeyer and Müller (1989) to test hydrodynamical schemes in curvilinear coordinates. We solve this problem using a 3D Cartesian grid.

The initial conditions consist of a uniform sphere of radius r_0 and density ρ_0 at rest. The pressure p_0 is taken to be constant and very small

$$p_0 \ll \frac{4\pi G}{\gamma}\rho_0^2 r_0^2 \ . \tag{30.36}$$

We refer to such a nearly pressureless fluid as 'dust'. A perfect-gas equation of state is used, but the value of γ is not significant. Outflow boundary conditions are used for the gas, while isolated boundary conditions are used for the gravitational field.

The collapse of the dust sphere is self-similar; the cloud should remain spherical with uniform density as it collapses. The radius of the cloud, $r(t)$, should satisfy

$$\left(\frac{8\pi G}{3}\rho_0\right)^{1/2} t = \left(1-\frac{r(t)}{r_0}\right)^{1/2}\left(\frac{r(t)}{r_0}\right)^{1/2} + \sin^{-1}\left(1-\frac{r(t)}{r_0}\right)^{1/2} \tag{30.37}$$

(Colgate & White 1966). Thus. we expect to test three things with this problem: the ability of the code to maintain spherical symmetry during an implosion (in particular, no block boundary effects should be evident); the ability of the code to keep the density profile constant within the cloud; and the ability of the code to obtain the correct collapse factor. The second of these is particularly difficult, because the edge of the cloud is very sharp and because the Cartesian grid breaks spherical symmetry most dramatically at the center of the cloud, which is where all of the matter ultimately ends up.

Results of a `DustCollapse` run using FLASH 3.0 appear in Figure 30.60, which shows plots of density and the X component of velocity in menacing color scheme. The values are plotted at the end of the run from an X-Y plane in the center of the physical domain; density is in logarithmic scale. This run used a resolution of 128^3, and the results were compared against a similar run using FLASH 2.5. We have also included figures from an earlier higher resolution run using FLASH2 which used 4^3 top-level blocks and seven levels of refinement, for an effective resolution of 2048^3. In both the runs, the multipole Poisson solver was used with a maximum multipole moment $\ell = 0$. The initial conditions used $\rho_0 = 10^9$ g cm^{-3} and $r_0 = 6.5 \times 10^8$ cm. In Figure 30.61a, the density, pressure, and velocity are scaled by 2.43×10^9 g cm^{-3}, 2.08×10^{17} dyn cm^{-2}, and 7.30×10^9 cm s^{-1}, respectively. In Figure 30.61b they are scaled by 1.96×10^{11} g cm^{-3}, 2.08×10^{17} dyn cm^{-2}, and 2.90×10^{10} cm s^{-1}. Note that within the cloud, the profiles are very isotropic, as indicated by the small dispersion in each profile. Significant anisotropy is only present for low-density material flowing in through the Cartesian boundaries. In particular, it is encouraging that the velocity field remains isotropic all the way into the center of the grid; this shows the usefulness of refining spherically symmetric problems near $r = 0$. However, as material flows inward past refinement boundaries, small ripples develop in the density profile due to interpolation errors. These remain spherically symmetric but increase in amplitude as they are compressed. Nevertheless, they are still only a few percent in relative magnitude by the second frame. The other numerical effect of note is a slight spreading at the edge of the cloud. This does not appear to worsen significantly with time. If one takes the radius at which the density drops to one-half its central value as the radius of the cloud, then the observed collapse factor agrees with our expectation from (30.37). Overall our results, including the numerical effects, agree well with those of Mönchmeyer and Müller (1989).

This problem is configured to use the perfect-gas equation of state (`gamma`) with `gamma` set to 1.67 and is run in a three-dimensional box. The problem uses the specialized refinement marking routine supplied under the Grid interface of `Grid_markRefineSpecialized` which refines blocks containing the center of the cloud.

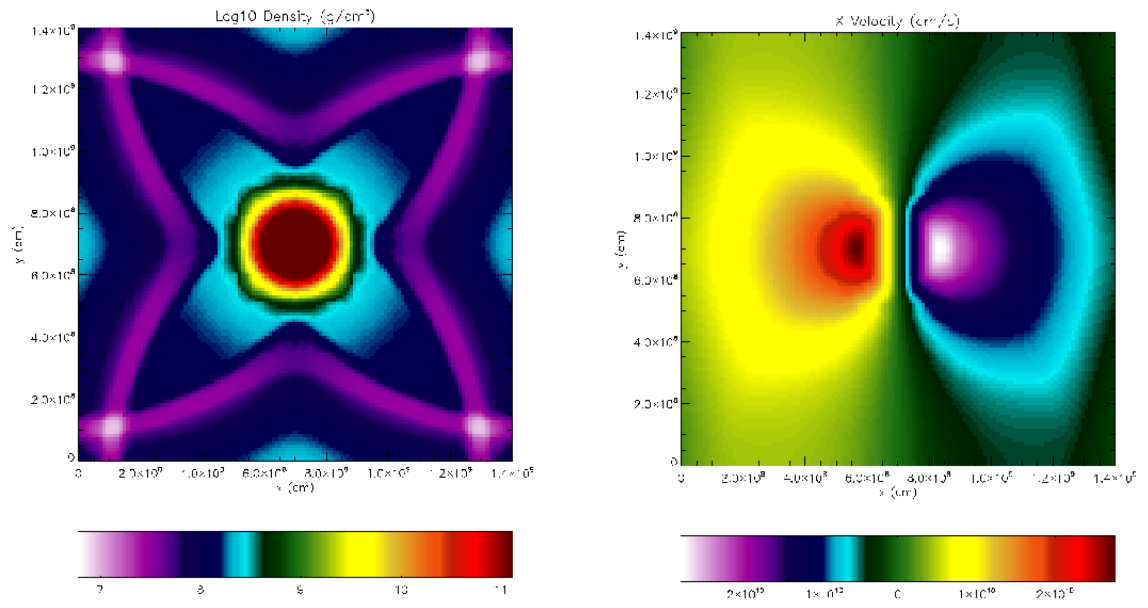

(a) (b)

Figure 30.60: XY plane of Density (a) and X component of Velocity (b) are shown at the center of the domain for the `DustCollapse` problem. The velocity is in normal scale, while density is logscale.

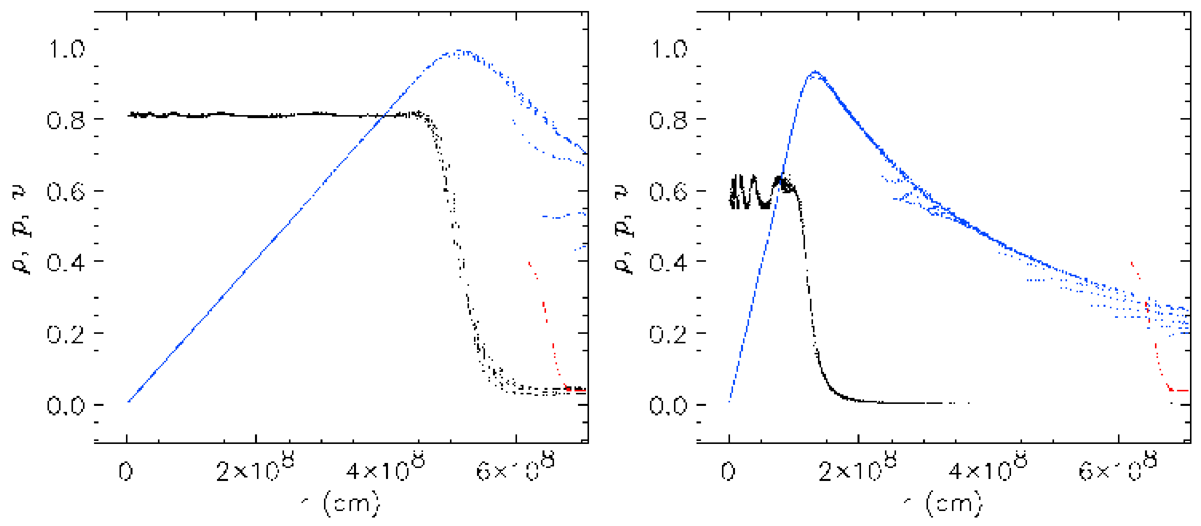

(a) (b)

Figure 30.61: Density (black), pressure (red), and velocity (blue) profiles in the homologous dust collapse problem at (a) $t = 0.0368$ sec and (b) $t = 0.0637$ sec. The density, pressure, and velocity are scaled as discussed in the text.

30.3.3 Huang-Greengard Poisson Test

The PoisTest problem tests the convergence properties of the multigrid Poisson solver on a multidimensional, highly (locally) refined grid. This problem is described by Huang and Greengard (2000). The source function consists of a sum of thirteen two-dimensional Gaussians

$$\rho(x, y) = \sum_{i=1}^{13} e^{-\sigma_i [(x-x_i)^2 + (y-y_i)^2]} , \tag{30.38}$$

where the constants σ_i, x_i, and y_i are given in Table 30.11. The very large range of widths and ellipticities of these peaks forces the mesh structure to be highly refined in some places. The density field and block structure are shown for a 14-level mesh in Figure 30.62.

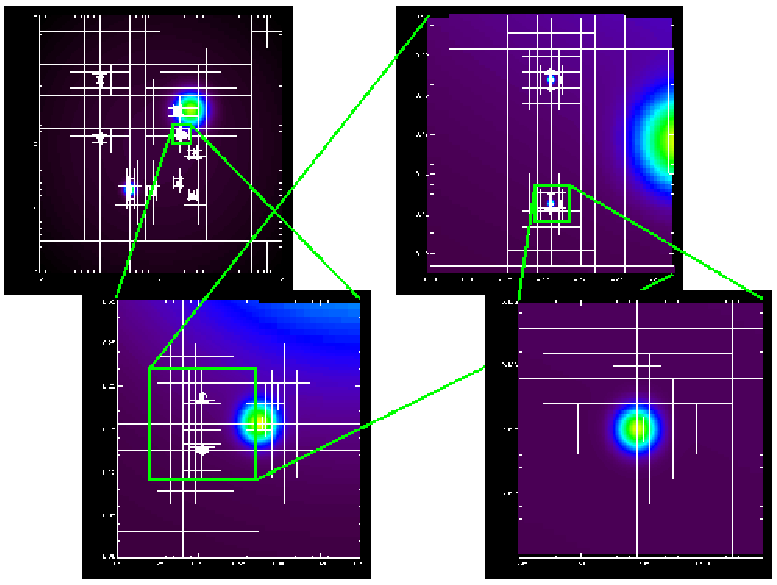

Figure 30.62: Density field and block structure for a 14-level mesh applied to the Huang-Greengard PoisTest problem. The effective resolution of the mesh is $65,536^2$.

Table 30.11: Constants used in the poistest problem.

i	1	2	3	4	5	6	7
x_i	0	-1	-1	0.28125	0.5	0.3046875	0.3046875
y_i	0	0.09375	1	0.53125	0.53125	0.1875	0.125
σ_i	0.01	4000	20000	80000	16	360000	400000
i	8	9	10	11	12	13	
x_i	0.375	0.5625	-0.5	-0.125	0.296875	0.5234375	
y_i	0.15625	-0.125	-0.703125	-0.703125	-0.609375	-0.78125	
σ_i	2000	18200	128	49000	37000	18900	

The PoisTest problem uses one additional runtime parameters sim_smlRho, the smallest allowed value of density. Runtime parameters from the Multigrid unit (both Gravity and GridSolvers) are relevant; see Section 8.10.2.6.

30.3.4 MacLaurin

The gravitational potential at the surface of, and inside a homogeneous spheroid called a "MacLaurin spheroid" is expressible in terms of analytical functions. This handy result was first determined by MacLaurin (1801), and later summarized by, amongst others, Chandrasekhar (1989). These properties allow validation of the FLASH4 gravitational solvers against the analytical solutions.

As a test case, an oblate ($a_1 = a_2 > a_3$) Maclaurin spheroid, of a constant density $\rho = 1$ in the interior, and $\rho = \epsilon \to 0$ outside (in FLASH4 smlrho is used). The spheroid is motionless and in hydrostatic equilibrium. The gravitational potential of such object is analytically calculable, and is:

$$\phi(\mathbf{x}) = \pi G\rho \left[2A_1a_1^2 - A_1(x^2+y^2) + A_3(a_3^2 - z^2)\right] \ , \tag{30.39}$$

for a point inside the spheroid. Here

$$A_1 = \frac{\sqrt{1-e^2}}{e^3}\sin^{-1} e - \frac{1-e^2}{e^2} \ , \tag{30.40}$$

$$A_3 = \frac{2}{e^2} - \frac{2\sqrt{1-e^2}}{e^3}\sin^{-1} e \ , \tag{30.41}$$

where e is the ellipticity of a spheroid:

$$e = \sqrt{1 - \left(\frac{a_3}{a_1}\right)^2} \ . \tag{30.42}$$

For a point outside the spheroid, potential is:

$$\phi(\mathbf{x}) = \frac{2a_3}{e^2}\pi G\rho \left[a_1 e \tan^{-1} h - \frac{1}{2}\left((x^2+y^2)\left(\tan^{-1} h - \frac{h}{1+h^2}\right) + 2z^2(h - \tan^{-1} h)\right)\right] \ , \tag{30.43}$$

where

$$h = \frac{a_1 e}{\sqrt{a_3^2 + \lambda}} \ , \tag{30.44}$$

and λ is the positive root of the equation

$$\frac{x^2}{a_1^2+\lambda} + \frac{y^2}{a_2^2+\lambda} + \frac{z^2}{a_3^2+\lambda} = 1 \ . \tag{30.45}$$

This test is also useful because the spheroid has spherical symmetry in the X–Y plane, but also lack of such symmetry in X–Z and Y–Z planes. The density distribution of the spheroid is shown in Equation 30.3.4. Spherical symmetry is simple to reproduce with a solution using multipole expansion. However, the non-symmetric solution requires an infinite number of multipole moments, while the code calculates solution up to a certain l_{max}, specified by the user as runtime parameter mpole_lmax. The error is thus expected to be dominated by the first non-zero term in the remainder of expansion. Also, the solution for any point inside the spheroid is the sum of monopole and dipole moments.

The simulation is calculated on a MacLaurin spheroid with eccentricity $e = 0.9$; several other values for eccentricity were tried with results qualitatively the same. All tests used 3D Cartesian coordinates. The gravitational potential is calculated on an adaptive mesh, and the relative error is investigated:

$$\epsilon = \left|\frac{\phi_{\text{analytical}} - \phi_{\text{FLASH}}}{\phi_{\text{analytical}}}\right| \tag{30.46}$$

from zone to zone.

As expected, increasing spatial resolution improves the solution quality, but here we focus on how the solution depends on the choice of l_max, the cutoff ℓ in (8.15). In Figure 30.64–30.64 the gravitational potential for the Maclaurin spheroid, the FLASH4 solution, and relative errors for several l_{max}'s are shown. A similar figure produced for $l_{max} = 1$ shows no difference from Figure 30.64, indicating that the last dipole term in the multipole expansion does not contribute to the accuracy of the solution but does increase computational

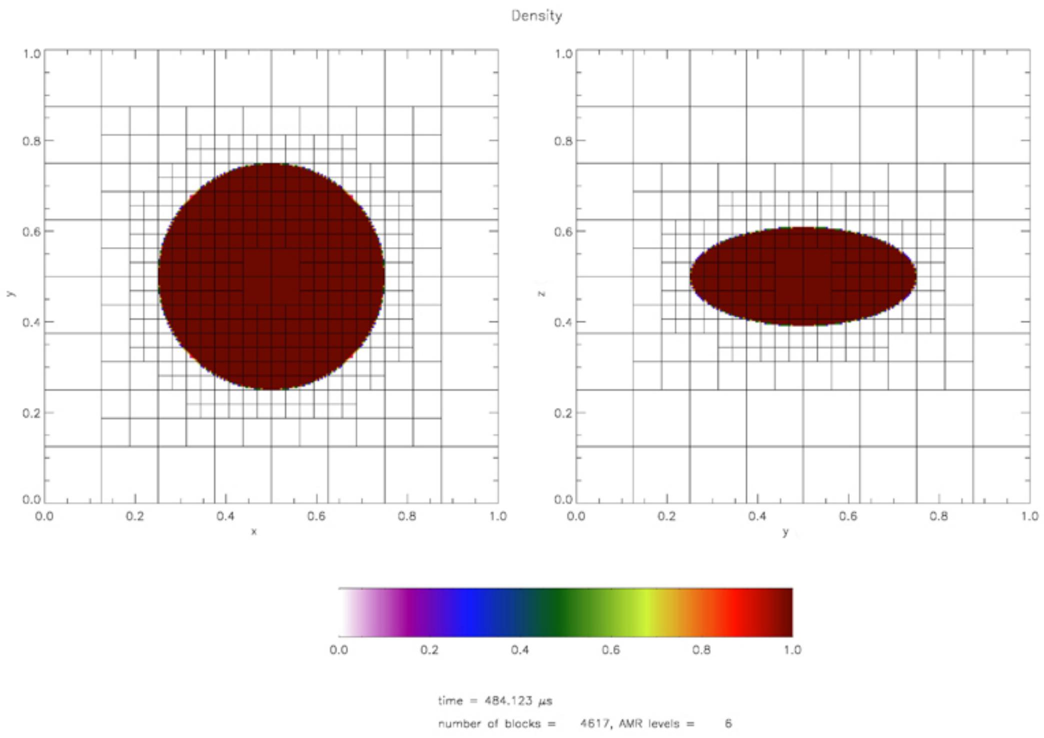

Figure 30.63: Density of the MacLaurin spheroid (left X–Y plane, right Y–Z plane) with ellipticity $e = 0.9$. The FLASH4 block structure is shown on top.

l_{max}	min(ϵ)	max(ϵ)	relative L^2_{in} norm	relative L^2_{out} norm	approx. time [s]
0	$4.5\ 10^{-6}$	0.182	$7.1\ 10^{-2}$	$6.8\ 10^{-2}$	9.8
1	$4.5\ 10^{-6}$	0.182	$7.1\ 10^{-2}$	$6.8\ 10^{-2}$	14.5
2	$9.8\ 10^{-6}$	0.062	$1.4\ 10^{-2}$	$1.7\ 10^{-2}$	34.7
4	$1.0\ 10^{-8}$	0.026	$4.0\ 10^{-3}$	$5.0\ 10^{-3}$	55.4
6	$6.1\ 10^{-9}$	0.013	$1.6\ 10^{-3}$	$2.5\ 10^{-3}$	134.9
8	$7.8\ 10^{-9}$	0.007	$8.7\ 10^{-4}$	$1.2\ 10^{-3}$	210.2
10	$6.7\ 10^{-9}$	0.004	$5.5\ 10^{-4}$	$7.0\ 10^{-4}$	609.7

Table 30.12: Minimal and maximal relative error in all zones of the simulation, calculated using (30.46). Last row is approximate time for one full timestep (gravity only).

cost. Because gravity sources are all of the same sign, and the symmetry of the problem, all odd-l moments are zero: reasonable, physically motivated values for setting mpole_lmax should be an even number.

In the X–Y plane, where the solution is radially symmetric, the first monopole term is enough to qualitatively capture the correct potential. As expected, the error is the biggest on the spheroid boundary, and decreases both outwards and inwards. Increasing the maximum included moment reduces errors. However, in other non-symmetric planes, truncating the potential to certain l_{max} leads to an error whose leading term will be the spherical harmonic of order $l_{max} + 2$, as can be nicely seen in the lower right sections of Figure 30.64 – 30.66. Increasing l_{max} reduces the error, but also increases the required time for computation. This computational increase is not linear because of the double sum in (8.17). Luckily, convergence is rather fast, and already for $l_{max} = 4$, there are only few zones with relative error bigger than 1%, while for the most of the computational domain the error is several orders of magnitude less.

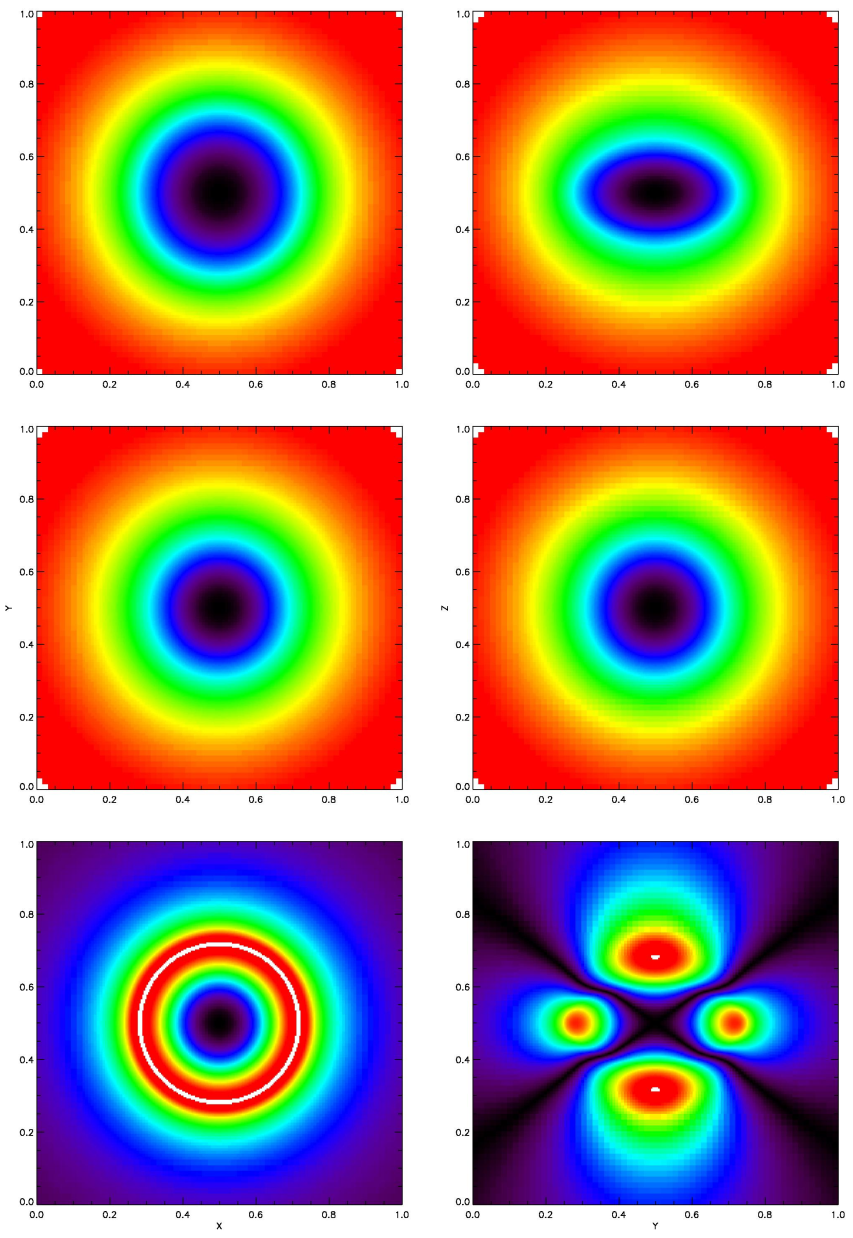

Figure 30.64: Maclaurin spheroid: $l\_max = 0$, 6 refinement levels. Left column is X–Y plane, cut through z=0.5, right column is Y–Z plane cut through x=0.5 . From top to bottom: analytical solution for the gravitational potential introduced on FLASH grid; solution of FLASH multipole solver; relative error.

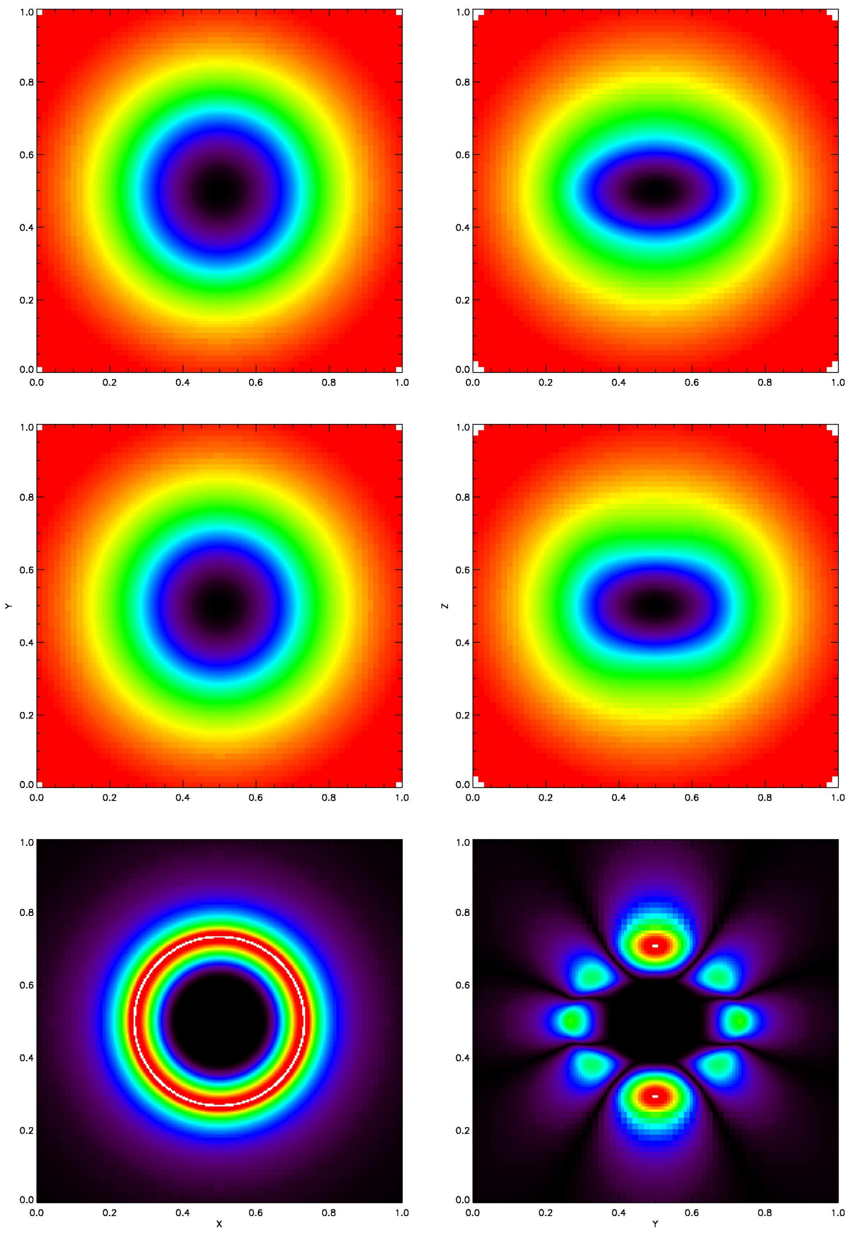

Figure 30.65: Maclaurin spheroid: $l\_max = 2$, 6 refinement levels. Left column is X–Y plane, cut through z=0.5, right column is Y–Z plane cut through x=0.5 . From top to bottom: analytical solution for the gravitational potential introduced on FLASH grid; solution of FLASH multipole solver; relative error.

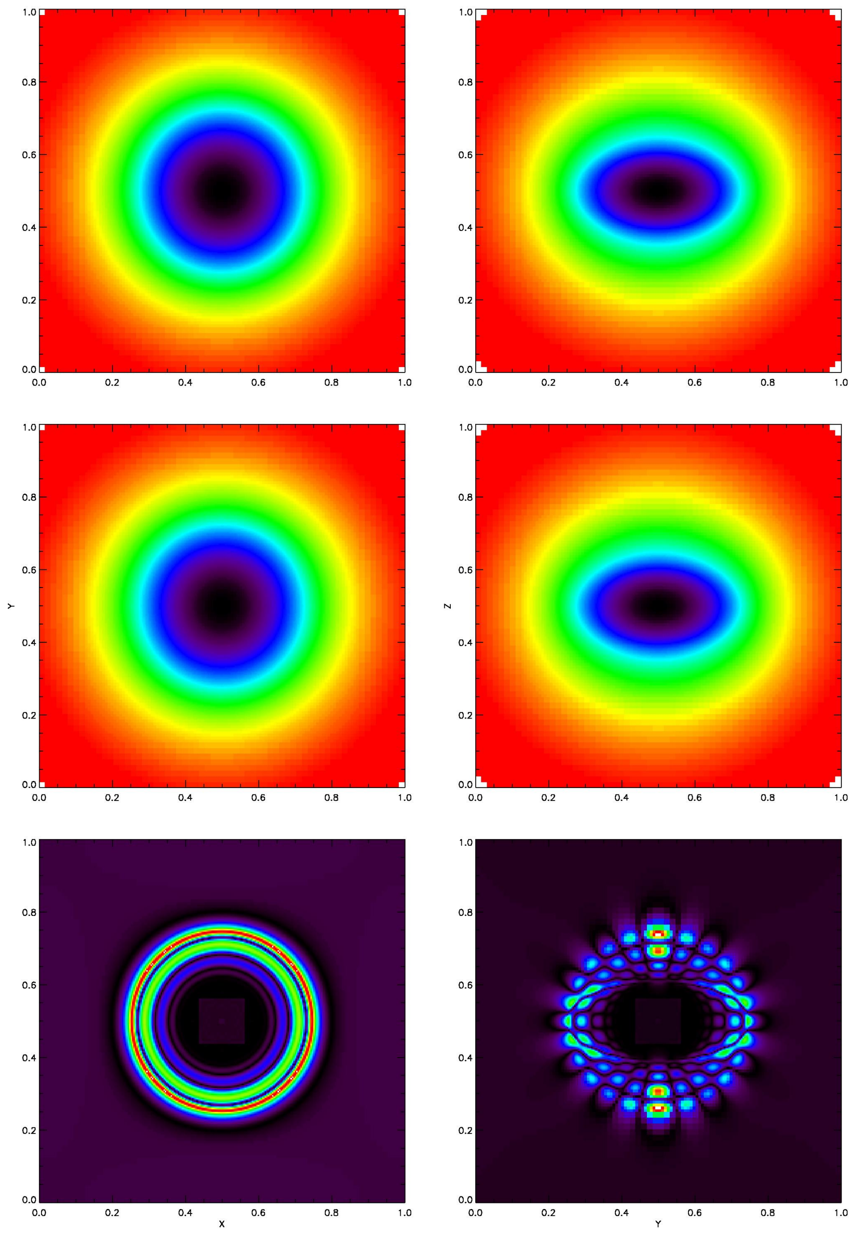

Figure 30.66: Maclaurin spheroid: $l\_max = 10$, 6 refinement levels. Left column is X–Y plane, cut through z=0.5, right column is Y–Z plane cut through x=0.5 . From top to bottom: analytical solution for the gravitational potential introduced on FLASH grid; solution of FLASH multipole solver; relative error.

30.4 Particles Test Problems

These problems are primarily designed to test the functioning of the particle tracking routines within FLASH4.

30.4.1 Two-particle `Orbit`

The `Orbit` problem tests the mapping of particle positions to gridded density fields, the mapping of gridded potentials onto particle positions to obtain particle forces, and the time integration of particle motion. The initial conditions consist of two particles of unit mass and separation r_0 located at positions $(x, y, z) = (0.5(L_x \pm r_0), 0.5L_y, 0.5L_z)$, where (L_x, L_y, L_z) are the dimensions of the computational volume. The initial particle velocity vectors are parallel to the y-axis and have magnitude

$$|v| = \sqrt{\frac{2GM}{r_0}} \ , \tag{30.47}$$

if a constant gravitational field due to a point mass M at $(0.5L_x, 0.5L_y, 0.5L_z)$ is employed, or

$$|v| = \frac{1}{2}\sqrt{\frac{2G}{r_0}} \ , \tag{30.48}$$

if the particles are self-gravitating. The correct behavior is for the particles to orbit the center of the grid in a circle with constant velocity. Figure 30.67 shows a typical pair of particle trajectories for this problem

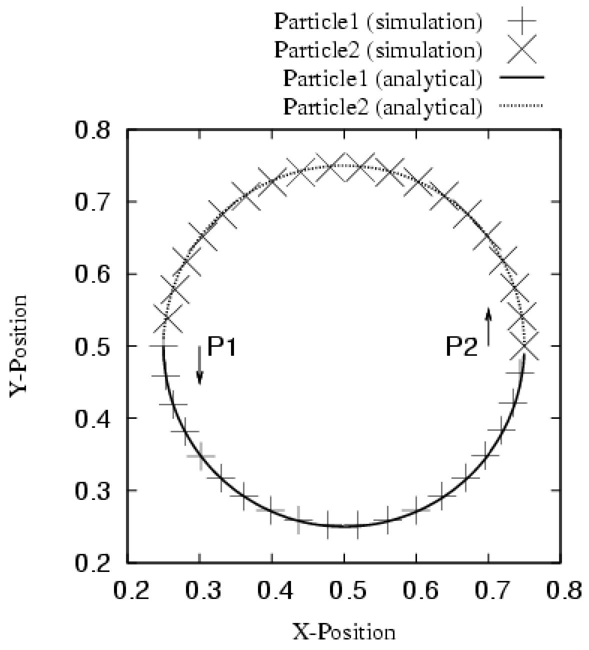

Figure 30.67: Particle trajectories in the `Orbit` test problem for a 3D grid at a fixed refinement level of 2. There is no motion along the z-axis.

No specific gravity unit is required by the problem configuration file, because the problem is intended to be run with either a fixed external field or the particles' own field. If the particles are to orbit in an external field (`ext_field = .true.`), the field is assumed to be a central point-mass field (`physics/-Gravity/GravityMain/PointMass`), and the parameters for that unit should be assigned appropriate values. If the particles are self-gravitating (`ext_field = .false.`), the `physics/Gravity/GravityMain/Poisson` unit should be included in the code, and a Poisson solver that supports isolated boundary conditions should be used (`grav_boundary_type = "isolated"`).

In either case, long-range forces for the particles must be turned on, or else they will not experience any accelerations at all. This can be done using the particle-mesh method by including the unit `Particles/ParticlesMain/active/longRange/gravity/ParticleMesh`.

FLASH Transition

Although the Multipole solver can work with the Orbit problem, the solutions are very poor. We strongly recommend the use of Multigrid solver with this problem.

As of FLASH 2.1 both the multigrid and multipole solvers support isolated boundary conditions. This problem should be run in three dimensions.

Grid interpolation

The FLASH2 user guide recommends that this problem be run with conservative, quadratic interpolants (such as `mesh/amr/paramesh2.0/quadratic_cartesian`) and monotonicity enforcement turned off (`monotone = .false.`). In FLASH4, you should use the default 2nd order monotonic interpolation scheme (see Section 8.6.2) in `PARAMESH` 4.

The two-particle orbit problem uses the runtime parameters listed in Table 30.13 in addition to the regular ones supplied with the code.

Table 30.13: Runtime parameters used in the `orbit` test problem.

Variable	Type	Default	Description
`separation`	real	0.5	Initial particle separation (r_0)
`ext_field`	logical	`.false.`	Whether to make the particles self-gravitating or to have them orbit in an external potential. In the former case `GravityMain/Poisson` should be used; in the latter, `GravityMain/PointMass.`

30.4.2 Zel'dovich Pancake

The cosmological pancake problem (Zel'dovich 1970), `Pancake`, provides a good simultaneous test of the hydrodynamics, particle dynamics, Poisson solver, and cosmological expansion modules. Analytic solutions well into the nonlinear regime are available for both N-body and hydrodynamical codes (Anninos & Norman 1994), permitting an assessment of the code's accuracy. After caustic formation the problem provides a stringent test of the code's ability to track thin, poorly resolved features and strong shocks using most of the basic physics needed for cosmological problems. Also, as pancakes represent single-mode density perturbations, coding this test problem is useful as a basis for creating more complex cosmological initial conditions.

We set the initial conditions for the pancake problem in the linear regime using the analytic solution given by Anninos and Norman (1994). In a universe with $\Omega_0 = 1$ at redshift z, a perturbation of wavenumber

k which collapses to a caustic at redshift $z_c < z$ has comoving density and velocity given by

$$\rho(x_e;z) = \bar{\rho}\left[1+\frac{1+z_c}{1+z}\cos\left(kx_\ell\right)\right]^{-1} \tag{30.49}$$

$$v(x_e;z) = -H_0(1+z)^{1/2}(1+z_c)\frac{\sin kx_\ell}{k}\ , \tag{30.50}$$

where $\bar{\rho}$ is the comoving mean density. Here x_e is the distance of a point from the pancake midplane, and x_ℓ is the corresponding Lagrangian coordinate, found by iteratively solving

$$x_e = x_\ell - \frac{1+z_c}{1+z}\frac{\sin kx_\ell}{k}\ . \tag{30.51}$$

The temperature solution is determined from the density under the assumption that the gas is adiabatic with ratio of specific heats γ:

$$T(x_e;z) = (1+z)^2\bar{T}_{\rm fid}\left[\left(\frac{1+z_{\rm fid}}{1+z}\right)^3\frac{\rho(x_e;z_{\rm fid})}{\rho(x_e;z)}\right]^{\gamma-1}\ . \tag{30.52}$$

The mean temperature $\bar{T}_{\rm fid}$ is specified at a redshift $z_{\rm fid}$.

Dark matter particles are initialized using the same solution as the gas. The Lagrangian coordinates x_ℓ are assigned to lie on a uniform grid. The corresponding perturbed coordinates x_e are computed using (30.51). Particle velocities are assigned using (30.50).

At caustic formation ($z = z_c$), planar shock waves form in the gas on either side of the pancake midplane and begin to propagate outward. A small region at the midplane is left unshocked. Immediately behind the shocks, the comoving density and temperature vary approximately as

$$\rho(x_e;z) \approx \bar{\rho}\frac{18}{\left(kx_\ell\right)^2}\frac{\left(1+z_c\right)^3}{\left(1+z\right)^3} \tag{30.53}$$

$$T(x_e;z) \approx \frac{\mu H_0^2}{6k_Bk^2}\left(1+z_c\right)\left(1+z\right)^2\left(kx_\ell\right)^2\ .$$

At the midplane, which undergoes adiabatic compression, the comoving density and temperature are approximately

$$\rho_{\rm center} \approx \bar{\rho}\left[\frac{1+z_{\rm fid}}{1+z}\right]^3\left[\frac{3H_0^2\mu}{k_B\bar{T}_{\rm fid}k^2}\frac{\left(1+z_c\right)^4\left(1+z\right)^3}{1+z_{\rm fid}}\right]^{1/\gamma} \tag{30.54}$$

$$T_{\rm center} \approx \frac{3H_0^2\mu}{k_Bk^2}\left(1+z\right)^2\left(1+z_c\right)^4\frac{\bar{\rho}}{\rho_{\rm center}}\ .$$

An example FLASH calculation of the post-caustic gas solution appears in Figure 30.68.

Because they are collisionless, the particles behave very differently than the gas. As particles accelerate toward the midplane, their phase profile develops a backwards "S" shape. At caustic formation the velocity becomes multivalued at the midplane. The region containing multiple streams grows in size as particles pass through the midplane. At the edges of this region (the caustics, or the inflection points of the "S"), the particle density is formally infinite, although the finite force resolution of the particles keeps the height of these peaks finite. Some of the particles that have passed through the midplane fall back and form another pair of caustics, twisting the phase profile again. Because each of these secondary caustics contains five streams of particles rather than three, the second pair of density peaks are higher than the first pair. This caustic formation process repeats arbitrarily many times in the analytic solution. In practice, the finite number of particles and the finite force resolution limit the number of caustics that are observed. An example FLASH calculation of the post-caustic particle solution appears in Figure 30.69.

The 2D `pancake` problem in FLASH4 uses the runtime parameters listed in Table 30.14 in addition to the regular ones supplied with the code.

This problem uses periodic boundary conditions and is intrinsically one-dimensional, but it can be run using Cartesian coordinates in 1D, 2D, or 3D, with the pancake midplane tilted with respect to the coordinate axes if desired.

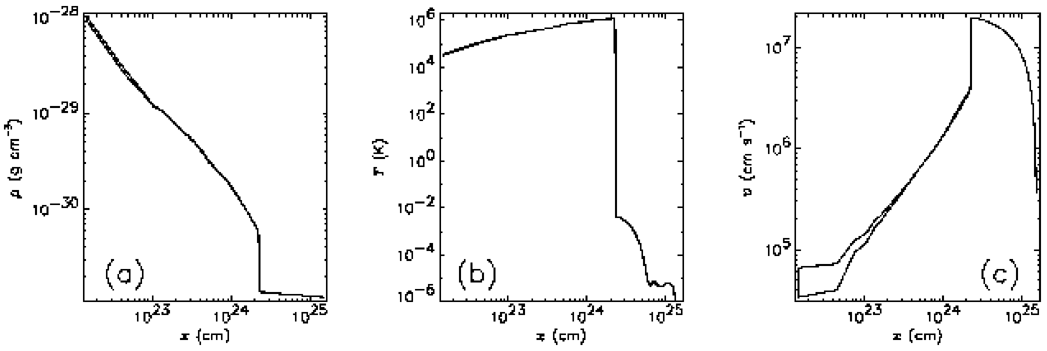

Figure 30.68: Example solution for the gas in a mixed particle/gas Zel'dovich `Pancake` problem. A comoving wavelength λ = 10 Mpc, caustic redshift z_c = 5, fiducial redshift z_fid = 200, and fiducial temperature T_fid = 550 K were used together with a Hubble constant of 50 km s^{-1} Mpc^{-1}. The cosmological model was flat with a baryonic fraction of 0.15. Results are shown for redshift $z = 0$. An adaptive mesh with an effective resolution of 1024 cells was used. Other parameters for this run were as described in the text. The distance x is measured from the pancake midplane. (a) Gas density. (b) Gas temperature. (c) Gas velocity.

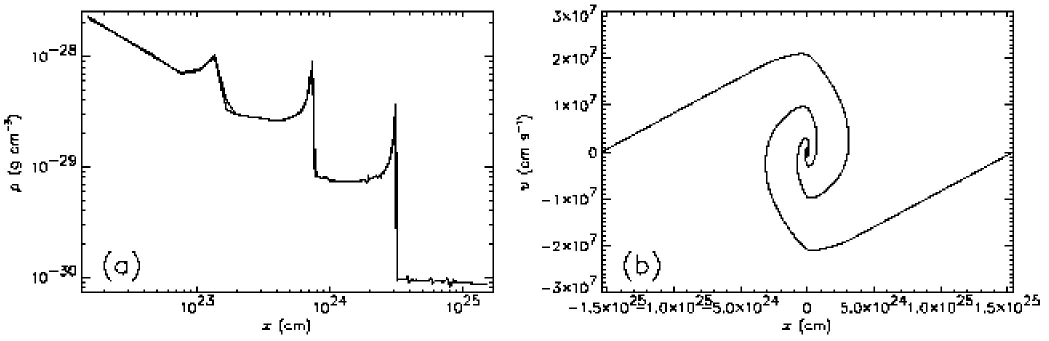

Figure 30.69: Example solution for the dark matter in a mixed particle/gas Zel'dovich pancake. Perturbation and cosmological parameters were the same as in Figure 30.68. Results are shown for redshift $z = 0$. An adaptive mesh with an effective resolution of 1024 cells was used. The number of particles used was 8192. Other parameters for this run were as described in the text. Distance x is measured from the pancake midplane. (a) Dark matter density. (b) Dark matter phase diagram showing particle positions x and velocities v.

Table 30.14: Runtime parameters used with the 2D `pancake` test problem.

Variable	Type	Default	Description
`lambda`	real	3.0857×10^{25}	Wavelength of the initial perturbation ($2\pi/k$)
`zcaustic`	real	5.	Redshift at which pancake forms a caustic (z_c)
`Tfiducial`	real	550.	Fiducial gas temperature (T_fid)
`zfiducial`	real	200.	Redshift at which gas temperature is T_fid (z_fid)
`xangle`	real	0.	Angle made by pancake normal with the x-axis (degrees)
`yangle`	real	90.	Angle made by pancake normal with the y-axis (degrees)
`pt_numX`	integer	128	Number of particles along x-side of initial particle "grid"

pt_numY	integer	128	Number of particles along y-side of initial particle “grid”
pt_numZ	integer	1	Number of particles along z-side of initial particle “grid”

30.4.3 Modified Huang-Greengard Poisson Test

The `PoisParticles` problem is designed to generate a refined grid from the distribution of particles in the computational domain. In other words, create a grid which is more refined in places where there is a clustering of particles. It is a modified form of the `PoisTest` simulation described in Section 30.3.3. Recall that the `PoisTest` problem involves the creation of a highly refined grid, which is used to test grid refinement.

In the `PoisParticles` problem, the density stored in the grid is used as an indicator of where to create new particles. Here, the number of particles created in each region of the grid is proportional to the grid density, *i.e.*, more particles are created in regions where there is a high density. Each new particle is assigned a mass, which is taken from the density in the grid, so that mass is conserved.

The `flash.par` parameters shown in Table 30.15 specify that the grid should refine until at most 5 particles exist per block. This creates a refined grid similar to the `Poistest` problem.

Table 30.15: Runtime parameters used with the `PoisParticles` test problem.

Variable	Type	Value	Description
refine_on_particle_count	logical	.true.	On/Off flag for refining the grid according to particle count.
max_particles_per_blk	integer	5	Grid refinement criterion which specifies maximum number of particles per block.

30.5 Burn Test Problem

30.5.1 Cellular Nuclear Burning

The `Cellular` Nuclear Burning problem is used primarily to test the function of the Burn simulation unit. The problem exhibits regular steady-state behavior and is based on one-dimensional models described by Chappman (1899) and Jouguet (1905) and Zel’dovich (Ostriker 1992), von Neumann (1942), and Doring (1943). This problem is solved in two dimensions. A complete description of the problem can be found in a recent paper by Timmes, Zingale et al(2000).

A 13 isotope α-chain plus heavy-ion reaction network is used in the calculations. A definition of what we mean by an α-chain reaction network is prudent. A strict α-chain reaction network is only composed of (α,γ) and (γ,α) links among the 13 isotopes ^{4}He, ^{12}C, ^{16}O, ^{20}Ne, ^{24}Mg, ^{28}Si, ^{32}S, ^{36}Ar, ^{40}Ca, ^{44}Ti, ^{48}Cr, ^{52}Fe, and ^{56}Ni. It is essential, however, to include (α,p)(p,γ) and (γ,p)(p,α) links in order to obtain reasonably accurate energy generation rates and abundance levels when the temperature exceeds $\sim 2.5\times10^{9}$ K. At these elevated temperatures the flows through the (α,p)(p,γ) sequences are faster than the flows through the (α,γ) channels. An (α,p)(p,γ) sequence is, effectively, an (α,γ) reaction through an intermediate isotope. In our α-chain reaction network, we include 8 (α,p)(p,γ) sequences plus the corresponding inverse sequences through the intermediate isotopes ^{27}Al, ^{31}P, ^{35}Cl, ^{39}K, ^{43}Sc, ^{47}V, ^{51}Mn, and ^{55}Co by assuming steady state proton flows.

The two-dimensional calculations are performed in a planar geometry of size 256.0 cm by 25.0 cm. The initial conditions consist of a constant density of 10^{7} g cm^{-3}, temperature of 2×10^{8} K, composition of pure carbon X(^{12}C)=1, and material velocity of $v_x = v_y$= 0 cm s^{-1}. Near the x=0 boundary the initial conditions are perturbed to the values given by the appropriate Chapman-Jouguet solution: a density of 4.236×10^{7} g cm^{-3}, temperature of 4.423×10^9 K, and material velocity of $v_x = 2.876\times10^8$ cm s^{-1}. Choosing different values or different extents of the perturbation simply change how long it takes for the initial conditions to achieve a near ZND state, as well as the block structure of the mesh. Each block contains 8 grid points in the x-direction, and 8 grid points in the y-direction. The default parameters for cellular burning are given in Table 30.16.

Table 30.16: Runtime parameters used with the `Cellular` test problem.

Variable	Type	Default	Description
`xhe4`	real	0.0	Initial mass fraction of He4
`xc12`	real	1.0	Initial mass fraction of C12
`xo16`	real	0.0	Initial mass fraction of O16
`rhoAmbient`	real	1×10^7	Density of cold upstream material.
`tempAmbient`	real	2×10^8	Temperature of cold upstream material.
`velxAmbient`	real	0.0	X-velocity of cold upstream material.
`rhoPerturb`	real	4.236×10^7	Density of the post shock material.
`tempPerturb`	real	4.423×10^9	Temperature of the post shock material.
`velxPerturb`	real	2.876×10^8	X-velocity of the post shock material.
`radiusPerturb`	real	25.6	Distance below which the perturbation is applied.
`xCenterPerturb`	real	0.0	X-position of the origin of the perturbation
`yCenterPerturb`	real	0.0	Y-position of the origin of the perturbation
`zCenterPerturb`	real	0.0	Z-position of the origin of the perturbation
`usePseudo1d`	logical	`.false.`	Defaults to a spherical configuration. Set to `.true.` if you want to use a 1d configuration, that is copied in the y and z directions.
`noiseAmplitude`	real	1.0×10^{-2}	Amplitude of the white noise added to the perturbation.
`noiseDistance`	real	5.0	The distance above the starting radius to which white noise is added.

The initial conditions and perturbation given above ignite the nuclear fuel, accelerate the material, and produce an over-driven detonation that propagates along the x-axis. The initially over-driven detonation is damped to a near ZND state on short time-scale. After some time, which depends on the spatial resolution and boundary conditions, longitudinal instabilities in the density cause the planar detonation to evolve into a complex, time-dependent structure. Figure 30.70 shows the pressure field of the detonation after 1.26×10^{-7} s. The interacting transverse wave structures are particularly vivid, and extend about 25 cm behind the shock front. Figure 30.71 shows a close up of this traverse wave region. Periodic boundary conditions are used at the walls parallel to the y-axis while reflecting boundary conditions were used for the walls parallel to the x-axis.

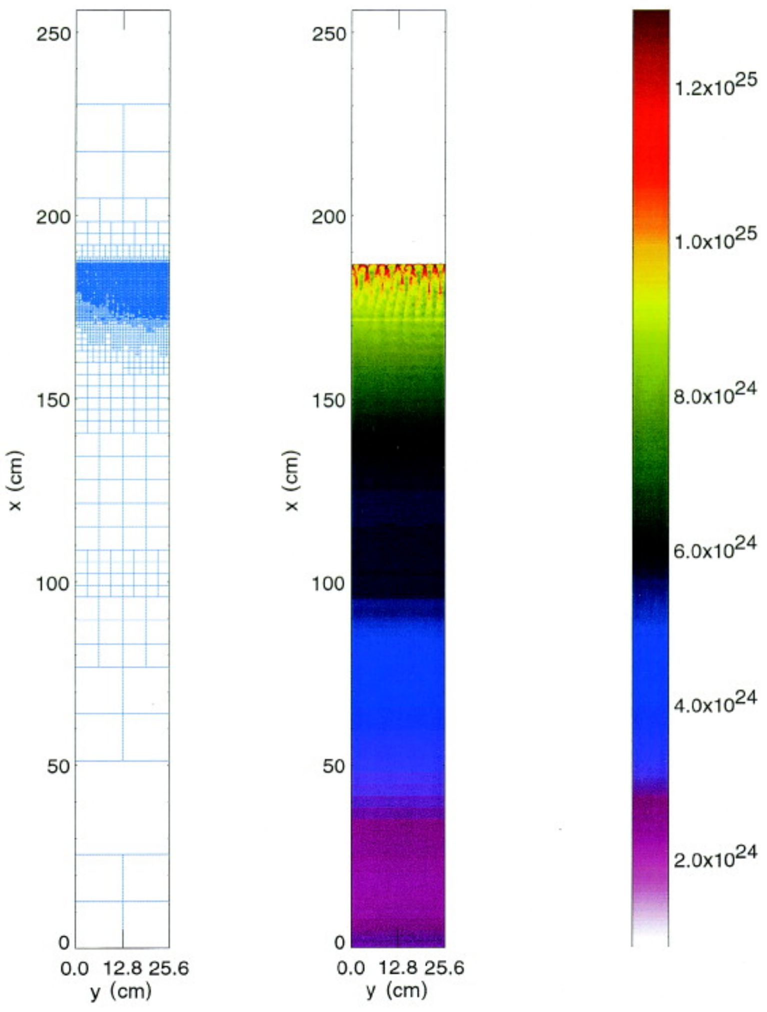

Figure 30.70: Steady-state conditions of the `Cellular` nuclear burn problem.

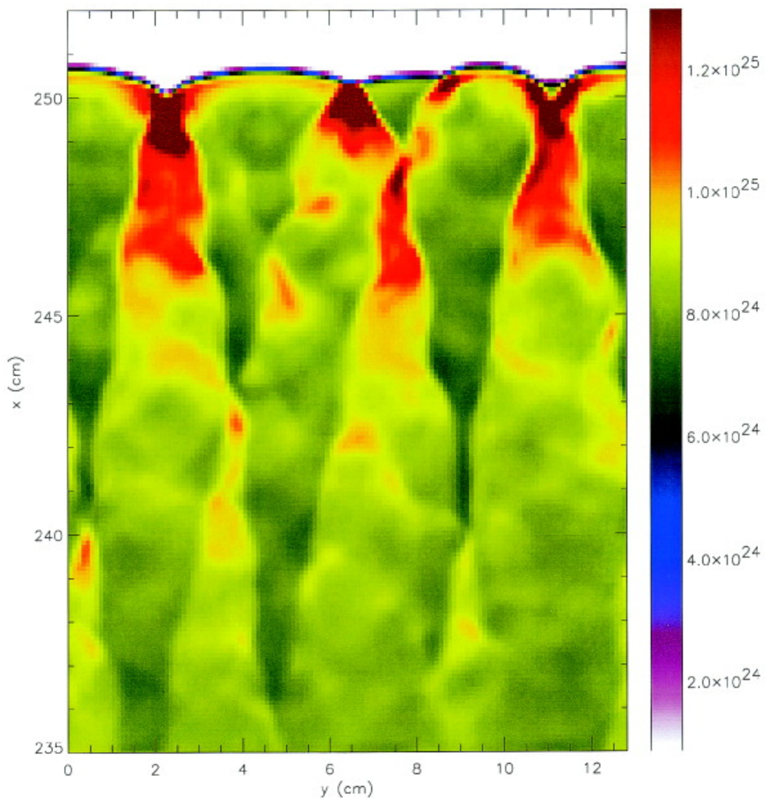

Figure 30.71: Close-up of the detonation front in steady-state for the `Cellular` nuclear burn problem.

30.6 RadTrans Test Problems

There are currently two simulations included in FLASH which involve the `RadTrans` unit with multigroup diffusion. These simulations are not comparisons to analytic solutions - instead they are simple tests designed to demonstrate the correct usage of the multigroup diffusion capability in FLASH.

30.6.1 Infinite Medium, Energy Equilibration

The simulation directory for this test is `MGDInfinite`. This is a fairly simple simulation which has no spatial gradients. Separate ion/electron/radiation temperatures are set throughout the domain initially. Over time, the temperatures should approach one another. The electrons and the radiation field exchange energy through emission and absorption, and the `HeatExchange` unit controls the rate at which the electrons and ions equilibrate with one another. The radiation field is represented using four radiation energy groups.

A sample setup line is:

```
./setup -auto MGDInfinite -1d +hdf5typeio +mtmmmt +mgd +uhd3t \
        -with-unit=physics/materialProperties/Opacity/OpacityMain/Constant \
        species=be,poli,xe mgd_meshgroups=4
```

Figure 30.72 shows the temperatures as a function of time.

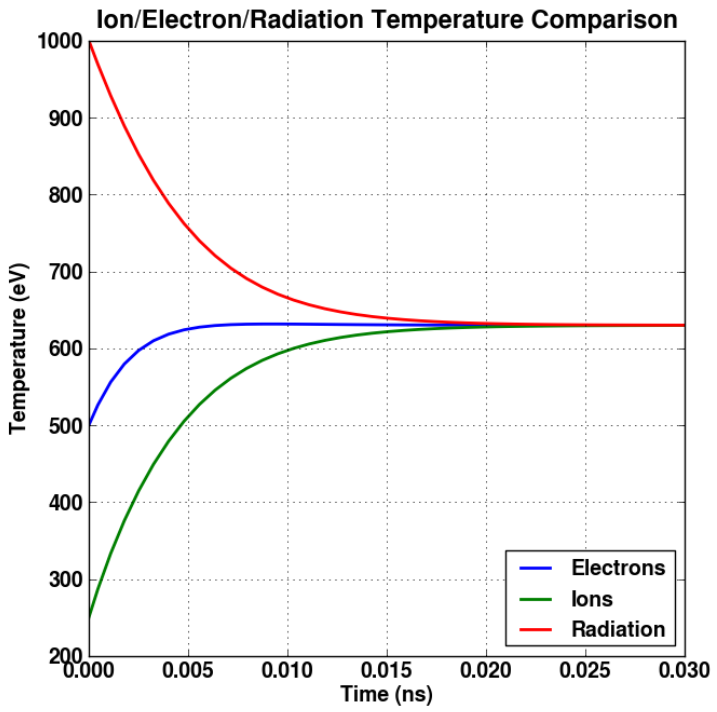

Figure 30.72: Temperatures as a function of time for the Infinite medium, Energy Equilibration simulation

30.6.2 Radiation Step Test

The simulation directory for this test is `MGDStep`. This simulation involves four group radiation diffusion and electron conduction. A constant opacity is used in this simulation. The transport opacity is set to a very small value to simulate a vacuum. This is a 1D test where the initial electron and radiation temperatures are discontinuous. Flux limiters are used for both the electrons and radiation. Over time, energy flows from the hotter region to the colder region. At the same time, the radiation temperature decreases as energy is absorbed by the electrons. Figure 30.73 shows the final temperature profiles for this simulation. There is a relatively sharp drop-off for each curve caused by the use of flux limiters. The drop-off can be made sharper by increasing the number of cells used in the simulation.

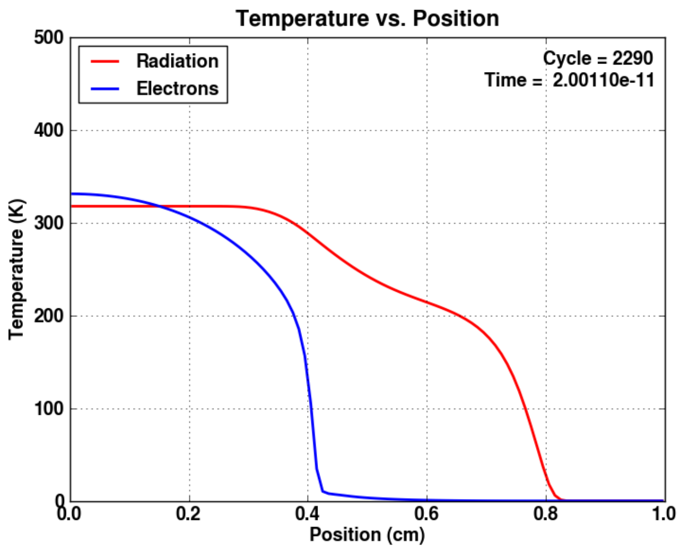

Figure 30.73: Radiation and electron temperatures as a function of position for the `MGDStep` at 20 ps.

30.7 Other Test Problems

30.7.1 The non-equilibrium ionization test problem

The `neitest` problem tests the ability of FLASH to calculate non-equilibrium ionization (NEI) ion abundances. It simulates a stationary plasma flow through a temperature step profile. The solutions were checked using an independent stationary code based on a fifth order Runge–Kutta method with adaptive stepsize control by step-doubling (see Orlando *et al.* (1999)).

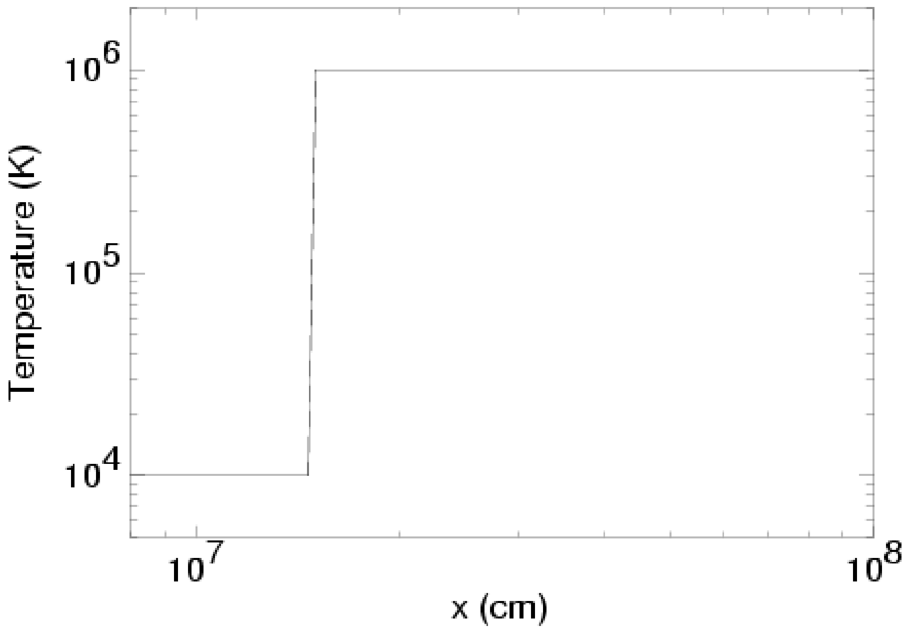

Figure 30.74: Temperature profile assumed for the test.

The test assumes a plasma with a mass density of 2×10^{-16} gm cm^{-3} flowing with a constant uniform velocity of 3×10^5 cm s^{-1} through a temperature step between 10^4 K and 10^6 K (*cf.* Figure 30.74). The plasma is in ionization equilibrium before going through the jump in the region at $T = 10^4$ K. The population fractions in equilibrium are obtained from the equations

$$[n_i^Z]_{eq} S_i^Z = [n_{i+1}^Z]_{eq} \alpha_{i+1}^Z \quad (i = 1, ..., l_Z - 1) \tag{30.55}$$

$$\sum_{i=1}^{l_Z} [n_i^Z]_{eq} = A_Z n_p \tag{30.56}$$

The presence of a temperature jump causes a strong pressure difference, which in turn should cause significant plasma motions. Since the purpose is to test the NEI module, it is imposed that the pressure difference does not induce any plasma motion and, to this end, the hydro variables (namely, T, ρ, $\mathbf{v}$) are not updated. In practice, the continuity equations are solved with uniform density and velocity, while the momentum and energy equations are ignored.

Figure 30.75 shows the population fractions for the 12 most abundant elements in astrophysical plasmas derived with the stationary code (Orlando *et al.* (1999)). The out of equilibrium ionization conditions are evident for all the elements just after the flow goes through the temperature jump.

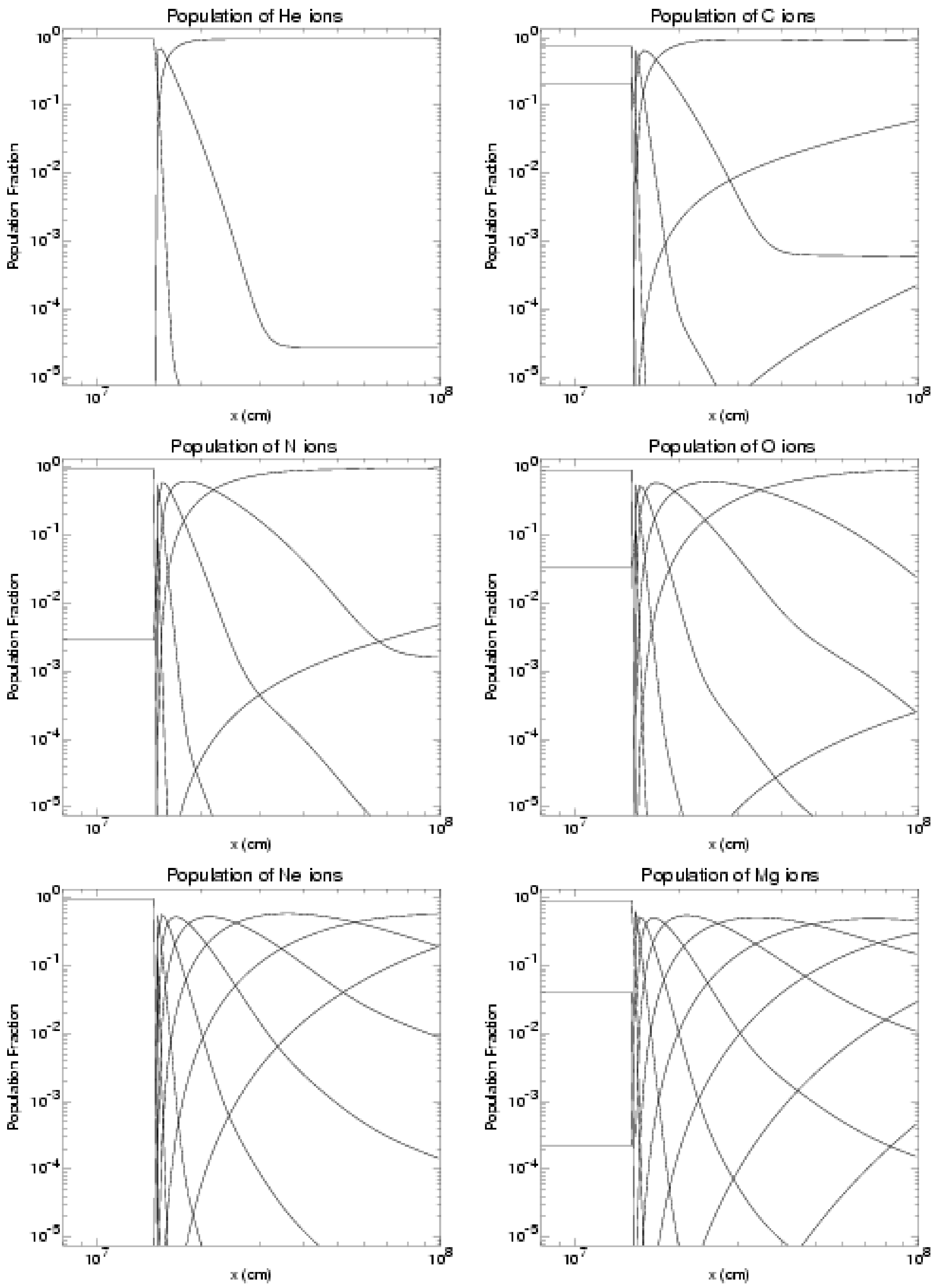

Figure 30.75: Numerical solutions of the stationary code. The figure shows the population fractions vs. space for the 12 elements most abundant in astrophysical plasmas assuming a stationary flow through a temperature jump.

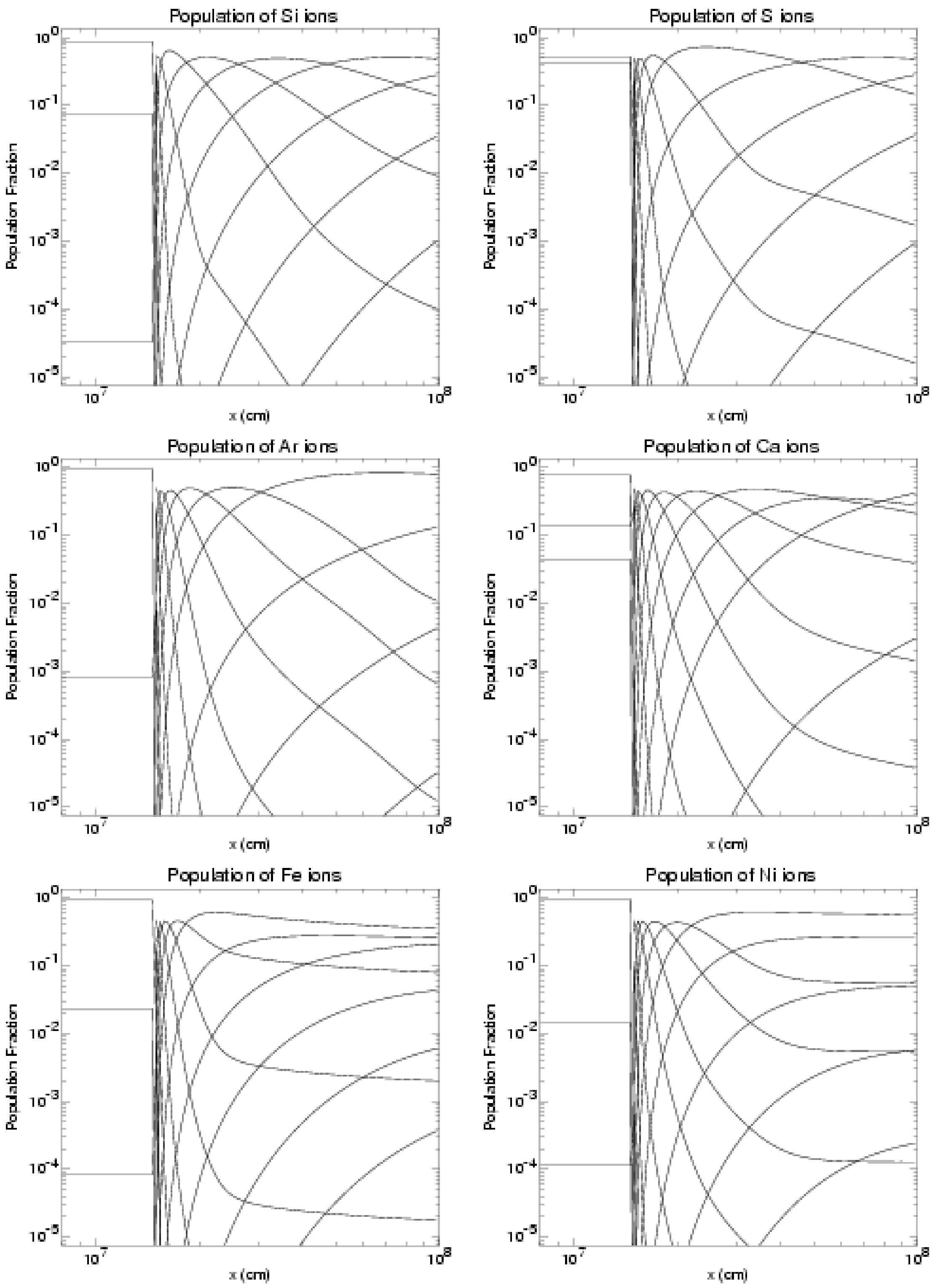

Figure 30.75: ... continued ...

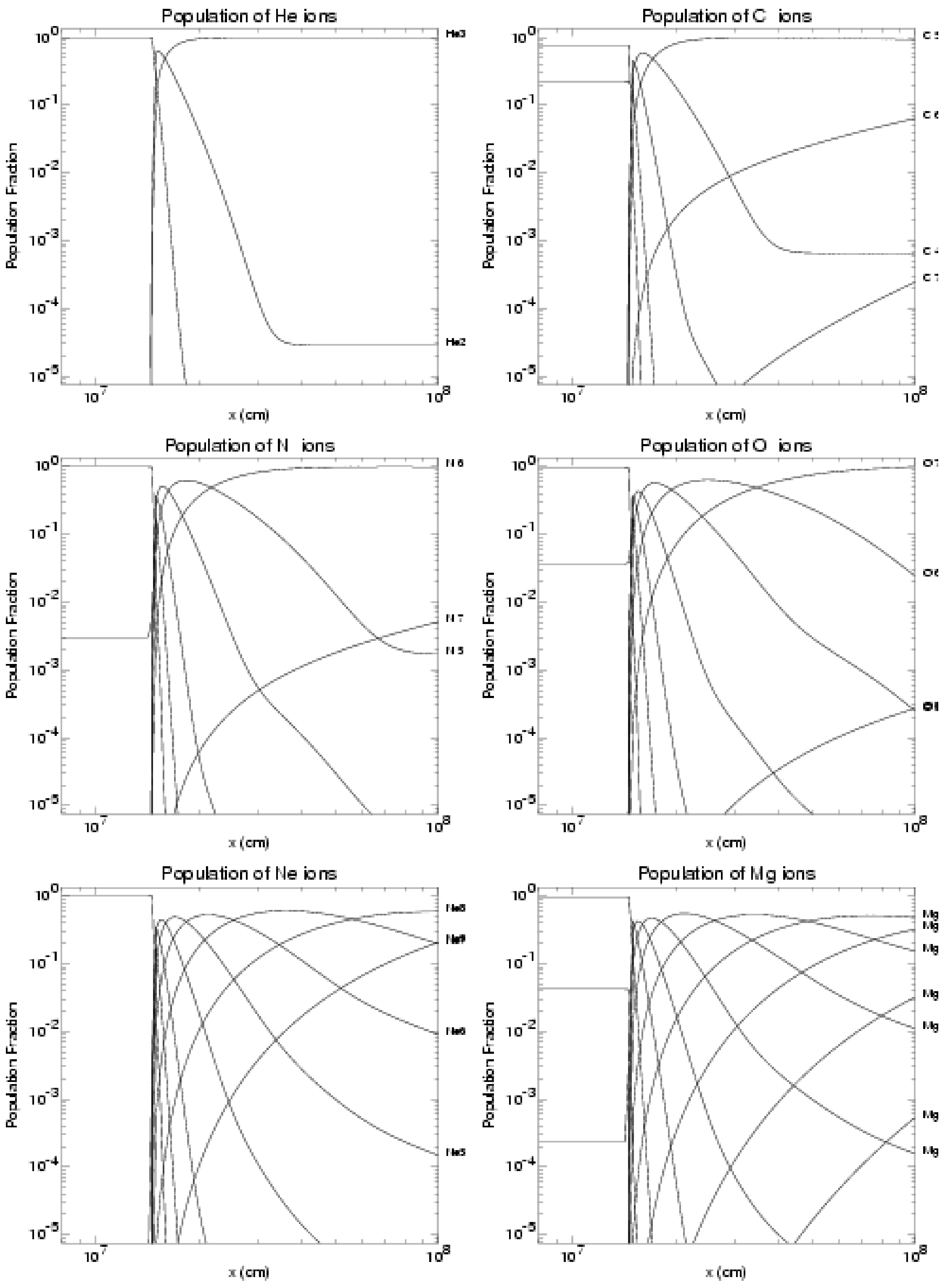

Figure 30.76: As in Figure 30.75 for the solutions of the FLASH code.

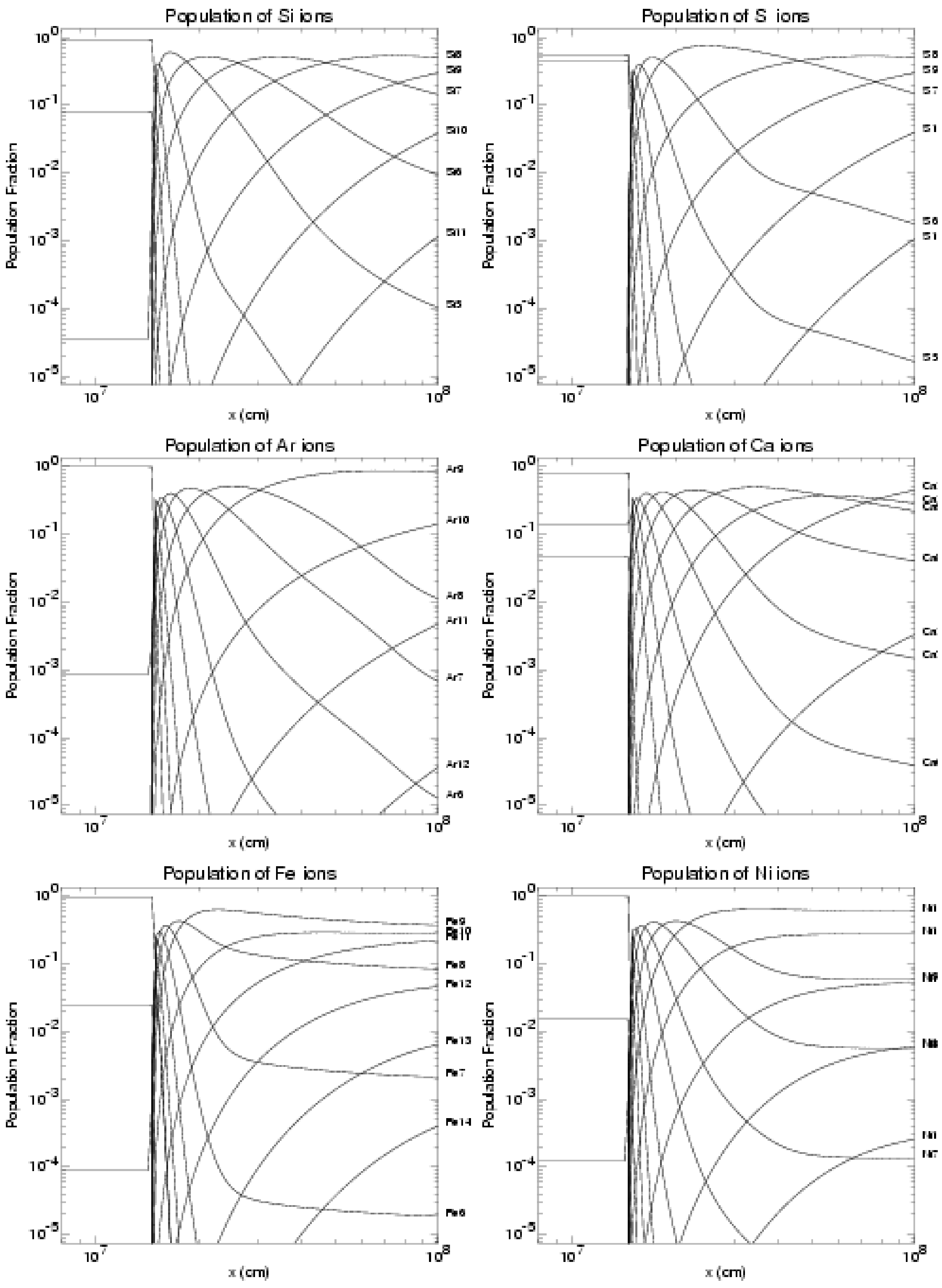

Figure 30.76: ... continued ...

The same problem was solved with the NEI module of the FLASH code, assuming that the plasma is initially in ionization equilibrium at $t = t_0$ over all the spatial domain. After a transient lasting approximately 700 s, in which the population fractions evolve due to the plasma flow through the temperature jump, the system reaches the stationary configuration. Outflow boundary conditions (zero-gradient) are assumed at both the left and right boundaries. Figure 30.76 shows the population fraction vs. space after 700 s.

30.7.2 The Delta-Function Heat Conduction Problem

The `ConductionDelta` problem tests the basic function of the `Diffuse` unit, in particular its use for thermal conduction, in connection with the `Conductivity` material property unit. It can be easily modified to examine the effects of Viscosity, of non-constant conductivity, and of combining these diffusive effects with hydrodynamics.

In its default configuration, `ConductionDelta` models the time development of a temperature peak that at some time $t_{\rm ini}$ has the shape of a delta function in 1D or 3D, subject to heat conduction (with constant coefficient) only. An ideal gas EOS is assumed. When using a flux-based `Diffuse` interface, the setup includes the `Hydro` code unit, but changes of the solution due to hydrodynamical effects are completely suppressed by zeroing all hydrodynamic fluxes each time before diffusive fluxes are computed (using `updateHydroFluxes` = `.FALSE.`); diffusive fluxes are then computed either by calling `Diffuse_therm` (in the `+splitHydro` case) or by an calling an internal routine (such as `hy_uhd_addThermalFluxes`) of the `Hydro` unit.

The theoretical solution of this initial value problem is known: For any $t > t_{\rm ini}$, the temperature profile is a Gaussian that spreads self-similarly over time. In particular in 1D, if the initial condition is defined as

$$T(x, t_{\rm ini}) = Q\delta(x) \quad , \tag{30.57}$$

then

$$T(x,t) = \frac{Q}{(4\pi\chi(t - t_{\rm ini}))^{1/2}} e^{-x^2/4\chi(t-t_{\rm ini})} \tag{30.58}$$

(with χ the constant coefficient of diffusivity), see for example Zel'dovich and Raizer Ch. X.

See the end of Section 18.1 for alternative ways of configuring the test problem, using either a flux-based or a standalone `Diffuse` interface.

30.7.3 The HydroStatic Test Problem

The `Hydrostatic` problem tests the basic function of hydrostatic boundary conditions implemented in the `Grid` unit, in connection with a `Hydro` implementation. It is essentially a 1D problem, but can be configured as 1 1D, 2D, or 3D setup. It can be easily modified to include additional physical effects, by including additional code units in the setup.

In its default configuration, `HydroStatic` is set up with constant `Gravity`. The domain is initialized with density, pressure, *etc.*, fields representing an analytical solution of the hydrostatic problem with the given gravitational acceleration, essentially following the barometric formula.

This initial condition is then evolved in time. Ideally, the solution would remain completely static, and nothing should move. The deviation from this ideal behavior that occurs in practice is a measure of the quality of the discretization of the initial condition, of the hydrodynamics implementation, and of the boundary conditions. The effect of the latter, in particular, can be examined by visualizing artifacts that develop near the boundaries (in particular, velocity artifacts), and studying their dependence on the choice of boundary condition variant.

30.7.4 Hybrid-PIC Test Problems

A classic plasma model problem is that of an ion beam into a plasma (Winske 1986). Work by Matthew (1994) describes a two-dimensional simulation of a low density ion beam through a background plasma. The initial condition has a uniform magnetic field, with a beam of ions, number density n_b, propagating along the field with velocity $v_b = 10v_A$, where $v_A = B/\sqrt{\mu_0 n m_i}$ is the Alfvén velocity, through a background (core) plasma of number density n_c. Both the background and beam ions have thermal velocities $v_{th} = v_A$. Here

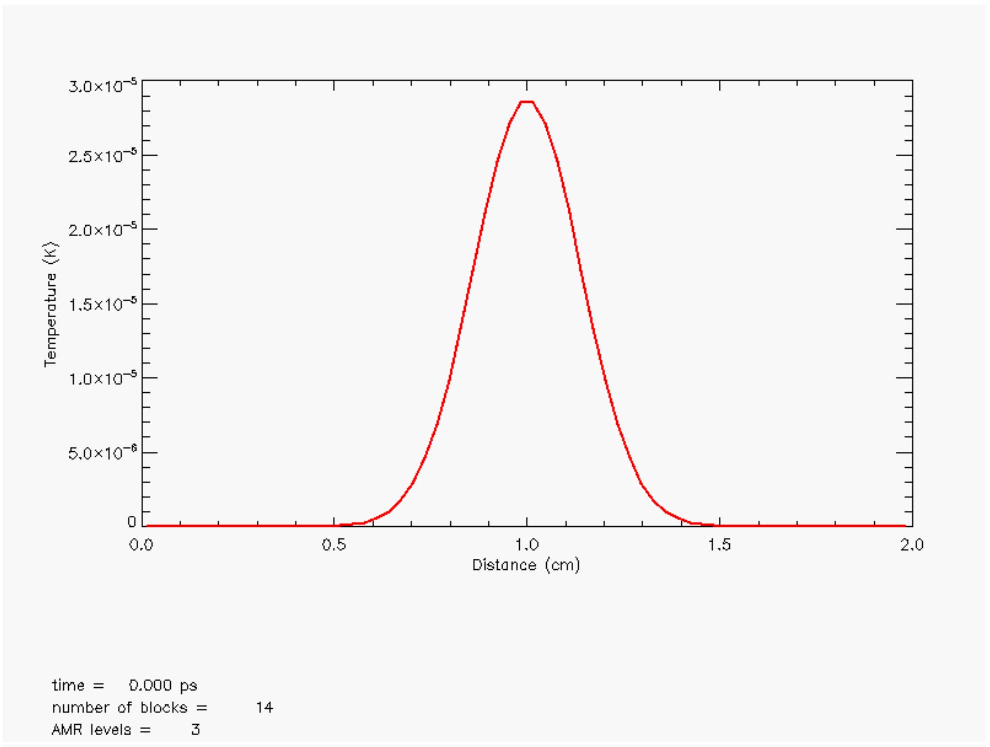

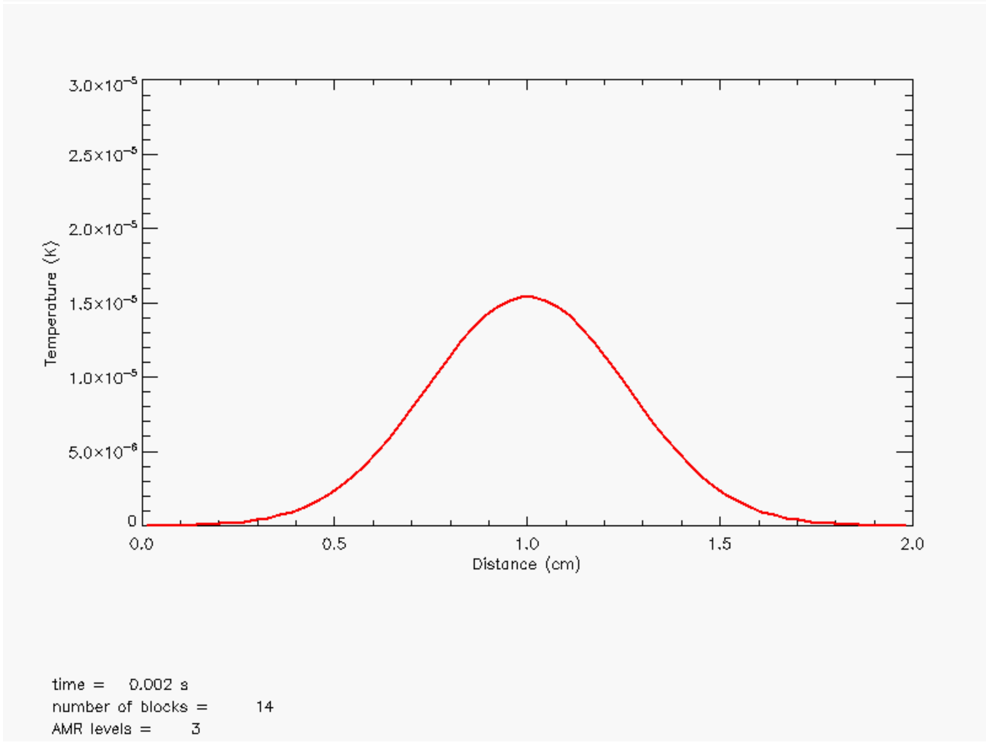

Figure 30.77: Temperature profile of the Delta-Function Heat Conduction Problem at two times. $t\_\mathrm{ini} = -1\,\mathrm{ms}$, top: $t = 0\,\mathrm{ms}$, bottom: $t = 2.46\,\mathrm{ms}$.

we study what is denoted a *resonant beam* with $n_b = 0.015\,n_c$ and $v_c = -0.2\,v_A$. Electron temperature is assumed to be zero, so the electron pressure term in the electric field equation of state is zero. The weight of the macroparticles are chosen such that there is an equal number of core and beam macroparticles, each beam macroparticles thus represent fewer real ions than the core macroparticles. The number of magnetic field update subcycles is nine.

30.7.4.1 One-dimensional ion beam

The spatial extent of the domain is 22016 km along the x-axis, divided up in 256 cells with periodic boundary conditions. The core number density is $n_c = 7$ cm^{-3}. The magnetic field magnitude is $B = 6$ nT directed along the x-axis, which give an Alfvén velocity of 50 km/s and an ion inertial length of δ_i=86 km, where $\delta_i = v_A/\Omega_i$ and $\Omega_i = q_i B/m_i$ is the ion gyrofrequency. The time step is 0.0865 s = $0.05\,\Omega_i^{-1}$, and the cell size is δ_i. The number of particles per cell is 32. In Fig. 30.78 we show a velocity space plot of the macro-ions at time $t = 34.6$ s $\approx 20\,\Omega_i^{-1}$. This can be compared to Fig. 5 in Winske (1984).

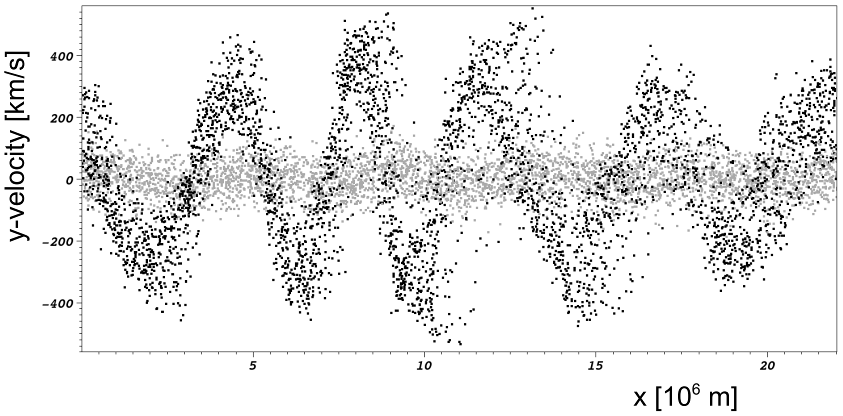

Figure 30.78: Velocity space plot for a one-dimensional ion beam. Velocity along the y-axis as a function of position at time $t = 34.6$ s $\approx 20\,\Omega\_i^{-1}$. Each gray dot is a core macro-ion, and each black dot is a beam macro-ion.

30.7.4.2 Two-dimensional ion beam

In the two-dimensional case we have a square grid with sides of length 22016 km, and 128 cells in each direction with periodic boundary conditions. The time step is 0.0216 s = $0.05\,\Omega_i^{-1}$, and the cell widths are $2\delta_i$. The number of particles per cell is 16. Otherwise the setup is identical to the one-dimensional case. In Fig. 30.79 we show the magnitude of the magnetic field y-component at time $t = 77.85$ s $\approx 46\,\Omega_i^{-1}$. This can be compared to Fig. 5 in Winske (1986).

30.7.5 Full-physics Laser Driven Simulation

The `LaserSlab` simulation provides an example of how to run a realistic, laser driven, simulation of an HEDP experiment. It exercises a wide range of HEDP physics including:

- 3T unsplit hydrodynamics in $R - z$ geometry
- Electron thermal conduction with Spitzer conductivities
- Ion/electron equilibration
- Radiation Diffusion with tabulated opacity
- Laser Ray Tracing
- Tabulated Equation of State

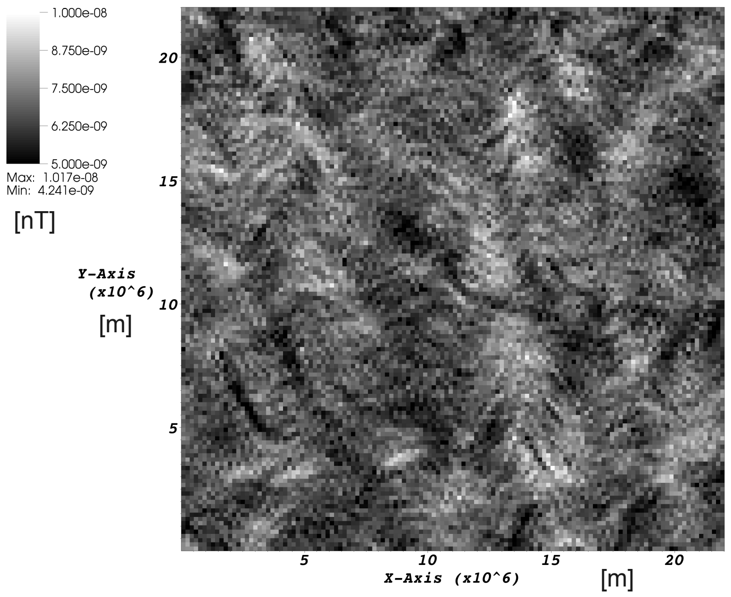

Figure 30.79: The magnetic field y-component for a two-dimensional ion beam at time $t = 77.85\text{ s} \approx 46\,\Omega\_i^{-1}$.

This simulation has no analytic solutions associated with it. Rather, it is designed to demonstrate the HEDP capabilities that are available in FLASH.

The simulation models a single laser beam illuminating a solid Aluminum disc in $R - z$ geometry. The laser is focused on the z-axis and enters the domain at a 45 degree angle. The simulation contains two materials (or "species" in FLASH terminology). These are called `CHAM` (short for chamber) and `TARG` (short for target). The `TARG` species models the Aluminum disc. The laser travels through a low density Helium region before reaching the Aluminum. The properties of the `CHAM` species are set to model the low density Helium. A schematic showing the initial conditions is shown in Figure 30.80. The laser rays enter just above the lower-right corner of the domain and travel until they are absorbed or reflected. The beam intensity is not uniform across the beam cross section. Rather, it has a super-Gaussian intensity profile with a 10 micron spot radius.

The following setup line is used for this simulation:

```
./setup -auto LaserSlab -2d -nxb=16 -nyb=16 +hdf5typeio \
        species=cham,targ +mtmmmt +laser +uhd3t +mgd mgd_meshgroups=6 \
        -parfile=example.par
```

where:

- `-2d` and `+cylindrical` tells FLASH that this is a 2D simulation
- `-nxb=16` and `-nyb=16` sets the AMR block size to 16 by 16
- `+hdf5typeio` enables a newer version of IO that writes to HDF5 files. `HDF5TypeIO` is faster that other IO implementations in FLASH and is also more user friendly when generating figures using external tools, such as VisIt.
- `species=cham,targ` Creates two species named `CHAM` and `TARG` using the setup argument *instead of* the `SPECIES` keyword in the `Simulation Config` file. This is required for using the Multispecies opacity unit and is more user friendly since it allows many options to be specified in the runtime parameters file. See Section 11.4 for more information.

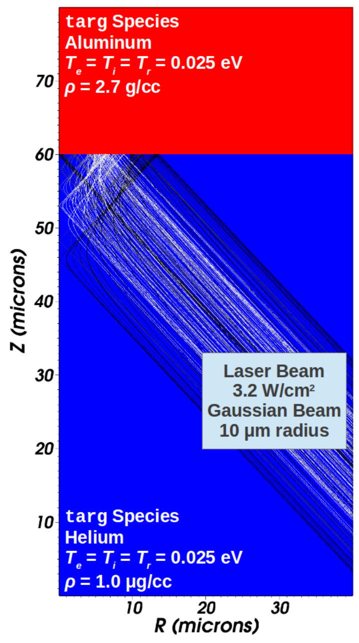

Figure 30.80: Schematic showing the initial conditions in the `LasSlab` simulation.

- `+mtmmmt` Activates the Multi-Temperature, Multi-Material, Multi-Type EOS in FLASH. This EOS lets users select a different EOS model (such as gamma-law or tabulated) for each species in the simulation through the runtime parameters file. (see)
- `+laser` Activates laser ray tracing (see Section 17.4).
- `+mgd` and `mgd_meshgroups=6` activates multigroup radiation diffusion and tells FLASH that there will be *maximum* of six groups per mesh (see Chapter 24)
- `+uhd3t` Activates the 3T unsplit hydro solver (see Section 14.1.4)
- `-parfile=example.par` Chooses a parameter file that is different than the default

The remainder of this section will describe how each physics unit functions and how the runtime parameters are chosen for this simulation. Images of the results will also be shown at the end of this section.

30.7.5.1 Initial Conditions and Material Properties

The section “Initial Conditions” section in the runtime parameter file, “example.par”, sets parameters which define the initial state of the fluid and also set the properties of the materials. The first runtime parameters in this section are:

```
sim_targetRadius = 200.0e-04
sim_targetHeight = 20.0e-04
sim_vacuumHeight = 60.0e-04
```

These options define the space occupied by the target material (the `targ` species, Aluminum for this simulation). The Aluminum disc extends from:

$$0 < R < \texttt{sim\_targetRadius} \;\text{ and} \tag{30.59}$$

$$\texttt{sim\_vacuumHeight} < z < \texttt{sim\_vacuumHeight} + \texttt{sim\_targetHeight}, \tag{30.60}$$

where all parameters are in centimeters.

The next section sets the initial fluid state in the target region and also sets the properties of the targ species to match Aluminum. The relevant options are:

```
# Target material defaults set for Aluminum at room temperature:
sim_rhoTarg  = 2.7                   # Set target material density (solid Al)
sim_teleTarg = 290.11375             # Set initial electron temperature
sim_tionTarg = 290.11375             # Set initial ion temperature
sim_tradTarg = 290.11375             # Set initial radiation temperature
ms_targA = 26.9815386                # Set average atomic mass
ms_targZ = 13.0                      # Set average atomic number
ms_targZMin = 0.02                   # Set minimum allowed ionization level
eos_targEosType = "eos_tab"          # Set EOS model to tabulated EOS
eos_targSubType = "ionmix4"          # Set EOS table file to IONMIX 4 format
eos_targTableFile = "al-imx-003.cn4" # Set tabulated EOS file name
```

The initial density is chosen to match solid Aluminum. The initial ion, electron, and radiation temperatures are set to room temperature (290 K, 0.025 eV). The runtime parameters ms_targA and ms_targZ set the average atomic mass and atomic number of the targ species. Note that in the past, this information was specified by modifying the Simulation_initSpecies subroutine. This information can now be specified using runtime parameters since the species=cham,targ setup variable was used (see Section 11.4 for more information). The parameter ms_targZMin sets the minimum ionization level for targ. Without this parameter, the initial ionization would be nearly zero and the slab would be subcritical with respect to the laser light. The laser rays would penetrate deeply into the slab and could possible travel through it with no heating. This can be avoided by putting a lower limit on the ionization level. The final three parameters control the behavior of the MTMMMT EOS with respect to targ. The option eos_targEosType sets the EOS model to use for the Aluminum. In this case, we have chosen to use a tabulated EOS which is in the IONMIX4 format. Finally, we specify the name of the file which contains the EOS data. The file "al-imx-003.cn4" can be found in the LaserSlab simulation directory in the source tree. The IONMIX4 format, described in Section 22.4.6, is not human readable. However, the file "al-imx-003.imx.gz" contains a human readable representation of this EOS and opacity data.

A similar set of runtime parameter options exist for the cham species:

```
# Chamber material defaults set for Helium at pressure 1.6 mbar:
sim_rhoCham  = 1.0e-05
sim_teleCham = 290.11375
sim_tionCham = 290.11375
sim_tradCham = 290.11375
ms_chamA = 4.002602
ms_chamZ = 2.0
eos_chamEosType = "eos_tab"
eos_chamSubType = "ionmix4"
eos_chamTableFile = "he-imx-005.cn4"
```

The initial Helium density, sim_rhoCham is chosen to be fairly low. This ensures that the Helium remains relatively transparent to the laser light (see Section 17.4.2 for a description of how the laser energy absorption coefficient is computed).

For both the targ and cham species, the initial state of the fluid is defined using a density with three temperatures. The initial EOS mode is set using the eosModeInit runtime parameter. It is set to "dens_temp_gather". This tells FLASH that the initial state will be specified using the density and the temperature.

30.7.5.2 Multigroup Radiation Diffusion Parameters

This simulation uses multigroup radiation diffusion (MGD) to model the radiation field. This involves setting parameters which control the MGD package itself and setting parameters which control how opacities for the two species are computed. The MGD settings from the parameter file are:

```
rt_useMGD       = .true.
rt_mgdNumGroups = 6
rt_mgdBounds_1  = 1.0e-01
rt_mgdBounds_2  = 1.0e+00
rt_mgdBounds_3  = 1.0e+01
rt_mgdBounds_4  = 1.0e+02
rt_mgdBounds_5  = 1.0e+03
rt_mgdBounds_6  = 1.0e+04
rt_mgdBounds_7  = 1.0e+05
rt_mgdFlMode    = "fl_harmonic"
rt_mgdFlCoef    = 1.0

rt_mgdXlBoundaryType = "reflecting"
rt_mgdXrBoundaryType = "vacuum"
rt_mgdYlBoundaryType = "vacuum"
rt_mgdYrBoundaryType = "reflecting"
rt_mgdZlBoundaryType = "reflecting"
rt_mgdZrBoundaryType = "reflecting"
```

The first option turns on MGD. The second parameter sets the number of radiation energy groups in the simulation, six in this case. Note that this number must be less than or equal to the value of the `mgd_meshgroups` setup variable. This restriction can be relaxed through the use of mesh replication (see Section 24.1.2). The runtime parameters beginning with `rt_mgdBounds_` define the group boundaries for each energy group in electron-volts. The parameters `rt_mgdFlMode` and `rt_mgdFlCoef` set the flux limiter coefficient (see Section 18.1.3 and Section 24.1 for more information). The final six parameters set the boundary conditions for all groups.

The next set of parameters tell FLASH how to compute opacities for each material. In general, the total cell opacity is a number density weighted average of the opacity of each species in the cell. The parameters which control the behavior of the opacity unit for this simulation are:

```
useOpacity     = .true.

### SET CHAMBER (HELIUM) OPACITY OPTIONS ###
op_chamAbsorb   = "op_tabpa"
op_chamEmiss    = "op_tabpe"
op_chamTrans    = "op_tabro"
op_chamFileType = "ionmix4"
op_chamFileName = "he-imx-005.cn4"

### SET TARGET (ALUMINUM) OPACITY OPTIONS ###
op_targAbsorb   = "op_tabpa"
op_targEmiss    = "op_tabpe"
op_targTrans    = "op_tabro"
op_targFileType = "ionmix4"
op_targFileName = "al-imx-003.cn4"
```

The first parameter tells FLASH that opacities will be computed. The next five parameters control how opacities are computed for the `cham` species (Helium) and the final five control the `targ` species (Aluminum). These options tell FLASH to use the IONMIX4 formatted opacity file "he-imx-005.cn4" for Helium and "al-imx-003.cn4" for Aluminum. Section 22.4.5.1 provides a detailed description of how these parameters are used. Note that the number of groups and group structure in these opacity files must be consistent with the `rt_mgdNumGroups` and `rt_mgdBounds` parameters that were described above.

30.7.5.3 Laser Parameters

This section describes the runtime parameters which control the behavior of the laser in FLASH. Modeling laser energy deposition using ray tracing is fairly complicated and requires large numbers of input parameters. It is highly recommended that you read through the section describing the behavior of the laser model in FLASH to learn more about how the ray tracing algorithms actually work (see Section 17.4).

This simulation uses a single laser beam which travels at an angle of 45 degrees from the z-axis. The "Laser Parameters" section of the runtime parameters file contains all of the options relevant to defining the laser beam. The first set of parameters are:

```
useEnergyDeposition = .true. # Turn on laser energy deposition
ed_maxRayCount      = 10000  # Set maximum number of rays/cycle/proc to 2000
ed_gradOrder        = 2      # Turn on laser ray refraction
```

The first parameter activates the laser model.

The `ed_maxRayCount` parameter sets the maximum number of rays which can be stored on a given process at once. It tells FLASH how much space to set aside for storing rays. In the case of a single process simulation, `ed_maxRayCount` must be less than the total number of rays launched on each cycle. The total number of rays launched is set by the `ed_numRays_###` parameters, described below. Finally, the parameter `ed_gradOrder` controls how the electron number density and temperature are interpolated within a cell. A value of two specifies linear interpolation.

The next set of parameters are:

```
ed_laser3Din2D           = .true.
ed_laser3Din2DwedgeAngle = 0.1
```

Setting `ed_laser3Din2D` to `.true.` activates the 3D-in-2D ray trace algorithm. This means that in this simulation, the beams are defined in 3D geometry and the laser rays are traced in 3D. The total energy deposited is then projected back on the $R - z$ plane. This can significantly improve the accuracy of the ray trace when compared to 2D-in-2D ray-tracing. The exception to this is the case of a single beam centered on the z-axis and traveling along the z axis. In this case, there is no difference between 3D-in-2D and 2D-in-2D ray tracing algorithms. In this example, the rays travel at a 45 degree angle. Thus, the 3D-in-2D ray-trace is needed. When using the 3D-in-2D ray trace, `ed_laser3Din2DwedgeAngle` sets the wedge angle. It should be set to a number between 0.1 and 1.0 degrees. See Section 17.4.8.

The next set of parameters are:

```
ed_useLaserIO             = .true.
ed_laserIOMaxNumPositions = 10000
ed_laserIONumRays         = 128
```

These parameters make use of the LaserIO package in FLASH for visualizing laser rays (see Section 17.4.10.4). These options tell FLASH to write out the trajectory of 128 rays to the plot files. The runtime parameter `plotFileIntervalStep` is set to 100 which tells FLASH to write plot files every 10 cycles. Later in this section, instructions and examples for plotting the laser ray data will be presented.

Next, a single laser pulse is defined. Each laser pulse (in this case, there is only one) represents a specific time history of the power and multiple pulses can be defined. The `LaserSlab` simulation has only a single laser beam which uses laser pulse number 1. The relevant runtime parameter options are:

```
# Define Pulse 1:
ed_numberOfSections_1 = 4
ed_time_1_1  = 0.0
ed_time_1_2  = 0.1e-09
ed_time_1_3  = 1.0e-09
ed_time_1_4  = 1.1e-09

ed_power_1_1 = 0.0
ed_power_1_2 = 1.0e+09
ed_power_1_3 = 1.0e+09
ed_power_1_4 = 0.0
```

The laser pulse is defined as a piecewise linear function. The parameter `ed_numSections_1` is set to four, meaning the laser power is defined using four different time/power points. The four time and power pairs are defined using the `ed_time_1_#` and `ed_power_1_#` parameters where the times are in seconds and the powers are specified in Watts. In this case a square pulse is defined with a gradual rise, termination over 0.1 ns. The peak power is 10^9 W and the pulse lasts for a total of 1.1 ns.

The next set of parameters define the laser beam itself. The trailing _1 in the parameter names indicate that these parameters are associated with the first beam (in this case, the only beam):

```
ed_lensX_1                     =  1000.0e-04
ed_lensY_1                     =  0.0e-04
ed_lensZ_1                     = -1000.0e-04
ed_lensSemiAxisMajor_1         =  10.0e-04
ed_targetX_1                   =  0.0e-04
ed_targetY_1                   =  0.0e-04
ed_targetZ_1                   =  60.0e-04
ed_targetSemiAxisMajor_1       =  10.0e-04
ed_targetSemiAxisMinor_1       =  10.0e-04
ed_pulseNumber_1               =  1
ed_wavelength_1                =  1.053
ed_crossSectionFunctionType_1 = "gaussian2D"
ed_gaussianExponent_1          =  4.0
ed_gaussianRadiusMajor_1       =  7.5e-04
ed_gaussianRadiusMinor_1       =  7.5e-04
ed_numberOfRays_1              =  4096
ed_gridType_1                  = "radial2D"
ed_gridnRadialTics_1           =  64
ed_semiAxisMajorTorsionAngle_1=  0.0
ed_semiAxisMajorTorsionAxis_1 = "x"
```

The parameters `ed_targetX_1`, `ed_targetY_1`, and `ed_targetZ_1` define the coordinate of the center of the laser focal spot. Notice that even though this is a 2D simulation, three coordinates are specified. That is because this while most of the FLASH solvers will operate in 2D, $R-z$ geometry, the laser ray trace operates in 3D Cartesian geometry. For specifying the laser focal spot center, "X" refers to the R direction in the FLASH simulation (which is also called the "X" direction for many FLASH runtime parameters, regardless of the geometry). The `ed_targetZ_1` parameter is referring to the z direction in the $R-z$ simulation. This is actually the "Y" direction for other FLASH runtime parameters. Finally, the "Z" direction for the 3D-in-2D ray trace parameters is the direction pointing out of the computer screen. This same naming convention is used for the parameters `ed_lensX_1`, `ed_lensY_1`, and `ed_lensZ_1`. These parameters specify the center of the lens. On each time step, all rays are traced from a location on the lens to the focal spot. The lens must be defined so that it exists entirely *outside* of the domain. The parameters `ed_targetSemiAxisMajor_1` and `ed_targetSemiAxisMinor_1` set the radius of the laser spot. The laser beam can have an elliptical shape. In this case the two parameters will have different values, but usually, a circular beam is desired. In this case, the beam will have a circular shape and a 10 micron radius. The parameter `ed_lensSemiAxisMajor_1` sets the radius of the focal spot. The laser beam is associated with pulse number 1 (the only pulse in this case) using the parameter `ed_pulseNumber_1`. The parameter `ed_wavelength_1` specifies the wavelength, in microns, of the laser light. The `ed_numberOfRays_1` parameter tells FLASH to launch 4096 rays for the first beam every time the `EnergyDeposition` subroutine is called. When using unsplit hydrodynamics (as in this case), this routine is called a single time per cycle. When using split hydrodynamics, it is called twice.

Taken together, the parameters:

- `ed_crossSectionFunctionType_1`,
- `ed_gaussianExponent_1`,
- `ed_gaussianRadiusMajor_1`, and
- `ed_gaussianRadiusMinor_1`

define the spatial variation of the intensity across the beam. When ed_crossSectionFunctionType_1 is set to "gaussian2D", the intensity profile is a supergaussian described by:

$$I(r) = I_0 \exp\left\{ - \left[\left(\frac{x}{R_x} \right)^2 + \left(\frac{y}{R_y} \right)^2 \right]^{\gamma/2} \right\} \qquad (30.61)$$

where:

- R_x =ed_gaussianRadiusMajor_1,
- R_y =ed_gaussianRadiusMinor_1, and
- γ =ed_gaussianExponent_1.

In our case, we've set up a beam with a super-Gaussian profile ($gamma = 4$) and an e-folding length of 7.5 microns. Since $R_x = R_y$ we have a circular beam and not an elliptical beam. The user does not directly specify I_0. Rather, the user specifies the total beam power (as described above). This then sets I_0 through the integral relation:

$$P = 2\pi \int_0^R drrI(r), \qquad (30.62)$$

The parameters ed_semiAxisMajorTorsionAngle_1 and ed_semiAxisMajorTorsionAxis_1 only need to change for non-circular beams.

Finally, the user must specify how rays will be spatially distributed across the beam. The ed_numberOfRays_1 parameter sets the total number of rays to launch on each time step for each beam. Now we have to decide how to distribute those rays cross the cross-section of the laser beam. The parameter ed_gridType_1 is set to "radial2D". This means the rays will be laid out on the circular cross-section of the beam with some radial and angular spacing. The area of the beam is divided into regions of equal radius and angle. The parameter ed_gridnRadialTics_1 is set to 64 meaning that there are 64 radial slices in the beam cross section. Therefore, there are: $4096/64 = 64$ angular slices.

30.7.5.4 Examining LaserSlab Simulation Output

This section describes how the output can be visualized using VisIt and through other means. LaserIO code in FLASH can be used to visualize ray paths (see Section 17.4.10.4 for more information). The LaserIO unit can only be used with parallel HDF5 IO implementations. The +hdf5typeio setup option is consistent with this. The runtime parameters:

```
ed_useLaserIO              = .true.
ed_laserIOMaxNumPositions = 10000
ed_laserIONumRays          = 128
```

tell FLASH to use LaserIO and to write out the trajectory of 128 rays to the plot files so they can be visualized in VisIt. Notice that this is a small subset of the total number of rays that are actually launched. Writing out all of the rays is inadvisable since it will have numerous negative effects on performance when large number of rays are used in the simulation. In this case, plot files are written every 0.1 ns and the simulation is run for 2 ns cycles (as indicated by the parameter tmax). Thus, the following plot files are generated:

```
lasslab_hdf5_plt_cnt_0000
lasslab_hdf5_plt_cnt_0001
...
lasslab_hdf5_plt_cnt_0199
lasslab_hdf5_plt_cnt_0200
```

These HDF5 files contain the ray trajectories for each of the plot time steps (cycles 1, 11, ... 191, and 201 in this case). Unfortunately, at this time, the FLASH VisIt plugin does not natively support ray visualization.

The ray data must be extracted from the plot files in placed in a form that VisIt does understand. The `extract_rays.py` script, found in the `tools/scripts` directory, performs this operation. Note, however, that `extract_rays.py` requires the NumPy and PyTables python packages to operate.

After this example `LaserSlab` simulation is run, the extract˙rays.py script can be used as shown:

```
>>> extract_rays.py lasslab_hdf5_plt_cnt_*
Processing file: lasslab_hdf5_plt_cnt_0000
Processing file: lasslab_hdf5_plt_cnt_0001
...
Processing file: lasslab_hdf5_plt_cnt_0198
Processing file: lasslab_hdf5_plt_cnt_0199
Processing file: lasslab_hdf5_plt_cnt_0200
No ray data in "lasslab_hdf5_plt_cnt_0200" skipping...
```

Note that a warning message was printed for the last plot file. This occurs because there is no ray data for a plot file written on the last cycle of a simulation. This is a limitation of the LaserIO package. The script generates files in the VTK format named:

```
  lasslab_las_0000.vtk
  lasslab_las_0001.vtk
  ...
  lasslab_las_0198.vtk
  lasslab_las_0199.vtk
```

These files contain meshes which define the ray trajectories in a format understood by VisIt.

The ray data can be plotted on top of the computational mesh. In VisIt, load the `lasslab_las_*.vtk` database. Add the "RayPower˙Watts" Pseudocolor plot. The "RayPower˙Watts" plot colors the trajectories based on the *power* of each ray in units of Watts. Thus, the power of any one ray at any given time should be less than the beam powers specified in the runtime parameters file.

An example showing the ray powers and trajectories is shown in Figure 30.80. The trajectory of 128 laser rays has been drawn. The rays are colored based on their powers.

Computing the Number Density and Average Ionization

For a simulation using the MTMMMT EOS, the electron number density itself is not directly represented in the solution vector. Rather, for mostly historical reasons, FLASH only keeps track of the variables `YE` and `SUMY`, which are defined as:

$$\texttt{YE} = \frac{\bar{Z}}{\bar{A}}\,, \quad \texttt{SUMY} = \frac{1}{\bar{A}}$$

where $\bar{Z}$ is the average ionization level and $\bar{A}$ is the average atomic mass of the cell. Thus, one can compute the average ionization and electron number density from these quantities. For example:

$$\begin{aligned}
\bar{A} &= \frac{1}{\texttt{SUMY}}, \\
\bar{Z} &= \frac{\texttt{YE}}{\texttt{SUMY}}, \\
n_{\text{ion}} &= N_A \frac{\rho}{\bar{A}} = \texttt{SUMY}\, N_A \rho, \\
n_{\text{ele}} &= N_A \bar{Z} \frac{\rho}{\bar{A}} = \texttt{YE}\, N_A \rho
\end{aligned}$$

Where N_A is Avogadros number, n_{ion} is the ion number density, n_{ele} is the electron number density, and ρ is the mass density (`DENS` in FLASH). These quantities can be plotted in VisIt using expressions.

Another useful tool in visualizing the behavior of the laser is the FLASH variable `DEPO`. This variable stores the laser energy deposited in a cell on a particular time step per unit mass. The division by mass removes the geometric factor present in the ray power. The amount of laser energy entering the domain and the amount of laser energy exiting the domain can be used to compute the fraction of laser energy that is deposited. The energy entering and exiting the domain is shown for each cycle and integrated over the entire simulation in the file "lasslab˙LaserEnergyProfile.dat". This file is produced whenever the laser ray tracing package is active in FLASH.

30.8 3T Shock Simulations

FLASH has the ability to simulate plasmas which have separate ion, electron, and radiation temperatures (see Chapter 13). Usually, simulations which multiple temperatures have several physics models active including:

- Electron thermal conduction
- Ion/Electron equilibration
- Radiation emission, absorption, and diffusion

This section contains a series of simulations which verify FLASH through comparisons with analytic solutions of steady shocks where various assumptions are active. Unfortunately, no single analytic solution contains three distinct temperatures with realistic physical coefficients. Thus, each simulation is performed with a different set of assumptions active. Taken together, they adequately exercise the 3T capabilities in FLASH.

30.8.1 Shafranov Shock

The Shafranov problem (Shafranov, 1957) is a one-dimensional problem that provides a good verification for structure of 1D shock waves in a two-temperature plasma with separate ion and electron temperatures. The Shafranov shock solutions takes as input a given upstream condition and shock speed. It then computes the downstream conditions and a shock profile. The solution is fairly sophisticated in that it takes into account electron thermal conduction and ion/electron equilibration. An assumption is made that the electron entropy is continuous across the shock. Thus, immediately downstream of the shock, the ion-temperature is substantially higher than the electron temperature. Far downstream, the temperature equilibrate. Electron conduction creates a preheat region upstream of the shock. An gamma-law EOS is used (typically with $\gamma = 5/3$).

Unfortunately, the Shafranov shock solution can only be simplified to an ODE which must be numerically integrated. The `ShafranovShock` simulation directory includes analytic solutions for several materials including Hydrogen, Helium, and Xenon in the files `plasma_shock.out`, `plasma_shock_Z2.out`, and `plasma_shock_Z54.out` respectively.

Several solutions are compared here for the fully-ionized Helium case with the following initial/boundary conditions:

- Upstream Ion/Electron Temperature: 5 eV
- Upstream Density: 0.0018 g/cc
- Upstream Velocity: 0.0 cm/s
- Shock Speed: 1.623415272E+07 cm/s

Figure 30.81, Figure 30.82, and Figure 30.83, shows the electron/ion temperature, density, and velocity at 0.15 ns for three cases:

- Analytic Solution: This is the analytic solution for the steady shock. This solution is used to initialize the FLASH simulations. The simulations are correct to the extent that they are able to maintain this shock profile.

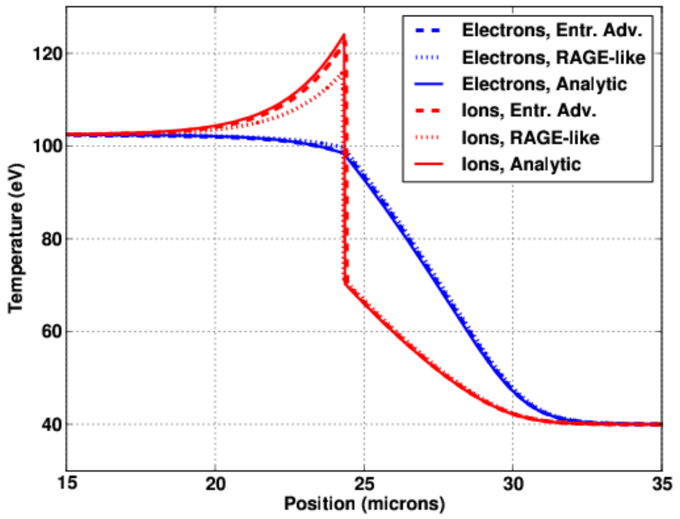

Figure 30.81: Electron and ion temperatures from Shafranov shock simulation

- Entropy Advection Solution: This is a 1D FLASH simulation using the split hydrodynamics solver in "entropy advection" mode as described in Section 14.1.4.1.
- RAGE-like Solution: This is a 1D FLASH simulation using the split hydrodynamics solver in "RAGE-like" mode as described in Section 14.1.4.2.

The figures show that the both the entropy advection and RAGE-like FLASH simulation are able to maintain the correct shock speeds. However, the entropy advection approach closely matches the correct analytic ion temperature profile while the RAGE-like simulation a peak ion temperature that is too low. This is the expected behavior since the RAGE-like mode does not attempt to ensure that electrons are adiabatically compressed by the shock.

This simulation can be setup with the following setup command:

```
# For the Entropy Advection Case:
./setup ShafranovShock -auto -1d +pm4dev +3t -parfile=flash_Z2.par

# For the RAGE-like Case:
./setup ShafranovShock -auto -1d +pm4dev +3t -parfile=ragelike_Z2.par
```

30.8.2 Non-Equilibrium Radiative Shock

The non-equilibrium radiative shock solution is an analytical solution to a steady, 1D, radiative shock where $T_e = T_i$ but $T_e \neq T_r$. It is presented in (Lowrie, 2008). A constant opacity is assumed, making this a *gray* simulation. The "analytic" solution is fairly complex and reduces to an ODE which must be evaluated numerically. This ODE is evaluated for a given set of upstream conditions and a given Mach number (evaluated relative to the upstream sound speed). A gamma-law equation of state is assumed.

The FLASH implementation of this simulation resides in the `GrayDiffRadShock` simulation directory. The simulation can be set up using the following command:

```
./setup -auto GrayDiffRadShock -1d +pm4dev +splitHydro +3t mgd_meshgroups=1
```

The simulation is performed using 3T hydrodynamics with the multigroup radiation diffusion (MGD) unit (see Chapter 24). A single radiation energy group is used with opacities set to $\sigma_a = \sigma_e = 423$ cm^{-1} and

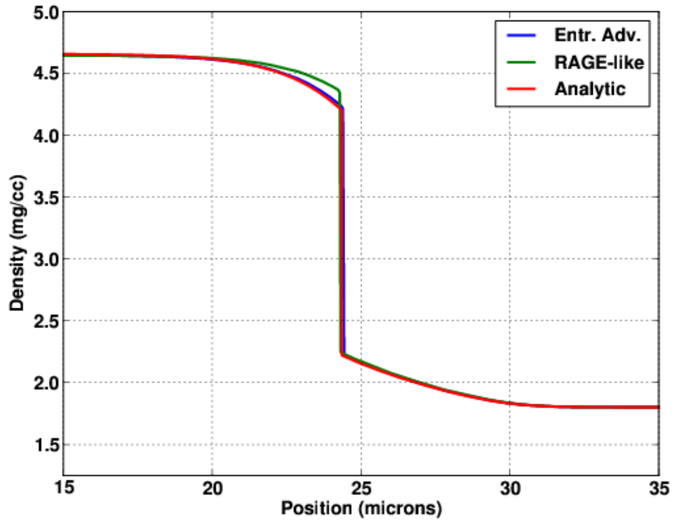

Figure 30.82: Mass density from Shafranov shock simulation

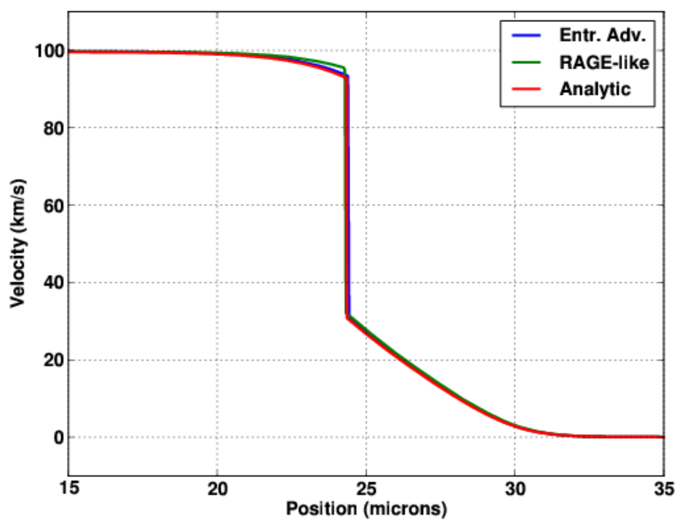

Figure 30.83: Velocity from Shafranov shock simulation

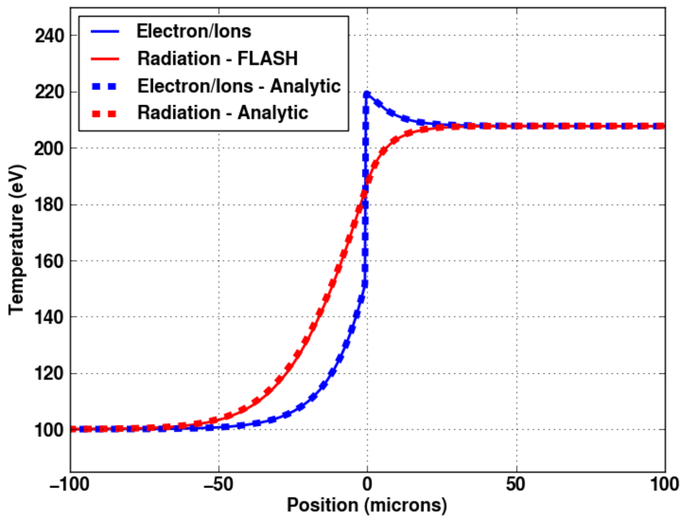

Figure 30.84: Temperatures from non-equilibrium radiative shock simulation. The FLASH results are compared to analytic solution.

$\sigma_t = 788\ \text{cm}^{-1}$ (see Section 22.4.1). A $\gamma = 5/3$ gamma-law EOS is used with $Z = 1$ and $A = 2$. The electron and ion temperatures are forced to equilibrium by using the Spitzer `Heatexchange` implementation (see: Section 17.5.1) where the ion/electron equilibration time has been reduced by a factor of 10^6 by setting the `hx_ieTimeCoef` runtime parameter.

The initial conditions are defined by a step function where the jump occurs at $x = 0$. The upstream ($x < 0$) and downstream ($x > 0$) conditions are chosen so that the shock remains stationary. The correct jump conditions are to maintain a stationary mach two shock are:

- $\rho_0 = 1.0$ g/cc
- $T_0 = 100$ eV
- $u_0 = 2.536e + 07$ cm/s
- $\rho_1 = 2.286$ g/cc
- $T_1 = 2.078$ eV
- $u_1 = 1.11e + 07$ cm/s

where the subscript 1 represents downstream conditions and the subscript 0 represents upstream conditions. The runtime parameter `sim_P0` representing the ratio of radiation to matter pressure is set to 10^{-4}.

The verification test is successful to the extent that FLASH is able to maintain a stationary shock with the correct steady state spatial profile as shown in Figure 8 of (Lowrie, 2008). This is an excellent verification test in that no special modifications to the FLASH code are needed to perform this test. The simulation is run for 4.25 ns which is enough time for the initial step function profile to reach a steady state solution. Figure 30.84 compares the temperatures in the FLASH simulation to the analytic solution. Figure 30.85 compares density to the analytic solution. Excellent agreement is obtained.

30.8.3 Blast Wave with Thermal Conduction

The ReinickeMeyer blast wave solution (Reinicke, 1991) models a blast wave in a single temperature fluid with thermal conduction. The semi-analytic solution reduces to an ODE which must be integrated numerically.

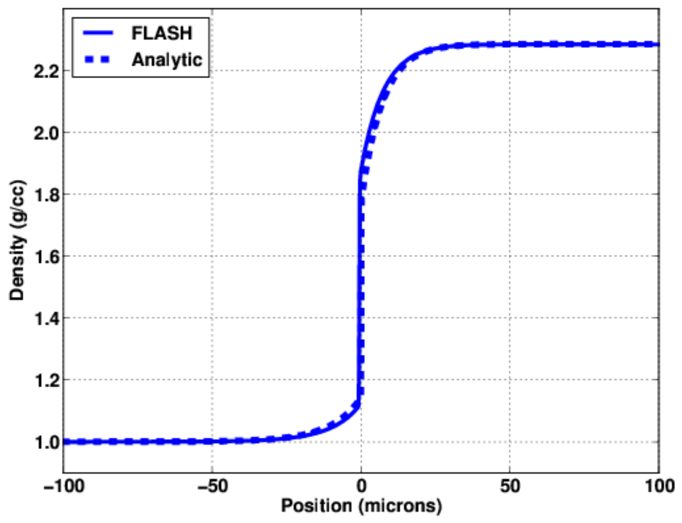

Figure 30.85: Mass density from non-equilibrium radiative shock simulation. The FLASH result is compared to the analytic solution.

Figure 30.86 compares a FLASH simulation to the analytic solution (obtained from `cococubed.asu.edu/code_pages/vv.shtml` after 0.3242 ns for a particular set of initial conditions. Excellent agreement is obtained with the analytic solution. The image shows that at this time the blast wave is at approximately 0.45 cm and the conduction front is at 0.9 cm. The simulation can be set up using the following command:

```
./setup -auto ReinickeMeyer -1d +pm4dev +spherical -parfile=flash_SPH1D.par
```

The shortcut `+splitHydro` may have to be added to reproduce the presented results.

30.9 Matter+Radiation Simulations

Here are some simulations that use the **RadFLAH** (radiation-fluxlimiter-aware hydro) variant of unsplit `Hydro`. They differ from generic 3T simulations in that there is no phyiscal distinction between the temperatures of electrons and ions; that is, electrons and ions are understood as forming a “matter” component. The “matter” component can have a different temperature from radiation.

30.9.1 Radiation-Inhibited Bondi Accretion

This setup can be used as a 1D spherical version of the radiation-inhibited Bondi accretion problem described by Krumholz et al (2007). The simulation can be set up using the following command:

```
./setup radflaHD/BondiAccretion -1d -auto +spherical -nxb=16 +mgd mgd_meshgroups=1 \
        species=h1 ManualSpeciesDirectives=True +parallelio +uhd3tr \
        -without-unit=physics/Hydro/HydroMain/unsplit
```

Note that this setup differs significantly from the one described in Krumholz et al (2007), by using 1D instead of 3D geometry, and by excluding the central region from the domain instead of representing the accreting mass at the origin as a sink (or “star”) particle.

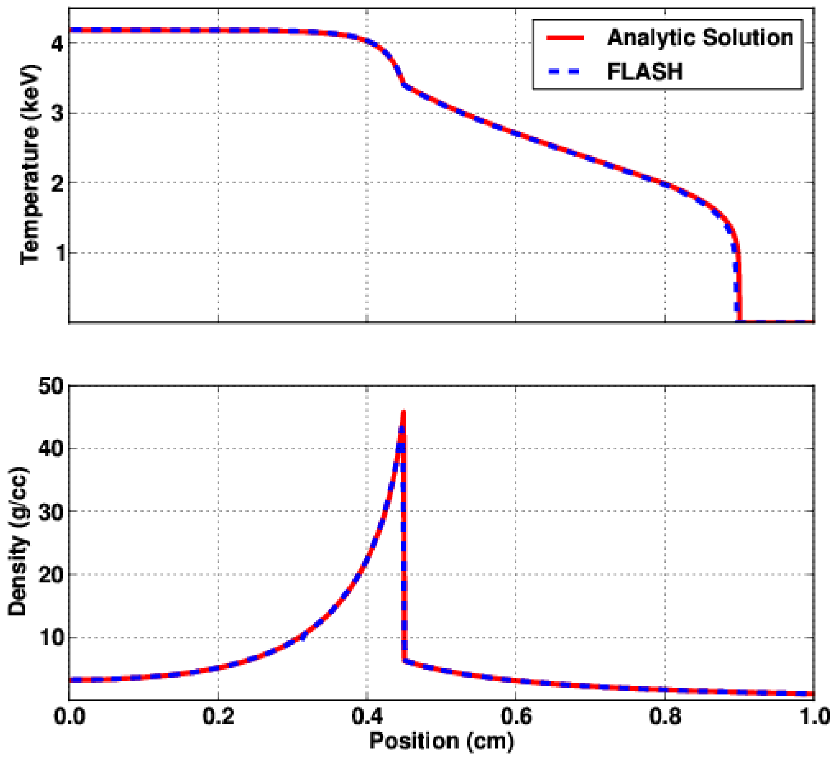

Figure 30.86: Mass density and temperature from ReinickeMeyer blast wave FLASH simulation compared to analytic solution.

30.9.2 Radiation Blast Wave

This setup can be used to reproduce the Radiation Blast Wave problem described in the Castro II paper by Zhang et al (2011). The simulation can be set up using the following command for using the default MGD solver:

```
./setup radflaHD/RadBlastWave -1d -auto +spherical -nxb=16 +mgd mgd_meshgroups=1 \
        species=h1 ManualSpeciesDirectives=True +parallelio +uhd3tr
```

For Case II of Zhang et al (2011), the following variant, using the experimental ExpRelax MGD solver implementation, may give better results:

```
./setup radflaHD/RadBlastWave -1d -auto +spherical -nxb=16 +mgd mgd_meshgroups=1 \
        species=h1 ManualSpeciesDirectives=True +parallelio +uhd3tr RadTransImpl=ExpRelax
```

Part X

Tools

Two tools are included in the release of `FLASH` to assist users with analysis of data. The first, `sfocu`, provides a way to compare output files. The second, `fidlr3.0`, provides visualization and analysis tools by using the proprietary IDL package.

Chapter 31

VisIt

The developers of `FLASH` also highly recommend VisIt, a free parallel interactive visualization package provided by Lawrence Livermore National Laboratory (see `https://wci.llnl.gov/codes/visit/`). VisIt runs on Unix and PC platforms, and can handle small desktop-size datasets as well as very large parallel datasets in the terascale range. VisIt provides a native reader to import `FLASH2.5` and FLASH3. Version 1.10 and higher natively support FLASH3. For VisIt versions 1.8 or less, FLASH3 support can be obtained by installing a tarball patch available at `http://flash.uchicago.edu/site/flashcode/user_support/visit/`. Full instructions are also available at that site.

Chapter 32

Serial FLASH Output Comparison Utility (`sfocu`)

`Sfocu` (Serial Flash Output Comparison Utility) is mainly used as part of an automated testing suite called `flashTest` and was introduced in FLASH version 2.0 as a replacement for focu.

`Sfocu` is a serial utility which examines two FLASH checkpoint files and decides whether or not they are "equal" to ensure that any changes made to FLASH do not adversely affect subsequent simulation output. By "equal", we mean that

- The leaf-block structure matches – each leaf block must have the same position and size in both datasets.
- The data arrays in the leaf blocks (`dens`, `pres`...) are identical.
- The number of particles are the same, and all floating point particle attributes are identical.

Thus, `sfocu` ignores information such as the particular numbering of the blocks and particles, the timestamp, the build information, and so on.

`Sfocu` can read `HDF5` and `PnetCDF` FLASH checkpoint files. Although `sfocu` is a serial program, it is able to do comparisons on the output of large parallel simulations. `Sfocu` has been used on irix, linux, AIX and OSF1.

32.1 Building `sfocu`

The process is entirely manual, although Makefiles for certain machines have been provided. There are a few compile-time options which you set via the following preprocessor definitions in the Makefile (in the `CDEFINES` macro):

`NO_HDF5` build without HDF5 support

`NO_NCDF` build without PnetCDF support

`NEED_MPI` certain parallel versions of HDF5 and all versions of PnetCDF need to be linked with the MPI library. This adds the necessary `MPI_Init` and `MPI_Finalize` calls to `sfocu`. There is no advantage to running `sfocu` on more than one processor; it will only give you multiple copies of the same report.

32.2 Using `sfocu`

The basic and most common usage is to run the command `sfocu <file1> <file2>`. The option `-t <dist>` allows a distance tolerance in comparing bounding boxes of blocks in two different files to determine which are the same (which have data to compare to one another). You might need to widen your terminal to view the output, since it can be over 80 columns. Sample output follows:

```
A: 2006-04-25/sod_2d_45deg_4lev_ncmpi_chk_0001
B: 2005-12-14/sod_2d_45deg_4lev_ncmpi_chk_0001
Min Error: inf(2|a-b| / max(|a+b|, 1e-99) )
Max Error: sup(2|a-b| / max(|a+b|, 1e-99) )
Abs Error: sup|a-b|
Mag Error: sup|a-b| / max(sup|a|, sup|b|, 1e-99)
Block shapes for both files are: [8,8,1]
Mag-error tolerance: 1e-12
Total leaf blocks compared: 541 (all other blocks are ignored)
-----+------------+-----------++-----------+-----------+-----------++-----------+-----------+-----------+
Var  | Bad Blocks | Min Error ||             Max Error             ||             Abs Error             |
-----+------------+-----------++-----------+-----------+-----------++-----------+-----------+-----------+
     |            |           ||   Error   |     A     |     B     ||   Error   |     A     |     B     |
-----+------------+-----------++-----------+-----------+-----------++-----------+-----------+-----------+
dens | 502        | 0         || 1.098e-11 | 0.424     |  0.424    || 4.661e-12 | 0.424     | 0.424     |
eint | 502        | 0         || 1.1e-11   | 1.78      |  1.78     || 1.956e-11 | 1.78      | 1.78      |
ener | 502        | 0         || 8.847e-12 | 2.21      |  2.21     || 1.956e-11 | 2.21      | 2.21      |
gamc | 0          | 0         || 0         | 0         |  0        || 0         | 0         | 0         |
game | 0          | 0         || 0         | 0         |  0        || 0         | 0         | 0         |
pres | 502        | 0         || 1.838e-14 | 0.302     |  0.302    || 1.221e-14 | 0.982     | 0.982     |
temp | 502        | 0         || 1.1e-11   | 8.56e-09  |  8.56e-09 || 9.41e-20  | 8.56e-09  | 8.56e-09  |
velx | 516        | 0         || 5.985     | 5.62e-17  | -1.13e-16 || 2.887e-14 | 0.657     | 0.657     |
vely | 516        | 0         || 2         | 1e-89     | -4.27e-73 || 1.814e-14 | 0.102     | 0.102     |
velz | 0          | 0         || 0         | 0         |  0        || 0         | 0         | 0         |
mfrc | 0          | 0         || 0         | 0         |  0        || 0         | 0         | 0         |
-----+------------+-----------++-----------+-----------+-----------++-----------+-----------+-----------+
-----+------------+-----------++-----------+-----------+-----------++-----------+-----------+-----------+
Var  | Bad Blocks | Mag Error ||                 A                 ||                 B                 |
-----+------------+-----------++-----------+-----------+-----------++-----------+-----------+-----------+
     |            |           ||    Sum    |    Max    |    Min    ||    Sum    |    Max    |    Min    |
-----+------------+-----------++-----------+-----------+-----------++-----------+-----------+-----------+
dens | 502        | 4.661e-12 ||  1.36e+04 | 1         |  0.125    ||  1.36e+04 | 1         |  0.125    |
eint | 502        | 6.678e-12 ||  7.3e+04  | 2.93      |  1.61     ||  7.3e+04  | 2.93      |  1.61     |
ener | 502        | 5.858e-12 ||  8.43e+04 | 3.34      |  2        ||  8.43e+04 | 3.34      |  2        |
gamc | 0          | 0         ||  4.85e+04 | 1.4       |  1.4      ||  4.85e+04 | 1.4       |  1.4      |
game | 0          | 0         ||  4.85e+04 | 1.4       |  1.4      ||  4.85e+04 | 1.4       |  1.4      |
pres | 502        | 1.221e-14 ||  1.13e+04 | 1         |  0.1      ||  1.13e+04 | 1         |  0.1      |
temp | 502        | 6.678e-12 ||  0.000351 | 1.41e-08  |  7.75e-09 ||  0.000351 | 1.41e-08  |  7.75e-09 |
velx | 516        | 3.45e-14  ||  1.79e+04 | 0.837     | -6.09e-06 ||  1.79e+04 | 0.837     | -6.09e-06 |
vely | 516        | 2.166e-14 ||  1.79e+04 | 0.838     | -1.96e-06 ||  1.79e+04 | 0.838     | -1.96e-06 |
velz | 0          | 0         ||  0        | 0         |  0        ||  0        | 0         |  0        |
mfrc | 0          | 0         ||  3.46e+04 | 1         |  1        ||  3.46e+04 | 1         |  1        |
-----+------------+-----------++-----------+-----------+-----------++-----------+-----------+-----------+
FAILURE
```

“Bad Blocks” is the number of leaf blocks where the data was found to differ between datasets. Four different error measures (min/max/abs/mag) are defined in the output above. In addition, the last six columns report the sum, maximum and minimum of the variables in the two files. Note that the sum is physically meaningless, since it is not volume-weighted. Finally, the last line permits other programs to parse the `sfocu` output easily: when the files are identical, the line will instead read `SUCCESS`.

It is possible for `sfocu` to miss machine-precision variations in the data on certain machines because of compiler or library issues, although this has only been observed on one platform, where the compiler produced code that ignored IEEE rules until the right flag was found.

Chapter 33

Drift

33.1 Introduction

Drift is a debugging tool added to FLASH to help catch programming mistakes that occur while refactoring code in a way that *should not* change numerical behavior. Historically, simulation checkpoints have been used to verify that results obtained after a code modification have not affected the numerics. But if changes are observed, then the best a developer can do to narrow the bug hunting search space is to look at pairs of checkpoint files from the two different code bases sequentially. The first pair to compare unequal will tell you that somewhere between that checkpoint and its immediate predecessor something in the code changed the numerics. Therefor, the search space can only be narrowed to the limit allow by the checkpointing interval, which in FLASH, without clever calls to IO sprinkled about, is at best once per time cycle.

Drift aims to refine that granularity considerably by allowing comparisons to be made upon every modification to a block's contents. To achieve this, drift intercepts calls to `Grid_releaseBlkPtr`, and inserts into them a step to checksum each of the variables stored on the block. Any checksums that do not match with respect to the last checksums recorded for that block are logged to a text file along with the source file and line number. The developer can then compare two drift logs generated by the different runs using `diff` to find the first log entry that generates unequal checksums, thus telling the developer which call to `Grid_releaseBlkPtr` first witnessed divergent values.

The following are example excerpts from two drift logs. Notice the checksum value has changed for variable `dens` on block 18. This should clue the developer in that the cause of divergent behavior lies somewhere between `Eos_wrapped.F90:249` and `hy_ppm_sweep.F90:533`.

```
inst=2036                                 inst=2036
step=1                                    step=1
src=Eos_wrapped.F90:249                   src=Eos_wrapped.F90:249
blk=57                                    blk=57
 dens E8366F6E49DD1B44                     dens E8366F6E49DD1B44
 eint 89D635E5F46E4CE4                     eint 89D635E5F46E4CE4
 ener C6ED4F02E60C9E8F                     ener C6ED4F02E60C9E8F
 pres 6434628E2D2E24E1                     pres 6434628E2D2E24E1
 temp DB675D5AFF7D48B8                     temp DB675D5AFF7D48B8
 velx 42546C82E30F08B3                     velx 42546C82E30F08B3

inst=2100                                 inst=2100
step=1                                    step=1
src=hy_ppm_sweep.F90:533                  src=hy_ppm_sweep.F90:533
blk=18                                    blk=18
 dens A462F49FFC3112DE                     dens 5E52D67C5E93FFF1
 eint 9CD79B2E504C7C7E                     eint 9CD79B2E504C7C7E
 ener 4A3E03520C3536B9                     ener 4A3E03520C3536B9
 velx 8193E8C2691A0725                     velx 8193E8C2691A0725
 vely 86C5305CB7DE275E                     vely 86C5305CB7DE275E
```

33.2 Enabling drift

In FLASH, drift is disabled by default. Enabling drift is done by hand editing the Flash.h file generated by the setup process. The directive line `#define DRIFT_ENABLE 0` should be changed to `#define DRIFT_ENABLE 1`. Once this has been changed, a recompilation will be necessary by executing `make`.

With drift enabled, the FLASH executable will generate log files in the same directory it is executed in. These files will be named `drift.<rank>.log`, one for each MPI process.

The following runtime parameters are read by drift to control its behavior:

Parameter	Default	Description
`drift_trunc_mantissa`	2	The number of least significant mantissa bits to zero out before hashing a floating point value. This can be used to stop numerical noise from altering checksum values.
`drift_verbose_inst`	0	The instance index at which drift should start logging checksums per call to `Grid_releaseBlkPtr`. Before this instance is hit, only user calls to `Driver_driftUnk` will generate log data. A value of zero means never log checksums per block. Instance counting is described below.
`drift_tuples`	.false.	A boolean switch indicating if drift should write logs in the more human readable ”non-tuples” format or the machine friendly ”tuples” format that can be read in by the `driftDee` script found in the `tools/` directory. Generally the ”non-tuples” format is a better choice to use with tools such as `diff`.

33.3 Typical workflow

Drift has two levels of output verbosity, let us refer to them as verbose and not verbose. When in non-verbose mode, drift will only generate output when directly told to do so through the `Driver_driftUnk` API call. This call tells drift to generate a checksum for each `unk` variable over all blocks in the domain and then log those checksums that have changed since the last call to `Driver_driftUnk`. Verbose mode also generates this information and additionally includes the per-block checksums for every call to `Grid_releaseBlkPtr`. Verbose mode can generate *a lot* of log data and so should only be activated when the simulation nears the point at which divergence originates. This is the reason for the `drift_verbose_inst` runtime parameter.

Drift internally maintains an ”instance” counter that is incremented with every intercepted call to `Grid_releaseBlkPtr`. This is drift's way of enumerating the program states. When comparing two drift logs, if the first checksum discrepancy occurs at instance number 1349 (arbitrary), then it is clear that somewhere between the 1348'th and 1349'th call to `Grid_releaseBlkPtr` a divergent event occurred.

The suggested workflow once drift is enabled is to first run both simulations with verbose mode off (`dirft_verbse_inst`=0). The main `Driver_evolveFlash` implementations have calls to `Driver_driftUnk` between all calls to FLASH unit advancement routines. So the default behavior of drift will generate multiple unk-wide checksums for each variable per timestep. These two drift logs should be compared to find the first entry with a mismatched checksum. Each entry generated by `Driver_driftUnk` will contain an instance range like in the following:

```
step=1
from=Driver_evolveFlash.F90:276
unks inst=1234 to 2345
 dens 9CF3C169A5BB129C
 eint 9573173C3B51CD12
 ener 028A5D0DED1BC399
 ...
```

The line "`unks inst=1349 to 2345`" informs us these checksums were generated sometime after the 2345'th call to `Grid_releaseBlkPtr`. Assume this entry is the first such entry to not match checksums with its counterpart. Then we know that somewhere between instance 1234 and 2345 divergence began. So we set `drift_verbose_inst = 1234` in the runtime parameters file of each simulation and then run them both again. Now drift will run up to instance 1234 as before, only printing at calls to `Driver_driftUnk`, but starting with instance 1234 each call to `Grid_releaseBlkPtr` will induce a per block checksum to be logged as well. Now these two drift files can be compared to find the first difference, and hopefully get you on your way to hunting down the cause of the bug.

33.4 Caveats and Annoyances

The machinery drift uses to intercept calls to `Grid_releaseBlkPtr` is lacking in sophistication, and as such can put some unwanted constraints on the code base. The technique used is to declare a preprocessor `#define` in `Flash.h` to expand occurrences of `Grid_releaseBlkPtr` to something larger that includes `__FILE__` and `__LINE__`. This is how drift is able to correlate calls to `Grid_releaseBlkPtr` with the originating line of source code. Unfortunately this technique places a very specific restriction on the code once drift is enabled. The trouble comes from the types of source lines that may refer to a subroutine without calling it. The primary offender being `use` statements with `only` clauses listing the module members to import into scope. Because macro expansion is dumb with respect to context, it will expand occurrences of `Grid_releaseBlkPtr` in these `use` statements, turning them into syntactic rubbish. The remedy for this issue is to make sure the line `#include "Flash.h"` comes after all statements involving `Grid_releaseBlkPtr` but not calling it, and before all statements that are calls to `Grid_releaseBlkPtr`. In practice this is quite easy. With only one subroutine per file, there will only be one line like:

```
use Grid\_interface, only: ..., Grid\_releaseBlkPtr, ...
```

and it will come before all calls to `Grid_releaseBlkPtr`, so just move the `#include "Flash.h"` after the `use` statements. The following is an example:

Incorrect	Correct
`#include "Flash.h"`	`subroutine Flash_subroutine()`
`subroutine Flash_subroutine()`	`  use Grid_interface, only: Grid_releaseBlkPtr`
`  use Grid_interface, only: Grid_releaseBlkPtr`	`  implicit none`
`  implicit none`	`#include "Flash.h"`
`  [...]`	`  [...]`
`  call Grid_releaseBlkPtr(...)`	`  call Grid_releaseBlkPtr(...)`
`  [...]`	`  [...]`
`end subroutine Flash_subroutine`	`end subroutine Flash_subroutine`

If such a solution is not possible because no separation between all `use` and `call` statements exists, then there are two remaining courses of action to get the source file to compile. One, hide these calls to `Grid_releaseBlkPtr` from drift by forceably disabling the macro expansion. To do so, just add the line `#undef Grid_releaseBlkPtr` after `#include "Flash.h"`. The second option is to carry out the macro expansion by hand. This also requires disabling the macro with the undef just mentioned, but then also rewriting each call to `Grid_releaseBlkPtr` just as the preprocessor would. Please consult `Flash.h` to see the text that gets substituted in for `Grid_releaseBlkPtr`.

Chapter 34

FLASH IDL Routines (fidlr3.0)

`fidlr3.0` is a set of routines to read and plot data files produced by FLASH. The routines are written in the graphical display language IDL (Interactive Data Language) and require the IDL program from Research Systems Inc. (`http://www.rsi.com`). These routines include programs which can be run from the IDL command line to read 1D, 2D, or 3D FLASH datasets, interactively analyze datasets, and interpolate them onto uniform grids.

However, some of these routines are not described in this release of the documentation because they have not been thoroughly tested with FLASH4. A graphical user interface (GUI) to these routines (**`xflash3`**) is provided, which enables users to read FLASH AMR datasets and make plots of the data. Both plotfiles and checkpoint files, which differ only in the number and numerical precision of the variables stored, are supported.

`fidlr3.0` supports Cartesian, cylindrical, polar and spherical geometries. The proper geometry should be detected by **`xflash3`** using the geometry attribute in the file header. System requirements for running `fidlr3.0` are: IDL version 5.6 and above, and the HDF5 library. The routines also have limited support for data files written with `netCDF`, although this output format has not been thoroughly tested. The routines are intended to be backwards-compatible with `FLASH2`, although again extensive testing has not been performed.

34.1 Installing and Running fidlr3.0

`fidlr3.0` is distributed with FLASH and is contained in the `tools/fidlr3.0/` directory. These routines were written and tested using IDL v6.1 for Linux. They should work without difficulty on any UNIX machine with IDL installed—any functionality of `fidlr3.0` under Windows is purely coincidental. Due to copyright difficulties with GIF files, output image files are in PNG or Postscript format. Most graphics packages, like xv or the GIMP, should be able to convert between PNG format and other commonly used formats.

Installation of `fidlr3.0` requires defining some environment variables, making sure your IDL path is properly set, and compiling the support for HDF5 files. These procedures are described below.

34.1.1 Setting Up fidlr3.0Environment Variables

The FLASH `fidlr3.0` routines are located in the `tools/fidlr3.0/` subdirectory of the FLASH root directory. To use them you must set two environment variables. First set the value of `XFLASH3_DIR` to the location of the FLASH IDL routines; for example, under `csh`, use

```
setenv XFLASH3_DIR flash-root-path/tools/fidlr3.0
```

where *flash-root-path* is the absolute path of the FLASH3 root directory. This variable is used in the plotting routines to find the customized color table and setup parameters for `xflash3`.

Next, make sure that you have an `IDL_DIR` environment variable set. This should point to the directory in which the IDL distribution is installed. For example, if IDL is installed in *idl-root-path*, then you would define

```
setenv IDL_DIR idl-root-path .
```

Finally, you need to tell IDL where to find the `fidlr3.0` routines. This is accomplished through the `IDL_PATH` environment variable

```
setenv IDL_PATH ${XFLASH3_DIR}:${IDL_DIR}:${IDL_DIR}/lib .
```

If you already have an `IDL_PATH` environment variable defined, just add `XFLASH3_DIR` to the beginning of it. You may wish to include these commands in your `.cshrc` (or the analogous versions in your `.profile` file, depending on your shell) to avoid having to reissue them every time you log in. It is important that the `${XFLASH3_DIR}` come before the IDL directories in the path and that the `${IDL_DIR}/lib` directory be included as well.

34.1.2 Running IDL

`fidlr3.0` uses 8-bit color tables for all of its plotting. On displays with higher color depths, it may be necessary to use color overlays to get the proper colors on your display. For SGI machines, launching IDL with the `start.pro` script will enable 8-bit pseudocolor overlays. For Linux boxes, setting the X color depth to 24-bits per pixel and launching IDL with the `start_linux.pro` script usually produces proper colors.

```
 prompt> idl start_linux
```

34.2 `xflash3`: A Widget Interface to Plotting FLASH Datasets

The main interface to the `fidlr3.0` routines for plotting FLASH datasets is `xflash3`. Typing `xflash3` at the IDL command prompt will launch the main `xflash3` widget, shown in Figure 34.1.

```
IDL> xflash3
```

`xflash3` produces colormap plots of FLASH data with optional overlays of velocity vectors, contours, and the block structure. The basic operation of `xflash3` is to specify a single output file (either checkpoint or plotfile) as a prototype for the FLASH simulation. The prototype is probed for the list of variables it contains, and then the remaining plot options become active.

`xflash3` can output to the screen, Postscript, or a PNG image file. If the data is significantly higher resolution than the output device, `xflash3` will sub-sample the image by one or more levels of refinement before plotting.

Once the image is plotted, the *query* (2-d data only) and *1-d slice* buttons will become active. Pressing *query* and then clicking anywhere in the domain will pop up a window containing the values of all the FLASH variables in the cell nearest the cursor. The query function uses the actual FLASH data—not the interpolated/uniformly gridded data generated for the plots. Pressing *1-d slice* and then left-clicking on the plot will produce a 1-d slice vertically through the point. Right-clicking on the domain produces a horizontal slice through the data.

The widget is broken into several sections, with some features initially disabled. Not all options are available in all dimensions, or in this release of FLASH4. These sections are explained below.

34.2.1 File Menu

The file to be visualized is composed of the path, the basename (the same base name used in the flash.par file) with any file type information appended to it (*e.g.* `'hdf5_chk_'`) and the range of suffixes through which to loop. By default, `xflash3` sets the path to the working directory from which IDL was started. `xflash3` requires a prototype file to work on a dataset. The prototype can be any of the files in the dataset that has the same name structure (*i.e.* everything is the same but the suffix) and contains the same variables.

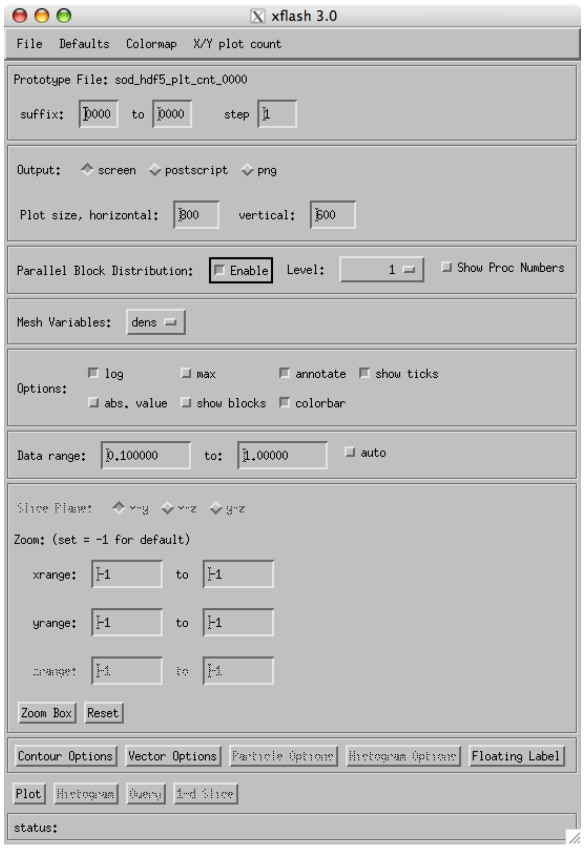

Prototype File: sod_hdf5_plt_cnt_0000
suffix: 0000 to 0000 step 1
Output: screen postscript png
Plot size, horizontal: 800 vertical: 600
Parallel Block Distribution: Enable Level: 1 Show Proc Numbers
Mesh Variables: dens
Options: log max annotate show ticks abs. value show blocks colorbar
Data range: 0.100000 to: 1.00000 auto
Slice Plane: x-y x-z y-z
Zoom: (set = -1 for default)
xrange: -1 to -1
yrange: -1 to -1
zrange: -1 to -1
status:

Figure 34.1: The main `xflash3` widget.

34.2.1.1 File/Open prototype...

The *Open prototype...* menu option will bring up the file selection dialog box (see Figure 34.2). Once a plotfile or checkpoint prototype is selected, the remaining options on the xflash widget become active, and the variable list box "Mesh Variables" is populated with the list of variables in the file (see Figure 34.3).

`xflash3` will automatically determine if the file is an HDF5 or netCDF file and read the 'unknown names' dataset to get the variable list. Some derived variables will also appear on the list (for example, sound speed), if the dependent variables are contained in the datafile. These derived variables are currently inoperable in 3-D.

34.2.2 Defaults Menu

The *Defaults* menu allows you to select one of the predefined problem defaults. This choice is provided for the convenience of users who want to plot the same problem repeated using the same data ranges. This menu item will load the options (data ranges, velocity parameters, and contour options) for the problem as specified in the `xflash_defaults` procedure. When `xflash3` is started, `xflash_defaults` is executed to read in the known problem names. The data ranges and velocity defaults are then updated. To add a problem to `xflash3`, only the `xflash_defaults` procedure needs to be modified. The details of this procedure are provided in the comment header in `xflash_defaults`. It is not necessary to add a problem in order to plot a dataset, since all default values can be overridden through the widget.

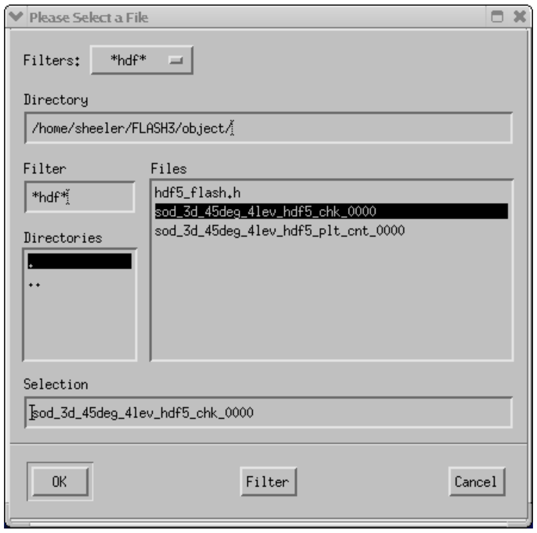

```
Filters: *hdf*
Directory
/home/sheeler/FLASH3/object/
Filter          Files
*hdf*           hdf5_flash.h
                sod_3d_45deg_4lev_hdf5_chk_0000
                sod_3d_45deg_4lev_hdf5_plt_cnt_0000
Directories
.
..
Selection
sod_3d_45deg_4lev_hdf5_chk_0000
```

Figure 34.2: The `xflash3` file selection dialog.

34.2.3 Colormap Menu

The *colormap menu* lists the colormaps available to `xflash3`. These colormaps are stored in the file `flash_colors.tbl` in the `fidlr3.0` directory and differ from the standard IDL colormaps. The first 12 colors in the colormaps are reserved by `xflash3` to hold the primary colors used for different aspects of the plotting. These colormaps are used for 2-d and 3-d data only. At present, there is no control over the line color in 1-d.

34.2.4 X/Y plot count Menu

The *X/Y plot count* menu specifies how many plots to put on a single page when looping over suffixes in a dataset. At present, this only works for 2-d data. Note, the query and 1-d slice operations will not work if there are multiple plots per page.

34.2.5 Plotting options available from the GUI

Various options are available on the `xflash3` user interface to change the appearance of the plots.

34.2.5.1 File Options

The first section below the menu bar specifies the file options. This allows you to specify the range of files in the dataset (*i.e.* the suffixes) to loop over. The optional *step* parameter can be used to skip over files when looping through the dataset. For example, to generate a “movie” of the checkpoint files from initial conditions to checkpoint number 17, enter `0000` in the first `suffix:` box, and enter `0017` in the box following `to`. Leave the step at the default of 1 to visualize every output.

34.2.5.2 Output Options

A plot can be output to the screen (default), a Postscript file, or a PNG file. The output filenames are composed from the basename + variable name + suffix. For outputs to the screen or PNG, the *plot size* options allow you to specify the image size in pixels. For Postscript output, `xflash3` chooses portrait or landscape orientation depending on the aspect ratio of the domain.

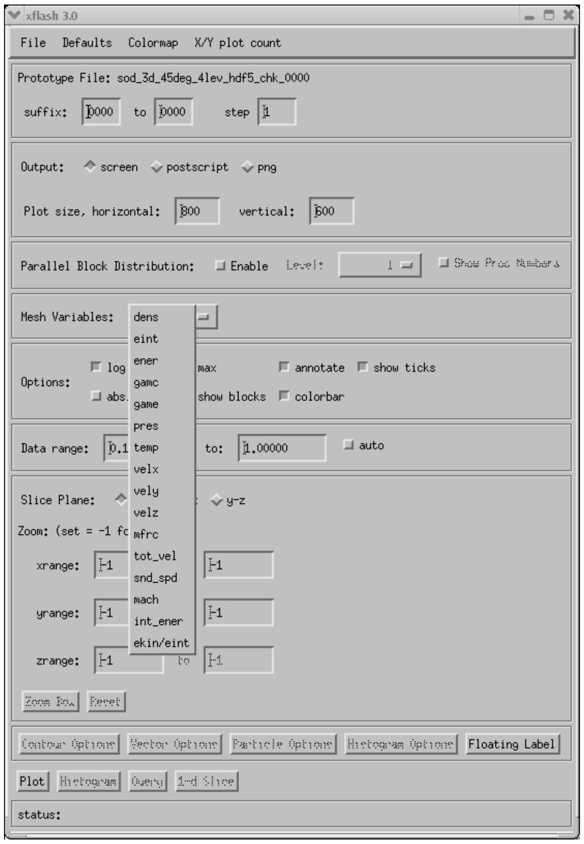
Prototype File: sod_3d_45deg_4lev_hdf5_chk_0000
suffix: 0000 to 0000 step 1
Plot size, horizontal: 800 vertical: 600
Data range: 0.1 to: 1.00000
xrange: -1 -1
yrange: -1 -1
zrange: -1 to -1

Figure 34.3: The `xflash3` main window after a prototype has been selected, showing the variable list.

34.2.5.3 Parallel Block Distribution Options

A plot of the parallel block distribution on the physical domain can be created. To use this feature, select the "Enable" toggle button located in the "Parallel Block Distribution" row of the xflash GUI. If more than one processor has been used to generate the simulation results, the different levels of refinement in the simulation can then be selected from a drop down menu. The menu shows which processors hold which blocks at a given level of refinement. Each processor is denoted by a unique color. Additionally, the processor number can be superimposed on the plot by selecting the "Show Plot Numbers" checkbox.

34.2.5.4 Mesh Variables

The variables dropbox lists the mesh, or grid variables stored in the 'unknown names' record in the data file and any derived variables that `xflash3` knows how to construct from these variables (*e.g.* sound speed). This selection allows you to choose the variable to be plotted. By default, `xflash3` reads all the variables in a file in 1- and 2-d datasets, so switching the variable to plot can be done without re-reading. At present, there is no easy way to add a derived variable. Both the widget routine (`xflash3.pro`) and the plotting backend (`xplot#d_amr.pro`) will need to be told about any new derived variables. Users wishing to add derived variables should look at how the total velocity (`tot_vel`) is computed.

34.2.5.5 Options

The options block allows you to toggle various options on/off. Table 34.1 lists the various options available.

Table 34.1: `xflash3` options

log	Plot the base-10 log of the variable.
max	When a sequence of files is defined in the file options, plot the maximum of the variable in each cell over all the files.
annotate	Toggle the title and time information on the plot.
show ticks	Show the axis tick marks on the plot.
abs. value	Plot the absolute value of the dataset. This operation is performed before taking the log.
show blocks	Draw the zone boundaries on the plot.
colorbar	Plot the colorbar legend for the data range.

34.2.5.6 Data Range

These fields allow you to specify the range of the variable to plot. Data outside of the range will be set to the minimum or maximum values of the colormap. If the *auto* box is checked, the limits will be ignored, and the data will be scaled to the minimum and maximum values of the variable in the dataset.

34.2.5.7 Slice Plane

The slice plane group is only active for 3-d datasets. This option allows you to select a plane for plotting in (x-y, x-z, y-z).

34.2.5.8 Zoom

The zoom options allow you to set the domain limits for the plot. A value of -1 uses the actual limit of the domain. For 3-d plots, only one field will be available in the direction perpendicular to the slice plane. The *zoom box* button puts a box cursor on the plot and allows you to select a region to zoom in on by positioning and resizing the box with the mouse. Use the left mouse button to move the center of the zoom box. Use the middle button to resize the box. Finally, right-click with the mouse when you are satisfied with the zoom box selection. (Note that you must choose the "Plot" button again to see the results of the selected zoom. The *reset* button will reset the zoom limits.

34.2.6 Plotting buttons

Several buttons are located at the bottom of the `xflash3` user interface which pop up additional windows. Most of these set additional groups of options, but the actual commands to create plots are located on the bottom row.

34.2.6.1 Contour Options Button

This button launches a dialog box that allows you to select up to 4 contour lines to plot on top of the colormap plot (see Figure 34.4). The variable, value, and color are specified for each reference contour. To plot a contour, select the check box next to the contour number. This will allow you to set the variable from which to make the contour, the value of the contour, and the color. This option is available in 2-d only at present.

34.2.6.2 Vector Options Button

This button launches a dialog box that allows you to set the options used to plot vectors on the plot (see Figure 34.5). This option is usually utilized to overplot velocity vectors. First select the *plot vectors* checkbox to enable the other options. Choose the variables to generate vectors with the *x-component* and *y-component* pull-down boxes. These choices are set to `velx` and `vely` by default. *typical vector* sets the vector length to

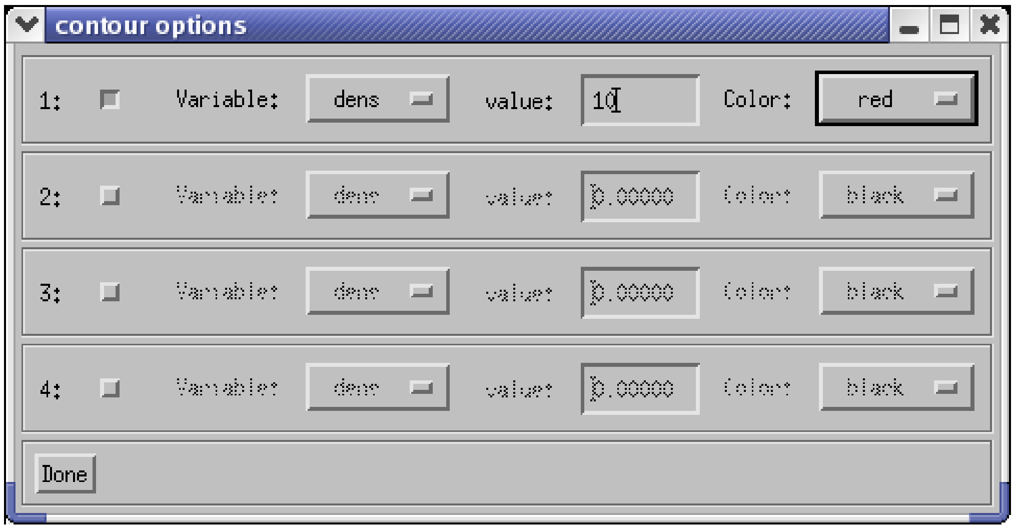

1: Variable: dens value: 10 Color: red

2: Variable: dens value: 0.00000 Color: black

3: Variable: dens value: 0.00000 Color: black

4: Variable: dens value: 0.00000 Color: black

Figure 34.4: The `xflash3` contour option subwidget.

which to scale the vectors, and *minimum vector* and *maximum vector* specify the range of vectors for which to plot. *xskip* and *yskip* allow you to thin out the arrows. This option is available in 2-d only.

34.2.6.3 Particle Options Button

This button enables the user to set options for plotting particles. Since particle-handling routines are not present in this release of FLASH4, this option is disabled in `xflash3`.

34.2.6.4 Histogram Options Button

This button pops up a dialog box that allows you to set the histogram options. Currently, only the number of bins and the scale of the y-axis can be set. This option is disabled in this release of FLASH3.

34.2.6.5 Floating Label Button

This button pops up a dialog box that allows you to add annotation to the plot. First select the *use floating label* checkbox to enable the other options. Choose the size of the text in pixels, the thickness of the font, and the color of the text. Also select the relative position on the screen. The *multiple plots* button allows different annotation to be placed on each of plot displayed.

34.2.6.6 Plot Button

Create the colormap plot after selecting the desired options described above. The status of the plot will appear on the status bar at the bottom.

34.2.6.7 Histogram Button

Create a histogram of the data. This option is disabled in this release of FLASH3.

34.2.6.8 Query Button

The query button becomes active once the plot is created. Click on *Query* and then click somewhere in the domain to generate a popup window listing the data values at the cursor location (see Figure 34.6). Use the *Close* button to dismiss the results.

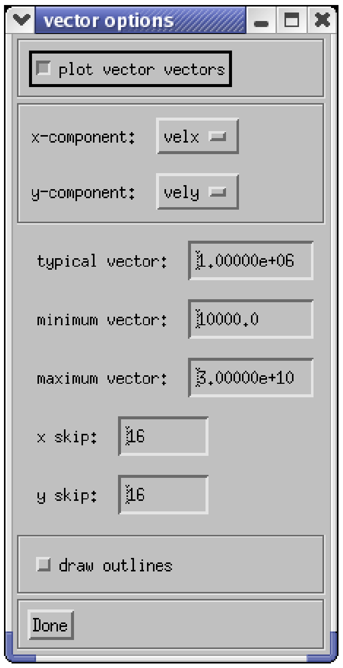

plot vector vectors

x-component: velx

y-component: vely

typical vector: 1.00000e+06

minimum vector: 10000.0

maximum vector: 3.00000e+10

x skip: 16

y skip: 16

draw outlines

Figure 34.5: The `xflash3` velocity option subwidget.

34.2.6.9 1-d Slice Button

This button is available for 2-d and 3-d datasets only. Clicking on *1-d Slice* and then left-clicking in the domain will plot a one-dimensional slice of the current variable vertically through the point selected. A right-click will produce a horizontal slice. This function inherits the options chosen in the *Options* block.

34.3 Comparing two datasets

From the IDL prompt, a plot showing visual difference can be created with the command `diff3`. Comparisons can be made between any two variables in different files or within the same file. However, this command currently is supported ONLY for two-dimensional datasets. For example, the command:

```
IDL> diff3, '<path_to_file>/flash_hdf5_0001','dens', '<path_to_file>/flash_hdf5_0002','dens'
```

plots the difference between the 'dens' variable in two different Flash files.

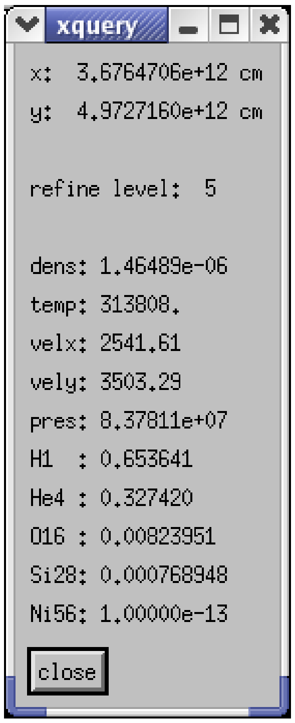

```
x:  3.6764706e+12 cm
y:  4.9727160e+12 cm

refine level:  5

dens: 1.46489e-06
temp: 313808.
velx: 2541.61
vely: 3503.29
pres: 8.37811e+07
H1  : 0.653641
He4 : 0.327420
O16 : 0.00823951
Si28: 0.000768948
Ni56: 1.00000e-13
```

Figure 34.6: The `xflash3` query widget, displaying information for a cell.

Chapter 35

convertspec3d

The Spect3D software, developed by Prism Scientific Computing:

`http://www.prism-cs.com/Software/Spect3D/Spect3D.htm`

is a widely used tool that can be used to model simulated diagnostic responses generated by radiation hydrodynamics codes. The simulated images mimic common diagnostics fielded in many HEDP experiments. The `convertspec3d` python script can be used to convert FLASH output into input for the Spect3D code.

35.1 Installation

The `convertspec3d` script is written in python and depends on several popular python packages. The dependencies include:

- Python 2.7
- PyTables
- The python NETCDF package: `http://code.google.com/p/netcdf4-python/`
- The setuptools package

Once these dependencies are installed, you can install the `convertspec3d` script. To do so, enter the `tools` directory of the FLASH source tree and enter:

```
  python setup.py install
```

By default, this will try to install the FLASH python tools to a system wide location. You will need root/administrator privileges for this. If you are on a system where you do not have root privileges, just enter:

```
  python setup.py install --user
```

for a user space installation. Type `convertspec3d` in the command line an you should see some help information - if the installation went well. For example, you should see something like:

```
> convertspect3d
usage: convertspec3d [-h] --species SPECIES [--extra EXTRA]
                     file_names [file_names ...]
convertspec3d: error: too few arguments
```

35.2 Usage

To describe the usage of the script, it will be assumed that the user is modeling a laser driven HEDP experiment. The example will be based on the `LaserSlab` simulation described in 30.7.5. The script essentially assumes you are running a simulation using the MTMMMT EOS, where the plasma electron number density and ion number density can be determined using the `SUMY` and `YE` variables. Spect3D requires this information for most applications. The simulation must have material information where species are used to model each material. In the case of the `LaserSlab` simulation, there are two species: `cham` and `targ`.

The script takes, as arguments, a list of one or more FLASH checkpoint/plot files and converts each of these files. The new files have the same names as the old files, but have a `.exo` extension. For example, the checkpoint file `lasslab_hdf5_chk_0000` would be converted into the file `lasslab_hdf5_chk_0000.exo`. The minimal information required by the script is the list of the FLASH output files and a list of the species. For example, for the `LaserSlab` simulation described in section 30.7.5, the command for convert the checkpoint files would be:

```
%> convertspec3d lasslab_hdf5_chk_* --species=cham,targ
```

You should then see a series of `.exo` files generated. The new files contain the following information by default:

- The electron temperature in eV
- The ion temperature in eV
- The electron number density in 1/cc
- The ion number density in 1/cc
- The mass density in g/cc
- The "partial" mass density for each species (i.e. the fraction of the total density in each cell accounted for by each species)

With this information, users can run many Spect3D simulations.

If FLASH plot files are being converted, they must contain certain variables. The required variables are:

- `dens`
- `tele`
- `tion`
- `sumy`
- `ye`
- The variables for each species. In this example, `cham` and `targ`

In addition to simulating diagnostic responses, Spect3D can also plot simulation code output directly. Thus, even though Spect3D doesn't require it, users might want to plot the radiation temperature, or some other variable, in Spect3D. The `--extra` command line argument for `convertspec3d` allows users to add additional variables. For example, let's extend the `convertspec3d` command to include the total specific internal energy and radiation temperature:

```
%> convertspec3d lasslab_hdf5_chk_* --species=cham,targ --extra=trad,eint
```

Part XI

Going Further with FLASH

Chapter 36

Adding new solvers

Adding new solvers (either for new or existing physics) to FLASH starts with a new subdirectory at an appropriate location in the source tree. If the solver provides an alternative implementation for the already supported physics, then the subdiretory should be added below the main sub-unit directory for that sub-unit. For example, adding a *Constant* implementation to the *Heatexchange* unit requires adding a subdirectory Constant under "source/physics/sourceTerms/Heatexchange/HeatexchangeMain". If the solver is adding new physics to the code, a new capitalized subdirectory should be placed under the *physics* subdirectory, effectively creating a new unit, and its API should be defined by placing the null implementations of the relevant functions in the subdirectory. The implementations themselves should go into the *UnitMain* subdirectory placed in the unit. For exampe adding a *Heat* unit the to code requires putting a directory *Heat* under "source/physics", and adding files *Heat_init.F90*, *Heat_finalize.F90* and at least one "doer" function such as *Heat.F90* with null implementations of the corresponding functions. Other than the source files, a *Makefile* and a *Config* file may need to be added to the subdirectory. If the solver is a new unit, both those files will be needed at the *Unit* and *UnitMain* levels. If the solver is an alternative implementaion, the files may or may not be needed. See `http://flash.uchicago.edu/site/flashcode/user_support/flash_howtos/ExampleFlashUnit/` for the architecture of a unit.
`Makefile`: The Makefile snippet added to any directory should reflect all the files in the subdirectory that are not inherited from a higher level directory. At the API level, the Makefile should include all the functions that constitute the API for the unit. At any lower level, those functions should not be included in the Makefile, instead all the local files at that level should be included. The implemented source files appear at *UnitMain* or some other peer level (if there is more than one sub-unit in the unit). An example of Makefile for a unit "Heat" with only three functions is as follows:

```
# Makefile for Heat unit API
Heat = Heat_init.o Heat_finalize.o Heat.o
```

All the subdirectories lying below this level have their Makefiles use macro concatenation to add to the list. For example, if the implementation of the Heat unit adds one file he_getTemp.F90 in the HeatMain implementation, the corresponding Makefile will be

```
# Makefile for HeatMain sub-unit
Heat += Heat\_data.o he_getTemp.o
```

Note that the sub-unit's Makefile only makes reference to files provided at its own level of the directory hierarchy, and the units will have at least one data module (in this instance Heat_data) which contains all the unit scope data. If the sub-unit provides special versions of routines to override those supplied by the any implementation at a higher level directory in the unit, they do not need to be mentioned again in the object list,

`Config`: Create a configuration file for the unit, sub-unit or alternative implementation you are creating. All configuration files in a sub-unit path are used by `setup`, so a sub-unit inherits its parent unit's configuration. `Config` should declare any runtime parameters you wish to make available to the code when this unit is included. It should indicate which (if any) other units your unit requires in order to function, and it should indicate which (if any) of its sub-units should be used as a default if none is specified when `setup` is run. The configuration file format is described in Section 3.1.

This is all that is necessary to add a unit or sub-unit to the code. If you are creating a new solver for an existing physics unit, the unit itself should provide the interface layer to the rest of the code. As long as your sub-unit provides the routines expected by the interface layer, the sub-unit should be ready to work. However, if you are adding a new unit, you will need to add calls to your API routines elsewhere in the code as needed. The most likley place where these calls will need to the be placed will be in the `Driver` unit

It is difficult to give complete general guidance; here we simply note a few things to keep in mind. If you wish to be able to turn your unit on or off without recompiling the code, create a new runtime parameter (*e.g.*, `useUnit`) at the API level of the your unit. You can then test the value of this parameter before calling your API routines from the main code. For example, the `Burn` unit routines are only called if (`useBurn==.true.`). (Of course, if the `Burn` unit is not included in the code, setting `useBurn` to true will result in empty subroutine calls.)

You will need to add `Unit_data.F90` file which will contain all the data you want to have visible everywhere within the unit. Note that this data is not supposed to be visible outside the unit. You may wish have `Driver_initFlash` call your unit's initialiation routine and `Driver_finalizeFlash` to call your unit's finalize routine.

If your solver introduces a constraint on the timestep, you should create a routine named `Unit_`*computeDt*() that computes this constraint. Add a call to this routine in `Drive_computeDt.F90` (part of the `Driver` unit). Your routine should operate on a single block and take three parameters: the timestep variable (a real variable which you should set to the smaller of itself and your constraint before returning), the minimum timestep location (an integer array with five elements), and the block identifier (an integer). Returning anything for the minimum location is optional, but the other timestep routines interpret it in the following way. The first three elements are set to the coordinates within the block of the cell contributing the minimum timestep. The fourth element is set to the block identifier, and the fifth is set to the current processor identifier. This information tags, along with the timestep constraint, when blocks and solvers are compared across processors, and it is printed on stdout by the master processor along with the timestep information as FLASH advances.

If your solver is time-dependent, you will need to add a call to your solver in the `Drive_evolveFlash` routine. Limit the entry points into your unit to the API functions. It is a FLASH architecture requirement, violating this will make the code unmaintainable and will make it hard to get support from the code developers.

Chapter 37

Porting FLASH to other machines

Porting FLASH to new architectures should be fairly straightforward for most Unix or Unix-like systems. For systems which look nothing like Unix or which have no ability to interpret the setup script or makefiles, extensive reworking of the meta-code which configures and builds FLASH would be necessary. We do not treat such systems here; rather than do so, it would be simpler for us to do the port ourselves.

For Unix-like systems, you should make sure that your system has `csh`, a `gmake` that permits included makefiles, `awk`, `sed`, and `Python`. Next, create a directory in `sites/` with the name of your site. It is best to name your site according to the output from the `hostname -f` command (it will return something like code.uchicago.edu) so that the setup script can automatically determine your site without you needing to manually specify the `-site` setup script option. Copy a `Makefile.h` from a pre-existing site directory into your new site directory.

37.1 Writing a `Makefile.h`

To reflect your system, you must modify the different macros defined in `Makefile`:

`FCOMP` : the name of the Fortran 90 compiler

`CCOMP` : the name of the C compiler

`CPPCOMP` : the name of the C++ compiler

`LINK` : the name of the linker (usually the Fortran compiler should serve as the linker)

`PP` : a flag (if any) that should precede a preprocessor directive (typically -D)

`FFLAGS_OPT` : the Fortran compilation flags to produce an optimized executable. These are the flags used when -auto is given to setup.

`FFLAGS_DEBUG` : the Fortran compilation flags to produce an executable that can be used with a debugger (*e.g.* totalview). These flags are used when -debug is passed to setup.

`FFLAGS_TEST` : Fortran compilation flags to produce an executable suitable for testing. These usually involve less optimization. These flags are used when -test is passed to setup.

`CFLAGS_OPT` : the optimized set of compilation flags for C/C++ code.

`CFLAGS_DEBUG` : the debug compilation flags for C/C++ code.

`CFLAGS_TEST` : the test compilation flags for C/C++ code.

`LFLAGS_OPT` : linker flags used with the `_OPT` compilation flags. This usually ends in '-o' to rename the executable.

`LFLAGS_DEBUG` : linker flags used with the `_DEBUG` compilation.

`LFLAGS_TEST` : linker flags used with the `_TEST` compilation.

`LIB_OPT` : libraries to link in with the `_OPT` compilation. This should include the MPI library if an MPI wrapper for the linker was not used (*e.g.* `mpif90`).

`LIB_DEBUG` : libraries to link in the with the `_DEBUG` compilation.

`LIB_TEST` : libraries to link in with the `_TEST` compilation.

`LIB_HDF5` the necessary link line required to link in the `HDF5` library. This will look something like

```
-L /path/to/library -lhdf5
```

For example, here's how you might modify the macros defined in the `Makefile.h` for code.uchicago.edu. The first part of `Makefile.h` defines the paths for the MPI wrapper script and various I/O and numerical libraries.

```
MPI_PATH   = /opt/mpich2/intel/1.4.1p1
HDF5_PATH  = /opt/hdf5/intel/1.8.7
HYPRE_PATH = /opt/hypre/intel/2.7.0b
NCMPI_PATH = /opt/netcdf/intel/1.2.0
```

These should be modified to reflect the locations on your system. Next we setup the compilers and linker. We almost always use the Fortran 90 compiler as the linker, so the Fortran libraries are automatically linked in.

```
FCOMP   = \${MPI_PATH}/bin/mpif90
CCOMP   = \${MPI_PATH}/bin/mpicc
CPPCOMP = \${MPI_PATH}/bin/mpicxx
LINK    = \${MPI_PATH}/bin/mpif90

# pre-processor flag
PP     = -D
```

These commands will need to be changed if your compiler names are different. You are encouraged to use the compiler wrapper scripts instead of the compilers directly. Note that some older versions of MPICH do not recognize `.F90` as a valid extension. For these, you can either update MPICH to a later version or edit `mpif90` and add `.F90` to the line that checks for a valid extension. The `PP` macro refers to the pre-processor and should be set to the flag that the compiler uses to pass information to the C preprocessor (usually `-D`).

We define three different setups of compiler flags as described earlier: the "`_OPT`" set for normal, fully optimized code, the "`_DEBUG`" set for debugging FLASH, and the "`_TEST`" set for regression testing. This latter set usually has less optimization. These three sets are picked with the `-auto`, `-debug`, and `-test` flags to `setup` respectively.

```
FFLAGS_OPT   = -c -g -r8 -i4 -O3 -real_size 64 -diag-disable 10120
FFLAGS_DEBUG = -c -g -r8 -i4 -O0 -check bounds -check format \
-check output_conversion -warn all -warn error -real_size 64 -check uninit \
-traceback -fp-stack-check -diag-disable 10120 -fpe0 -check pointers
FFLAGS_TEST  = \${FFLAGS_OPT} -fp-model precise
F90FLAGS =

CFLAGS_OPT   = -c -O3 -g -D_LARGEFILE64_SOURCE -D_FORTIFY_SOURCE=2 \
-diag-disable 10120
CFLAGS_DEBUG = -c -O0 -g -traceback -debug all -debug extended \
-D_LARGEFILE64_SOURCE -diag-disable 10120 -ftrapuv -fp-stack-check
CFLAGS_TEST  = \${CFLAGS_OPT} -fp-model precise
```

Next come the linker flags. Typically, these have only `-o` to rename the executable, and some debug flags (*e.g.* `-g`) for the "_DEBUG" set.

```
LFLAGS_OPT   = -diag-disable 10120 -O3 -o
LFLAGS_DEBUG = -diag-disable 10120 -o
LFLAGS_TEST  = \${LFLAGS_OPT}
```

There are library macros for any libraries that are required by a specific FLASH unit (*e.g.* HDF5).

```
CFLAGS_MPI   = -I\$(MPI_PATH)/include
CFLAGS_HDF5  = -I\${HDF5_PATH}/include -DH5_USE_16_API
CFLAGS_NCMPI = -I\$(NCMPI_PATH)/include
FFLAGS_HYPRE = -I\${HYPRE_PATH}/include

LIB_MPI   =
LIB_HDF5 = -L\$(HDF5_PATH)/lib -lhdf5_fortran -lhdf5 -lz
LIB_NCMPI = -L\$(NCMPI_PATH)/lib -lpnetcdf
LIB_HYPRE = -L\${HYPRE_PATH}/lib -lHYPRE
```

Finally, we have a macro to specify any platform dependent code and some macros for basic file manipulation and library tools.

```
MACHOBJ =

MV = mv -f
AR = ar -r
RM = rm -f
CD = cd
RL = ranlib
ECHO = echo
```

On most platforms, these will not need to be modified.

Chapter 38

Multithreaded FLASH

38.1 Overview

We have added the capability to run multiple threads of execution within each MPI task. The multithreading is made possible by usage of OpenMP which is described at `www.openmp.org`. For information about building a multithreaded FLASH application please refer to Section 5.8.

The OpenMP parallel regions do not cover all FLASH units in FLASH4. At this time we have only focussed on the units which are exercised most heavily in typical FLASH applications: these are the split and unsplit hydrodynamics solvers, the unsplit magnetohydrodynamic solvers, Gamma law and multigamma EOS, Helmholtz EOS, Multipole solver (improved version (support for 2D cylindrical and 3D cartesian)) and energy deposition. The level of OpenMP coverage will increase in future releases.

The setup script will prevent you from setting up invalid threaded applications by exiting with a conflict error. We have added the conflicts to prevent using, for example, a non thread-safe EOS in a OpenMP parallel region. Example setup lines can be found in `sites/code.uchicago.edu/openmp_test_suite/test.info`.

38.2 Threading strategies

We have experimented with two different threading strategies for adding an extra layer of parallelism to the standard MPI decomposition described in Chapter 8.

The first strategy makes use of the fact that the solution updates on different Paramesh blocks are independent, and so, multiple threads can safely update the solution on different blocks at the same time. This is a coarse-grained threading approach which is only applicable to Paramesh. It can be included in a FLASH application by adding `threadBlockList=True` to the FLASH setup line.

```
  call Grid_getListOfBlocks(LEAF,blockList,blockCount)
  !\$omp do schedule(static)
  do b=1,blockCount
     blockID = blockList(b)
     call update_soln_on_a_block(blockID)
```

The second strategy parallelises the nested do loops in the kernel subroutines such that different threads are updating the solution on independent cells from the same block at the same time. This is a fine-grained threading approach which is applicable to both Paramesh and UG. It can be included in a FLASH application by adding `threadWithinBlock=True` to the FLASH setup line. Notice that we parallelise the outermost do loop for a given dimensionality to improve cache usage for each thread.

```
#if NDIM == 3
        !\$omp do schedule(static)
#endif
        do k=k0-2,kmax+2
```

```
#if NDIM == 2
           !\$omp do schedule(static)
#endif
           do j=j0-2,jmax+2
#if NDIM == 1
              !\$omp do schedule(static)
#endif
              do i=i0-2,imax+2
                 soln(i,j,k) = ....
```

The final threading option is only applicable to the energy deposition unit. In this unit we assign different rays to each thread, where the number of rays assigned is dynamic because the work per ray is not fixed. It can be included in a FLASH application by adding `threadRayTrace=True` to the FLASH setup line

It is perfectly fine to mix these setup options except for `threadBlockList=True` and `threadWithin-Block=True`.

38.3 Running multithreaded FLASH

38.3.1 OpenMP variables

There are OpenMP environmental variables which control the threaded runtime. The most frequntly used is `OMP_NUM_THREADS` which controls the number of OpenMP threads in each parallel region. It should be exported to your environment from your current shell. In the following example we specify that each OpenMP parallel region will be executed by 4 threads (assuming bash shell)

```
export OMP_NUM_THREADS=4
```

You may also need to set `OMP_STACKSIZE` to increase the stack size of the threads created by the OpenMP runtime. This is because some test problems exceed the default limit which leads to a segmentation fault from an innocent piece of source code. In practice we have only encountered this situation in a White Dwarf Supernova simulation with block list threading on a machine which had a default stack size of 4MB. For safety we now set a default value of 16MB for all of our runs to provide plenty of stack space for each thread.

```
export OMP_STACKSIZE=16M
```

If you need to use a job submission script to run FLASH on compute nodes then you should export the OpenMP variables in your job submission script.

38.3.2 FLASH variables

There are FLASH runtime parameters which can be set to `.true.` or `.false.` to turn on/off the parallel regions in different units. They are

Unit	**Block list threading**	**Within block threading**	**Ray trace threading**
Hydro	`threadHydroBlockList`	`threadHydroWithinBlock`	N/A
EOS	N/A	`threadEosWithinBlock`	N/A
Multipole	`threadMpoleBlockList`	`threadMpoleWithinBlock`	N/A
Energy Deposition	N/A	N/A	`threadRayTrace`

There is no parameter for block list threading of EOS because, quite simply, there is no block list in EOS. In many FLASH simulations the EOS subroutines are only called from the hydrodynamic subroutines which means the EOS will be called in parallel if you thread the Hydro unit block list loop.

In general you do not need to worry about these runtime parameters because the default values will be set according to the setup variable passed to the setup script. This means that if you setup a Sedov simulation with block list threading then `threadHydroBlockList` will default to `.true.` and `threadHydroWithinBlock` will default to `.false.`. The runtime control of parallel regions may be useful if we ever need to investigate a possible multithreaded bug in a particular unit.

38.3.3 FLASH constants

There are FLASH constant runtime parameters which describe the threading strategies included in your FLASH application. The constants are named `threadBlockListBuild`, `threadWithinBlockBuild` and `threadRayTraceBuild`. We query these constants in the unit initialization file (e.g. `Hydro_init.F90`) to verify that your FLASH application supports the parallel regions requested by the runtime parameters in 38.3.2. If the parallel regions are not supported you will get a warning message in your FLASH log file and the parallel regions will be disabled. If this happens you can still use the requested parallel regions but you must re-setup FLASH with the appropriate threading strategy. In general you do not need to worry about the existence of these constants because if you setup the application with, say, block list threading it only makes sense for you to adjust the block list threading runtime parameters in your flash.par.

A nice property of using constant runtime parameters instead of pre-processor defines is that `-noclobber` rebuilds are extremely fast. This means you can resetup a `threadBlockList` application with `threadWithin-Block` and only rebuild the handful of source files that actually changed. If we used pre-processor defines to identify the thread strategy then we would have to rebuild every single file because any file could make use of the define. We actually take advantage of the forced rebuild from changing/adding/removing a pre-processor define when we switch from a threaded to a non-threaded application. We do this because OpenMP directives are conditionally compiled when a compiler option such as `-fopenmp` (GNU) is added to the compile line. Any source file could contain OpenMP and so we must do a complete rebuild to ensure correctness. We force a complete rebuild by defining `FLASH_OPENMP` in `Flash.h` for any type of multithreaded build.

38.4 Verifying correctness

The hybrid (MPI+OpenMP) tests using only the multithreaded Hydro and Eos units have the nice property that they **can** give identical results to the corresponding MPI only test. I emphasise **can** because it is possible for an optimized build of the MPI+OpenMP application to give a different answer to the MPI only application. This is because the OpenMP directives can impede the compiler from optimizing the floating point calculations. Therefore, to obtain an exact match between an unthreaded and threaded test you should add a compiler option which prevents the compiler from making any aggressive floating point transformations. For the Intel compiler we needed to add `-fp-model precise` to both the MPI-only and MPI+OpenMP compiler flags to get the same answer. It should be possible to get identical answers for tests like Sod 30.1.1 and Sedov 30.1.4.

This approach does not hold if you use the multithreaded Multipole or energy deposition unit because the floating point accumulation order is different to the order in the unthreaded versions. In the multithreading of the Multipole solver we give each thread its own private moments array and then accumululate the private moment arrays into a single moments array. Similarly, in the energy deposition unit we give each thread a private energy deposition array which is then accumulated into `DEPO_VAR` mesh variable. It is reasonable to expect a small discrepancy, e.g. a magnitude error of 1E-14 in `DEPO_VAR`, in a single time step, but be aware that over a large number of time steps the accumulation of small differences can become much larger.

38.5 Performance results

We present some performance results for each of the multithreaded FLASH units. It is important to note that the multithreaded speedup of each unit is not necessarily representative of a full application because a full application spends time in units which are not (currently) threaded, such as Paramesh, Particles and I/O.

All of the experiments are run on Eureka, a machine at Argonne National Laboratory, which contains 100 compute nodes each with 2 x quad-core Xeon w/32GB RAM. We make use of 1 node and run FLASH with 1 MPI task and 1-8 OpenMP threads.

38.5.1 Multipole solver

We tested the MacLaurin Spheroid problem described in Section 30.3.4 with the new Multipole solver described in Section 8.10.2.2 using three FLASH applications: one with Paramesh and block list threading, one with Paramesh and within block threading and one with UG and within block threading. The FLASH setup lines are

```
./setup unitTest/Gravity/Poisson3 -auto -3d -maxblocks=600 -opt \
+pm4dev +newMpole +noio threadBlockList=True timeMultipole=True

./setup unitTest/Gravity/Poisson3 -auto -3d -maxblocks=600 -opt \
+pm4dev +newMpole +noio threadWithinBlock=True timeMultipole=True

./setup unitTest/Gravity/Poisson3 -auto -3d +ug -opt +newMpole +noio \
threadWithinBlock=True timeMultipole=True -nxb=64 -nyb=64 -nzb=64
```

The effective resolution of the experiments are the same: the Paramesh experiments have `lrefine_max=4` and blocks containing 8 internal cells along each dimension and the UG experiment has a single block containing 64 internal cells along each dimension. We add the setup variable `timeMultipole` to include a custom implementation of `Gravity_potentialListOfBlocks.F90` which repeats the Poisson solve 100 times.

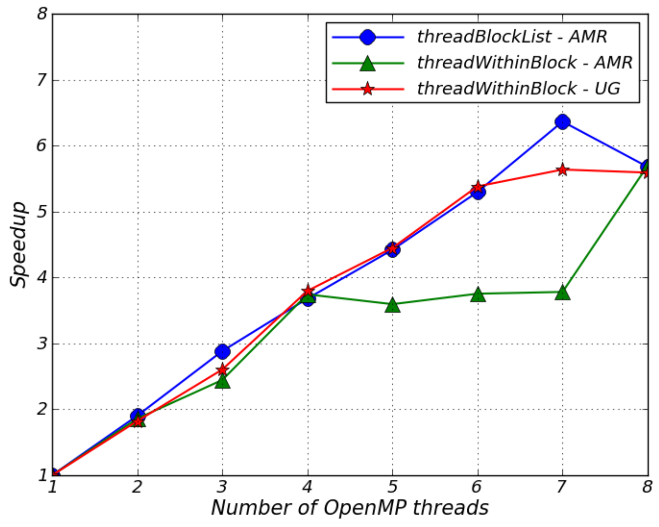

Figure 38.1: Speedup of the threaded Multipole solver in the Maclaurin Spheroid test problem.

The results in Figure 38.1 demonstrate multithreaded speedup for three different configurations of FLASH. The speedup for the AMR `threadWithinBlock` application is about the same for 4 threads as it is for 5,6 and 7 threads. This is because we parallelize only the slowest varying dimension with a static loop schedule and so some threads are assigned 64 cells per block whilst others are assigned 128 cells per block. We do not see the same issue with the UG `threadWithinBlock` application because the greater number of cells per block avoids the significant load imbalance per thread.

38.5.2 Helmholtz EOS

We tested the Helmholtz EOS unit test described in Section 16.6 with a UG and a NoFBS FLASH application. The FLASH setup lines are

```
./setup unitTest/Eos/Helmholtz -auto -3d +ug threadWithinBlock=True \
timeEosUnitTest=True +noio
```

```
./setup unitTest/Eos/Helmholtz -auto -3d +nofbs threadWithinBlock=True \
timeEosUnitTest=True +noio
```

The `timeEosUnitTest` setup variable includes a version of `Eos_unit.F90` which calls `Eos_wrapped` 30,000 times in `MODE_DENS_TEMP`.

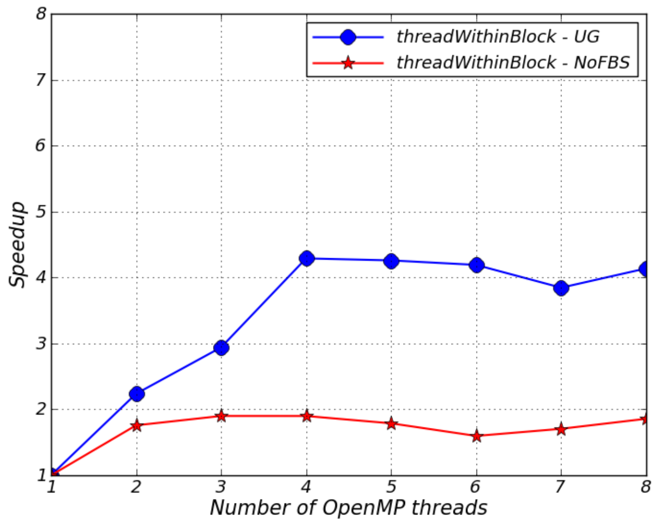

Figure 38.2: Speedup of the threaded Helmholtz EOS in the EOS unit test.

The results in Figure 38.2 show that the UG version gives better speedup than the NoFBS version. This is most likely because the NoFBS version contains dynamic memory allocation / deallocation within `Eos_wrapped`.

The UG application does not show speedup beyond 4 threads. This could be because the work per thread for each invocation of `Eos_wrapped` is too small, and so it would be interesting to re-run this exact test with blocks larger than $8 \times 8 \times 8$ cells. Unfortunately the Helmholtz EOS unit test does not currently support larger blocks – this is a limitation of the Helmholtz EOS unit test and not Helmholtz EOS.

38.5.3 Sedov

We ran 2d and 3d multithreaded versions of the standard Sedov simulation described in Section 30.1.4. We tested both split and unsplit hydrodynamic solvers and both `threadBlockList` and `threadWithinBlock` threading strategies. The 2d setup lines are

```
./setup Sedov -2d -auto +pm4dev -parfile=coldstart_pm.par \
-nxb=16 -nyb=16 threadBlockList=True +uhd

./setup Sedov -2d -auto +pm4dev -parfile=coldstart_pm.par \
-nxb=16 -nyb=16 threadWithinBlock=True +uhd

./setup Sedov -2d -auto +pm4dev -parfile=coldstart_pm.par \
-nxb=16 -nyb=16 threadBlockList=True

./setup Sedov -2d -auto +pm4dev -parfile=coldstart_pm.par \
-nxb=16 -nyb=16 threadWithinBlock=True
```

and the 3d setup lines are

```
./setup Sedov -3d -auto +pm4dev -parfile=coldstart_pm_3d.par \
+cube16 threadBlockList=True +uhd

./setup Sedov -3d -auto +pm4dev -parfile=coldstart_pm_3d.par \
+cube16 threadWithinBlock=True +uhd

./setup Sedov -3d -auto +pm4dev -parfile=coldstart_pm_3d.par \
+cube16 threadBlockList=True

./setup Sedov -3d -auto +pm4dev -parfile=coldstart_pm_3d.par \
+cube16 threadWithinBlock=True
```

The results are shown in Figures 38.3 and 38.4. The speedup graph is based on times obtained from the "hydro" timer label in the FLASH log file.

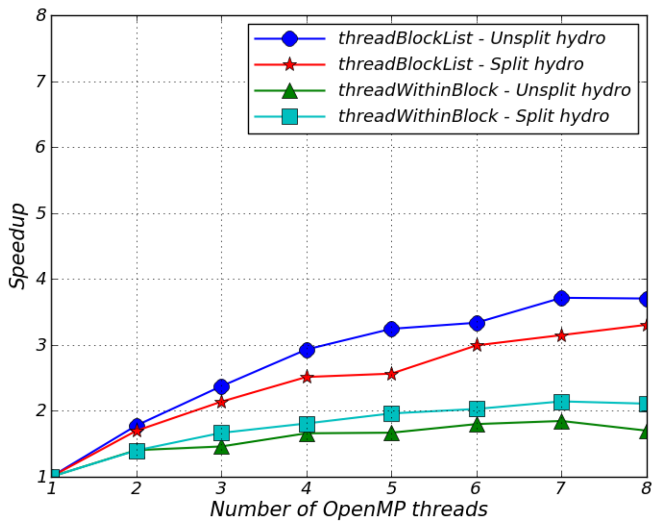

Figure 38.3: Speedup of the threaded hydrodynamic solvers in a 2d Sedov test.

Part of the reason for loss of speedup in Figures 38.3 and 38.4 is that the hydrodynamic solvers in FLASH call Paramesh subroutines to exchange guard cells and conserve fluxes. Paramesh is not (yet) multithreaded and so we call these subroutines with a single thread. All other threads wait at a barrier until the single thread has completed execution.

The unsplit hydro solver has one guardcell fill per hydro timestep and the split hydro solver has NDIM guardcell fills per hydro timestep (one per directional sweep). The extra guardcell fills are part of the reason that the split applications generally give worse speedup than the unsplit applications.

38.5.4 LaserSlab

We finish with a scaling test for the ray trace in the energy deposition unit. We setup the LaserSlab simulation described in Section 30.7.5 with the additional setup option `threadRayTrace=True`. The setup line and our parameter modifications are

```
./setup LaserSlab -2d -auto +pm4dev -geometry=cylindrical \
-nxb=16 -nyb=16 +mtmmmt +laser +mgd +uhd3t species=cham,targ \
mgd_meshgroups=6 -without-unit=flashUtilities/contiguousConversion \
-without-unit=flashUtilities/interpolation/oneDim \
```

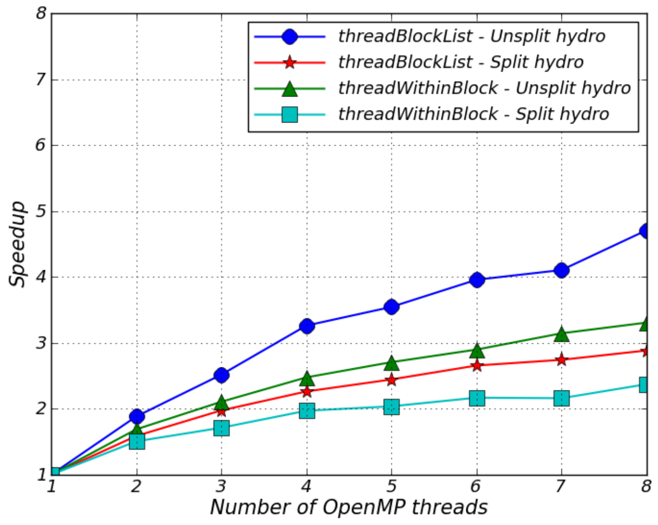

Figure 38.4: Speedup of the threaded hydrodynamic solvers in a 3d Sedov test.

```
-parfile=coldstart_pm_rz.par threadRayTrace=True +noio

ed_maxRayCount = 80000
ed_numRays_1 =  50000
nend = 20
```

The speedup is calculated from times obtained from the "Transport Rays" label in the FLASH log file and the speedup graph is shown in Figure 38.5. The timer records how long it takes to follow all rays through the complete domain during the timestep. As an aside we remove the flashUtilities units in the setup line to keep the number of line continuation characters in a setup script generated Fortran file less than 39. This is just a workaround for picky compilers; another strategy could be a compiler option that allows compilation of Fortran files containing more than 39 continuation characters.

38.6 Conclusion

At the current time we have only really exposed an extra layer of parallelism in FLASH and have not yet focused on tuning the multithreading. We do not have enough experience to suggest the most efficient ways to run the multithreaded code, however, we can suggest some things that may help the efficiency. In an application setup with `threadBlockList` it makes sense to maintain at least 5 blocks per thread. This is because the computational load imbalance between thread A being assigned 1 block and thread B being assigned 2 blocks is larger than thread A being assigned 5 blocks and thread B being assigned 6 blocks. In an application setup with `threadWithinBlock` you should probably use larger blocks, perhaps $16 \times 16 \times 16$ or even $32 \times 32 \times 32$, so that each thread has more cells to work on.

As a closing note, you should be aware of the amount of time spent in the threaded FLASH units compared to the non-threaded FLASH units in your particular FLASH application - perfect speedup in a threaded unit may be insignificant if most of the time is spent in a non-threaded FLASH unit.

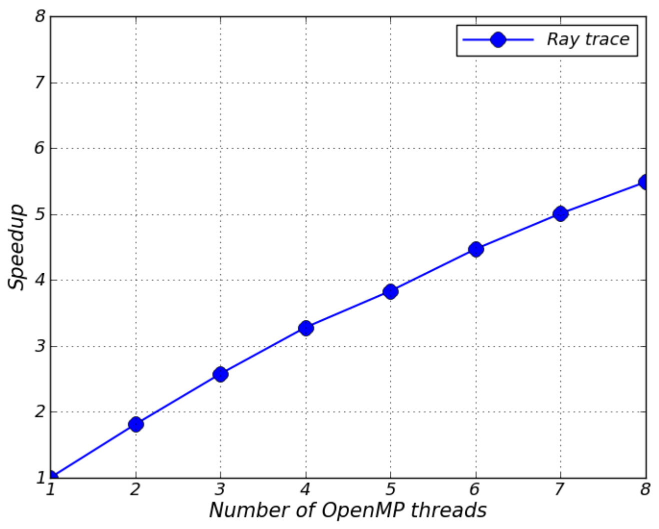

Figure 38.5: Speedup of the energy deposition ray trace in the LaserSlab test.

References

Anninos, W. Y., & Norman, M. L. 1994, ApJ, 429, 434

Aparicio, J. M. 1998, ApJS, 117, 627

Atzeni, S. and Meyer-Ter-Vehn, J. 2004, The Physics of Inertial Fusion: Beam Plasma Interaction, Hydrodynamics, Hot Dense Matter (Oxford Science Publications)

Armfield, S. & Street, R. 2002, Int. J. Numer. Meth. Fluids, 38, 255-282

Bader, G. & Deuflhard, P. 1983, NuMat, 41, 373

Balsara, D. S., 2001, JCP, 174, 614

Balsara, D. S. 2004, ApJS, 151, 149

Balsara, D. S., & Spicer, D. S. 1999, JCP, 149, 270

Bardeen, J. M., Bond, J. R., Kaiser, N., & Szalay, A. S. 1986, ApJ, 304, 15

Barnes, J. & Hut, P. 1986, Nature, 324, 446

Berger, M. J. & Collela, P. 1989, JCP, 82, 64

Berger, M. J. & Oliger, J. 1984, JCP, 53, 484

Blinnikov, S. I., Dunina-Barkovskaya, N. V., & Nadyozhin, D. K. 1996, ApJS, 106, 171

Boris, J. P. & Book, D. L. 1973, JCP, 11, 38

Bonnor, W. B. 1956, MNRAS, 116, 351

Brackbill, J. & Barnes, D. C. 1980 JCP, 35, 426

Braginskii, S. I. 1965 Rev. Plasma Phys., 1, 205

Brandt, A. 1977, Math. Comp., 31, 333

Brio, M. & Wu, C. C. 1988 JCP, 75, 400

Brown, P. N., Byrne, G. D., & Hindmarsh, A. C. 1989, SIAM J. Sci. Stat. Comput., 10, 1038

Brysk, H., Campbell, P.M., Hammerling, P. 1974, Plasma Physics, 17, 473

Bunn, E. F. & White, M. 1997, ApJ, 480, 6

Burgers, J. M. 1969, Flow Equations for Composite Gases (New York: Academic)

Nakamura, K. *et al.* 2010, J. Phys., G 37, 075021 (also `http://pdg.lbl.gov/2010/reviews/contents_sports.html`)

Caughlan, G. R. & Fowler, W. A. 1988, Atomic Data and Nuclear Data Tables, 40, 283

Chandrasekhar, S. 1961, Hydrodynamic and Hydromagnetic Stability (Oxford: Clarendon)

Chandrasekhar, S. 1939, An Introduction to the Study of Stellar Structure (Toronto: Dover)

Chandrasekhar, S. 1987, Ellipsoidal Figures of Equilibrium (New York: Dover)

Chapman, D. L. 1899, Philos. Mag., 47, 90

Chapman, S. & Cowling, T. G. 1970, The Mathematical Theory of Non-uniform Gases (Cambridge: CUP)

Christy, R. F. 1966, ApJ, 144, 108

Cohen, E. R. & Taylor, B. N. 1987, Rev.Mod.Phys., 59, 1121

Colella, P. & Glaz, H. M. 1985, JCP, 59, 264

Colella, P. & Woodward, P. 1984, JCP, 54, 174

Colgate, S. A., & White, R. H. 1966, ApJ, 143, 626

Colin, O. & Ducros, F. & Veynante, D. & Poinsot, T. 2000, Physics of Fluids, 12, 7, 1843

Couch, S. M., Graziani, C. & Flocke, N. 2013, ApJ, 778, 181

Decyk, V. K., Norton, C. D., & Szymanski, B. K. 1997, ACM Fortran Forum, 16 (also http://www.cs.rpi.edu/~szymansk/oof90.html)

DeZeeuw, D. & Powell, K. G. 1993, JCP, 104, 56

Doring, W. 1943, Ann. Phys., 43, 421

Dubey, A., Daley, C., ZuHone, J., Ricker, P. M., Weide, K. & Graziani, C. 2012, ApJS, 201, 27

Duff, I. S., Erisman, A. M., & Reid, J. K. 1986, Direct Methods for Sparse Matrices (Oxford: Clarendon Press)

Einfeldt, B., Munz, C. D., Roe, P. L., & Sjögreen, B. 1991, JCP, 92, 273–295

Emery, A. F. 1968, JCP, 2, 306

Eswaran, V. and Pope, S. B. 1988, Computers & Fluids, 16, 257–278

Evans, C. R. & Hawley, J. F. 1988, ApJ, 332, 659

Ewald, P. P. 1921, Ann. Phys., 64, 253

Federrath, C., Banerjee, R., Clark, P. C. & Klessen, R. S. 2010, ApJ 713, 269

Federrath, C., Roman-Duval, J., Klessen, R. S., Schmidt, W., Mac Low, M.-M. 2010, A&A, 512, A81

Fletcher, C. A. J. 1991, Computational Techniques for Fluid Dynamics, 2d ed. (Berlin: Springer)

Flocke, N. 2015, ACM Transactions on Mathematical Software, 41, Article 30

Forester, C. K. 1977, JCP, 23, 1

Foster, P. N., & Chevalier, R. A. 1993, ApJ, 416, 303

Fryxell, B. A., Müller, E., & Arnett, D. 1989, in Numerical Methods in Astrophysics, ed. P. R. Woodward (New York: Academic)

Fryxell, B., Olson, K., Ricker, P., Timmes, F. X., Zingale, M., Lamb, D. Q., MacNeice, P., Rosner, R., Truran, J. W., & Tufo, H. 2000, ApJS, 131, 273

Gardiner, T., & Stone, J. 2005, JCP, 205, 509

Gittings, M., et al. 2008, Computational Science and Discovery, 1, 015005

Godunov, S. K. 1959, Mat. Sbornik, 47, 271

Harten, A. 1983, JCP, 49, 357–393

Hawley, J. F. 2000, ApJ, 528, 462

Holmström, M., Fatemi, S., Futaana, Y., & Nilsson, H. 2012, The interaction between the Moon and the solar wind. Earth, Planets and Space, 74, 237–245

Holmström, M. 2013, Handling vacuum regions in a hybrid plasma solver. Numerical modeling of space plasma flows (ASTRONUM-2012), ASP Conference Series, vol. 474, 202–207. arXiv:1301.0272

Hu, W. & Sugiyama, N. 1996, ApJ, 471, 542

Huang, J. & Greengard, L. 2000, SIAM. J. Sci. Comput., 21, 1551

Huba, J.D. 2009, NRL Plasma Formulary (NRL/PU/6790–11-551).

Iben, I. Jr. 1975, ApJ, 196, 525

Itoh, N., Hayashi, H., Nishikawa, A., & Kohyama, Y. 1996, ApJS, 102, 411

Jackson, A. P. & Townsley, D. M. & Calder, A. C. 2014, ApJ, 784, 174

James, R. A. 1977, JCP, 25, 71

Jeans, J. H. 1902, Phil. Trans. Roy. Soc. (London), 199, 1

Jouguet, E. 1905, J. Math. Pure Appl., 1, 347

Kaiser, T. B. 2000, Phys. Rev. E, 61, 895

Khokhlov, A. M. 1997, Naval Research Lab memo 6406-97-7950

Krumholz, M., Klein, R., McKee, C., & Bolstad, J. 2007, ApJ, 667, 626

Kurganov, A., Noelle, S., & Petrova, G. 2001, SIAM. J. 23, 707

Kurganov, A., & Tadmor, E. 2000, JCP, 160, 241

Lacey, C. G. & Cole, S. 1993, MNRAS, 262, 627

Ledvina, S., Ma, Y.-J., and Kallio, E., Modeling and Simulating Flowing Plasmas and Related Phenomena, Space Sci. Rev., 143–189, 2008.

Lee, D. 2006, Ph.D. Dissertation, Univ. of Maryland

Lee, D. & Deane, A. 2009, JCP, 228, 952

Lee, D. 2012, JCP, submitted

Lee, Y. T. & More, R. M. 1984, Phys. Fluids, 27, 1273

Li, S., & Li, H. 2004, JCP, 199, 1

Li, S. 2005, JCP, 203, 344–357

Löhner, R. 1987, Comp. Meth. App. Mech. Eng., 61, 323

LeVeque, R. J. 1992, Numerical Methods for Conservation Laws, Birkhäuser.

LeVeque, R. J. 1997, JCP, 131, 327

LeVeque, R. J. 1998, “Nonlinear Convservation Laws and Finite Volume Methods”, LeVeque, R. J., Mihalas, D., Dorfi, E. A., Mueller, E. (ed.), Computational Methods for Astrophysical Fluid Flow, Springer.

Lowrie, R. 2008, Shock Waves, 18, 129

MacLaurin, C. 1801, A Treatise on Fluxions, (W. Baynes), Available on http://books.google.com

MacNeice, P., Olson, K. M., Mobarry, C., de Fainchtein, R., & Packer, C. 1999, CPC, 126, 3

Marder, B. 1987, JCP, 68, 48

Martií, J. M., Müller, E., 2003, Living Rev. Relativ., 6, 7, .

Martin, D. & Cartwright, K., “Solving Poisson’s Equation using Adaptive Mesh Refinement.” (http://seesar.lbl.gov/anag/staff/martin/AMRPoisson.html)

Martin, D., & Cartwright, K. 1996, “Solving Poisson’s Equation using Adaptive Mesh Refinement”, Technical Report No. UCB/ERL M96/66

Matthews, A. P., Current Advance Method and Cyclic Leapfrog for 2D Multispecies Hybrid Plasma Simulations, Journal of Computational Physics, 112, 102–116, 1994.

Mignone, A., Plewa, T., Bodo, G. 2005, ApJ, 160, 199

Mignone, A., Bodo, G., Massaglia, S., Matsakos, T., Tesileanu, O., Zanni, C., & Ferrari, A. 2007, ApJS, 170, 228.

Miyoshi, T. & Kusano K. 2005, JCP, 208, 315–344

Mönchmeyer, R., & Müller, E. 1989, A&A, 217, 351

Müller, E., & Steinmetz, M. 1995, Comp. Phys. Comm., 89, 45

Munz, C. D., Omnes, P., Schneider, R., Sonnendrücker, & Voß, U. 2000, JCP, 161, 484

Nadyozhin, D. K. 1974, Nauchnye informatsii Astron, Sov. USSR, 32, 33

Noh, W. F. 1987, JCP, 72, 78

Orszag, S. A., Tang, C.-M., 1979, JFM, 90, 129

Ostriker, J.P., ed. 1992, Selected Works of Yakov Borisovich Zeldovich (Princeton Univ. Press)

Paczyńsky B., & Wiita, P. J. 1980, A&A, 88, 23.

Parashar M., 1999, private communication (http://www.caip.rutgers.edu/~parashar/DAGH)

Plewa, T. & Müller, E. 1999, A&A, 342, 179.

Potekhin, A. Y., Chabrier, G., & Yakovlev, D. G. 1997, A&A323, 415

Powell, K. G., Roe, P. L., Linde, T. J. , Gombosi, T. I., & DeZeeuw, D. L. 1999, JCP, 154, 284

Press, W. H., Teukolsky, S. A., Vetterling, W. T., & Flannery, B. P. 1992, Numerical Recipes in Fortran, 2d ed. (Cambridge: CUP)

Price, D. J. & Federrath, C. 2010, MNRAS, 406, 1659

Pritchett, Philip L., Particle-in-cell Simulations of Magnetosphere Electrodynamics, IEEE Transactions on Plasma Science, 28, 6, 1976–1990, 2000.

Quirk, J. J., in Upwind and High-Resolution Schemes, ed. M. Yousuff Hussaini, Bram van Leer, and John Van Rosendale, 1997, (Berlin: Springer).

Reinicke, P. and Meyer-ter-Vehn, J. 1991, Phys. Fluids A, 3, 1807

Ricker, P. M. 2008, arXiv: 0710.4397, ApJS, 176, 293

Ross, R., Nurmi, D., Cheng, A. & Zingale, M. 2001, Proceedings of SC2001.

Salmon, J. K. & Warren, M. S. 1994, JCP, 111, 136

Schulz-Rinne, C. W, Collins, J. P., and Glaz, H. M. 1993, SIAM J. Sci. Comput. 14, 1394.

Sedov, L. I. 1959, Similarity and Dimensional Methods in Mechanics (New York: Academic)

Shu, C.-W. 1998, in Advanced Numerical Approximation of Nonlinear Hyperbolic Equations, ed. A. Quarteroni, Lecture Notes in Mathematics, 1697, (Berlin: Springer)

Shu, C.-W. & Osher, S. 1989, JCP, 83, 32

Skinner, M. A., & Ostriker, E. C. ApJS, 188, 290

Spitzer, L. 1962, Physics of Fully Ionized Gases. (New York: Wiley)

Sportisse, B. 2000, JCP, 161, 140

Springel, V. 2005, MNRAS, 364, 1105

Sod, G. 1978, JCP, 27, 1

Strang, G. 1968, SIAM J. Numer. Anal., 5, 506

Timmes, F. X. 1992, ApJ, 390, L107

Timmes, F. X. 1999, ApJS, 124, 241

Timmes, F. X. 2000, ApJ, 528, 913

Timmes, F. X. & Arnett, D. 2000, ApJS, 125, 294

Timmes, F. X. & Brown, E. 2002 (in preparation)

Timmes, F. X. & Swesty, F. D. 2000, ApJS, 126, 501

Timmes, F. X. & Zingale, M. & Olson, K. & Fryxell, B. & Ricker, P. & Calder, A. C. & Dursi, L. J. & Tufo, H. & MacNeice, P. & Truran, J. W. & Rosner, R. 2000, ApJ543, 938

Toro, E. F. 1999, Riemann Solvers and Numerical Methods for Fluid Dynamics, 2nd Ed. (New York: Springer)

Tóth, G. 2000, JCP, 161, 605

Townsley, D. M. & Calder, A. C. & Asida, S. M. & Seitenzahl, I. R. & Peng, F. & Vladimirova, N. & Lamb, D. Q. & Truran, J. W. 2007, ApJ, 668, 1118

Trottenberg, U., Oosterlee, C., & Schüller, A. 2001, Multigrid (San Diego: Academic Press)

Tzeferacos, P., Fatenejad, M., Flocke, N., Gregori, G., Lamb, D. Q., Lee, D., Meinecke, J., Scopatz, A., & Weide, K. 2012 HEDP, 8, 322, doi:10.1016/j.hedp.2012.08.001

Uhlenbeck, G. E. & Ornstein, L. S. 1930, Phys. Rev. 36, 823

van der Vorst, H. 1992, "Bi-CGSTAB: A Fast and Smoothly Converging Variant of Bi-CG for the Solution of Nonsymmetric Linear Systems", SIAM J. Sci. and Stat. Comput., 13:2, 631-644

van Leer, B. 1979, JCP, 32, 101

Vanella, M., Rabenold, P. & Balaras, E. 2010, J. Comput. Phys., 229:18, 6427-6449

von Neumann, J. 1942, ORSD Rep. No. 549

Velikovich, A. L., Giuliani, J. L., Zalesak, S. T., Thornhill, J. W., & Gardiner, T. A. 2012, Phys. Plasmas, 19, 012707

Vladimirova, N. & Weirs, G. & Ryzhik, L. 2006, Combustion Theory and Modelling, 10, 727

Wallace, R. K., Woosley, S. E., & Weaver, T. A. 1982, ApJ, 258, 696

Warren, M. S. & Salmon, J. K. 1993, in Proc. Supercomputing 1993 (Washington, DC: IEEE Computer Soc.)

Weaver, T. A., Zimmerman, G. B., & Woosley, S. E. 1978, ApJ, 225, 1021

Williams, F. A. 1988, Combustion Theory (Menlo Park: Benjamin-Cummings)

Williamson, J. H. 1980, JCP, 35, 48

Winske, D. and Leroy, M. M., Diffuse ions produced by electromagnetic ion beam instabilities, Journal of Geophysical Research, 89, 2673–2688, 1984.

Winske, D. and Quest, K. B., Electromagnetic Ion Beam Instabilities: Comparison of one- and two-dimensional simulations, Journal of Geophysical Research, 91, 8789–8797, 1986.

Woodward, P. & Colella, P. 1984, JCP, 54, 115

Xin, J. 2000, SIAM Rev., 42, 161

Yakovlev, D. G., & Urpin, V. A. (YU) 1980 24, 303

Yang. J. & Balaras, E. 2006, J. Comput. Phys., 215:1, 12-40

Yee, H. C., Vinokur, M., and Djomehri, M. J. 2000, JCP, 162, 33

Yee, K. S., IEEE Trans. Antenna Propagation, 1966, AP-14, 302

Zachary, A., Malagoli, A., Colella, P. 1994, SIAM, 15, 263

Zalesak, S. T. 1987, in Advances in Computer Methods for Partial Differential Equations VI, eds. Vichnevetsky, R. and Stepleman, R. S. (IMACS), 15

Zel'dovich, Ya. B. 1970, A&A, 5, 84

Zel'dovich, Ya. B. and Raizer, Yu. P. 2002, Physics of Shock Waves and High-Temperature Hydrodynamic Phenomena, Dover

Zhang, W., Howell, L., Almgren, A., Burrows, A., & Bell, J. 2011, ApJS, 196, 20

Zingale, M., Dursi, L. J., ZuHone, J., Calder, A. C., Fryxell, B., Plewa, T., Truran, J. W., Caceres, A., Olson, K., Ricker, P. M., Riley, K., Rosner, R., Siegel, A., Timmes, F. X., and Vladimirova, N. 2002, ApJS, 143, 539

Runtime Parameters

FLASH4 API

Index